Title
Nickel-Catalyzed Arylations of Amides

Permalink
https://escholarship.org/uc/item/0cs6s1m6

Author
Boit, Timothy B

Publication Date
2021

Peer reviewed|Thesis/dissertation

UNIVERSITY OF CALIFORNIA

Los Angeles

Nickel-Catalyzed Arylations of Amides

A dissertation submitted in partial satisfaction of the

requirements for the degree Doctor of Philosophy

in Chemistry

by

Timothy Bartlett Boit

2021

ABSTRACT OF THE DISSERTATION

Nickel-Catalyzed Arylations of Amides

by

Timothy B. Boit

Doctor of Philosophy in Chemistry

University of California, Los Angeles, 2021

Professor Neil Kamal Garg, Chair

This dissertation describes the development of nickel-catalyzed arylations of amides via amide C–N bond activation. Although amide C–N bonds have traditionally been considered relatively inert, recent progress in the metal-catalyzed activation of this bond has enabled cross-couplings of amide electrophiles. Herein, efforts to achieve a general nickel-catalyzed Suzuki–Miyaura cross-coupling of aliphatic amides and a strategy to improve the practicality of this parent methodology are described. Furthermore, a one-pot reductive arylation of amides wherein two different nucleophiles are added to the amide carbonyl carbon is reported. This reaction, which proceeds by way of a sequential nickel-catalyzed Suzuki–Miyaura coupling and base-catalyzed reduction cascade process, directly converts amide starting materials to chiral secondary alkyl–

aryl alcohol products. Each of the methodologies presented is expected to expand the field of amide C–N bond activation methodologies and highlight the synthetic utility of amide building blocks for C–C bond-forming cross-coupling reactions.

Chapter one outlines the current state of the art in nickel and iron-catalyzed cross-couplings of traditionally inert electrophiles. Specifically, recent advances in base-metal-catalyzed reactions of phenol, aniline, ester, and amide derivatives that proceed via aryl or acyl C–O/C–N bond activation are described. This brief review should provide context for the subsequent studies presented in this dissertation. Furthermore, summarizing recent efforts in this field is expected to highlight the utility of base-metal-catalyzed cross-couplings of traditionally-inert electrophiles in organic synthesis.

Chapters two and three describe the development of nickel-catalyzed Suzuki–Miyaura cross-couplings of aliphatic amide derivatives. Chapter two details a general nickel-catalyzed arylation of aliphatic amides, where mild cleavage of the aliphatic amide C–N bond is made possible using a nickel(0)–N-heterocyclic carbene (NHC) catalyst–ligand system. The methodology specifically focuses on the union of heterocyclic fragments to assemble poly-heterocyclic ketone scaffolds. In addition, a stereoretentive Suzuki–Miyaura coupling is described, wherein amides bearing epimerizable α-stereocenters undergo the reaction with minimal erosion of stereochemistry. Chapter three outlines a strategy for performing nickel-catalyzed Suzuki–Miyaura couplings of aliphatic amides on the benchtop. In this approach, air- and moisture-sensitive reagents are stored in paraffin capsules, allowing for air-sensitive transition-metal-catalyzed cross-couplings to be carried out without the need for glovebox manipulations. Both studies are anticipated to advance the utility of amides as acyl synthons for C–C bond-forming cross-coupling reactions.

Chapters four and five concern the development of a base-catalyzed reduction of aryl ketones and its application toward a one-pot reductive arylation of aliphatic amides. In chapter four, the use of an electron-rich benzylic alcohol reductant to achieve a Meerwein–Ponndorf–Verley (MPV)-type reduction of ketones is reported. This approach avoids the use of the hydride source as the solvent, proceeds under mildly basic conditions, reduces aromatic and *O*- and *S*-containing heteroaromatic ketones, and delivers enantioenriched alcohol products through a stereospecific reduction when using an enantioenriched reductant. These studies expand the field of base-catalyzed MPV-type reductions of carbonyls and address several limitations associated with prior methodologies. Chapter five describes the the application of this mild ketone reduction protocol toward a one-pot reductive arylation of amides. Specifically, this methodology, which proceeds by way of a nickel-catalyzed Suzuki–Miyaura coupling of aliphatic amides and subsequent base-catalyzed transfer hydrogenation of ketone intermediates, provides direct access to chiral secondary alkyl–aryl alcohols from amide starting materials. This study represents the first catalytic method for the direct intermolecular addition of two different nucleophiles to the amide carbonyl carbon. Moreover, these efforts are expected to promote the development of additional catalytic approaches to directly convert carboxylic acids and their derivatives to functional groups bearing stereogenic centers.

Kendall N. Houk

Hosea Martin Nelson

Yi Tang

Neil Kamal Garg, Committee Chair

University of California, Los Angeles

2021

It's the sides of the mountain which sustain life, not the top.

– Robert M. Pirsig

For Anna

TABLE OF CONTENTS

LIST OF FIGURES

CHAPTER ONE

CHAPTER THREE

CHAPTER FOUR

CHAPTER FIVE

LIST OF TABLES

LIST OF ABBREVIATIONS

α	alpha
β	beta
γ	gamma
λ	wavelength
μ	micro
π	pi
δ	chemical shift
Δ	heat
(Het)	hetero
[H]	reduction
[O]	oxidation
$[\alpha]_D$	specific rotation at wavelength of sodium D line
°C	degrees Celsius
Å	angstrom
AcOH	acetic acid
$AlCl_3$	aluminum trichloride
Alk	alkyl
APCI	atmospheric-pressure chemical ionization
app.	apparent
aq.	aqueous
Ar	aryl
Au	gold
B(pin)	pinacol borane
Benz-ICy•HCl	1,3-dicyclohexylbenzimidazolium chloride
BF_3•Et_2O	boron trifluoride diethyl etherate
Bn	benzyl
$BnNH_2$	benzylamine

Boc	*tert*-butoxycarbonyl
Boc$_2$O	di-*tert*-butyl dicarbonate
Bu	butyl
Bz	benzoyl
c	centi
c	concentration for specific rotation measurements
C	carbon
C$_6$D$_6$	deuterated benzene
C$_6$H$_6$	benzene
CaH$_2$	calcium hydride
cal	calorie
calcd	calculated
cat.	catalytic or catalyst
CD$_3$CN	deuterated acetonitrile
CDCl$_3$	deuterated chloroform
CF$_3$	trifluoromethyl
CH$_2$Cl$_2$	dichloromethane
CH$_3$	methyl
CH$_3$CN	acetonitrile
CHCl$_3$	chloroform
CO$_2$	carbon dioxide
cod	1,5-cyclooctadiene
d	doublet
DART	direct analysis in real time
DMAP	4-dimethylaminopyridine
DMF	*N,N*-dimethylformamide
DMSO	dimethyl sulfoxide
dppf	1,1′-bis(diphenylphosphino)ferrocene
EDC	1-ethyl-3-(3-dimethylaminopropyl)carbodiimide
EDC•HCl	1-ethyl-3-(3-dimethylaminopropyl)carbodiimide hydrochloride
eds.	editors
EDTA	ethylenediaminetetraacetic acid
ee	enantiomeric excess
equiv	equivalent

ESI	electrospray ionization
Et	ethyl
Et$_2$O	diethyl ether
Et$_3$N	triethylamine
EtOAc	ethyl acetate
FAQ	frequently asked questions
FT	Fourier transform
g	gram(s)
GC-MS	gas chromatography mass spectrometry(er)
h	hour(s)
H	proton
hν	light
HCl	hydrochloric acid
Hf	hafnium
HMB	hexamethylbenzene
HOBt	hydroxybenzatriazole
HPLC	high-performance liquid chromatography
HRMS	high resolution mass spectroscopy
Hz	hertz
i-Bu	isobutyl
i-Pr	*iso*-propyl
i-PrNH$_2$	*iso*-propyl amine
i-PrOAc	*iso*-propyl acetate
i-PrOH	*iso*-propyl alcohol
I$_2$	iodine
ICy•HCl	1,3-dicyclohexylimidazolium chloride
IPr	1,3-Bis(2,6-diisopropylphenyl)-imidazol-2-ylidene
IR	infrared (spectroscopy)
J	coupling constant
K$_3$PO$_4$	potassium phosphate tribasic
KO*t*-Bu	potassium *tert*-butoxide
KRED	ketoreductase
L	liter
LDA	lithium diisopropylamide
LiAlH$_4$	lithium aluminum hydride

LiCl	lithium chloride
LiHMDS	lithium bis(trimethylsilyl)amide
m	multiplet or milli or meter
M	molecular mass, molar, or metal
m-	meta
m/z	mass to charge ratio
Me	methyl
$MgSO_4$	magnesium sulfate
MHz	megahertz
min	minute(s)
Mo	molybdenum
mol	mole(s)
mp	melting point
MS	molecular sieves
N	normal
n-Bu	butyl (linear)
n-BuLi	butyl (linear) lithium
N_2	nitrogen gas
Na^0	sodium metal
$Na_2S_2O_3$	sodium thiosulfate
Na_2SO_4	sodium sulfate
NADP	nicotinamide adenine dinucleotide phosphate
NaH	sodium hydride
$NaHCO_3$	sodium bicarbonate
NaOH	sodium hydroxide
NaO*t*-Bu	sodium *tert*-butoxide
NH_4Cl	ammonium chloride
NHC	*N*-heterocyclic carbene
Ni	nickel
nM	nanomolar
NMR	nuclear magnetic resonance
NOESY	nuclear overhauser effect spectroscopy
o-	ortho
OMe	methoxy
p-	para

Pd	palladium
PDB	protein data bank
Ph	phenyl
PhCOCF$_3$	2,2,2-trifluoroacetophenone
PhH	benzene
PhMe	toluene
Piv	pivaloyl
PPh$_3$	triphenylphosphine
ppm	parts per million
Pr	Propyl
Pt	platinum
PTFE	polytetrafluoroethylene
q	quartet
quint.	quintet
rac	racemic
R$_f$	retention factor
rpm/RPM	revolutions per minute
Ru	ruthenium
s	singlet or second
sat.	saturated
sext.	sextet
SFC	supercritical fluid chromatography
SiPr	1,3-Bis(2,6-diisopropylphenyl)-1,3-dihydro-2*H*-imidazol-2-ylidene
SiPr•HCl	1,3-Bis(2,6-diisopropylphenyl)-1,3-dihydro-2*H*-imidazol-2-ylidene hydrochloride
SmI$_2$	samarium diiodide
t	triplet
t-Bu	*tert*-butyl
t-BuNH$_2$	*tert*-butyl amine
t-BuOH	*tert*-butyl alcohol
TA	teaching assistant
TBDPS	*tert*-butyldiphenylsilyl
TBDPSCl	*tert*-butyldiphenylchlorosilane
TCI	Tokyo Chemical Industry Co.

temp	temperature
THF	tetrahydrofuran
Ti	titanium
TLC	thin layer chromatography
TMB	1,3,5-trimethoxybenzene
TMSCl	chlorotrimethylsilane
t_R	retention time
Trit	trityl
Ts	tosyl
UATR	universal attenuated total reflectance
UHP	ultra-high purity
UV	ultraviolet
WT	wild-type
$ZnEt_2$	diethyl zinc
Zr	zirconium

ACKNOWLEDGEMENTS

Any body of work, even a modest one such as this, requires help and input from many people to complete. I am also indebted to the failed experiments, the rabbit holes, the dead ends, and unfruitful collaborations that didn't make it into the following chapters, but from which I learned a great deal. Life lessons that I've either stumbled upon or, more often, learned from a friend or colleague also won't receive the formal recognition they deserve in this dissertation. Though I will likely overlook some people, I hope to recognize those who have helped me through my chemistry career thus far.

I first owe thanks to Dr. Rajeeva Singh and Prof. Ben Gorske, who encouraged my initial interest in chemistry. To this day, Rajeeva is far more concerned with the books I am reading than anything I am doing in the lab. To him, institutionalized science is merely another outlet for his natural curiosity. In this regard, Rajeeva encouraged me to approach problems at the bench with interest and care. My undergraduate advisor, Ben Gorske, presented experimental chemistry to me as a challenge of diligence and industry. Unsurprisingly, this attitude appealed to my competitive side and I gladly took the bait. Indeed, I enjoy organic synthesis in part because it can be physically taxing. These two perspectives have come to represent the yin and yang of how I view chemistry and I find that I do my best work when they are balanced.

I owe the majority of my development as a critical thinker and professional to my doctoral advisor, Prof. Neil Garg. Beyond being a gifted chemistry teacher, Neil has a remarkable talent for showing his students how to effectively manage their time and efficiently dissect complex problems. These practical and analytical tools are now indispensable to my life inside and outside of the laboratory. Neil is also an exceptionally clear thinker and communicator and expects his students to meet his high standards. In striving to elevate my writing and presentation skills, my

appreciation for these crafts has grown dramatically and they now constitute highly rewarding aspects of having a career in the sciences. Neil has also impressed me with his capacity for change. Over my five years, he has transformed from boss, to mentor, to friend. At our first meeting Neil told me that above all else, he aims to make sure those around him know that he is dependable. He has certainly succeeded in convincing me of that. Neil is a good person to have in your corner and I am immensely grateful for his unwavering support over the past five years.

I would also like to acknowledge the rest of my doctoral committee: Professors Ken Houk, Hosea Nelson, and Yi Tang. Their collective support, advice, and mentorship throughout my graduate career was invaluable, and I thank them for serving on my committee.

The most important component of the Garg Lab is the people. Every member of the lab has left a lasting impression on me. With many, I have formed good friendships. I am indebted to everyone in the Garg lab for inspiring a culture of generosity and hard work.

Postdoctoral scholars occupy a unique niche in the laboratory environment. Largely detached from laboratory politics, they can be trusted sources of support and guidance for fatigued graduate students. Moreover, having already completed graduate school, they often have a noticeable familiarity with the feeling of failure. The reassurances of a postdoc to keep swimming when there's no land in sight can go a long way.

In my five years, the Garg lab has benefited from a number of strong postdoctoral scholars. Drs. Sophie Rachine, Maude Giroud, and Veronica Tona represented the European bloc and introduced several unforgettable phrases to the group including "I'm swimming in a cup of water." Drs. Nathan Adamson and Daniel Nasrallah are the most recent postdocs to join the group and have already demonstrated their abilities as effective synthetic chemists and teachers. I've had the honor of working with Dr. Logan Bachmann in several contexts including on chemistry projects,

a collaboration with the Bill & Melinda Gates Foundation, and synthetic exercises. Ever humble about his extensive chemical knowledge, Logan is one of my favorite people to learn from and I look forward to seeing what he takes on after leaving the Garg lab.

Dr. Evan Darzi was a postdoctoral scholar in the Garg lab during my first three years in graduate school and has had a profound impact on my scientific and personal growth. We worked in adjoining hoods and I greatly benefited from Darzi's aptitude as an experimentalist and teacher. Darzi is without a doubt the most resourceful and clever chemist I have ever met. He embodies the spirit of "work smart, not hard" and has a real talent for accumulating lots of information from very few experiments. Beyond that, Darzi was born to be the front man of a 90's rock band and his magnetic personality coupled with an incorrigible cheekiness makes him just plain fun to be around. While working next to him, I absorbed a few core lessons on resourcefulness, pushing the limits of one's chemistry, and being a good colleague. Never one to dwell on the past, he also helped me develop tools for remaining positive when chemistry or life go south. I'm incredibly grateful that Darzi, as he loves to remind me with tongue-in-cheek, is "there for me."

My first year in the Garg lab was in part characterized by the exceptionally strong graduating class of Jesus Moreno, Jose Medina, Nick Weires, and Mike Corsello. Nick was my direct mentor and he showed me the ropes of synthetic organic chemistry and methodology development. A meticulous experimentalist, he instilled in me a determination to be thorough and detailed at the bench. In addition, Nick is an exceptional writer and taught me essence of technical scientific writing. He also turned out to be one of the funniest people I have ever met. That first summer of graduate school in a room with Jacob, Yamano, and Nick, I regularly had to catch my breath from laughing so hard. I also formed a strong connection with Mike Corsello. An important common ground between us is the appreciation of knowledge for its own sake. Mike can deftly

transition between intellectual sparring partner or compassionate comrade and has the wisdom to know which role his friends need him to play.

I am grateful to have overlapped with Elias Picazo, Emma Baker-Tripp, and Junyong Kim for two years during my graduate career. All three were absolute powerhouses in the lab and also excellent role models for how to navigate graduate school with a healthy optimism and a fulfilling life away from the bench. I had the pleasure of working with Junyong for two years and his experience was instrumental in getting several projects off the ground.

The class of '19 also had some incredible people. By his fifth year, Lucas Morrill had emerged as a formidable synthetic chemist and possessed a chemical intuition that we all inherently trusted. As a fellow Bostonian, Lucas was always game to talk about the Celtics, Sox, or Pats, and I'm glad for the part I played in getting him more interested in European soccer. Joyann Barber was unapologetically upbeat all the time and it was hard to frown when you saw her in the morning. In contrast, Bryan Simmons was perfectly sardonic and I found his grounded feedback invaluable as I prepared documents for grant applications or candidacy.

Besides my own class, I always felt closest to the class of students directly above me. Rob Susick and I bonded over a shared love of esoteric music, the outdoors, and armchair philosophy. Michael Yamano continues to be a source of inspiration for me in my professional life. Unquestionably brilliant, Michael is also one of the hardest working chemists I've met. I spent many hours pitching hypothetical projects to Yamano only to watch him effortlessly dismantle them; this is how I learned to separate the wheat from the chaff. Jordan Dotson is another chemist I consider to be an intellectual shepherd of my graduate school experience. Jordon taught us all the value of having a deep understanding of physical organic chemistry. Moreover, Jordan's humble and caring demeanor is immediately disarming and makes him an incredibly effective

teacher. From the very start, I felt a kinship with Jacob Dander. That bond was strengthened by living together at Los Leones and supporting one another as we ran the gauntlet that accompanied developing nickel-catalyzed methods. Although his taste in movies is questionable, I trust his judgement on nearly every other subject. Jacob is a gifted logician and has a hilarious story for almost any occasion. I would just as soon choose him to be my debate partner as my drinking buddy. His steadfast moral compass has also been a source of comfort to me when my own feels unsure. Finally, we are both indebted to Jacob's better half, Ryan Kauffman. Ryan is an incredibly warm and caring individual whose jaw-dropping artistic talent serves Jacob and I the slice of humility we so often need.

I have been fortunate to share this journey with outstanding classmates. Melissa Ramirez has been a positive force in the lab throughout our time in graduate school. Her warm authenticity and consistent work ethic endear her to all of her colleagues. I am indebted to Melissa for supporting me as Lecture Series Representative for UCLA's Organization for Cultural Diversity in the Sciences (OCDS) this past year. Being a part of this organization has been a highlight of my final year in graduate school. Sarah Anthony is the Garg lab member with the greatest longevity and is a reliable go-to with any questions concerning UCLA or Garg lab traditions. A southern California native, she is also easy-going and always down for a good laugh. At the bench, Sarah has an inspiring work ethic and an impressively broad synthetic skill set. The Garg lab will certainly miss her wealth of laboratory experience and party-organization skills.

It's not an original observation that at some point in the Garg lab, you transition to being one of the "old folks." Having just barely summitted a series of treacherous peaks yourself, you're then expected to throw the rope down for others and learn how to guide them up.

The Garg lab is in good hands with the class of students directly below ours. Francesca, or simply "Fran," is one of the nicest people I have ever met. I have a lot of respect for Fran's quiet strength as she makes a daily choice to embrace optimism over the more excusable pessimism that can permeate our field. Jason Chari is an enigma to me and I delight in my confusion. I once asked him what he thinks about while regularly completing bike rides of over 100 miles and other superhuman feats of endurance. In his typically matter-of-factness, Jason said he knew he'd simply be disappointed if he quit. He is similarly indefatigable in the lab. The class is rounded out by Rachel Knapp. Rachel is undeniably cool, making her something of an anomaly in academia. She is also a staunch pragmatist, highlighted by her enthusiasm for L. L. Bean products. Perhaps most importantly, Rachel is a dependable friend and colleague, and a trusted source of advice for many students including myself. This past year, I had the good fortune to work with her as part of a collaboration with the Bill & Melinda Gates Foundation. Rachel not only has a firm grasp of synthetic chemistry, but an equally sharp mind for understanding people.

The class of '23 boasts several forces of nature. Katie Spence, aka the "Wild Card," is absolutely fearless and I look forward to joining her crew if there is ever an apocalyptic event. Andrew Kelleghan is a uniquely gifted synthetic chemist and I appreciate his capacity to distill many chemical concepts down to their first principles. The final member of the group, Milauni Mehta, is an incredibly close friend unless she is within earshot, in which case we are *best* friends. I had the distinct honor of being a mentor to Milauni during her earlier years in the lab. We have worked together on three separate projects during my graduate career. Those projects cemented a ride-or-die comradery between us that was a great source of encouragement and support when chemistry wasn't working. Having a front row seat to her evolution as a chemist and professional has been one of the most rewarding aspects of my graduate career.

The current second-year class is also comprised of strong individuals. Matt McVeigh is an authority on all things Texas and the type of colleague you want to get a beer with after work. Laura Wonilowicz has my respect forever after witnessing some of the beastly columns she has run so far as a graduate student. Ana Bulger, who I'm convinced possesses the world's most finely tuned bullshit detector, has also been a good friend since her arrival in the lab. This past year, Ana, Jacob Dander, and I co-wrote a review, which directly benefited from Ana's capacity to pick apart and improve our writing. And though neither I, nor anyone else, will ever live up to Dander in Ana's eyes, I'm glad she has nevertheless accepted my friendship.

The current group of first-year students, Dominick Witkowski, Arismel Tena-Meza, and Luca McDermott, have the proper ingredients to succeed in the Garg lab: optimism, hard work, and a willingness to be a team-player. I look forward to seeing their future successes.

Finally, I would like to thank the love of my life, Anna Bearman. Our relationship began in fits and starts well before graduate school and I kept her at a comfortable distance, as I did with everyone else in my life. At some point, Anna got tired of my battling my hesitation from a distance and moved in with me before I knew what happened. With her by my side, the past (nearly) four years have been the happiest and most fulfilling of my life as I have learned to live without fear or mistrust. She knows me better than I know myself and I love her more than I could ever express in words. She is my earth, moon, stars, and sun. In Los Angeles, we have had the space and time to grow together, and it has been precious. Now, eager to return to the rocks and pines of the east coast, we are an inseparable team. In the next leg of our journey, as in all of our adventures, I will happily supply the wind in our sails and trust Anna at the helm.

Chapter 1 is a version of Boit, T. B.; Dander, J. E.; Bulger, A. S.; Garg, N. K. *ACS Catal.* **2020**, *10,* 12109–12129. Boit, Dander, Bulger, and Garg were responsible for the manuscript.

Chapter 2 is a version of Boit, T. B.; Weires, N. A.; Kim, J.; Garg, N. K. *ACS Catal.* **2018**, *8*, 1003–1005. Boit, Weires, and Kim were responsible for experimental work.

Chapter 3 is a version of Mehta, M. M.; Boit, T. B.; Dander, J. E.; Garg, N. K. *Org. Lett.* **2020**, *22*, 1–5. Mehta, Boit, and Dander were responsible for experimental work.

Chapter 4 is a version of Boit, T. B.; Mehta, M. M.; Garg, N. K. *Org, Lett.* **2019**, *1*, 6447–6451. Boit and Mehta were responsible for experimental work.

Chapter 5 is a version of Boit, T. B.; Mehta, M. M.; Kim, J.; Baker, E. L.; Garg, N. K. *Angew. Chem., Int. Ed.* **2021**, *60*, 2472–2477. Boit, Mehta, Kim, and Baker were responsible for experimental work.

BIOGRAPHICAL SKETCH

Education:

University of California, Los Angeles, CA
- Ph.D. in Organic Chemistry, anticipated Spring 2021
- TRDRP Graduate Research Fellow, July 2018 – Present
- Current GPA: 4.00/4.00

Bowdoin College, Brunswick, ME
- B.A. in Chemistry and Physics, June 2016
- Cumulative GPA: 3.65/4.00

Professional and Academic Experience:

Graduate Research Assistant: University of California, Los Angeles, CA
- July 2016 – present; Advisor: Prof. Neil K. Garg.
- Established the scope of the nickel-catalyzed Suzuki–Miyaura cross-coupling of aliphatic amides and achieved the first stereoretentive Suzuki–Miyaura coupling of amides. These efforts established the first general catalytic (hetero)arylation of aliphatic amides.
- Developed a paraffin encapsulation strategy to achieve the nickel-catalyzed Suzuki–Miyaura cross-coupling of aliphatic amides on the benchtop. This methodology obviates the need to set up the reactions in a glovebox, rendering it more practical and user-friendly.
- Discovered a one-pot reductive arylation of amides. This methodology converts amides into chiral secondary alcohols through a nickel-catalyzed cross-coupling and transfer hydrogenation cascade, and represents the first catalytic intermolecular addition of two distinct nucleophiles to an amide in a single operational step.
- Developed a base-catalyzed Meerwein–Ponndoff–Verley (MPV) reduction of hetero(aromatic) ketones. This approach avoids using the hydride source as the solvent and has the potential to deliver enantioenriched alcohol products.
- Collaborated with the Bill & Melinda Gates Foundation to conceive new synthetic routes toward essential medicines. Several of the routes were evaluated in the laboratory.
- Designed collaborative studies with the Bouchard and Annabi labs at UCLA in pursuit of novel hyperpolarized ^{15}N contrast agents and water-soluble visible light-absorbing photoinitiators, respectively.

Course Instructor: University of California, Los Angeles, CA.
- Undergraduate elective course: "Catalysis in Modern Drug Discovery" (Summer 2020).
- Proposed, designed, and taught a six-week course on the fundamentals of catalysis and its applications in the syntheses of small molecule drugs.

Graduate Teaching Assistant: University of California, Los Angeles, CA.
- Undergraduate organic chemistry laboratory sections (Fall 2016 / Spring, Fall 2017).
- Undergraduate organic NMR spectroscopy instrumentation assistant (Winter 2017).
- Taught students organic reaction mechanisms, synthetic laboratory techniques, and how to perform and analyze 1D and 2D NMR spectroscopy experiments.

Undergraduate Research Assistant: Bowdoin College, Brunswick, ME.
- June 2014 – June 2016; Advisor: Prof. Benjamin C. Gorske.
- Synthesized novel classes of oxo- and thioamide-containing *N*-substituted glycine oligomers (peptoids) toward the development of peptoids with defined α-helical secondary structures.

Honors and Awards:

- Donald J. Cram Dissertation Award, 2021
- Education Innovation Award, UCLA, 2020
- Ralph and Charlene Bauer Award, UCLA, 2020
- Michael E. Jung Excellence in Teaching Award, UCLA, 2020
- Tobacco-Related Disease Research Program (TRDRP) of California, Predoctoral Research Fellowship Award, 2018–2021.
- Excellence in Second Year Academics and Research Award, UCLA, 2019.
- Graduate Dean's Scholar Award, UCLA, 2016–2017.
- Honors in Chemistry, Bowdoin College, 2016.
- ACS Award Organic Chemistry, Bowdoin College, 2015–2016.
- Hypercube Award, Bowdoin College, 2015.
- Sarah and James Bowdoin Scholar, Bowdoin College, 2013.

Publications:

1. **Reductive Arylation of Amides via a Nickel-Catalyzed Suzuki–Miyaura Coupling and Transfer Hydrogenation Cascade**. Timothy B. Boit,[†] Milauni M. Mehta,[†] Junyong Kim, Emma L. Baker, and Neil K. Garg. *Angew. Chem., Int. Ed.* **2021**, *60*, 2472–2477.

2. **Activation of C–O and C–N Bonds using Non-Precious Metal Catalysis**. Timothy B. Boit,[†] Jacob E. Dander,[†] Ana S. Bulger,[†] and Neil K. Garg. *ACS Catal.* **2020**, *10*, 12109–12126.

3. **Treating a Global Health Crisis with a Dose of Synthetic Chemistry**. Melissa A. Hardy, Brandon A. Wright, J. Logan Bachman, Timothy B. Boit, Hannah M. S. Haley, Rachel R. Knapp, Robert F. Lusi, Taku Okada, Veronica Tona, Neil K. Garg, and Richmond Sarpong. *ACS Central Sci.* **2020**, *6*, 1017–1030.

4. **From Glovebox to Benchtop**. Timothy B. Boit, Katie. A. Spence, and Neil K. Garg. *Nature Catal.* **2020**, *3*, 2–3.

5. **Nickel-Catalyzed Suzuki–Miyaura Coupling of Aliphatic Amides on the Benchtop**. Milauni M. Mehta,[†] Timothy B. Boit,[†] Jacob E. Dander,[†] and Neil K. Garg. *Org. Lett.* **2020**, *22*, 1–5.

6. **Base-Mediated Meerwein–Ponndorf–Verley Reduction of Aromatic and Heterocyclic Ketones**. Timothy B. Boit, Milauni M. Mehta, and Neil K. Garg. *Org. Lett.* **2019**, *21*, 6447–6451.

7. **Nickel-Catalyzed Suzuki–Miyaura Coupling of Aliphatic Amides**. Timothy B. Boit,[†] Nicholas A. Weires,[†] Junyong Kim,[†] and Neil K. Garg. *ACS Catal.* **2018**, *8*, 1003–1008.

[†]Authors Contributed Equally.

CHAPTER ONE

Activation of Aryl and Acyl C–O and C–N Bonds Using Non-Precious-Metal Catalysis

Timothy B. Boit,[†] Ana S. Bulger,[†] Jacob E. Dander,[†] and Neil K. Garg.

1.1 Introduction

Metal-catalyzed cross-couplings represent one of the most important reaction platforms in modern synthetic chemistry (Figure 1.1A).[1] Although the field enjoys a rich history, there remains fervent interest in expanding the frontiers of cross-coupling chemistry. Some areas of current exploration include the development of new modes of reactivity (dual catalysis,[2] photoredox catalysis,[3] cross-electrophile couplings,[4] chemoenzymatic transformations,[5] etc.), stereoselective couplings,[6] and the utilization of new classes of electrophiles. With respect to the latter, non-precious metal catalysis has been particularly enabling.
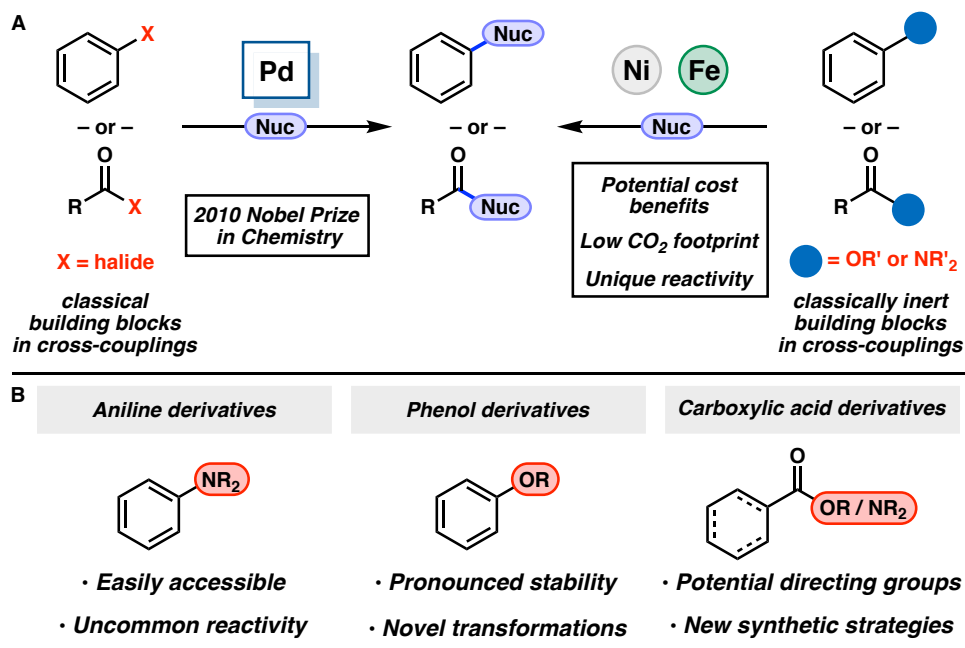
Figure 1.1. (A) Classical building blocks and those historically considered inert under traditional cross-coupling conditions. (B) Overview of recently explored electrophiles in cross-coupling reactions.

In addition to potential cost, toxicity, and environmental benefits relative to precious metal alternatives, non-precious metal catalysts can effect unique and challenging transformations (Figure 1.1A).[7] In particular, iron[7a–f,j] and nickel[7f–j] catalysis have become focal points in this arena. At the time our laboratory began in 2007, nickel-catalyzed cross-couplings were known, but significantly underexplored compared to palladium-catalyzed variants. Since 2007, more than 1200 manuscripts involving nickel-catalyzed cross-couplings have been published.[8] Moreover, several reviews covering advances in nickel catalysis have been published over the past decade, highlighting the rapid growth of the field.[7] This expansion has largely been driven by recognition of nickel's ability to participate in single-electron processes[9] and to activate strong bonds[10] historically considered inert in cross-coupling reactions.[7e,f,11] Notably, the use of non-traditional building blocks (e.g., aniline-, phenol-, and carboxylic acid-derivatives) in cross-couplings offers several advantages owing to their abundance, bench stability, utility as directing groups, and

orthogonal reactivity to more common aryl and acyl halide electrophiles (Figure 1.1B). As a result, these methodologies can enable novel disconnections and improvements in synthetic strategy.

In the context of strong bond activation,[12] our laboratory has been particularly interested in the activation and cross-coupling of phenol, amide, and ester electrophiles, using nickel or iron catalysis. Herein, we highlight our laboratory's contributions in this area, which are summarized in Figure 1.2. First, we consider cross-couplings of phenol-derived pivalates, carbonates, carbamates, and sulfamates to form C–N and C–C bonds (Figure 1.2A). Additionally, we discuss our efforts to develop nickel-catalyzed activations of esters and amides (Figures 1.2B and 1.2C, respectively). Where illustrative, we also outline some of the many contributions from others in the field. Lastly, we provide insight into potential future directions in these areas.
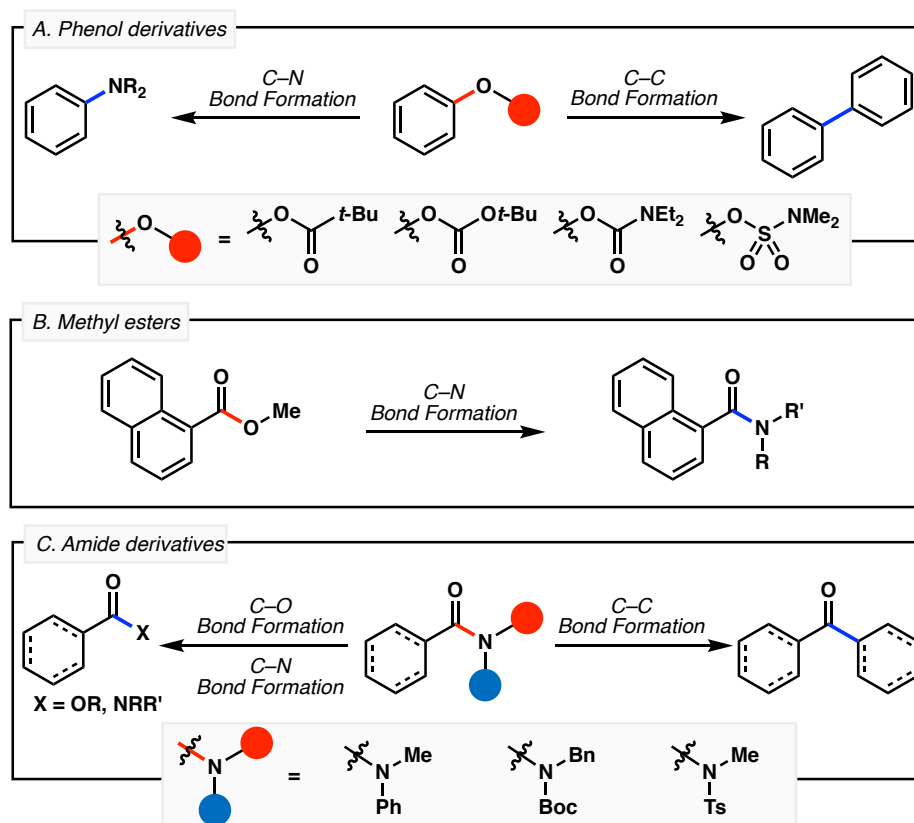
Figure 1.2. The scope of this review, which focuses on the activation of phenol, amide, and ester electrophiles.

1.2 Activation of Aryl C–O Bonds

The use of phenol-derivatives in cross-couplings is particularly attractive due to their broad availability, stability, and utility as directing groups in aromatic ring functionalization (Figure 1.3).[13] Although cross-couplings of aryl sulfonates are common,[14] methodologies that employ inexpensive phenol derivatives that are unreactive under Pd-catalysis and can serve as directing groups offer practical and conceptual advantages.[15,16,17,18] For example, phenolic electrophiles could be leveraged in conjunction with orthogonal cross-coupling handles to allow for the facile construction of privileged polyfunctionalized aromatics.[19] Although couplings of aryl and vinyl methyl ethers had been described by Wenkert and Chatani, respectively,[20,21,22,23,24] when our laboratory opened in 2007, cross-couplings of simple O-acylated phenols were unknown.
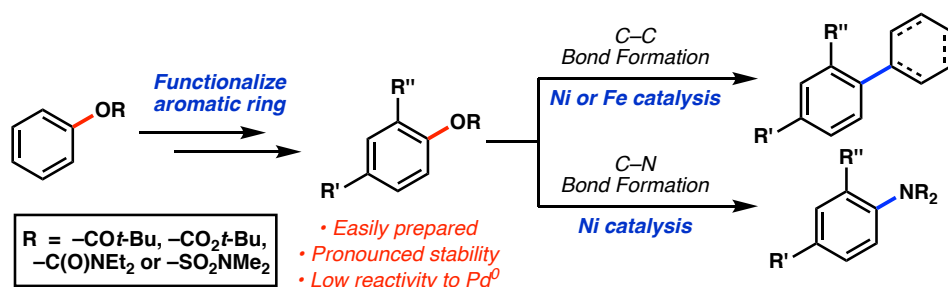
Figure 1.3. Overview of our laboratory's studies on using phenol derivatives as cross-coupling electrophiles in base-metal-catalyzed C–C and C–N bond-forming reactions.

Our initial efforts in this area focused on nickel-catalyzed C–C and C–N bond-forming reactions of pivalates, carbonates, and carbamates (Figure 1.4).[25] We first developed the nickel-catalyzed Suzuki–Miyaura coupling of aryl pivalates. Of note, this reaction avoids competitive activation of the acyl C–O bond, which has been observed in related cross-couplings of aryl ethers.[26,27] An example of the pivalate cross-coupling methodology is shown in Figure 1.4 involving the synthesis of disubstituted naphthalene derivative **1.4**. First, regioselective bromination of naphthyl-1-pivalate at C4 gave naphthyl bromide **1.1**, which underwent Suzuki–

Miyaura coupling with indolylboronic ester **1.2** to deliver indole **1.3**. Subsequently, nickel-catalyzed cross-coupling of aryl pivalate **1.3** with phenylboronic acid gave **1.4** in 88% yield.[28] This concise route to **1.4** underscores the value of *O*-acylated phenols as orthogonal cross-coupling electrophiles in the synthesis of polyaromatic molecules.[19] In a subsequent study, we found that aryl *tert*-butylcarbonates could serve as cross-coupling electrophiles, as illustrated by the nickel-catalyzed coupling of carbonate **1.5** to forge biaryl **1.6** in 65% yield.[29]

Aryl carbamates also proved to be versatile electrophiles in C–C and C–N bond-forming cross-coupling reactions, as demonstrated by the examples shown in Figure 1.4.[29] Importantly, this substrate class can be used to functionalize the ortho position on aromatic rings via directed lithiation.[30] Using $NiCl_2(PCy_3)_2$, naphthyl carbamate **1.7** smoothly underwent nickel-catalyzed cross-coupling to furnish biaryl product **1.8** in 86% yield.[29] The corresponding amination of aryl carbamates was enabled by the use of *N*-heterocyclic carbene ligand, SIPr, and could be used to generate naphthylmorpholine **1.11** in excellent yield.[31] Developing methodologies to construct sp^2–sp^3 C–C bonds represents another frontier in cross-couplings.[32] Toward this end, we turned to iron catalysis to achieve the Kumada coupling of aryl carbamates,[33,34] which allowed for the formation of sterically-hindered sp^2–sp^3 C–C bonds, such as that found in **1.12**.[35] Finally, a catalytic reduction of aryl carbamates (**1.7** → **1.14**, Figure 1.4) was achieved using inexpensive 1,1,3,3-tetramethyldisiloxane (TMDSO) as the reductant,[36] thereby providing a means to achieve the deoxygenation of aromatic rings. In addition, one can perform net cine substitution processes using directed ortho-metallation/functionalization, followed by reductive removal of the carbamate. Since our initial studies in this area, there have been a number of other contributions from other groups toward expanding the scope and mechanistic understanding of cross-couplings of *O*-acylated phenol-derivatives.[37]
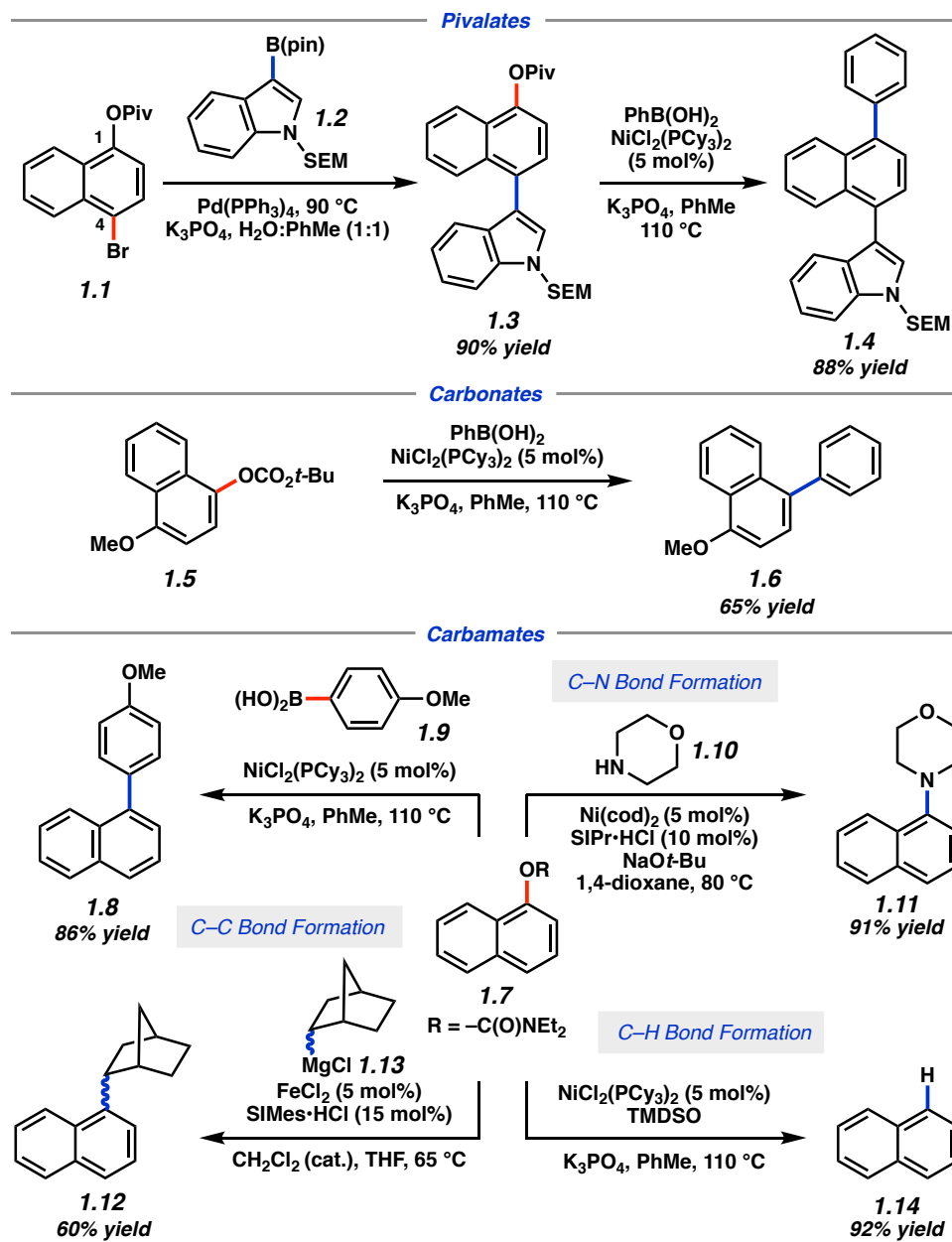
Figure 1.4. Select examples of Ni- and Fe-catalyzed cross-couplings of pivalates, carbonates, and carbamates reported by our laboratory.

The cross-coupling of sulfamate electrophiles presented another attractive opportunity, as they are also common directing groups in ortho-metalation reactions as established by Snieckus.[30] Nickel-catalyzed Kumada couplings of aryl sulfamates had been reported,[18] but milder C–C and C–N bond-forming cross-couplings of these substrates were unknown. With regard to the former

challenge, sulfamates proved to be viable substrates in nickel-catalyzed Suzuki–Miyaura cross-couplings. In fact, subsequent experimental and computational studies carried out in collaboration with the Houk group revealed aryl sulfamates to be more reactive electrophiles in comparison to aryl carbamates.[38] Importantly, this transformation avoids the use of highly basic and nucleophilic organometallic reagents, allowing for coupling of vinyl sulfamate **1.15** to give substituted cyclohexenone **1.17** in 78% yield (Figure 1.5).[29] Sulfamates were also competent electrophiles in iron-catalyzed Kumada couplings, as shown by the formation of tricyclic product **1.19** in 82% yield.[35] Additionally, the use of aryl sulfamates in catalytic amination reactions highlights their versatility as cross-coupling handles, and allowed for the rapid synthesis of linezolid (**1.22**) from fluorosulfamate **1.20**. Following sulfamate-directed ortho-functionalization,[29] aryl sulfamate **1.20** underwent a nickel-catalyzed cross-coupling with morpholine (**1.10**) to deliver arylated amine **1.21** in 84% yield.[39] As previously mentioned, subsequent computational and experimental efforts from others in the field have greatly contributed to the rapid growth in understanding and scope of base-metal-catalyzed cross-couplings of non-traditional phenol-derived electrophiles.[37k,40]
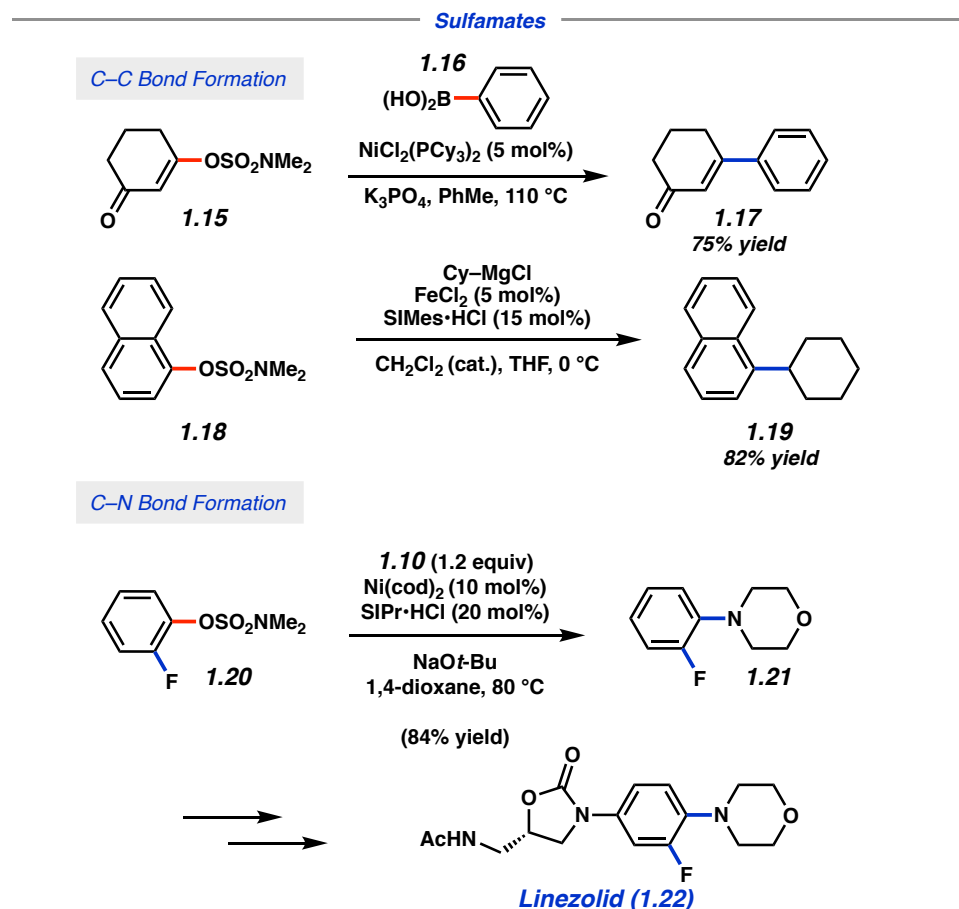
Figure 1.5. Select examples of nickel- and iron-catalyzed cross-couplings of sulfamates reported by our laboratory.

A common limitation of nickel-catalyzed methodologies, including those developed by our own laboratory, is the air- and moisture-sensitivity of the precatalysts and/or ligands employed. To avoid the need for glovebox manipulations in the nickel-catalyzed amination of carbamates and sulfamates, we investigated the use of a variety of air-stable Ni(II) complexes.[41] NiCl$_2$(DME) (**1.23**) and PhB(pin) were identified as a suitable precatalyst and mild reductant, respectively, to achieve a range of nickel-catalyzed aminations on the benchtop. For example, the methodology tolerated electron-deficient and heterocyclic substrates as well as a variety of amine nucleophiles, giving rise to **1.21** and **1.24**–**1.26** in 50–98% yields (Figure 1.6).[42] Recognizing that the use of

industrially-friendly solvents could further enhance the practicality of this methodology through a collaboration with the ACS Green Chemistry Institute's Pharmaceutical Roundtable, we evaluated the coupling of (hetero)aryl sulfamates with amine nucleophiles in 2-methyl-THF using nickel-catalysis.[43] The robustness of this method was evidenced by the gram-scale coupling of trifluoromethyl aryl sulfamate **1.27** with morpholine (**1.10**) to give arylated amine **1.28** in 97% yield using only 3 mol% NiCl$_2$(DME).
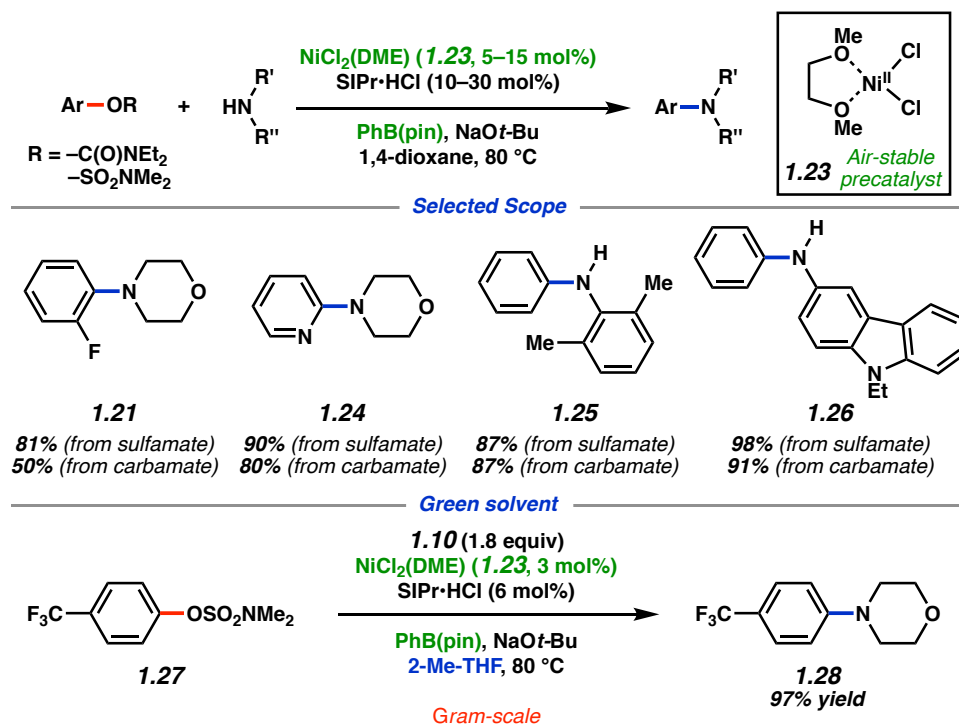
Figure 1.6. Benchtop aminations of aryl sulfamates and carbamates and gram-scale coupling of **1.27** in a green solvent.

1.3 Activation of Aryl C–N Bonds

Although not a focus of our laboratory's research, base-metal-catalyzed cross-couplings of aniline derivatives also represent an active field of inquiry (Figure 1.7). Historically, aniline-derived diazonium salts have been extensively employed in palladium-catalyzed cross-couplings.[44,45] However, the use of safer and more robust aniline-derivatives in coupling reactions

has recently garnered significant attention.[46] MacMillan and coworkers reported a nickel-catalyzed Suzuki–Miyaura coupling of aryltrimethylammonium triflates in 2003,[47] building upon the foundational report by Wenkert on Kumada couplings of these species.[48] More recently, Shi described a directing group-free nickel-catalyzed Suzuki–Miyaura coupling of *N,N*-dimethylaryl amines, overcoming a key limitation in comparable Ru-catalyzed reactions.[49,50] Moreover, a nickel-catalyzed Suzuki–Miyaura coupling of azoles was published by Robins,[51] which allowed for the synthesis of important arylated purine nucleoside analogs **1.29** and **1.30** in good yields.[52] Finally, the Nakao group and others have investigated transition-metal-catalyzed cross-couplings of nitroarenes and this strategy has been applied toward the syntheses of polycyclic aromatic hydrocarbons.[53] We are optimistic that base-metal-catalyzed aryl C–N bond activation will continue to see use in complex molecule synthesis.
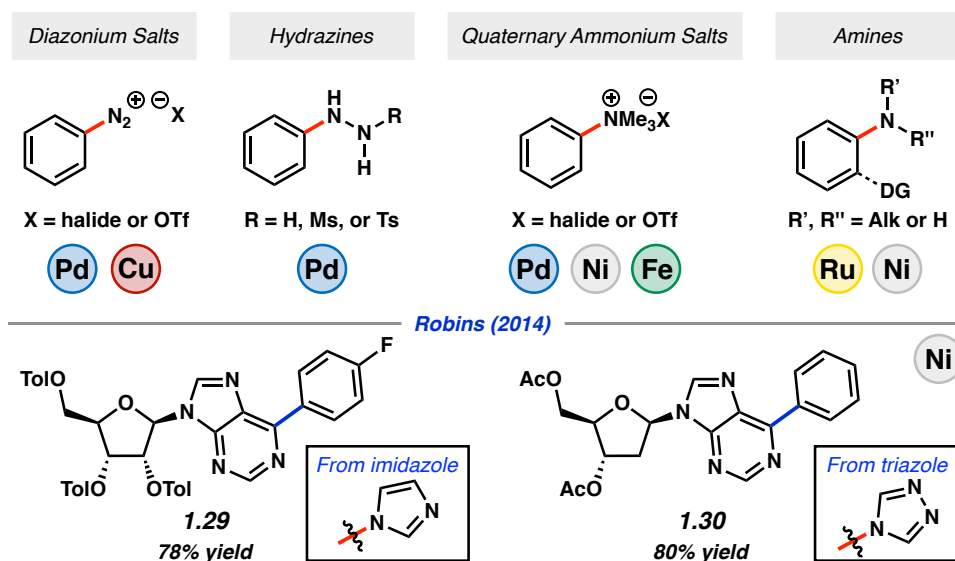
Figure 1.7. Overview of aniline derivatives employed in metal-catalyzed cross-coupling reactions.

1.4 Activation of Acyl C–O Bonds

Interest in the metal-catalyzed cleavage of the acyl C–O bonds of esters dates back to Yamamoto's seminal 1976 report utilizing stoichiometric nickel complexes.[54] Although cross-

couplings of esters, including decarboxylative variants pioneered by Itami[55] and Gooßen,[56] have since established the feasibility of metal-catalyzed acyl C–O bond activation for subsequent functional group interconversion, these reports were limited to the coupling of structurally or electronically activated substrates. Specifically, aryl esters employed in these couplings featured metal-chelating[57] or electron-withdrawing[58] *O*-substituents to facilitate oxidative addition (Figure 1.8).[59] These substrates are often synthesized from carboxylic acid precursors and are generally more reactive than alkyl esters. In contrast, simple methyl esters are naturally abundant, commercially available, and unreactive under Pd-catalysis. As a result, chemists could consider sequential cross-coupling strategies that take advantage of this orthogonal reactivity.
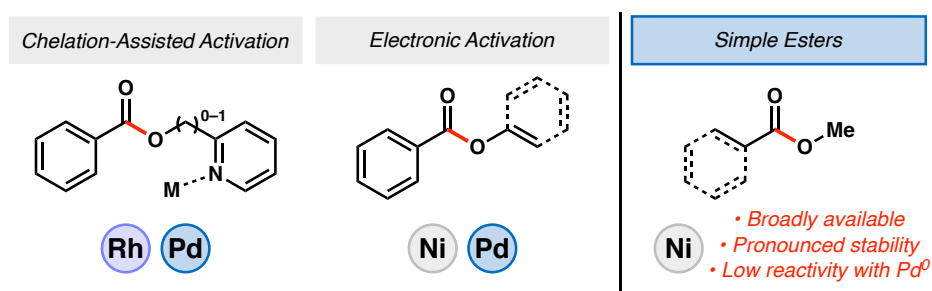
Figure 1.8. Historical approaches to metal-catalyzed ester acyl C–O bond activation and advantages of alkyl esters as substrates.

At the time our laboratory entered this field,[60] cross-couplings of methyl esters were unknown. Notably, these transformations feature high kinetic barriers to oxidative additions due to resonance stabilization of the acyl C–O bond.[61] However, we hypothesized that the unique reactivity of nickel(0) in the activation of strong bonds[7e,f,10,11] may allow for catalytic cross-couplings of methyl esters. Noting the importance of amide bond formations in industry,[62] we first pursued a nickel-catalyzed amidation of methyl esters.[60] Ultimately, the combined use of a Ni/NHC catalyst and Al(O*t*-Bu)$_3$ additive was found to effect the desired transformation. Computations performed by the Houk group[60] indicated that the Al(O*t*-Bu)$_3$ additive facilitates the

rate-limiting oxidative addition step and drives product formation through the generation of a favorable Lewis acid-base complex with the amide product. Although this methodology was limited to the activation of naphthyl-derived substrates, its utility was illustrated in the synthesis of complex anilide **1.33** (Figure 1.9). Treatment of **1.31**, which was prepared via sequential Buchwald–Hartwig and DCC couplings of a suitable methyl naphthoate precursor, with optimized amidation conditions generated anilide **1.33** in 60% yield without observable epimerization. This sequence highlights the mildness of the methodology and illustrates the utility of late-stage methyl ester activations in complex molecule synthesis.

Further studies have improved the efficiency and scope of nickel-catalyzed amidations of methyl esters. Newman and coworkers have described an additive-free variant of this methodology utilizing elevated temperatures.[63] In doing so, they were able to achieve amidations of enantioenriched aliphatic methyl esters to access products like furanylamide **1.34** in high yields (Figure 1.9). A range of aromatic substrates could also be coupled utilizing these conditions, allowing for the improved synthesis of α-amino-3-hydroxy-5-methyl-4-isoxazolepropionic acid receptors (AMPAR) positive modulator **1.35**. In a subsequent survey of NHC ligands in this transformation,[64] the same group reported the selective amidation of an alkyl methyl ester in the presence of an aryl methyl ester to form **1.36** in 65% yield. A reductive cross-coupling of nitroarenes and methyl esters has also been described.[65] Notably, nitroarenes are widely used in industry as inexpensive precursors to aryl amines. In an impressive application of this methodology, Hu and coworkers treated known ester **1.37** with their optimized Ni/Zn conditions to generate (–)-rhazinilam **1.38** in 59% yield.[65,66] As a result, the synthesis of the natural product was completed with improved step economy and comparable efficiency.

Figure 1.9. Recent advances in the nickel-catalyzed amidation of methyl esters.

Additional advances have broadened the scope of bond formations possible using nickel-catalyzed activations of methyl esters (Figure 1.10). Similar to Heck-type reactions of amides developed in our lab (vida infra),[67] Newman recently reported domino Heck reactions of methyl esters that form a C–C bond intramolecularly as well as a terminating C–C or C–H bond in a single catalytic transformation.[68] The generation of indanones **1.40** and **1.41** in 51% and 79% yields, respectively, from methyl ester substrate **1.39** highlights the potential utility of this methodology in divergent synthesis. Furthermore, nickel-catalyzed activations of methyl esters that proceed with decarbonylation have been reported. Specifically, the Rueping laboratory has utilized methyl esters

to generate a variety of aryl stannanes, such as substituted pyridine **1.44**.[69] A decarbonylative methylation of aryl methyl esters was reported by Yamaguchi and coworkers, and was utilized to access 2-methylindole **1.45** in 48% yield.[70] We anticipate that the exploration of new bond formations and modes of reactivities will continue to be an important driver of innovation in this field.
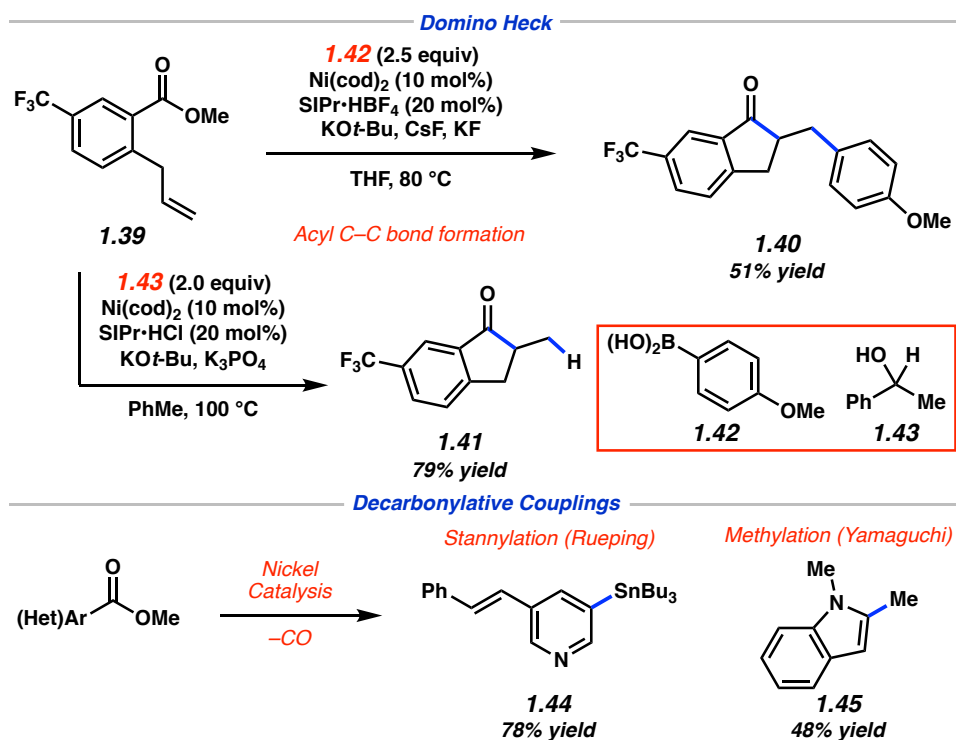
Figure 1.10. Nickel-catalyzed domino Heck and decarbonylative cross-couplings of methyl esters.

1.5 Activation of Acyl C–N Bonds

Although amide C–N bond cleavage is common in Nature, synthetic methods for activation of the amide C–N bond remain challenging due to well-understood resonance effects (Figure 1.11).[71] The pronounced stsability of amides, however, renders them ideal functional handles to be carried through multi-step synthetic sequences. Moreover, as they are also common directing groups in C–H activations,[72] strategies to merge amide-directed C–H functionalization with

subsequent late-stage C–N bond activation could allow for the rapid assembly of molecular architectures.

Recognizing the potential utility of amides as useful synthetic handles, a number of strategies for the functional group interconversion of amides have been reported.[73] For example, the use of amides featuring chelating *N*-substituents such as *N*-methoxy-*N*-methylamides or "Weinreb amides,"[71a,74] has enabled the single addition of organometallic nucleophiles to amides to access ketone products. Additionally, single-electron reduction of imides can generate reactive radical anion intermediates for subsequent functionalizations.[75] Notably, electrophilic activation of amides to generate versatile imidate intermediates has a rich history, with many elegant examples of this strategy being showcased by the Maulide group in recent years.[76] Another strategy for amide activation involves hydrosilylation using Vaska's complex (IrCl(CO)(PPH$_3$)$_2$), which has been leveraged by the Dixon group[77] and others[78] for a variety of reductive functionalizations of tertiary amides. Finally, our group and others have been interested in amide activation through direct oxidative addition by a transition-metal catalyst into the amide C–N bond for subsequent cross-coupling reactions. Although unknown at the time our lab entered the field in 2015, we envisioned that this latter approach could provide an alternative synthetic tool for the activation of amides that avoids the use of either highly nucleophilic or electrophilic reagents.[7g,79]
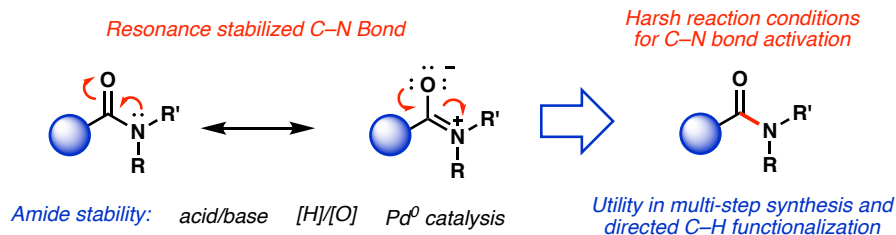
Figure 1.11. The resonance stabilization and potential synthetic utility of amide C–N bond activations.

Beginning with our first disclosure in 2015,[80] our laboratory has reported several nickel-catalyzed transformations that proceed with amide C–N bond activation. Our early investigations focused on the use of amide substrates derived from aromatic carboxylic acids (which are often referred to as "aryl amides" and are distinct from *N*-aryl amides mentioned below), with select examples shown in Figure 1.12. We identified the conversion of amides to esters, a historically challenging transformation that often proceeds under harshly acidic or basic conditions,[71a] as an exciting starting point for our studies.[80]

In collaboration with the Houk lab, we first computationally and experimentally investigated the effect of amide *N*-substituents in the nickel-catalyzed conversion of benzamides to methyl benzoate. These studies revealed two salient features of this transformation. First, *N*-substituents had a profound influence on the change in Gibbs free energy values for the overall reactions (ΔG). Although esterifications of *N,N*-dialkyl benzamides were calculated to be largely thermodynamically unfavorable or thermoneutral, esterifications of *N*-aryl amides were found to be thermodynamically favorable, with a calculated ΔG of –6.8 kcal/mol for the conversion of *N*-phenyl-*N*-methyl benzamide to methyl benzoate. The effect of amide *N*-substituents on the oxidative addition barrier using nickel catalysis with commercially available NHC ligand SIPr[81] was also evaluated computationally. In comparison to the calculated barriers for *N*-dialkyl amides, those for *N*-aryl amides were estimated to be more reasonable, with the oxidative addition barrier for *N*-phenyl-*N*-methyl benzamide calculated to be 26 kcal/mol. Overall, the computational predictions were supported by experiments as we observed quantitative yield in the nickel-catalyzed conversion of *N*-phenyl-*N*-methyl benzamide to methyl benzoate. These initial collaborative studies with the Houk lab greatly informed our understanding of the impact of *N*-substituents on the performance of amides in various nickel-catalyzed transformations. Moreover,

the Szostak group has bolstered the field by provided valuable insight into the physical properties and reactivity of non-planar, or "twisted", amides (in particular, glutaramides).[79a,82]

Using *N*-alkyl-*N*-phenyl benzamides, we found the use of nickel precatalyst / ligand combination of Ni(cod)$_2$ / SIPr allowed for the mild coupling of with a range of alcohol nucleophiles to furnish ester products, such as menthyl ester **1.46**, in high yields (Figure 1.12).[80] We then explored additional C–heteroatoms bond-forming reactions of *N,N*-alkyl, phenyl benzamides using nickel catalysis. Although water could not be directly employed as a nucleophile to access carboxylic acids from amides,[83] we designed a one-pot, two-step net-hydrolysis reaction. Specifically, in situ generation of a silyl ester, followed by subsequent deprotection provided carboxylic acids, such as **1.47**, in good yields using mild reaction conditions.[84] We were also interested in overcoming the longstanding challenge of secondary amide transamidation utilizing our nickel catalysis platform.[85] Toward this end, a two-step, Boc-activation/nickel catalysis approach enabled the catalytic transamidation of secondary amides, notably providing ready access to amino-acid derived amide **1.48** on gram-scale.[86] Reasoning that these reactions could proceed through a Ni(0)/Ni(II) catalytic cycle, a hypothesis supported by DFT calculations performed by the Houk group, we became interested in leveraging well-established M(0)/M(II) cross-coupling platforms to form C–C bonds.[80] Indeed, we found that and aryl amides could smoothly undergo nickel-catalyzed Suzuki–Miyaura (*N*-alkyl-*N*-Boc amides) and Negishi (*N*-Me-*N*-tosyl and *N*-benzyl-*N*-Boc amides) couplings to form biaryl and aryl–alkyl ketones, respectively.[87,88] Notably, both of these methodologies proved to be scalable, providing gram-scale access to ketones **1.49**, an antiproliferative tubulin-binding agent,[89] and **1.50**, a key intermediate in Pfizer's synthesis of a glucagon receptor modulator,[90] respectively.

17
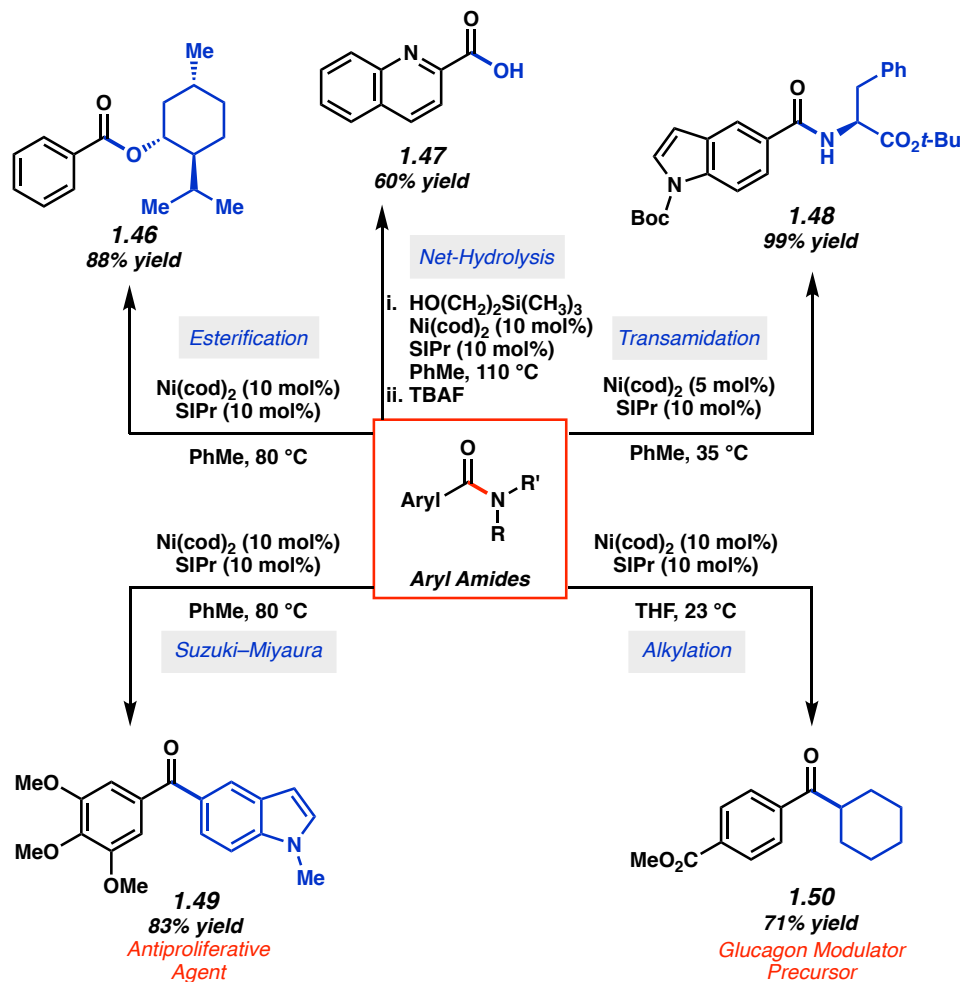
Figure 1.12. Recent advances in the nickel-catalyzed activation of aryl amide C–N bonds by our laboratory.

Nickel-catalyzed cross-couplings of amides that build stereocomplexity represent an important frontier of the field. Through the development of intramolecular Mizoroki–Heck cyclizations, we achieved the synthesis of indanones bearing α-quaternary stereocenters from *N*-benzyl-*N*-Boc amides (Figure 1.13).[67] Notably, this methodology provided diastereoselective access to indanone **1.52**, establishing vicinal stereocenters, one of which is quaternary, in a single transformation. Stanley and coworkers have extended this strategy to include domino-Heck reactions incorporating boron nucleophiles.[91] We were also interested in pursuing methodologies that generate stereocenters at the originating amide carbonyl carbon through the net addition of

two nucleophiles. Ultimately, a one-pot chemoenzymatic synthesis of enantioenriched alcohols was achieved through the combined use of nickel- and biocatalysis in a collaboration with Codexis.[92] For example, enantioenriched diarylmethanol **1.54** was accessed in 72% yield and 97% ee utilizing the methodology, which combined a Suzuki–Miyaura cross-coupling and ketoreductase (KRED)-mediated reduction in a one-pot, sequential process. These studies validated the utility of amide C–N bond activation in stereocomplexity-generating transformations. We view the development of asymmetric methods as a fruitful area for further exploration in this field.
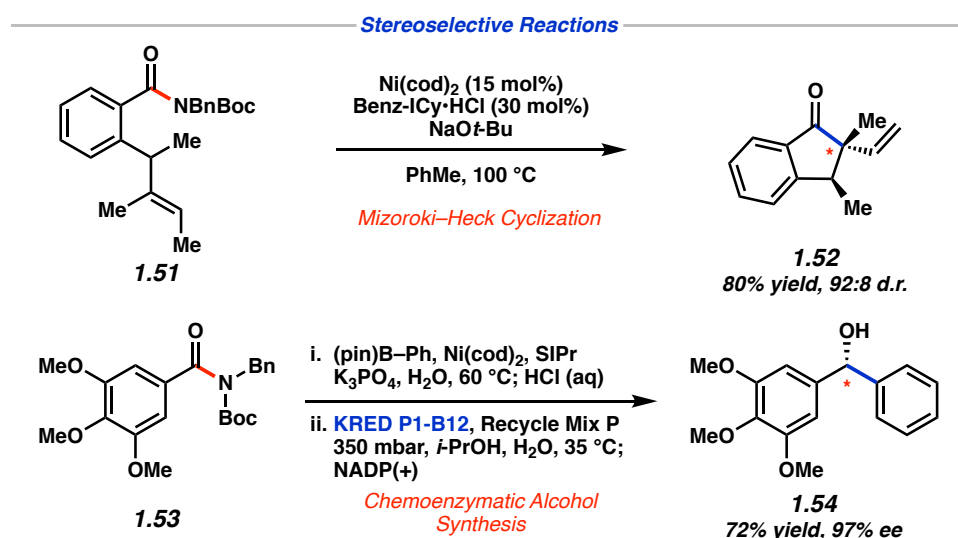
Figure 1.13. Asymmetric reactions of aryl amides developed by our laboratory.

Notably, the aforementioned methodologies were limited to the activation of aryl amide substrates. The activation of amides derived from aliphatic carboxylic acids (often referred to as "aliphatic amides") presents an even greater challenge as a result of increased steric requirements and a presumed lack of catalyst–substrate pre-complexation.[93] In considering esterifications of aliphatic amides, the use of terpyridine as the ligand proved effective in a collaborative study with Boehringer–Ingelheim (Figure 1.14).[94] This methodology provided efficient access to steroidal ester **1.55**, and could be used in a macrocyclic ring-opening to form ester **1.56**. Subsequently, we

evaluated C–C and C–N bond-forming reactions of alkyl amides through the use of the electron-rich NHC ligand precursor, Benz-Icy•HCl.[81,95,96,97] Specifically, we developed a Suzuki–Miyaura coupling of aliphatic amides, which provided access to ketone **1.57** from an enantioenriched amide with minimal racemization. Importantly, this methodology affords enolizable ketone products, which can then be further elaborated. For example, a Suzuki–Miyaura cross-coupling of a tetrahydropyranyl amide and concatenate Fischer indolization provided spiroindolenine **1.58** in rapid fashion. Transamidation of aliphatic secondary amides was also possible using this catalytic system, following C–N bond activation via *N*-functionalization. Of note, the stereoretentive transamidation of a prolinamide to provide secondary amide **1.59** in 60% yield and 99% ee was possible utilizing the methodology.[95] With the development of these protocols, our laboratory established the viability of aliphatic amides in C–O, C–C, and C–N bond-forming reactions using nickel catalysis.
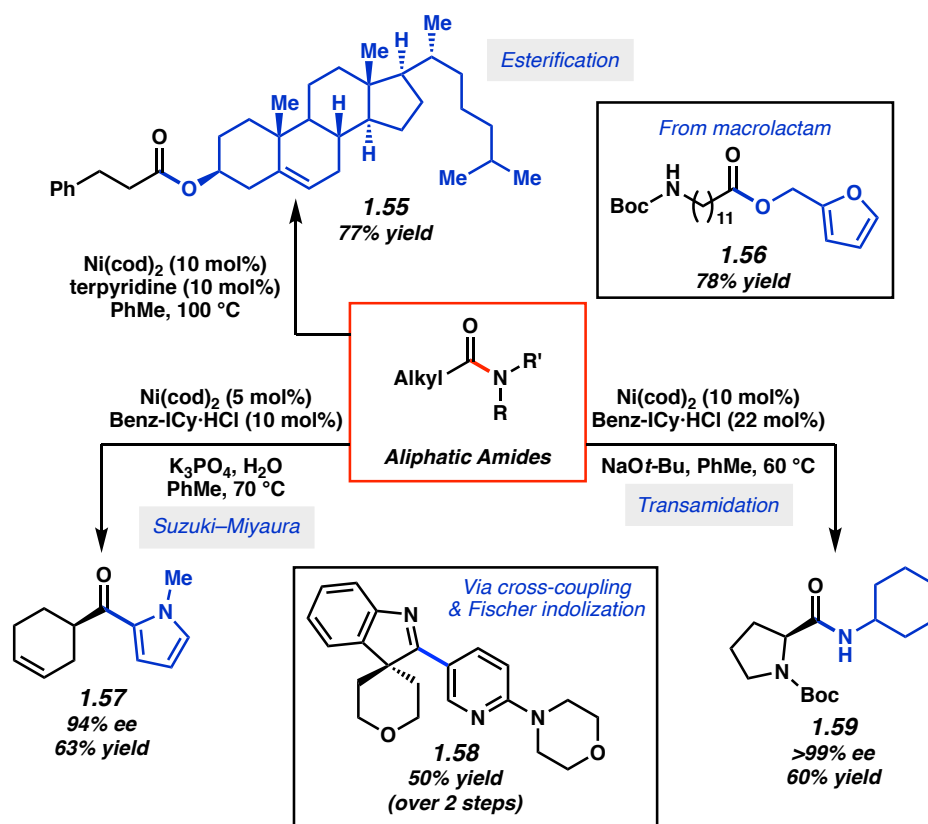
Figure 1.14. Recent advances in the nickel-catalyzed activation of aliphatic amide C–N bonds by our laboratory.

As previously noted, our laboratory has an interest in improving the practicality of nickel-catalyzed methods. Toward this end, we sought to optimize the catalytic efficiency of the esterification of amides reported by our laboratory.[98] A highlight of this collaborative effort with AbbVie, which combined experimentation and kinetic modeling,[99] was the realization of a 5 gram-scale coupling of aryl amide **1.60** and menthol (**1.61**) at a reduced temperature (45 °C vs. 80 °C) using <1 mol% Ni(cod)$_2$ to give ester **1.46** in 97% yield (Figure 1.15). Another key challenge in the area of nickel catalysis lies in the development of glovebox-free cross-couplings.[100] Encapsulating air- and moisture-sensitive reagents in paraffin wax has been an effective means to carry out transition-metal-catalyzed reactions on the benchtop,[101,102] including in undergraduate instructional laboratories.[103] In this regard, we successfully employed paraffin–Ni(cod)$_2$/Benzy-

ICy•HCl capsules in the benchtop Suzuki–Miyaura coupling of piperidinyl amide **1.62** to give

polyheterocyclic ketone **1.64** in 73% yield on gram-scale. We are hopeful that future advances in

these areas will promote greater use of base-metal catalysis in academia and industry.
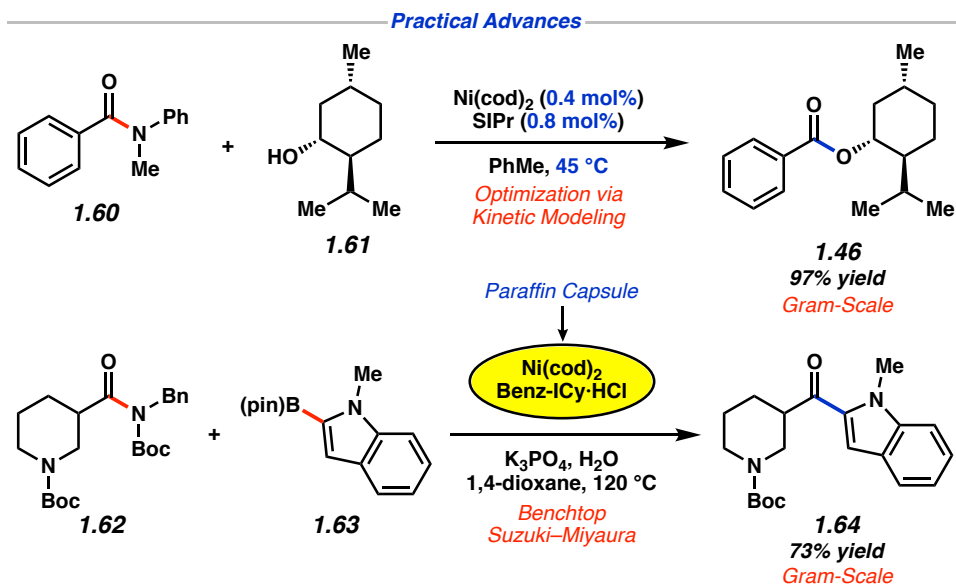
Figure 1.15. Practical advances in nickel-catalyzed activations of amides disclosed by our laboratory.

The field of amide C–N bond activation using transition metal catalysis, including

breakthroughs with palladium catalysis led by Szostak,[104] has flourished in recent years,

particularly when considering the introduction of alternative amide electrophiles and novel modes

of reactivity. More than 85 studies involving transition-metal-catalyzed amide C–N bond

activation have been reported since our initial study in 2015.[105] Select examples of amide

derivatives that have been employed successfully by other groups in nickel-catalyzed cross-

couplings are shown in Figure 1.16.[106] Amides have also seen use as acyl synthons in emerging

cross-coupling manifolds, testifying to the rapid growth of this field. For instance, Hu and

coworkers demonstrated a nickel-catalyzed reductive transamidation of *N,N*-Bn,Boc benzamides

using nitroarenes.[66,107] Notably, this methodology was tolerant of a range of functional groups,

including aryl bromides, allowing for the formation of aryl amide **1.67** in 69% yield. Additionally, Molander and coworkers reported a Ni/Ir dual-catalytic photoredox approach to access alkyl–alkyl ketones such as 1,4-dicarbonyl **1.70**.[108] Finally, a number of Ni-catalyzed decarbonylative reactions of amides have been reported, expanding the scope of functional groups directly accessible from amides, as illustrated by the synthesis of compounds **1.71**–**1.73**.[109,110,111] The continued exploration of new modes of reactivity and bond-forming reactions is critical to advancing amides as useful building blocks in complex molecule synthesis.
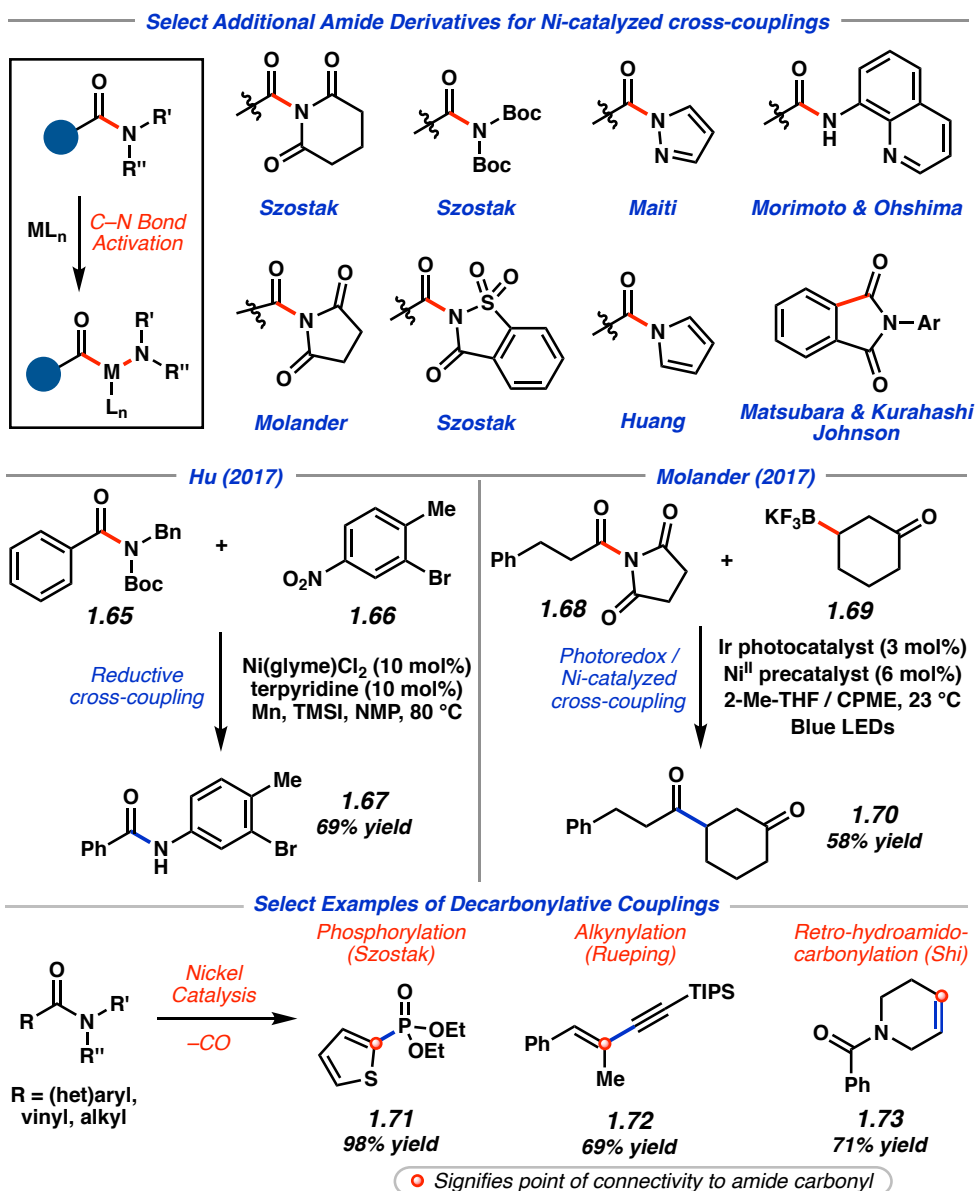
Figure 1.16. *N*-substituent variation, alternative reaction modes, and decarbonylative reactions of amides utilizing nickel catalysis.

1.6 Outlook and Future Directions

Although the field of base-metal-catalyzed activation of strong bonds has grown rapidly in recent years, there remains tremendous opportunity for future discovery. For example, expanding the scope of substrates that can undergo activation to include (sp³)C–O/N electrophiles[112,113] and developing catalytic systems to activate amides, phenols, and anilines without the need for

electron-withdrawing or chelating substituents[114] could allow chemists to directly manipulate common moieties in commodity chemicals and natural products. Another frontier for this field lies in the application of cross-couplings involving the activation of strong bonds to the synthesis of complex molecules. In this regard, the development of both chemo- and stereoselective reactions is expected to be highly enabling. Additionally, collaborations between academia and industry as well as amongst academic research groups would help achieve the future directions outlined above and expedite the adoption of novel methodologies in industrial settings.[115] Finally, computational investigations into reaction mechanisms and selectivities will undoubtedly lead to improvements in existing methodologies, inspire the development of others, and lead to the disclosure of tools to predict selectivities and outcomes in these transformations. Of note, although nickel catalysis has seen widespread use in the activation of strong bonds, there remains significant interest in exploring the utility of alternative non-precious metal catalysts in this arena and more broadly in cases where it could lower the cost of drug manufacturing.[115,116] We also envision that the optimization of reaction conditions and catalyst loadings, the discovery of new inexpensive ligand frameworks,[117] and the disclosure of well-defined, air-stable pre-catalysts[118] will promote the use of base-metal catalysis in academia and industry. We hope and anticipate that strong bond activation using base-metal catalysts will continue to thrive as a field and be viewed as an increasingly valuable strategy in organic synthesis.

1.7 Notes and References

(1) (a) Suzuki, A.; Cross-coupling reactions of organoboranes: an easy way to construct C–C bonds. *Angew. Chem., Int. Ed.* **2011**, *50*, 6723–6737. (b) Negishi, zE. Magical power of transition metals: past, present, and future. *Angew. Chem., Int. Ed.* **2011**, *50*, 6738–6764. (c) Seechurn, C. C. C. J.; Kitching, M. O.; Colacot, T. J.; Snieckus, V. Palladium-catalyzed cross-coupling: a historical contextual perspective to the 2010 Nobel Prize. *Angew. Chem., Int. Ed.* **2012**, *51*, 5062–5085.

(2) For representative reviews, see: (a) Duschek, A.; Kirsch, S. F. Combining the concepts: dual catalysis with carbophilic Lewis acids. *Angew. Chem., Int. Ed.* **2008**, *47*, 5703–5705. (b) Hirner, J. J.; Shi, Y.; Blum, S. A. Organogold reactivity with palladium, nickel, and rhodium: transmetalation, cross-coupling and dual catalysis. *Acc. Chem. Res.* **2011**, *44*, 603–613. (c) Hanna, L. E.; Jarvo, E. R. Selective cross-electrophile coupling by dual catalysis. *Angew. Chem., Int. Ed.* **2015**, *54*, 15618–15620. (d) Afewerki, S.; Córdova, A. Combinations of aminocatalysts and metal catalysts: a powerful cooperative approach in selective organic synthesis. *Chem. Rev.* **2016**, *116*, 13512–13570. (e) Krautwald, S.; Carreira, E. M. Stereodivergence in asymmetric catalysis. *J. Am. Chem. Soc.* **2017**, *139,* 5627–5639. (f) Romiti, F.; del Pozo, J.; Paioti, P. H. S.; Gonsales, S. A.; Li, X.; Hartrampf, F. W. W.; Hoveyda, A. H. Different strategies for designing dual-catalytic enantioselective processes: from fully cooperative to non-cooperative systems. *J. Am. Chem. Soc.* **2019**, *141*, 17952–17961.

(3) For representative reviews, see: (a) Zhiwei, Z.; Ahnemna, D. T.; Chu, L.; Terrett, J. A.; Doyle, A. G.; MacMillan, D. W. C. Merging photoredox with nickel catalysis: coupling of α-

carboxyl sp^3-carbons with aryl halides. *Science* **2014**, *345*, 437–440. (b) Twilton, J.; Le, C.; Zhang, P.; Shaw, M. H.; Evans, R. W.; MacMillan D. W. C. The merger of transition metal and photocatalysis. *Nat. Rev. Chem.* **2017**, *1*, 0052. (c) Hopkinson, M. N.; Tlahuext-Aca, A.; Glorius, F. Merging visible light photoredox and gold catalysis. *Acc. Chem. Res.* **2016**, *49*, 2261–2272. (d) Douglas, J. J.; Sevrin, M. J.; Stephenson, C. R. J. Visible light photocatalysis: applications and new disconnections in the synthesis of pharmaceutical agents. *Org. Process. Res. Dev.* **2016**, *20*, 1134–1147.

(4) For representative reviews, see: (a) Lucas, E. L.; Jarvo, E. R. Stereospecific and stereoconvergent cross-couplings between alkyl electrophiles. *Nat. Rev. Chem.* **2017**, *1*, 65. (b) Weix, D. J. Methods and mechanisms for cross-electrophile coupling of Csp^2 halides with alkyl electrophiles. *Acc. Chem. Res.* **2015**, *48*, 1767–1775. (c) Hanna, L. E.; Jarvo, E. R. Selective cross-electrophile coupling by dual catalysis. *Angew. Chem., Int. Ed.* **2015**, *54*, 15618–15620. (d) Everson, D. A.; Weix, D. J. Cross-electrophile coupling: principles of reactivity and selectivity. *J. Org. Chem.* **2014**, *79*, 4793–4798.

(5) For representative publications on combining chemo- and biocatalysis, see: (a) Rudroff, F.; Mihovilovic, M. D.; Gröger, H.; Snajdrova, R.; Iding, H.; Bornscheuer, W. T. Opportunities and challenges for combining chemo- and biocatalysis. *Nat. Catal.* **2018**, *1*,12–22. (b) Denard, C. A.; Hartwig, J. F.; Zhao, H. Multistep one-pot reactions combining biocatalysis and chemical catalysts for asymmetric synthesis. *ACS Catal.* **2013**, *3*, 2856–2864. (c) Gröger, H.; Hummel, W. Combining the 'two worlds' of chemocatalysis and biocatalysis towards multi-step one-pot processes in aqueous media. *Curr. Opin. Chem. Biol.* **2014**, *19,* 171–179. (d) Ríos-Lombardía, N.; García-Álvarez, J.; González-Sabín, J. One-pot combination of metal-

and biocatalysis in water for the synthesis of chiral molecules. *Catalysts* **2018**, *8*, 75. (e) Sirasani, G.; Tong, L.; Balskus, E. P. A biocompatible alkene hydrogenation merges organic synthesis with microbial metabolism. *Angew. Chem., Int. Ed.* **2014**, *53*, 7785–7788. (f) Wallace, S.; Balskus, E. P. Interfacing microbial styrene production with a biocompatible cyclopropanation reaction. *Angew. Chem., Int. Ed.* **2015**, *54*, 7106–7109.

(6) For representative publications, see: (a) Lucas, E. L.; Jarvo, E. R. Keeping track of the electrons. *Acc. Chem. Res.* **2018**, *51*, 567–572. (b) Brozek, L. A.; Ardolino, M. J.; Morken, J. P. Diasterocontrol in asymmetric allyl–allyl cross-coupling: stereocontrolled reaction of prochiral allylboronates with prochiral allyl chlorides. *J. Am. Chem. Soc.* **2011**, *133*, 16778–16781. (c) Kainz, Q. M.; Matier, C. D.; Bartoszewicz, A.; Zultanski, S. L.; Peters, J. C.; Fu, G. C. Asymmetric copper-catalyzed C–N cross-couplings induced by visible light. *Science* **2016**, *351*, 681–684. (d) Wang, Z.; Yin, H.; Fu, G. C. Catalytic enantioconvergent coupling of secondary and tertiary electrophiles with olefins. *Nature* **2018**, *563*, 379–383. (e) Huo, H.; Gorsline, B. J.; Fu, G. C. Catalyst-controlled doubly enantioconvergent coupling of racemic alkyl nucleophiles and electrophiles. *Science* **2020**, *367*, 559–564.

(7) (a) Bolm, C.; Legros, J.; Le Paih, J.; Zani, L. Iron-catalyzed reactions in organic synthesis. *Chem. Rev.* **2004**, *104*, 6217−6254. (b) Enthaler, S.; Junge, K.; Beller, M. Sustainable metal catalysis with iron: from rust to rising star? *Angew. Chem., Int. Ed.* **2008**, *47*, 3317−3321. (c) Bauer, E. B. Recent advances in iron catalysis in organic synthesis. *Curr. Org. Chem*. **2008**, *12*, 1341−1369. (d) Fürstner, A.; Iron catalysis in organic synthesis: A critical assessment of what is takes to make this base metal a multitasking champion. *ACS Central Sci.* **2016**, *2*, 778–789. (e) Fürstner, A.; Leitner A.; Méndez, M.; Krause, H. Iron-catalyzed cross-coupling

reactions. *J. Am. Chem. Soc.* **2002**, *124*, 13856–13863. (f) Mesganaw, T.; Garg, N. K. Ni- and Fe-catalyzed cross-coupling reactions of phenol derivatives. *Org. Process Res. Dev.* **2013**, *17*, 29−39. (g) Tasker, S. Z.; Standley, E. A.; Jamison, T. F. Recent advances in homogeneous nickel catalysis. *Nature* **2014**, *509*, 299−309. (h) Ananikov, V. P. Nickel: the "Spirited Horse" of transition metal catalysis. *ACS Catal.* **2015**, *5*, 1964–1971. (i) Dander, J. E.; Garg, N. K. Breaking amides using nickel catalysis. *ACS. Catal.* **2017**, *7*, 1413–1423. (j) Su, B.; Cao, Z.-C.; Shi, Z.-J. Exploration of earth-abundant transition metals (Fe, Co, and Ni) as catalysts in unreactive chemical bond activations. *Acc. Chem. Res.* **2015**, *48*, 886–896.

(8) On the basis of a SciFinder search for the research topic "nickel cross-coupling" and narrowing the search to only journal articles (i.e. excluding review articles) published between 2008 and 2020 (accessed July 30, 2020).

(9) Nickel readily participates in radical pathways due to the relatively stability of open-shell nickel-complexes. For theoretical and experimental studies, see: (a) Poli, R.; Cacelli, I. Orbital splitting and pairing energy in open-shell organometallics: A study of two families of 16-electron complexes [Cp2M] (M = Cr, Mo, W) and [CpM(PH3)] (M = Co, Rh, Ir). *Eur. J. Inorg. Chem.* **2005**, 2324–2331. (b) Tsou, T. T.; Kochi, J. Mechanism of oxidative addition. Reaction of nickel(0) complexes with aromatic halides. *J. Am. Chem. Soc.* **1979**, *101*, 6319–6332. (c) Schley, N. D.; Fu, G. C. Nickel-catalyzed Negishi arylations of propargylic bromides: A mechanistic investigation. *J. Am. Chem. Soc.* **2014**, *136*, 16588–16593.

(10) In comparison to palladium, nickel has a smaller atomic radius, is less electronegative, and is more easily oxidized. In turn, oxidative addition is more facile to Ni(0) relative to Pd(0). For theoretical and experimental studies, see: (a) Mann, J. B.; Meek, T. L.; Knight, E. T.; Capitani,

J. F.; Allen, L. C. Configuration energies of the d-block elements. *J. Am. Chem. Soc.* **2000**, *122*, 5132–5317. (b) Lide, D. R. CRC handbook of chemistry and physics, 87th ed.; CRC Press: 2008. Chapter 4 p. 1 (c) Batsanov, S. S. Van der Waals radii of elements. *Inorg. Mater.* **2001**, *37*, 871−885. (d) Hartwig, J. F. *Organotransition Metal Chemistry: From Bonding to Catalysis*; Murdzek, J., Eds.; University Science Books: Mill Valley, CA, 2010; p 8.

(11) (a) Diccianni, J.; Lin, W.; Diao, T. Mechanisms of nickel-catalyzed coupling reactions and applications in alkene functionalization. *Acc. Chem. Res.* **2020**, *53*, 906–919. (b) Diccianni, J. B.; Diao, T. Mechanisms of nickel-catalyzed cross-coupling reactions. *Trends. Chem.* **2019**, *1*, 830–844.

(12) In the context of this Viewpoint, we consider a "strong bond" as one that has been traditionally inert to oxidative addition using palladium catalysis.

(13) (a) Rosen, B. M.; Quasdorf, K. W.; Wilson, D. A.; Zhang, N.; Resmerita, A.-M.; Garg, N. K.; Percec, V. Nickel-catalyzed cross-couplings involving carbon–oxygen bonds. *Chem. Rev.* **2011**, *111*, 1346–1416. (b) Yu, D.-G.; Li, B.-J.; Shi, Z.-J. Exploration of new C–O electrophiles in cross-coupling reactions. *Acc. Chem. Res.* **2010**, *43*, 1486−1495. (c) Li, B.-J.; Yu, D.-G.; Sun, C.-L.; Shi, Z.-J. Activation of "inert" alkenyl/aryl C–O bond and its applications in cross-coupling reactions. *Chem. Eur. J.* **2011**, *17*, 1728−1759. (d) Gooßen, L. J.; Gooßen, K.; Stanciu, C. C(aryl)–O activation of aryl carboxylates in nickel-catalyzed biaryl syntheses. *Angew. Chem., Int. Ed.* **2009**, *48*, 3569–3571.

(14) For reviews, see: (a) Miyaura, N.; Suzuki, A. Palladium-catalyzed cross-coupling reactions of organoboron compounds. *Chem. Rev.* **1995**, *95*, 2457–2483. (b) Suzuki, A. J Recent advances in the cross-coupling reactions of organoboron derivatives with organic

electrophiles. *Organomet. Chem.* **1999**, *576*, 147–168. (c) Miyaura, N. In *Advances in Metal-Organic Chemistry*; Liebeskind, L. S., Ed.; JAI: London, 1998; Vol. 6, p. 187–243. (d) Suzuki, A. In *Metal-Catalyzed Cross-Coupling Reactions*; Diederich, F., Stang, P. J., Eds.; Wiley-VCH: New York, 1998; p. 761–813. (e) Stanforth, S. P. Catalytic cross-coupling reactions in biaryl synthesis. *Tetrahedron* **1998**, *54*, 263–303.

(15) Approximate reagent costs by Aldrich Chemical Co., Inc. are: (a) Triflic anhydride = $280 per mol. (b) Methanesulfonyl chloride = $12 per mol. (c) Trimethylacetyl chloride (pivaloyl chloride) = $15 per mol. (d) Iodomethane = $68 per mol.

(16) Although aryl sulfonates have been established as viable cross-coupling partners, their utility in ortho-lithiation reactions is limited. For examples of alkyl benzenesulfonates as directing groups in ortho-metalation reactions, see: (a) Bonfiglio, J. N. Directed ortho-lithiation of alkyl arene sulfonates. *J. Org. Chem.* **1986**, *51*, 2833–2835. (b) Spangler, L. A. A novel method for the preparation of 2,6-disubstituted benzenesulfonates and benzenesulfonyl chlorides utilizing the powerful alkyl sulfonate ortho directing group. *Tetrahedron Lett.* **1996**, *37*, 3639–3642.

(17) For examples of aryl mesylates and tosylates in cross-coupling reactions, see: (a) Zim, D.; Lando, V. R.; Dupont, J.; Monteiro, A. L. NiCl$_2$(PCy$_3$)$_2$: A simple and efficient catalyst precursor for the Suzuki cross-coupling of aryl tosylates and arylboronic acids. *Org. Lett.* **2001**, *3*, 3049–3051. (b) Tang, Z.-Y; Hu, Q.-S. Room-temperature Ni(0)-catalyzed cross-coupling reactions of aryl arenesulfonates with arylboronic acids. *J. Am. Chem. Soc.* **2004**, *126*, 3058–3059. (c) Percec, V.; Golding, G. M.; Smidrkal, J.; Weichold, O. NiCl$_2$(dppe)-catalyzed cross-coupling of aryl mesylates, arenesulfonates, and halides with arylboronic

acids. *J. Org. Chem.* **2004**, *69*, 3447– 3452. (d) Zhang, L.; Meng, T.; Wu, J. Palladium-catalyzed Suzuki−Miyaura cross-couplings of aryl tosylates with potassium aryltrifluoroborates. *J. Org. Chem.* **2007**, *72*, 9346–9349. (e) Munday, R. H.; Martinelli, J. R.; Buchwald, S. L. Palladium-catalyzed carbonylation of aryl tosylates and mesylates. *J. Am. Chem. Soc.* **2008**, *130*, 2754–2755.

(18) Macklin, T. K.; Snieckus, V. Directed ortho metalation methodology. The *N,N*-dialkyl aryl *O*-sulfamate as a new directed metalation group and cross-coupling partner for Grignard reagents. *Org. Lett.* **2005**, *7*, 2519–2522.

(19) Polyfunctionalized aromatics are important scaffolds in medicines, ligands for catalysis, and materials chemistry. For examples, see: (a) Kotha, S.; Lahiri, K.; Kashinath, D. Recent applications of the Suzuki–Miyaura cross-coupling reaction in organic synthesis. *Tetrahedron* **2002**, *58*, 9633–9695. (b) Kertesz, M.; Choi, C. H.; Yang, S. Conjugated polymers and aromaticity. *Chem. Rev.* **2005**, *105*, 3448–3481. (c) Martin, R.; Buchwald, S. L. Palladium-catalyzed Suzuki–Miyaura cross-coupling reactions employing dialkylbiaryl phosphine ligands. *Acc. Chem. Res.* **2008**, *41*, 1461–1473. (d) Surry, D. S.; Buchwald, S. L. Biaryl phosphane ligands in palladium-catalyzed amination. *Angew. Chem., Int. Ed.* **2008**, *47*, 6338–6361.

(20) (a) Wenkert, E.; Michelotti, E. L.; Swindell, C. S. Nickel-induced conversion of carbon-oxygen into carbon-carbon bonds. One-step transformations of enol ethers into olefins and aryl ethers into biaryls. *J. Am. Chem. Soc*. **1979**, *101*, 2246–2247. (b) Wenkert, E.; Michelotti, E. L.; Swingdell, C. S.; Tingoli, M. Transformation of carbon-oxygen into carbon-carbon bonds mediated by low-valent nickel species. *J. Org. Chem.* **1984**, *49*, 4894–4899.

(21) Dankwardt, J. W. Nickel-catalyzed cross-coupling of aryl Grignard reagents with aromatic alkyl ethers: an efficient synthesis of unsymmetrical biaryls. *Angew. Chem., Int. Ed.* **2004**, *43*, 2428–2432.

(22) Guan, B.-T.; Xiang, S.-K.; Wu, T.; Sun, Z.-P.; Wang, B.-Q.; Zhao, K.-Q.; Shi, Z.-J. Methylation of arenes via Ni-catalyzed aryl C–O/F activation. *Chem. Commun.* **2008**, 1437–1439.

(23) Tobisu, M.; Shimasaki, T.; Chatani, N. Nickel-catalyzed cross-coupling of aryl methyl ethers with aryl boronic esters. *Angew. Chem., Int. Ed.* **2008**, *47*, 4866–4869.

(24) More recently, Sergeev and Hartwig disclosed the nickel-catalyzed hydrogenolysis of diaryl ethers: Sergeev, A. G.; Hartwig, J. F. Selective, nickel-catalyzed hydrogenolysis of aryl ethers. *Science* **2011**, *322*, 439–443.

(25) The Suzuki–Miyaura coupling of aryl pivalates was simultaneously reported by our laboratory and the laboratory of Shi: Guan, B.-T.; Wang, Y.; Li, B.-J.; Yu, D.-G.; Shi, Z.-J. Biaryl construction via Ni-catalyzed C−O activation of phenolic carboxylates. *J. Am. Chem. Soc.* **2008**, *130*, 14468–14470.

(26) (a) Ishizu, J.; Yamamoto, T.; Yamamoto, A. Selective cleavage of C–O bonds in esters through oxidative addition to Ni(0) complexes. *Chem. Lett.* **1976**, 1091–1094. (b) Yamamoto, T.; Ishizu, J.; Kohara, T.; Komiya, S.; Yamamoto, A. Oxidative addition of aryl carboxylates to nickel(0) complexes involving cleavage of the acyl-oxygen bond. *J. Am. Chem. Soc.* **1980**, *102*, 3758–3764.

(27) In general, while evaluating the feasibility of new methodologies, we often employ naphthyl substrates as oxidative addition to these substrates tends to be more facile.

(28) Quasdorf, K. W.; Tian. X.; Garg, N. K. Cross-coupling reactions of aryl pivalates with boronic acids. *J. Am. Chem. Soc.* **2008**, *130*, 14422–14423.

(29) Quasdorf, K. W.; Riener, M.; Petrova, K. V.; Garg, N. K. Suzuki–Miyaura coupling of aryl carbamates, carbonates, and sulfamates. *J. Am. Chem. Soc.* **2009**, *131*, 17748–17749.

(30) Snieckus, V. Directed ortho metalation. Tertiary amide and O-carbamate directors in synthetic strategies for polysubstituted aromatics. *Chem. Rev.* **1990**, *90*, 879–933.

(31) Mesganaw, T.; Silberstein, A. L.; Ramgren, S. D.; Fine Nathel, N. F.; Hong, X.; Liu, P.; Garg, N. K. Nickel-catalyzed amination of aryl carbamates and sequential site-selective cross-couplings. *Chem. Sci.* **2011***, 2,* 1766–1771.

(32) For reviews in the area of sp^2–sp^3 C–C cross-couplings, see: (a) Tellis, J. C.; Kelley, C. B.; Primer, D. N.; Jouffroy, M.; Patel, N. R.; Molander, G. A. Single-electron transmetalation via photoredox/nickel dual catalysis: unlocking a new paradigm for sp^3−sp^2 cross-coupling. *Acc. Chem. Res.* **2016**, *49*, 1429–1439. (b) Iwasake, T.; Kambe, N. Ni-catalyzed C–C couplings using alkyl electrophiles. *Top. Curr. Chem.* **2016**, *374*, 1–36. (c) Miyaura, N.; Suzuki, A. Palladium-catalyzed cross-coupling reactions of organoboron compounds. *Chem. Rev.* **1995**, *95*, 2457–2483.

(33) For examples of iron-catalyzed alkylations of aryl halides, triflates, and sulfonates, see: (a) Fürstner, A.; Leitner, A. Iron-catalyzed cross-coupling reactions of alkyl-Grignard reagents with aryl chlorides, tosylates, and triflates. *Angew. Chem., Int. Ed.* **2002**, *41*, 609–612. (b) Fürstner, A.; Leitner, A.; Méndez, M.; Krause, H. Iron-catalyzed cross-coupling reactions. *J. Am. Chem. Soc.* **2002**, *124*, 13856–13863. (c) Fürstner, A.; Martin, R.; Krause, H.; Günter, S.; Goddard, R.; Lehmann, C. W. Preparation, structure, and reactivity of nonstabilized

organoiron compounds. Implications for iron-catalyzed cross coupling reactions. *J. Am. Chem. Soc.* **2008**, *130*, 8773–8787.

(34) For the iron-catalyzed alkylation of heteroaromatic sulfonates and phosphates, see: (a) Gøgsig, T. M.; Lindhardt, A. T.; Skrydstrup, T. Heteroaromatic sulfonates and phosphates and electrophiles in iron-catalyzed cross-couplings. *Org. Lett.* **2009**, *11*, 4886–4888. (b) Kleimark, J.; Larsson, P.-F.; Emamy, P.; Hedström, A.; Norrby, P.-O. Low temperature studies of iron-catalyzed cross-coupling of alkyl Grignard reagents with aryl electrophiles. *Adv. Synth. Catal.* **2012**, *354*, 448–456.

(35) Silberstein, A. L.; Ramgren, S. D.; Garg, N. K. Iron-catalyzed alkylations of aryl sulfamates and carbamates. *Org. Lett.* **2012**, *14*, 3796–3799.

(36) Mesganaw, T.; Fine Nathel, N. F.; Garg, N. K. Cine substitution of arenes using the aryl carbamate as a removable directing group. *Org. Lett*. **2012**, *14*, 2918–2921.

(37) (a) Yoshikai, N.; Matsuda, H.; Nakamura, E. Hydroxyphosphine ligand for nickel-catalyzed cross-coupling through nickel/magnesium bimetallic cooperation. *J. Am. Chem. Soc.* **2009**, *131*, 9590–9599. (b) Li, B.-J.; Wu, Z.-H.; Guan, B.-T.; Sun, C.-L.; Wang, B.-Q.; Shi, Z.-J. Cross-coupling of alkenyl/aryl carboxylates with Grignard reagent via Fe-catalyzed C–O bond activation. *J. Am. Chem. Soc.* **2009**, *131*, 14656–14657. (c) Xu, L.; Li, B.-J.; Wu, Z.-H.; Lu, X.-Y.; Guan, B.-T.; Wang, B.-Q.; Zhao, K.-Q.; Shi, Z.-J.; Nickel catalyzed efficient and practical Suzuki–Miyaura coupling of alkenyl and aryl carbamates with aryl boroxines. *Org. Lett.* **2010**, *12*, 884–887. (d) Shimasaki, T.; Tobisu, M.; Chatani, N. Nickel-catalyzed amination of aryl pivalates by the cleavage of aryl C–O bonds. *Angew. Chem., Int. Ed.* **2010**, *49*, 2929–2932. (e) Tobisu, M.; Yamakawa, K.; Shimasaki, T.; Chatani, N. Nickel-catalyzed

reductive cleavage of aryl–oxygen bonds in alkoxy- and pivaloxyarenes using hydrosilanes as a mild reducing agent. *Chem. Commun.* **2011**, *47*, 2946–2948. (f) Zhao, F.; Yu, D.-G.; Zhu, R.-Y.; Xi, Z.; Shi, Z.-J. Cross-coupling of aryl/alkenyl silyl ethers with Grignard reagents through nickel-catalyzed C–O bond activation. *Chem. Lett.* **2011**, *40*, 1001–1003. (g) Yu, D. G.; Shi, Z.-J. Mutual activation: Suzuki–Miyaura coupling through direct cleavage of the sp^2 C–O bond of naphtholate. *Angew. Chem., Int. Ed.* **2011**, *50*, 7097–7100. (h) Huang, K.; Yu, D.-G.; Zheng, S.-F.; Wu, Z.-H.; Shi, Z.-J. *Chem. Eur. J.* **2011**, *17*, 786–791. (i) Zhao, F.; Zhang, Y.-F.; Wen, J.; Yu, D.-G.; Wei, J.-B.; Xi, Z.; Shi, Z.-J. Programmed selective sp^2 C–O bond activation toward multiarylated benzenes. *Org. Lett.* **2013**, *15*, 3230–3233. (j) Hong, X.; Liang, Y.; Houk, K. N. Mechanisms and origins of switchable chemoselectivity of Ni-catalyzed C(aryl)–O and C(acyl)–O activation of aryl esters with phosphine ligands. *J. Am. Chem. Soc.* **2014**, *136*, 2017–2025. (k) Yue, H.; Guo, L.; Liu, X.; Rueping, M. Nickel-catalyzed synthesis of primary aryl and heteroaryl amines via C–O bond cleavage. *Org. Lett.* **2017**, *19*, 1788–1791.

(38) Quasdorf, K. W.; Antoft-Finch, A.; Liu, P.; Silberstein, A. L.; Komaromi, A.; Blackburn, T.; Ramgren, S. D.; Houk, K. N.; Snieckus, V.; Garg, N. K. Suzuki–Miyaura cross-coupling of aryl carbamates and sulfamates: experimental and computational studies. *J. Am. Chem. Soc*. **2011**, *133*, 6352–6363.

(39) Ramgren, S. D.; Silberstein, A. L.; Yang, Y.; Garg, N. K. Nickel-catalyzed amination of aryl sulfamates. *Angew. Chem., Int. Ed.* **2011**, *50*, 2171–2173.

(40) (a) Jezorek, R. L.; Zhang, N.; Leowanawat, P.; Bunner, M. H.; Gutsche, N.; Pesti, A. K. R.; Olsen, J. T.; Percec, V. Air-stable nickel precatalysts for fast and quantitative cross-coupling

of aryl sulfamates with aryl neopentylglycolboronates at room temperature. *Org. Lett.* **2014**, *16*, 6326–6239. (b) Beromi, M. M.; Nova, A.; Balcells, D.; Brasacchio, A. M.; Brudvig, G. W.; Guard, L. M.; Hazari, N.; Vinyard, D. J. Mechanistic study of an improved Ni precatalyst for Suzuki–Miyaura reactions of aryl sulfamates: Understanding the role of Ni(I) species. *J. Am. Chem. Soc.* **2017**, *139*, 922–936. (c) Zhang, N.; Hoffman, D. J.; Gutsche, N.; Gupta, J.; Percec, V. Comparison of arylboron-based nucleophiles in Ni-catalyzed Suzuki–Miyaura cross-coupling with aryl mesylates and sulfamates. *J. Org. Chem.* **2012**, *77*, 5956–5964. (d) Muto, K.; Yamaguchi, J.; Lei, A.; Itami, K. Isolation, structure, and reactivity of an arylnickel(II) pivalate complex in catalytic C–H/C–O biaryl coupling. *J. Am. Chem. Soc.* **2013**, *135*, 16384–16387. (e) Leowanawat, P.; Zhang, N.; Safi, M.; Hoffman, D. J.; Fryberger, M. C.; George, A.; Percec, V. *trans*-Chloro(1-naphthyl)bis(triphenylphosphine)nickel(II)/PCy$_3$ catalyzed cross-coupling of aryl and heteroaryl neopentylglycolboronates with aryl and heteroaryl mesylates and sulfamates at room temperature. *J. Org. Chem.* **2012**, *77*, 2885–2982. (f) Leowanawat, P.; Zhang, N.; Percec, V. Nickel catalyzed cross-coupling of aryl C–O based electrophiles with aryl neopentylglycolboronates. *J. Org. Chem.* **2012**, *77*, 1018–1025. (g) Leowanawat, P.; Zhang, N.; Resmerita, A.-M.; Rosen, B. M.; Percec, V. Ni(COD)$_2$/PCy$_3$ Catalyzed cross-coupling of aryl and heteroaryl neopentylglycolboronates with aryl and heteroaryl mesylates and sulfamates in THF at room temperature. *J. Org. Chem.* **2011**, *76*, 9946–9955.

(41) For representative publications on the development of air-stable Ni(II) precatalysts, see: (a) Standley, E. A. and Jamison, T. F. Simplifying nickel(0) catalysis: an air-stable nickel precatalyst for the internally selective benzylation of terminal alkenes. *J. Am. Chem. Soc.*

2013, *135*, 1585–1592. (b) Strieth-Kalthoff, F.; Longstreet, A. R.; Weber, J. M.; Jamison, T. F. Bench-stable *N*-heterocyclic carbene nickel precatalysts for C–C and C–N bond-forming reactions. *ChemCatChem* **2018**, *10*, 1–6. (c) Weber, J. M.; Longstreet, A. R.; Jamison, T. F. Bench-stable nickel precatalysts with Heck-type activation. *Organometallics* **2018**, *37*, 2716–2722. (d) Shields, J. D.; Gray, E. E.; Doyle, A. G. A modular, air-stable nickel precatalyst. *Org. Lett.* **2015**, *17,* 2166−2169.

(42) Hie, L.; Ramgren, S.D.; Mesganaw, T.; Garg, N.K. Nickel-catalyzed amination of aryl sulfamates and carbamates using an air-stable precatalyst. *Org. Lett.* **2012**, *14*, 4182–4185.

(43) Nathel, N. F. N.; Kim, J.; Hie, L.; Jiang, X.; Garg, N.K. Nickel-catalyzed amination of aryl chlorides and sulfamates in 2-methyl THF. *ACS Catal.* **2014**, *4*, 3289–3293.

(44) Roglans, A.; Pla-Quintana, A.; Moreno-Mañas, M. Diazonium salts as substrates in palladium-catalyzed cross-coupling reactions. *Chem. Rev.* **2006**, *106*, 4622−4643.

(45) Though Cu(I) catalyzed reactions of aryl diazononium salts are well-established, these transformations typically proceed via single-electron-transfer and aryl radical reactivity rather than through traditional M(0)/M(II) cross-coupling catalytic cycles.

(46) For a comprehensive review, see: Ouyang, K.; Hao, W.; Zhang, W.-X.; Xi, Z. Transition-metal-catalyzed cleavage of C–N single bonds. *Chem. Rev.* **2015**, *115*, 12045–12090.

(47) Blakey, S. B.; MacMillan, D. W. C. The first Suzuki cross-couplings of aryltrimethylammonium salts. *J. Am. Chem. Soc.* **2003**, *125*, 6046−6047.

(48) Wenkert, E.; Han, A.-L.; Jenny, C.-J. Nickel-induced conversion of carbon−nitrogen into carbon−carbon bonds. one-step transformations of aryl, quaternary ammonium salts into alkylarenes and biaryls. *J. Chem. Soc., Chem. Commun.* **1988**, 975−976.

(49) Cao, Z.-C.; Xie, S.-J.; Fang, H.; Shi, Z.-J. Ni-catalyzed cross-coupling of dimethyl aryl amines with arylboronic esters under reductive conditions. *J. Am. Chem. Soc.* **2018**, *140*, 13575−13579.

(50) For examples, see: (a) Ueno, S.; Chatani, N.; Kakiuchi, F. Ruthenium-catalyzed carbon−carbon bond formation via the cleavage of an unreactive aryl carbon−nitrogen bond in aniline derivatives with organoboronates. *J. Am. Chem. Soc.* **2007**, *129*, 6098–6099. (b) Koreeda, T.; Kochi, T.; Kakiuchi, F. Cleavage of C−N bonds in aniline derivatives on a ruthenium center and its relevance to catalytic C−C bond formation. *J. Am. Chem. Soc.* **2009**, *131*, 7238–7239. (c) Koreeda, T.; Kochi, T.; Kakiuichi, F. Substituent effects on stoichiometric and catalytic cleavage of carbon–nitrogen bonds in aniline derivatives by ruthenium–phosphine complexes. *Organometallics* **2013**, *32*, 682–690. (d) Koreeda, T.; Kochi, T.; Kakuichi, F. Ruthenium-catalyzed reductive deamination and tandem alkylation of aniline derivatives. *J. Organomet. Chem.* **2013**, *741−742*, 148−152. (e) Zhao, Y.; Snieckus, V. Beyond directed ortho metalation: ruthenium-catalyzed amide-directed C_{Ar}−N activation/C−C coupling reaction of anthranilamides with organoboronates. *Org. Lett*. **2014**, *16*, 3200−3203.

(51) Liu, J.; Robins, M. J. Azoles as Suzuki cross-coupling leaving groups: syntheses of 6-arylpurine 2′-deoxynucleosides and nucleo- sides from 6-(imidazol-1-yl)- and 6-(1,2,4-triazol-4-yl)purine derivatives. *Org. Lett.* **2004**, *6*, 3421−3423.

(52) For reports on the application of nucleoside analogs as potential therapeutics or chemical probes, see: (a) Hocek, M.; Holy, A.; Votruba, I.; Dvořáková, H. Synthesis and cytostatic activity of substituted 6-phenylpurine bases and nucleosides: application of the Suzuki–

Miyaura cross-coupling reactions of 6-chloropurine derivatives with phenylboronic acids. *J. Med. Chem.* **2000**, *43*, 1817–1825. (b) Perez, O. D.; Chang, Y.-T.; Rosania, G.; Sutherlin, D.; Schultz, P. G. Inhibition and reversal of myogenic differentiation by purine-based microtubule assembly inhibitors. *Chem. Biol.* **2002**, *9*, 475–483.

(53) Notably, Pd-catalyzed cross-couplings of nitroarenes have been reported by Nakao and coworkers. (a) Ramu Yadav, M.; Nagaoka, M.; Kashihara, M.; Zhong, R.-L.; Miyazaki, T.; Sakaki, S.; Nakao, Y. The Suzuki–Miyaura coupling of nitroarenes. *J. Am. Chem. Soc.* **2017**, *139*, 9423–9426. (b) Inoue, F.; Kashihara, M.; Ramu Yadav, M; Nakao, Y. Buchwald–Hartwig amination of nitroarenes. *Angew. Chem., Int. Ed.* **2017**, *56*, 13307–13309. (c) Rocard, L.; Hatych, D.; Chartier, T.; Cauchy, T.; Hudhomme, P. Original Suzuki−Miyaura coupling using nitro derivatives for the synthesis of perylenediimide-based multimers. *Eur. J. Org. Chem.* **2019**, 7635−7643. (d) Zhou, F.; Zhou, F.; Su, R.; Yang, Y.; You, J. Build-up of double carbohelicenes using nitroarenes: Dual role of the nitro Functionality as an activating and leaving group. *Chem. Sci.* **2020**, *11*, 7424−7428. (e) Muto, K.; Okita, T.; Yamaguchi, J. Transition-metal-catalyzed denitrative coupling of nitroarenes. *ACS Catal.* **2020**, *10*, 9856–9871.

(54) Yamamoto, T.; Ishizu, J.; Kohara, T.; Komiya, S.; Yamamoto, A. Oxidative addition of aryl carboxylates to nickel (0) complexes involving cleavage of the acyl–oxygen bond. *J. Am. Chem. Soc.* **1980**, *102*, 3758–3764.

(55) (a) Amaike, K.; Muto, K.; Yamaguchi, J.; Itami, K. Decarbonylative C–H coupling of azoles and aryl esters: unprecedented nickel catalysis and applications to the synthesis of Muscoride A. *J. Am. Chem. Soc.* **2012**, *134*, 13573–13576. (b) Meng, L.; Kamada, Y.;

Muto, K.; Yamaguchi, J.; Itami, K. C–H alkenylation of azoles with enols and esters by nickel catalysis. *Angew. Chem., Int. Ed.* **2013**, *52*, 10048–10051. (c) Muto, K.; Yamaguchi, J.; Musaev, D. G.; Itami, K. Decarbonylative organoboron cross-coupling of esters by nickel catalysis. *Nat. Commun.* **2015**, *6*, 7508. (d) Muto, K. Hatakeyama, R.; Itami, K.; Yamaguchi, J. Palladium-catalyzed decarbonylative cross-coupling of azinecarboxylates with arylboronic acids. *Org. Lett.* **2016**, *18*, 5106–5109.

(56) (a) Gooßen, L. J.; Paetzold, J. Pd-catalyzed decarbonylative olefination of aryl esters: towards a waste-free Heck reaction. *Angew. Chem., Int. Ed.* **2002**, *41*, 1237–1241. (b) Gooßen, L. J.; Paetzold, J. Decarbonylative Heck olefination of enol esters: salt-free and environmentally friendly access to vinyl arenes. *Angew. Chem., Int. Ed.* **2004**, *43*, 1095–1098.

(57) For the chelation-assisted transition-metal-catalyzed activation of esters, see (a) Chatani, N.; Tatamidani, H.; Ie, Y.; Kakiuchi, F.; Murai, S. The ruthenium-catalyzed reductive decarboxylation of esters: catalytic reactions involving the cleavage of acyl–oxygen bonds of esters. *J. Am. Chem. Soc.* **2001**, *123*, 4849–4850. (b) Tatamidani, H.; Yokota, K.; Kakiuchi, F.; Chatani, N. Catalytic cross-coupling reaction of esters with organoboron compounds and decarbonylative reduction of esters with $HCOONH_4$: A new route to acyl transition metal complexes through the cleavage of acyl–oxygen bonds in esters. *J. Org. Chem.* **2004**, *69*, 5615–5621. (c) Tatamidani, H.; Kakiuchi, F.; Chatani, N. A new ketone synthesis by palladium-catalyzed cross-coupling reactions of esters with organoboron compounds. *Org. Lett.* **2004**, *6*, 3597–3599.

(58) For the use of electronically-activated esters in transition-metal-catalyzed couplings, see: (a) Refs. 55 and 56. (b) LaBerge, N. A.; Love, J. A. Nickel-catalyzed decarbonylative coupling

of aryl esters and arylboronic acids. *Eur. J. Org. Chem.* **2015**, 5546–5553. (c) Halima, T. B.; Vandavasi, J. K.; Shkoor, M.; Newman, S. G. A cross-coupling approach to amide bond formation from esters. *ACS Catal.* **2017**, *7*, 2176–2180. (d) Kruckenberg, A.; Wadepohl, H.; Gade, L. H. Bis(diisospropylphosphinomethyl)amine nickel(II) and nickel(0) complexes: coordination chemistry, reactivity, and catalytic decarbonylative C–H arylation of benzoxazole. *Organometallics* **2013**, *32*, 5153–5170. (e) Yue, H.; Guo, L.; Liao, H.-H.; Cai, Y.; Zhu, C.; Rueping, M. Catalytic ester and amide to amine interconversion: nickel-catalyzed decarbonylative amination of esters and amides by C–O and C–C bond activation. *Angew. Chem., Int. Ed.* **2017**, *56*, 4282–4285. (f) Yu, H.; Guo, L.; Lee, S.-C.; Liu, X.; Rueping, M. Selective reductive removal of ester and amide groups from arenes and heteroarenes through nickel-catalyzed C–O and C–N bond activation. *Angew. Chem., Int. Ed.* **2017**, *56*, 3972–3976. (g) Halima, T. B.; Zhang, W.; Yalaoui, I.; Hong, X.; Yang, Y.; Houk, K. N.; Newman, S. G. Palladium-catalyzed Suzuki–Miyaura coupling of aryl esters. *J. Am. Chem. Soc.* **2017**, *139*, 1311–1318.

(59) For transition-metal-catalyzed cross-couplings of acid anhydrides, see: (a) Wang, D.; Zhang, Z. Palladium-catalyzed cross-coupling reactions of carboxylic anhydrides with organozinc reagents. *Org. Lett.* **2003**, *5*, 4645−4648. (b) Cook, M. J.; Rovis, T. Enantioselective rhodium-catalyzed alkylative desymmetrization of 3,5-dimethylglutaric anhydride. *Synthesis* **2009**, *2*, 335−338. (c) Bercot, E. A.; Rovis, T. A mild and efficient catalytic alkylative monofunctionalization of cyclic anhydrides. *J. Am. Chem. Soc.* **2002**, *124*, 174−175. (d) Bercot, E. A.; Rovis, T. Highly efficient nickel-catalyzed cross-coupling of succinic and glutaric anhydrides with organozinc reagents. *J. Am. Chem. Soc.* **2005**, *127*, 247−254. (d)

Johnson, J. B.; Cook, M. J.; Rovis, T. Ligand differentiated complementary Rh-catalyst systems for the enantioselective desymmetrization of meso-cyclic anhydrides. *Tetrahedron* **2009**, *65*, 3202−3210. (f) Rogers, R. L.; Moore, J. L.; Rovis, T. Alkene-directed regioselective nickel-catalyzed cross-coupling of cyclic anhydrides with diorganozinc reagents. *Angew. Chem., Int. Ed.* **2007**, *46*, 9301−9304. (g) Bercot, E. A.; Rovis, T. A palladium-catalyzed enantioselective alkylative desymmetrization of meso-succinic anhydrides. *J. Am. Chem. Soc.* **2004**, *126*, 10248−10249. (h) Johnson, J. B.; Yu, R. T.; Fink, P.; Bercot, E. A.; Rovis, T. Selective substituent transfer from mixed zinc reagents in Ni-catalyzed anhydride alkylation. *Org. Lett.* **2006**, *8*, 4307−4310. (i) Johnson, J. B.; Bercot, E. A.; Rowley, J. M.; Coates, G. W.; Rovis, T. Ligand-dependent catalytic cycle and role of styrene in nickel-catalyzed anhydride cross-coupling: evidence for turnover-limiting reductive elimination. *J. Am. Chem. Soc.* **2007**, *129*, 2718−2725. (j) Cook, M. J.; Rovis, T. Rhodium-catalyzed enantioselective desymmetrization of meso-3,5-dimethyl glutaric anhydride: A general strategy to *syn*-deoxypolypropionate synthons. *J. Am. Chem. Soc.* **2007**, *129*, 9302−9303. (k) Stephan, M. S.; Teunissen, A. J. J. M.; Verzijl, G. K. M.; de Vries, J. G. Heck reactions without salt formation: aromatic carboxylic anhydrides as arylating agents. *Angew. Chem., Int. Ed.* **1998**, *37*, 662–664. (l) Gooßen, L. J.; Ghosh, K. Palladium-catalyzed synthesis of aryl ketones from boronic acids and carboxylic acids or anhydrides. *Angew. Chem., Int. Ed.* **2001**, *40*, 3458–3460. (m) Kajita, Y.; Kurahashi, T.; Matsubara, S. Nickel-catalyzed decarbonylative addition of anhydrides to alkynes. *J. Am. Chem. Soc.* **2008**, *130*, 17226–17227.

(60) Hie, L.; Nathel, N. F. N.; Hong, X.; Yang, Y.-F.; Houk, K. N.; Garg, N. K. Nickel-catalyzed activation of acyl C–O bonds of methyl esters. *Angew. Chem., Int. Ed.* **2016**, *55*, 2810–2814.

(61) Carey, F. A.; Sundberg, R. J. *Advanced Organic Chemistry Part A: Structure and Mechanisms.* Springer: New York, 2000; p. 9–11.

(62) Brown, D. G.; Boström, J. Analysis of past and present synthetic methodologies on medicinal chemistry: where have all the new reactions gone? *J. Med. Chem.* **2016**, *59*, 4443–4458.

(63) Halima, T. B. Masson-Makdissi, J.; Newman, S. G. Nickel-catalyzed amide bond formation from methyl esters. *Angew. Chem., Int. Ed.* **2018**, *57*, 12925–12929.

(64) Zheng, Y.-L.; Newman, S. G. Methyl esters as cross-coupling electrophiles: direct synthesis of amide bonds. *ACS Catal.* **2019**, *9*, 4426–4433.

(65) Cheung, C. W.; Leendert, P.; Hu, X. Direct amination of esters with nitroarenes. *Nat. Commun.* **2017**, *8*, 14878.

(66) Hu and coworkers note that, rather than proceeding via nickel-catalyzed oxidative addition to the acyl C–O bond, this transformation likely proceeds through a nickel nitrene intermediate, which could undergo insertion into the acyl C–O bond to generate a Ni(II) amido species. See ref. 65 for further discussion of the mechanism.

(67) Medina, J. M.; Moreno, J.; Racine, S.; Du, S.; Garg, N. K. Mizoroki–Heck cyclizations of amide derivatives for the introduction of quaternary centers. *Angew. Chem., Int. Ed.* **2017**, *56*, 6567–6571.

(68) Zheng, Y.-L.; Newman, S. G. Nickel-catalyzed domino Heck-type reactions using methyl esters as cross-coupling electrophiles. *Angew. Chem., Int. Ed.* **2019**, *58*, 18159–18164.

(69) Yue, H.; Zhu, C.; Rueping, M. Catalytic ester to stannane functional group interconversion via decarbonylative cross-coupling of methyl esters. *Org. Lett.* **2018**, *20*, 385–388.

(70) Okita, T.; Muto, K.; Yamaguchi, J. Decarbonylative methylation of aromatic esters by a nickel catalyst. *Org. Lett.* **2018**, *20*, 3132–3135.

(71) (a) *The Amide Linkage: Structural Significance in Chemistry, Biochemistry, and Materials Science*; Greenberg, A., Breneman, C. M., Liebman, J. F., Eds.; Wiley: Hoboken, NJ, 2003; p. 33–43. (b) Pauling, L.; Corey, R. B.; Branson, H. R. The structure of proteins: two hydrogen-bonded helical configurations of the polypeptide chain. *Proc. Natl. Acad. Sci. USA* **1951**, *37*, 205−211.

(72) For select examples of amide-directed C−H functionalization, see: Rouquet, G.; Chatani, N. Catalytic functionalization of $C(sp^2)$–H and $C(sp^3)$–H bonds by using bidentate directing groups. *Angew. Chem., Int. Ed.* **2013**, *52*, 11726−11743 and references therein.

(73) Kaiser, D.; Bauer, A.; Lemmerer, M.; Maulide, N. Amide activation: An emerging tool for chemoselective synthesis. *Chem. Soc. Rev.* **2018**, *47*, 7899–7925.

(74) (a) Nahm, S.; Weinreb, S. M. N-methoxy-N-methylamides as effective acylating agents. *Tetrahedron Lett.* **1981**, *22*, 3815–3818.

(75) (a) Jensen, C. M.; Lindsay, K. B.; Taaning, R. H.; Karaffa, J.; Hansen, A. M.; Skrydstrup. Can decarbonylation of acyl radicals be overcome in radical addition reactions? En route to a solution employing *N*-acyl oxazolidinones and SmI_2/H_2O. *J. Am. Chem. Soc.* **2005**, *127*, 6544–6545. (b) Shi, S.; Lalancette, R.; Szostak, R.; Szostak, M. Highly chemoselective synthesis of indolizidine lactams by SmI_2-induced umpolung of the amide bond via aminoketyl radicals: Efficient entry to alkaloid scaffolds. *Chem. Eur. J.* **2016**, *22*, 11949–11953. (c) Huang, H.-M.; Procter, D. J. Radical-radical cyclization cascades of barbiturates triggered by electron-transfer reduction of amide-type carbonyls. *J. Am. Chem. Soc.* **2016**,

138, 7770–7775. (d) Huang, H.-M.; Procter, D. J. Dearomatizing radical cyclizations and cyclization cascades triggered by electron-transfer reduction of amide-type carbonyls. *J. Am. Chem. Soc.* **2017**, *139*, 1661–1667. (e) Huang, H.-M; Bonilla, P.; Procter, D.-J. Selective construction of quaternary stereocentres in radical cyclisation cascades triggered by electron-transfer reduction of amide-type carbonyls. *Org. Biomol. Chem.* **2017**, *15*, 4159–4164.

(76) For select examples, see: (a) Madelaine, C.; Valerio, V.; Maulide, N. Unexpected electrophilic rearrangements of amides: A stereoselective entry to challenging substituted lactones. *Angew. Chem., Int. Ed.* **2010**, *49*, 1583–1586. (b) Peng, B.; Geerdrink D.; Maulide, N. Electrophilic rearrangements of chiral amides: A traceless asymmetric α-allylation. *J. Am. Chem. Soc.* **2013**, *135*, 14968–14971. (c) Tona, V.; Maryasin, B.; de la Torre, A.; Sprachmann, J.; González, L.; Maulide, N. Direct regioselective synthesis of tetrazolium salts by activation of secondary amides under mild conditions. *Org. Lett.* **2017**, *19*, 2662–2665.

(77) (a) Gregory, A. W.; Chambers, A.; Hawkins, A.; Jakubec, P.; Dixon, D. J. Iridium-catalyzed reductive nitro-Mannich cyclization. *Chem.-Eur. J.* **2015**, *21*, 111−114. (b) Fuentes de Arriba, Á . L.; Lenci, E.; Sonawane, M.; Formery, O.; Dixon, D. J. Iridium-catalyzed reductive Strecker reaction for late-stage amide and lactam cyanation. *Angew. Chem., Int. Ed.* **2017**, *56*, 3655−3659. (c) Xie, L.-G.; Dixon, D. J. Tertiary amine synthesis via reductive coupling of amides with Grignard reagents. *Chem. Sci.* 2017, 8, 7492− 7497. (d) Gabriel, P.; Xie, L.-G.; Dixon, D. J. Iridium-catalyzed reductive coupling of Grignard reagents and tertiary amides. *Org. Synth.* **2019**, *96*, 511−527. (e) Xie, L. G.; Dixon, D. J. Iridium-catalyzed reductive Ugi-type reactions of tertiary amides. *Nat. Commun.* **2018**, *9*, 2841. (f) Gabriel, P.; Gregory, A. W.; Dixon, D. J. Iridium-catalyzed aza-spirocyclization of indole-tethered amides: An

interrupted Pictet−Spengler reaction. *Org. Lett.* **2019**, *21*, 6658−6662. (g) For a review, see: Mathea-Raven, D.; Gabriel, P.; Leitch, J. A.; Almehmadi, Y. A.; Yamazaki, K.; Dixon, D. J. Catalytic reductive functionalization of tertiary amides using Vaska's complex: Synthesis of complex tertiary amine building blocks and natural products. *ACS Catal.* **2020**, *10*, 8880–8897.

(78) (a) Nakajima, M.; Sato, T.; Chida, N. Iridium-catalyzed chemoselectivu-Ravene reductive nucleophilic addition to *N*-,ethoxyamides. *Org. Lett.* **2015**, *17*, 1696−1699. (b) Huang, P.-Q.; Ou, W.; Han, F. Chemoselective reductive alkynylation of tertiary amides by Ir and Cu(I) bis-metal sequential catalysis. *Chem. Commun.* **2016**, *52*, 11967−11970. (c) Hu, X.-N.; Shen, T.-L.; Cai, D.-C.; Zheng, J.-F.; Huang, P.-Q. The iridium-catalysed reductive coupling reaction of tertiary lactams/amides with isocyanoacetates. *Org. Chem. Front.* **2018**, *5*, 2051−2056. (d) Takahashi, Y.; Sato, T.; Chida, N. Iridium-catalyzed reductive nucleophilic addition to tertiary amides. *Chem. Lett.* **2019**, *48*, 1138−1141.

(79) For recent reviews, see: (a) Meng, G.; Shi, S.; Szostak, M. Cross-coupling of amides by N−C bond activation. *Synlett* **2016**, *27*, 2530−2540. (b) Takise, R.; Muto, K.; Yamaguchi, J. Cross-coupling of aromatic esters and amides. *Chem. Soc. Rev.* **2017**, *46*, 5864−5888. (c) Kaiser, D.; Bauer, A.; Lemmerer, M.; Maulide, N. Amide activation: an emerging tool for chemoselective synthesis. *Chem. Soc. Rev.* **2018**, *47*, 7899−7925.

(80) Hie, L.; Fine Nathel, N. F.; Shah, T. K.; Baker, E. L.; Hong, X.; Yang, Y.; Liu, P.; Houk, K. N.; Garg, N. K. Conversion of amides to esters by nickel-catalysed activation of amide C–N bonds. *Nature* **2015**, *524*, 79–83.

(81) (a) Huynh, H. V. Electronic properties of *N*-heterocyclic carbenes and their experimental determination. *Chem. Rev.* **2018**, *118*, 9457–9492. (b) Dröge, T.; Glorius, F. The measure of all rings–*N*-heterocyclic carbenes. *Angew. Chem., Int. Ed.* **2010**, *49*, 6940–6952. (c) Kelly III, R. A; Clavier, H.; Guidice, S.; Scott, N. M.; Stevens, E. D.; Bordner, J.; Samardjiev, I.; Hoff, C. D.; Cavallo, L.; Nolan, S. P. Determination of *N*-heterocyclic carbene (NHC) steric and electronic parameters using the [(NHC)Ir(CO)$_2$Cl] system. *Organometallics* **2008**, *27*, 202–210. (d) Gómez-Suárez, A.; Nelson, D. J.; Nolan, S. P. Quantifying and understanding the steric properties of *N*-heterocyclic carbenes. *Chem. Commun.* **2017**, *53*, 2650–2660.

(82) Liu, C.; Szostak, M. Twisted amides: From obscurity to broadly useful transition-metal-catalyzed reactions by N–C amide bond activation. *Chem. Eur. J.* **2017**, *23*, 7157–7173.

(83) Using our previously established conditions for the nickel-catalyzed esterification of amides, the use of H$_2$O as a nucleophile delivered no product. Moreover, in the presence of benzoic acid, the nickel-catalyzed esterification of *N*-Ph,Me benzamide failed to deliver product, indicating catalyst poisoning.

(84) Knapp, R. R.; Bulger, A. S.; Garg, N. K. Nickel-catalyzed conversion of amides to carboxylic acids. *Org. Lett.* **2020**, *22*, 2833–2837.

(85) Transamidation of secondary amides has been historically difficult due to the resonance stability of amides and the often thermoneutral nature of this conversion. For further reading on this topic, see: (a) Lanigan, R. M.; Sheppard, T. D. Recent developments in amide synthesis: direct amidation of carboxylic acids and transamidation reactions. *Eur. J. Org. Chem.* **2013**, 7453–7465. (b) Musci, Z.; Chass, G. A.; Csizmadia, I. G. Amidicity change as

a significant driving force and thermodynamic selection rule of transamidation reactions. A synergy between experiment and theory. *J. Phys. Chem. B* **2008**, *112*, 7885–7893.

(86) Baker, E. L.; Yamano, M. M.; Zhou, Y.; Anthony, S. M.; Garg, N. K. A two-step approach to achieve secondary amide transamidation enabled by nickel catalysis. *Nat. Commun.* **2016**, *7*, 1–5.

(87) Weires, N. A.; Baker, E. L.; Garg, N. K. Nickel-catalyzed Suzuki–Miyaura coupling of amides. *Nat. Chem.* **2016**, *8*, 75–79.

(88) Simmons, B. J.; Weires, N. A.; Dander, J. E.; Garg, N. K. Nickel-catalyzed alkylation of amide derivatives. *ACS Catal*. **2016**, *6*, 3176–3179.

(89) Hu, L.; Jiang, J.; Qu, J.; Li, Y.; Jin, J.; Li, Z.; Boykin, D. W. Novel potent antimitotic heterocyclic ketones: synthesis, antiproliferative activity, and structure–activity relationships. *Bioorg. Med. Chem. Lett.* **2007**, *17*, 3613–3617.

(90) Apnes, G. E.; Didluk, M. T.; Filipski, K. J.; Guzman-Perez, A.; Lee, E. C. Y.; Pfefferkorn, J. A.; Stevens, B. D.; Tu, M. M. Glucagon Receptor Modulators. U.S. Patent 20120202834, Aug. 9, 2012.

(91) Walker, Jr., J. A.; Vickerman, K. L.; Humke, J. N.; Stanley, L. M. Ni-catalyzed alkene carboacylation via amide C–N bond activation. *J. Am. Chem. Soc.* **2017**, *139*, 10228–10231.

(92) Dander, J. E.; Giroud, M.; Racine, S.; Darzi, E. R.; Alvizo, O.; Entwistle, D.; Garg, N. K. Chemoenzymatic conversion of amides to enantioenriched alcohols in aqueous medium. *Communications Chemistry* **2019**, *2*, 82.

(93) Computations suggest that the active Ni–NHC catalyst coordinates to aryl substrates prior to amide C–N bond activation, thereby lowering the entropic cost associated with the barrier to oxidative addition (see ref. 80).

(94) Hie, L.; Baker, E. L.; Anthony, S. M.; Desrosiers, J.; Senanayake, C.; Garg, N. K. Nickel-catalyzed esterification of aliphatic amides. *Angew. Chem., Int. Ed.* **2016**, *55*, 15129–15132.

(95) Dander, J. E.; Baker, E. L.; Garg, N. K. Nickel-catalyzed transamidation of aliphatic amide derivatives. *Chem. Sci.* **2017**, *8*, 6433–6438.

(96) Boit, T. B.; Weires, N. A.; Kim, J.; Garg, N. K. Nickel-catalyzed Suzuki–Miyaura coupling of aliphatic amides. *ACS Catal.* **2018**, *8*, 1003–1008.

(97) The NHC ligand, Benz-ICy, is formed from the precursor salt, Benz-ICy•HCl, via deprotonation in situ: Arduengo III, A. J.; Harlow, R. L.; Kline M. A stable crystalline carbene. *J. Am. Chem. Soc.* **1991**, *113*, 361–363.

(98) Weires, N. A.; Caspi, D. D.; Garg, N. K. Kinetic modeling of the nickel-catalyzed esterification of amides. *ACS Catal.* **2017**, *7*, 4381–4385.

(99) Our collaborator, Dan Caspi, employed *DynoChem* software to model the kinetics of the transformation and perform *in silico* simulations to calculate ideal reaction conditions.

(100) For air-stable Ni(0)–olefin precatalysts recently reported by the Cornellaand Engle labs, see: (a) Tran, V. T.; Li, Z.-Q.; Apolinar, O.; Derosa, J.; Joannou, M. V.; Wisniewski, S. R.; Eastgate, M. D.; Engle, K. M. Ni(COD)(DQ): an air-stable 18-electron Ni(0)-olefin precatalyst. *Angew. Chem., Int. Ed.* **2020**, *59*, 7409–7413. (b) Nattmann, L; Saeb, R.; Nöthling, N.; Cornella, J. An air-stable binary Ni(0)-olefin catalyst. *Nat. Catal.* **2020**, *3*, 6–13.

(101) (a) Sather, A. C.; Lee, H. G.; Colombe, J. R.; Zhang, A.; Buchwald, S. L. Dosage delivery of sensitive reagents enables glove- box free synthesis. *Nature* **2015**, *524*, 208−211. (b) Fang, Y.; Liu, Y.; Ke, Y.; Guo, C.; Zhu, N.; Mi, X.; Ma, Z.; Hu, Y. A new chromium-based catalyst coated with paraffin for ethylene oligomerization and the effect of chromium state on oligomerization selectivity. *Appl. Catal., A* **2002**, *235*, 33−38. (c) Taber, D. F.; Frankowski, K. J. Grubbs' catalyst in paraffin: an air-stable preparation for alkene metathesis. *J. Org. Chem.* **2003**, *68*, 6047−6048.

(102) Mehta, M. M.; Boit, T. B.; Dander, J. E.; Garg, N. K. Ni-catalyzed Suzuki–Miyaura cross-coupling of aliphatic amides on the benchtop. *Org. Lett.* **2020**, *22*, 1–5.

(103) For additional examples of using a paraffin-encapsulation strategy from our laboratory, see: (a) Dander, J. E.; Weires, N. A.; Garg, N. K. Benchtop delivery of Ni(cod)$_2$ using paraffin capsules. *Org. Lett.* **2016**, *18*, 3934–3936. (b) Dander, J. E.; Morill, L. A.; Nguyen, M. M.; Chen, S.; Garg, N. K. Breaking amide C–N bonds in an undergraduate organic chemistry laboratory. *J. Chem. Ed.* **2019**, *96*, 776–780.

(104) For Pd-catalyzed amide C−N bond activations, see: (a) Li, X.; Zou, G. Acylative Suzuki coupling of amides: acyl-nitrogen activation via synergy of independently modifiable activating groups. *Chem. Commun.* **2015**, *51*, 5089−5092. (b) Yada, A.; Okajima, S.; Murakami, M. Palladium-catalyzed intramolecular insertion of alkenes into the carbon−nitrogen bond of β-lactams. *J. Am. Chem. Soc.* **2015**, *137*, 8708−8711. (c) Meng, G.; Szostak, M. Palladium-catalyzed Suzuki−Miyaura coupling of amides by carbon−nitrogen cleavage: general strategy for amide N−C bond activation. *Org. Biomol. Chem.* **2016**, *14*, 5690−5705. (d) Meng, G.; Szostak, M. General olefin synthesis by the palladium-catalyzed

Heck reaction of amides: sterically-controlled chemoselective N−C activation. *Angew. Chem., Int. Ed.* **2015**, *54*, 14518−14522. (e) Meng, G.; Szostak, M. Sterically controlled Pd-catalyzed chemoselective ketone synthesis via N−C cleavage in twisted amides. *Org. Lett.* **2015**, *17*, 4364−4367. (f) Liu, C.; Meng, G.; Liu, Y.; Liu, R.; Lalancette, R.; Szostak, R.; Szostak, M. *N*-Acylsaccharins: stable electrophilic amide-based acyl transfer reagents in Pd-catalyzed Suzuki−Miyaura coupling via N−C cleavage. *Org. Lett.* **2016**, *18*, 4194−4197. (g) Lei, P.; Meng, G.; Szostak, M. General method for the Suzuki−Miyaura cross-coupling of amides using commercially available, air- and moisture-stable palladium/ NHC (NHC = *N*-heterocyclic carbene) complexes. *ACS Catal.* **2017**, *7*, 1960−1965. (h) Liu, C.; Liu, Y.; Liu, R.; Lalancette, R.; Szostak, R.; Szostak, M. Palladium-catalyzed Suzuki−Miyaura cross-coupling of *N*-mesylamides by N−C cleavage: electronic effect of the mesyl group. *Org. Lett.* **2017**, *19*, 1434−1437. (i) Liu, C.; Meng, G.; Szostak, M. *N*- Acylsaccharins as amide-based arylating reagents via chemoselective N−C cleavage: Pd-catalyzed decarbonylative Heck reaction. *J. Org. Chem.* **2016**, *81*, 12023−12030. (j) Meng, G.; Shi, S.; Szostak, M. Palladium-catalyzed Suzuki−Miyaura cross-coupling of amides via site-selective N−C bond cleavage by cooperative catalysis. *ACS Catal.* **2016**, *6*, 7335−7339. (k) Cui, M.; Wu, H.; Jian, J.; Wang, H.; Liu, C.; Stelck, D.; Zeng, Z. Palladium-catalyzed Sonogashira coupling of amides: access to ynones via C−N bond cleavage. *Chem. Commun.* **2016**, *52*, 12076−12079. (l) Wu, H.; Li, Y.; Cui, M.; Jian, J.; Zeng, Z. Suzuki coupling of amides via palladium-catalyzed C−N cleavage of *N*-acylsaccharins. *Adv. Synth. Catal.* **2016**, *358*, 3876−3880. (m) Shi, S.; Szostak, M. Decarbonylative cyanation of amides by palladium catalysis. *Org. Lett.* **2017**, *19*, 3095−3098. (n) Lei, P.; Meng, G.; Ling, Y.; An, J.; Szostak, M. Pd-PEPPSI: Pd-NHC

precatalyst for Suzuki−Miyaura cross-coupling reactions of amides. *J. Org. Chem.* **2017**, *82*, 6638−6646. (o) Meng, G.; Szostak, R.; Szostak, M. Suzuki−Miyaura cross-coupling of *N*-acylpyrroles and pyrazoles: planar, electronically activated amides in catalytic N−C cleavage. *Org. Lett.* **2017**, *19*, 3596−3599. (p) Meng, G.; Lalancette, R.; Szostak, R.; Szostak, M. N-Methylamino pyrimidyl amides (MAPA): highly reactive, electronically-activated amides in catalytic N−C(O) cleavage. *Org. Lett.* **2017**, *19*, 4656−4659. (q) Osumi, Y.; Liu, C.; Szostak, M. *N*-Acylsuccinimides: twist-controlled, acyl transfer reagents in Suzuki− Miyaura cross-coupling by N−C amide bond activation. *Org. Biomol. Chem.* **2017**, *15*, 8867−8871. (r) Lei, P.; Meng, G.; Ling, Y.; An, J.; Nolan, S. P.; Szostak, M. General method for the Suzuki−Miyaura cross-coupling of primary amide-derived electrophiles enabled by [Pd(NHC)(cin)−Cl] at room temperature. *Org. Lett.* **2017**, *19*, 6510−6513. (s) Li, X.; Zou, G. Palladium-catalyzed acylative cross-coupling of amides with diarylboronic acids and sodium tetraarylborates. *J. Organomet. Chem.* **2015**, *794*, 136−145. (t) Liu, C.; Li, G.; Shi, S.; Meng, G.; Lalancette, R.; Szostak, R.; Szostak, M. Acyl and decarbonylative Suzuki coupling of *N*-acetyl amides: electronic tuning of twisted, acyclic amides in catalytic carbon−nitrogen bond cleavage. *ACS Catal.* **2018**, *8*, 9131−9139. (u) Meng, G.; Szostak, M. Palladium/NHC (NHC = *N*-heterocyclic carbene)-catalyzed β-alkyl Suzuki cross-coupling of amides by selective N−C bond cleavage. *Org. Lett.* **2018**, *20*, 6789−6793. (v) Shi, S.; Szostak, M. Decarbonylative borylation of amides by palladium catalysis. *ACS Omega* **2019**, *4*, 4901−4907. (w) Zhou, T.; Li, G.; Nolan, S. P.; Szostak, M. [Pd(NHC)(acac)Cl]: well-defined, air-stable, and readily available precatalysts for Suzuki and Buchwald−Hartwig cross-coupling (transamidation) of amides and esters by N−C/O−C activation. *Org. Lett.* **2019**, *21*, 3304−3309. (x) Rahman, M.

M.; Buchspies, J.; Szostak, M. *N*-Acylphthalimides: efficient acyl coupling reagents in Suzuki−Miyaura cross-coupling by N−C cleavage catalyzed by Pd-PEPPSI precatalysts. *Catalysts* **2019**, *9*, 129. (y) Liu, C.; Lalancette, R.; Szostak, R.; Szostak, M. Sterically hindered ketones via palladium-catalyzed Suzuki−Miyaura cross-coupling of amides by N−C(O) activation. *Org. Lett.* **2019**, *21*, 7976−7981. (z) Li, G.; Zhou, T.; Poater, A.; Cavallo, L.; Nolan, S. P.; Szostak, M. Buchwald−Hartwig cross-coupling by air-and moisture-stable [Pd(NHC)(allyl)Cl] pre-catalysts: catalyst evaluation and mechanism. *Catal. Sci. Technol.* **2020**, *10*, 710–716.

(105) Conservatively estimated on the basis of SciFinder search results (accessed July 30, 2020).

(106) (a) Shi, S.; Szostak, M. Nickel-catalyzed diaryl ketone synthesis by N−C bond cleavage: direct Negishi cross-coupling of primary amides by site-selective *N,N*-di-Boc activation. *Org. Lett.* **2016**, *18*, 5872−5875. (b) Shi, S.; Szostak, M. Efficient synthesis of diaryl ketones by nickel-catalyzed Negishi cross-coupling of amides via carbon−nitrogen bond cleavage at room temperature accelerated by solvent effect. *Chem. Eur. J.* **2016**, *22*, 10420−10424. (c) Dey, A.; Sasmal, S.; Seth, K.; Lahiri, G. K.; Maiti, D. Nickel-catalyzed deamidative step-down reduction of amides to aromatic hydrocarbons. *ACS Catal.* **2017**, *7*, 433−437. (d) Ni, S.; Zhang, W.; Mei, H.; Han, J.; Pan, Y. Ni-catalyzed reductive cross-coupling of amides with aryl iodide electrophiles via C−N bond activation. *Org. Lett.* **2017**, *19*, 2536−2539. (e) Shi, S.; Szostak, M. Nickel-catalyzed Negishi cross-coupling of *N*-acylsuccinimides: stable, amide-based, twist-controlled acyl transfer reagents via N−C activation. *Synthesis* **2017**, *49*, 3602−3608. (f) Huang, P.-Q.; Chen, H. Ni-catalyzed cross-coupling reactions of *N*-acylpyrrole-type amides with organoboron reagents. *Chem. Commun.* **2017**, *53*,

12584−12587. (g) Deguchi, T.; Xin, H.-L.; Morimoto, H.; Ohshima, T. Direct catalytic alcoholysis of unactivated 8-aminoquinoline amides. *ACS Catal.* **2017**, *7*, 3157−3161.

(107) Cheung, C. W.; Ploeger, M. L.; Hu, X. Nickel-catalyzed reductive transamidation of secondary amides with nitroarenes. *ACS Catal.* **2017**, *7*, 7092–7096.

(108) Amani, J.; Alam, R.; Badir, S.; Molander, G. A. synergistic visible-light photoredox/nickel-catalyzed synthesis of aliphatic ketones via N–C cleavage of imides. *Org. Lett.* **2017**, *19*, 2426−2429.

(109) Srimontree, W.; Chatupheeraphat, A.; Liao, H.-H.; Rueping, M. Amide to alkyne interconversion via a nickel/copper-catalyzed deamidative cross-coupling of aryl and alkenyl amides. *Org. Lett.* **2017**, *19*, 3901–3094.

(110) (c) Hu, J.; Wang, M.; Pu, X.; Shi, Z. Nickel-catalysed retro-hydroamidocarbonylation of aliphatic amides to olefins. *Nat. Commun.* **2017**, *8*, 14993.

(111) Liu, C.; Szostak, M. Decarbonylative phosphorylation of amides by palladium and nickel catalysis: The Hirao cross-coupling of amide derivatives. *Angew. Chem., Int. Ed.* **2017**, *56*, 12718–12722.

(112) For cross-couplings of acyclic alkyl C–O electrophiles, see: (a) Robbins, W. R.; Hartwig, J. F.; Sterically controlled alkylation of arenes through iridium-catalyzed C–H borylation. *Angew. Chem. Int. Ed.* **2013**, *52*, 933–937. (b) Lucas, E. L.; Jarvo, E. R. Stereospecific and stereoconvergent cross-couplings between alkyl electrophiles. *Nat. Rev. Chem.* **2017**, *1*, 0065. (c) Zhang, S.; Taylor, B. L. H.; Ji, C.; Gao, Y.; Harris, M. R.; Hanna, L. E.; Jarvo, E. R.; Houk, K. N.; Hong, X. Mechanism and origins of ligand-controlled stereoselectivity of Ni-catalyzed Suzuki–Miyaura coupling with benzylic esters: A computational study. *J. Am.*

Chem. Soc. **2017**, *139*, 12994–13005. (d) Shugrue, C. R.; Sculimbrene, B. R.; Jarvo, E. R.; Mercado, B. Q.; Miller, S. J. Outer-sphere control for divergent multicatalysis with common catalytic moieties. *J. Org. Chem.* **2019**, *84*, 1664–1672. (e) Sanford, A. B.; Tollefson, E. J.; Jarvo, E. R. Stereospecific cross-coupling reactions provide conformationally-biased arylalkanes with anti-leukemia activity. *Isr. J. Chem.* **2020**, *60*, 402–405. (f) Sanford, A. B.; Thane, T. A.; McGinnis, T. M.; Chen, P.-P.; Hong, X.; Jarvo, E. R. Nickel-catalyzed alkyl–alkyl cross-electrophile coupling reaction of 1,3-dimesylates for the synthesis of alkylcyclopropanes. *J. Am. Chem. Soc.* **2020**, *142*, 5017–5023. (g) Zhou, Q.; Srinivas, H. D.; Dasgupta, S.; Watson, M. P. Nickel-catalyzed cross-couplings of benzylic pivalates with arylboroxines: Stereospecific formation of diarylalkanes and triarylmethanes. *J. Am. Chem. Soc.* **2013**, *135*, 3307–3310.

(113) For cross-couplings of alkyl C–N electrophiles, see: (h) Calet, S.; Urso, F.; Alper, H. Enantiospecific and stereospecific rhodium(I)-catalyzed carbonylation and ring expansion of aziridines. Asymmetric synthesis of β-lactams and the kinetic resolution of aziridines. *J. Am. Chem. Soc.* **1989**, *111*, 931−934. (i) Ney, J. E.; Wolfe, J. P. Synthesis and reactivity of azapalladacyclobutanes. *J. Am. Chem. Soc.* **2006***, 128*, 15415−15422. (j) Lin, B. L.; Clough, C. R.; Hillhouse, G. L. Interactions of aziridines with nickel complexes: Oxidative-addition and reductive-elimination reactions that break and make C−N bonds. *J. Am. Chem. Soc.* **2002**, *124*, 2890−2891. (k) Huang, C.-Y.; Doyle, A. G. Nickel-catalyzed Negishi alkylations of styrenyl aziridines. *J. Am. Chem. Soc.* **2012**, *134*, 9541−9544. (l) Nielsen, D. K.; Huang, C.-Y.; Doyle, A. G. Directed nickel-catalyzed Negishi cross-Coupling of alkyl aziridines. *J. Am. Chem. Soc.* **2013**, *135*, 13605−13609. (m) Huang, C.-Y.; Doyle, A. G. Electron-deficient

olefin ligands enable generation of quaternary carbons by Ni-catalyzed cross-coupling. *J. Am. Chem. Soc.* **2015**, *137*, 5638−5641.

(114) (a) Liu, C.; Li, G.; Shi, S.; Meng, G.; Lalancette, R.; Szostak, R.; Szostak, M. Acyl and decarbonylative Suzuki coupling of N-acetyl amides: electronic tuning of twisted, acyclic amides in catalytic carbon–nitrogen bond cleavage. *ACS Catal.* **2018**, *8*, 9131–9139. (b) Iranpoor, N.; Panahi, F.; Jamedi, F. Nickel-catalyzed one-pot synthesis of biaryls from phenols and arylboronic acids via C–O activation using TCT reagent. *J. Organomet. Chem.* **2015**, *781*, 6–10. (c) Chen, L.; Lang, H.; Fang, L.; Zhu, M.; Liu, J.; Yu, J.; Wang, L. Nickel-catalyzed one-pot Suzuki–Miyaura cross-coupling of phenols and arylboronic acids mediated by *N,N*-ditosylaniline. *Eur. J. Org. Chem.* **2014**, 4953–4957. (d) Chen, G.; Huang, J.; Gao, L.; Han, F. Nickel-catalyzed cross-coupling of phenols and arylboronic acids through an in situ phenol activation mediated by PyBroP. *Chem. Eur. J.* **2011**, *17*, 4038–4042. (e) Oger, N.; d'Halluin, M.; Grognec, E.L.; Felpin, F. Using aryl diazonium salts in palladium-catalyzed reactions under safer conditions. *Org. Process. Res. Dev.* **2014**, *18*, 1786–1801.

(115) Hardy, M. A.; Wright, B. A.; Bachman, J. L.; Boit, T. B.; Haley, H. M. S.; Knapp, R. R.; Lusi, R. F.; Okada, T.; Tona, V.; Garg, N. K.; Sarpong, R. Treating a global health crisis with a dose of synthetic chemistry. *ACS Cent. Sci.* **2020**, *6*, 1017–1030.

(116) For reviews on cross-couplings catalyzed by base-metals, see: (a) Thapa, S.; Shrestha, B.; Gurung, S. K.; Giri, R. Copper-catalysed cross-coupling: an untapped potential. *Org. Biomol. Chem.* **2015**, *13*, 4816–4827. (b) Cahiez, G.; Moyeux, A. Cobalt-catalyzed cross-coupling reactions. *Chem. Rev.* **2010**, *110*, 1435–1462. (c) Mako, T. L.; Byers, J. A. Recent advances

in iron-catalysed cross-coupling reactions and their mechanistic underpinning. *Inorg. Chem. Front.* **2016**, *3*, 766–790.

(117) Expensive NHC ligands are often required for nickel-catalyzed activations of strong bonds.

(118) Hazari, N.; Melvin, P. R.; Beromi, M. M. Well-defined nickel and palladium precatalysts for cross-coupling. *Nat. Rev. Chem.* **2017**, *1*, 25.

Nickel-Catalyzed Suzuki–Miyaura Coupling of Aliphatic Amides

Timothy B. Boit,[†] Nicholas A. Weires,[†] Junyong Kim,[†] and Neil K. Garg.

2.1 Abstract

We report the Ni-catalyzed Suzuki–Miyaura coupling of aliphatic amide derivatives. Prior studies have shown that aliphatic amide derivatives can undergo Ni-catalyzed carbon–heteroatom bond formation, but Ni-mediated C–C bond formation using aliphatic amide derivatives has remained difficult. The coupling disclosed herein is tolerant of considerable variation with respect to both the amide-based substrate and the boronate coupling partner, and proceeds in the presence of heterocycles and epimerizable stereocenters. Moreover, a gram-scale Suzuki–Miyaura coupling/Fischer indolization sequence demonstrates the ease with which unique poly-heterocyclic scaffolds can be constructed, particularly by taking advantage of the enolizable ketone functionality present in the cross-coupled product. The methodology provides an efficient means to form C–C bonds from aliphatic amide derivatives using non-precious metal catalysis and offers a general platform for the hetero-arylation of aliphatic acyl electrophiles.

2.2 Introduction

The facile unification of molecular fragments via C–C bond formation represents an important and challenging objective in transition metal catalysis.[1] Although the field has been largely dominated by the coupling of aryl electrophiles, there has been a recent resurgence in developing analogous methods using stable acyl electrophiles. More specifically, esters and

amides have emerged as useful synthetic building blocks in a variety of acyl cross-coupling manifolds. Recent breakthroughs in the area include the Suzuki–Miyaura coupling of phenyl esters reported independently by Newman and Szostak, which proceeds using palladium catalysis,[2,3] in addition to numerous amide C–N bond activation studies using either palladium or nickel.[4,5,6,7,8,9]

We and others have been especially interested in using nickel catalysis to enable facile C–C bond formation from amide derivatives. Such methods provide new strategies for the synthesis of ketones which complement Weinreb's methodology,[10] but importantly avoid the use of highly basic or pyrophoric reagents. Previously, we have shown that nickel catalysis can promote the cross-coupling of Ts- or Boc- activated benzamide derivatives in C–C bond forming reactions.[4b,4d,4k] These cross-coupling platforms have allowed for the efficient coupling of *aryl* amide electrophiles, however, the corresponding activation of *aliphatic* amides is more challenging. Prior computational studies suggest that the use of aliphatic amides is inherently more difficult because of the high kinetic barrier of activation associated with oxidative addition into the resonance-stabilized C–N bond.[4a] Indeed, achievements in cross-couplings of aliphatic amides using Ni catalysis is limited to carbon-heteroatom bond formation.[4h,o] Molander and coworkers have also reported an elegant coupling of *N*-acyl succinimides with alkyl trifluoroborate salts employing a dual-metal photoredox approach using nickel and an iridium photocatalyst,[9] which nicely complements the method described herein.[11,12]

With the aim of developing a general cross-coupling manifold to build C–C bonds from aliphatic amides, we targeted the Suzuki–Miyaura coupling shown in Figure 2.1. From the outset, we opted to focus our efforts on the coupling of heterocyclic fragments due to their prevalence in bioactive molecules. Certain heterocycles can be challenging to employ in metal-mediated cross couplings as they are known to ligate metal catalysts and inhibit reactivity.[1b] Moreover, only a

handful of isolated examples of hetero-arylative Suzuki–Miyaura couplings of aliphatic acyl electrophiles exist[13] (i.e., anhydrides,[13a,b] thioesters,[13c,d] acid chlorides[13e,f]), and a general platform for the hetero-arylation of aliphatic acyl electrophiles has not been developed. In this paper, we describe the nickel-catalyzed Suzuki–Miyaura coupling of aliphatic amide derivatives. Importantly, this methodology provides rapid access to functionalizable heterocyclic scaffolds while expanding the scope of synthetically useful transformations involving amide derivatives and non-precious metal catalysis.
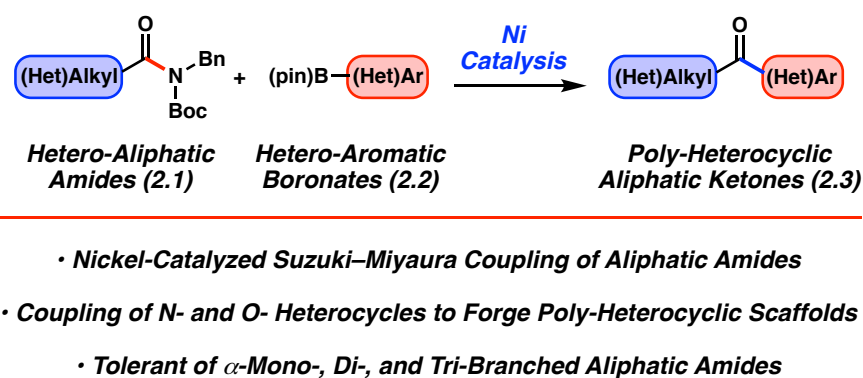
Figure 2.1. Suzuki–Miyaura hetero-arylation of aliphatic amides to construct poly-heterocyclic scaffolds.

2.3 Evaluation of Ligand Effects in the Suzuki–Miyaura Coupling

To initiate our study, we examined the coupling of piperidine derivative **2.4**[14] with *N*-methylpyrrole-2-boronic acid pinacol ester (**2.5**), as shown in Figure 2.2. Our initial attempts to employ the *N*-heterocyclic carbene (NHC) ligand SIPr (**2.7**), which we had previously shown to be competent in the Suzuki–Miyaura coupling of aromatic amide derivatives,[4b] were met with difficulty, as no trace of the desired ketone product **2.6** was formed at 50 °C (entry 1). Moreover, increasing the temperature to 120 °C only led to partial decomposition of substrate **2.4** (entry 2). Next, we screened several ligand frameworks that have been used in the context of nickel-catalyzed couplings. Interestingly, efforts to utilize the ligand terpyridine (**2.8**), which had been

shown to facilitate the nickel-catalyzed esterification of aliphatic amide derivatives,[4h] were also

unfruitful (entry 3). Gratifyingly, however, use of the NHC precursor ICy•HBF$_4$ (**2.9**) was found

to promote the desired Suzuki–Miyaura coupling, and delivered ketone **2.6** in 95% yield (entry 4).

Ligand **2.9** has been used in other nickel-catalyzed processes,[5b,5f,15] including in the Heck reaction

of benzamide derivatives.[4k] Finally, the related NHC precursor Benz-ICy•HCl (**2.10**) was

evaluated and found to give similarly useful results (entry 5). As NHC precursor **2.10** was found

to be broadly effective in subsequent scouting experiments, it was used in our further studies.[16]

Finally, although we focus on the use of *N*-Bn,Boc amides in this study, it should be noted that the

methodology is not limited to the use of the *N*-benzyl group. For example, coupling of *N*-*i*Pr,Boc

cyclohexamide with boronate **2.5** under the optimized conditions gave the corresponding ketone

in 72% yield.

Figure 2.2. Evaluation of reaction conditions for the nickel-catalyzed coupling of aliphatic amide **2.4** with boronate **2.5** to furnish ketone **2.6**. [a]Conditions: Ni(cod)$_2$ (5 mol%), **2.7**–**2.10** (10 mol%), substrate **2.4** (1.0 equiv), boronate **2.5** (2.5 equiv), K$_3$PO$_4$ (4.0 equiv), toluene (1.0 M), and H$_2$O (2.0 equiv) heated at the indicated temperature for 16 h. Yields were determined by ^{1}H NMR analysis using hexamethylbenzene as an internal standard.

2.4 Scope of the Coupling with Hetero-Aliphatic Amides and Hetero-Aryl Boronates

With the optimized conditions in hand, we explored the scope of the coupling with respect to both the hetero-aliphatic amide-derived substrate and the hetero-aryl boronate to afford a variety of bis-heterocyclic ketone products (Figure 2.3). The reaction was found to be widely tolerant of *N*-heterocyclic boronate nucleophiles, including pyrrole, quinoline, indole, pyrazole, and morpholino-pyridine moieties, as demonstrated by the formation of **2.6** and **2.11**–**2.16**, all in good yields. Moreover, an isomeric piperidine amide substrate could be utilized, allowing for the

formation of pyrrolo- and pyrazolo-ketones **2.17** and **2.18**, respectively. Alternatively, the pyrrolidine heterocycle could also be employed to generate ketones **2.19** and **2.20** in 82% and 90% yields, respectively. Finally, substrates derived from both 4- and 3-isomers of tetrahydropyran carboxylic acid were shown to be competent in the coupling, furnishing ketones **2.21**–**2.25** in good to excellent yields. The formation of **2.25** highlights the use of an oxygen-containing heterocyclic boronate in the coupling reaction. It is also worth noting that non-heterocyclic aryl boronates, such as 2-naphthyl and phenyl boronic esters, could be employed in the Suzuki–Miyaura coupling as demonstrated by the formation of **2.26** and **2.27**, respectively. In addition, o-Me, p-CF$_3$, and p-CO$_2$Me substituents were tolerated on the phenyl boronate, giving rise to ketones **2.28**–**2.30**, respectively.[17]
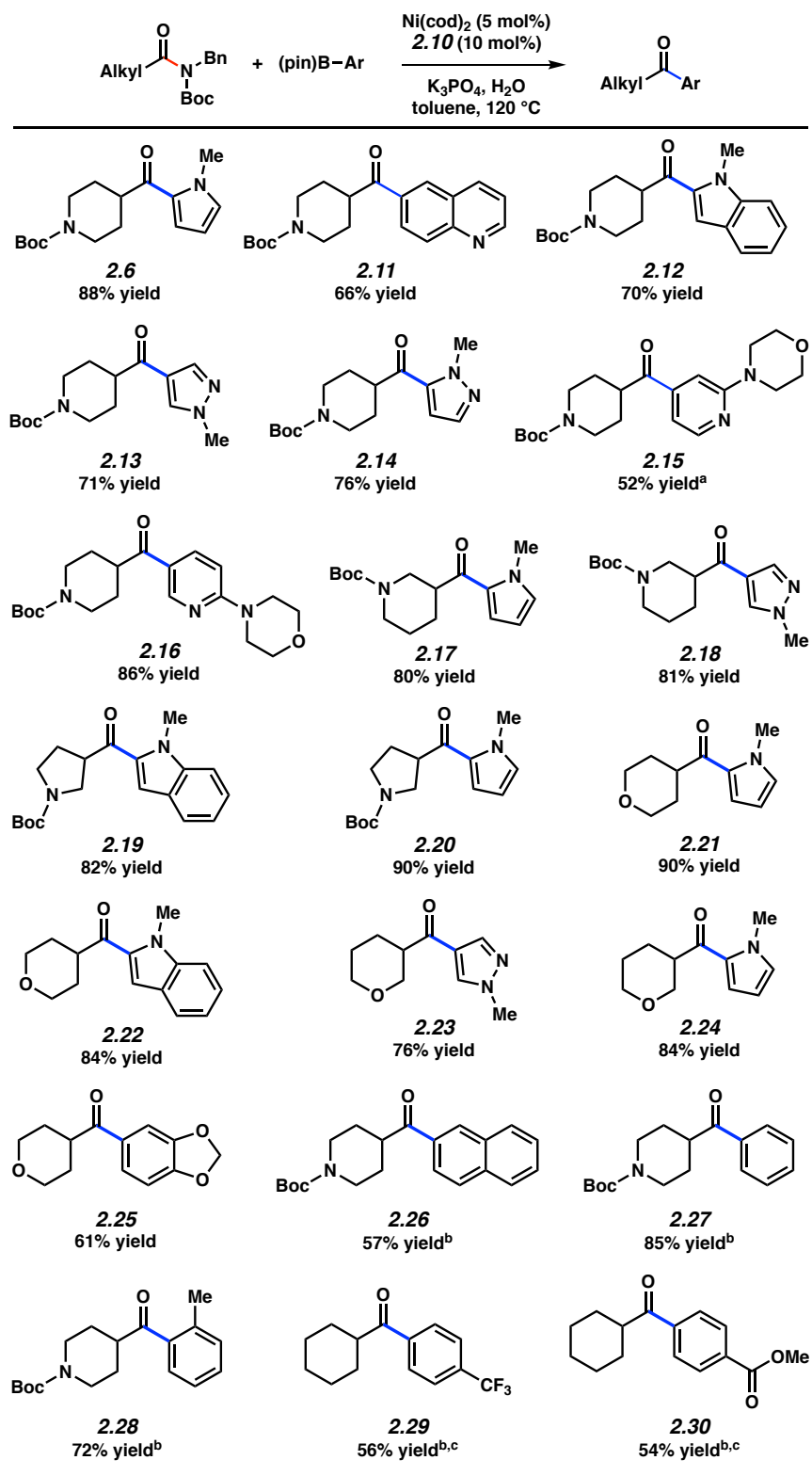
Figure 2.3. Scope of the Suzuki–Miyaura coupling with hetero-aliphatic amide substrates and aryl boronates. Conditions: Ni(cod)$_2$ (5 mol %), **2.10** (10 mol %), substrate (1.0 equiv), boronate (2.5 equiv), K$_3$PO$_4$ (4.0 equiv), toluene (1.0 M), and H$_2$O (2.0 equiv) heated at 120 °C for 16 h. Unless

otherwise noted, yields reflect the average of two isolation experiments. [a]Reaction run using 3.3 equiv of the boronate. [b]Yield determined by ^{1}H NMR analysis using hexamethylbenzene as an external standard. [c]Reaction run for 24 h using 5.0 equiv of the boronate.

2.5 Scope of the Coupling with Non-Heterocyclic Aliphatic Amide Substrates

The scope of the hetero-arylative coupling with boronate **2.5** was also evaluated with respect to several non-heterocyclic aliphatic amide derivatives (Figure 2.4). Substrates derived from dihydrocinnamic and decanoic acids coupled in high yields to furnish ketones **2.31** and **2.32**, respectively. Additionally, α-branched carbocyclic amides also underwent efficient couplings, providing pyrrolo-ketones **2.33** and **2.34**. Finally, sterically encumbered carboxamides could also be employed in the coupling, as demonstrated by the production of *tert*-butyl ketone **2.35** in excellent yield.
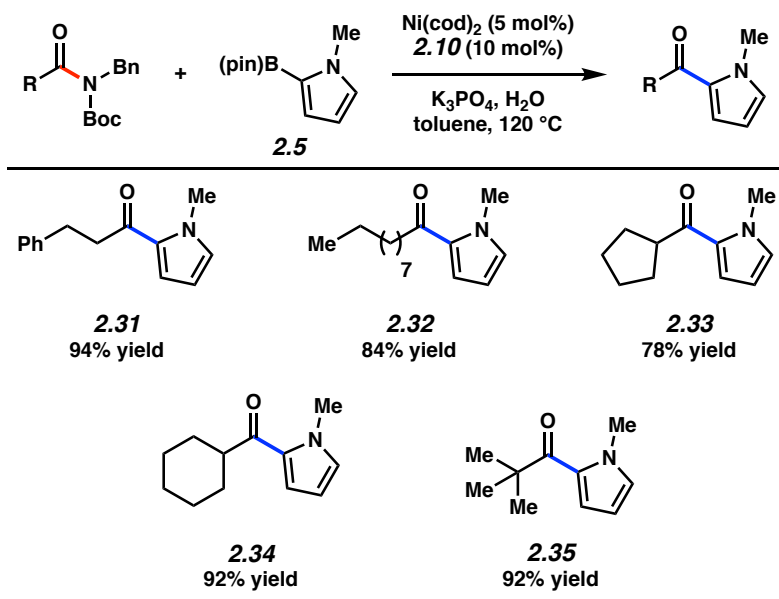
Figure 2.4. Scope of the coupling with non-heterocyclic aliphatic amide substrates and boronate **2.5**. Yields reflect the average of two isolation experiments. Conditions: Ni(cod)$_2$ (5 mol %), **2.10** (10 mol %), substrate (1.0 equiv), boronate **2.5** (2.5 equiv), K$_3$PO$_4$ (4.0 equiv), toluene (1.0 M), and H$_2$O (2.0 equiv) heated at 120 °C for 16 h. Yields reflect the average of two isolation experiments.

2.6 Evaluation of Ligand Effects in the Coupling of Benzamide Derivatives

Although our manuscript focuses on *aliphatic* amides for the reasons mentioned earlier, we were curious if our optimal reaction conditions could be applied to a benzamide substrate (Figure 2.5). We have reported earlier the coupling of *N*-Bn,Boc benzamide **2.36** with phenylboronic acid pinacol ester **2.37** using a Ni/SIPr system at 50 ºC. This gives ketone **2.38** in 96% yield (entry 1).[4b] We performed the corresponding coupling of **2.36** and **2.37** using the Ni/Benz-ICy catalyst system. At 50 °C, we obtained only a 14% yield of the cross-coupled product, **2.38** (entry 2). We also performed the cross-coupling using the Ni/Benz-ICy catalyst system at 120 ºC, which furnished **2.38** in 60% yield (entry 3).[18] As such, for practioners of this methodology, we recommend the use of Ni/SIPr at 50 °C to achieve the Suzuki–Miyaura coupling of benzamide-type substrates[4b] and the use of the conditions reported herein (i.e., Ni/Benz-ICy at 120 °C) for aliphatic amides.

Entry	Temp.	Mol % Ni	Ligand (mol%)	Yield of 2.38
1[a]	50 °C	5 mol%	*SIPr* (2.7, 5 mol%)	96%
2[b,c]	50 °C	5 mol%	*Ben-ICy·HCl* (2.10, 10 mol%)	14%
3[b,c]	120 °C	5 mol%	*Ben-ICy·HCl* (2.10, 10 mol%)	60%
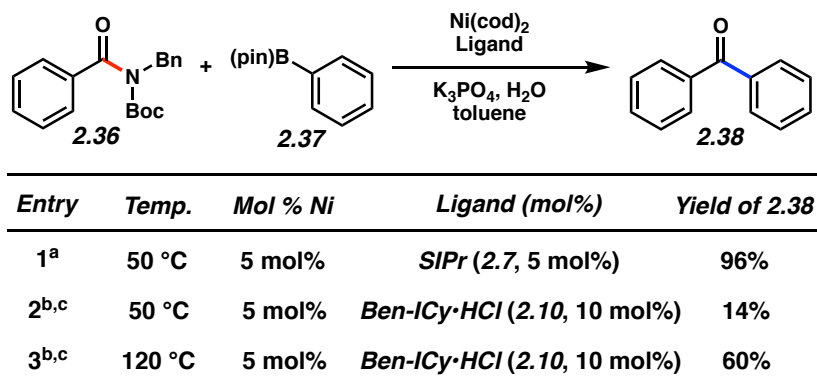
Figure 2.5. Suzuki–Miyaura coupling of amide **2.36** with boronate **2.37** using Ni/SIPr and Ni/Benz-ICy catalyst systems. [a]Conditions: Ni(cod)$_2$ (5 mol %), **2.7** (5 mol %), substrate (1.0 equiv), boronate **2.37** (1.2 equiv), K$_3$PO$_4$ (2.0 equiv), toluene (1.0 M), and H$_2$O (2.0 equiv) heated at 50 °C for 24 h. [b]Reaction run using Ni(cod)$_2$ (5 mol %), **2.10** (10 mol %), substrate (1.0 equiv), boronate **2.37** (2.5 equiv), K$_3$PO$_4$ (4.0 equiv), toluene (1.0 M), and H$_2$O (2.0 equiv) heated at the indicated temperature for 16 h. [c]Yields reflect the average of two experiments. Yields were determined by ^{1}H NMR analysis using hexamethylbenzene as an external standard.

2.7 Discovery and Optimization of a Stereoretentive Suzuki–Miyaura coupling

We also questioned if the methodology would be amenable to the coupling of an amide substrate containing a defined chiral center α to the carbonyl. As such, we attempted the coupling between amide **2.39** and boronate **2.5** (Figure 2.6). Although the use of standard conditions (i.e., 120 ºC for 16 h) gave the desired ketone product **2.40** in 68% yield, roughly 20% epimerization was also observed. We found that by carrying out the reaction at 90 ºC for 2 h, the epimerization could be avoided. Thus, ketone **2.40** was obtained in 70% yield, without observable formation of the *syn* diastereomer. Moreover, the tolerance of the ester (and other functional groups)[19] underscores the complementarity of this methodology to the Weinreb ketone synthesis,[10] where such electrophilic functional groups typically do not withstand the use of highly basic and nucleophilic organometallic reagents. Importantly, this result provides the first example of an amide or ester Suzuki–Miyaura coupling that proceeds smoothly in the presence of an epimerizable stereocenter α to the amide carbonyl. The tolerance of the method to defined stereocenters α to the carbonyl was also evaluated using enantioenriched cyclohexenyl amide **2.41**. Using standard conditions (i.e., 120 ºC for 16 h), the desired ketone **2.42** was obtained in 81% yield, but only in 14% *ee*. By lowering the temperature of the reaction to 70 ºC, the desired coupling of **2.41** with boronate **2.5** proceeded in good yield and with significant preservation of stereochemical information. We hypothesize that the observed epimerization stems from the basicity of the deprotonated Benz-ICy•HCl (**2.10**). In fact, subjection of enantioenriched **2.42** to the free NHC in toluene at 120 ºC for 4 h led to complete racemization of the substrate. In contrast, the corresponding experiments performed with Benz-ICy•HCl (**2.10**) or K_3PO_4 led to no or minimal observable loss in *ee*, respectively. It should also be noted that ketone product **2.42** was observed to racemize more readily than amide **2.41** under the standard reaction conditions (see section

2.10.2.5 for details). Nonetheless, these results demonstrate the mildness of the reaction conditions and bode well for future synthetic applications.
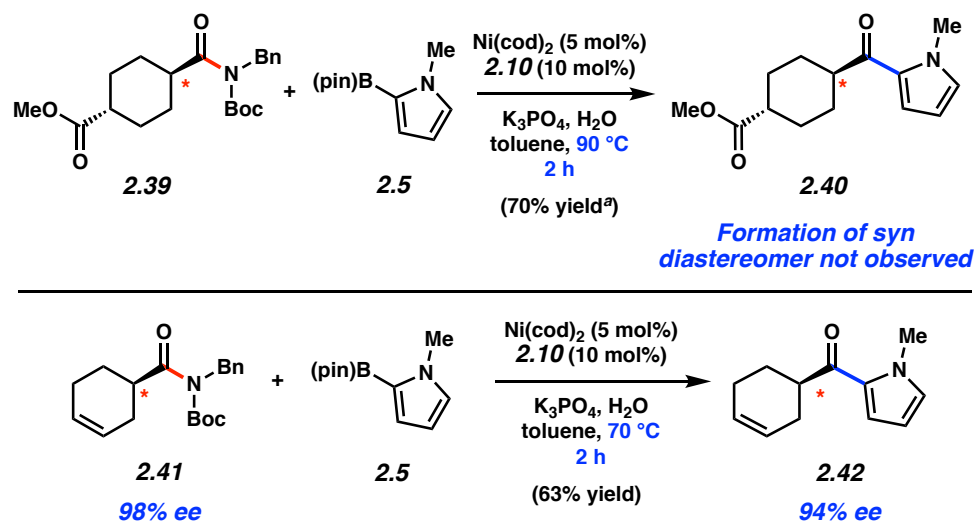
Figure 2.6. Stereoretentive Suzuki–Miyaura couplings of amide **2.39** and enantioenriched amide **2.41**. Yield reflects the average of two isolation experiments. Conditions: Ni(cod)$_2$ (5 mol %), **2.10** (10 mol %), substrate (1.0 equiv), boronate **2.5** (2.5 equiv), K$_3$PO$_4$ (4.0 equiv), toluene (1.0 M), and H$_2$O (2.0 equiv) heated at 70 °C for 2 h. Yield reflects the average of two isolation experiments. [a]Reaction run at 90 °C for 2 h. Yield determined by ^{1}H NMR analysis using hexamethylbenzene as an external standard.

2.8 Gram-Scale Suzuki–Miyaura Coupling and Subsequent Fischer Indolization

In comparison to more classical aryl-aryl couplings, the products obtained from this methodology possess enolizable ketones, which serve as valuable synthetic handles. As a demonstration of this benefit, we performed a gram-scale Suzuki–Miyaura coupling and subsequent Fischer indolization reaction to construct a polyheterocyclic spiroindolenine scaffold (Figure 2.7). Spiroindolenines are commonly seen in bioactive molecules[20] and also serve as valuable synthetic intermediates.[21] In this case, Suzuki–Miyaura coupling of tetrahydropyran carboxamide **2.43** with boronate **2.44** took place on gram scale under conditions employing reduced boronate, catalyst, and ligand loadings (1.2 equiv, 2.5 and 5 mol%, respectively) to furnish ketone **2.45** in 82% yield. Next, ketone **2.45** was transformed into spirocycle **2.47** in 61% yield by

reaction with phenylhydrazine (**2.46**) in the presence of TFA by way of a Fischer indolization.[22]

The rapid construction of poly-heterocyclic spiroindolenine **2.47**,[23] hinging upon the classical reactivity of enolizable ketones, underscores the utility of the Suzuki–Miyaura coupling of aliphatic amides and further demonstrates the ease with which a variety of unique heterocyclic compounds can be fashioned.
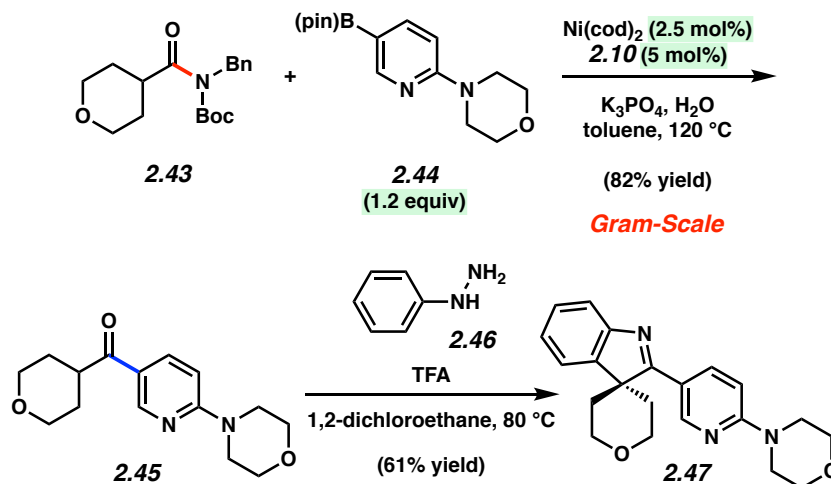
Figure 2.7. Sequential gram-scale Suzuki–Miyaura coupling and Fischer indolization to provide **2.47**.

2.9 Conclusions

We have developed the nickel-catalyzed Suzuki–Miyaura coupling of aliphatic amides. The coupling was found to be tolerant of variation in both coupling partners, and can be employed in the presence of heterocycles, epimerizable stereocenters, and sensitive functional groups (e.g., esters). The synthetic utility of this methodology was further demonstrated on gram-scale via a Suzuki–Miyaura coupling/Fischer indolization sequence to form poly-heterocyclic spiroindolenine **2.47**. These studies offer a general platform for the hetero-arylation of aliphatic acyl electrophiles, while contributing to the repertoire of synthetic transformations involving amide derivatives and non-precious metal catalysis. Moreover, given their stability towards a

variety of conditions, we view amides as having significant potential utility as synthons in the derivatization of biomolecules and multistep synthetic efforts.

2.10 Experimental Section

2.10.1 Materials and Methods

Unless stated otherwise, reactions were conducted in flame-dried glassware under an atmosphere of nitrogen or argon and commercially obtained reagents were used as received. Non-commercially available substrates were synthesized following protocols specified in Section 2.10.2 in the Experimental Procedures. Prior to use, toluene was purified by distillation and taken through five freeze-pump-thaw cycles, and phenylhydrazine (**2.46**) was passed over a plug of basic alumina. Benzylamine was obtained from Sigma–Aldrich. Boronate esters **2.5**, **2.57**, **2.58**, **2.59**, **2.60**, **2.61**, **2.63**, **2.37**, **2.64**, **2.66**, **2.67**, and **2.44** and carboxylic acids **2.48**, **2.49**, **2.51**, **2.53**, **2.54**, **2.56** were obtained from Combi-Blocks. Boronate ester **2.62**[24] was prepared according to literature procedures. Ni(cod)$_2$, SIPr (**2.7**), terpyridine (**2.8**), ICy•HBF$_4$ (**2.9**), and Benz-ICy•HCl (**2.10**) were obtained from Strem Chemicals. K$_3$PO$_4$ was obtained from Acros. Reaction temperatures were controlled using an IKAmag temperature modulator, and unless stated otherwise, reactions were performed at room temperature (approximately 23 °C). Thin-layer chromatography (TLC) was conducted with EMD gel 60 F254 pre-coated plates (0.25 mm for analytical chromatography and 0.50 mm for preparative chromatography) and visualized using a combination of UV, anisaldehyde, iodine, and potassium permanganate staining techniques. Silicycle Siliaflash P60 (particle size 0.040–0.063 mm) was used for flash column chromatography. ^{1}H NMR spectra were recorded on Bruker spectrometers (at 300, 400 and 500 MHz) and are reported relative to residual solvent signals. Data for ^{1}H NMR spectra are reported as follows: chemical shift (δ ppm), multiplicity, coupling constant (Hz), integration. Data for ^{13}C NMR are reported in terms of chemical shift (at 75 and 125 MHz). IR spectra were recorded on a Perkin-Elmer UATR Two FT-IR spectrometer and are reported in terms of frequency absorption (cm^{-1}). DART-MS spectra were

collected on a Thermo Exactive Plus MSD (Thermo Scientific) equipped with an ID-CUBE ion source and a Vapur Interface (IonSense Inc.). Both the source and MSD were controlled by Excalibur software v. 3.0. The analyte was spotted onto OpenSpot sampling cards (IonSense Inc.) using $CHCl_3$ as the solvent. Ionization was accomplished using UHP He plasma with no additional ionization agents. The mass calibration was carried out using Pierce LTQ Velos ESI (+) and (–) Ion calibration solutions (Thermo Fisher Scientific). Determination of enantiopurity was carried out using either a Mettler Toledo SFC (supercritical fluid chromatography) or Agilent HPLC using a Daicel ChiralPak OJ-H column. Optical rotations were measured with a Rudolph Autopol III Automatic Polarimeter.

2.10.2 Experimental Procedures

2.10.2.1 Syntheses of Amide Substrates

Representative Procedure for the synthesis of amide substrates from Tables 2.1 and 2.2 and Figures 2.2, 2.3, 2.6, and 2.7 (synthesis of amide 2.4 is used as an example).
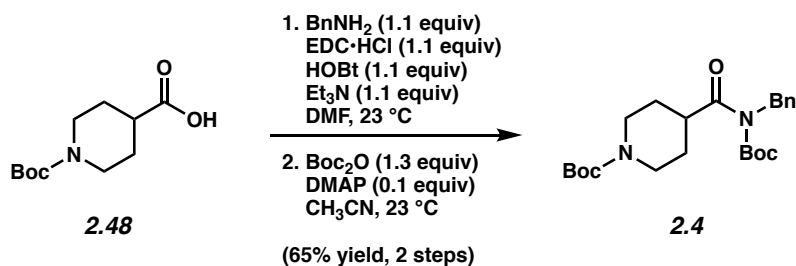
To a mixture of carboxylic acid **2.48** (3.00 g, 13.1 mmol, 1.0 equiv), EDC•HCl (2.76 g, 14.4 mmol, 1.1 equiv), HOBt (1.94 g, 14.4 mmol, 1.1 equiv), triethylamine (1.99 mL, 14.4 mmol, 1.1 equiv) and DMF (131 mL, 0.1 M) was added benzylamine (1.57 mL, 14.4 mmol, 1.1 equiv). The resulting mixture was stirred at 23 °C for 16 h, and then diluted with deionized water (250 mL) and transferred to a separatory funnel with EtOAc (150 mL) and brine (50 mL). The aqueous

layer was extracted with EtOAc (3 x 150 mL), then the organic layers were combined and washed with deionized water (3 x 125 mL), dried over Na_2SO_4, and evaporated under reduced pressure. The resulting crude solid material was used in the subsequent step without further purification.

To a flask containing the crude material from the previous step was added DMAP (148 mg, 1.21 mmol, 0.1 equiv) followed by acetonitrile (60.0 mL, 0.2 M). Boc_2O (3.43 g, 15.7 mmol, 1.3 equiv) was added in one portion and the reaction vessel was flushed with N_2, then the reaction mixture was allowed to stir at 23 °C for 16 h. The reaction was quenched by addition of saturated aqueous $NaHCO_3$ (200 mL), transferred to a separatory funnel with EtOAc (200 mL) and H_2O (200 mL), and extracted with EtOAc (3 x 100 mL). The organic layers were combined, dried over Na_2SO_4, and evaporated under reduced pressure. The resulting crude residue was purified by flash chromatography (9:1 Hexanes:EtOAc) to yield amide **2.4** (3.59 g, 65% yield, over two steps) as white solid. Amide **2.4**: mp: 83–85 °C; R_f 0.39 (5:1 Hexanes:EtOAc); ^{1}H NMR (500 MHz, $CDCl_3$): δ 7.31–7.26 (m, 2H), 7.24–7.18 (m, 3H), 4.86 (s, 2H), 4.12 (br s, 2H), 3.59 (tt, J = 11.2, 3.6, 1H), 2.88–2.70 (m, 2H), 1.91–1.79 (m, 2H), 1.65 (qd, J = 12.2, 4.0, 2H), 1.45 (s, 9H), 1.40 (s, 9H); ^{13}C NMR (125 MHz, $CDCl_3$): δ 178.2, 154.8, 153.1, 138.4, 128.5, 127.5, 127.2, 83.5, 79.6, 47.8, 43.8, 43.0, 29.0, 28.6, 28.0; IR (film): 2976, 2932, 2861, 1731, 1689 cm^{-1}; HRMS-APCI (m/z) [M + H]$^+$ calcd for $C_{23}H_{35}N_2O_5$, 419.25405; found 419.25413.

Note: Supporting information for the syntheses of some amides shown in Figures 2.3, 2.4, 2.5 and 2.6 have previously been reported: **2.65**,[4h] **2.68**,[4h] **2.69**,[4h] **2.70**,[4h] **2.71**,[4h] **2.36**,[4b] **2.41**,[4o] **rac-2.41**,[4o] and **2.72**.[4o] Syntheses for the remaining substrates shown in Figures 2.3, 2.4, 2.6, and 2.7 are as follows:

Any modifications of the conditions shown in the representative procedure above are

specified in the following schemes.
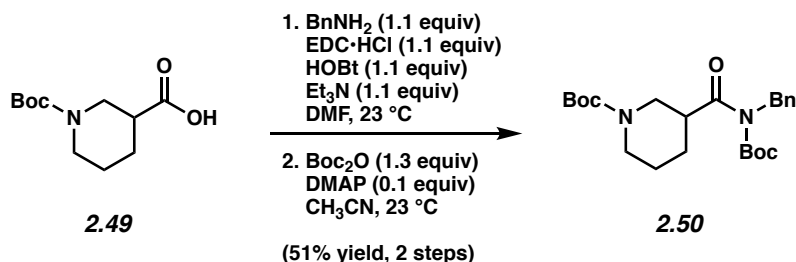
Amide 2.50. Purification by flash chromatography (9:1 Hexanes:EtOAc) generated amide **2.50**

(51% yield, over two steps) as a white solid. Amide **2.50**: mp: 73–75 ºC; R_f 0.43 (5:1

Hexanes:EtOAc); ^{1}H NMR (500 MHz, CDCl3): δ 7.31–7.26 (m, 2H), 7.24–7.19 (m, 3H), 4.92–

4.78 (m, 2H), 4.26–3.94 (m, 2H), 3.51 (tt, J = 10.6, 3.6, 1H), 2.99 (dd, J = 12.5, 11.0, 1H), 2.75

(br s, 1H), 2.10 (br s, 1H), 1.74–1.68 (m, 1H), 1.62–1.48 (m, 2H), 1.45 (s, 9H), 1.40 (s, 9H); [13]C

NMR (125 MHz, CDCl3, 15 of 17 observed): δ 177.2, 154.8, 152.9, 138.3, 128.5, 127.5, 127.3,

83.6, 79.7, 47.7, 43.5, 28.7, 28.6, 28.0, 24.7; IR (film): 2977, 2935, 2862, 1732, 1687 cm^{-1}; HRMS-

APCI (*m/z*) [M + H]$^+$ calcd for $C_{23}H_{35}N_2O_5$, 419.25405; found 419.25304.
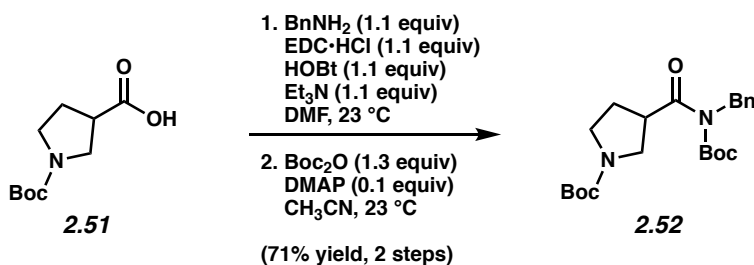
Amide 2.52. Purification by flash chromatography (9:1 Hexanes:EtOAc) generated amide **2.52**

(71% yield, over two steps) as a colorless oil. Amide **2.52**: R_f 0.47 (5:1 Hexanes:EtOAc); ^{1}H NMR

(500 MHz, CDCl3): δ 7.32–7.27 (m, 2H), 7.25–7.19 (m, 3H), 4.88 (s, 2H), 4.08 (quint, J = 7.1,

1H), 3.67 (br s, 1H), 3.56 (dd, J = 10.8, 6.3, 1H), 3.53–3.45 (m, 1H), 3.43–3.33 (m, 1H), 2.15 (br

s, 2H), 1.46 (s, 9H), 1.42 (s, 9H); ^{13}C NMR (125 MHz, CDCl$_3$, 15 of 16 observed): δ 176.2, 154.6,

153.2, 138.3, 128.5, 127.6, 127.4, 83.8, 79.4, 49.3, 48.0, 45.6, 29.4, 28.7, 28.1; IR (film): 2979,

2887, 1731, 1693, 1366, 1143 cm^{-1}; HRMS-APCI (m/z) [M + H]$^+$ calcd for C$_{22}$H$_{33}$N$_2$O$_5$,

405.23840; found 405.23794.

*Note: ^{1}H and ^{13}C NMR spectra of amide **2.52** were obtained at 57 °C.*
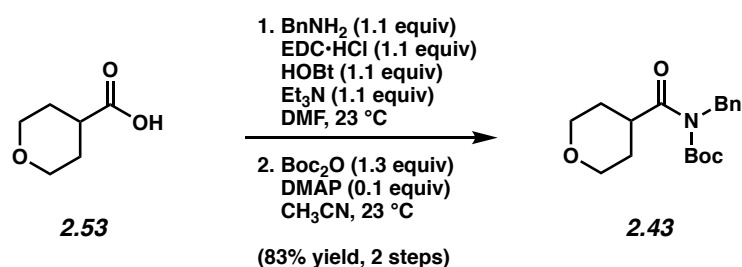
Amide 2.43. Purification by flash chromatography (14:1 Hexanes:EtOAc) generated amide **2.43**

(83% yield, over two steps) as a white solid. Amide **2.43**: mp: 52–54 ºC; R$_f$ 0.59 (5:1

Hexanes:EtOAc); ^{1}H NMR (500 MHz, CDCl$_3$): δ 7.32–7.27 (m, 2H), 7.25–7.19 (m, 3H), 4.87 (s,

2H), 4.03–3.97 (m, 2H), 3.74–3.65 (m, 1H), 3.48 (td, J = 11.5, 2.4, 2H), 1.91–1.75 (m, 4H), 1.40

(s, 9H); ^{13}C NMR (125 MHz, CDCl$_3$): δ 178.1, 153.1, 138.4, 128.5, 127.5, 127.3, 83.4, 67.5, 47.8,

42.2, 29.7, 28.0; IR (film): 2962, 2842, 1728, 1688, 1366, 1143 cm^{-1}; HRMS-APCI (m/z) [M +

H]$^+$ calcd for C$_{18}$H$_{26}$NO$_4$, 320.18563; found 320.18538.
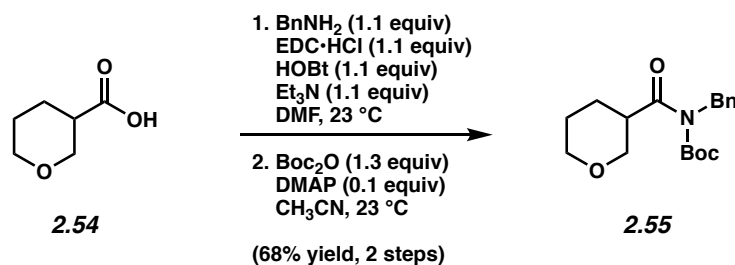
Amide 2.55. Purification by flash chromatography (14:1 Hexanes:EtOAc) generated amide **2.55** (68% yield, over two steps) as a white solid. Amide **2.55**: mp: 49–50 ºC; R$_f$ 0.38 (5:1 Hexanes:EtOAc); ^{1}H NMR (500 MHz, CDCl$_3$): δ 7.31–7.26 (m, 2H), 7.25–7.18 (m, 3H), 4.87 (d, J = 14.9, 1H), 4.81 (d, J = 14.9, 1H), 4.10–4.01 (m, 1H), 3.95–3.87 (m, 1H), 3.72–3.63 (m, 1H), 3.55 (t, J = 10.4, 1H), 3.44 (td, J = 10.8, 3.4, 1H), 2.13–2.04 (m, 1H), 1.81–1.63 (m, 3H), 1.42 (s, 9H); ^{13}C NMR (125 MHz, CDCl$_3$): δ 176.7, 153.0, 138.3, 128.5, 127.6, 127.3, 83.7, 70.1, 68.4, 47.7, 44.0, 28.0, 27.3, 25.3; IR (film): 2977, 2847, 1732, 1685, 1371, 1146 cm^{-1}; HRMS-APCI (*m/z*) [M + H]$^+$ calcd for C$_{18}$H$_{26}$NO$_4$, 320.18563; found 320.18577.
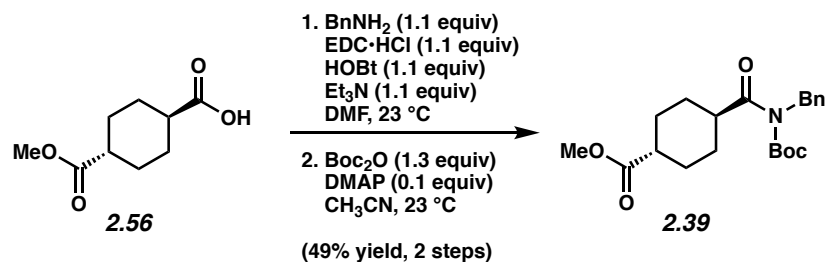
Amide 2.39. Purification by flash chromatography (9:1 Hexanes:EtOAc) generated amide **2.39** (49% yield, over two steps) as a white solid. Amide **2.39**: mp: 65–67 ºC; R$_f$ 0.49 (5:1 Hexanes:EtOAc); ^{1}H NMR (500 MHz, CDCl$_3$): δ 7.31–7.26 (m, 2H), 7.24–7.20 (m, 3H), 4.85 (s, 2H), 3.67 (s, 3H), 3.43–3.36 (m, 1H), 2.37–2.0 (m, 1H), 2.10–1.96 (m, 4H), 1.58–1.46 (m, 4H), 1.41 (s, 9H); ^{13}C NMR (125 MHz, CDCl$_3$): δ 179.1, 176.2, 153.1, 138.5, 128.5, 127.6, 127.2, 83.4,

51.7, 47.8, 44.1, 42.8, 29.0, 28.4, 28.0; IR (film): 2977, 2946, 2865, 1728, 1689 cm^{-1}; HRMS-

APCI (*m/z*) [M + H]$^+$ calcd for $C_{21}H_{30}NO_5$, 376.21185; found 376.21140.

2.10.2.2 Initial Survey of Ligands and Relevant Control Experiments
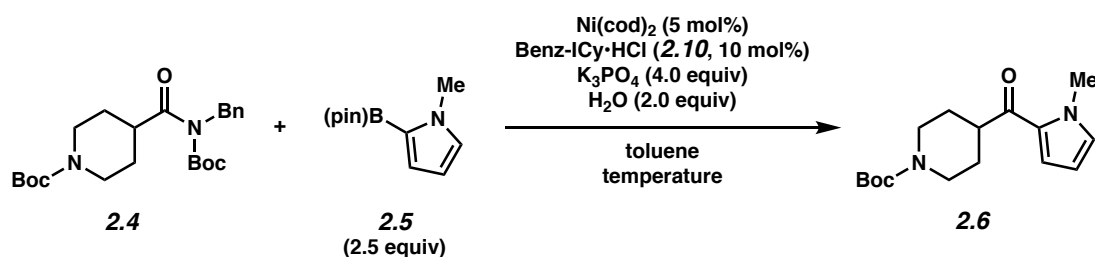
Representative Procedure for Suzuki–Miyaura Reactions from Table 2.1 (coupling of amide 2.4 and *N*-methylpyrrole-2-boronic acid pinacol ester (2.5) is used as an example). A 1-dram vial was charged with anhydrous powdered K_3PO_4 (170 mg, 0.800 mmol, 4.0 equiv) and a magnetic stir bar. The vial and contents were flame-dried under reduced pressure, then allowed to cool under N_2. Amide substrate **2.4** (83.8 mg, 0.200 mmol, 1.0 equiv), *N*-methylpyrrole-2-boronic acid pinacol ester (**2.5**) (104 mg, 0.500 mmol, 2.5 equiv), and hexamethylbenzene (9.6 mg, 0.59 mmol, 0.30 equiv) were added. The vial was flushed with N_2, then water (7.2 µL, 0.400 mmol, 2.0 equiv), which had been sparged with N_2 for 10 min, was added. The vial was taken into a glove box and charged with Ni(cod)$_2$ (2.8 mg, 0.010 mmol, 5 mol%) and Benz-ICy•HCl (**2.10**, 6.4 mg, 0.020 mmol, 10 mol%). Subsequently, toluene (0.20 mL, 1.0 M) was added. The vial was sealed with a Teflon-lined screw cap, removed from the glove box, and stirred vigorously (800 rpm) at 120 °C for 16 h. After cooling to 23 °C, the mixture was diluted with hexanes (0.5 mL) and filtered over a plug of silica gel (10 mL of EtOAc eluent). The volatiles were removed under reduced pressure, and the yield was determined by ^{1}H NMR analysis with hexamethylbenzene as an internal standard.

Any modifications of the conditions shown in the representative procedure

above are specified below in Table 2.1.

Table 2.1. Initial survey of ligands and relevant control experiments.[a]

| | **Experimental Results** | |
Reaction Conditions	**2.4**	**2.6**
2.5 (2.5 equiv), K₃PO₄ (4.0 equiv), H₂O (2.0 equiv) Ni(cod)₂ (5 mol%), SIPr (*2.7*, 10 mol%), toluene (1.0 M), 50 °C, 16 h	100%	0%
2.5 (2.5 equiv), K₃PO₄ (4.0 equiv), H₂O (2.0 equiv) Ni(cod)₂ (5 mol%), SIPr (*2.7*, 10 mol%), toluene (1.0 M), 120 °C, 16 h	52%[b]	0%
2.5 (2.5 equiv), K₃PO₄ (4.0 equiv), H₂O (2.0 equiv) Ni(cod)₂ (5 mol%), terpyridine (*2.8*, 10 mol%), toluene (1.0 M), 120 °C, 16 h	50%[b]	0%
2.5 (2.5 equiv), K₃PO₄ (4.0 equiv), H₂O (2.0 equiv) Ni(cod)₂ (5 mol%), ICy·HBF₄ (*2.9*, 10 mol%), toluene (1.0 M), 120 °C, 16 h	0%	95%
2.5 (2.5 equiv), K₃PO₄ (4.0 equiv), H₂O (2.0 equiv) Ni(cod)₂ (5 mol%), Benz-ICy·HCl (*2.10*, 10 mol%), toluene (1.0 M), 120 °C, 16 h	0%	95%
Control Experiments:		
2.5 (2.5 equiv), K₃PO₄ (4.0 equiv), H₂O (2.0 equiv) toluene (1.0 M), 120 °C, 16 h	25%[b]	0%
2.5 (2.5 equiv), K₃PO₄ (4.0 equiv), H₂O (2.0 equiv) Benz-ICy·HCl (*2.10*, 10 mol%), toluene (1.0 M), 120 °C, 16 h	25%[b]	0%
2.5 (2.5 equiv), K₃PO₄ (4.0 equiv), H₂O (2.0 equiv) Ni(cod)₂ (5 mol%), toluene (1.0 M), 120 °C, 16 h	5%[b]	0%

[a] Yields were determined by ¹H NMR analysis using hexamethylbenzene as an internal standard.
[b] Substantial amounts of the corresponding Boc-cleavage product (des-Boc amide starting material) were observed due to the elevated reaction temperature.

2.10.2.3 Scope of Methodology
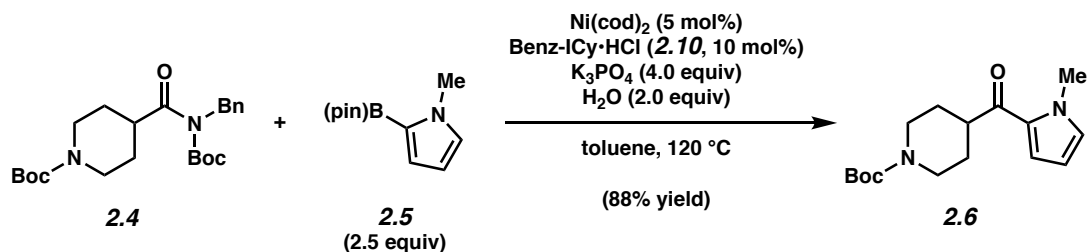
Representative Procedure (coupling of amide 2.4 and *N*-methylpyrrole-2-boronic acid pinacol ester (2.5) is used as an example). Ketone 2.6. A 1-dram vial was charged with anhydrous powdered K_3PO_4 (170 mg, 0.800 mmol, 4.0 equiv) and a magnetic stir bar. The vial and contents were flame-dried under reduced pressure, then allowed to cool under N_2. Amide substrate **2.4** (83.8 mg, 0.200 mmol, 1.0 equiv) and *N*-methylpyrrole-2-boronic acid pinacol ester (**2.5**) (104 mg, 0.500 mmol, 2.5 equiv) were added. The vial was flushed with N_2, then water (7.2 μL, 0.400 mmol, 2.0 equiv), which had been sparged with N_2 for 10 min, was added. The vial was taken into a glove box and charged with Ni(cod)$_2$ (2.8 mg, 0.010 mmol, 5 mol%) and Benz-ICy•HCl (**2.10**, 6.4 mg, 0.020 mmol, 10 mol%). Subsequently, toluene (0.20 mL, 1.0 M) was added. The vial was sealed with a Teflon-lined screw cap, removed from the glove box, and stirred vigorously (800 rpm) at 120 °C for 16 h. After cooling to 23 °C, the mixture was diluted with hexanes (0.5 mL) and filtered over a plug of silica gel (10 mL of EtOAc eluent). The volatiles were removed under reduced pressure, and the crude residue was purified by flash chromatography (19:1 Hexanes:EtOAc → 14:1 Hexanes:EtOAc → 9:1 Hexanes:EtOAc) to yield ketone product **2.6** (88% yield, average of two experiments) as a white solid. Ketone **2.6**: mp: 77–80 °C; R_f 0.18 (5:1 Hexanes:EtOAc); ¹H NMR (500 MHz, CDCl$_3$): δ 7.00–6.95 (m, 1H), 6.85–6.80 (m, 1H), 6.16–6.11 (m, 1H), 4.18 (br s, 2H), 3.93 (s, 3H), 3.20–3.10 (m, 1H), 2.93–2.70 (m, 2H), 1.85–1.66 (m, 4H), 1.46 (s, 9H); ¹³C NMR (125 MHz, CDCl$_3$): δ 193.1, 154.9, 131.6, 129.8, 118.9, 108.1, 79.7,

44.8, 43.6, 38.0, 29.1, 28.6; IR (film): 2929, 2859, 1686, 1646, 1408, 1168 cm^{-1}; HRMS-APCI

(*m/z*) [M + H]$^{+}$ calcd for C$_{16}$H$_{25}$N$_2$O$_3$, 293.18597; found 293.18535.

Any modifications of the conditions shown in the representative procedure above are specified in the following schemes, which depict all of the results shown in Figures 2.3, 2.4, 2.5, 2.6, and 2.7.
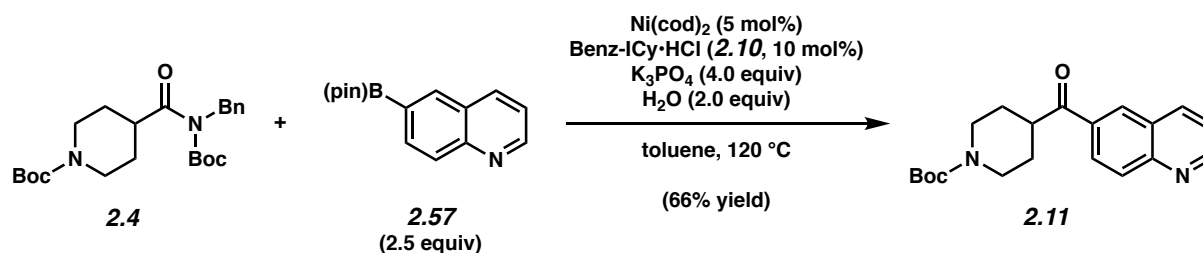
Ketone 2.11. Purification by flash chromatography (1:1 Hexanes:EtOAc → 1:2 Hexanes:EtOAc) generated ketone **2.11** (66% yield, average of two experiments) as a clear oil. Ketone **2.11**: R$_f$ 0.33 (1:1 Hexanes:EtOAc); ^{1}H NMR (500 MHz, CDCl$_3$): δ 9.02 (dd, *J* = 4.2, 1.7, 1H), 8.44 (d, *J* = 1.9, 1H), 8.29 (dd, *J* = 8.3, 1.3, 1H), 8.23 (dd, *J* = 8.8, 1.9, 1H), 8.18 (d, *J* = 8.8, 1H), 7.50 (dd, *J* = 8.3, 4.2, 1H), 4.20 (br s, 2H), 3.56 (tt, *J* = 11.1, 3.7, 1H), 3.04–2.85 (m, 2H), 1.98–1.84 (m, 2H), 1.82–1.74 (m, 2H), 1.47 (s, 9H); ^{13}C NMR (125 MHz, CDCl$_3$, 14 of 16 observed): δ 201.6, 154.8, 152.8, 150.2, 137.7, 133.8, 130.5, 129.6, 128.0, 127.7, 122.2, 79.9, 43.9, 28.6; IR (film): 2972, 2859, 1676, 1423, 1366, 1161 cm^{-1}; HRMS-APCI (*m/z*) [M + H]$^{+}$ calcd for C$_{20}$H$_{25}$N$_2$O$_3$, 341.18597; found 341.18465.
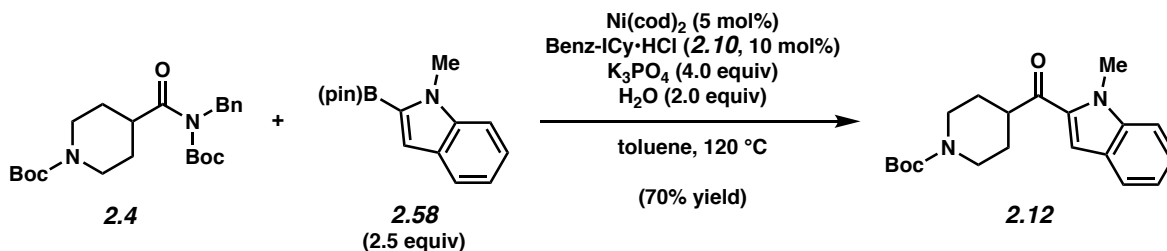
Ketone 2.12. Purification by flash chromatography (19:1 Hexanes:EtOAc → 14:1 Hexanes:EtOAc → 9:1 Hexanes:EtOAc) generated ketone **2.12** (70% yield, average of two experiments) as a white solid. Ketone **2.12**: R_f 0.25 (5:1 Hexanes:EtOAc). Spectral data match those previously reported.[4]
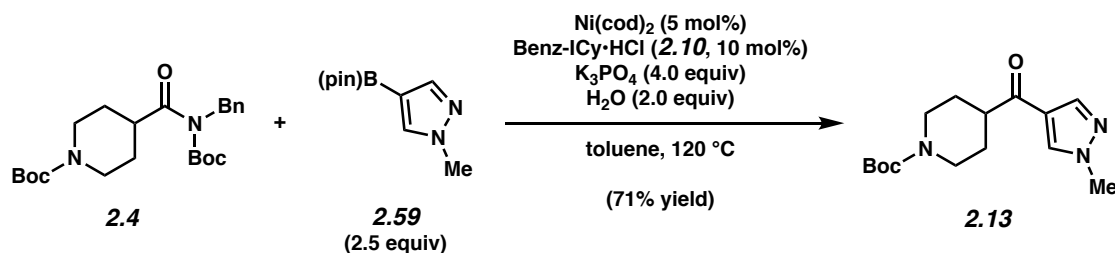
Ketone 2.13. Purification by flash chromatography (49:1 PhH:CH$_3$CN → 19:1 PhH:CH$_3$CN → 1:1 Hexanes:EtOAc → 1:3 Hexanes:EtOAc) generated ketone **2.13** (71% yield, average of two experiments) as a white solid. Ketone **2.13**: mp: 99–101 °C; R_f 0.24 (1:3 Hexanes:EtOAc); ^{1}H NMR (500 MHz, CDCl$_3$): δ 7.89 (s, 1H), 7.88 (s, 1H), 4.15 (br s, 2H), 3.94 (s, 3H), 3.27 (tt, J = 11.1, 3.9, 1H), 2.93–2.73 (m, 2H), 1.93–1.63 (m, 4H), 1.46 (s, 9H); ^{13}C NMR (125 MHz, CDCl$_3$, 10 of 11 observed): δ 196.4, 154.8, 140.4, 132.8, 123.0, 79.8, 46.3, 39.6, 28.6, 28.4; IR (film): 2977, 2937, 2859, 1671, 1540, 1168 cm^{-1}; HRMS-APCI (*m/z*) [M + H]$^+$ calcd for C$_{15}$H$_{24}$N$_3$O$_3$, 294.18122; found 294.18073.
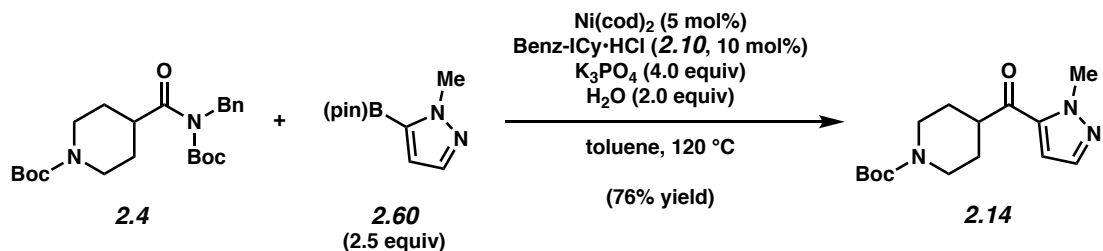
Ketone 2.14. Purification by flash chromatography (4:1 Hexanes:EtOAc → 3:1 Hexanes:EtOAc) generated ketone **2.14** (76% yield, average of two experiments) as a clear oil. Ketone **2.14**: R_f 0.42 (2:1 Hexanes:EtOAc); ^{1}H NMR (500 MHz, CDCl$_3$): δ 7.48 (d, J = 2.1, 1H), 6.84 (d, J = 2.1, 1H), 4.16 (s, 5H), 3.12 (tt, J = 11.3, 3.7, 1H), 2.93–2.75 (m, 2H), 1.89–1.76 (m, 2H), 1.75–1.66 (m, 2H), 1.46 (s, 9H); ^{13}C NMR (125 MHz, CDCl$_3$, 9 of 11 observed): δ 193.5, 154.8, 137.8, 137.6, 111.2, 79.9, 46.3, 40.6, 28.6; IR (film): 2955, 2860, 1677, 1423, 1366, 1321, 1169 cm^{-1}; HRMS-APCI (m/z) [M + H]$^+$ calcd for C$_{15}$H$_{24}$N$_3$O$_3$, 294.18122; found 294.18035.
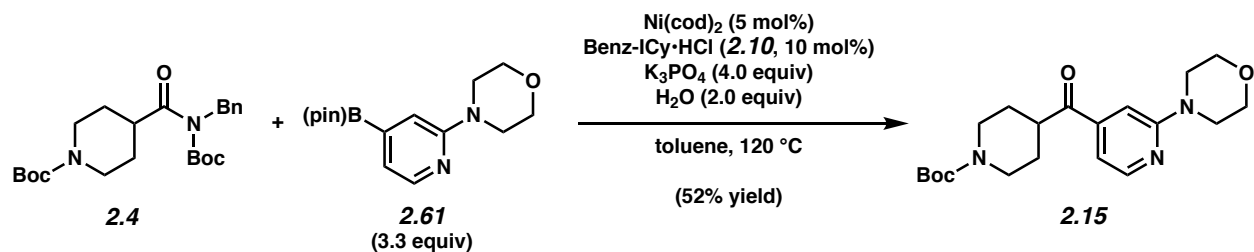
Ketone 2.15. Purification by flash chromatography (2:1 Hexanes:EtOAc) generated ketone **2.15** (52% yield, average of two experiments) as a yellow oil. Ketone **2.15**: R_f 0.31 (2:1 Hexanes:EtOAc); ^{1}H NMR (500 MHz, CDCl$_3$): δ 8.33 (dd, J = 5.1, 0.8, 1H), 7.03 (s, 1H), 7.00 (dd, J = 5.2, 1.2, 1H), 4.13 (br s, 2H), 3.85–8.80 (m, 4H), 3.59–3.54 (m, 4H), 3.27 (tt, J = 11.1, 3.6, 1H), 2.97–2.80 (m, 2H), 1.91–1.77 (m, 2H), 1.70–1.60 (m, 2H); ^{13}C NMR (125 MHz, CDCl$_3$, 13 of 14 observed): δ 202.5, 160.5, 154.8, 149.3, 144.1, 111.1, 104.7, 79.9, 66.8, 45.6, 44.2, 28.6,

28.2; IR (film): 2969, 2854, 1688, 1426, 1241, 1166 cm^{-1}; HRMS-APCI (*m/z*) [M + H]$^+$ calcd for C$_{20}$H$_{30}$N$_3$O$_4$, 376.22308; found 376.22152.
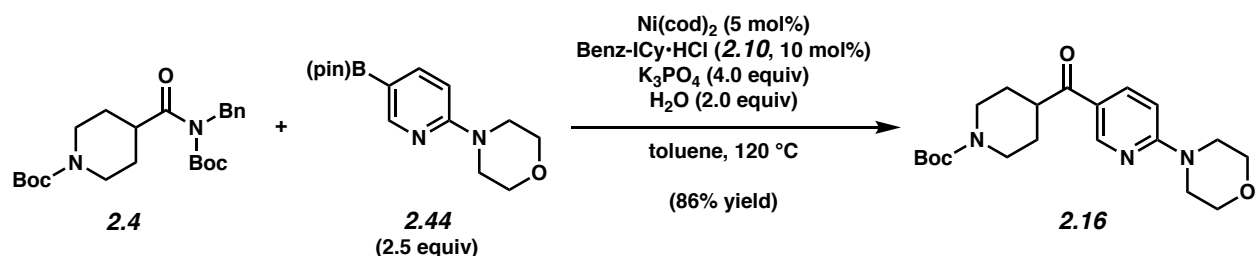
Ketone 2.16. Purification by flash chromatography (5:1 Hexanes:EtOAc → 9:1 CH$_2$Cl$_2$:MeOH) generated ketone **2.16** (86% yield, average of two experiments) as a white solid. Ketone **2.16**: mp: 131–133 °C; R$_f$ 0.52 (1:3 Hexanes:EtOAc); ^{1}H NMR (500 MHz, CDCl$_3$): δ 8.82–8.72 (m, 1H), 3.26 (dd, *J* = 9.1, 2.5, 1H), 6.69–6.58 (m, 1H), 4.17 (br s, 2H), 3.86–3.77 (m, 4H), 3.73–3.64 (m, 4H), 3.27 (tt, *J* = 11.1, 3.8, 1H), 2.99–2.71 (m, 2H), 1.94–1.64 (m, 4H), 1.46 (s, 9H); ^{13}C NMR (125 MHz, CDCl$_3$, 12 of 14 observed): δ 199.4, 160.9, 154.9, 150.4, 137.9, 121.5, 105.9, 79.8, 66.7, 45.0, 43.3, 28.6; IR (film): 2969, 2857, 1686, 1593, 1418, 1216, 1168 cm^{-1}; HRMS-APCI (*m/z*) [M + H]$^+$ calcd for C$_{20}$H$_{30}$N$_3$O$_4$, 376.22308; found 376.22247.

Ketone 2.17. Purification by flash chromatography (19:1 Hexanes:EtOAc → 14:1 Hexanes:EtOAc → 9:1 Hexanes:EtOAc) generated ketone **2.17** (80% yield, average of two experiments) as a white solid. Ketone **2.17**: mp: 86–88 °C; R$_f$ 0.19 (5:1 Hexanes:EtOAc); ^{1}H NMR

(500 MHz, CDCl$_3$): δ 7.08–7.02 (m, 1H), 6.82 (br s, 1H), 6.17–6.12 (m, 1H), 4.40–4.00 (m, 2H), 3.93 (s, 3H), 3.22–3.09 (m, 1H), 2.99–2.78 (m, 1H), 2.76–2.61 (m, 1H), 2.02–1.92 (m, 1H), 1.78–1.69 (m, 2H), 1.57–1.50 (m, 1H), 1.47 (s, 9H); ^{13}C NMR (125 MHz, CDCl$_3$): δ 192.0, 154.9, 131.7, 129.9, 119.5, 108.3, 79.7, 47.8, 47.1, 45.3, 44.0, 37.9, 28.6, 28.4, 24.8; IR (film): 2937, 2862, 1690, 1645, 1408 cm^{-1}; HRMS-APCI (*m/z*) [M + H]$^+$ calcd for C$_{16}$H$_{25}$N$_2$O$_3$, 293.18597; found 293.18458.

*Note: Ketone **2.17** was obtained as a mixture of conformers. These data represent empirically observed chemical shifts from the ^{13}C NMR spectrum.*
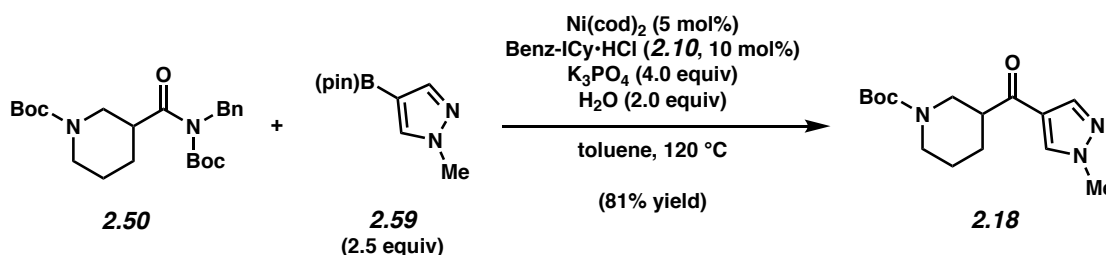
Ketone 2.18. Purification by flash chromatography (9:1 Hexanes:EtOAc → 5:1 Hexanes:EtOAc → 2:1 Hexanes:EtOAc → 1:1 Hexanes:EtOAc) generated ketone **2.18** (81% yield, average of two experiments) as a white solid. Ketone **2.18**: mp: 96–97 ºC; R$_f$ 0.19 (1:1 Hexanes:EtOAc); ^{1}H NMR (500 MHz, CDCl$_3$): δ 7.93 (s, 1H), 7.91 (br s, 1H), 4.40–4.01 (m, 2H), 3.94 (s, 3H), 3.05–2.65 (m, 3H), 2.03–1.95 (m, 1H), 1.79–1.64 (m, 2H), 1.55–1.43 (m, 10H); ^{13}C NMR (125 MHz, CDCl$_3$): δ 195.3, 154.8, 140.6, 132.8, 123.1, 79.9, 46.7, 45.0, 43.9, 39.5, 28.6, 27.8, 24.8; IR (film): 2939, 2862, 1683, 1663, 1540, 1148 cm^{-1}; HRMS-APCI (*m/z*) [M + H]$^+$ calcd for C$_{15}$H$_{24}$N$_3$O$_3$, 294.18122; found 294.17877.

*Note: Ketone **2.18** was obtained as a mixture of conformers. These data represent empirically observed chemical shifts from the ^{13}C NMR spectrum.*
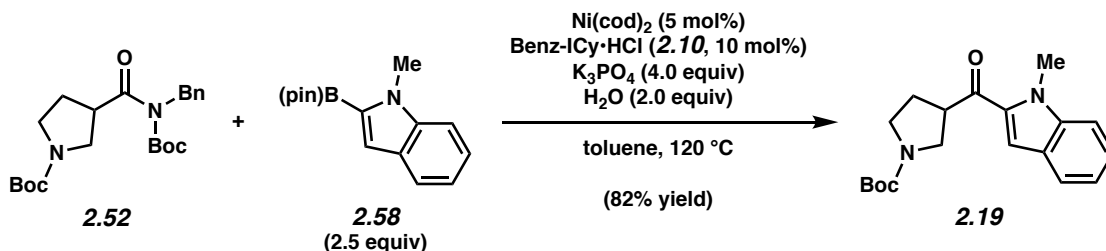
Ketone 2.19. Purification by flash chromatography (4:1 Hexanes:EtOAc) generated ketone **2.19** (82% yield, average of two experiments) as a clear oil. Ketone **2.19**: R_f 0.26 (4:1 Hexanes:EtOAc); ^{1}H NMR (500 MHz, CDCl$_3$): δ 7.70 (br s, 1H), 7.39 (br s, 2H), 7.33 (br s, 1H), 7.17 (br s, 1H), 4.08 (s, 3H), 4.04–3.91 (m, 1H), 3.82–3.65 (m, 1H), 3.65–3.39 (m, 3H), 2.35–2.12 (m, 2H), 1.47 (s, 9H); ^{13}C NMR (125 MHz, CDCl$_3$): δ 193.1, 192.9, 154.5, 140.5, 134.2, 126.4, 125.9, 123.1, 121.1, 112.0, 110.6, 79.5, 49.0, 48.9, 47.3, 46.3, 45.8, 45.6, 32.4, 29.7, 29.4, 28.6; IR (film): 2974, 2882, 1688, 1658, 1393, 1166, 1118 cm^{-1}; HRMS-APCI (*m/z*) [M + H]$^+$ calcd for C$_{19}$H$_{25}$N$_2$O$_3$, 329.18597; found 329.18463.

*Note: Ketone **2.19** was obtained as a mixture of conformers. These data represent empirically observed chemical shifts from the ^{13}C NMR spectrum.*
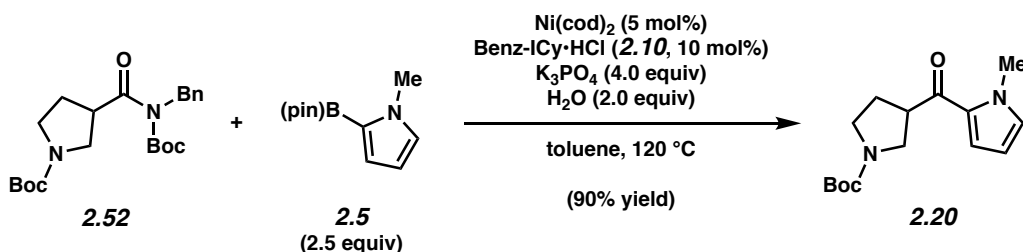
Ketone 2.20. Purification by flash chromatography (4:1 Hexanes:EtOAc) generated ketone **2.20** (90% yield, average of two experiments) as a clear oil. Ketone **2.20**: R_f 0.18 (4:1 Hexanes:EtOAc); ^{1}H NMR (500 MHz, CDCl$_3$): δ 6.97 (br s, 1H), 6.83 (br s, 1H), 6.14 (br s, 1H), 3.93 (s, 3H), 3.83–3.44 (m, 4H), 3.38 (br s, 1H), 2.28–2.12 (m, 1H), 2.08 (br s, 1H), 1.45 (s, 9H); ^{13}C NMR (125

MHz, CDCl$_3$): δ 189.9, 189.7, 154.5, 131.9, 130.2, 119.6, 108.4, 79.4, 49.0, 48.9, 46.4, 45.9, 45.6, 45.5, 37.9, 29.5, 29.4, 28.6; IR (film): 2977, 2882, 1686, 1643, 1401, 1366, 1118 cm^{-1}; HRMS-APCI (*m/z*) [M + H]$^+$ calcd for C$_{15}$H$_{23}$N$_2$O$_3$, 279.17032; found 279.17976.

*Note: Ketone **2.20** was obtained as a mixture of conformers. These data represent empirically observed chemical shifts from the ^{13}C NMR spectrum.*
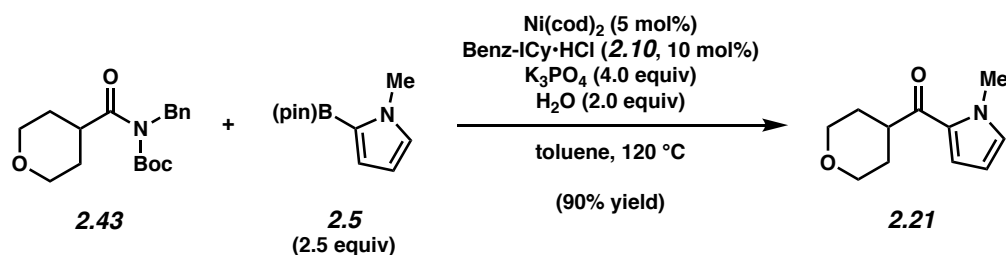
Ketone 2.21. Purification by flash chromatography (5:1 Hexanes:EtOAc) generated ketone **2.21** (90% yield, average of two experiments) as a white solid. Ketone **2.21**: mp: 72–74 °C; R$_f$ 0.21 (4:1 Hexanes:EtOAc); ^{1}H NMR (500 MHz, CDCl$_3$): δ 7.00–6.95 (m, 1H), 6.82 (s, 1H), 6.15–6.10 (m, 1H), 4.09–4.00 (m, 2H), 3.94 (s, 3H), 3.51 (t, *J* = 11.8, 2H), 3.26 (tt, *J* = 11.5, 3.8, 1H), 1.91 (qd, *J* = 12.4, 4.3, 2H), 1.70 (d, *J* = 13.4, 2H); ^{13}C NMR (125 MHz, CDCl$_3$): δ 192.9, 131.6, 129.8, 118.9, 108.1, 67.6, 43.8, 38.0, 29.7; IR (film): 2952, 2847, 1642, 1408, 1306, 1094 cm^{-1}; HRMS-APCI (*m/z*) [M + H]$^+$ calcd for C$_{11}$H$_{16}$NO$_2$, 194.11756; found 194.11707.
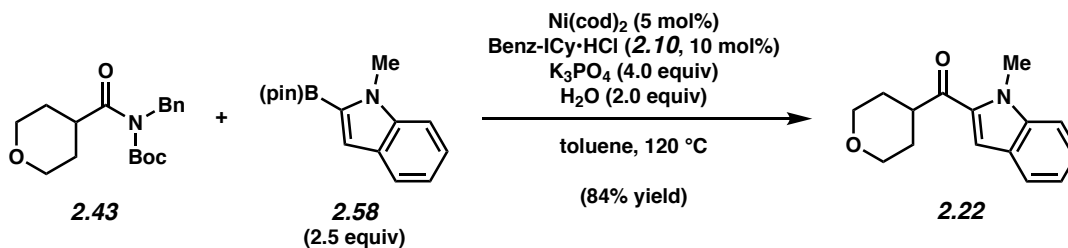
Ketone 2.22. Purification by flash chromatography (5:1 Hexanes:EtOAc) generated ketone **2.22** (84% yield, average of two experiments) as a white solid. Ketone **2.22**: mp: 63–66 °C; R$_f$ 0.35 (4:1

Hexanes:EtOAc); ^{1}H NMR (500 MHz, CDCl$_3$): δ 7.70 (d, J = 8.1, 1H), 7.39 (d, J = 3.6, 2H), 7.33

(s, 1H), 7.19–7.14 (m, 1H), 4.12–4.09 (m, 1H), 4.07 (s, 4H), 3.57 (t, J = 11.7, 2H), 3.48 (tt, J =

11.5, 3.6, 1H), 1.96 (qd, J = 12.4, 4.2, 2H), 1.81 (d, J = 13.2, 2H); ^{13}C NMR (125 MHz, CDCl$_3$):

δ 196.0, 140.4, 133.8, 126.1, 125.9, 123.0, 120.9, 111.1, 110.6, 67.5, 44.7, 32.4, 29.8; IR (film):

2954, 2844, 1656, 1511, 1386, 1118 cm^{-1}; HRMS-APCI (m/z) [M + H]$^+$ calcd for C$_{15}$H$_{18}$NO$_2$,

244.13321; found 244.13264.
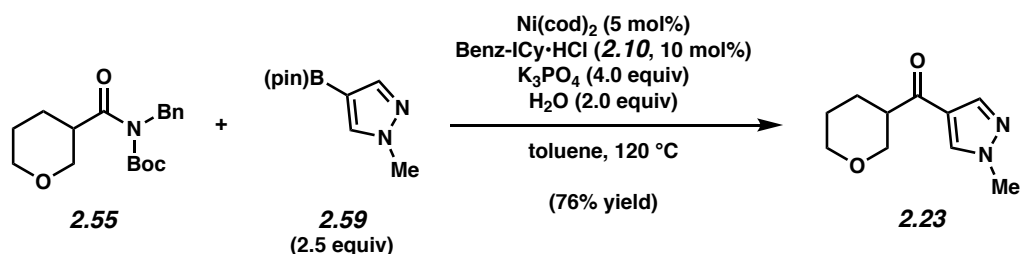
Ketone 2.23. Purification by flash chromatography (1:2 Hexanes:EtOAc) generated ketone **2.23**

(76% yield, average of two experiments) as a yellow solid. Ketone **2.23**: mp: 83–84 °C; R$_f$ 0.25

(1:2 Hexanes:EtOAc); ^{1}H NMR (500 MHz, CDCl$_3$): δ 7.89 (s, 1H), 7.87 (s, 1H), 4.04 (d, J = 11.1,

1H), 3.96–3.86 (m, 4H), 3.50 (t, J = 10.9, 1H), 3.43–3.34 (m, 1H), 3.20–3.11 (m, 1H), 1.97 (d, J

= 12.7, 1H), 1.86–1.73 (m, 1H), 1.73–1.63 (m, 2H); ^{13}C NMR (125 MHz, CDCl$_3$): δ 195.2, 140.4,

132.8, 123.3, 69.8, 68.2, 47.2, 39.5, 26.6, 25.2; IR (film): 2947, 2852, 1656, 1541, 1401, 1188,

1080 cm^{-1}; HRMS-APCI (m/z) [M + H]$^+$ calcd for C$_{10}$H$_{15}$N$_2$O$_2$, 165.11280; found 165.11223.
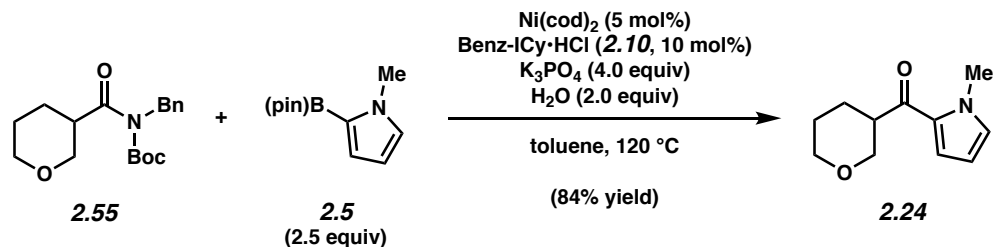
Ketone 2.24. Purification by flash chromatography (4:1 Hexanes:EtOAc) generated ketone **2.24** (84% yield, average of two experiments) as a clear oil. Ketone **2.24**: R_f 0.30 (4:1 Hexanes:EtOAc); ^{1}H NMR (500 MHz, CDCl$_3$): δ 7.04–7.00 (m, 1H), 6.81 (s, 1H), 6.15–6.10 (m, 1H), 4.09–4.02 (m, 1H), 3.98–3.92 (m, 1H), 3.91 (s, 3H), 3.52 (t, J = 10.9, 1H), 3.44–3.33 (m, 2H), 2.00–1.93 (m, 1H), 1.84 (qd, J = 12.1, 4.3, 1H), 1.78–1.65 (m, 2H); ^{13}C NMR (125 MHz, CDCl$_3$): δ 191.8, 131.7, 130.1, 119.5, 108.2, 70.6, 68.3, 45.7, 37.9, 27.1, 25.4; IR (film): 2947, 2849, 1638, 1406, 1201, 1065 cm^{-1}; HRMS-APCI (m/z) [M + H]$^+$ calcd for C$_{11}$H$_{16}$NO$_2$, 194.11756; found 194.11699.
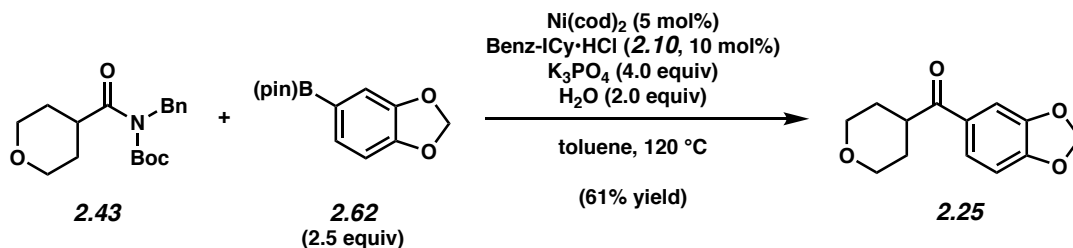
Ketone 2.25. Purification by flash chromatography (30:15:1 Hexanes:EtOAc:TEA) generated ketone **2.25** (61% yield, average of two experiments) as a white solid. Ketone **2.25**: mp: 97–98 °C; R_f 0.35 (2:1 Hexanes:EtOAc); ^{1}H NMR (500 MHz, CDCl$_3$): δ 7.55 (dd, J = 8.2, 1.8, 1H), 7.42 (d, J = 1.8, 1H), 6.86 (d, J = 8.2, 1H), 6.04 (s, 2H), 4.05 (ddd, J = 11.4, 4.0, 2.4, 2H), 3.54 (td, J = 11.7, 2.2, 2H), 3.40 (tt, J = 11.2, 3.8, 1H), 1.92–1.83 (m, 2H), 1.77–1.72 (m, 2H); ^{13}C NMR (125 MHz, CDCl$_3$): δ 200.0, 151.9, 148.5, 130.7, 124.5, 108.3, 108.1, 102.0, 67.5, 42.6, 29.4; IR (film):

2955, 2847, 1670, 1440, 1258, 1241, 1114 cm^{-1}; HRMS-APCI (m/z) [M + H]$^+$ calcd for C$_{13}$H$_{15}$O$_4$, 235.09649; found 235.09592.
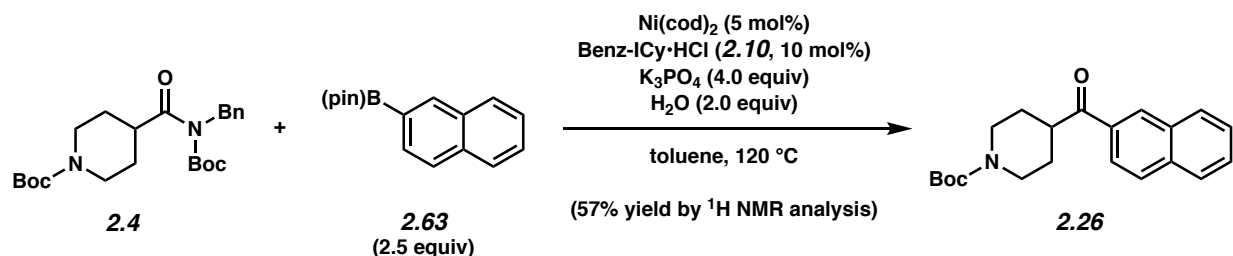
Ketone 2.26. ^{1}H NMR analysis of the crude reaction mixture indicated a 57% yield of ketone **2.26** relative to hexamethylbenzene internal standard. Purification by preparative thin-layer chromatography (4:1 Hexanes:EtOAc) provided an analytical sample of ketone **2.26** as a white amorphous solid. Ketone **2.26**: R$_f$ 0.29 (4:1 Hexanes:EtOAc); ^{1}H NMR (500 MHz, CDCl$_3$): δ 8.45 (s, 1H), 8.02–7.96 (m, 2H), 7.93–7.86 (m, 2H), 7.63–7.54 (m, 2H), 4.20 (br s, 2H), 3.58 (tt, J = 11.1, 3.7, 1H), 3.04–2.87 (m, 2H), 1.97–1.84 (m, 2H), 1.82–1.71 (m, 2H), 1.48 (s, 9H); ^{13}C NMR (125 MHz, CDCl$_3$): δ 202.2, 154.9, 135.7, 133.3, 132.7, 129.8, 129.7, 128.8, 128.7, 127.9, 127.0, 124.3, 79.8, 43.7, 43.3, 28.7, 28.6; IR (film): 3060, 2975, 2930, 2858, 1682 cm^{-1}; HRMS-APCI (m/z) [M + H]$^+$ calcd for C$_{21}$H$_{26}$NO$_3$, 340.19072; found 340.19041.
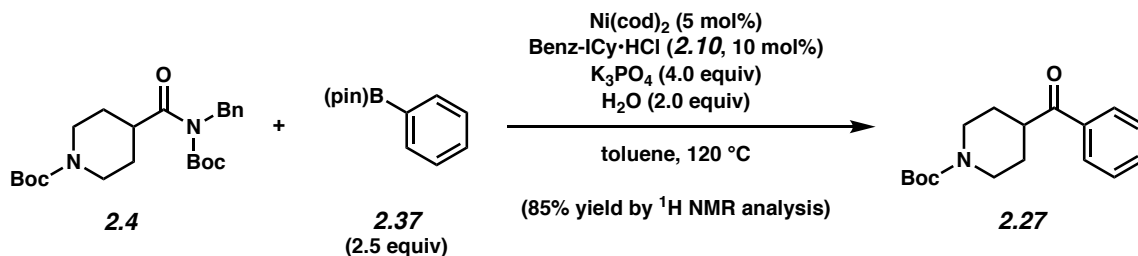
Ketone 2.27. ^{1}H NMR analysis of the crude reaction mixture indicated an 85% yield of ketone **2.27** relative to hexamethylbenzene internal standard. Purification by preparative thin-layer

chromatography (3:1 Hexanes:EtOAc) provided an analytical sample of ketone **2.27** as a white amorphous solid. Ketone **2.27**: R_f 0.21 (5:1 Hexanes:EtOAc). Spectral data match those previously reported.[25]
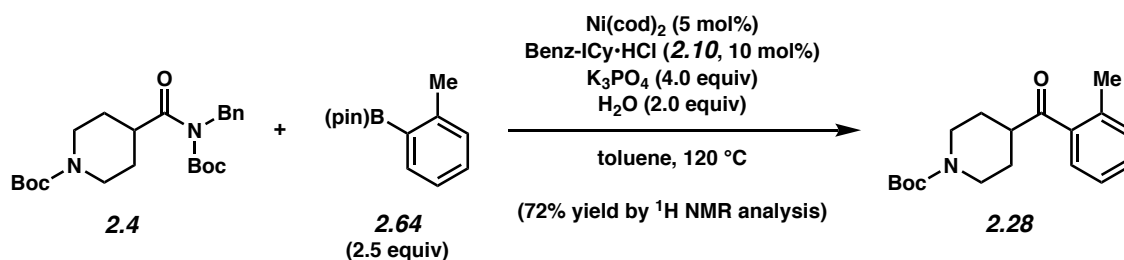
Ketone 2.28. ^{1}H NMR analysis of the crude reaction mixture indicated a 72% yield of ketone **2.28** relative to hexamethylbenzene internal standard. Purification by preparative thin-layer chromatography (4:1 Hexanes:EtOAc) provided an analytical sample of ketone **2.28** as a clear oil. Ketone **2.28**: R_f 0.42 (3:1 Hexanes:EtOAc). Spectral data match those previously reported.[4]
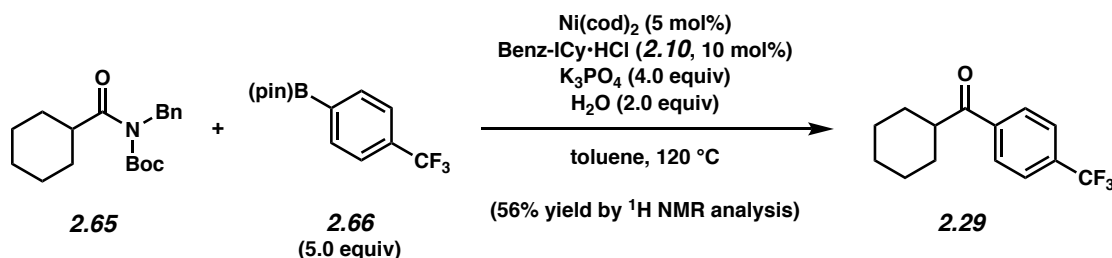
Ketone 2.29. ^{1}H NMR analysis of the crude reaction mixture indicated a 56% yield of ketone **2.29** relative to hexamethylbenzene internal standard. Purification by preparative thin-layer chromatography (9:1 Hexanes:EtOAc) provided an analytical sample ketone **29** as a white solid. Ketone **2.29**: R_f 0.56 (9:1 Hexanes:EtOAc). Spectral data match those previously reported.[26]
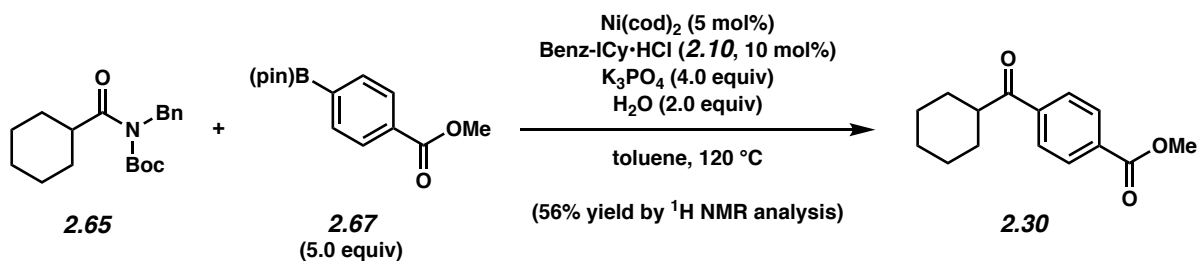
Ketone 2.30. ^{1}H NMR analysis of the crude reaction mixture indicated a 38% yield of ketone **2.30** relative to hexamethylbenzene internal standard. Purification by preparative thin-layer chromatography (9:1 Hexanes:EtOAc) provided an analytical sample of ketone **2.30** as a white solid. Ketone **2.30**: R_f 0.39 (9:1 Hexanes:EtOAc). Spectral data match those previously reported.[27]
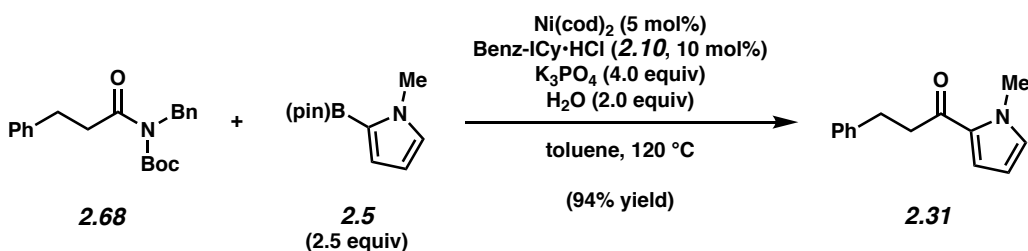
Ketone 2.31. Purification by flash chromatography (19:1 Hexanes:EtOAc → 14:1 Hexanes:EtOAc → 9:1 Hexanes:EtOAc) generated ketone **2.31** (94% yield, average of two experiments) as a clear oil. Ketone **2.31**: R_f 0.43 (5:1 Hexanes:EtOAc). Spectral data match those previously reported.[28]
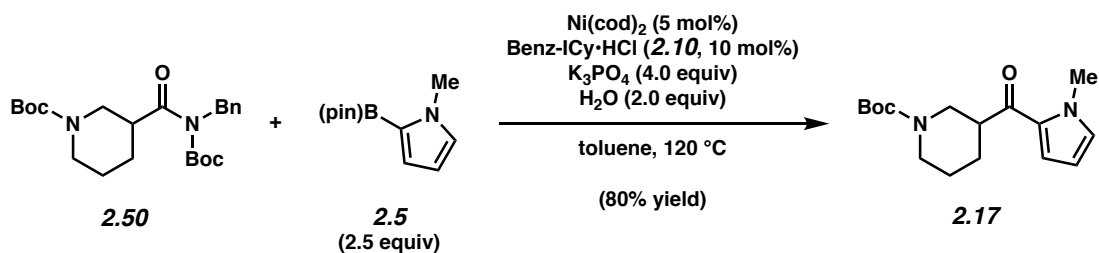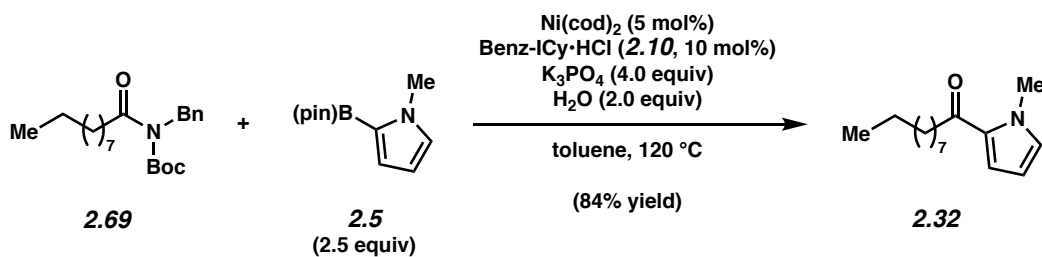

Ketone 2.32. Purification by flash chromatography (24:1 Hexanes:EtOAc) generated ketone **2.32** (84% yield, average of two experiments) as a clear oil. Ketone **2.32**: R_f 0.52 (5:1 Hexanes:EtOAc);

^{1}H NMR (500 MHz, CDCl$_3$): δ 6.95 (dd, J = 4.1, 1.7, 1H), 6.80–6.77 (m, 1H), 6.11 (dd, J = 4.1, 2.5, 1H), 3.94 (s, 3H), 2.77–2.73 (m, 2H), 1.69 (quint, J = 7.5, 2H), 1.39–1.20 (m, 12H), 0.88 (t, J = 7.1, 3H); ^{13}C NMR (125 MHz, CDCl$_3$): δ 192.0, 131.0, 130.9, 119.0, 107.9, 39.3, 37.9, 32.0, 29.7, 29.633, 29.627, 29.5, 25.5, 22.8, 14.3; IR (film): 2955, 2923, 2853, 1649, 1528 cm^{-1}; HRMS-APCI (m/z) [M + H]$^+$ calcd for C$_{15}$H$_{26}$NO, 236.20089; found 236.20080.
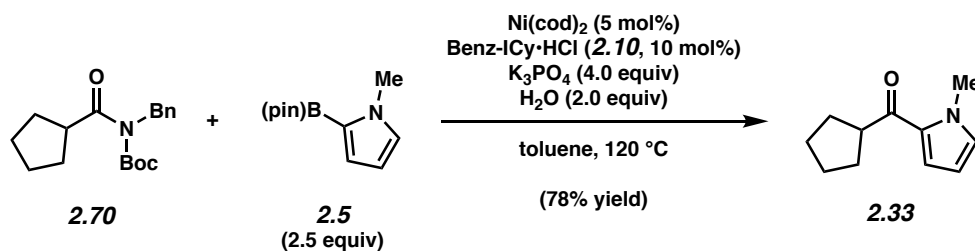
Ketone 2.33. Purification by flash chromatography (24:1 Hexanes:EtOAc → 19:1 Hexanes:EtOAc) generated ketone **2.33** (78% yield, average of two experiments) as a clear oil. Ketone **2.33**: R$_f$ 0.50 (5:1 Hexanes:EtOAc). Spectral data match those previously reported.[29]
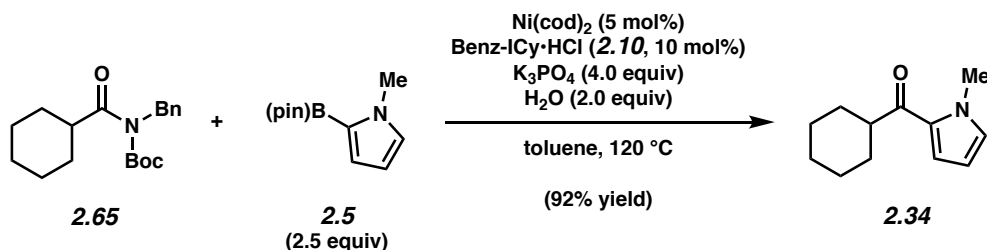
Ketone 2.34. Purification by flash chromatography (14:1 Hexanes:EtOAc) generated ketone **2.34** (92% yield, average of two experiments) as a clear oil. Ketone **2.34**: R$_f$ 0.28 (14:1 Hexanes:EtOAc). Spectral data match those previously reported.[30]
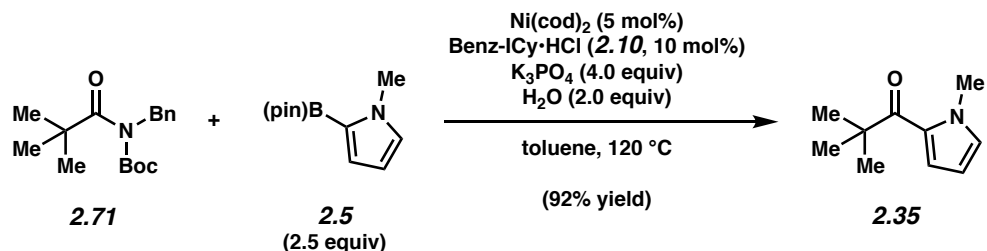
Ketone 2.35. Purification by flash chromatography (19:1 Hexanes:EtOAc) generated ketone **2.35** (92% yield, average of two experiments) as a clear oil. Ketone **2.35**: R_f 0.66 (4:1 Hexanes:EtOAc). Spectral data match those previously reported.[31]
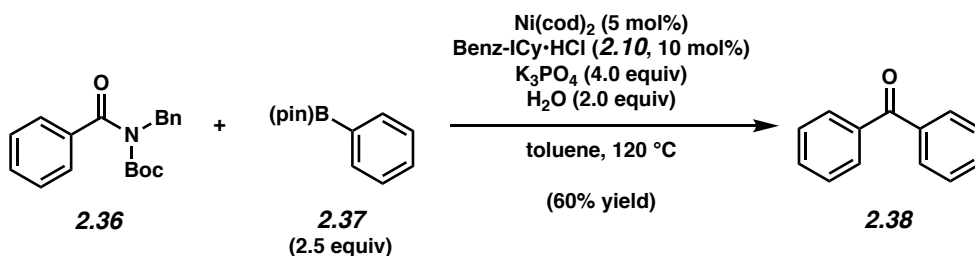
Ketone 2.38. Purification by thin-layer chromatography (5:1 Hexanes:EtOAc) generated ketone **2.38** (the reported yield was based on ^{1}H NMR analysis using hexamethylbenzene as an external standard) as a white solid. Ketone **2.38**: R_f 0.56 (5:1 Hexanes:EtOAc). Spectral data match those previously reported.[4b]
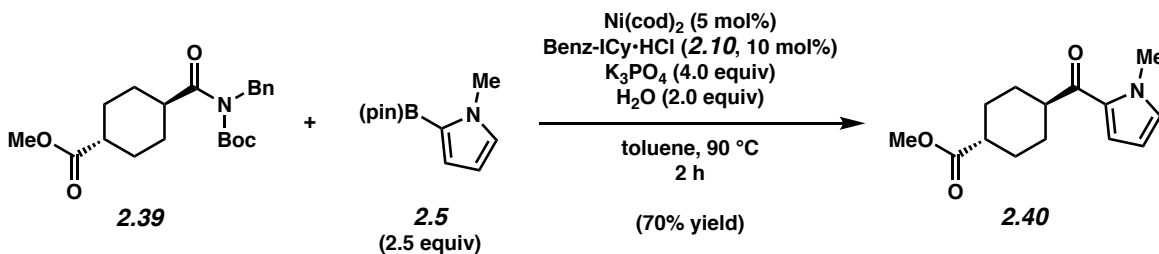
Ketone 2.40. Purification by flash chromatography (49:1 CHCl$_3$:CH$_3$CN) generated ketone **2.40** (the reported yield was based on ^{1}H NMR analysis using hexamethylbenzene as an external standard) as a white solid. Ketone **2.40**: R_f 0.48 (19:1 CHCl$_3$:CH$_3$CN); ^{1}H NMR (500 MHz,

CDCl$_3$): δ 6.97 (dd, J = 4.1, 1.7, 1H), 6.83–6.80 (m, 1H), 6.13 (dd, J = 4.1, 2.5, 1H), 3.93 (s, 3H),

3.68 (s, 3H), 3.06–2.99 (m, 1H), 2.38–2.30 (m, 1H), 2.14–2.05 (m, 2H), 1.98–1.88 (m, 2H), 1.63–

1.49 (m, 4H); ^{13}C NMR (125 MHz, CDCl$_3$): δ 194.3, 176.3, 131.5, 130.0, 118.9, 108.0, 51.7, 45.9,

42.7, 37.9, 29.0, 28.5; IR (film): 2942, 2862, 1730, 1645, 1408, 1251 cm^{-1}; HRMS-APCI (m/z)

[M + H]$^+$ calcd for C$_{14}$H$_{20}$NO$_3$, 250.14377; found 250.14273.
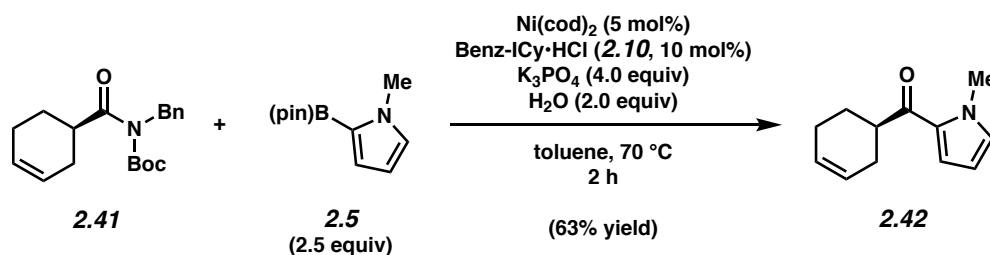
Ketone 2.42. Purification by flash chromatography (19:1 Hexanes:EtOAc → 14:1

Hexanes:EtOAc) generated ketone **2.42** (63% yield, average of two experiments) as a clear oil.

Ketone **2.42**: R$_f$ 0.46 (5:1 Hexanes:EtOAc); ^{1}H NMR (500 MHz, CDCl$_3$): δ 6.99 (dd, J = 4.1, 1.6,

1H), 6.83–6.80 (m, 1H), 6.13 (dd, J = 4.1, 2.4, 1H), 5.79–5.70 (m, 2H), 3.95 (s, 3H), 3.32–3.25

(m, 1H), 2.39–2.30 (m, 1H), 2.20–2.11 (m, 3H), 1.96–1.90 (m, 1H), 1.79–1.69 (m, 1H); ^{13}C NMR

(125 MHz, CDCl$_3$): δ 194.8, 131.3, 130.3, 126.6, 126.2, 119.0, 108.0, 42.7, 38.0, 28.6, 26.4, 25.2;

IR (film): 3107, 3023, 2931, 2838, 1643, 1527 cm^{-1}; HRMS-APCI (m/z) [M + H]$^+$ calcd for

C$_{12}$H$_{16}$NO, 190.12264; found 190.12245. [α]$^{20.7}_{D}$ –6.20 ° (c = 1.00, CHCl$_3$).
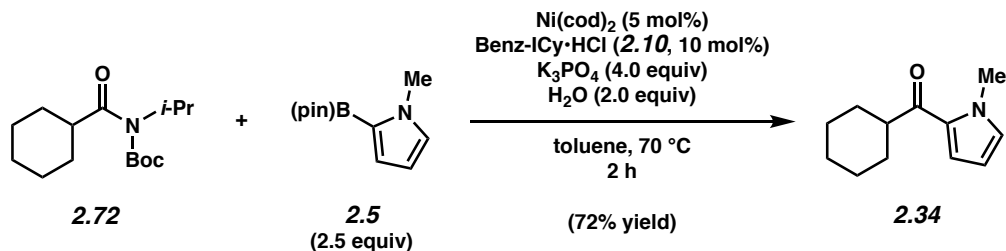
Ketone 2.34. Purification by column chromatography (49:1 Hexanes:EtOAc) generated ketone **2.34** (the reported yield was based on ^{1}H NMR analysis using hexamethylbenzene as an external standard) as a clear oil. Ketone **2.34**: R_f 0.28 (14:1 Hexanes:EtOAc). Spectral data match those previously reported.[30]

2.10.2.4 Verification of Enantiopurity

2.10.2.4.1 Synthesis of Racemic Ketone
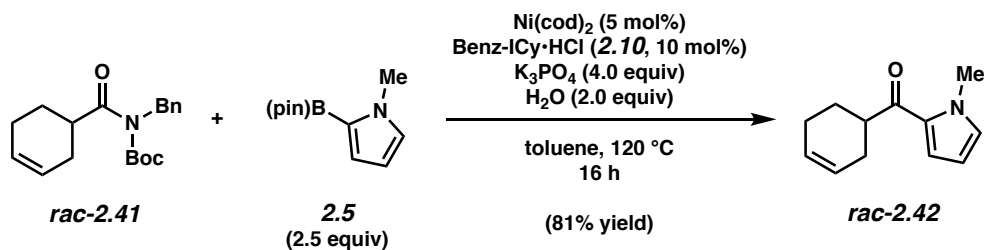
Ketone rac-2.42. Purification by flash chromatography (19:1 Hexanes:EtOAc → 14:1 Hexanes:EtOAc) generated ketone **rac-2.42** (81% yield, average of two experiments) as a clear oil. Spectral data match those previously reported (see section 2.10.2.3).

2.10.2.4.2 Chiral SFC Assays

Table 2.2. Conditions and results of chiral SFC analysis of amide starting materials.
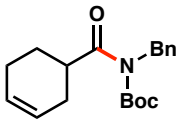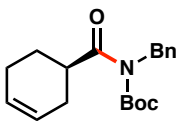
Compound	Method Column/Temp.	Solvent	Method Flow Rate	Retention Times (min)	Enantiomeric Ratio (er)
rac-2.41	Daicel ChiralPak OJ-H/35 °C	1% isopropanol in CO_2	1 mL/min	9.29/10.63	50:50
2.41	Daicel ChiralPak OJ-H/35 °C	1% isopropanol in CO_2	1 mL/min	9.57/10.54	99:1

Figure 2.8. SFC trace of *rac*-**2.41** (Table 2.2, Entry 1).

Index	Name	Start [Min]	Time [Min]	End [Min]	RT Offset [Min]	Quantity [% Area]	Height [µV]	Area [µV.Min]	Area [%]
1	UNKNOWN	9.29	10.10	10.63	0.00	50.11	449.1	223.3	50.106
2	UNKNOWN	10.63	11.18	12.08	0.00	49.89	422.0	222.4	49.894
Total						100.00	871.2	445.7	100.000
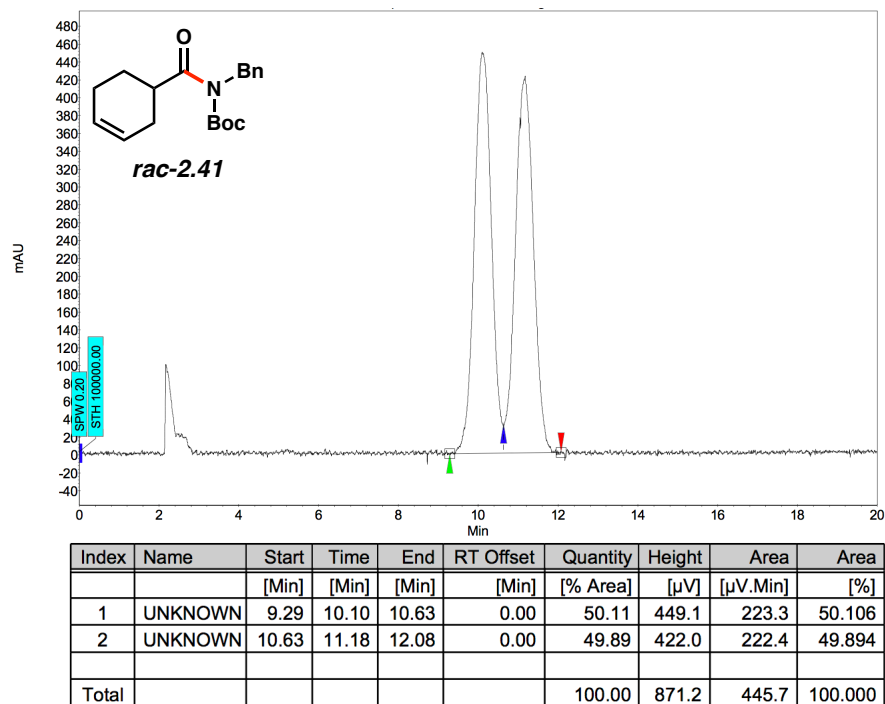
Figure 2.9. SFC trace of **2.41** (Table 2.2, Entry 2).
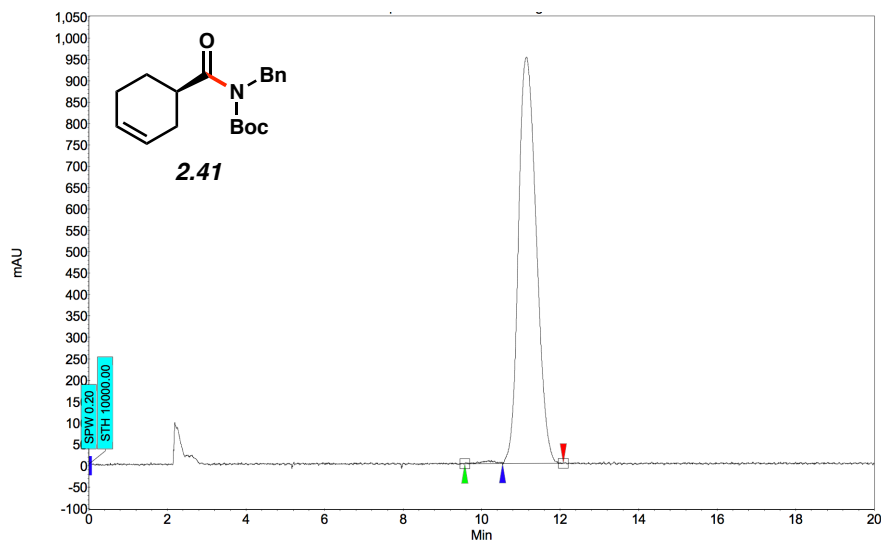
Index	Name	Start	Time	End	RT Offset	Quantity	Height	Area	Area
		[Min]	[Min]	[Min]	[Min]	[% Area]	[µV]	[µV.Min]	[%]
1	UNKNOWN	9.57	10.18	10.54	0.00	0.56	7.1	2.8	0.556
2	UNKNOWN	10.54	11.15	12.08	0.00	99.44	950.0	498.7	99.444
Total						100.00	957.2	501.5	100.000

Table 2.3. Conditions and results of chiral SFC analysis of ketone products.

Compound	Method Column/Temp.	Solvent	Method Flow Rate	Retention Times (min)	Enantiomeric Ratio (er)
rac-2.42	Daicel ChiralPak OJ-H/35 °C	5% isopropanol in CO_2	2 mL/min	6.72/7.33	50:50
2.42	Daicel ChiralPak OJ-H/35 °C	5% isopropanol in CO_2	2 mL/min	6.69/7.12 6.82/7.29	99:2 96:4

98

Figure 2.10. SFC trace of *rac*-**2.42** (Table 2.3, Entry 1).
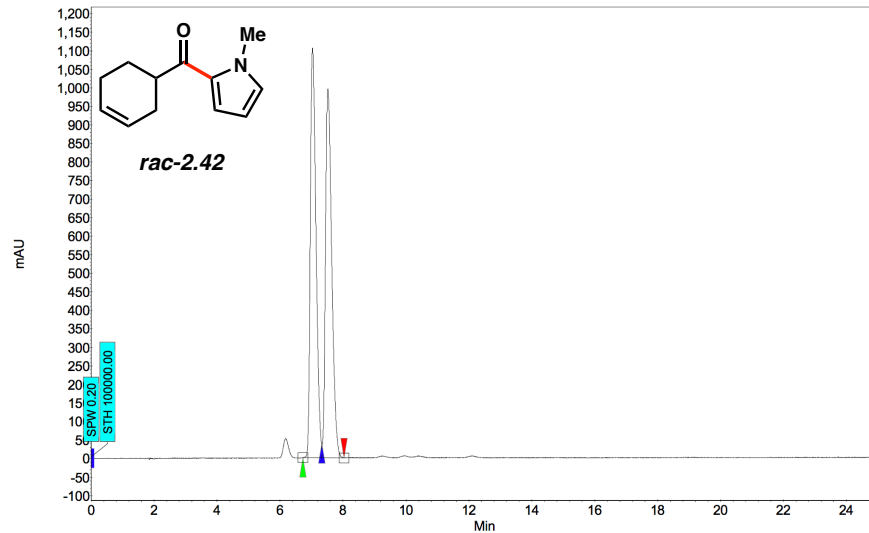
Index	Name	Start	Time	End	RT Offset	Quantity	Height	Area	Area
		[Min]	[Min]	[Min]	[Min]	[% Area]	[µV]	[µV.Min]	[%]
1	UNKNOWN	6.72	7.03	7.33	0.00	50.11	1104.5	231.5	50.113
2	UNKNOWN	7.33	7.52	8.04	0.00	49.89	994.7	230.5	49.887
Total						100.00	2099.2	462.0	100.000

Figure 2.11. SFC trace of **2.42** (Table 2.3, Entry 2).
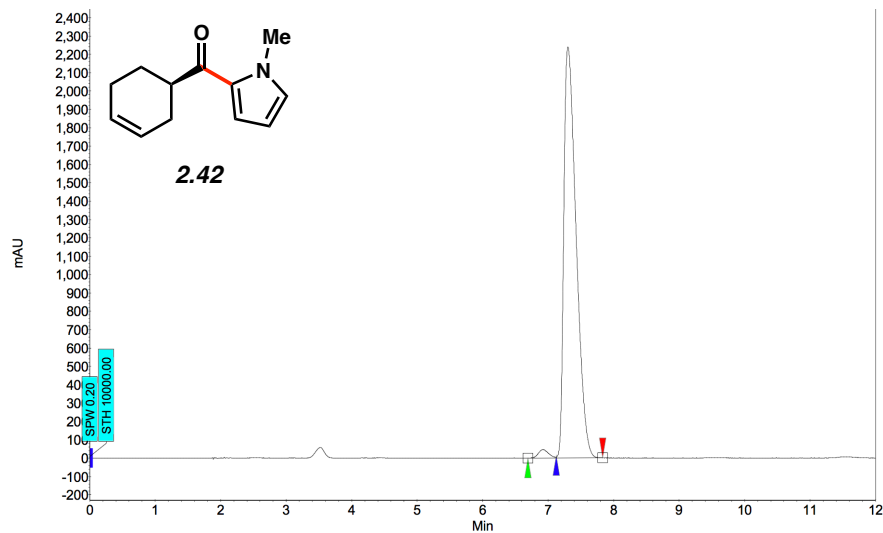
Index	Name	Start	Time	End	RT Offset	Quantity	Height	Area	Area
		[Min]	[Min]	[Min]	[Min]	[% Area]	[µV]	[µV.Min]	[%]
1	UNKNOWN	6.69	6.92	7.12	0.00	1.66	46.1	8.2	1.656
2	UNKNOWN	7.12	7.30	7.83	0.00	98.34	2239.4	485.6	98.344
Total						100.00	2285.5	493.8	100.000

99

Figure 2.12. SFC trace of **2.42** (Table 2.3, Entry 2).

Index	Name	Start	Time	End	RT Offset	Quantity	Height	Area	Area
		[Min]	[Min]	[Min]	[Min]	[% Area]	[µV]	[µV.Min]	[%]
1	UNKNOWN	6.82	7.08	7.29	0.00	4.17	47.1	10.2	4.168
2	UNKNOWN	7.29	7.54	8.05	0.00	95.83	908.7	235.6	95.832
Total						100.00	955.8	245.9	100.000

2.10.2.5 Erosion of Stereochemistry Control Experiments

2.10.2.5.1 Suzuki–Miyaura Coupling using Enantioenriched Amide Substrate
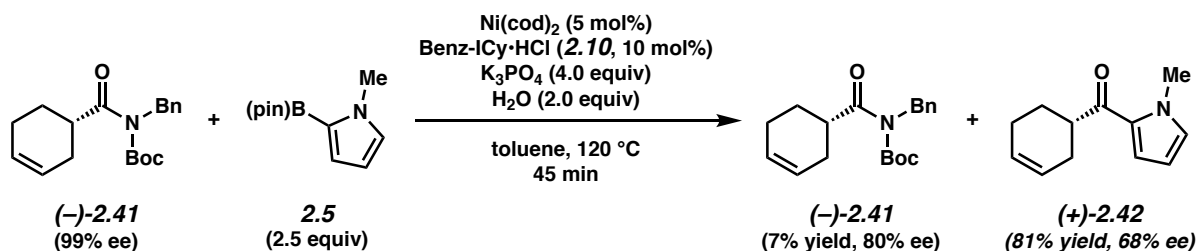
Amide 2.41 & Ketone 2.42. Purification by flash chromatography (Hexanes → 49:1 Hexanes:EtOAc → 24:1 Hexanes:EtOAc → 16:1 Hexanes:EtOAc) afforded recovered amide substrate **2.41** in 80% ee and ketone **2.42** in 68% ee (the reported yield was based on ^{1}H NMR analysis using hexamethylbenzene as an external standard) as clear oils. Spectral data match those previously reported (see section 2.10.2.3).

2.10.2.5.2 Chiral HPLC Assays

Table 2.4. Conditions and results of chiral HPLC analysis of amide starting materials.
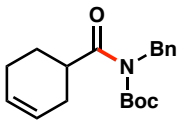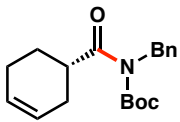
Compound	Method Column/Temp.	Solvent	Method Flow Rate	Retention Times (min)	Enantiomeric Ratio (er)
rac-2.41	Daicel ChiralPak OJ-H/23 °C	1% isopropanol in hexanes	1 mL/min	14.51/16.14	50:50
(–)-2.41	Daicel ChiralPak OJ-H/23 °C	1% isopropanol in hexanes	1 mL/min	14.08/15.61	90:10

Figure 2.13. HPLC trace of *rac-***2.41** (Table 2.4, Entry 1).
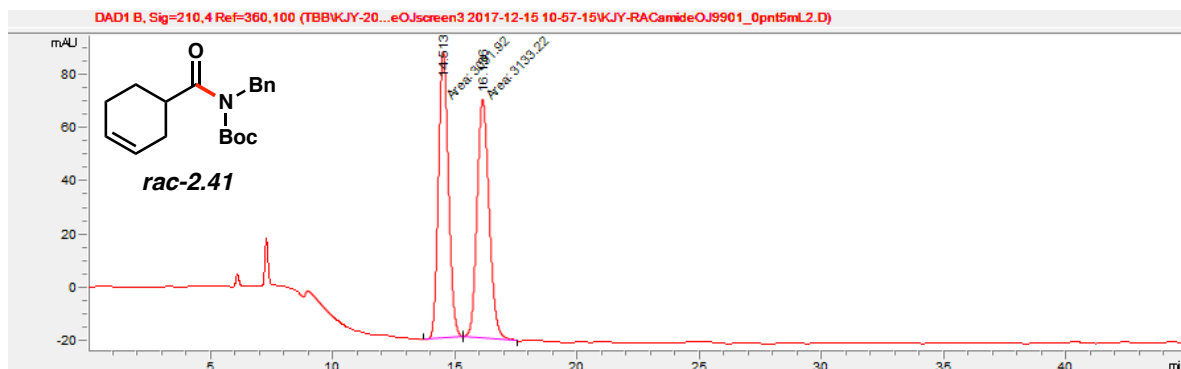
#	Time	Area	Height	Width	Area%	Symmetry
1	14.513	3091.9	108.2	0.4765	49.668	0.859
2	16.136	3133.2	90.2	0.5787	50.332	0.827

Figure 2.14. HPLC trace of **(–)-2.41** (Table 2.4, Entry 2).
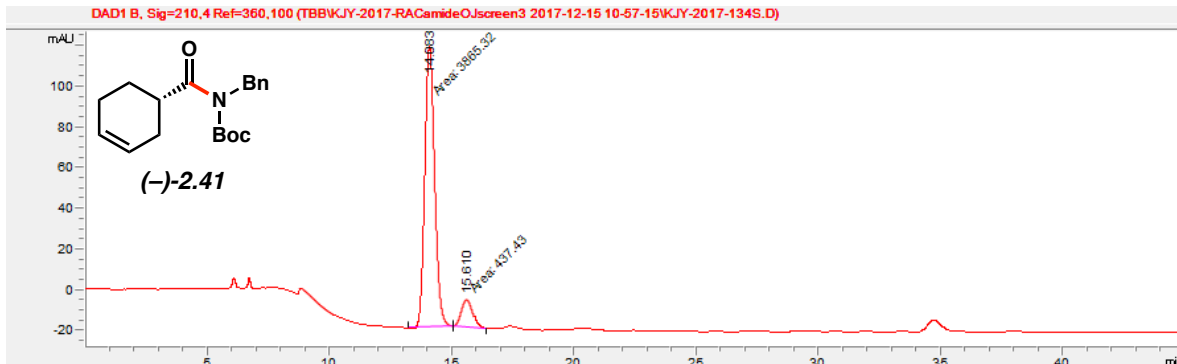
#	Time	Area	Height	Width	Area%	Symmetry
1	14.083	3865.3	138.1	0.4666	89.834	0.841
2	15.61	437.4	13.6	0.5372	10.166	0.848

Table 2.5. Conditions and results of chiral HPLC analysis of ketone products.

Compound	Method Column/Temp.	Solvent	Method Flow Rate	Retention Times (min)	Enantiomeric Ratio (er)
rac-2.42	Daicel ChiralPak OJ-H/23 °C	10% isopropanol in hexanes	1 mL/min	6.04/6.43	50:50
(+)-2.42	Daicel ChiralPak OJ-H/23 °C	10% isopropanol in hexanes	1 mL/min	6.05/6.46	84:16

102

Figure 2.15. HPLC trace of *rac*-**2.42** (Table 2.5, Entry 1).

#	Time	Area	Height	Width	Area%	Symmetry
1	6.041	967.6	140.3	0.1149	49.989	0.799
2	6.432	968	129.5	0.1246	50.011	0.805
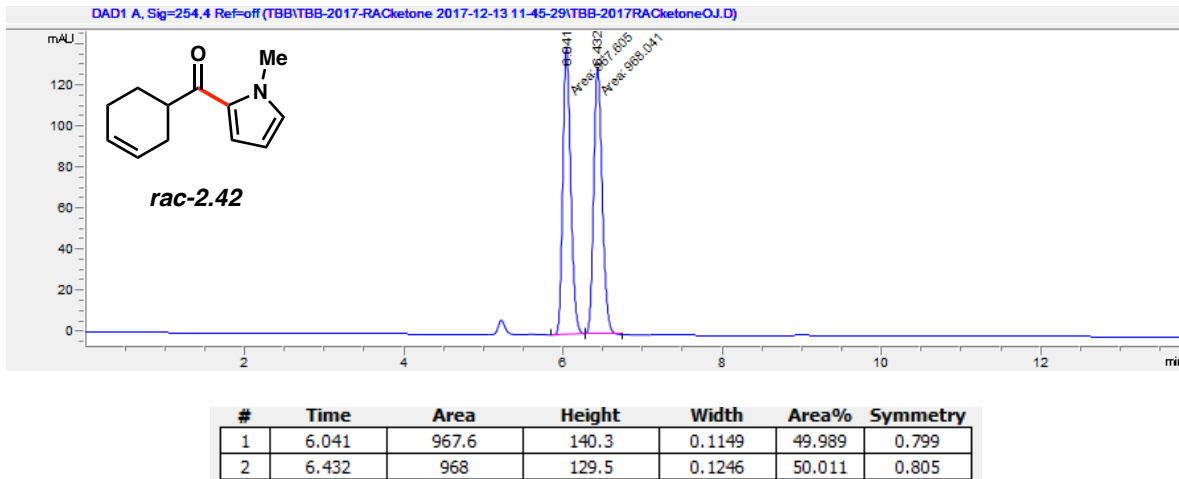
Figure 2.16. HPLC trace of **(+)-2.42** (Table 2.5, Entry 2).

#	Time	Area	Height	Width	Area%	Symmetry
1	6.056	1736.6	249.8	0.1159	83.718	0.788
2	6.455	337.7	45.3	0.1243	16.282	0.807
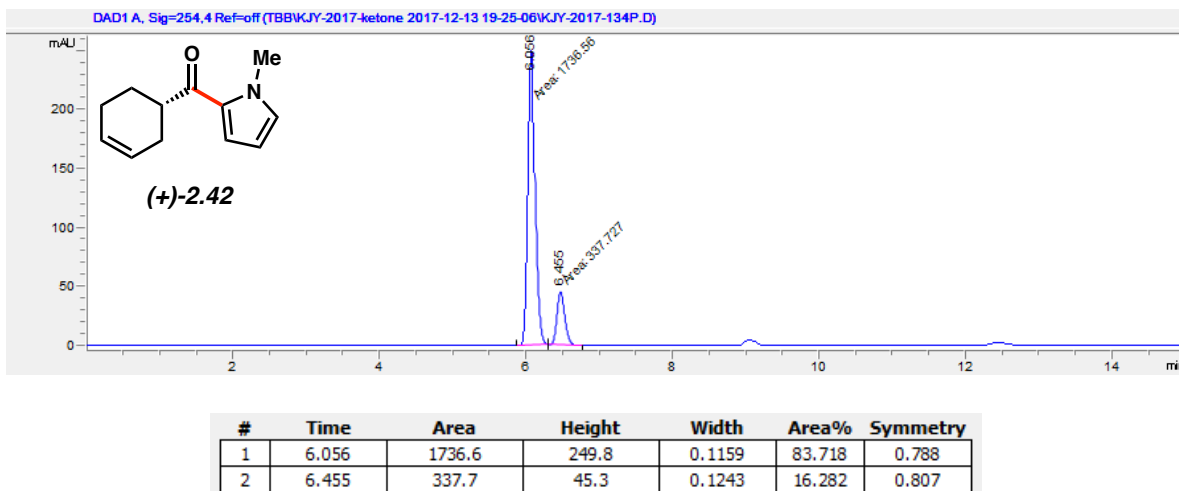
2.10.2.5.3 Elucidation of Origin of Erosion of α-Stereocenter

Table 2.6. Evaluation of impact of reaction components on erosion of α-stereocenter[a]

2.42-reactant (96% ee) → *2.42-product*
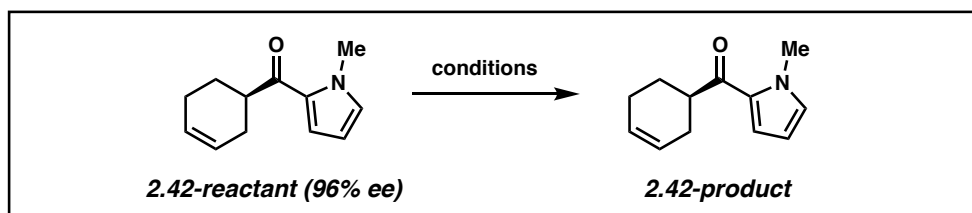
Entry	Control Experiment Conditions	Experimental Results ee of 2.42-product
1	K₃PO₄ (4.0 equiv), H₂O (2.0 equiv) toluene (1.0 M), 120 °C, 4 h	88%
2	Ni(cod)₂ (5 mol%) toluene (1.0 M), 120 °C, 16 h	92%
3	Benz-ICy·HCl (*2.10*, 10 mol%) toluene (1.0 M), 120 °C, 4 h	96%
4	Ni(cod)₂ (5 mol%), Benz-ICy·HCl (*2.10*,10 mol%), NaOtBu (9 mol%) toluene (1.0 M), 120 °C, 4 h	51%[a]
5	Benz-ICy·HCl (*2.10*,10 mol%), NaOtBu (9 mol%) toluene (1.0 M), 120 °C, 4 h	0%[b]

[a] Ni(cod)₂, Benz-ICy•HCl, and NaOtBu were stirred for 1 h in toluene at 23 ºC to generate active catalyst prior to addition to ketone substrate. [b] Benz-ICy•HCl and NaOtBu were stirred for 1 h in toluene at 23 ºC to generate free NHC prior to addition to ketone substrate.

2.10.2.5.4 Chiral HPLC Assays

Table 2.7. Conditions and results of chiral HPLC analysis of amides starting materials and ketones products.
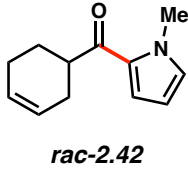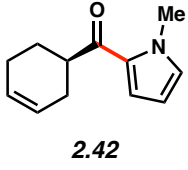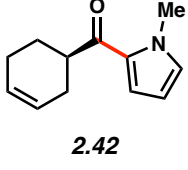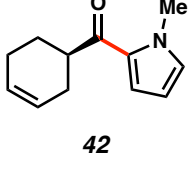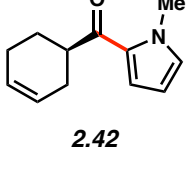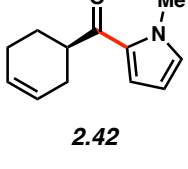
Compound	Control Experiment Entry	Method Column/ Temp.	Solvent	Method Flow Rate	Retention Times (min)	Enantiomeric Ratio (er)
rac-2.42	-	Daicel ChiralPak OJ-H/23 °C	10% isopropanol in hexanes	1 mL/min	6.041/6.432	50:50
2.42	1	Daicel ChiralPak OJ-H/23 °C	10% isopropanol in hexanes	1 mL/min	6.063/6.455	6:94
2.42	2	Daicel ChiralPak OJ-H/23 °C	10% isopropanol in hexanes	1 mL/min	6.064/6.456	4:96
42	3	Daicel ChiralPak OJ-H/23 °C	10% isopropanol in hexanes	1 mL/min	6.073/6.464	2:98
2.42	4	Daicel ChiralPak OJ-H/23 °C	10% isopropanol in hexanes	1 mL/min	6.074/6.466	24:76
2.42	5	Daicel ChiralPak OJ-H/23 °C	10% isopropanol in hexanes	1 mL/min	6.092/6.488	50:50

Figure 2.17. HPLC trace of *rac*-**2.42**.
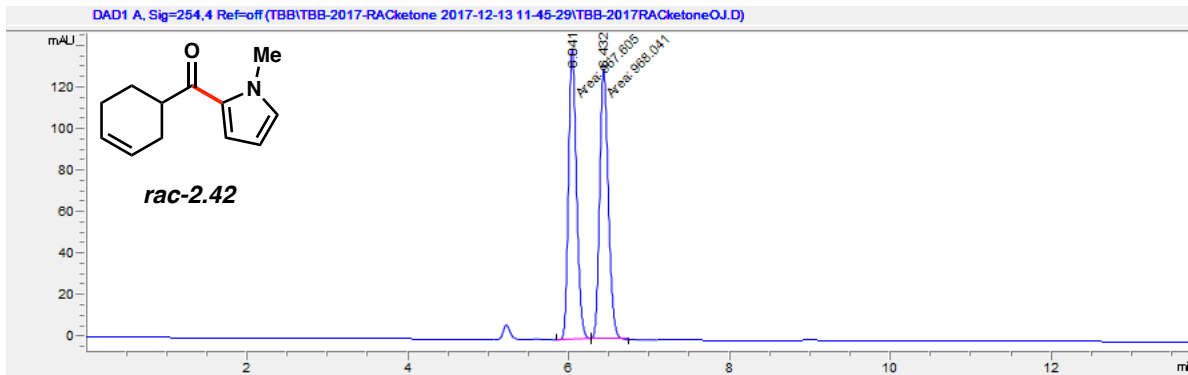
#	Time	Area	Height	Width	Area%	Symmetry
1	6.041	967.6	140.3	0.1149	49.989	0.799
2	6.432	968	129.5	0.1246	50.011	0.805

Figure 2.18. HPLC trace of **2.42** (Table 2.6, Entry 1).
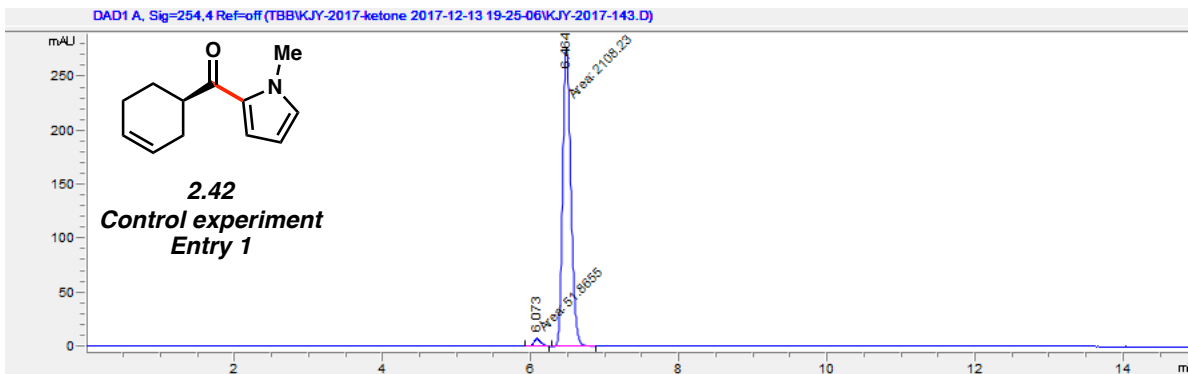
#	Time	Area	Height	Width	Area%	Symmetry
1	6.073	51.9	7.6	0.1144	2.401	0.839
2	6.464	2108.2	276.1	0.1273	97.599	0.796

Figure 2.19. HPLC trace of **2.42** (Table 2.6, Entry 2).
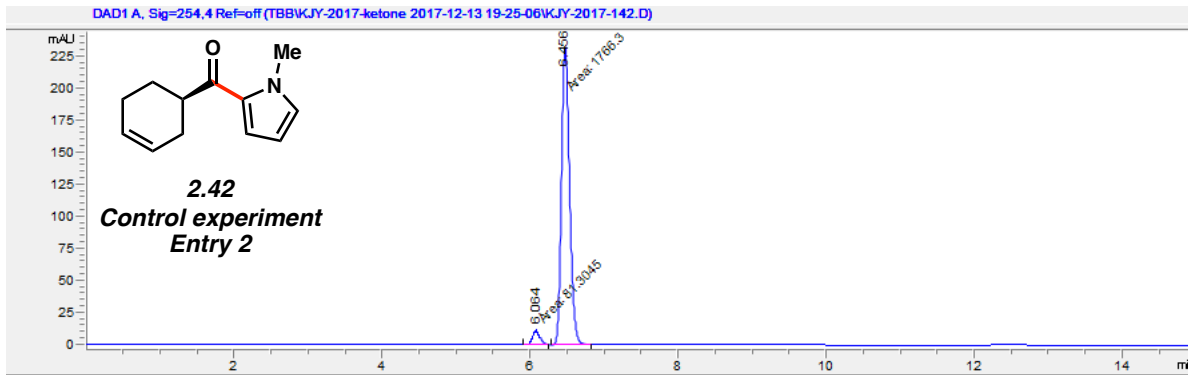
#	Time	Area	Height	Width	Area%	Symmetry
1	6.063	99.3	14.1	0.1172	5.607	0.819
2	6.455	1670.9	219.9	0.1267	94.393	0.799

Figure 2.20. HPLC trace of **2.42** (Table 2.6, Entry 3).
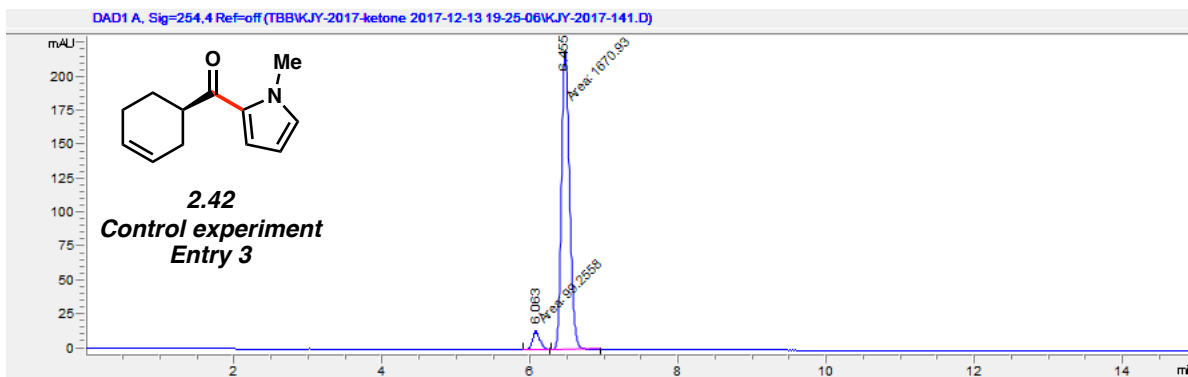
#	Time	Area	Height	Width	Area%	Symmetry
1	6.064	81.3	11.6	0.1168	4.401	0.798
2	6.456	1766.3	232.5	0.1266	95.599	0.798

Figure 2.21. HPLC trace of **2.42** (Table 2.6, Entry 4).

#	Time	Area	Height	Width	Area%	Symmetry
1	6.074	468.5	67.7	0.1154	24.245	0.808
2	6.466	1463.8	193.6	0.126	75.755	0.799
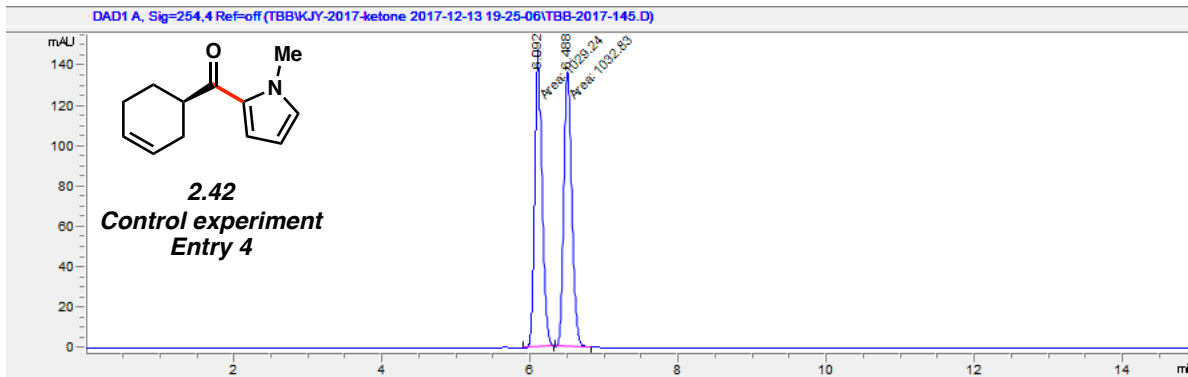
Figure 2.22. HPLC trace of **2.42** (Table 2.6, Entry 5).

#	Time	Area	Height	Width	Area%	Symmetry
1	6.092	1029.2	147.7	0.1161	49.913	0.796
2	6.488	1032.8	136.8	0.1259	50.087	0.801

108
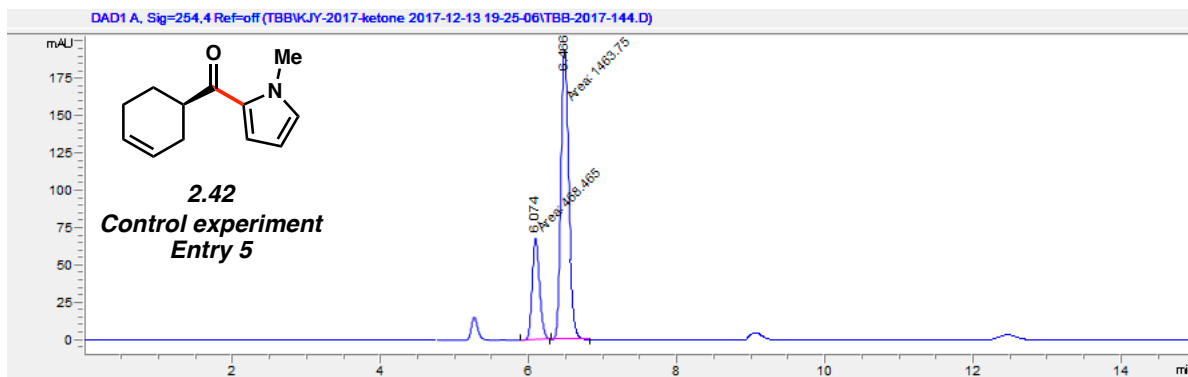
2.10.2.6 Robustness Screen

Table 2.8. Evaluation of functional group compatibility in the Suzuki reaction.[a]
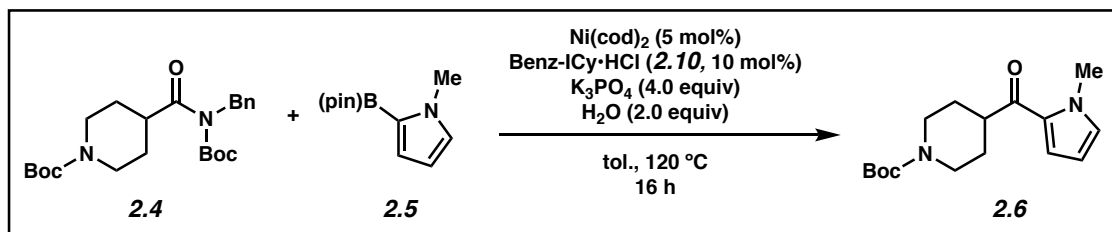
Entry	Additive	Yield of *2.6* (%)	Additive Remaining (%)	SM Remaining (%)	Entry	Additive	Yield of *2.6* (%)	Additive Remaining (%)	SM Remaining (%)
1	None	95	N.D.	0	8	(phenol)	0	42	0
2	(2-methyl-2-propanol)	70	N.D.[b]	0	9	(benzoic acid)	68	0	0
3	(Ph-NH-*n*-Bu)	58	73	0	10	(benzamide)	0	30	0
4	(*t*-Bu acetate)	66	N.D.[b]	0	11	(N-methylbenzamide)	66	66	0
5	(3-phenylpropanal)	0	8	46	12	Ph≡Et	71	4	0
6	(acetophenone)	67	73	0	13	(cyclohexene oxide)	26	N.D.[b]	0
7	Me-CN	0	N.D.[b]	0					

[a] Conditions: Ni(cod)$_2$ (5 mol%), Benz-ICy•HCl (10 mol%), substrate (1.0 equiv), PhB(pin) (2.5 equiv), K$_3$PO$_4$ (4.0 equiv), toluene (1.0 M), H$_2$O (2.0 equiv), and additive (1.0 equiv) at 120 °C for 16 h. Yields of coupled product, remaining additive, and remaining starting material were determined by ^{1}H NMR analysis using hexamethylbenzene as an internal standard. [b] Not determined due to low boiling point.

2.10.2.7 Gram-Scale Suzuki–Miyaura Reaction and Subsequent Fischer Indolization
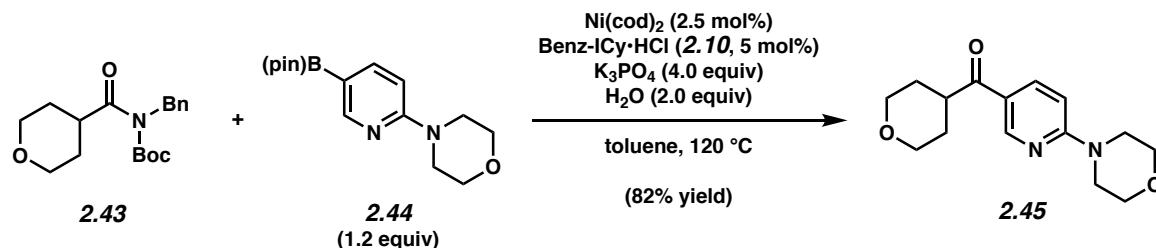
Ketone 2.45. A 20 mL scintillation vial was charged with anhydrous powdered K$_3$PO$_4$ (2.66 g, 12.5 mmol, 4.0 equiv) and a magnetic stir bar. The vial and contents were flame-dried under reduced pressure, then allowed to cool under N$_2$. Amide substrate **2.43** (1.00 g, 3.14 mmol, 1.0 equiv) and 2-morpholinopyridine-5-boronic acid pinacol ester (**2.44**) (1.09 g, 3.76 mmol, 1.2 equiv) were added. The vial was flushed with N$_2$, then water (113 µL, 6.27 mmol, 2.0 equiv), which had been sparged with N$_2$ for 10 min, was added. The vial was taken into a glove box and charged with Ni(cod)$_2$ (21.6 mg, 0.0784 mmol, 2.5 mol%) and Benz-ICy•HCl (**2.10**, 50.0 mg, 0.157 mmol, 5 mol%). Subsequently, toluene (3.14 mL, 1.0 M) was added. The vial was sealed with a Teflon-lined screw cap, removed from the glove box, and stirred vigorously (800 rpm) at 120 °C for 16 h. After cooling to 23 °C, the mixture was diluted with hexanes (7 mL) and filtered over a plug of silica gel (100 mL of EtOAc eluent). The volatiles were removed under reduced pressure, and the crude residue was purified by flash chromatography (3:1 Hexanes:EtOAc → 19:1 CH$_2$Cl$_2$:MeOH) to yield ketone product **2.45** (707 mg, 82% yield) as an off-white solid. Ketone **2.45**: mp: 122–124 ℃; R$_f$ 0.36 (4:1 PhH:CH$_3$CN); ^{1}H NMR (500 MHz, CDCl$_3$): δ 8.79 (d, J = 2.2, 1H), 8.06 (dd, J = 9.1, 2.4, 1H), 6.63 (d, J = 9.1, 1H), 4.09–4.02 (m, 2H), 3.84–3.78 (m, 4H), 3.71–3.65 (m, 4H), 3.54 (td, J = 11.7, 2.2, 2H), 3.37 (tt, J = 11.2, 3.8, 1H), 1.96–1.84 (m, 2H), 1.79–1.71 (m, 2H); ^{13}C NMR (125 MHz, CDCl$_3$): δ 199.2, 160.7, 150.4, 137.9, 121.5, 105.9, 67.5, 66.7,

45.0, 42.4, 29.3; IR (film): 2955, 2920, 2850, 1663, 1596 cm^{-1}; HRMS-APCI (*m/z*) [M + H]$^+$ calcd

for $C_{15}H_{21}N_2O_3$, 277.15467; found 277.15256.
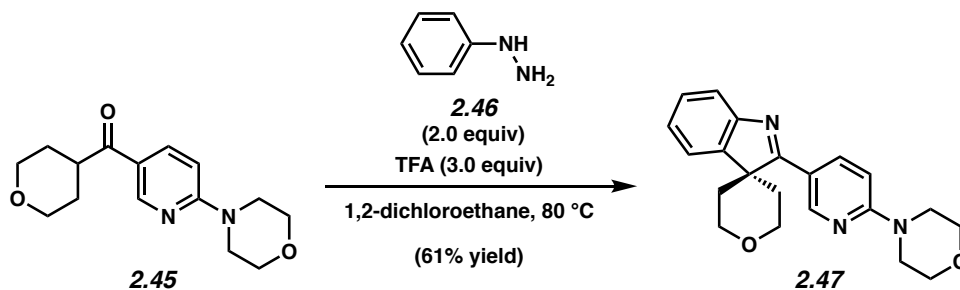
Indolenine 2.47. A 20 mL scintillation vial was charged with ketone **2.45** (707 mg, 2.56 mmol,

1.0 equiv) and a magnetic stir bar. Subsequently, 1,2-dichloroethane (12.0 mL, 0.21 M),

phenylhydrazine **2.46** (503 μL, 5.12 mmol, 2.0 equiv), and TFA (588 μL, 7.69 mmol, 3.0 equiv)

were added. The vial was sealed with a Teflon-lined screw cap and stirred at 80 °C for 16 h. After

cooling to 23 °C, the volatiles were removed under reduced pressure, and the crude residue was

purified by flash chromatography (3:1 Hexanes:EtOAc → 1:1 Hexanes:EtOAc → 100% EtOAc)

to yield indolenine **2.47** (546 mg, 61% yield) as a tan solid. Indolenine **2.47**: mp: 186–189 ºC; R$_f$

0.26 (4:1 PhH:CH$_3$CN); ^{1}H NMR (500 MHz, CDCl$_3$): δ 9.11 (d, *J* = 2.2, 1H), 8.49 (dd, *J* = 9.1,

2.5, 1H), 7.92 (d, *J* = 7.4, 1H), 7.69 (d, *J* = 7.3, 1H), 7.41 (td, *J* = 7.6, 1.1, 1H), 7.22 (td, *J* = 7.5,

1.1, 1H), 6.73 (d, *J* = 9.1, 1H), 4.23–4.08 (m, 4H), 3.87–3.81 (m, 4H), 3.70–3.64 (m, 4H), 2.77–

2.67 (m, 2H), 1.36 (d, *J* = 14.1, 2H); ^{13}C NMR (125 MHz, CDCl$_3$): δ 179.2, 159.5, 154.1, 148.9,

145.9, 138.2, 128.3, 124.8, 123.6, 121.2, 118.4, 106.4, 66.8, 64.0, 54.5, 45.2, 31.6; IR (film): 2960,

2921, 2858, 1596, 1499 cm^{-1}; HRMS-APCI (*m/z*) [M + H]$^+$ calcd for $C_{21}H_{24}N_3O_2$, 350.18630;

found 350.18529.

2.11 Spectra Relevant to Chapter Two:

Nickel-Catalyzed Suzuki–Miyaura Coupling of Aliphatic Amides

Timothy B. Boit,[†] Nicholas A. Weires,[†] Junyong Kim,[†] and Neil K. Garg.

Purified Product, 1H NMR

7.298 7.296 7.293 7.286 7.282 7.279 7.270 7.267 7.263 7.240 7.237 7.235 7.227 7.223 7.218 7.208 7.205 7.201 7.191
4.861
4.121
3.624 3.617 3.610 3.602 3.595 3.588 3.580 3.573 3.565
2.793
1.858 1.835 1.694 1.686 1.670 1.662 1.645 1.638 1.621 1.612 1.450 1.396

Current Data Parameters
NAME   TBB-1-214p
EXPNO   1
PROCNO   1

F2 - Acquisition Parameters
Date_   20170327
Time   13.17 h
INSTRUM   av500
PROBHD   Z119248_0002 (
PULPROG   zg30
TD   65536
SOLVENT   CDCl3
NS   8
DS   0
SWH   10000.000 Hz
FIDRES   0.305176 Hz
AQ   3.2767999 sec
RG   12.14
DW   50.000 usec
DE   10.00 usec
TE   298.0 K
D1   2.00000000 sec
TD0   1
SFO1   500.1330008 MHz
NUC1   1H
P1   10.00 usec
PLW1   13.50000000 W

F2 - Processing parameters
SI   65536
SF   500.1300121 MHz
WDW   EM
SSB   0
LB   0.30 Hz
GB   0
PC   1.00

2.004 3.000   2.000 2.032 1.013 2.043   2.026 2.113 9.009 9.093

Figure 2.23 ¹H NMR (500 MHz, CDCl₃) of compound **2.4**.

Purified Product, 13C NMR

178.233   154.847 153.084   138.391 128.453 127.460 127.238   83.461 79.561   47.755 43.817 43.041   28.974 28.572 27.992

Current Data Parameters
NAME   TBB-1-214p
EXPNO   13
PROCNO   1

F2 - Acquisition Parameters
Date_   20170327
Time   13.35 h
INSTRUM   av500
PROBHD   Z119248_0002 (
PULPROG   zgpg30
TD   65536
SOLVENT   CDCl3
NS   300
DS   2
SWH   31250.000 Hz
FIDRES   0.953674 Hz
AQ   1.0485760 sec
RG   204.54
DW   16.000 usec
DE   18.00 usec
TE   298.0 K
D1   2.00000000 sec
D11   0.03000000 sec
TD0   1
SFO1   125.7722511 MHz
NUC1   13C
P1   10.50 usec
PLW1   23.00000000 W
SFO2   500.1330008 MHz
NUC2   1H
CPDPRG[2   waltz16
PCPD2   80.00 usec
PLW2   13.50000000 W
PLW12   0.21094000 W
PLW13   0.10610000 W

F2 - Processing parameters
SI   131072
SF   125.7577748 MHz
WDW   EM
SSB   0
LB   1.00 Hz
GB   0
PC   1.40

Figure 2.24 ¹³C NMR (125 MHz, CDCl₃) of compound **2.4**.

113

7.298 7.283 7.268 7.237 7.222 7.216 7.200
4.908 4.878 4.817 4.787 4.164 4.035 3.535 3.529 3.521 3.514 3.507 3.500 3.493 3.486 3.479 3.011 2.986 2.963 2.745 2.105 1.724 1.718 1.704 1.699 1.612 1.609 1.588 1.574 1.563 1.543 1.528 1.521 1.450 1.403

Boc—N, O, Boc
N
Bn

2.50

Current Data Parameters
NAME   TBB-1-082p
EXPNO   4
PROCNO   1

F2 - Acquisition Parameters
Date_   20170327
Time   13.54 h
INSTRUM   av500
PROBHD   Z119248_0002 (
PULPROG   zg30
TD   65536
SOLVENT   CDCl3
NS   8
DS   0
SWH   10000.000 Hz
FIDRES   0.305176 Hz
AQ   3.2767999 sec
RG   12.14
DW   50.000 usec
DE   10.00 usec
TE   298.0 K
D1   2.00000000 sec
TD0   1
SFO1   500.1330008 MHz
NUC1   1H
P1   10.00 usec
PLW1   13.50000000 W

F2 - Processing parameters
SI   65536
SF   500.1300121 MHz
WDW   EM
SSB   0
LB   0.30 Hz
GB   0
PC   1.00

10 9 8 7 6 5 4 3 2 1 0 ppm

1.988 3.010   2.030   2.024 1.000 0.996 1.007   0.995 1.072 2.099 9.058 9.036

Figure 2.25 ^{1}H NMR (500 MHz, CDCl$_3$) of compound **2.50**.

177.199   154.849 152.890   138.334 128.480 127.522 127.258   83.610 79.651   47.686 43.457   28.710 28.583 28.005 24.676

Current Data Parameters
NAME   TBB-1-082p
EXPNO   2
PROCNO   1

F2 - Acquisition Parameters
Date_   20170327
Time   13.02 h
INSTRUM   av500
PROBHD   Z119248_0002 (
PULPROG   zgpg30
TD   65536
SOLVENT   CDCl3
NS   550
DS   2
SWH   31250.000 Hz
FIDRES   0.953674 Hz
AQ   1.0485760 sec
RG   204.54
DW   16.000 usec
DE   18.00 usec
TE   298.0 K
D1   2.00000000 sec
D11   0.03000000 sec
TD0   1
SFO1   125.7722511 MHz
NUC1   13C
P1   10.50 usec
PLW1   23.00000000 W
SFO2   500.1330008 MHz
NUC2   1H
CPDPRG[2   waltz16
PCPD2   80.00 usec
PLW2   13.50000000 W
PLW12   0.21094000 W
PLW13   0.10610000 W

F2 - Processing parameters
SI   131072
SF   125.7577721 MHz
WDW   EM
SSB   0
LB   1.00 Hz
GB   0
PC   1.40

230 220 210 200 190 180 170 160 150 140 130 120 110 100 90 80 70 60 50 40 30 20 10 ppm

Figure 2.26 ^{13}C NMR (125 MHz, CDCl$_3$) of compound **2.50**.

114

Figure 2.27 ¹H NMR (500 MHz, CDCl₃) of compound **2.52**.

Figure 2.28 ¹³C NMR (125 MHz, CDCl₃) of compound **2.52**.
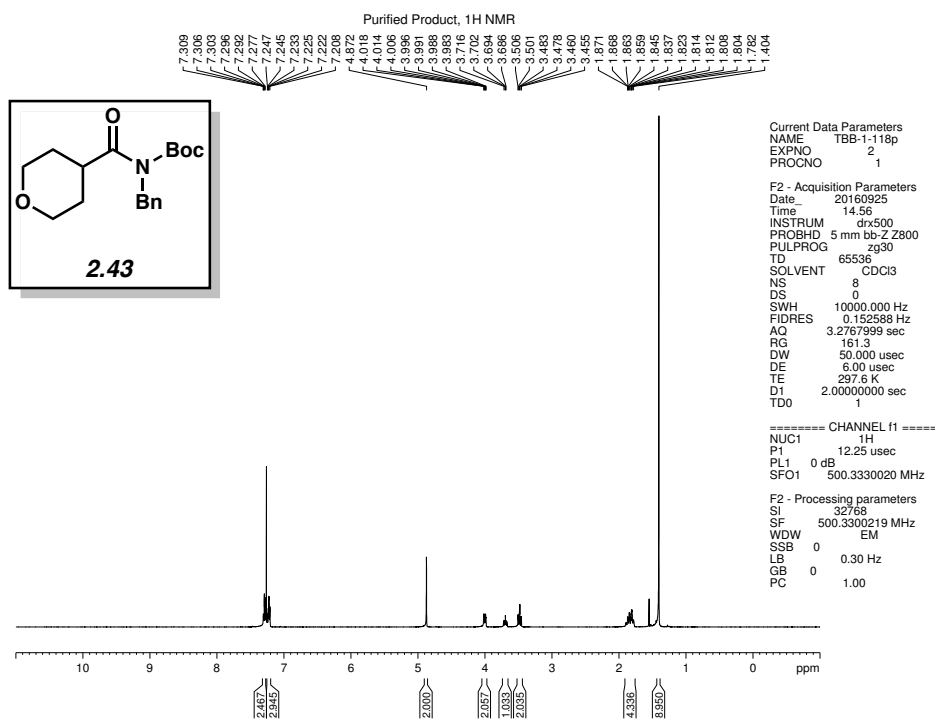
Figure 2.29 ¹H NMR (500 MHz, CDCl₃) of compound **2.43**.
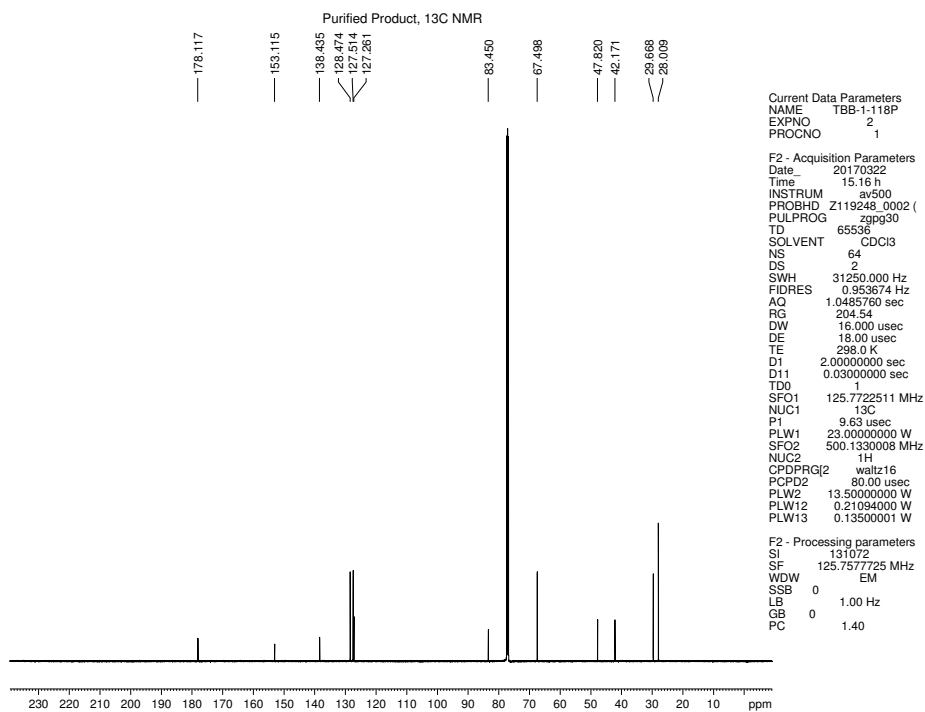
Figure 2.30 ¹³C NMR (125 MHz, CDCl₃) of compound **2.43**.
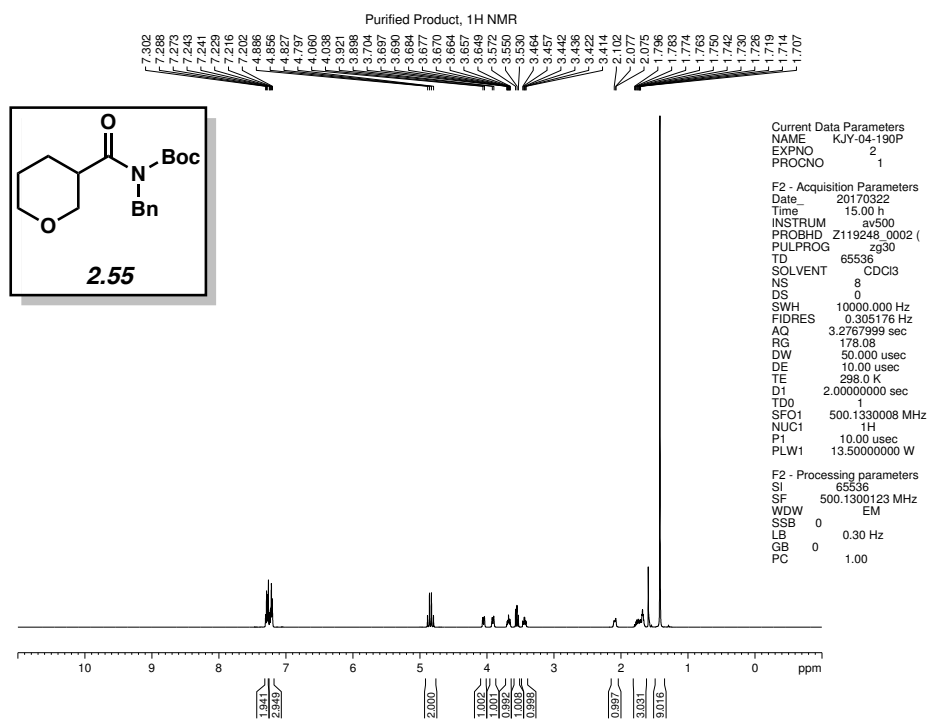
Figure 2.31 ^{1}H NMR (500 MHz, CDCl$_3$) of compound **2.55**.
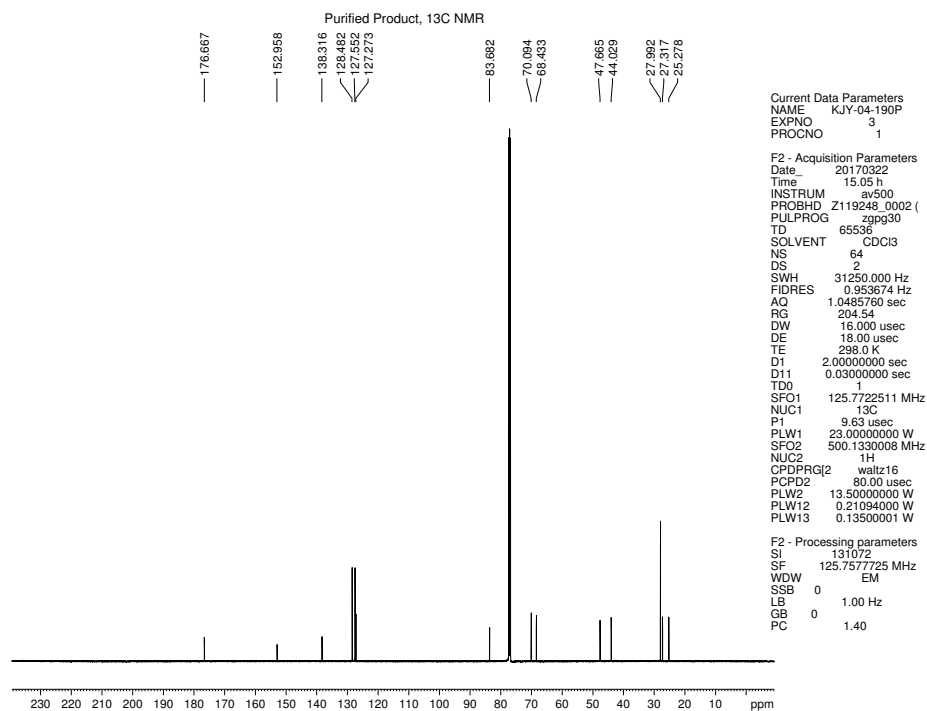
Figure 2.32 ^{13}C NMR (125 MHz, CDCl$_3$) of compound **2.55**.

117
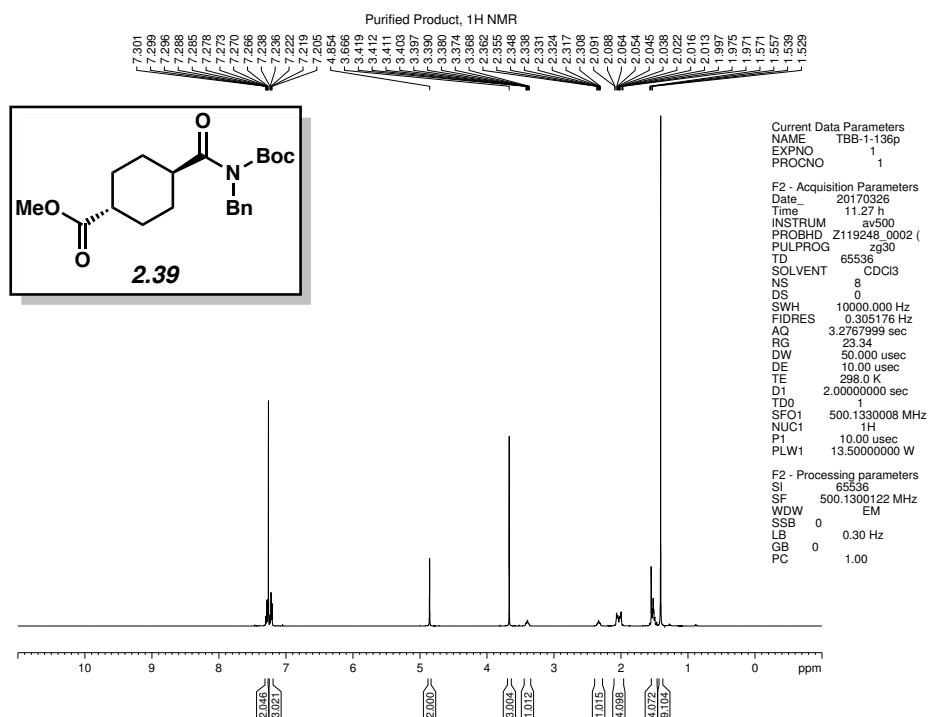
Figure 2.33 ^{1}H NMR (500 MHz, CDCl$_3$) of compound **2.39**.
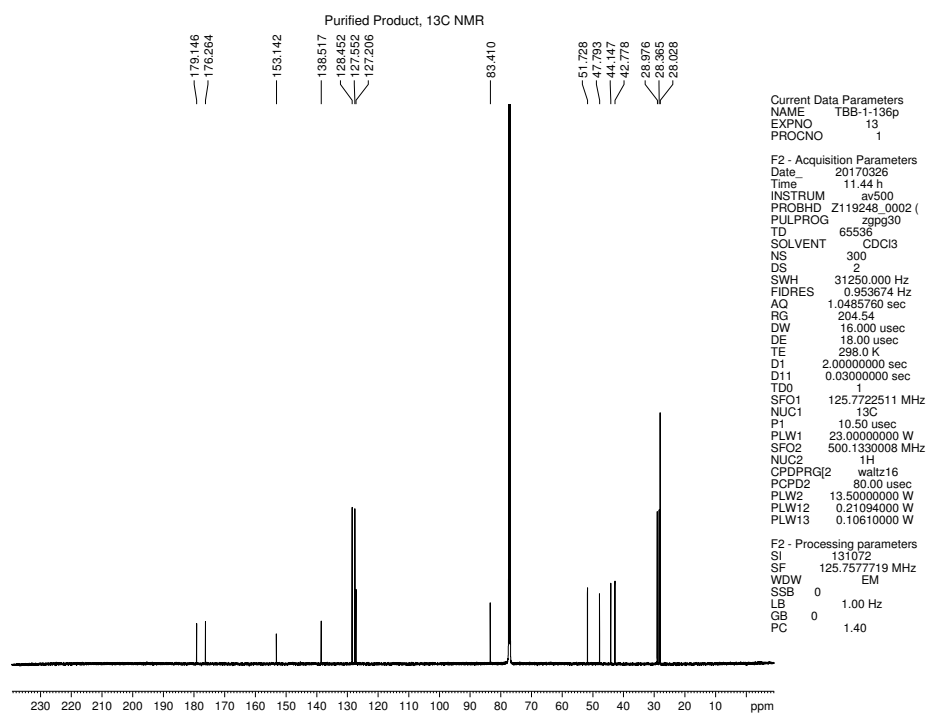
Figure 2.34 ^{13}C NMR (125 MHz, CDCl$_3$) of compound **2.39**.

Figure 2.35 ¹H NMR (500 MHz, CDCl₃) of compound **2.6**.
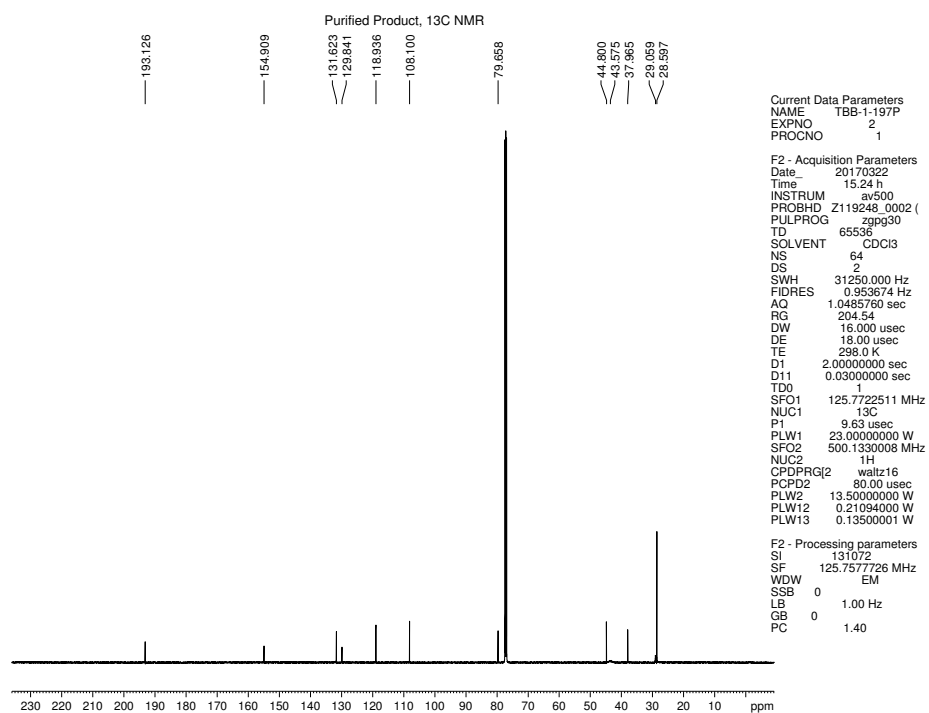
Figure 2.36 ¹³C NMR (125 MHz, CDCl₃) of compound **2.6**.

Figure 2.37 ^{1}H NMR (500 MHz, CDCl₃) of compound **2.11**.

Figure 2.38 ^{13}C NMR (125 MHz, CDCl₃) of compound **2.11**.
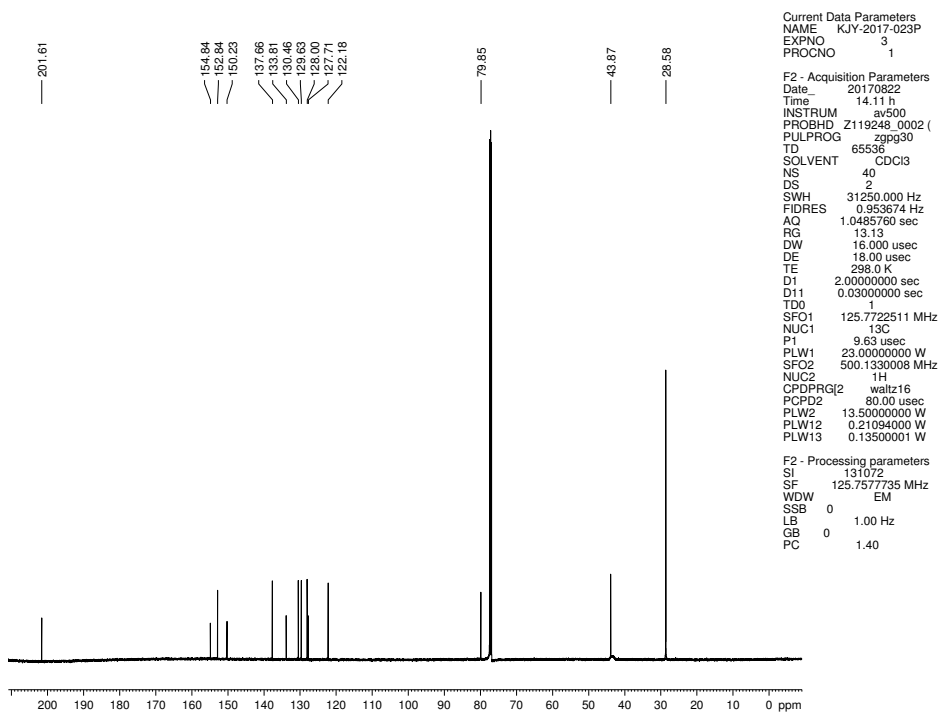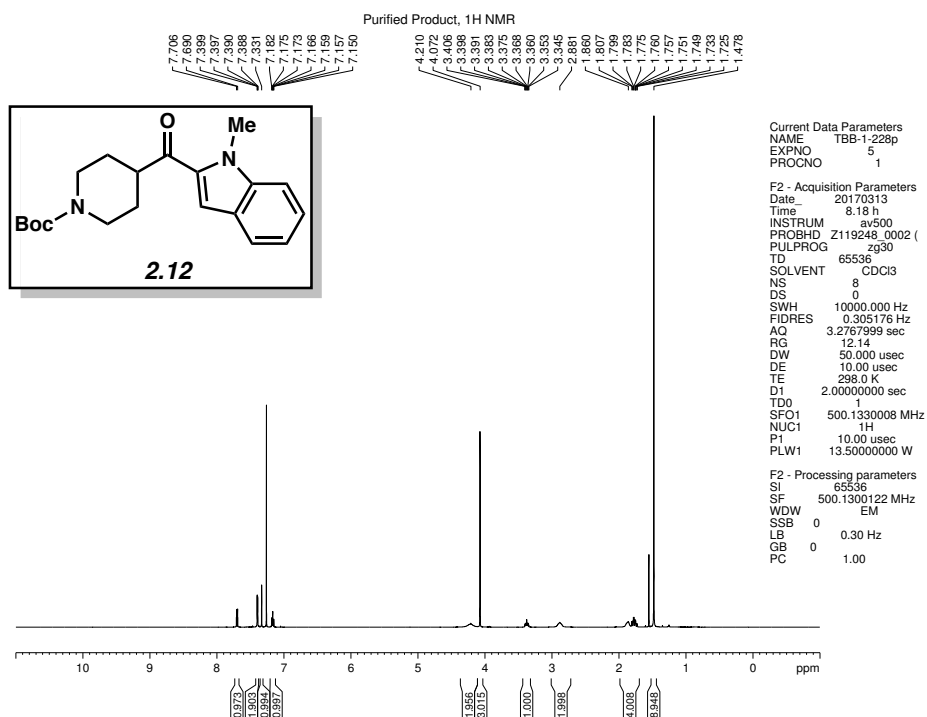
Figure 2.39 ^{1}H NMR (500 MHz, CDCl$_3$) of compound **2.12**.
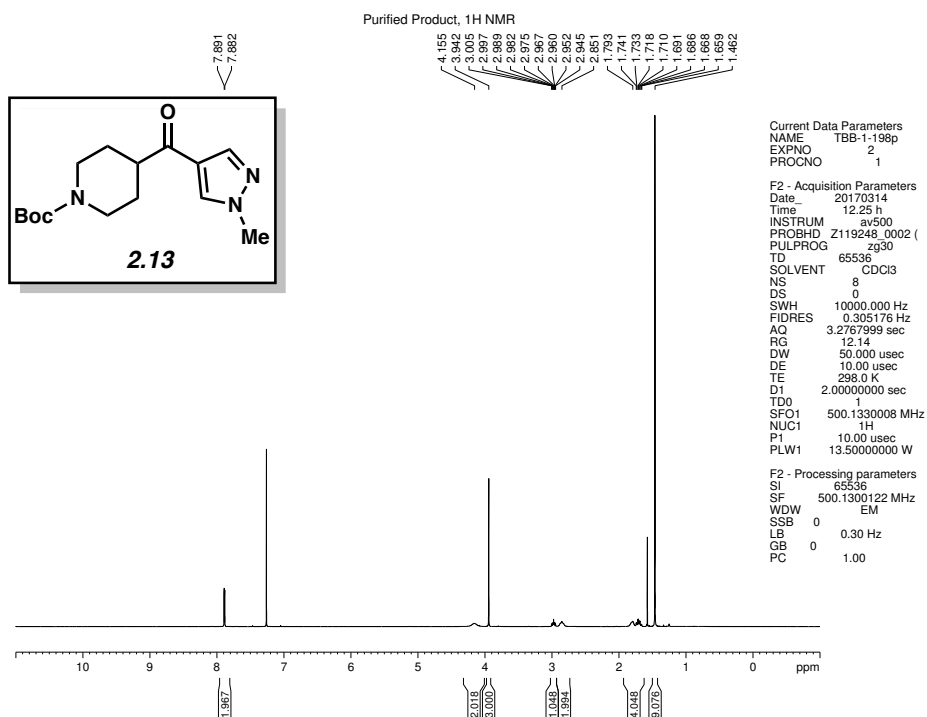
Figure 2.40 ^{1}H NMR (500 MHz, CDCl$_3$) of compound **2.13**.

196.400
154.839
140.405
132.796
123.041
79.768
46.262
39.558
28.588
28.421

Current Data Parameters
NAME   TBB-1-198p
EXPNO   13
PROCNO   1

F2 - Acquisition Parameters
Date_   20170314
Time   12.41 h
INSTRUM   av500
PROBHD Z119248_0002 (
PULPROG   zgpg30
TD   65536
SOLVENT   CDCl3
NS   225
DS   2
SWH   31250.000 Hz
FIDRES   0.953674 Hz
AQ   1.0485760 sec
RG   204.54
DW   16.000 usec
DE   18.00 usec
TE   298.0 K
D1   2.00000000 sec
D11   0.03000000 sec
TD0   1
SFO1   125.7722511 MHz
NUC1   13C
P1   10.50 usec
PLW1   23.00000000 W
SFO2   500.1330008 MHz
NUC2   1H
CPDPRG[2   waltz16
PCPD2   80.00 usec
PLW2   13.50000000 W
PLW12   0.21094000 W
PLW13   0.10610000 W

F2 - Processing parameters
SI   131072
SF   125.7577719 MHz
WDW   EM
SSB   0
LB   1.00 Hz
GB   0
PC   1.40

230 220 210 200 190 180 170 160 150 140 130 120 110 100 90 80 70 60 50 40 30 20 10 ppm

Figure 2.41 ^{13}C NMR (125 MHz, CDCl$_3$) of compound **2.13**.

7.481
7.477
6.838
6.834
4.155
3.145
3.138
3.130
3.123
3.115
3.108
3.100
3.093
3.085
2.842
1.832
1.809
1.730
1.721
1.706
1.697
1.682
1.679
1.674
1.671
1.461

2.14

Current Data Parameters
NAME   TBB-2017-030P
EXPNO   2
PROCNO   1

F2 - Acquisition Parameters
Date_   20170822
Time   14.24 h
INSTRUM   av500
PROBHD Z119248_0002 (
PULPROG   zg30
TD   65536
SOLVENT   CDCl3
NS   8
DS   0
SWH   10000.000 Hz
FIDRES   0.305176 Hz
AQ   3.2767999 sec
RG   26.59
DW   50.000 usec
DE   10.00 usec
TE   298.0 K
D1   2.00000000 sec
TD0   1
SFO1   500.1330008 MHz
NUC1   1H
P1   10.00 usec
PLW1   13.50000000 W

F2 - Processing parameters
SI   65536
SF   500.1300121 MHz
WDW   EM
SSB   0
LB   0.30 Hz
GB   0
PC   1.00

10   9   8   7   6   5   4   3   2   1   0 ppm

1.000
1.029
5.045
1.045
2.040
2.047
2.000
9.185

Figure 2.42 ^{1}H NMR (500 MHz, CDCl$_3$) of compound **2.14**.

122
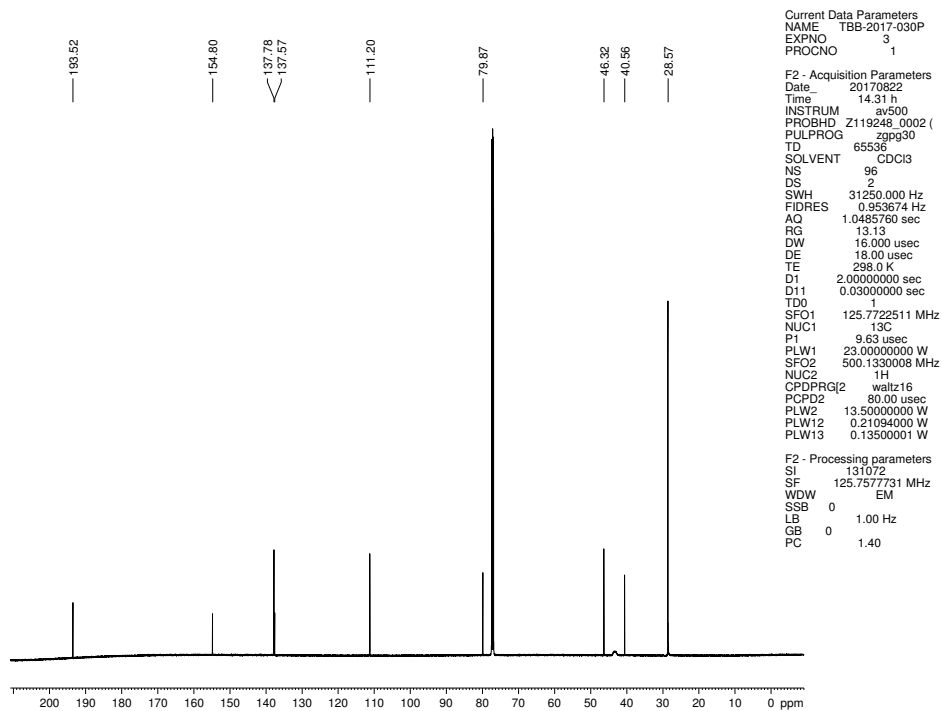
Figure 2.43 ¹³C NMR (125 MHz, CDCl₃) of compound **2.14**.

Figure 2.44 ¹H NMR (500 MHz, CDCl₃) of compound **2.15**.

202.50

160.54
154.79
149.32
144.09

111.12
104.71

79.87

66.80

45.58
44.19

28.56
28.17

Current Data Parameters
NAME   KJY-2017-025P
EXPNO   3
PROCNO   1

F2 - Acquisition Parameters
Date_   20170822
Time   14.20 h
INSTRUM   av500
PROBHD Z119248_0002 (
PULPROG   zgpg30
TD   65536
SOLVENT   CDCl3
NS   48
DS   2
SWH   31250.000 Hz
FIDRES   0.953674 Hz
AQ   1.0485760 sec
RG   13.13
DW   16.000 usec
DE   18.00 usec
TE   298.0 K
D1   2.00000000 sec
D11   0.03000000 sec
TD0   1
SFO1   125.7722511 MHz
NUC1   13C
P1   9.63 usec
PLW1   23.00000000 W
SFO2   500.1330008 MHz
NUC2   1H
CPDPRG[2   waltz16
PCPD2   80.00 usec
PLW2   13.50000000 W
PLW12   0.21094000 W
PLW13   0.13500001 W

F2 - Processing parameters
SI   131072
SF   125.7577733 MHz
WDW   EM
SSB   0
LB   1.00 Hz
GB   0
PC   1.40

Figure 2.45 ^{13}C NMR (125 MHz, CDCl$_3$) of compound **2.15**.

Purified Product, 1H NMR

8.783
8.779

8.063
8.045
8.040

6.638
6.621
6.620

4.167
3.822
3.812
3.806
3.802
3.690
3.679
3.670
3.299
3.292
3.277
3.270
3.262
3.255
3.248
3.240
2.869
1.796
1.749
1.741
1.726
1.718
1.699
1.676
1.669
1.465

Current Data Parameters
NAME   TBB-1-242p
EXPNO   1
PROCNO   1

F2 - Acquisition Parameters
Date_   20170312
Time   20.37 h
INSTRUM   av500
PROBHD Z119248_0002 (
PULPROG   zg30
TD   65536
SOLVENT   CDCl3
NS   8
DS   0
SWH   10000.000 Hz
FIDRES   0.305176 Hz
AQ   3.2767999 sec
RG   12.14
DW   50.000 usec
DE   10.00 usec
TE   298.0 K
D1   2.00000000 sec
TD0   1
SFO1   500.1330008 MHz
NUC1   1H
P1   10.00 usec
PLW1   13.50000000 W

F2 - Processing parameters
SI   65536
SF   500.1300122 MHz
WDW   EM
SSB   0
LB   0.30 Hz
GB   0
PC   1.00

1.000
1.003
1.012
2.070
4.077
4.047
1.012
2.069
4.167
9.348

Figure 2.46 ^{1}H NMR (500 MHz, CDCl$_3$) of compound **2.16**.

124

Purified Product, 13C NMR

199.425

160.687
154.879
150.371

137.859

121.517

105.890

79.751

66.734

45.047
43.343

28.595

Current Data Parameters
NAME   TBB-1-242p
EXPNO   13
PROCNO   1

F2 - Acquisition Parameters
Date_   20170312
Time   20.56 h
INSTRUM   av500
PROBHD Z119248_0002 (
PULPROG   zgpg30
TD   65536
SOLVENT   CDCl3
NS   203
DS   2
SWH   31250.000 Hz
FIDRES   0.953674 Hz
AQ   1.0485760 sec
RG   14.67
DW   16.000 usec
DE   18.00 usec
TE   298.0 K
D1   2.00000000 sec
D11   0.03000000 sec
TD0   1
SFO1   125.7722511 MHz
NUC1   13C
P1   9.63 usec
PLW1   23.00000000 W
SFO2   500.1330008 MHz
NUC2   1H
CPDPRG[2   waltz16
PCPD2   80.00 usec
PLW2   13.50000000 W
PLW12   0.21094000 W
PLW13   0.13500001 W

F2 - Processing parameters
SI   131072
SF   125.7577717 MHz
WDW   EM
SSB   0
LB   1.00 Hz
GB   0
PC   1.40

230 220 210 200 190 180 170 160 150 140 130 120 110 100 90 80 70 60 50 40 30 20 10 ppm

Figure 2.47 ^{13}C NMR (125 MHz, CDCl$_3$) of compound **2.16**.

Purified Product, 1H NMR

7.054
7.048
6.821
6.147
6.142
6.140
6.135
4.224
4.126
3.927
3.160
3.138
2.892
2.695
1.984
1.963
1.760
1.752
1.730
1.709
1.702
1.683
1.581
1.552
1.551
1.549
1.467

2.17

Note: Mixture of conformers present

Current Data Parameters
NAME   TBB-1-203p
EXPNO   1
PROCNO   1

F2 - Acquisition Parameters
Date_   20170326
Time   19.02 h
INSTRUM   av500
PROBHD Z119248_0002 (
PULPROG   zg30
TD   65536
SOLVENT   CDCl3
NS   8
DS   0
SWH   10000.000 Hz
FIDRES   0.305176 Hz
AQ   3.2767999 sec
RG   12.14
DW   50.000 usec
DE   10.00 usec
TE   298.0 K
D1   2.00000000 sec
TD0   1
SFO1   500.1330008 MHz
NUC1   1H
P1   10.00 usec
PLW1   13.50000000 W

F2 - Processing parameters
SI   65536
SF   500.1300121 MHz
WDW   EM
SSB   0
LB   0.30 Hz
GB   0
PC   1.00

10 9 8 7 6 5 4 3 2 1 0 ppm

0.981
0.968
0.968
2.031
3.000
1.009
0.986
1.030
1.018
2.053
0.857
9.148

Figure 2.48 ^{1}H NMR (500 MHz, CDCl$_3$) of compound **2.17**.

192.019

154.870

131.676
129.904

119.536

108.250

79.703

47.752
47.097
45.294
44.003
37.916
28.609
28.420
24.822

Current Data Parameters
NAME   TBB-1-203p
EXPNO   13
PROCNO   1

F2 - Acquisition Parameters
Date_   20170326
Time   19.34 h
INSTRUM   av500
PROBHD Z119248_0002 (
PULPROG   zgpg30
TD   65536
SOLVENT   CDCl3
NS   222
DS   2
SWH   31250.000 Hz
FIDRES   0.953674 Hz
AQ   1.0485760 sec
RG   204.54
DW   16.000 usec
DE   18.00 usec
TE   298.0 K
D1   2.00000000 sec
D11   0.03000000 sec
TD0   1
SFO1   125.7722511 MHz
NUC1   13C
P1   10.50 usec
PLW1   23.00000000 W
SFO2   500.1330008 MHz
NUC2   1H
CPDPRG[2   waltz16
PCPD2   80.00 usec
PLW2   13.50000000 W
PLW12   0.21094000 W
PLW13   0.10610000 W

F2 - Processing parameters
SI   131072
SF   125.7577736 MHz
WDW   EM
SSB   0
LB   1.00 Hz
GB   0
PC   1.40

230 220 210 200 190 180 170 160 150 140 130 120 110 100 90 80 70 60 50 40 30 20 10 ppm

Figure 2.49 ¹³C NMR (125 MHz, CDCl₃) of compound **2.17**.

7.927
7.909

4.247
4.091
3.939
2.980
2.959
2.861
2.716
2.003
1.976
1.763
1.735
1.713
1.688
1.558
1.529
1.525
1.516
1.508
1.500

2.18

*Note: Mixture of
conformers present*

Current Data Parameters
NAME   TBB-1-204p
EXPNO   2
PROCNO   1

F2 - Acquisition Parameters
Date_   20170124
Time   13.03 h
INSTRUM   av500
PROBHD Z119248_0002 (
PULPROG   zg30
TD   65536
SOLVENT   CDCl3
NS   8
DS   0
SWH   10000.000 Hz
FIDRES   0.305176 Hz
AQ   3.2767999 sec
RG   12.14
DW   50.000 usec
DE   10.00 usec
TE   298.0 K
D1   2.00000000 sec
TD0   1
SFO1   500.1330008 MHz
NUC1   1H
P1   10.00 usec
PLW1   13.50000000 W

F2 - Processing parameters
SI   65536
SF   500.1300146 MHz
WDW   EM
SSB   0
LB   0.30 Hz
GB   0
PC   1.00

10 9 8 7 6 5 4 3 2 1 0 ppm

1.000
0.900

2.033
3.036

3.070

1.052
2.070
10.165

Figure 2.50 ¹H NMR (500 MHz, CDCl₃) of compound **2.18**.

126

Figure 2.51 ^{13}C NMR (125 MHz, CDCl$_3$) of compound **2.18**.
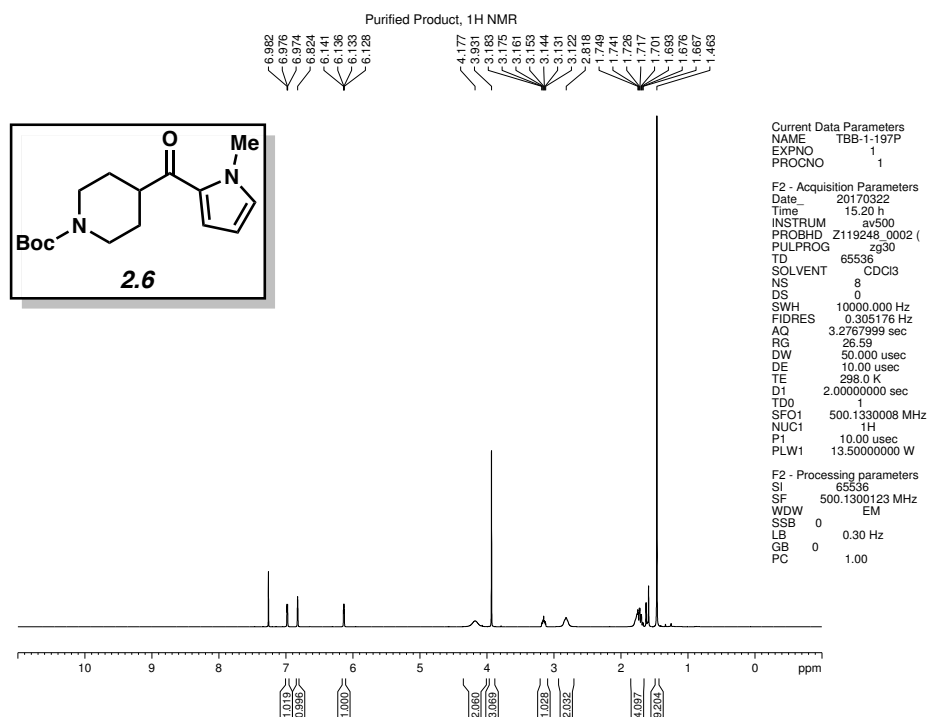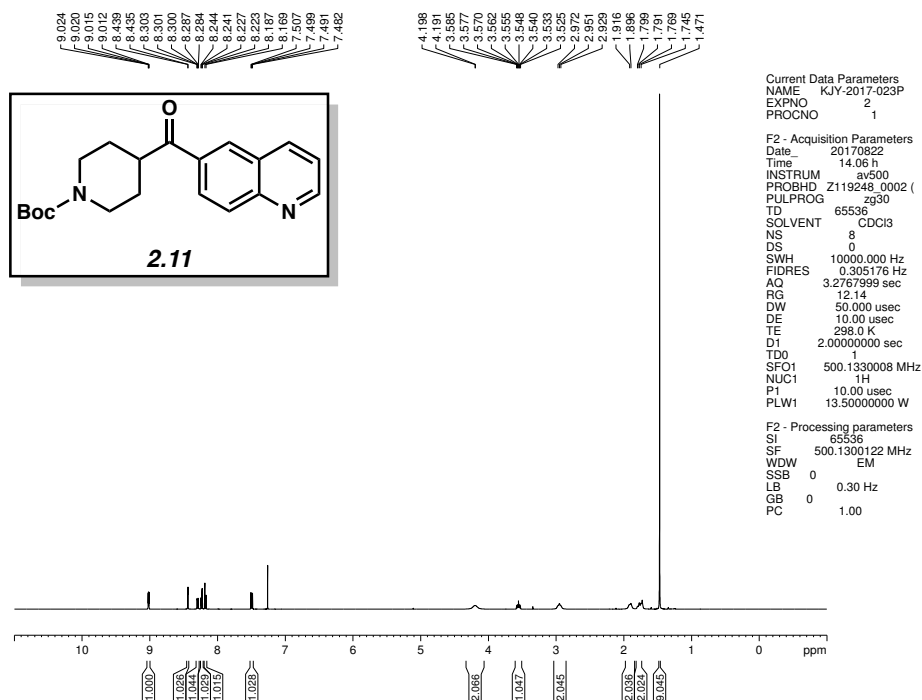

Figure 2.52 ^{1}H NMR (500 MHz, CDCl$_3$) of compound **2.19**.

193.074
192.895
154.503
140.474
134.182
126.445
125.859
123.109
121.064
111.971
110.561
79.525
48.996
48.917
47.252
46.316
45.803
45.589
32.416
29.678
29.442
28.642

Current Data Parameters
NAME   KJY-04-188P
EXPNO   3
PROCNO   1

F2 - Acquisition Parameters
Date_   20170313
Time   14.38 h
INSTRUM   av500
PROBHD Z119248_0002 (
PULPROG   zgpg30
TD   65536
SOLVENT   CDCl3
NS   40
DS   2
SWH   31250.000 Hz
FIDRES   0.953674 Hz
AQ   1.0485760 sec
RG   204.54
DW   16.000 usec
DE   18.00 usec
TE   298.0 K
D1   2.00000000 sec
D11   0.03000000 sec
TD0   1
SFO1   125.7722511 MHz
NUC1   13C
P1   9.63 usec
PLW1   23.00000000 W
SFO2   500.1330008 MHz
NUC2   1H
CPDPRG[2   waltz16
PCPD2   80.00 usec
PLW2   13.50000000 W
PLW12   0.21094000 W
PLW13   0.13500001 W

F2 - Processing parameters
SI   131072
SF   125.7577760 MHz
WDW   EM
SSB   0
LB   1.00 Hz
GB   0
PC   1.40

230 220 210 200 190 180 170 160 150 140 130 120 110 100 90 80 70 60 50 40 30 20 10 ppm

Figure 2.53 ^{13}C NMR (125 MHz, CDCl$_3$) of compound **2.19**.

6.975
6.833
6.139
3.934
3.759
3.744
3.712
3.691
3.573
3.518
3.385
2.203
2.188
2.164
2.147
2.084
1.450

2.20

Note: Mixture of conformers present

Current Data Parameters
NAME   KJY-04-186P
EXPNO   2
PROCNO   1

F2 - Acquisition Parameters
Date_   20170313
Time   14.46 h
INSTRUM   av500
PROBHD Z119248_0002 (
PULPROG   zg30
TD   65536
SOLVENT   CDCl3
NS   8
DS   0
SWH   10000.000 Hz
FIDRES   0.305176 Hz
AQ   3.2767999 sec
RG   12.14
DW   50.000 usec
DE   10.00 usec
TE   298.0 K
D1   2.00000000 sec
TD0   1
SFO1   500.1330008 MHz
NUC1   1H
P1   10.00 usec
PLW1   13.50000000 W

F2 - Processing parameters
SI   65536
SF   500.1300126 MHz
WDW   EM
SSB   0
LB   0.30 Hz
GB   0
PC   1.00

10 9 8 7 6 5 4 3 2 1 0 ppm

1.000
0.980
0.976
2.983
4.077
1.032
0.971
1.070
9.064

Figure 2.54 ^{1}H NMR (500 MHz, CDCl$_3$) of compound **2.20**.

Purified Product, 13C NMR

189.915
189.686
154.519
131.852
130.232
119.604
108.356
79.374
49.036
48.913
46.420
45.878
45.643
45.455
37.921
29.535
29.427
28.640

Current Data Parameters
NAME   KJY-04-186P
EXPNO   3
PROCNO   1

F2 - Acquisition Parameters
Date_   20170313
Time   14.49 h
INSTRUM   av500
PROBHD   Z119248_0002 (
PULPROG   zgpg30
TD   65536
SOLVENT   CDCl3
NS   40
DS   2
SWH   31250.000 Hz
FIDRES   0.953674 Hz
AQ   1.0485760 sec
RG   204.54
DW   16.000 usec
DE   18.00 usec
TE   298.0 K
D1   2.00000000 sec
D11   0.03000000 sec
TD0   1
SFO1   125.7722511 MHz
NUC1   13C
P1   9.63 usec
PLW1   23.00000000 W
SFO2   500.1330008 MHz
NUC2   1H
CPDPRG[2   waltz16
PCPD2   80.00 usec
PLW2   13.50000000 W
PLW12   0.21094000 W
PLW13   0.13500001 W

F2 - Processing parameters
SI   131072
SF   125.7577749 MHz
WDW   EM
SSB   0
LB   1.00 Hz
GB   0
PC   1.40

230 220 210 200 190 180 170 160 150 140 130 120 110 100 90 80 70 60 50 40 30 20 10 ppm

Figure 2.55 ^{13}C NMR (125 MHz, CDCl$_3$) of compound **2.20**.

Purified Product, 1H NMR

6.985
6.977
6.824
6.140
6.133
6.128
4.062
4.055
4.040
4.032
3.938
3.533
3.509
3.486
3.289
3.281
3.274
3.266
3.258
3.251
3.243
3.235
3.228
1.949
1.940
1.922
1.916
1.898
1.890
1.875
1.866
1.714
1.688

2.21

Current Data Parameters
NAME   KJY-04-175P
EXPNO   2
PROCNO   1

F2 - Acquisition Parameters
Date_   20170313
Time   15.05 h
INSTRUM   av500
PROBHD   Z119248_0002 (
PULPROG   zg30
TD   65536
SOLVENT   CDCl3
NS   8
DS   0
SWH   10000.000 Hz
FIDRES   0.305176 Hz
AQ   3.2767999 sec
RG   23.34
DW   50.000 usec
DE   10.00 usec
TE   298.0 K
D1   2.00000000 sec
TD0   1
SFO1   500.1330008 MHz
NUC1   1H
P1   10.00 usec
PLW1   13.50000000 W

F2 - Processing parameters
SI   65536
SF   500.1300127 MHz
WDW   EM
SSB   0
LB   0.30 Hz
GB   0
PC   1.00

10 9 8 7 6 5 4 3 2 1 0 ppm

1.000
0.979
0.976
2.045
2.993
2.021
1.001
2.027
2.045

Figure 2.56 ^{1}H NMR (500 MHz, CDCl$_3$) of compound **2.21**.

129

Purified Product, 13C NMR

192.891 131.556 129.778 118.862 108.070 67.573 43.845 37.955 29.713

Current Data Parameters
NAME   KJY-04-175P
EXPNO   3
PROCNO   1

F2 - Acquisition Parameters
Date_   20170313
Time   15.08 h
INSTRUM   av500
PROBHD Z119248_0002 (
PULPROG   zgpg30
TD   65536
SOLVENT   CDCl3
NS   40
DS   2
SWH   31250.000 Hz
FIDRES   0.953674 Hz
AQ   1.0485760 sec
RG   204.54
DW   16.000 usec
DE   18.00 usec
TE   298.0 K
D1   2.00000000 sec
D11   0.03000000 sec
TD0   1
SFO1   125.7722511 MHz
NUC1   13C
P1   9.63 usec
PLW1   23.00000000 W
SFO2   500.1330008 MHz
NUC2   1H
CPDPRG[2   waltz16
PCPD2   80.00 usec
PLW2   13.50000000 W
PLW12   0.21094000 W
PLW13   0.13500001 W

F2 - Processing parameters
SI   131072
SF   125.7577737 MHz
WDW   EM
SSB   0
LB   1.00 Hz
GB   0
PC   1.40

230 220 210 200 190 180 170 160 150 140 130 120 110 100 90 80 70 60 50 40 30 20 10 ppm

Figure 2.57 ^{13}C NMR (125 MHz, CDCl$_3$) of compound **2.21**.

Purified Product, 1H NMR

7.709 7.692 7.397 7.390 7.334 7.184 7.176 7.168 7.161 7.160 7.153 4.103 4.099 4.096 4.079 3.592 3.569 3.545 3.511 3.503 3.496 3.488 3.480 3.473 3.466 3.457 3.450 2.005 1.997 1.978 1.973 1.955 1.946 1.931 1.923 1.819 1.793

Current Data Parameters
NAME   KJY-04-179P
EXPNO   2
PROCNO   1

F2 - Acquisition Parameters
Date_   20170313
Time   14.53 h
INSTRUM   av500
PROBHD Z119248_0002 (
PULPROG   zg30
TD   65536
SOLVENT   CDCl3
NS   8
DS   0
SWH   10000.000 Hz
FIDRES   0.305176 Hz
AQ   3.2767999 sec
RG   21.37
DW   50.000 usec
DE   10.00 usec
TE   298.0 K
D1   2.00000000 sec
TD0   1
SFO1   500.1330008 MHz
NUC1   1H
P1   10.00 usec
PLW1   13.50000000 W

F2 - Processing parameters
SI   65536
SF   500.1300125 MHz
WDW   EM
SSB   0
LB   0.30 Hz
GB   0
PC   1.00

10 9 8 7 6 5 4 3 2 1 0 ppm

1.000 1.997 1.009 1.011   0.986 4.124   2.053 1.031   2.088 2.072

Figure 2.58 ^{1}H NMR (500 MHz, CDCl$_3$) of compound **2.22**.

130

Figure 2.59 ^{13}C NMR (125 MHz, CDCl[3]) of compound **2.22**.

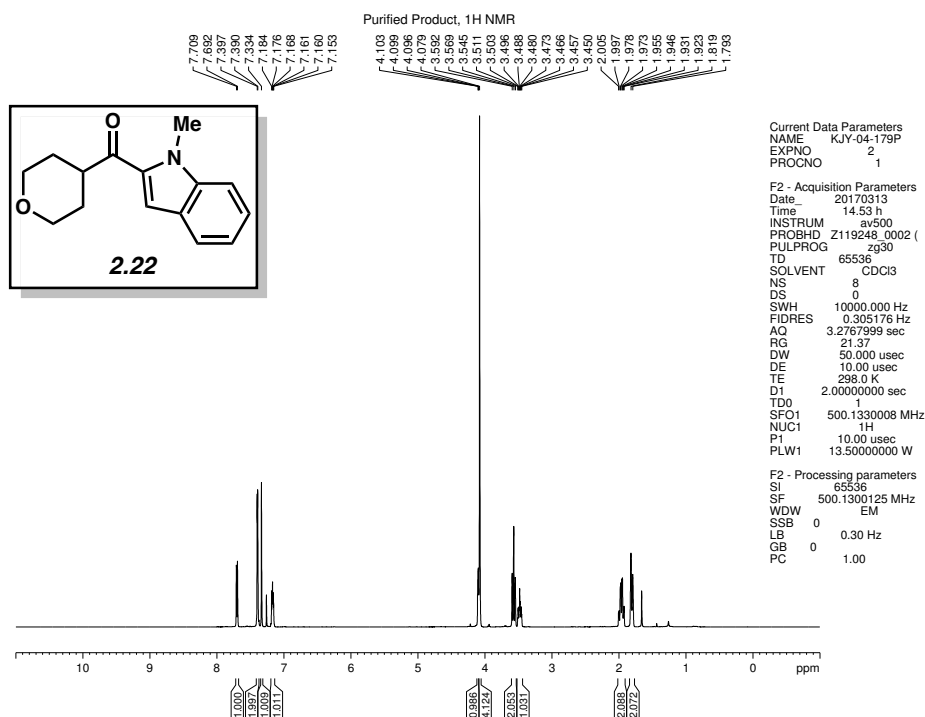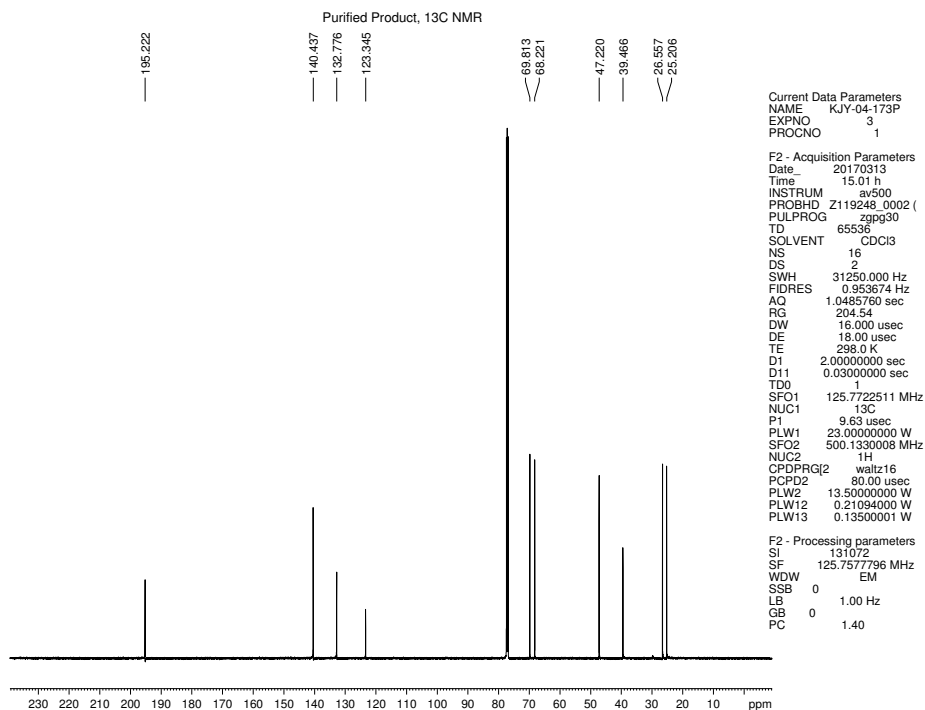*Figure 2.60* ^{1}H NMR (500 MHz, CDCl[3]) of compound **2.23**.

Purified Product, 13C NMR

195.222
140.437
132.776
123.345
69.813
68.221
47.220
39.466
26.557
25.206

Current Data Parameters
NAME   KJY-04-173P
EXPNO   3
PROCNO   1

F2 - Acquisition Parameters
Date_   20170313
Time   15.01 h
INSTRUM   av500
PROBHD Z119248_0002 (
PULPROG   zgpg30
TD   65536
SOLVENT   CDCl3
NS   16
DS   2
SWH   31250.000 Hz
FIDRES   0.953674 Hz
AQ   1.0485760 sec
RG   204.54
DW   16.000 usec
DE   18.00 usec
TE   298.0 K
D1   2.00000000 sec
D11   0.03000000 sec
TD0   1
SFO1   125.7722511 MHz
NUC1   13C
P1   9.63 usec
PLW1   23.00000000 W
SFO2   500.1330008 MHz
NUC2   1H
CPDPRG[2   waltz16
PCPD2   80.00 usec
PLW2   13.50000000 W
PLW12   0.21094000 W
PLW13   0.13500001 W

F2 - Processing parameters
SI   131072
SF   125.7577796 MHz
WDW   EM
SSB   0
LB   1.00 Hz
GB   0
PC   1.40

230 220 210 200 190 180 170 160 150 140 130 120 110 100 90 80 70 60 50 40 30 20 10 ppm

Figure 2.61 ^{13}C NMR (125 MHz, CDCl$_3$) of compound **2.23**.

Purified Product, 1H NMR

7.024
7.019
7.016
6.810
6.131
6.128
4.071
4.067
4.048
4.045
3.959
3.955
3.937
3.932
3.907
3.546
3.524
3.502
3.435
3.429
3.412
3.406
3.398
3.390
3.383
3.376
3.368
3.360
3.354
3.346
3.338
1.980
1.977
1.955
1.952
1.885
1.875
1.861
1.851
1.836
1.827
1.812
1.803
1.782
1.774
1.759
1.748

2.24

Current Data Parameters
NAME   KJY-04-197P
EXPNO   2
PROCNO   1

F2 - Acquisition Parameters
Date_   20170313
Time   14.26 h
INSTRUM   av500
PROBHD Z119248_0002 (
PULPROG   zg30
TD   65536
SOLVENT   CDCl3
NS   8
DS   0
SWH   10000.000 Hz
FIDRES   0.305176 Hz
AQ   3.2767999 sec
RG   12.14
DW   50.000 usec
DE   10.00 usec
TE   298.0 K
D1   2.00000000 sec
TD0   1
SFO1   500.1330008 MHz
NUC1   1H
P1   10.00 usec
PLW1   13.50000000 W

F2 - Processing parameters
SI   65536
SF   500.1300122 MHz
WDW   EM
SSB   0
LB   0.30 Hz
GB   0
PC   1.00

10   9   8   7   6   5   4   3   2   1   0   ppm

1.000
0.973
0.978
1.039
1.051
2.958
1.013
2.015
1.025
1.043
2.283

Figure 2.62 ^{1}H NMR (500 MHz, CDCl$_3$) of compound **2.24**.

132

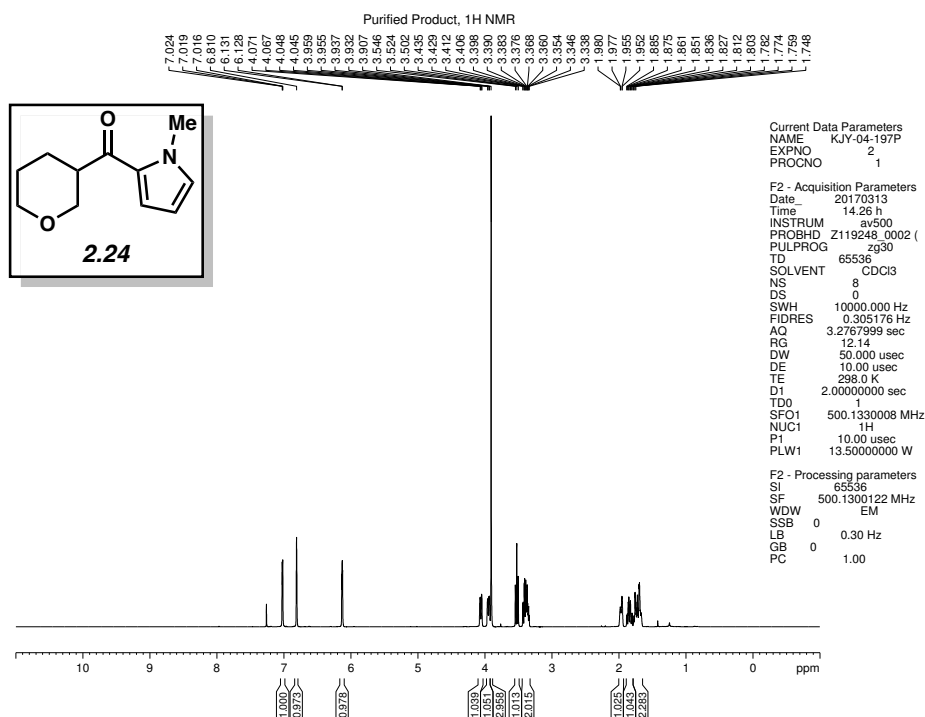*Figure 2.63* ¹³C NMR (125 MHz, CDCl₃) of compound **2.24**.

Figure 2.64 ¹H NMR (500 MHz, CDCl₃) of compound **2.25**.
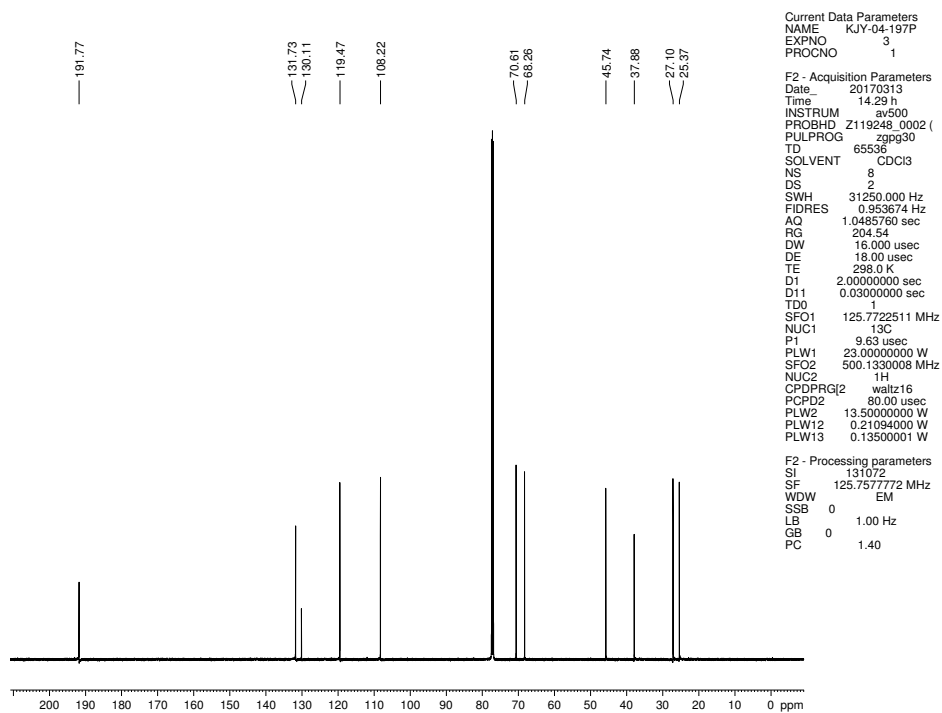
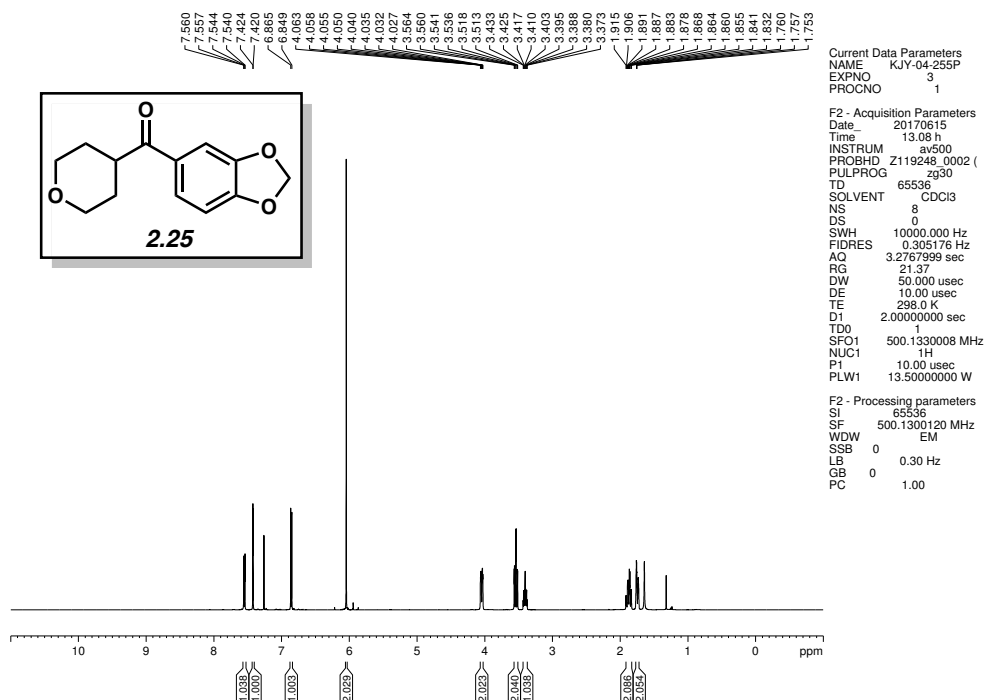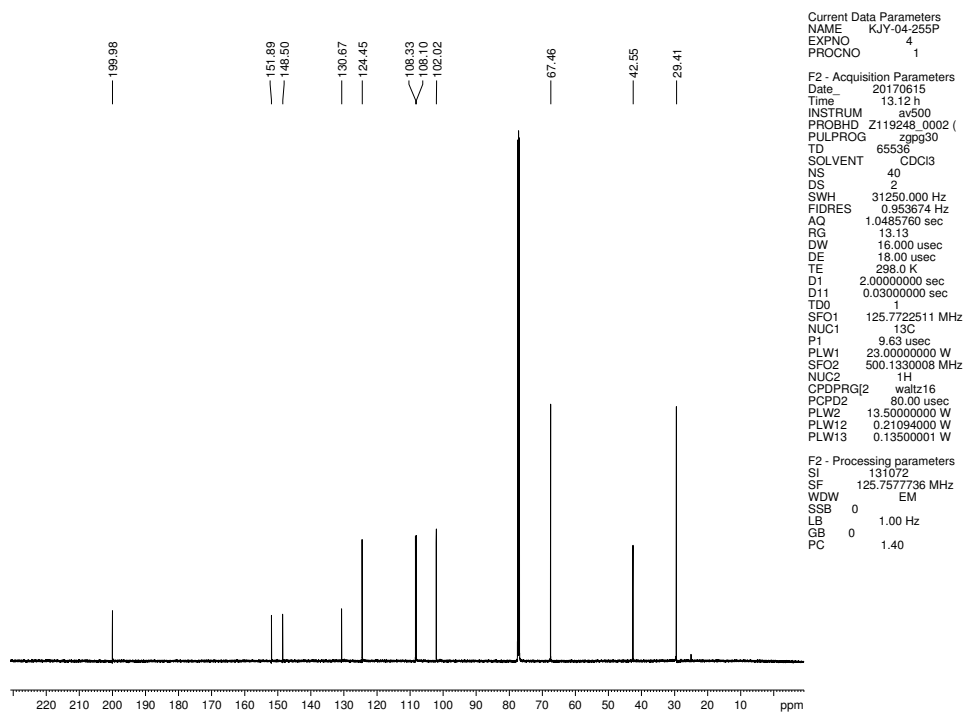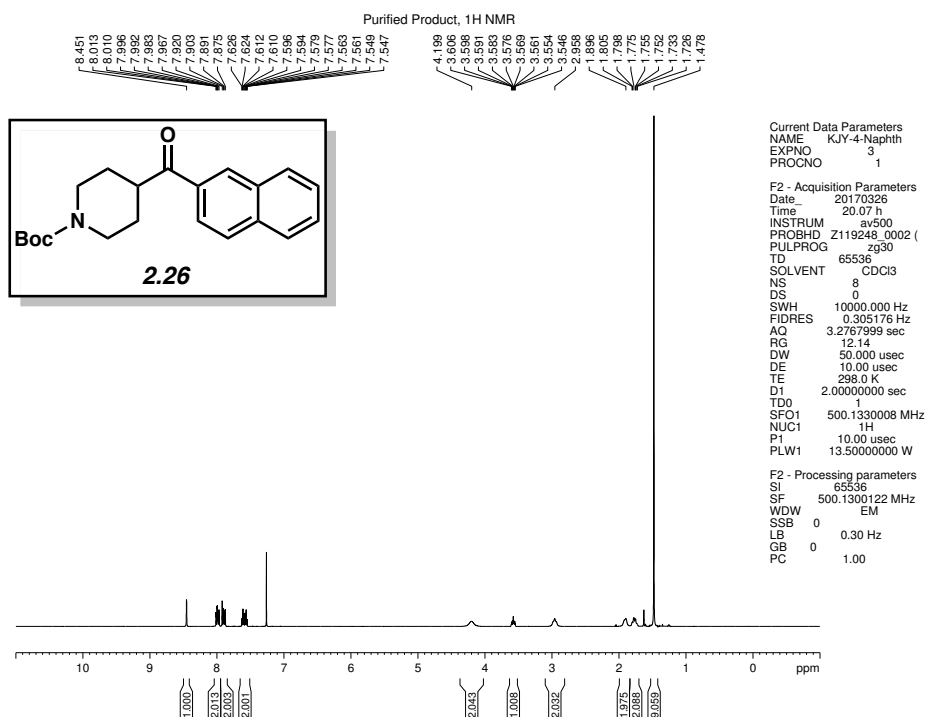Figure 2.65 ^{13}C NMR (125 MHz, CDCl$_3$) of compound **2.25**.

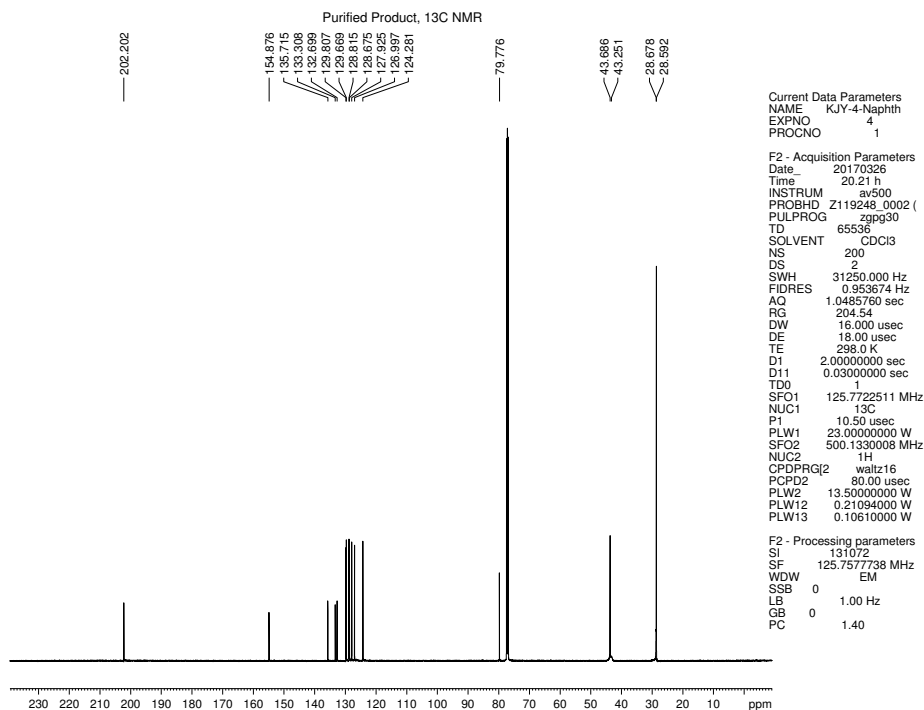Figure 2.66 ^{1}H NMR (500 MHz, CDCl$_3$) of compound **2.26**.

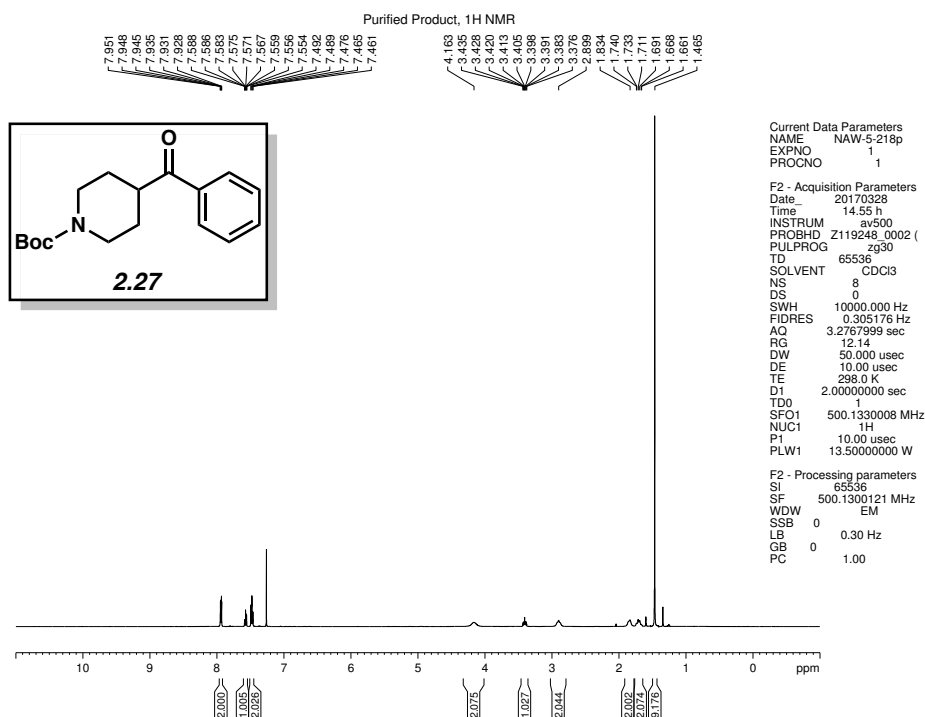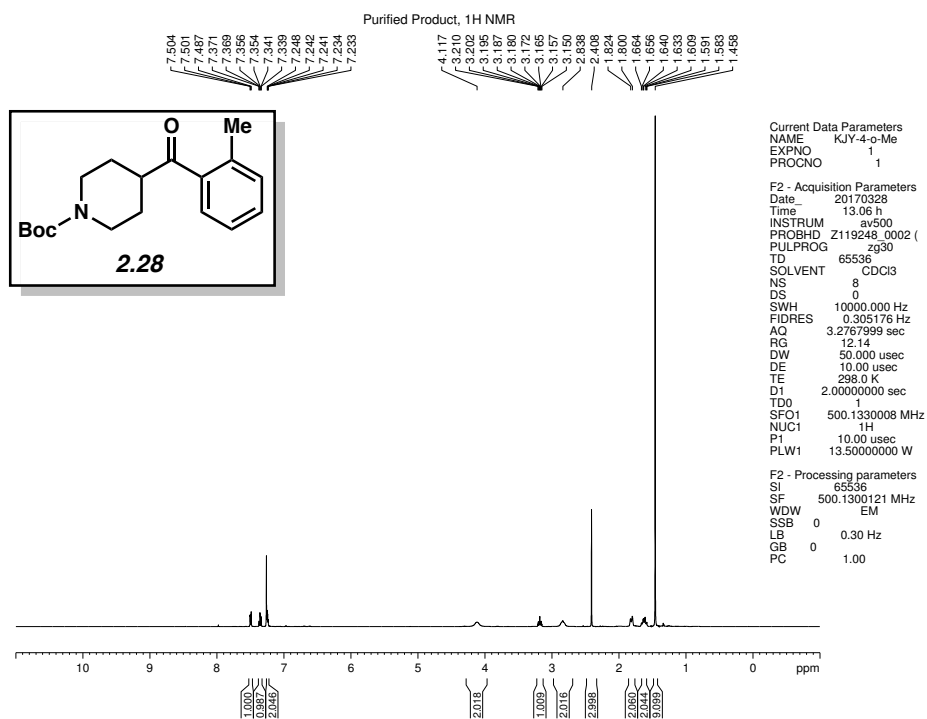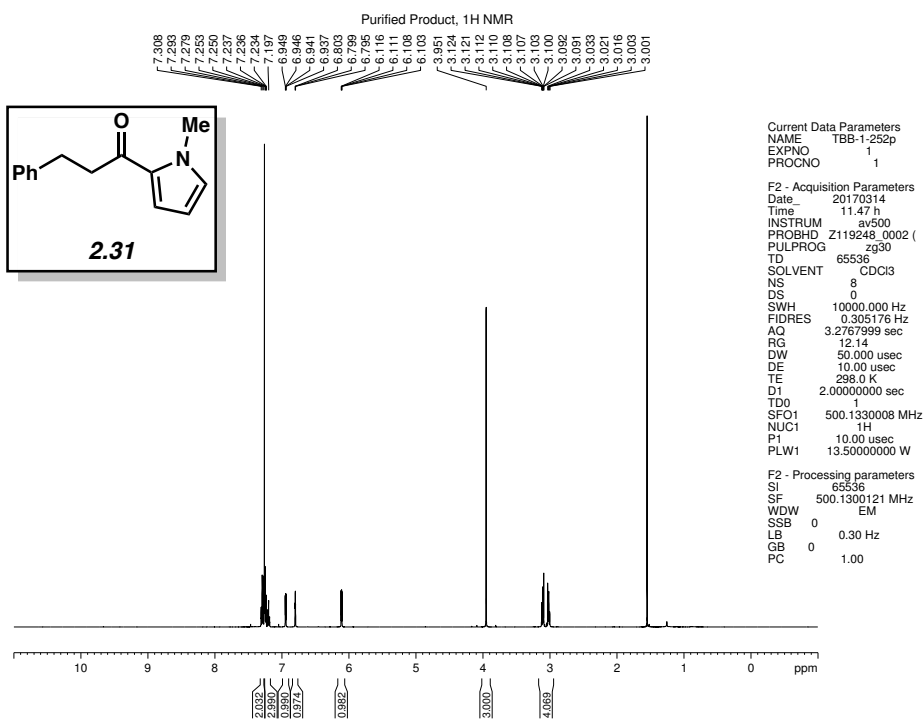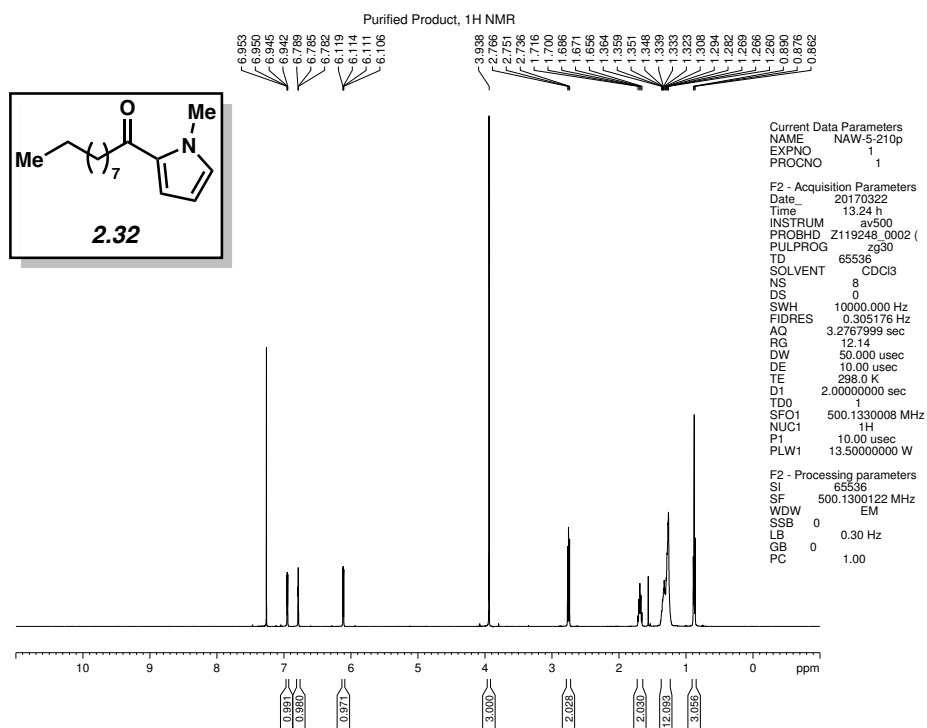*Figure 2.67* ^{13}C NMR (125 MHz, CDCl$_3$) of compound **2.26**.

Figure 2.68 ^{1}H NMR (500 MHz, CDCl$_3$) of compound **2.27**.

Figure 2.69 ^{1}H NMR (500 MHz, CDCl$_3$) of compound **2.28**.
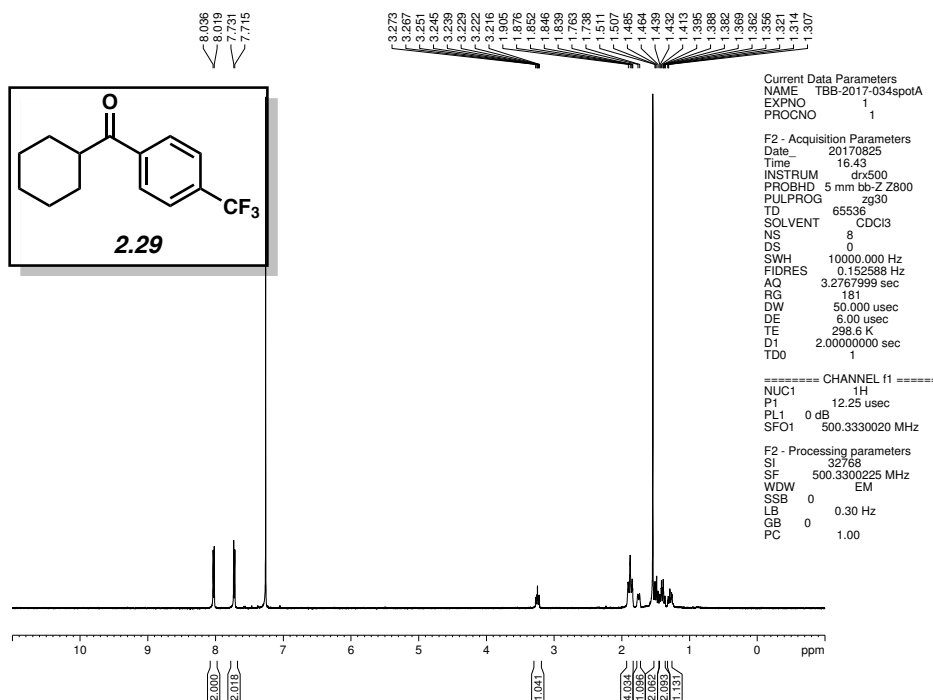
Figure 2.70 ^{1}H NMR (500 MHz, CDCl$_3$) of compound **2.29**.
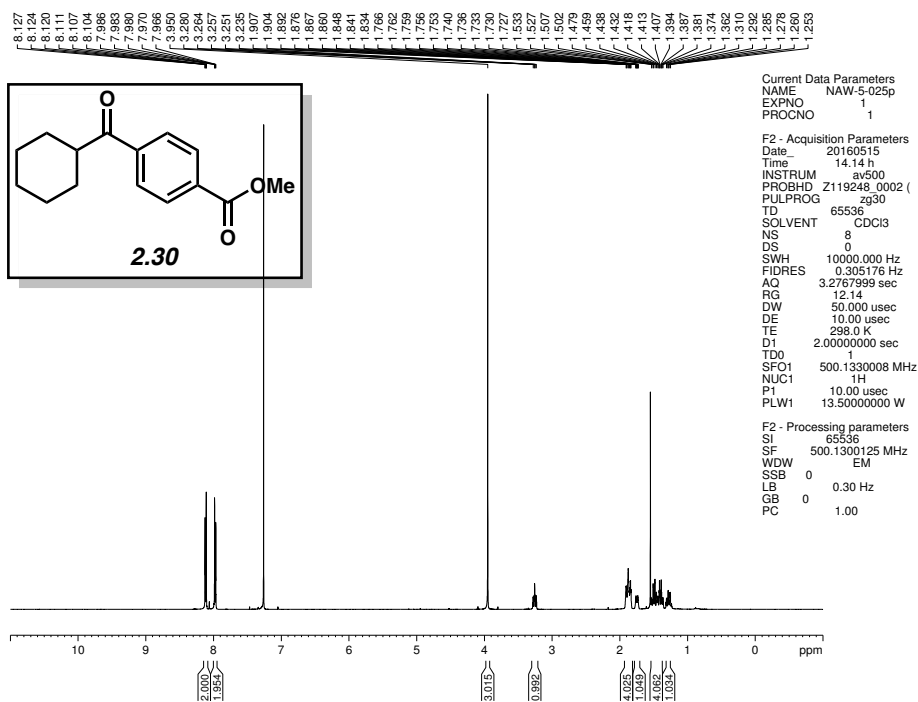
Figure 2.71 ¹H NMR (500 MHz, CDCl₃) of compound **2.30**.

Figure 2.72 ¹H NMR (500 MHz, CDCl₃) of compound **2.31**.

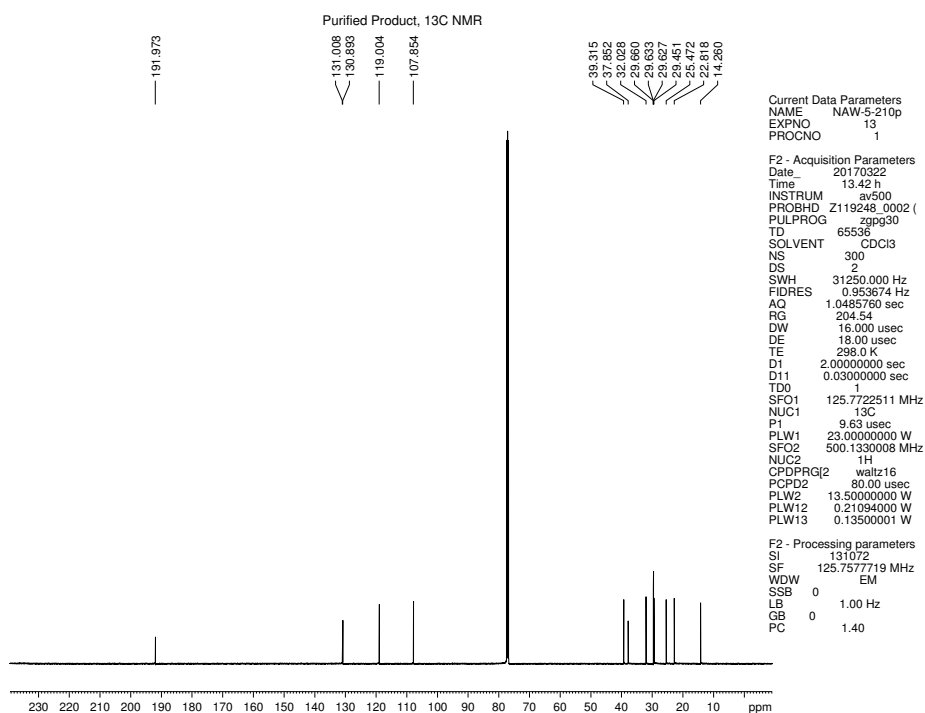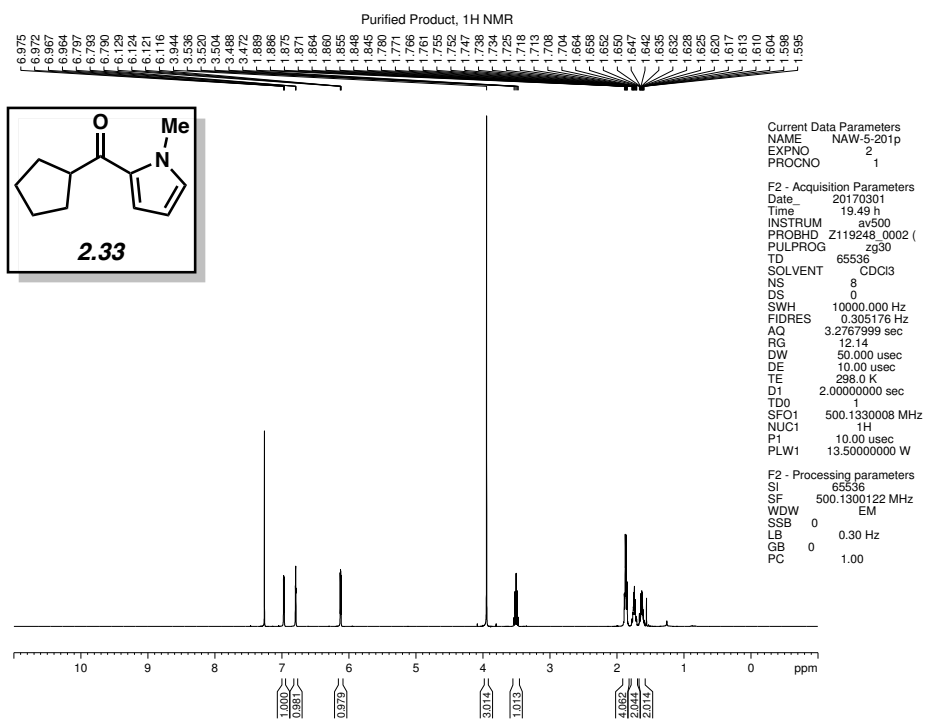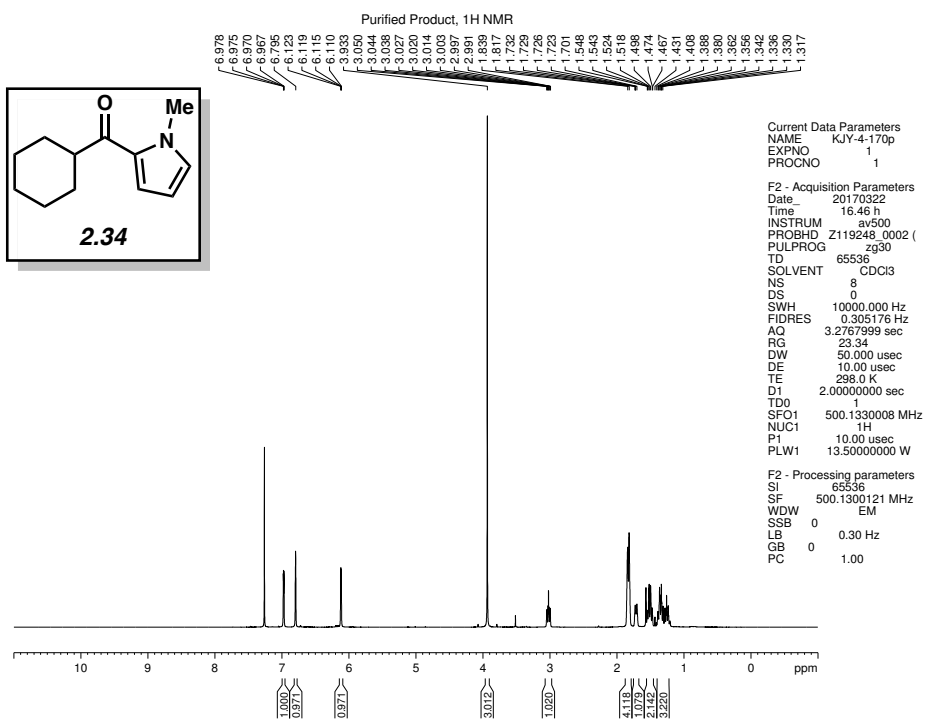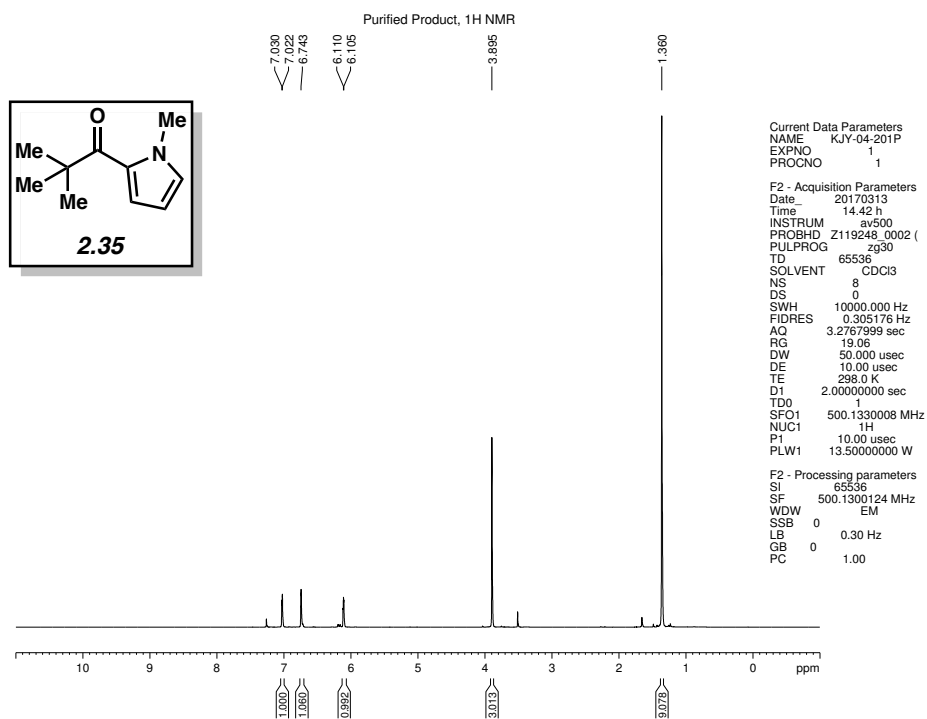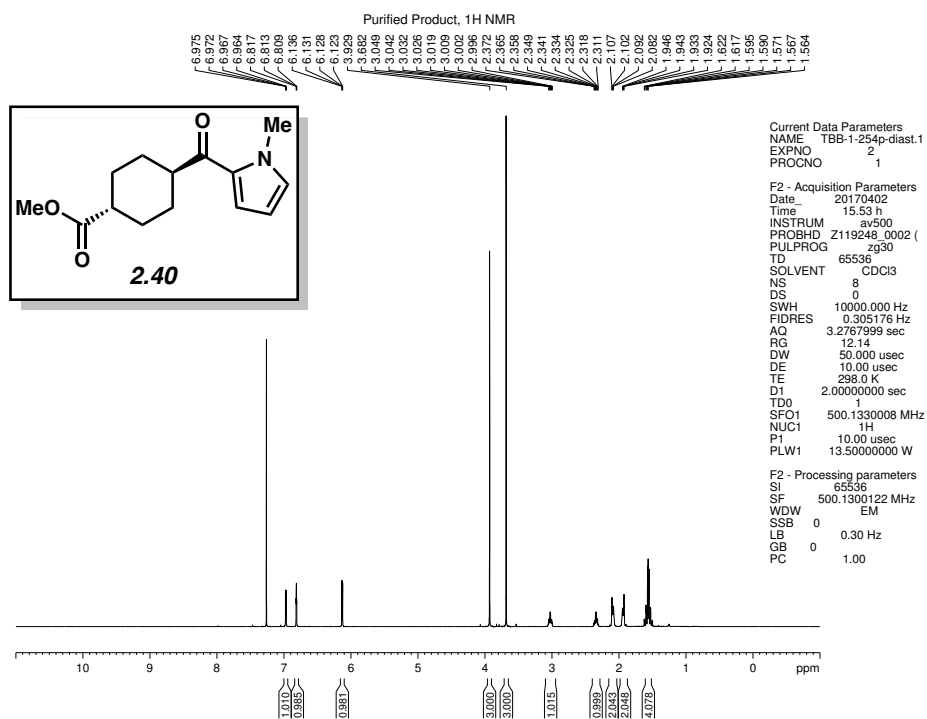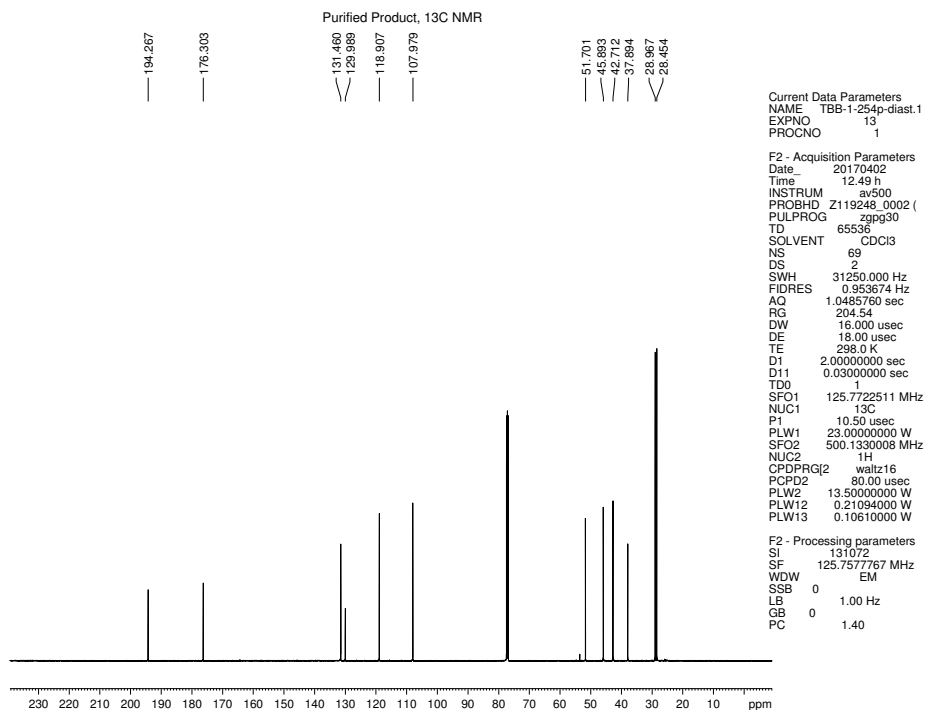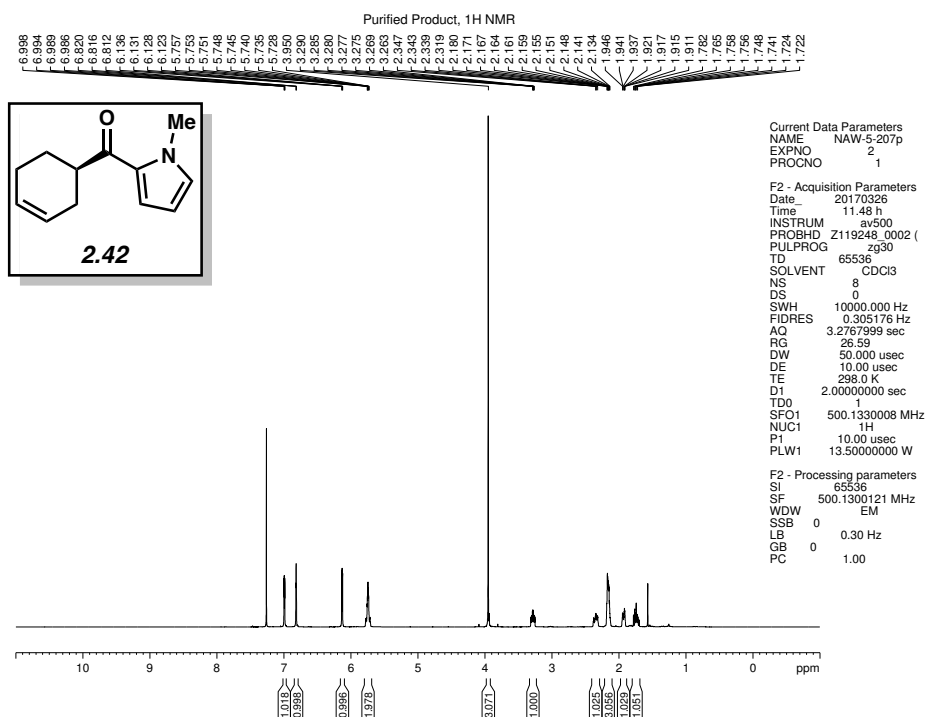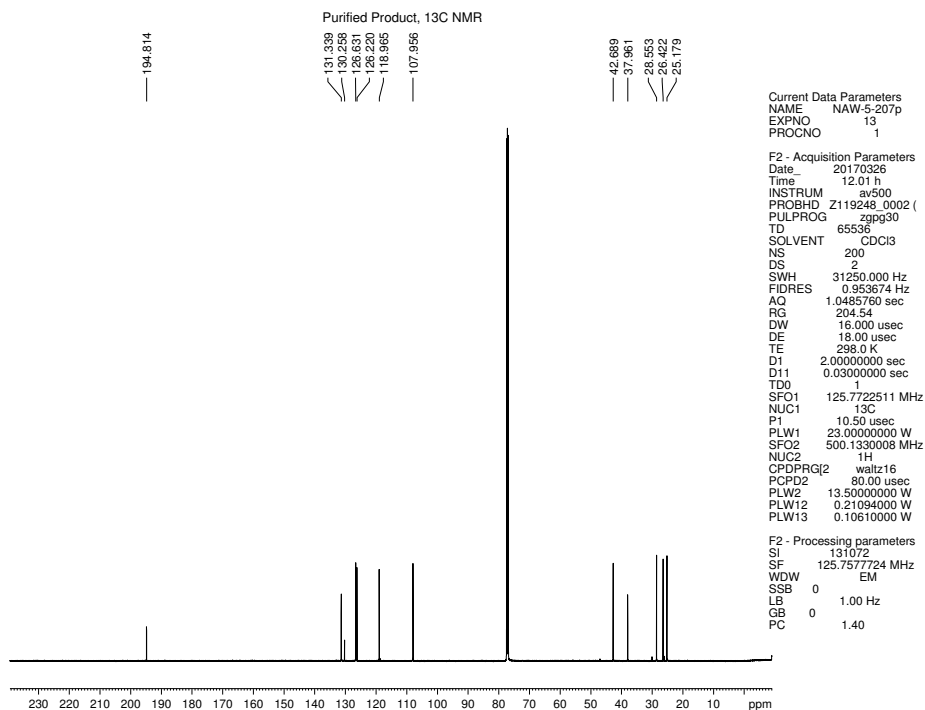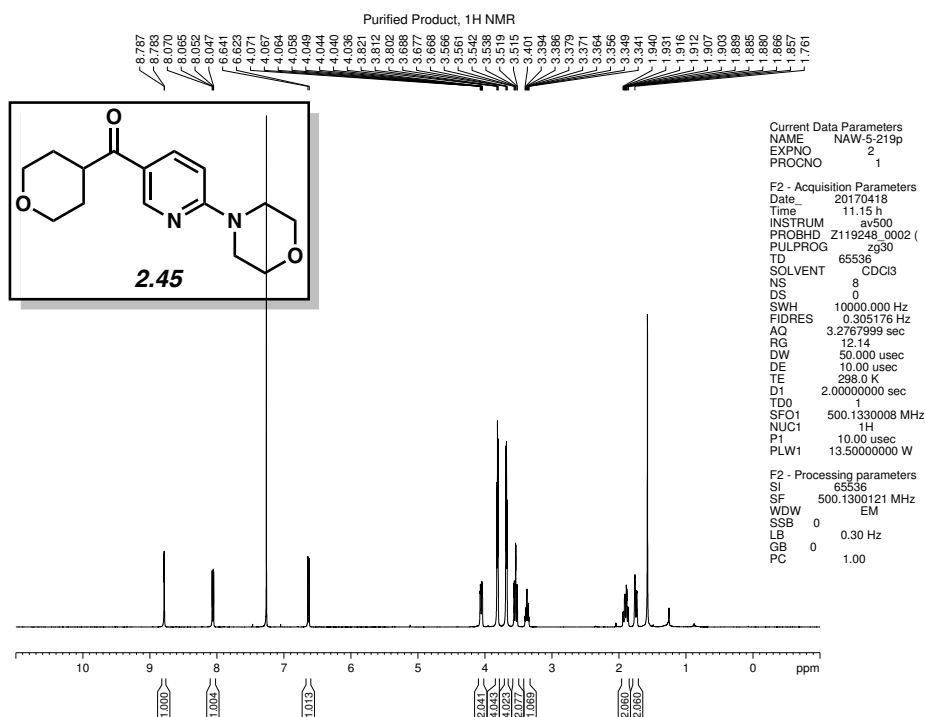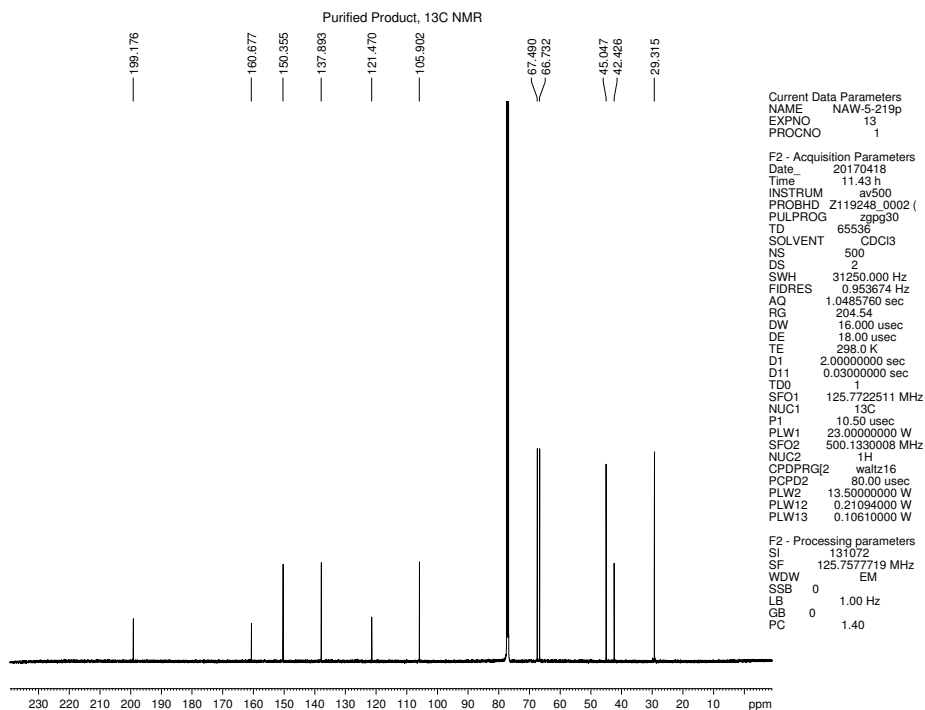Figure 2.73 ^{1}H NMR (500 MHz, CDCl$_3$) of compound **2.32**.

Figure 2.74 ^{13}C NMR (125 MHz, CDCl$_3$) of compound **2.32**.

Purified Product, 1H NMR

6.975, 6.972, 6.967, 6.964, 6.797, 6.793, 6.790, 6.129, 6.124, 6.121, 6.116, 3.944, 3.536, 3.520, 3.504, 3.488, 3.472, 1.889, 1.886, 1.875, 1.871, 1.864, 1.860, 1.855, 1.848, 1.845, 1.780, 1.771, 1.766, 1.761, 1.755, 1.752, 1.747, 1.738, 1.734, 1.725, 1.718, 1.713, 1.708, 1.704, 1.664, 1.658, 1.652, 1.650, 1.647, 1.642, 1.635, 1.632, 1.628, 1.625, 1.620, 1.617, 1.613, 1.610, 1.604, 1.598, 1.595

2.33

Current Data Parameters
NAME   NAW-5-201p
EXPNO   2
PROCNO   1

F2 - Acquisition Parameters
Date_   20170301
Time   19.49 h
INSTRUM   av500
PROBHD Z119248_0002 (
PULPROG   zg30
TD   65536
SOLVENT   CDCl3
NS   8
DS   0
SWH   10000.000 Hz
FIDRES   0.305176 Hz
AQ   3.2767999 sec
RG   12.14
DW   50.000 usec
DE   10.00 usec
TE   298.0 K
D1   2.00000000 sec
TD0   1
SFO1   500.1330008 MHz
NUC1   1H
P1   10.00 usec
PLW1   13.50000000 W

F2 - Processing parameters
SI   65536
SF   500.1300122 MHz
WDW   EM
SSB   0
LB   0.30 Hz
GB   0
PC   1.00

1.000 0.981 0.979   3.014 1.013   4.062 2.044 2.014

Figure 2.75 ^{1}H NMR (500 MHz, CDCl$_3$) of compound **2.33**.

Purified Product, 1H NMR

6.978, 6.975, 6.970, 6.967, 6.795, 6.123, 6.119, 6.115, 6.110, 3.933, 3.050, 3.044, 3.038, 3.027, 3.020, 3.014, 3.003, 2.997, 2.991, 1.839, 1.817, 1.732, 1.729, 1.726, 1.723, 1.701, 1.548, 1.543, 1.524, 1.518, 1.498, 1.474, 1.467, 1.431, 1.408, 1.388, 1.380, 1.362, 1.356, 1.342, 1.336, 1.330, 1.317

2.34

Current Data Parameters
NAME   KJY-4-170p
EXPNO   1
PROCNO   1

F2 - Acquisition Parameters
Date_   20170322
Time   16.46 h
INSTRUM   av500
PROBHD Z119248_0002 (
PULPROG   zg30
TD   65536
SOLVENT   CDCl3
NS   8
DS   0
SWH   10000.000 Hz
FIDRES   0.305176 Hz
AQ   3.2767999 sec
RG   23.34
DW   50.000 usec
DE   10.00 usec
TE   298.0 K
D1   2.00000000 sec
TD0   1
SFO1   500.1330008 MHz
NUC1   1H
P1   10.00 usec
PLW1   13.50000000 W

F2 - Processing parameters
SI   65536
SF   500.1300121 MHz
WDW   EM
SSB   0
LB   0.30 Hz
GB   0
PC   1.00

1.000 0.971   0.971   3.012   1.020   4.118 1.079 2.142 3.220

Figure 2.76 ^{1}H NMR (500 MHz, CDCl$_3$) of compound **2.34**.

7.030
7.022
6.743
6.110
6.105
3.895
1.360

Current Data Parameters
NAME   KJY-04-201P
EXPNO   1
PROCNO   1

F2 - Acquisition Parameters
Date_   20170313
Time   14.42 h
INSTRUM   av500
PROBHD Z119248_0002 (
PULPROG   zg30
TD   65536
SOLVENT   CDCl3
NS   8
DS   0
SWH   10000.000 Hz
FIDRES   0.305176 Hz
AQ   3.2767999 sec
RG   19.06
DW   50.000 usec
DE   10.00 usec
TE   298.0 K
D1   2.00000000 sec
TD0   1
SFO1   500.1330008 MHz
NUC1   1H
P1   10.00 usec
PLW1   13.50000000 W

F2 - Processing parameters
SI   65536
SF   500.1300124 MHz
WDW   EM
SSB   0
LB   0.30 Hz
GB   0
PC   1.00

Figure 2.77 ^{1}H NMR (500 MHz, CDCl$_3$) of compound **2.35**.

6.975
6.972
6.967
6.964
6.817
6.813
6.809
6.136
6.131
6.128
6.123
3.929
3.682
3.049
3.042
3.032
3.026
3.019
3.009
3.002
2.996
2.372
2.365
2.358
2.349
2.341
2.334
2.325
2.318
2.311
2.107
2.102
2.092
2.082
1.946
1.943
1.933
1.924
1.622
1.617
1.595
1.590
1.571
1.567
1.564

Current Data Parameters
NAME   TBB-1-254p-diast.1
EXPNO   2
PROCNO   1

F2 - Acquisition Parameters
Date_   20170402
Time   15.53 h
INSTRUM   av500
PROBHD Z119248_0002 (
PULPROG   zg30
TD   65536
SOLVENT   CDCl3
NS   8
DS   0
SWH   10000.000 Hz
FIDRES   0.305176 Hz
AQ   3.2767999 sec
RG   12.14
DW   50.000 usec
DE   10.00 usec
TE   298.0 K
D1   2.00000000 sec
TD0   1
SFO1   500.1330008 MHz
NUC1   1H
P1   10.00 usec
PLW1   13.50000000 W

F2 - Processing parameters
SI   65536
SF   500.1300122 MHz
WDW   EM
SSB   0
LB   0.30 Hz
GB   0
PC   1.00

Figure 2.78 ^{1}H NMR (500 MHz, CDCl$_3$) of compound **2.40**.

Figure 2.79 ¹³C NMR (125 MHz, CDCl₃) of compound **2.40**.

Figure 2.80 ¹H NMR (500 MHz, CDCl₃) of compound **2.42**.

Figure 2.81 ^{13}C NMR (125 MHz, CDCl$_3$) of compound **2.42**.

Figure 2.82 ^{1}H NMR (500 MHz, CDCl$_3$) of compound **2.45**.

Figure 2.83 ^{13}C NMR (125 MHz, CDCl$_3$) of compound **2.45**.
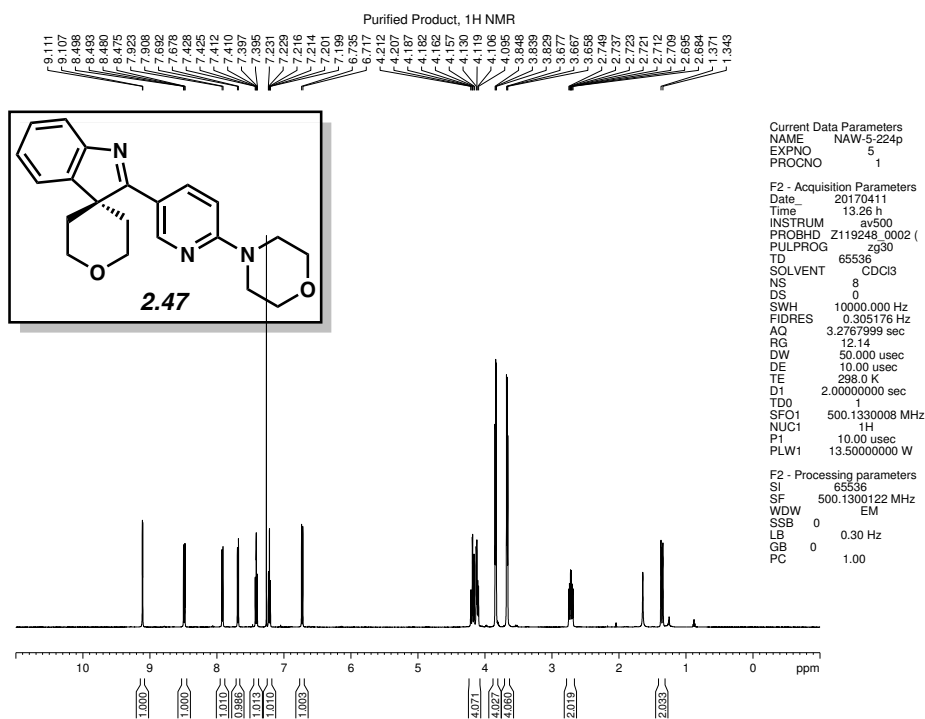
Figure 2.84 ^{1}H NMR (500 MHz, CDCl$_3$) of compound **2.47**.
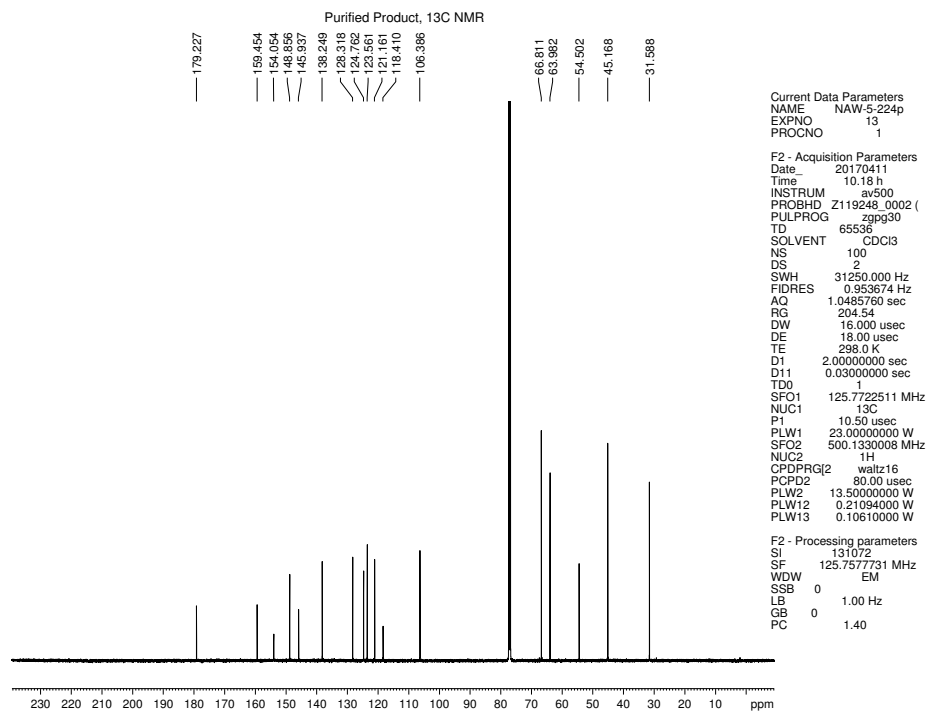
Figure 2.85 ¹³C NMR (125 MHz, CDCl₃) of compound **2.47**.

2.12 Notes and References

(1) (a) Miyaura, N. In *Metal-Catalyzed Cross-Coupling Reactions*, 2nd ed.; de Meijere, A.; Diederich, F., Eds.; Wiley-VCH: Weinheim, 2004; Vol. 1, p. v–vi, 41. (b) Kotschy, A.; Timári, T. *Heterocycles from Transition Metal Catalysis: Formation and Functionalization*; Springer: Dordrecht, 2005; p 176. (c) Littke, A. In *Modern Arylation Methods*; Ackermann, L., Ed.; Wiley-VCH: Weinheim, 2009; p 29. (d) Schröter, S.; Stock, C.; Bach, T. Regioselective Cross-Coupling Reactions of Polyhalogenated Heterocycles. *Tetrahedron* **2005**, *61*, 2245–2267.

(2) Recently, Szostak and Newman independently reported the Pd-catalyzed Suzuki–Miyaura coupling of phenol-derived esters. Both methods are highly focused on aryl esters, although four examples involving non-branched aliphatic substrates were disclosed in total between the two studies. One example utilizing an α-branched substrate was reported, albeit with some challenges noted by Newman. (a) Halima, T. B.; Zhang, W.; Yalaoui, T.; Hong, X.; Yang, Y.-F.; Houk, K. N.; Newman, S. G. Palladium-Catalyzed Suzuki–Miyaura Coupling of Aryl Esters. *J. Am. Chem. Soc.* **2017**, *139*, 1311–1318. (b) Lei, R.; Meng, G.; Shi, S.; Ling, Y.; An, J.; Szostak, R.; Szostak, M. Suzuki–Miyaura Cross-Coupling of Amides and Esters at Room Temperature: Correlation with Barriers to Rotation Around C–N and C–O Bonds. *Chem. Sci.* **2017**, *8*, 6525–6530.

(3) For additional non-decarbonylative transition metal-catalyzed reactions involving cleavage of the ester C–O bond, see: (a) Tatamidani, H.; Kakiuchi, F.; Chatani, N. A New Ketone Synthesis by Palladium-Catalyzed Cross-Coupling Reactions of Esters with Organoboron Compounds. *Org. Lett.* **2004**, *6*, 3597–3599. (b) Hie, L.; Fine Nathel, N. F.; Hong, X.; Yang,

Y.-F.; Houk, K. N.; Garg, N. K. Nickel-Catalyzed Activation of Acyl C−O Bonds of Methyl Esters. *Angew. Chem., Int. Ed.* **2016**, *55*, 2810–2814. (c) Yu, B.; Sun, H.; Xie, Z.; Zhang, G.; Xu, L.-W.; Zhang, W.; Gao, Z. Privilege Ynone Synthesis via Palladium-Catalyzed Alkynylation of "Super-Active Esters." *Org. Lett.* **2015**, *17*, 3298–3301. (d) LaBerge, N. A.; Love, J. A. Nickel-Catalyzed Decarbonylative Cou-pling of Aryl Esters and Arylboronic Acids. *Eur. J. Org. Chem.* **2015,** 5546–5553. (e) Tatamidani, H.; Yokota, K.; Kakiuchi, F.; Chatani, N. Catalytic Cross-Coupling Reaction of Esters with Organoboron Compounds and Decarbonylative Reduction of Esters with $HCOONH_4$: A New Route to Acyl Transition Metal Complexes through the Cleavage of Acyl−Oxygen Bonds in Esters. *J. Org. Chem.* **2004**, *69,* 5615–5621. (f) Desnoyer, A. N.; Friese, F. W.; Chiu, W.; Drover, M. W.; Patrick, B. O.; Love, J. A. Exploring Regioselective Bond Cleavage and Cross-Coupling Reactions using a Low-Valent Nickel Complex. *Chem. Eur. J.* **2016**, *22*, 4070–4077. (g) Shi, S.; Szostak, M. Pd-PEPPSI: A General Pd-NHC Precatalyst for Suzuki–Miyaura Cross-Coupling of Esters by C–O Cleavage. *Organometallics* **2017**, *36*, 3784–3789. (h) Dardir, A. H.; Melvin, P. R.; Davis, R. M.; Hazari, N.; Beromi, M. M. Rapidly Activating Pd-Precatalyst for Suzuki–Miyaura and Buchwald–Hartwig Couplings of Aryl Esters. *J. Org. Chem*. **2018**, *83*, 469–477. (i) For a recent review, see: Takise, R.; Muto, K.; Yamaguchi, J. Cross-Coupling of Aromatic Esters and Amides. *Chem. Soc. Rev.* **2017**, *46*, 5864–5888.

(4) For nickel-catalyzed reactions involving cleavage of the amide C–N bond, see: (a) Hie, L.; Fine Nathel, N. F.; Shah, T.; Baker, E. L.; Hong, X.; Yang, Y.-F.; Liu, P.; Houk, K. N.; Garg, N. K. Conversion of Amides to Esters by the Nickel-Catalysed Activation of Amide C–N Bonds. *Nature* **2015**, *524*, 79–83. (b) Weires, N. A.; Baker, E. L.; Garg, N. K. Nickel-

Catalysed Suzuki–Miyaura Coupling of Amides. *Nat. Chem*. **2016**, *8*, 75–79. (c) Baker, E. L.; Yamano, M. M.; Zhou, Y.; Anthony, S. M.; Garg, N. K. A Two-Step Approach to Achieve Secondary Amide Transamidation Enabled by Nickel Catalysis. *Nat. Commun*. **2016**, *7*, 11554–11558. (d) Simmons, B. J.; Weires, N. A.; Dander, J. E.; Garg, N. K. Nickel-Catalyzed Alkylation of Amide Derivatives. *ACS Catal*. **2016**, *6*, 3176–3179. (e) Dander, J. E.; Weires, N. A.; Garg, N. K. Benchtop Delivery of Ni(cod)$_2$ using Paraffin Capsules. *Org. Lett*. **2016**, *18*, 3934–3936. (f) Shi, S.; Szostak, M. Nickel-Catalyzed Diaryl Ketone Synthesis by N–C Cleavage: Direct Negishi Cross-Coupling of Primary Amides by Site-Selective *N,N*-Di-Boc Activation. *Org. Lett.* **2016**, *18*, 5872–5875. (g) Shi, S.; Szostak, M. Efficient Synthesis of Diaryl Ketones by Nickel-Catalyzed Negishi Cross-Coupling of Amides by Carbon–Nitrogen Bond Cleavage at Room Temperature Accelerated by a Solvent Effect. *Chem. Eur. J.* **2016**, *22*, 10420–10424. (h) Hie, L.; Baker, E. L.; Anthony, S. M.; Desrosiers, J.-N.; Senanayake, C.; Garg, N. K. Nickel-Catalyzed Esterification of Aliphatic Amides. *Angew. Chem., Int. Ed.* **2016**, *55*, 15129–15132. (i) Dey, A.; Sasmal, S.; Seth, K.; Lahiri, G. K.; Maiti, D. Nickel-Catalyzed Deamidative Step-Down Reduction of Amides to Aromatic Hydrocarbons. *ACS Catal.* **2017**, *7*, 433–437. (j) Ni, S.; Zhang, W.; Mei, H.; Han, J.; Pan, Y. Ni-Catalyzed Reductive Cross-Coupling of Amides with Aryl Iodide Electrophiles via C–N Bond Activation. *Org. Lett.* **2017**, *19*, 2536–2539. (k) Medina, J. M.; Moreno, J.; Racine, S.; Du, S.; Garg, N. K. Mizoroki–Heck Cyclizations of Amide Derivatives for the Introduction of Quaternary Centers. *Angew. Chem., Int. Ed.* **2017**, *56*, 6567–6571. (l) Hu, J.; Wang, M.; Pu, X.; Shi, Z. Nickel-Catalysed Retro-Hydroamidocarbonylation of Aliphatic Amides to Olefins. *Nat. Commun.* **2017**, *8*, 14993–14999. (m) Weires, N. A.; Caspi, D. D.; Garg, N. K. Kinetic

Modeling of the Nickel-Catalyzed Esterification of Amides. *ACS Catal.* **2017**, *7*, 4381–4385.

(n) Shi, S.; Szostak, M. Nickel-Catalyzed Negishi Cross-Coupling of N-Acylsuccinimides: Stable, Amide-Based, Twist-Controlled Acyl-Transfer Reagents via N–C Activation. *Synthesis* **2017**, *49*, 3602–3608. (o) Dander, J. E.; Baker, E. L.; Garg, N. K. Nickel-Catalyzed Transamidation of Aliphatic Amide Derivatives. *Chem. Sci.* **2017**, *8*, 6433–6438. (p) For a recent review, see: Dander, J. E.; Garg, N. K. Breaking Amides using Nickel Catalysis. *ACS Catal.* **2017**, *7*, 1413–1423.

(5) For nickel-catalyzed decarbonylative coupling reactions of amides, see: (a) Shi, S.; Meng, G.; Szostak, M. Synthesis of Biaryls through Nickel-Catalyzed Suzuki–Miyaura Coupling of Amides by Carbon–Nitrogen Bond Cleavage. *Angew. Chem., Int. Ed*. **2016**, *55*, 6959–6963. (b) Hu, J.; Zhao, Y.; Liu, J.; Zhang, Y.; Shi, Z. Nickel-Catalyzed Decarbonylative Borylation of Amides: Evidence for Acyl C−N Bond Activation. *Angew. Chem., Int. Ed.* **2016**, *55*, 8718–8722. (c) Srimontree, W.; Chatupheeraphat, A.; Liao, H.-H.; Rueping, M. Amide to Alkyne Interconversion via a Nickel/Copper-Catalyzed Deamidative Cross-Coupling of Aryl and Alkenyl Amides. *Org. Lett*. **2017**, *19*, 3091–3094. (d) Liu, C.; Szostak, M. Decarbonylative Phosphorylation of Amides by Palladium and Nickel Catalysis: The Hirao Cross-Coupling of Amide Derivatives. *Angew. Chem., Int. Ed.* **2017**, *56*, 12718–12722. (e) Yue, H.; Guo, L.; Liao, H.-H.; Cai, Y.; Zhu, C.; Rueping, M. Catalytic Ester and Amide to Amine Interconversion: Nickel-Catalyzed Decarbonylative Amination of Esters and Amides by C−O and C−C Bond Activation. *Angew. Chem., Int. Ed.* **2017**, *56*, 4282–4285. (f) Chatupheeraphat, A.; Liao, H.-H.; Lee, S.-C.; Rueping, M. Nickel-Catalyzed C–CN Bond Formation via Decarbonylative Cyanation of Esters, Amides, and Intramolecular Recombination Fragment

Coupling of Acyl Cyanides. *Org. Lett.* **2017**, *19*, 4255–4258. (g) Yue, H.; Guo, L.; Lee, S.-C.; Liu, X.; Rueping, M. Selective Reductive Removal of Ester and Amide Groups from Arenes and Heteroarenes through Nickel-Catalyzed C−O and C−N Bond Activation. *Angew. Chem., Int. Ed.* **2017**, *56*, 3972–3976.

(6) For palladium-catalyzed C–C bond forming reactions of amides, see: (a) Li, X.; Zou, G. Acylative Suzuki Coupling of Amides: Acyl-Nitrogen Activation via Synergy of Independently Modifiable Activating Groups. *Chem. Commun.* **2015**, *51*, 5089–5092. (b) Yada, A.; Okajima, S.; Murakami, M. Palladium-Catalyzed Intramolecular Insertion of Alkenes into the Carbon–Nitrogen Bond of β-Lactams. *J. Am. Chem. Soc.* **2015**, 137, 8708–8711. (c) Meng, G.; Szostak, M. Palladium-Catalyzed Suzuki–Miyaura Coupling of Amides by Carbon–Nitrogen Cleavage: General Strategy for Amide N–C Bond Activation. *Org. Biomol. Chem.* **2016**, *14*, 5690–5705. (d) Meng, G.; Szotak, M. General Olefin Synthesis by the Palladium-Catalyzed Heck Reaction of Amides: Sterically Controlled Chemoselective N–C Activation. *Angew. Chem., Int. Ed.* **2015**, *54*, 14518–14522. (e) Meng, G.; Szostak, M. Sterically Controlled Pd-Catalyzed Chemoselective Ketone Synthesis via N–C Cleavage in Twisted Amides. *Org. Lett.* **2015**, *17*, 4364–4367. (f) Liu, C.; Meng, G.; Liu, Y.; Liu, R.; Lalancette, R.; Szostak, R.; Szostak, M. N-Acylsaccharins: Stable Electrophilic Amide-Based Acyl Transfer Reagents in Pd-Catalyzed Suzuki–Miyaura Coupling via N–C Cleavage. *Org. Lett.* **2016**, *18*, 4194–4197. (g) Lei, P.; Meng, G.; Szostak, M. General Method for the Suzuki–Miyaura Cross-Coupling of Amides Using Commercially Available, Air- and Moisture-Stable Palladium/NHC (NHC = *N*-Heterocyclic Carbene) Complexes. *ACS Catal.* **2017**, *7*, 1960–1965. (h) Liu, C.; Liu, Y.; Liu, R.; Lalancette, R.; Szostak, R.; Szostak, M. Palladium-

Catalyzed Suzuki–Miyaura Cross-Coupling of N-Mesylamides by N–C Cleavage: Electronic Effect of the Mesyl Group. *Org. Lett.* **2017**, *19*, 1434–1437. (i) Liu, C.; Meng, G.; Szostak, M. *N*-Acylsaccharins as Amide-Based Arylating Reagents via Chemoselective N–C Cleavage: Pd-Catalyzed Decarbonylative Heck Reaction. *J. Org. Chem.* **2016**, *81*, 12023–12030. (j) Meng, G.; Shi, S.; Szostak, M. Palladium-Catalyzed Suzuki–Miyaura Cross-Coupling of Amides via Site-Selective N–C Bond Cleavage by Cooperative Catalysis. *ACS Catal.* **2016**, *6*, 7335–7339. (k) Cui, M.; Wu, H.; Jian, J.; Wang, H.; Liu, C.; Stelck, D.; Zeng, Z. Palladium-Catalyzed Sonogashira Coupling of Amides: Access to Ynones via C–N bond Cleavage. *Chem. Commun.* **2016**, *52*, 12076–12079. (l) Wu, H.; Li, Y.; Cui, M.; Jian, J.; Zeng, Z. Suzuki Coupling of Amides via Palladium-Catalyzed C–N Cleavage of *N*-Acylsaccharins. *Adv. Synth. Catal.* **2016**, *358*, 3876–3880. (m) Shi, S.; Szostak, M. Decarbonylative Cyanation of Amides by Palladium Catalysis. *Org. Lett*. **2017**, *19,* 3095–3098. n) Lei, P.; Meng, G.; Ling, Y.; An, J.; Szostak, M. Pd-PEPPSI: Pd-NHC Precatalyst for Suzuki–Miyaura Cross-Coupling Reactions of Amides. *J. Org. Chem.* **2017**, 82, 6638–6646. (o) Meng, G.; Szostak, R.; Szostak, M. Suzuki–Miyaura Cross-Coupling of *N*-Acylpyrroles and Pyrazoles: Planar, Electronically Activated Amides in Catalytic N–C Cleavage. *Org. Lett*. **2017**, *19*, 3596–3599. (p) Meng, G.; Lalancette, R.; Szostak, R.; Szostak, M. *N*-Methylamino Pyrimidyl Amides (MAPA): Highly Reactive, Electronically-Activated Amides in Catalytic N–C(O) Cleavage. *Org. Lett.* **2017***, 19*, 4656–4659*.* (q) Osumi, Y.; Szostak, M. *N*-Acylsuccinimides: Twist-Controlled, Acyl-Transfer Reagents in Suzuki–Miyaura Cross-Coupling by N–C Amide Bond Activation. *Org. Biomol. Chem*. **2017**, *15*, 8867–8871. (r) Lei, P.; Meng, G.; Ling, Y.; An, J.; Nolan, S. P.; Szostak, M. General Method for the Suzuki–Miyaura Cross-Coupling of Primary

Amide-Derived Electrophiles Enabled by [Pd(NHC)(cin)Cl] at Room Temperature. *Org. Lett.* **2017**, *19*, 6510–6513.

(7) For examples of Pd-catalyzed Suzuki–Miyaura coupling of aliphatic amides, see: Li, X.; Zou, G. Palladium-Catalyzed Acylative Cross-Coupling of Amides with Diarylborinic Acids and Sodium Tetraarylborates. *J. Organomet. Chem*. **2015**, *794*, 136–145.

(8) The field of nickel-catalyzed cross-couplings itself has gained tremendous interest in recent years due not only to the high natural abundance, low cost, and low CO_2 footprint of nickel, but also because of its ability to effect new or challenging transformations, including those involving activation of the amide C–N bond. For pertinent reviews on nickel catalysis, see: (a) Rosen, B. M.; Quasdorf, K. W.; Wilson, D. A.; Zhang, N.; Resmerita, A.-M.; Garg, N. K.; Percec, V. Nickel-Catalyzed Cross-Couplings Involving Carbon−Oxygen Bonds. *Chem. Rev*. **2011**, *111*, 1346−1416. (b) Tasker, S. Z.; Standley, E. A.; Jamison, T. F. Recent Advances in Homogeneous Nickel Catalysis. *Nature* **2014**, *509*, 299−309. (c) Mesganaw, T.; Garg, N. K. Ni- and Fe-Catalyzed Cross-Coupling Reactions of Phenol Derivatives. *Org. Process Res. Dev*. **2013**, *17*, 29−39. d) Ananikov, V. P. Nickel: The "Spirited Horse" of Transition Metal Catalysis. *ACS Catal*. **2015**, *5*, 1964−1971.

(9) Amani, J.; Alam, R.; Badir, S.; Molander, G. A. Synergistic Visible-Light Photoredox/Nickel-Catalyzed Synthesis of Aliphatic Ketones via N–C Cleavage of Imides. *Org. Lett.* **2017**, *19*, 2426–2429.

(10) Nahm, S.; Weinreb, S. M. *N*-Methoxy-*N*-Methylamides as Effective Acylating Agents. *Tetrahedron Lett*. **1981**, *22*, 3815–3818.

(11) As Molander's methodology utilizes *alkyl* boron reagents (see ref 9), and ours uses *aryl* boron reagents, the two methods offer different strategic approaches to access ketone products.

(12) The less activated *N*-Bn,Boc amides used in the present study are not competent substrates in the Ir/Ni photoredox-mediated couplings of *N*-acyl succinimides (see ref 9).

(13) (a) Gooßen, L. J.; Ghosh, K. Palladium-Catalyzed Synthesis of Aryl Ketones from Boronic Acids and Carboxylic Acids or Anhydrides. *Angew. Chem., Int. Ed.* **2001**, *40*, 3458–3460. (b) Gooßen, L. J.; Ghosh, K. Palladium-Catalyzed Synthesis of Aryl Ketones from Boronic Acids and Carboxylic Acids Activated in situ by Pivalic Anhydride. *Eur. J. Org. Chem.* **2002**, 3254–3257. (c) Yang, H.; Li, H.; Wittenberg, R.; Egi, M.; Huang, W.; Liebeskind, L. S. Ambient Temperature Synthesis of High Enantiopurity N-Protected Peptidyl Ketones by Peptidyl Thiol Ester−Boronic Acid Cross-Coupling. *J. Am. Chem. Soc.* **2007**, *129*, 1132–1140. (d) Lovell, K. M.; Vasiljevik, T.; Araya, J. J.; Lozama, A.; Prevatt-Smith, K. M; Day, V. W.; Dersch, C. M.; Rothman, R. B.; Butelman, E. R.; Kreek, M. J.; Prisinzano, T. E. Semisynthetic Neoclerodanes as Kappa Opioid Receptor Probes. *Bioorg. Med. Chem.* **2012**, *20*, 3100–3110. (e) Haddach, M.; McCarthy, J. R. A New Method for the Synthesis of Ketones: The Palladium-Catalyzed Cross-coupling of Acid Chlorides with Arylboronic Acids. *Tetrahedron Lett.* **1999**, *40*, 3109–3112. (f) Nique, F.; Hebbe, S.; Triballeau, N.; Peixoto, C.; Lefrancois, J.-M.; Jary, H.; Alvey, L.; Manioc, M.; Housseman, C.; Klaassen, H.; Van Beeck, K.; Guedin, D.; Namour, F.; Minet, D.; Van Der Aar, E.; Feyen, J.; Fletcher, S.; Blanque, R.; Robin-Jagerschmidt, C.; Deprez, P. Identification of a 4-(Hydroxymethyl)diarylhydantoin as a Selective Androgen Receptor Modulator. *J. Med. Chem.* **2012**, *55*, 8236–8247.

(14) The *N*-Bn,Boc amide derivatives employed in this study can be readily prepared from the corresponding carboxylic acids (i.e., benzyl amide formation, followed by treatment with Boc$_2$O) or directly from acid chlorides (i.e., using HN(Bn)Boc).

(15) For use of the Ni/ICy system in the Stille coupling of quaternary ammonium salts, see: Wang, D.-Y.; Kawahata, M.; Yang, Z.-K.; Miyamoto, K.; Komagawa, S.; Yamaguchi, K.; Wang, C.; Uchiyama, M. Stille Coupling via C–N Bond Cleavage. *Nat. Commun.* **2016**, *7*, 12937–12945.

(16) We attribute the improved competency of ligand **10** to its electron-rich nature, which ultimately renders oxidative addition more facile. For discussion of NHC ligands in transition metal catalysis, see: Hopkinson, M. N.; Richter, C.; Schedler, M.; Glorius, F. An Overview of *N*-Heterocyclic Carbenes. *Nature* **2014**, *510*, 485–496.

(17) For the relative nucleophilicities of substituted aryl boronates, see: a) Barder, T. E.; Walker, S. D.; Martinelli, J. R.; Buchwald, S. L. Catalysts for Suzuki−Miyaura Coupling Processes: Scope and Studies of the Effect of Ligand Structure. *J. Am. Chem. Soc.* **2005**, *127*, 4685–4696. b) Billingsley, K. L.; Buchwald, S. L. A General and Efficient Method for the Suzuki–Miyaura Coupling of 2-Pyridyl Nucleophiles. *Angew. Chem., Int. Ed.* **2008**, *47*, 4695–4698.

(18) The underpinnings behind the modest catalyst turnover (i.e., Figure 2.5, entries 2 and 3) is not presently understood.

(19) In addition to esters, ketones, tertiary alcohols, secondary amides, carboxylic acids, and epoxides are tolerated in this methodology, as determined by a robustness screen; see the SI for details.

(20) For bioactive spiroindolenines, see: (a) Weisbach, J. A.; Macko, E.; De Sanctis, N. J.; Cava, M. P.; Douglas, B. Synthesis and Pharmacology of Some *β*-Spiroindolenines and Indolines. *J. Med. Chem*. **1964**, *7*, 735–739. (b) Fourtillan, J.-B.; Violeau, B.; Karam, O.; Jouannetaud, M.-P.; Fourtillan, M.; Jacquesy, J.-C. *Melatoninergic Agonist Spiro[indolepyrrolidine] Derivatives, Process for Their Preparation and Their Use as Medicinal Products*, 1998, US576347. (c) Chowdhury, S.; Fu, J.; Liu, S.; Qi, J. *Spiro-Condensed Indole Derivatives as Sodium Channel Inhibitors*, 2010, WO2010/53998. (d) Li, X.-N.; Cai, X.-H.; Feng, T.; Li, Y.; Liu, Y.-P.; Luo, X.-D. Monoterpenoid Indole Alkaloids from *Gardneria ovata*. *J. Nat. Prod*. **2011**, *74*, 1073–1078. (e) Xu, Y.-J.; Pieters, L. Recent Developments in Antimalarial Natural Products Isolated from Medicinal Plants. *Mini. Rev. Med. Chem*. **2013**, *13*, 1056–1072. (f) Sweis, R. F.; Pliushchev, M.; Brown, P. J.; Guo, J.; Li, F.; Maag, D.; Petros, A. M.; Soni, N. B.; Tse, C.; Vedadi, M.; Michaelides, M. R.; Chiang, G. G.; Pappano, W. N. Discovery and Development of Potent and Selective Inhibitors of Histone Methyltransferase G9a. *ACS Med. Chem. Lett*. **2014**, *5*, 205–209.

(21) (a) Manske, R. H. F. *The Alkaloids, Chemistry and Physiology*, Academic Press, New York, 1981. (b) Cordell, G. A. *The Alkaloids: Chemistry and Biology*, Academic Press, San Diego, 1998. (c) Chadha, N.; Silakari, O. Indoles as Therapeutics of Interest in Medicinal Chemistry: Bird's Eye View. *Eur. J. Med. Chem.* **2017**, *134*, 159–184.

(22) For the classic Fischer indole synthesis, see: (a) Fischer, E.; Jourdan, F. Über die Hydrazine der Brenztraubensäure. *Ber. Dtsch. Chem. Ges.* **1883**, *16*, 2241−2245. (b) Fischer, E.; Hess, O.; Synthese von Indolderivaten. *Ber. Dtsch. Chem. Ges.* **1884**, *17*, 559−568.

(23) Indolino-spirotetrahydropyrans have been pursued as kinase inhibitors of the P13K-Akt pathway, ion channel modulators, 5-HT$_{2c}$ receptor agonists, HDAC inhibitors, and inhibitors of CMV DNA polymerase. (a) Gonzalez-Lopez de Turiso, F.; Shin, Y.; Brown, M.; Cardozo, M.; Chen, Y.; Fong, D.; Hao, X.; He, X.; Henne, K.; Hu, Y.-L.; Johnson, M. G.; Kohn, T.; Lohman, J.; McBride, H. J.; McGee, L. R.; Medina, J. C.; Metz, D.; Miner, K.; Mohn, D; Pattaropong, V.; Seganish, J.; Simard, J. L.; Wannberg, S.; Whittington, D. A.; Yu, G.; Cushing, T. D. Discovery and in Vivo Evaluation of Dual PI3Kβ/δ Inhibitors. *J. Med. Chem.* **2012**, 55, 7667–7685. (b) Brown, M.; Shin, Y.; Cushing, T. D.; Gonzalez-Lopez de Turiso, F.; He, X.; Kohn, T.; Lohman, J. W.; Pattaropong, V.; Seganish, J.; Shin, Y.; Simard, J. L. 2010, *Heterocyclic Compounds and Their Uses*, WO2010/151737. (c) Chen, G.; Cushing, T. D.; Fisher, B.; He, X.; Li, K.; Li, Z.; McGee, L. R.; Pattaropong, V.; Faulder, P.; Seganish, J. L.; Shin, Y. Alkynyl Alcohols as Kinase Inhibitors. WO2009/158011, 2009. (d) Padiya, K; Kamlesh, J; Nair, P. S.; Rivindra, R. R.; Chaure, G. S.; Gudade, G. B.; Parkale, S. S.; Manojkumar, V. L.; Swapnil, R. B.; Smita, A. B. Spirocyclic Compounds as Voltage-Gated Sodium Channel Modulators. WO2012/49555, 2012. (e) Semple, G.; Behan, D. P.; Feichtinger, K.; Glicklich, A.; Grottick, A. J.; Kam, M. M. S.; Kasem, M.; Lehmann, J.; Ren, A. S.; Schrader, T. O.; Shanahan, W. R.; Wong, A. S.-T.; Zhu, X. 5-HT$_{2c}$ Receptor Agonists and Compositions and Methods of Use. WO2015/66344, 2015. (f) Ng, P. Y.; Davis, H.; Bair, K. W.; Millan, D. S.; Rudintskaya, A.; Zheng, X.; Han, B.; Barczak, N.; Lancia Jr., D. 3-Spiro-7-Hydroxamic Acid Tetralins as HDAC Inhibitors. WO2016/168660, 2016. (g) Thibeault, C.; Rancourt, J.; Beaulieu, P. L.; Décor, A.; Grand-Maitre, C.; Kuhn, C.;

Villemure, E.; Leblanc, M.; Lacoste, J.-E.; Moreau, B.; Jolicoeur, E.; Surprenant, S.; Hucke, O. Inhibitors of Cytomegalovirus. WO2014/70976, 2014.

(24) Fier, P. S.; Luo, J.; Hartwig, J. F. Copper-Mediated Fluorination of Arylboronate Esters. Identification of a Copper(III) Fluoride Complex. *J. Am. Chem. Soc.* **2013**, *135*, 2552–2559.

(25) Allwood, D. M.; Blakemore, D. C.; Ley, S. V. Preparation of Unsymmetrical Ketones from Tosylhydrazones and Aromatic Aldehydes via Formyl C–H Bond Insertion. *Org. Lett.* **2014**, *16*, 3064–3067.

(26) Takemiya, A.; Hartwig, J. F. Palladium-Catalyzed Synthesis of Aryl Ketones by Coupling of Aryl Bromides with an Acyl Anion Equivalent. *J. Am. Chem. Soc*. **2006**, *128*, 14800–14801.

(27) Bechara, W. S.; Pelletier, G.; Charette, A. B. Chemoselective Synthesis of Ketones and Ketimines by Addition of Organometallic Reagents to Secondary Amides. *Nat. Chem*. **2012**, *4*, 228–234.

(28) Wakeham, R. J.; Taylor, J. E.; Bull, S. D.; Morris, J. A.; Williams, J. M. J. Iodide as an Activating Agent for Acid Chlorides in Acylation Reactions. *Org. Lett.* **2013**, *15*, 702–705.

(29) Clerici, F.; Gelmi, M. L.; Rossi, L. M. *N*-Arylsulfonylamidines. II: A New Synthesis of Ketones from *N*-Tosylamidines and Organolithium Compounds. *Synthesis* **1987**, 1025–1027.

(30) Barbero, M.; Cadamuro, S.; Degani, I.; Fochi, R.; Gatti, A.; Regondi, V. Pentaatomic Heteroaromatic Cations. 18. Acylation of Pyrrole and *N*-Methylpyrrole with 1,3-Benzoxathiolium Tetrafluoroborates. A High-Yield Method for the Synthesis of Diacylpyrroles. *J. Org. Chem.* **1988**, *53*, 2245–2250.

(31) Taylor, J. E.; Jones, M. D.; Williams, J. M. J.; Bull, S. D. Friedel−Crafts Acylation of Pyrroles and Indoles using 1,5-Diazabicyclo[4.3.0]non-5-ene (DBN) as a Nucleophilic Catalyst. *Org. Lett.* **2010**, *12*, 5740–5743.

CHAPTER THREE

Ni-Catalyzed Suzuki–Miyaura Cross-Coupling of Aliphatic Amides on the Benchtop

Milauni M. Mehta,[†] Timothy B. Boit,[†] Jacob E. Dander,[†] and Neil K. Garg.

3.1 Abstract

Suzuki–Miyaura cross-couplings of amides offer an approach to the synthesis of ketones that avoids the use of basic or pyrophoric nucleophiles. However, these reactions require glovebox manipulations, thus limiting their practicality. We report a benchtop protocol for Suzuki–Miyaura cross-couplings of aliphatic amides that utilizes a paraffin capsule containing a Ni(0) pre-catalyst and NHC ligand. This methodology is broad in scope, scalable, and provides a user-friendly approach to convert aliphatic amides to alkyl–aryl ketones.

3.2 Introduction

The conversion of carboxylic acid derivatives to ketones is a fundamental transformation in synthetic chemistry (Figure 3.1).[1] A common strategy to achieve this conversion is the Weinreb ketone synthesis, in which a *N*-methoxy-*N*-methyl amide undergoes net substitution with an organometallic nucleophile.[2] An alternative strategy lies in the development of transition metal-catalyzed cross-couplings of acyl electrophiles,[1c,3] which avoid the use of strongly basic and pyrophoric organometallic reagents. Our laboratory and others have shown that amides, which are well suited for multi-step synthesis due to their pronounced stability, are particularly useful in this

context.[4] Specifically, Ni-[5,6] and Pd-catalysis[7] have enabled the mild activation of the amide C–N bond for cross-coupling with boronic acids and esters,[8] as well as organozinc reagents.[9]

We recently reported a Ni-catalyzed Suzuki–Miyaura coupling of aliphatic amides to generate alkyl–aryl ketones (Figure 3.1, e.g. **3.1** + **3.2** → **3.3**).[10,11] This methodology is broad in scope, but requires the use of a glovebox, thus limiting its practical utility.[12] We questioned if a paraffin encapsulation strategy, analogous to that pioneered by Buchwald, could prove useful.[13] In this approach, air-sensitive reagents are stored in paraffin capsules, ultimately providing a user-friendly means to perform air-sensitive transition metal-catalyzed reactions. Previously, we showed the promise of this strategy for the Suzuki–Miyaura cross-coupling of a single benzamide-derived substrate utilizing paraffin–Ni(cod)$_2$/SIPr capsules.[14] However, this pre-catalyst and ligand combination is ineffective in the coupling of amides derived from aliphatic carboxylic acids.[10] Moreover, only a single example of a glovebox-free arylation of an aliphatic amide derivative has been reported, which uses a bench-stable Pd(II) pre-catalyst.[15] We report the realization of a paraffin encapsulation strategy to achieve the nickel-catalyzed Suzuki–Miyaura coupling of aliphatic amides on the benchtop.
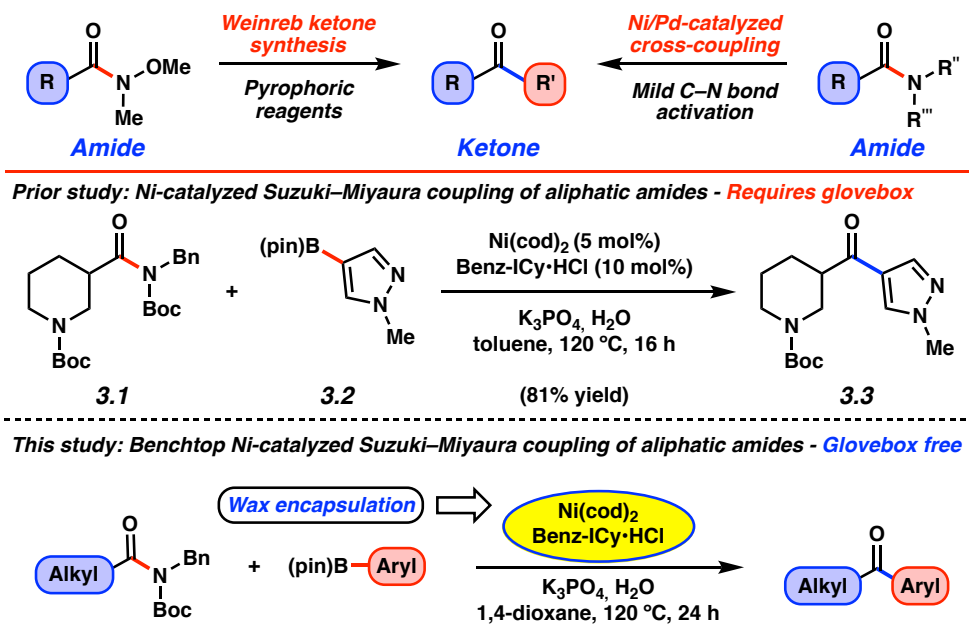
Figure 3.1. Methods for the conversion of amides to ketones, prior studies of Ni-catalyzed Suzuki–Miyaura couplings that utilize a glovebox, and paraffin encapsulation strategy for benchtop delivery (present study).

3.3 Reaction Discovery and Optimization

Our studies were initiated by preparing the desired paraffin capsules, using a molding process analogous to one we had previously reported (Figure 3.2).[14] These capsules were charged with Ni(cod)$_2$ and Benz-ICy•HCl, as this pre-catalyst/ligand combination had proven effective in our original studies on the Suzuki–Miyaura coupling of aliphatic amides using a glovebox.[10] Next, we assessed the utility of these capsules in the benchtop Suzuki–Miyaura coupling of amide **3.4** with *N*-methylpyrrole-2-boronic acid pinacol ester (**3.5**), using 5 mol% Ni. Unfortunately, the use of our literature conditions resulted in poor yield of ketone **3.6**.[16] Specifically, the coupling of **3.4** and **3.5** employing paraffin-encapsulated Ni(cod)$_2$/Benz-ICy•HCl, 2.5 equiv of **3.5**, toluene as the reaction solvent, and a stir rate of 400 RPM for 16 h at 120 °C provided ketone **3.6** in 28% ^{1}H NMR yield.[17] After extensive experimentation, it was found that employing higher equivalents of **3.5** (2.5 to 5.0), utilizing 1,4-dioxane as the reaction solvent, and extending the reaction time to 24

hours proved beneficial. This provided ketone **3.6** in 91% yield on the benchtop. Additionally,

these capsules displayed long-term air and moisture stability when stored outside of a glovebox.

After two months of storage, a benchtop coupling of **3.4** and **3.5** generated **3.6** in comparable

yield.[16] These capsules are currently undergoing commercialization to enable their widespread

use.[18]
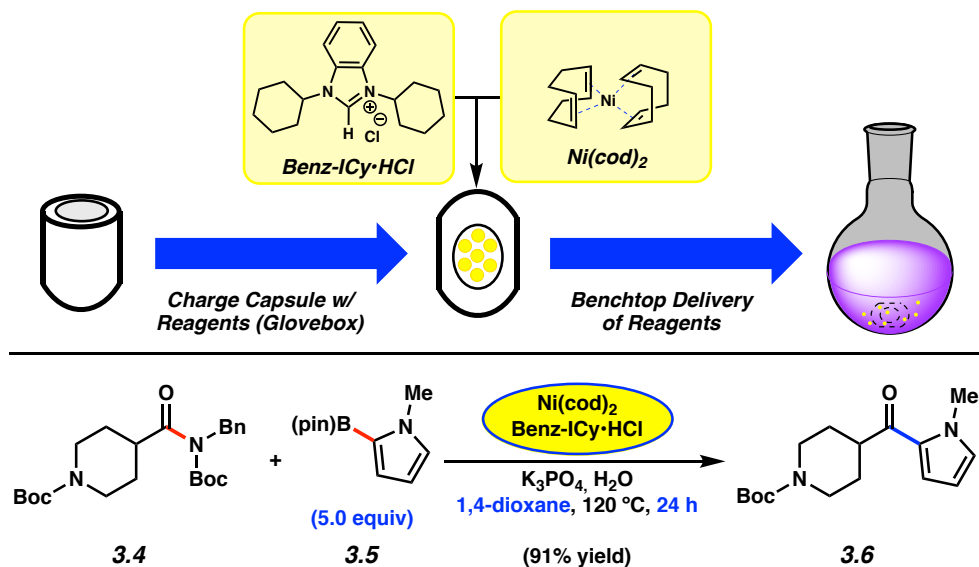
Figure 3.2. Preparation of Ni(cod)$_2$/Benz-ICy•HCl–paraffin capsules and their use in the benchtop Suzuki–Miyaura coupling of piperidinyl amide **3.4** and pyrrole boronic ester **3.5** under optimized conditions. Yield was determined by ^{1}H NMR analysis using 1,3,5-trimethoxybenzene as an external standard.

3.4 Scope of the Boronic Ester Coupling Partner

Having validated our encapsulation approach and arrived at optimized reaction conditions,

we evaluated the scope of this transformation with respect to the boronate ester coupling partner.

A variety of aryl boronate esters were assessed in couplings with piperidinylamide **3.4** (Figure

3.3). The methodology was found to be tolerant of medicinally privileged *N*-heterocyclic aryl

boronates[19] as evidenced by the formation of ketones **3.6**–**3.8**, in good to excellent yields.

Additionally, electron-poor *p*-CF$_3$ and sterically encumbered *o*-CH$_3$ substituted phenyl boronate

esters could be employed in the coupling, providing ketones **3.9** and **3.10** in 53% and 74% yields,

respectively. Boronate esters featuring extended aromatic ring systems were also competent

nucleophiles in the methodology, as demonstrated by the formation of naphthyl ketone **3.11** in

71% yield. Of note, in all cases, benchtop yields of the desired ketone products were comparable

to those obtained when using literature conditions requiring a glovebox (yields using the glovebox

protocol are shown in parentheses in Figure 3.3 and 3.4).[10]
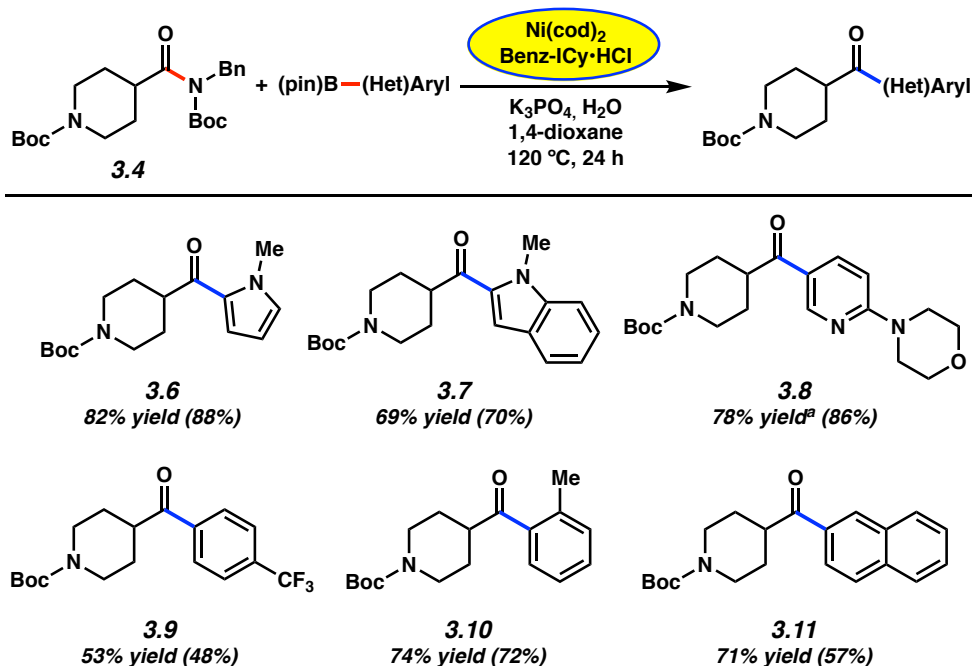
Figure 3.3. Scope of the boronic ester coupling partner. Unless otherwise noted, yields reflect the average of two isolation experiments. Yields in parentheses were obtained by carrying out the reaction in a glovebox utilizing literature conditions without encapsulating Ni(cod)$_2$ and Benz-ICy•HCl in paraffin. [a]Yield was determined by ^{1}H NMR analysis using 1,3,5-trimethoxybenzene as an external standard.

3.5 Scope of the Amide Substrate

We next surveyed a range of amide substrates in the Suzuki–Miyaura coupling with

pyrroloboronate **3.5** (Figure 3.4).[20] An additional piperidine-derived amide substrate could be used

in the coupling to furnish **3.12** in excellent yield. Furthermore, amides derived from isomeric 3-

and 4-tetrahydropyrancarboxylic acids were competent substrates, giving rise to ketones **3.13** and **3.14** in 79% and 84% yield, respectively. We also evaluated the coupling of non-heterocyclic amides. Linear and carbocyclic amides underwent the reaction smoothly, as demonstrated by the formation of **3.15** and **3.16** in 83% yield and 89% yield, respectively. Notably, steric bulk adjacent to the amide carbonyl did not hinder the Suzuki–Miyaura coupling as the use of a pivalamide substrate gave ketone **3.17** in 90% yield.
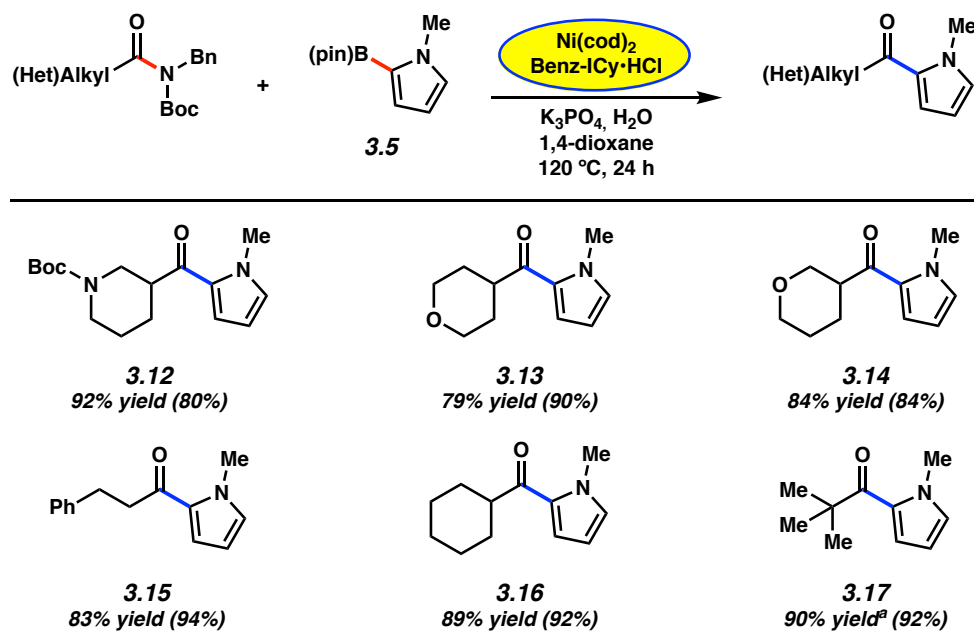
Figure 3.4. Scope of the amide substrate. Unless otherwise noted, yields reflect the average of two isolation experiments. Yields in parentheses were obtained by carrying out the reaction in a glovebox utilizing literature conditions without encapsulating Ni(cod)$_2$ and Benz-ICy•HCl in paraffin. [a]Yield was determined by ^{1}H NMR analysis using 1,3,5-trimethoxybenzene as an external standard.

3.6 Demonstration of Coupling on Gram-Scale

Finally, we assessed the Suzuki–Miyaura coupling of piperidine amide **3.1** with *N*-methylindole-2-boronic ester **3.18** on gram-scale as shown in Figure 3.5. Using 5 mol% Ni, the coupling proceeded smoothly to deliver ketone **3.19** in 73% yield. We view this result as promising

in the context of the scalable construction of biologically-relevant bis-heterocyclic ketones[19] where the enolizable alkyl–aryl ketone provides a valuable synthetic handle for further manipulation.
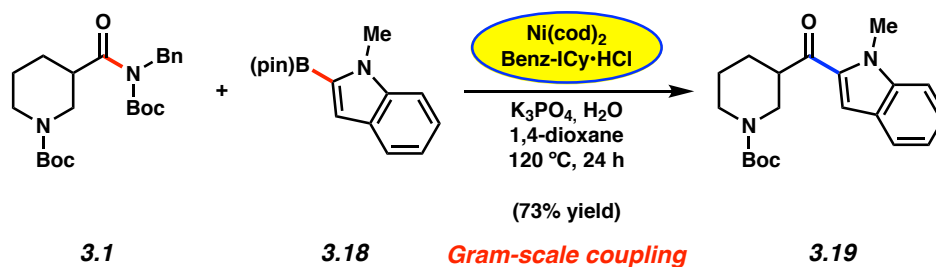
Figure 3.5. Gram-scale Suzuki–Miyaura coupling of amide **3.1** with boronate ester **3.18** to generate ketone **3.19**.

3.7 Conclusions

We have developed a benchtop protocol for the Suzuki–Miyaura cross-coupling of aliphatic amides to access alkyl–aryl ketones. Our strategy leverages mild Ni-catalyzed C–N bond activation to avoid the use of strongly basic and pyrophoric reagents typically employed in amide to ketone conversions. Additionally, the Ni(cod)$_2$/Benz-ICy•HCl–paraffin capsules, which are currently undergoing commercialization,[18] obviate the need to setup the reactions in a glovebox. Notably, this methodology enables the coupling of heterocyclic and aliphatic amides with a variety of aryl boronic esters for the formation of C–C bonds. Moreover, this transformation is scalable and, further, provides a valuable approach to the synthesis of alkyl–aryl ketones from amides, which benefits further from the use of base-metal catalysis and commercially available boronic ester nucleophiles. Thus, we hope these studies promote the use of Ni-mediated Suzuki–Miyaura couplings of aliphatic amides as a complement to traditional synthetic strategies.

3.8 Experimental Section

3.8.1 Materials and Methods

Unless stated otherwise, reactions were conducted in flame-dried glassware under an atmosphere of nitrogen or argon and commercially obtained reagents were used as received. Boronate esters **3.5**, **3.18**, **3.27**–**3.30** were obtained from Combi-Blocks. Ni(cod)$_2$ and Benz-ICy•HCl were obtained from Strem Chemicals. Potassium phosphate (K$_3$PO$_4$) was obtained from Acros. 1,4-Dioxane was obtained from Fisher Scientific and purified by distillation (over Na^0 and benzophenone) and degassed by sparging with N$_2$ for 1 h prior to use. Deionized water was degassed by sparging with N$_2$ for ≥10 min prior to use. Paraffin wax (mp 53–57 °C ASTM D 87) was obtained from Sigma-Aldrich and used as received. 1,3,5-trimethoxybenzene was obtained from Alfa Aesar and used as received. Reaction temperatures were controlled using an IKAmag temperature modulator, and unless stated otherwise, reactions were performed at room temperature (approximately 23 °C). Thin-layer chromatography (TLC) was conducted with EMD gel 60 F254 pre-coated plates (0.25 mm for analytical chromatography and 0.50 mm for preparative chromatography) and visualized using a combination of UV, anisaldehyde, iodine, and potassium permanganate staining techniques. Silicycle Siliaflash P60 (particle size 0.040–0.063 mm) was used for flash column chromatography. ^{1}H NMR spectra were recorded on Bruker spectrometers (400, 500, and 600 MHz) and are reported relative to residual solvent signals. Data for ^{1}H NMR spectra are reported as follows: chemical shift (δ ppm), multiplicity, coupling constant (Hz), integration. Data for ^{13}C NMR are reported in terms of chemical shift (at 125 MHz). IR spectra were recorded on a Perkin-Elmer UATR Two FT-IR spectrometer and are reported in terms of absorption frequency (cm^{-1}). DART-MS spectra were collected on a Thermo Exactive Plus MSD (Thermo Scientific) equipped with an ID-CUBE ion source and a Vapur Interface (IonSense Inc.).

Both the source and MSD were controlled by Excalibur software v. 3.0. The analyte was spotted onto OpenSpot sampling cards (IonSense Inc.) using $CHCl_3$, $CDCl_3$, or CH_2Cl_2 as the solvent. Ionization was accomplished using UHP He plasma with no additional ionization agents. The mass calibration was carried out using Pierce LTQ Velos ESI (+) and (–) Ion calibration solutions (Thermo Fisher Scientific).

Note: Supporting information for the syntheses of amides **3.1**, **3.4**, **3.20**, **3.21**,[5g] and **3.22–3.24**[10] have been published and spectral data match those previously reported.
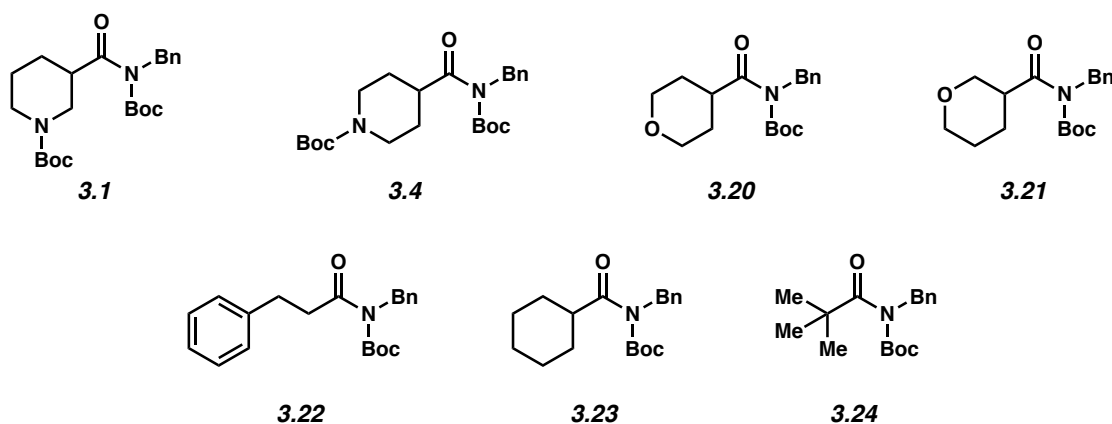
3.8.2 Experimental Procedures

3.8.2.1 Preparation of Paraffin Wax Capsules

Representative Procedure for the preparation of paraffin wax capsules for use in Sections 3.8.2.3 and 3.8.2.4. Paraffin wax (mp 53–57 °C ASTM D 87) was melted in a 250 mL beaker suspended in an oil bath maintained at 80 °C.
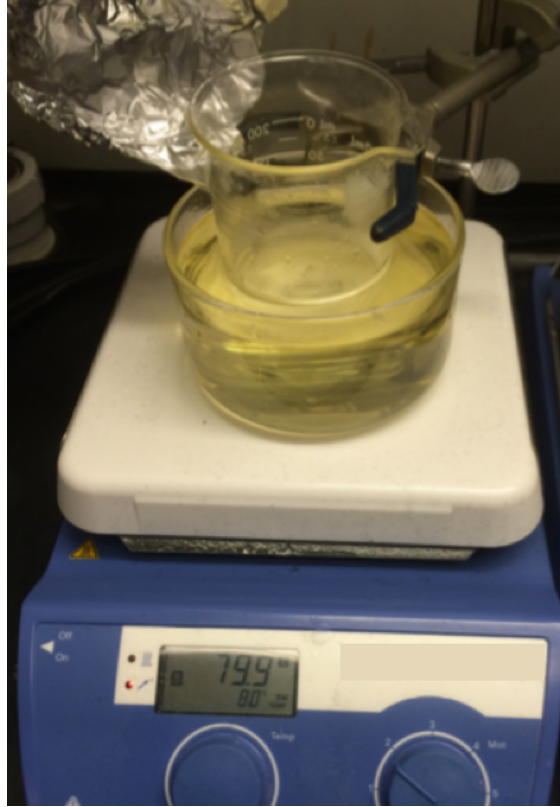
The molten paraffin was then pipetted into a standard brass mold (Brass Nipple, 1/8 in x close) using a 5 3/4 in glass pipette and pipette bulb.

After cooling, the resulting wax cylinder was removed from the brass mold and trimmed to approximately 1 cm in length using a razor blade.

Next, a cavity was bored in the wax cylinder using a standard drill bit (5/32 in, black oxide), taking care not to bore through the entire cylinder.

The resulting hollow and open capsule was brought into a glovebox, inserted into a 14/20 septum for ease of handling, and charged with Ni(cod)$_2$ (5.5 mg, 0.020 mmol, 5 mol%) and Benz-ICy•HCl (12.8 mg, 0.040 mmol, 10 mol%).

After charging the capsule, a warm metal spatula (maintained at approximately 80 °C using a hot plate in the glovebox) was used to melt the top of the capsule closed. Removal from the glovebox and re-dipping in molten wax twice (to ensure a proper seal) gave the desired capsules that were ready for use on the benchtop. The capsules were stored in a freezer maintained at –20 °C under an atmosphere of air until use.
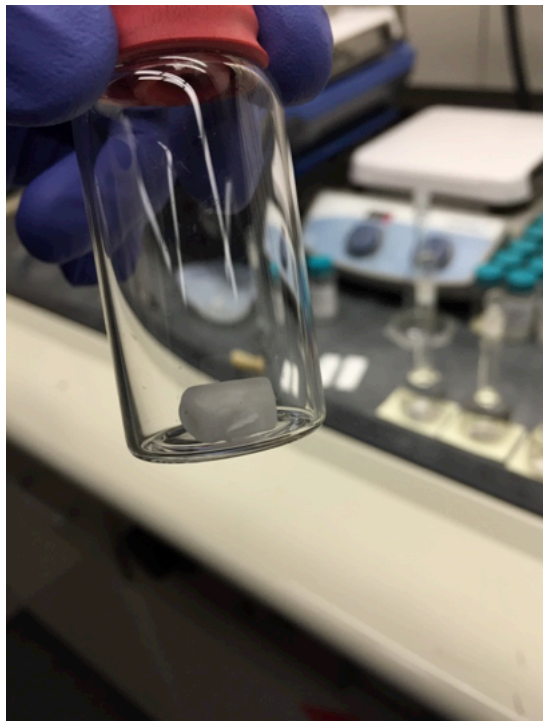
Note: Supporting information for the preparation of similar paraffin capsules has been previously disclosed.[14] Typically, paraffin wax capsules generated in this way were used within 1–2 weeks of being prepared. The stability of paraffin capsules to air and moisture was examined over a period of two months (See Section 3.8.2.3).

3.8.2.2 Preparation of Paraffin Wax Capsules for Gram-Scale Coupling

Representative Procedure for preparation of paraffin wax capsules for use in Section 3.8.2.5.

Paraffin wax (mp 53–57 °C ASTM D 87) was melted in a 250 mL beaker suspended in an oil bath maintained at 80 °C. The molten paraffin (approximately 4 mL) was then pipetted into a standard glass VWR culture tube (12 x 75 mm) using a 5 3/4 in glass pipette and pipette bulb. After cooling, the resulting wax cylinder was removed from the culture tube (by scoring and carefully breaking

the glass away from the paraffin) and trimmed to approximately 2.0 cm in length using a razor blade.

Next, a cavity was bored in the wax cylinder using a standard drill bit (15/64 in, black oxide), taking care not to bore through the entire cylinder.
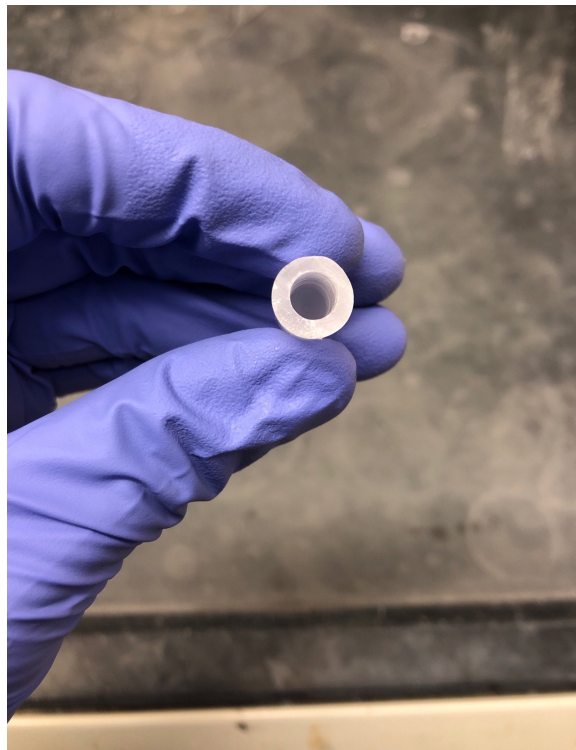
The resulting hollow and open capsule was brought into a glovebox and charged with Ni(cod)$_2$ (32.9 mg, 0.119 mmol, 5 mol%) and Benz-ICy•HCl (76.2 mg, 0.239 mmol, 10 mol%). After charging the capsule, a warm metal spatula (maintained at approximately 80 °C using a hot plate in the glovebox) was used to melt the top of the capsule closed. Removal from the glovebox and re-dipping in molten wax twice (to ensure a proper seal) gave the desired capsules that were ready for use on the benchtop (See Section 3.8.2.5)

Note: Supporting information for the preparation of similar gram-scale paraffin capsules has been previously disclosed.[14]

3.8.2.3 Optimization of Methodology
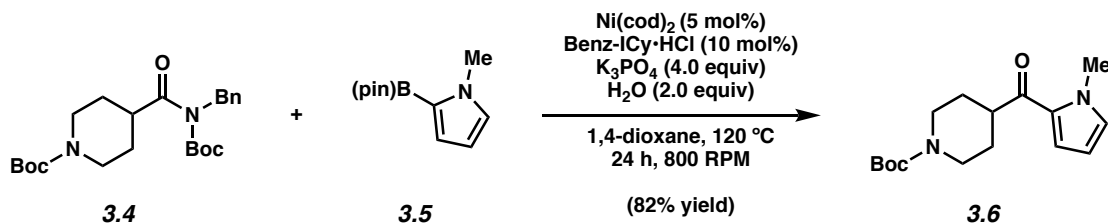
Representative Procedure for Table 3.1 (coupling of amide 3.4 and *N*-methylpyrrole-2-boronic acid pinacol ester (3.5) is used as an example). Ketone 3.6. A 2-dram vial was charged with anhydrous powder K_3PO_4 (340 mg, 1.60 mmol, 4.00 equiv) and a magnetic stir bar (egg-shaped 3/8 x 3/16 in). The vial and its contents were flame-dried under reduced pressure and

allowed to cool under N_2. The vial was then charged with amide substrate **3.4** (167 mg, 0.40 mmol, 1.00 equiv), *N*-methylpyrrole-2-boronic acid pinacol ester (**3.5**, 414 mg, 2.00 mmol, 5.00 equiv), and a paraffin wax capsule containing Ni(cod)$_2$ (5.50 mg, 0.02 mmol, 0.05 equiv) and Benz-ICy•HCl (12.8 mg, 0.04 mmol, 0.10 equiv) prepared as described in Section 3.8.2.1. The vial was purged with N_2 and subsequently deionized water (14.0 μL, 0.80 mmol, 2.00 equiv) and 1,4-dioxane (0.40 mL, 1.00 M) were added. The vial was capped with a Teflon-lined screw cap under a flow of N_2 and the reaction mixture was stirred vigorously (800 RPM) at 120 ºC for 24 h. After removing the vial from heat, the reaction mixture was transferred to a 100 mL pear-shaped flask containing 2.0 g of silica gel with hexanes (6 mL) and CH_2Cl_2 (6 mL). The mixture was adsorbed onto the silica gel under reduced pressure and filtered over a plug of silica gel (4.0 cm OD x 3.0 cm, 300 mL of hexanes eluent to remove paraffin, then 250 mL of EtOAc eluent). The volatiles were removed under reduced pressure and the yield of ketone **3.6** was determined by ^{1}H NMR analysis with 1,3,5-trimethoxybenzene as an external standard.[10]

Any modifications of the conditions shown in the representative procedure

above are specified below in Table 3.1.

Table 3.1. Optimization studies.
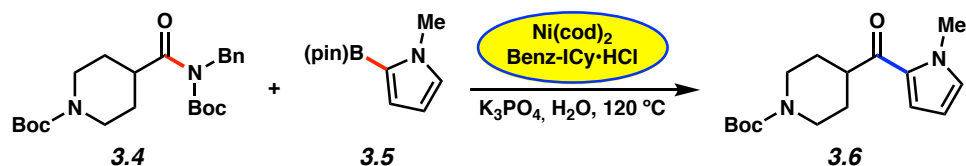
Entry	Solvent (1.0 M)	equiv. 3.5	Time	Stir Rate	Yield of 3.6[a]
1	toluene	2.5	16	400 RPM	28%
2	1,4-dioxane	2.5	16	400 RPM	71%
3	1,4-dioxane	5.0	24	800 RPM	91%
4[b]	1,4-dioxane	2 month stability test			97%

[a]Yields were determined by ^{1}H NMR analysis using 1,3,5-trimethoxybenzene as an external standard and reflect the average of two experiments. [b]Reaction performed using conditions outlined in Entry 3.

3.8.2.4 Scope of Methodology
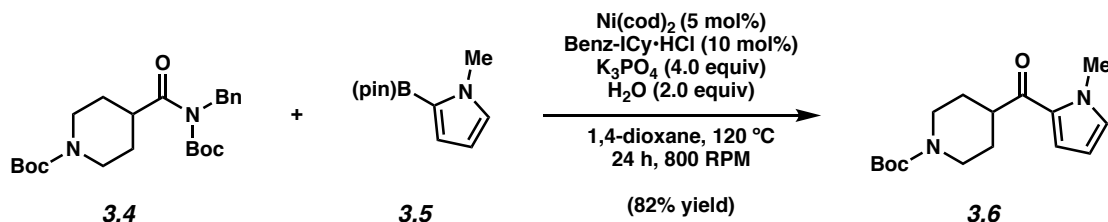
Representative Procedure for Figures 3.3 and 3.4 (coupling of amide 3.4 and *N*-methylpyrrole-2-boronic acid pinacol ester (3.5) is used as an example). Ketone 3.6. A 2-dram

vial was charged with anhydrous powder K_3PO_4 (340 mg, 1.60 mmol, 4.00 equiv) and a magnetic

stir bar (egg-shaped 3/8 x 3/16 in). The vial and its contents were flame-dried under reduced

pressure and allowed to cool under N_2. The vial was then charged with amide substrate **3.4** (167

mg, 0.40 mmol, 1.00 equiv), *N*-methylpyrrole-2-boronic acid pinacol ester (414 mg, 2.00 mmol,

5.0 equiv), and a paraffin wax capsule containing Ni(cod)$_2$ (5.50 mg, 0.02 mmol, 0.05 equiv) and

Benz-ICy•HCl (12.8 mg, 0.04 mmol, 0.10 equiv) prepared as described in Section 3.8.2.1. The

vial was purged with N_2 and subsequently deionized water (14.0 µL, 0.8 mmol, 2.00 equiv) and

1,4-dioxane (0.40 mL, 1.00 M) were added. The vial was capped with a Teflon-lined screw cap under a flow of N_2 and the reaction mixture was stirred vigorously (800 RPM) at 120 °C for 24 h. After removing the vial from heat, the reaction mixture was transferred to a 100 mL pear-shaped flask containing 2.0 g of silica gel with hexanes (6 mL) and CH_2Cl_2 (6 mL). The mixture was adsorbed onto the silica gel under reduced pressure and filtered over a plug of silica gel (4.0 cm OD x 3.0 cm, 300 mL of hexanes eluent to remove paraffin, then 250 mL of EtOAc eluent). The volatiles were removed under reduced pressure and the crude residue was purified by flash column chromatography (19:1 Hexanes:EtOAc → 9:1 Hexanes:EtOAc) to yield ketone **3.6** (82% yield, average of two experiments) as a yellow oil. Ketone **3.6**: R_f 0.25 (5:1 Hexanes:EtOAc). ^{1}H NMR (500 MHz, CDCl_3): δ 6.98 (dd, J = 4.1, 1.7, 1H), 6.83 (t, J = 2.0, 1H), 6.14 (dd, J = 2.6, 1.7, 1H), 4.18 (br s, 2H), 3.93 (s, 3H), 3.21–3.10 (m, 1H), 2.82 (br s, 2H), 1.85–1.64 (m, 4H), 1.47 (s, 9H). Spectral data match those previously reported.[10]

Any modifications of the conditions shown in the representative procedure above are specified in the following schemes, which depict all of the results shown in Figures 3.3 and 3.4.
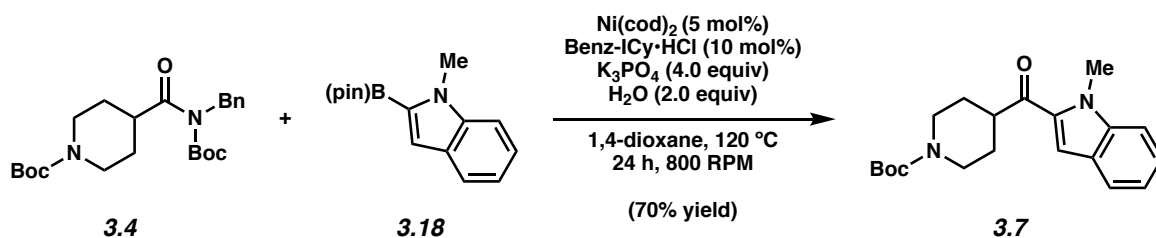
Ketone 3.7. Purification by flash chromatography (19:1 Hexanes:EtOAc → 9:1 Hexanes:EtOAc) generated ketone **3.7** (70% yield, average of two experiments) as a white solid. Ketone **3.7**: R_f 0.33 (5:1 Hexanes:EtOAc). ^{1}H NMR (500 MHz, CDCl_3): δ 7.70 (d, J = 7.9, 1H), 7.39 (d, J = 3.9, 2H),

7.33 (s, 1H), 7.20–7.14 (m, 1H) 4.21 (br s, 2H), 4.07 (s, 3H), 3.47–3.32 (m, 1H), 2.88 (br s, 2H), 1.86 (br s, 2H), 1.82–1.70 (m, 2H), 1.48 (s, 9H). Spectral data match those previously reported.[10]
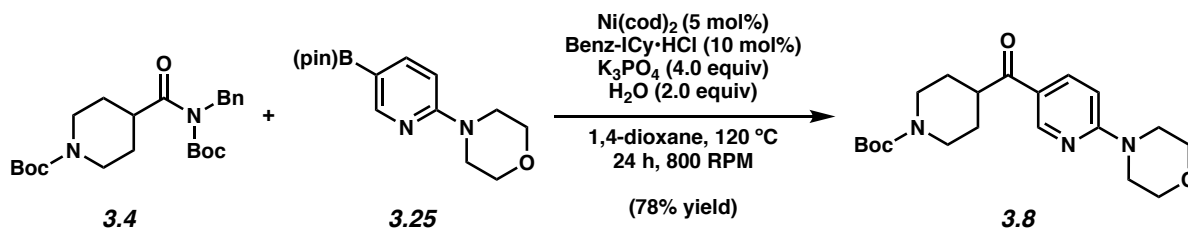
Ketone 3.8. ^{1}H NMR analysis of the crude reaction mixture indicated a 78% yield of ketone **3.8** relative to a 1,3,5-trimethoxybenzene external standard (average of two experiments). Purification by preparative thin-layer chromatography (1:1 Hexanes:EtOAc) provided an analytical sample of ketone **3.8** as a white solid. Ketone **3.8**: R_f 0.30 (1:1 Hexanes:EtOAc). ^{1}H NMR (500 MHz, CDCl$_3$): δ 8.78 (d, J = 2.6, 1H), 8.05 (dd, J = 9.1, 2.5, 1H), 6.63 (d, J = 9.1, 1H), 4.16 (br s, 2H), 3.81 (t, J = 5.2, 4H), 3.68 (t, J = 4.7, 4H), 3.32–3.21 (m, 1H), 2.87 (br s, 2H), 1.79 (br s, 2H), 1.76–1.65 (m, 2H), 1.46 (s, 9H). Spectral data match those previously reported.[10]
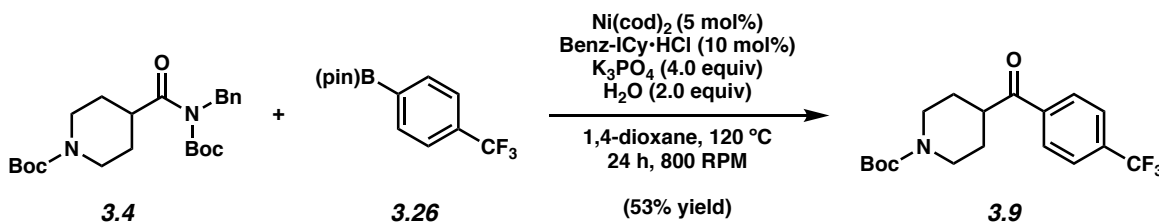
Ketone 3.9. Purification by flash chromatography (19:1 Hexanes:EtOAc → 9:1 Hexanes:EtOAc) generated ketone **3.9** (53% yield, average of two experiments) as a white solid. Ketone **3.9**: R_f 0.33 (5:1 Hexanes:EtOAc). ^{1}H NMR (500 MHz, CDCl$_3$): δ 8.03 (d, J = 8.4, 2H), 7.74 (d, J = 8.4, 2H), 4.16 (br s, 2H), 3.46–3.31 (m, 1H), 2.91 (br s, 2H), 1.85 (d, J = 13.3, 2H), 1.76–1.64 (m, 2H), 1.46 (d, J = 4.0, 9H). Spectral data match those previously reported.[10]
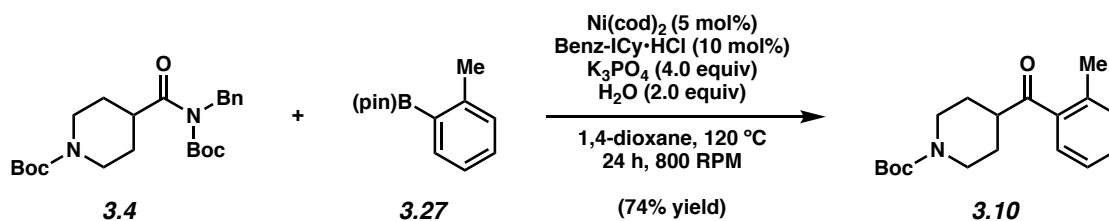
Ketone 3.10. Purification by flash chromatography (24:1 Hexanes:EtOAc → 5:1 Hexanes:EtOAc) generated ketone **3.10** (74% yield, average of two experiments) as a yellow oil. Ketone **3.10**: R_f 0.16 (9:1 Hexanes:EtOAc). ^{1}H NMR (600 MHz, CDCl$_3$): δ 7.50 (dd, J = 7.8, 1.4 Hz, 1H), 7.36 (td, J = 7.4, 1.3, 1H), 7.26–7.22 (m, 2H), 4.12 (br s, 2H), 3.18 (tt, J = 11.2, 3.6, 1H), 2.84 (br s, 2H), 2.41 (s, 3H), 1.81 (d, J = 13.1, 2H), 1.60–1.58 (m, 2H), 1.46 (s, 9H). Spectral data match those previously reported.[10]
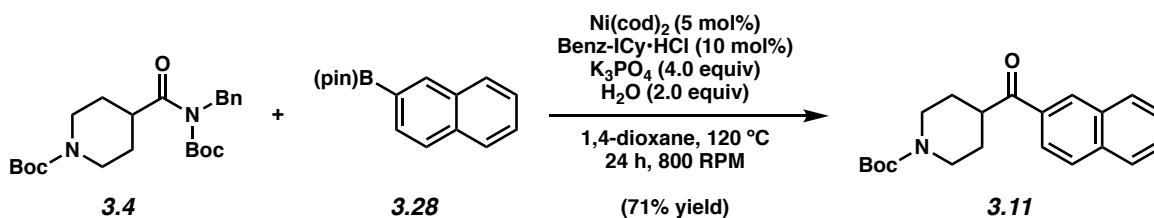
Ketone 3.11. Purification by flash chromatography (19:1 Hexanes:EtOAc → 14:1 Hexanes:EtOAc) generated ketone **3.11** (71% yield, average of two experiments) as a white solid. Ketone **3.11**: R_f 0.16 (9:1 Hexanes:EtOAc). ^{1}H NMR (500 MHz, CDCl$_3$): δ 8.45 (s, 1H), 8.04–7.85 (m, 4H), 7.65–7.53 (m, 2H), 4.20 (br s, 2H), 3.58 (tt, J = 11.2, 4.0, 1H), 2.96 (t, J = 2.8, 2H), 1.90 (br s, 2H), 1.83–1.69 (m, 2H), 1.48 (s, 9H). Spectral data match those previously reported.[10]
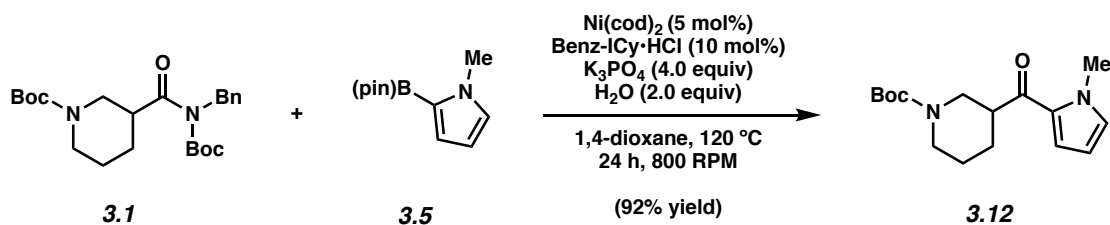
Ketone 3.12. Purification by flash chromatography (19:1 Hexanes:EtOAc → 9:1 Hexanes:EtOAc) generated ketone **3.12** (92% yield, average of two experiments) as a light brown oil. Ketone **3.12**: R_f 0.26 (5:1 Hexanes:EtOAc). ^{1}H NMR (400 MHz, CDCl$_3$): δ 7.05 (dd, J = 4.2, 1.6, 1H), 6.82 (t, J = 1.9, 1H), 6.14 (dd, J = 4.1, 2.5, 1H), 4.25 (br d, J = 13.5, 1H), 4.12 (br d, J = 11.7, 1H), 3.93 (br s, 3H), 3.16 (tt, J = 11.4, 3.6, 1H), 2.94–2.83 (m, 1H), 2.70 (td, J = 12.7, 2.4, 1H), 2.02–1.92 (m, 1H), 1.79–1.68 (m, 2H), 1.61–1.50 (m, 1H), 1.47 (s, 9H). Spectral data match those previously reported.[10]
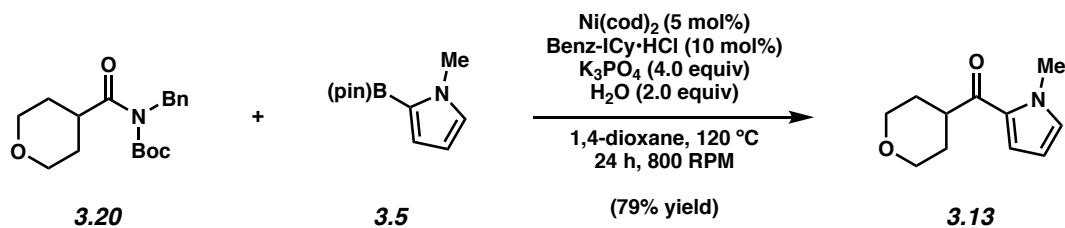
Ketone 3.13. Purification by sequential preparative thin-layer chromatography (9:1 Hexanes:EtOAc and 5:1 Hexanes:EtOAc) generated ketone **3.13** (79% yield, average of two experiments) as a white solid. Ketone **3.13**: R_f 0.17 (5:1 Hexanes:EtOAc). ^{1}H NMR (500 MHz, CDCl$_3$): δ 6.99 (dd, J = 4.1, 1.6, 1H), 6.83 (t, J = 1.9, 1H), 6.14 (dd, J = 4.1, 2.5, 1H), 4.09–4.00 (m, 2H), 3.94 (s, 3H), 3.52 (td, J = 11.8, 2.1, 2H), 3.26 (tt, J = 11.5, 3.8, 1H), 1.97–1.86 (m, 2H), 1.74–1.67 (m, 2H). Spectral data match those previously reported.[10]
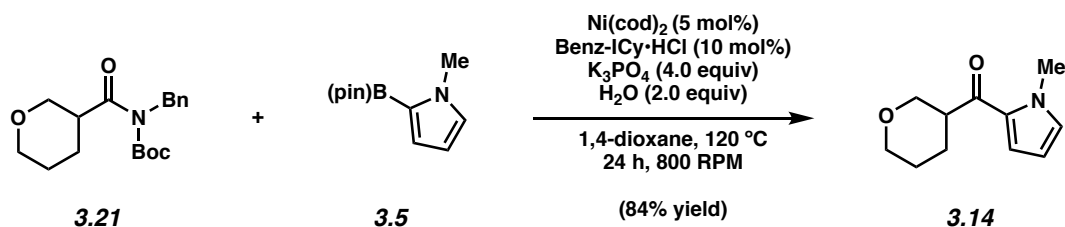
Ketone 3.14. Purification by flash chromatography (9:1 Hexanes:EtOAc) generated ketone **3.14** (84% yield, average of two experiments) as a colorless oil. Ketone **3.14**: R_f 0.22 (5:1 Hexanes:EtOAc). ^{1}H NMR (500 MHz, CDCl$_3$): δ 7.03 (dd, J = 4.2, 1.7, 1H), 6.82 (t, J = 1.9, 1H), 6.14 (dd, J = 4.2, 2.5, 1H), 4.10–4.04 (m, 1H), 3.99–3.93 (m, 1H), 3.92 (s, 3H), 3.53 (t, J = 10.8, 1H), 3.46–3.34 (m, 2H), 2.02–1.94 (m, 1H), 1.91–1.80 (m, 1H), 1.80–1.65 (m, 2H). Spectral data match those previously reported.[10]
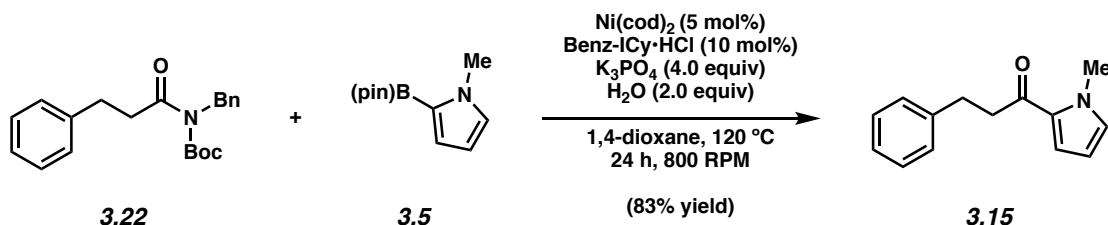
Ketone 3.15. Purification by flash chromatography (19:1 Hexanes:EtOAc) generated ketone **3.15** (83% yield, average of two experiments) as a colorless oil. Ketone **3.15**: R_f 0.40 (5:1 Hexanes:EtOAc). ^{1}H NMR (500 MHz, CDCl$_3$): δ 7.32–7.17 (m, 2H), 7.26–7.23 (m, 2H), 7.22–7.17 (m, 1H), 6.94 (dd, J = 4.1, 1.7, 1H), 6.80 (t, J = 1.9, 1H), 6.11 (dd, J = 4.1, 2.4, 1H), 3.95 (s, 3H), 3.14–3.08 (m, 2H), 3.05–2.99 (m, 2H). Spectral data match those previously reported.[10]
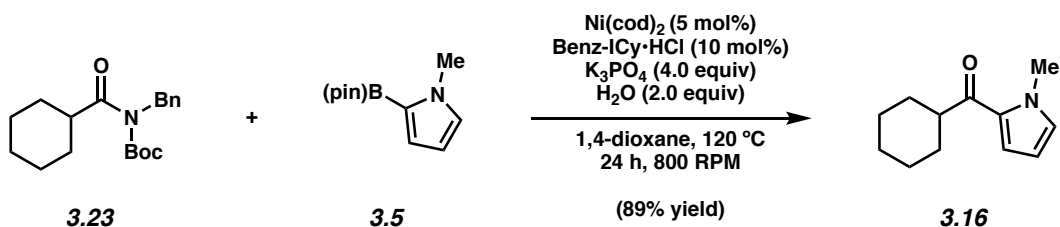
Ketone 3.16. Purification by flash chromatography (25:4:1 Hexanes:PhH:Et$_2$O) generated ketone **3.16** (89% yield, average of two experiments) as a colorless oil. Ketone **3.16**: R$_f$ 0.55 (5:1 Hexanes:EtOAc). ^{1}H NMR (500 MHz, CDCl$_3$): δ 6.97 (dd, J = 4.1, 1.7, 1H), 6.80 (t, J = 1.9, 1H), 6.12 (dd, J = 4.1, 2.5, 1H), 3.93 (s, 3H), 3.02 (tt, J = 11.7, 3.2, 1H), 1.88–1.79 (m, 4H), 1.76–1.67 (m, 1H), 1.56–1.45 (m, 2H), 1.41–1.30 (m, 2H), 1.29–1.19 (m, 1H). Spectral data match those previously reported.[10]
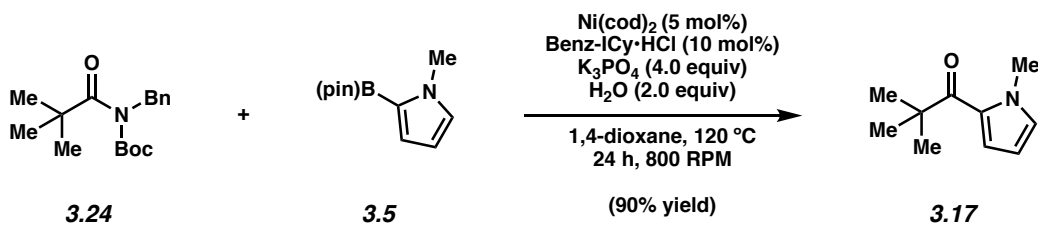
Ketone 3.17. ^{1}H NMR analysis of the crude reaction mixture indicated a 90% yield of ketone **3.17** relative to a 1,3,5-trimethoxybenzene external standard. Purification by preparative thin-layer chromatography (49:1 Cyclohexane:EtOAc), eluted twice, provided an analytical sample of ketone **3.17** as a colorless oil. Ketone **3.17**: R$_f$ 0.65 (4:1 Hexanes:EtOAc). ^{1}H NMR (500 MHz, CDCl$_3$): δ 7.03 (dd, J = 4.1, 1.6, 1H), 6.75 (t, J = 1.9, 1H), 6.11 (dd, J = 4.1, 2.5, 1H), 3.90 (s, 3H), 1.36 (m, 9H). Spectral data match those previously reported.[10]

180

3.8.2.5 Gram-Scale Benchtop Suzuki–Miyaura Cross-Coupling
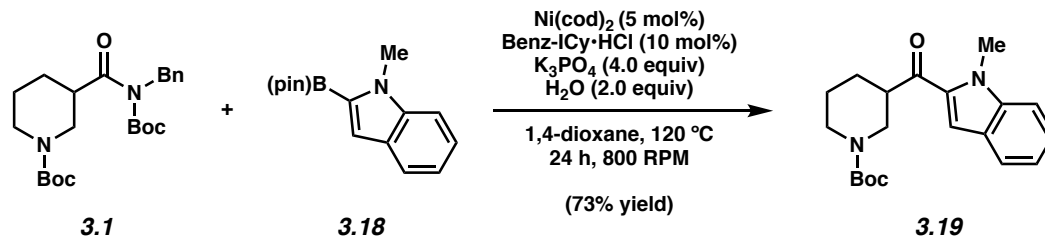
Ketone 3.19. A 20-mL scintillation vial was charged with anhydrous powder K_3PO_4 (2.03 g, 9.56 mmol, 4.00 equiv) and a magnetic stir bar (football shaped, 0.5 x 1.5 cm). The vial and its contents were flame-dried under reduced pressure and allowed to cool under N_2. The vial was charged with amide substrate **3.1** (1.00 g, 2.39 mmol, 1.00 equiv), boronic ester **3.18** (3.07 g, 11.9 mmol, 5.00 equiv), and a paraffin wax capsule containing $Ni(cod)_2$ (32.9 mg, 0.119 mmol, 0.050 equiv) and Benz-ICy•HCl (76.2 mg, 0.239 mmol, 0.100 equiv) prepared as described in Section 3.8.2.3. The vial was purged with N_2 and subsequently deionized water (86.1 µL, 4.78 mmol, 2.00 equiv) and 1,4-dioxane (2.39 mL, 1.00 M) were added. The vial was capped with a Teflon-lined screw cap under a flow of N_2 and the reaction mixture was stirred vigorously (800 RPM) at 120 °C for 24 h. After removing the vial from heat, the reaction mixture was transferred to a 100 mL pear-shaped flask containing 12.0 g of silica gel with hexanes (10 mL) and CH_2Cl_2 (10 mL). The mixture was adsorbed onto the silica gel under reduced pressure and filtered over a plug of silica gel (4.0 cm OD x 3.0 cm, 300 mL of hexanes eluent to remove paraffin, then 250 mL of EtOAc eluent). The volatiles were removed under reduced pressure and the crude residue was purified by flash column chromatography (14:1 Hexanes:Et$_2$O → 4:1 Hexanes:Et$_2$O) to yield ketone **3.19** (73% yield, average of two experiments) as a white amorphous solid. Ketone **3.19**: R$_f$ 0.25 (5:1 Hexanes:EtOAc); ^{1}H NMR (500 MHz, CDCl$_3$): δ 7.70 (d, J = 8.1, 1H), 7.44–7.34 (m, 3H), 7.20–7.11 (m, 1H), 4.32 (br s, 1H), 4.24–3.96 (m, 4H), 3.47–3.27 (m, 1H), 2.98 (br s, 1H), 2.74 (br s, 1H), 2.12–2.00 (m, 1H), 1.84–1.68 (m, 2H), 1.67–1.54 (m, 2H), 1.49 (s, 9H); ^{13}C NMR (125 MHz,

CDCl$_3$): δ 195.3, 154.9, 140.5, 133.9, 126.3, 125.9, 123.2, 121.0, 111.9, 110.5, 79.9, 47.9, 46.2, 44.9, 44.0, 32.4, 28.64, 28.61, 24.8; IR (film): 2973, 2938, 2861, 1691, 1656, 1614, 1423, 1168, 1146, 970 cm^{-1}; HRMS-APCI (m/z) [M + H]$^+$ calcd for C$_{20}$H$_{27}$N$_2$O$_3$, 343.2016; found 343.2010.

*Note: Ketone **3.19** was obtained as a mixture of conformers. These data represent empirically observed chemical shifts from the ^{13}C NMR spectrum.*

3.9 Spectra Relevant to Chapter Three:

Ni-Catalyzed Suzuki–Miyaura Cross-Coupling of Aliphatic Amides on the Benchtop

Milauni M. Mehta,[†] Timothy B. Boit,[†] Jacob E. Dander,[†] and Neil K. Garg.
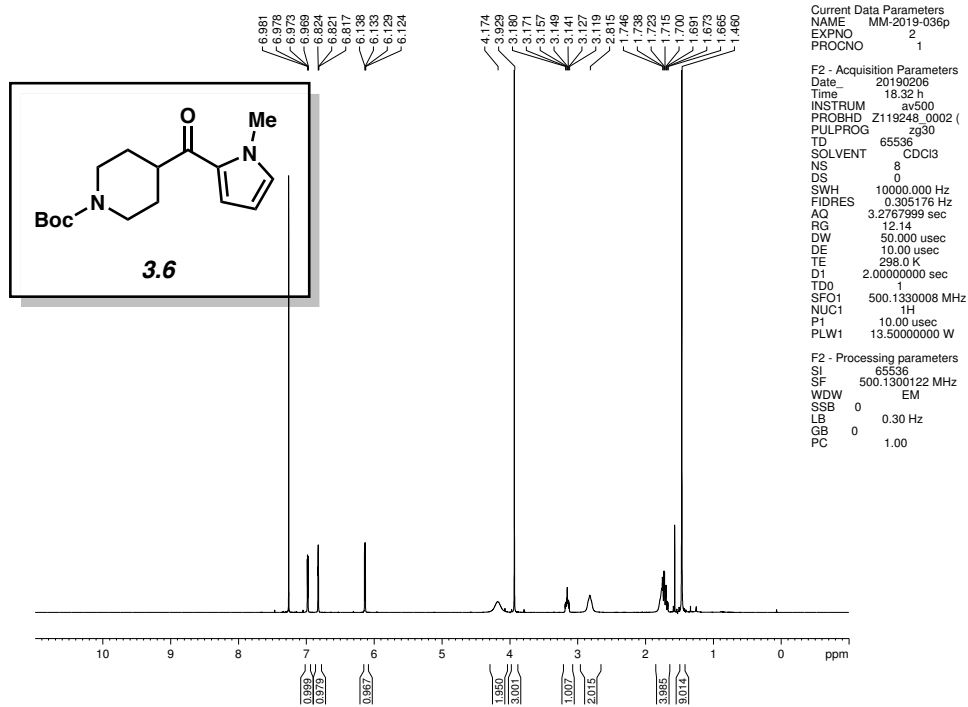
Figure 3.6 ^{1}H NMR (500 MHz, CDCl$_3$) of compound **3.6**.
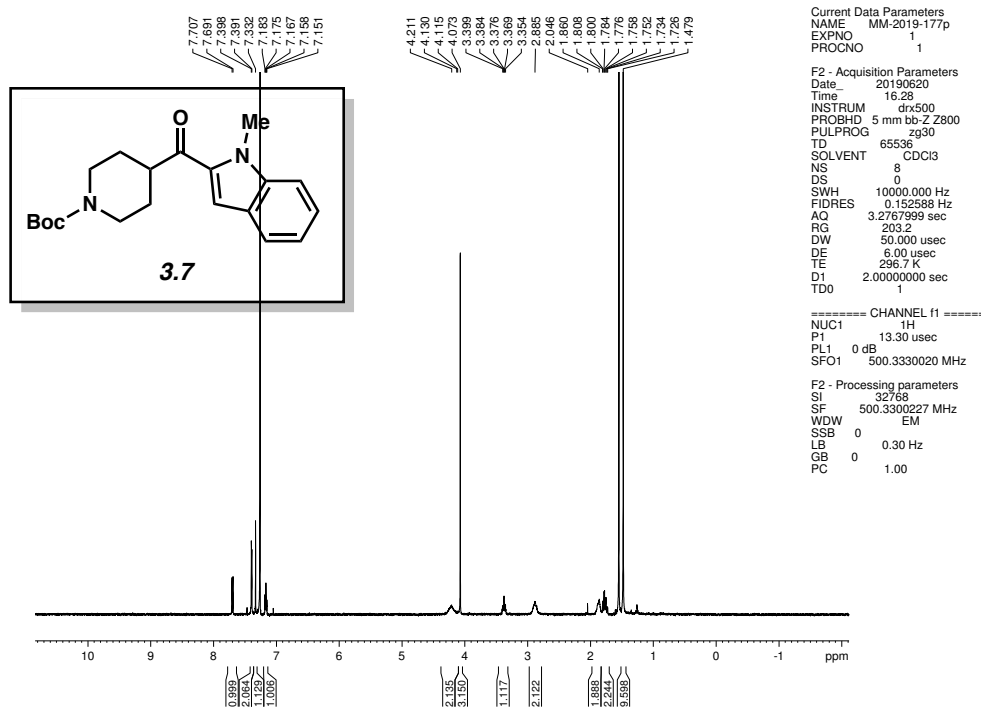
Figure 3.7 ^{1}H NMR (500 MHz, CDCl$_3$) of compound **3.7**.
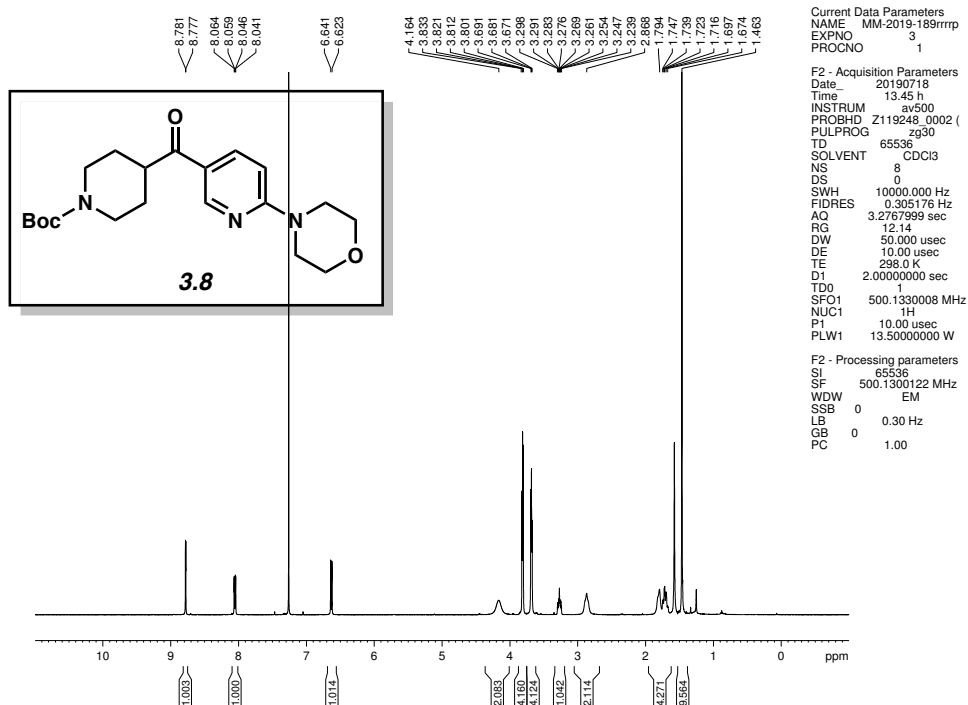
Figure 3.8 ^{1}H NMR (500 MHz, CDCl$_3$) of compound **3.8**.
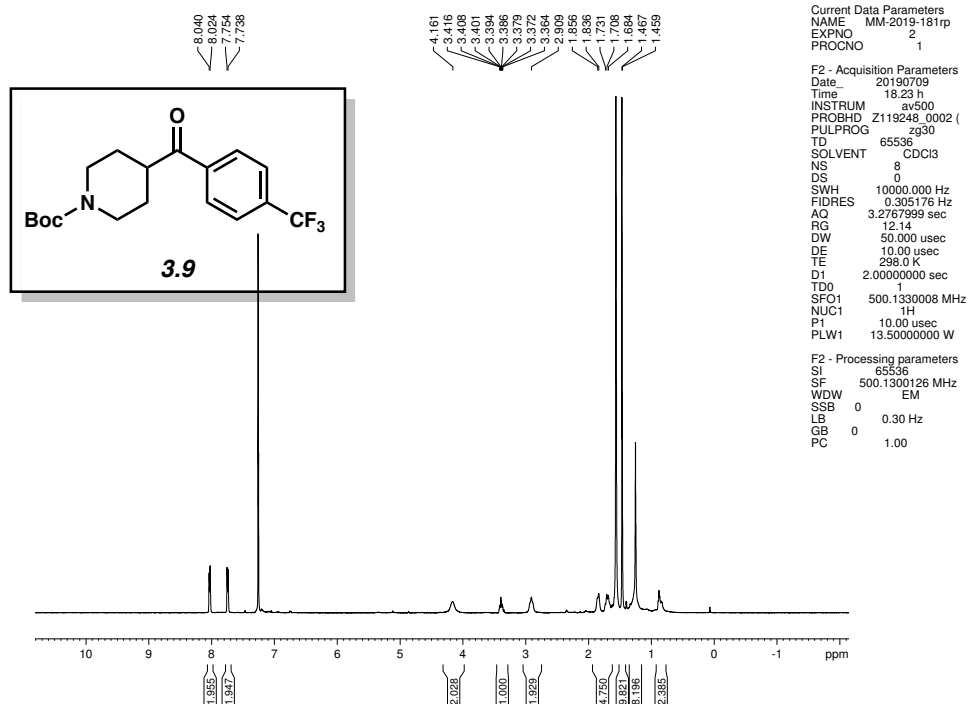
Figure 3.9 ^{1}H NMR (500 MHz, CDCl$_3$) of compound **3.9**.
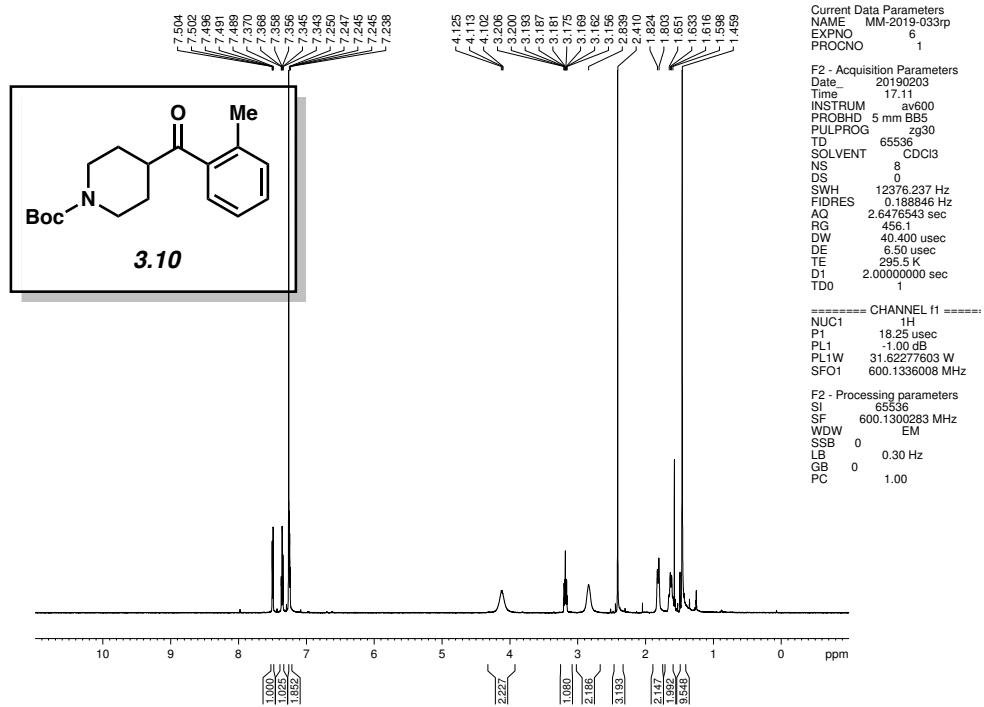
Figure 3.10 ^{1}H NMR (600 MHz, CDCl$_3$) of compound **3.10**.
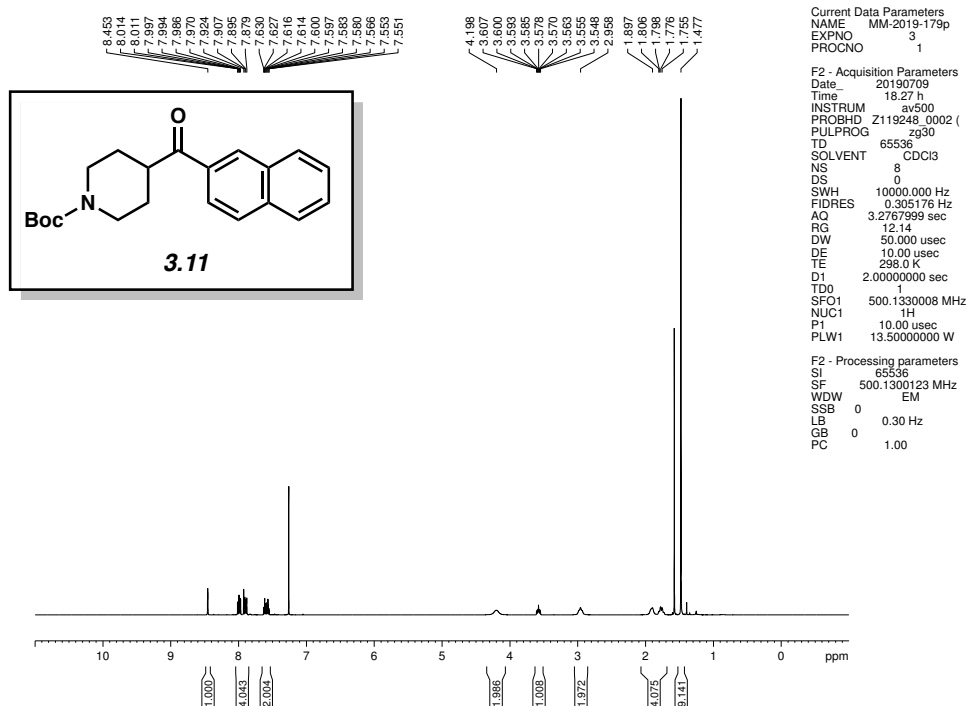
Figure 3.11 ^{1}H NMR (500 MHz, CDCl$_3$) of compound **3.11**.
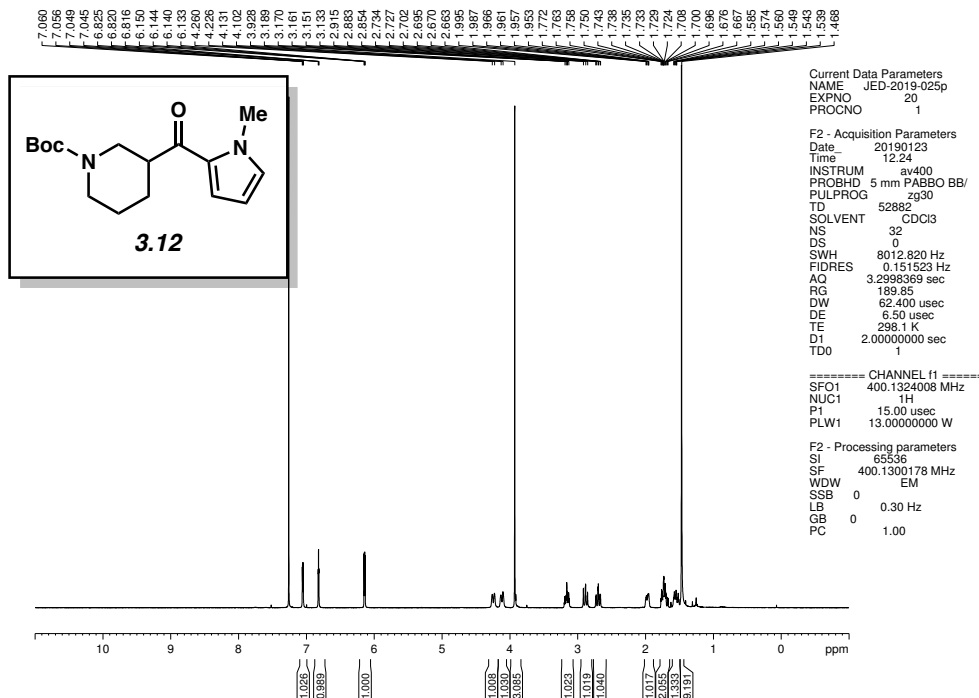
Figure 3.12 ^{1}H NMR (400 MHz, CDCl$_3$) of compound **3.12**.
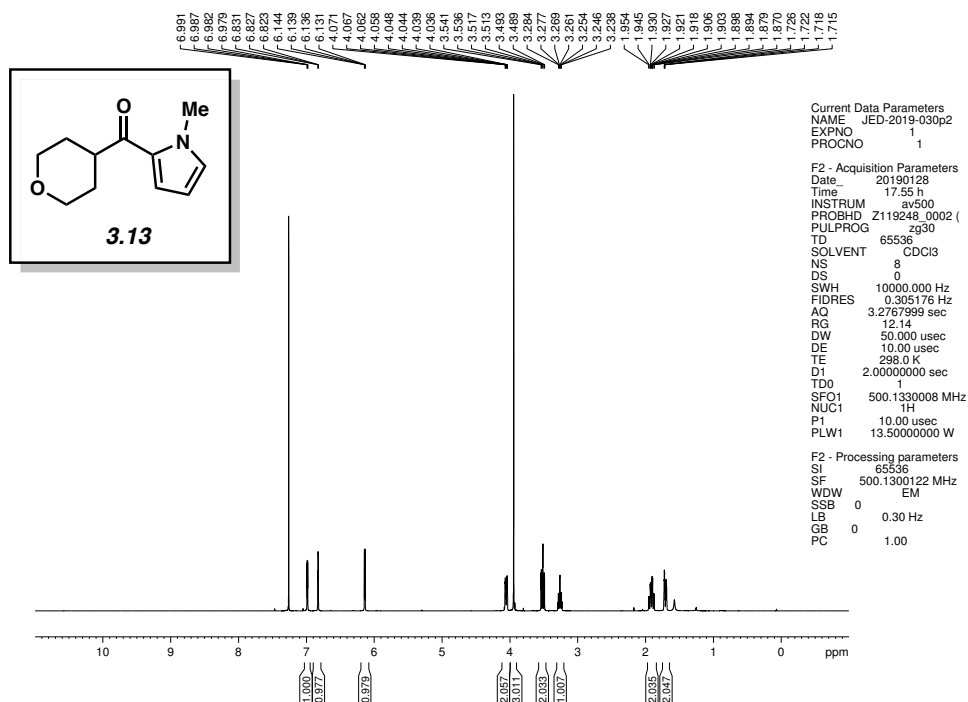
Figure 3.13 ^{1}H NMR (500 MHz, CDCl$_3$) of compound **3.13**.
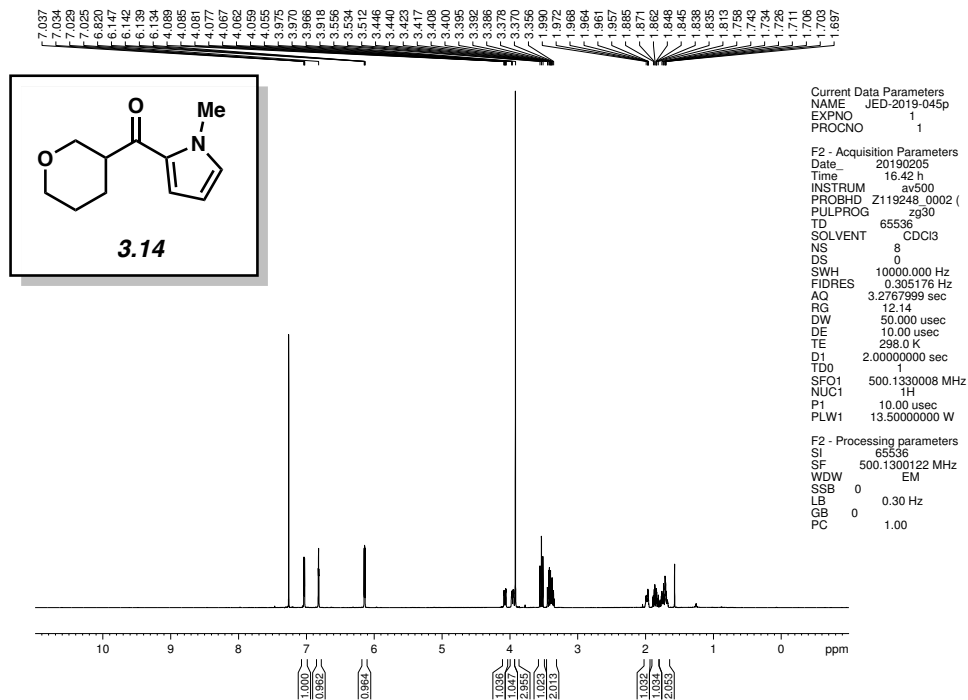
Figure 3.14 ^{1}H NMR (500 MHz, CDCl$_3$) of compound **3.14**.
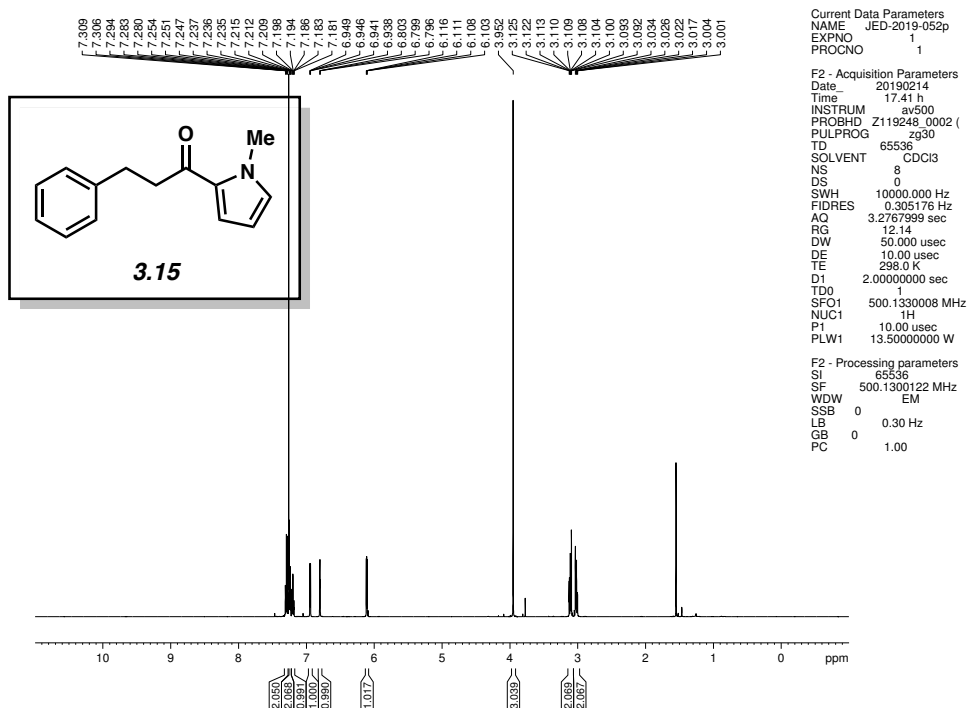
Figure 5.15 ^{1}H NMR (500 MHz, CDCl$_3$) of compound **3.15**.
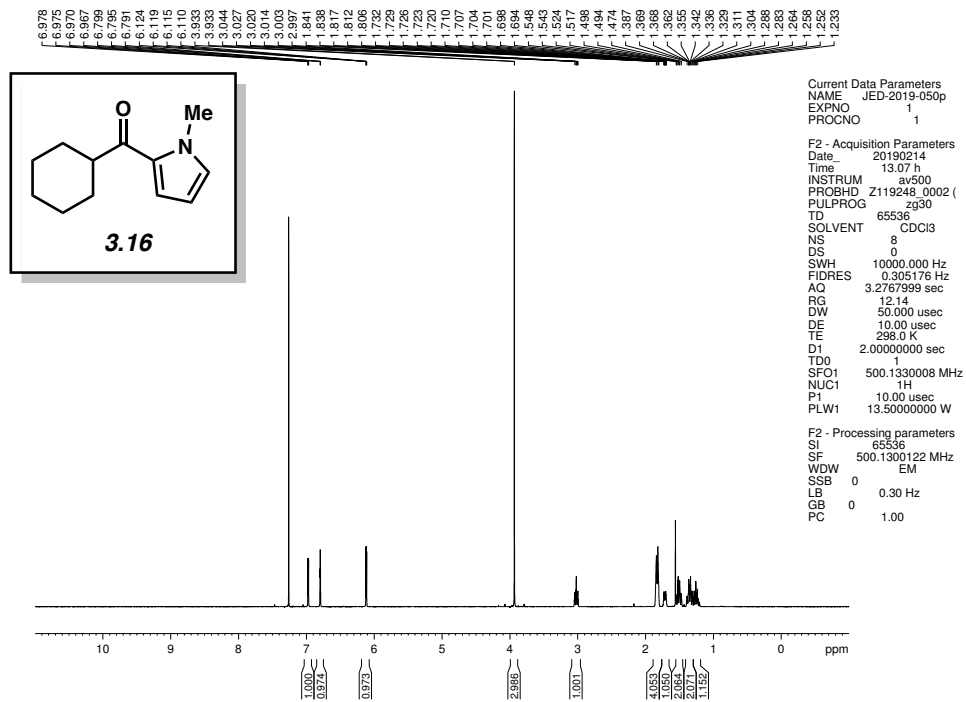
Figure 3.16 ^{1}H NMR (500 MHz, CDCl$_3$) of compound **3.16**.
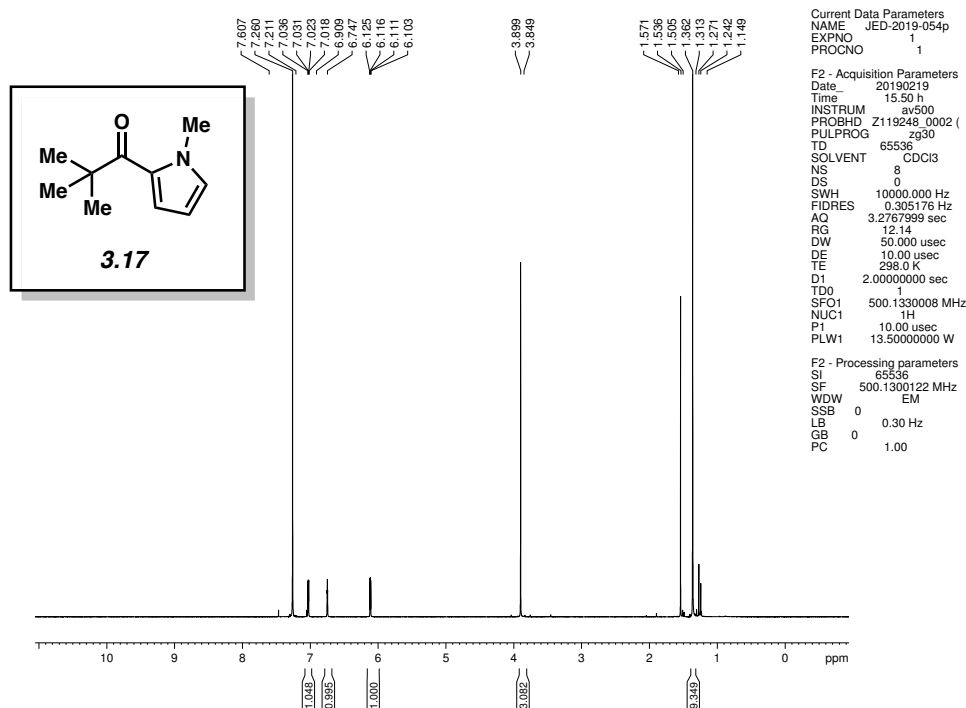
Figure 3.17 ^{1}H NMR (500 MHz, CDCl$_3$) of compound **3.17**.
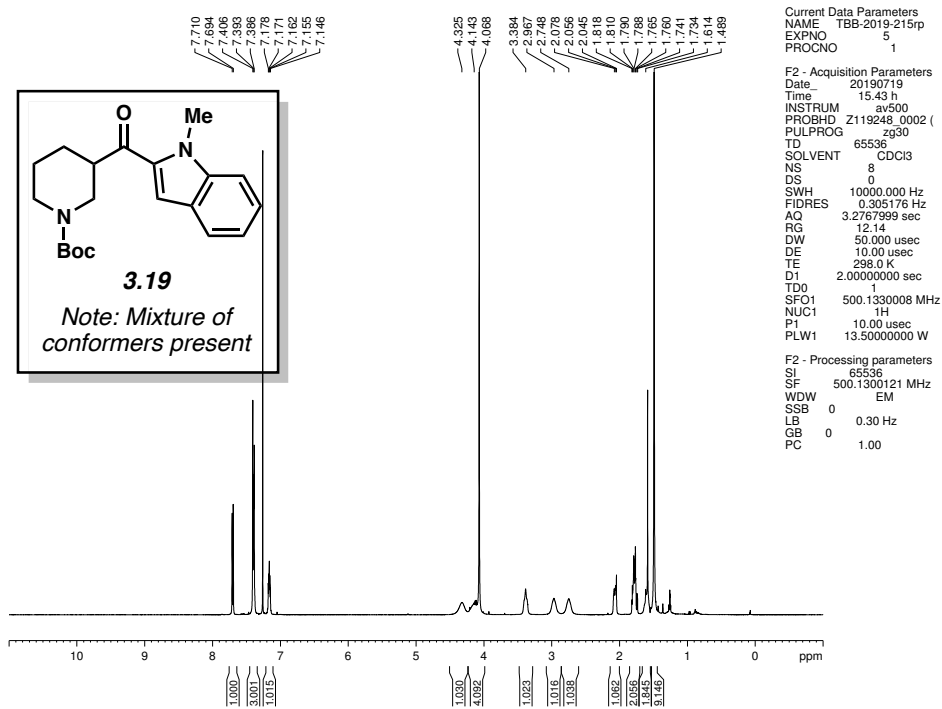
Figure 3.18 ^{1}H NMR (500 MHz, CDCl$_3$) of compound **3.19**.
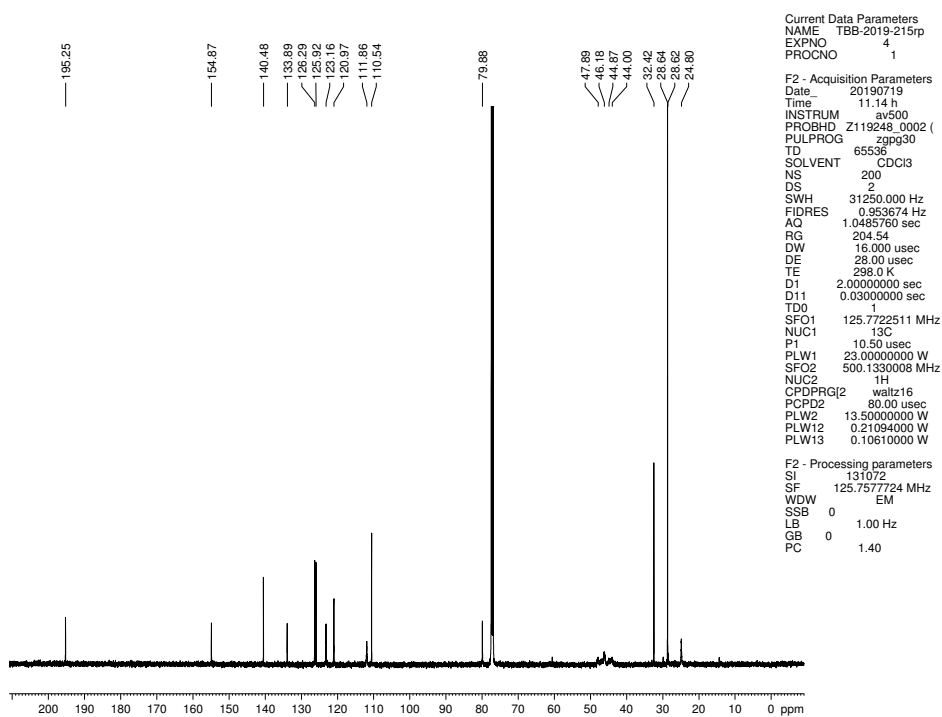
Figure 3.19 ^{13}C NMR (125 MHz, CDCl$_3$) of compound **3.19**.

3.10 Notes and References

(1) (a) Larock, R. C. Comprehensive Organic Transformations: A Guide to Functional Group Preparations; VCH: New York, 1989; pp 685−702. (b) Nicholson, J. W.; Wilson, A. D. Carboxylic. *J. Chem. Educ.* **2004**, *81*, 1362–1366. (c) Amani, J.; Molander, G. A. Direct Conversion of Carboxylic Acids to Alkyl Ketones. *Org. Lett.* **2017**, *19*, 3612–3615.

(2) (a) Nahm, S.; Weinreb, S. M. *N*-Methoxy-*N*-Methylamides as Effective Acylating Agents. *Tetrahedron Lett.* **1981**, *22*, 3815–3818. (b) Balasubramaniam, S.; Aidhen, I. S. The Growing Synthetic Utility of the Weinreb Amide. *Synthesis* **2002**, *23*, 3707–3738.

(3) For couplings of acyl halides, anhydrides, esters, and thioesters, see: (a) Labadie, J. W.; Tueting, D.; Stille, J. K. Synthetic Utility of the Palladium-Catalyzed Coupling Reaction of Acid Chlorides with Organotins. *J. Org. Chem.* **1983**, *48*, 4634−4642. (b) Stille, J. K. The Palladium-Catalyzed Cross-Coupling Reactions of Organotin Reagents with Organic Electrophiles. *Angew. Chem., Int. Ed.* **1986**, *25*, 508−524. (c) Stephan, M. S.; Teunissen, A. J. J. M.; de Vries, J. G. Heck Reactions without Salt Formation: Aromatic Carboxylic Anhydrides as Arylating Agents. *Angew. Chem., Int. Ed.* **1998**, *37*, 662−664. (d) Gooßen, L. J.; Ghosh, K. Palladium-Catalyzed Synthesis of Aryl Ketones from Boronic Acids and Carboxylic Acids Activated in situ by Pivalic Anhydride. *Angew. Chem., Int. Ed.* **2001**, *40*, 3458−3460. (e) Kakino, R.; Narahashi, H.; Shimizu, I.; Yamamoto, A. Palladium-Catalyzed Direct Conversion of Carboxylic Acids into Ketones with Organoboronic Acids Promoted by Anhydride Activators. *Bull. Chem. Soc. Jpn.* **2002**, *75*, 1333−1345. (f) Bykov, V. V.; Korolev, D. N.; Bumagin, N. A. Palladium-Catalyzed Reactions of Organoboron Compounds with Acyl Chlorides. *Russ. Chem. Bull.* **1997**, *46*, 1631−1632. (g) Zhang, L.; Wu, J.; Shi, L.; Xia,

C.; Li, F. *Tetrahedron Lett.* **2011**, *52*, 3897−3901. (h) Kakino, R.; Shimizu, I.; Yamamoto, A. Synthesis of Trifluoromethyl Ketones by Palladium-Catalyzed Cross-Coupling Reaction of Phenyl Trifluoroacetate with Organoboron Compounds. *Bull. Chem. Soc. Jpn.* **2001**, *74*, 371−376. (i) Cherney, A. H.; Reisman, S. E. Pd-Catalyzed Fukuyama Cross-Coupling of Secondary Organozinc Reagents for the Direct Synthesis of Unsymmetrical Ketones. *Tetrahedron* **2014**, *70*, 3259−3265. (j) Harada, T.; Kotani, Y.; Katsuhira, T.; Oku, A. Novel Method for Generation of Secondary Organozinc Reagent: Application to Tandem Carbon-Carbon Bond Formation Reaction of 1,1-Dibromoalkane. *Tetrahedron Lett.* **1991**, *32*, 1573−1576. (k) Negishi, E.-I.; Bagheri, V.; Chatterjee, S.; Luo, F.-T.; Miller, J. A.; Stoll, A. T. Palladium-Catalyzed Acylation of Organozincs and Other Organometallics as a Convenient Route to Ketones. *Tetrahedron Lett.* **1983**, *24*, 5181−5184. (l) Iwai, T.; Nakai, T.; Mihara, M.; Ito, T.; Mizuno, T.; Ohno, T. Pd-Catalyzed Cross-Coupling Reactions of Pyridine Carboxylic Acid Chlorides with Alkylzinc Reagents. *Synlett* **2009**, *20*, 1091−1094. (m) Grey, R. A. A Palladium-Catalyzed Synthesis of Ketones from Acid Chlorides and Organozinc Compounds. *J. Org. Chem.* **1984**, *49*, 2288−2289. (n) Bercot, E. A.; Rovis, T. A Mild and Efficient Catalytic Alkylative Monofunctionalization of Cyclic Anhydrides. *J. Am. Chem. Soc.* **2002**, *124*, 174−175. (o) Bercot, E. A.; Rovis, T. A Palladium-Catalyzed Enantioselective Alkylative Desymmetrization of *meso*-Succinic Anhydrides. *J. Am. Chem. Soc.* **2004**, *126*, 10248−10249. (p) Johnson, J. B.; Yu, R. T.; Fink, P.; Bercot, E. A.; Rovis, T. Selective Substituent Transfer from Mixed Zinc Reagents in Ni-Catalyzed Anhydride Alkylation. *Org. Lett.* **2006**, *8*, 4307−4310. (q) Tokuyama, H.; Yokoshima, S.; Yamashita, T.; Fukuyama, T. A Novel Ketone Synthesis by a Palladium-Catalyzed Reaction of Thiol Esters and Organozinc

Reagents. *Tetrahedron Lett.* **1998**, *39*, 3189−3192. (r) Mori, Y.; Seki, M. A Novel Procedure for the Synthesis of Multifunctional Ketones Through the Fukuyama Coupling Reaction Employing Dialkylzincs. *Tetrahedron Lett.* **2004**, *45*, 7343−7345. (s) Miyazaki, T.; Han-ya, Y.; Tokuyama, H.; Fukuyama, T. New Odorless Protocols for the Synthesis of Aldehydes and Ketones from Thiol Esters. *Synlett* **2004**, *3*, 477−480. (t) Dieter, R. K. Reaction of Acyl Chlorides with Organometallic Reagents: A Banquet Table of Metals for Ketone Synthesis. *Tetrahedron* **1999**, *55*, 4177–4236. (u) Shi, S.; Nolan, S. P.; Szostak, M. Well-Defined Palladium(II)–NHC Precatalysts for Cross-Coupling Reactions of Amides and Esters by Selective N–C/O–C Cleavage. *Acc. Chem. Res.* **2018**, *51*, 2589–2599. (v) Halima, T. B.; Zhang, W.; Yalaoui, T.; Hong, X.; Yang, Y.-F.; Houk, K. N.; Newman, S. G. Palladium-Catalyzed Suzuki–Miyaura Coupling of Aryl Esters. *J. Am. Chem. Soc.* **2017**, *139*, 1311–1318.

(4) For recent reviews, see: (a) Dander, J. E.; Garg, N. K. Breaking Amides using Nickel Catalysis. *ACS Catal.* **2017**, *7*, 1413−1423. (b) Meng, G.; Shi, S.; Szostak, M. Cross-Coupling of Amides by N–C Bond Activation. *Synlett* **2016**, *27*, 2530–2540. (c) Takise, R.; Muto, K.; Yamaguchi, J. Cross-Coupling of Aromatic Esters and Amides. *Chem. Soc. Rev.* **2017**, *46*, 5864–5888. (d) Kaiser, D.; Bauer, A.; Lemmerer, M.; Maulide, N. Amide Activation: An Emerging Tool for Chemoselective Synthesis. *Chem. Soc. Rev.* **2018**, *47*, 7899–7925.

(5) For nickel-catalyzed reactions proceeding with cleavage of the amide C−N bond, see: (a) Hie, L.; Fine Nathel, N. F.; Shah, T. K.; Baker, E. L.; Hong, X.; Yang, Y.-F.; Liu, P.; Houk, K. N.; Garg, N. K. Conversion of Amides to Esters by the Nickel-Catalysed Activation of Amide C–N Bonds. *Nature* **2015**, *524*, 79−83. (b) Weires, N. A.; Baker, E. L.; Garg, N. K. Nickel-

Catalysed Suzuki–Miyaura Coupling of Amides. *Nat. Chem.* **2016**, *8*, 75−79. (c) Baker, E. L.; Yamano, M. M.; Zhou, Y.; Anthony, S. M.; Garg, N. K. A Two-Step Approach to Achieve Secondary Amide Transamidation Enabled by Nickel Catalysis. *Nat. Commun.* **2016**, *7*, 11554. (d) Simmons, B. J.; Weires, N. A.; Dander, J. E.; Garg, N. K. Nickel-Catalyzed Alkylation of Amide Derivatives. *ACS Catal.* **2016**, *6*, 3176−3179. (e) Shi, S.; Szostak, M. Nickel-Catalyzed Diaryl Ketone Synthesis by N–C Cleavage: Direct Negishi Cross-Coupling of Primary Amides by Site-Selective *N,N*-Di-Boc Activation. *Org. Lett.* **2016**, *18*, 5872−5875. (f) Shi, S.; Szostak, M. Efficient Synthesis of Diaryl Ketones by Nickel-Catalyzed Negishi Cross-Coupling of Amides by Carbon–Nitrogen Bond Cleavage at Room Temperature Accelerated by a Solvent Effect. *Chem. Eur. J.* **2016**, *22*, 10420−10424. (g) Hie, L.; Baker, E. L.; Anthony, S. M.; Desrosiers, J.-N.; Senanayake, C.; Garg, N. K. Nickel-Catalyzed Esterification of Aliphatic Amides. *Angew. Chem., Int. Ed.* **2016**, *55*, 15129−15132. (h) Dey, A.; Sasmal, S.; Seth, K.; Lahiri, G. K.; Maiti, D. Nickel-Catalyzed Deamidative Step-Down Reduction of Amides to Aromatic Hydrocarbons. *ACS Catal.* **2017**, *7*, 433−437. (i) Ni, S.; Zhang, W.; Mei, H.; Han, J.; Pan, Y. Ni-Catalyzed Reductive Cross-Coupling of Amides with Aryl Iodide Electrophiles via C–N Bond Activation. *Org. Lett.* **2017**, *19*, 2536−2539. (j) Medina, J. M.; Moreno, J.; Racine, S.; Du, S.; Garg, N. K. Mizoroki–Heck Cyclizations of Amide Derivatives for the Introduction of Quaternary Centers. *Angew. Chem., Int. Ed.* **2017**, *56*, 6567−6571. (k) Hu, J.; Wang, M.; Pu, X.; Shi, Z. Nickel-Catalysed Retro-Hydroamidocarbonylation of Aliphatic Amides to Olefins. *Nat. Commun.* **2017**, *8*, 14993. (l) Weires, N. A.; Caspi, D. D.; Garg, N. K. (m) Shi, S.; Szostak, M. Nickel-Catalyzed Negishi Cross-Coupling of *N*-Acylsuccinimides: Stable, Amide-Based, Twist-Controlled Acyl-

Transfer Reagents via N–C Activation. *Synthesis* **2017**, *49*, 3602−3608. (n) Dander, J. E.; Baker, E. L.; Garg, N. K. Nickel-Catalyzed Transamidation of Aliphatic Amide Derivatives. *Chem. Sci.* **2017**, *8*, 6433−6438. (o) Huang, P.-Q.; Chen, H. Ni-Catalyzed Cross-Coupling Reactions of *N*-Acylpyrrole-Type Amides with Organoboron Reagents. *Chem. Commun.* **2017**, *53*, 12584−12587. (p) Deguchi, T.; Xin, H.-L.; Morimoto, H.; Ohshima, T. Direct Catalytic Alcoholysis of Unactivated 8-Aminoquinoline Amides. *ACS Catal.* **2017**, *7*, 3157−3161.

(6) For nickel-catalyzed decarbonylative coupling reactions of amides, see: (a) Shi, S.; Meng, G.; Szostak, M. Synthesis of Biaryls through Nickel-Catalyzed Suzuki–Miyaura Coupling of Amides by Carbon–Nitrogen Bond Cleavage. *Angew. Chem., Int. Ed.* **2016**, *55*, 6959−6963. (b) Hu, J.; Zhao, Y.; Liu, J.; Zhang, Y.; Shi, Z. Nickel-Catalyzed Decarbonylative Borylation of Amides: Evidence for Acyl C−N Bond Activation. *Angew. Chem., Int. Ed.* **2016**, *55*, 8718−8722. (c) Srimontree, W.; Chatupheeraphat, A.; Liao, H.-H.; Rueping, M. Amide to Alkyne Interconversion via a Nickel/Copper-Catalyzed Deamidative Cross-Coupling of Aryl and Alkenyl Amides. *Org. Lett.* **2017**, *19*, 3091−3094. (d) Liu, C.; Szostak, M. Decarbonylative Phosphorylation of Amides by Palladium and Nickel Catalysis: The Hirao Cross-Coupling of Amide Derivatives. *Angew. Chem., Int. Ed.* **2017**, *56*, 12718−12722. (e) Yue, H.; Guo, L.; Liao, H.-H.; Cai, Y.; Zhu, C.; Rueping, M. Catalytic Ester and Amide to Amine Interconversion: Nickel-Catalyzed Decarbonylative Amination of Esters and Amides by C−O and C−C Bond Activation. *Angew. Chem., Int. Ed.* **2017**, *56*, 4282−4285. (f) Chatupheeraphat, A.; Liao, H.-H.; Lee, S.-C.; Rueping, M. Nickel-Catalyzed C–CN Bond Formation via Decarbonylative Cyanation of Esters, Amides, and Intramolecular

Recombination Fragment Coupling of Acyl Cyanides. *Org. Lett.* **2017**, *19*, 4255−4258. (g) Yue, H.; Guo, L.; Lee, S.-C.; Liu, X.; Rueping, M. Selective Reductive Removal of Ester and Amide Groups from Arenes and Heteroarenes through Nickel-Catalyzed C−O and C−N Bond Activation. *Angew. Chem., Int. Ed.* **2017**, *56*, 3972−3976. (h) Lee, S.-C.; Guo, L.; Yue, H.; Liao, H.-H.; Rueping, M. Nickel-Catalyzed Decarbonylative Silylation, Borylation, and Amination of Arylamides via a Deamidative Reaction Pathway. *Synlett* **2017**, *28*, 2594−2598.

(7) For Pd-catalyzed amide C–N bond activation, see: (a) Li, X.; Zou, G. Acylative Suzuki Coupling of Amides: Acyl-Nitrogen Activation via Synergy of Independently Modifiable Activating Groups. *Chem. Commun.* **2015**, *51*, 5089−5092. (b) Yada, A.; Okajima, S.; Murakami, M. Palladium-Catalyzed Intramolecular Insertion of Alkenes into the Carbon–Nitrogen Bond of *β*-Lactams. *J. Am. Chem. Soc.* **2015**, *137*, 8708−8711. (c) Meng, G.; Szostak, M. Palladium-Catalyzed Suzuki–Miyaura Coupling of Amides by Carbon–Nitrogen Cleavage: General Strategy for Amide N–C Bond Activation. *Org. Biomol. Chem.* **2016**, *14*, 5690−5705. (d) Meng, G.; Szostak, M. General Olefin Synthesis by the Palladium-Catalyzed Heck Reaction of Amides: Sterically Controlled Chemoselective N–C Activation. *Angew. Chem., Int. Ed.* **2015**, *54*, 14518−14522. (e) Meng, G.; Szostak, M. Sterically Controlled Pd-Catalyzed Chemoselective Ketone Synthesis via N–C Cleavage in Twisted Amides. *Org. Lett.* **2015**, *17*, 4364−4367. (f) Liu, C.; Meng, G.; Liu, Y.; Liu, R.; Lalancette, R.; Szostak, R.; Szostak, M. *N*-Acylsaccharins: Stable Electrophilic Amide-Based Acyl Transfer Reagents in Pd-Catalyzed Suzuki–Miyaura Coupling via N–C Cleavage. *Org. Lett.* **2016**, *18*, 4194−4197. (g) Lei, P.; Meng, G.; Szostak, M. General Method for the Suzuki–Miyaura Cross-Coupling of Amides Using Commercially Available, Air- and Moisture-Stable Palladium/NHC (NHC

= *N*-Heterocyclic Carbene) Complexes. *ACS Catal.* **2017**, *7*, 1960−1965. (h) Liu, C.; Liu, Y.; Liu, R.; Lalancette, R.; Szostak, R.; Szostak, M. Palladium-Catalyzed Suzuki–Miyaura Cross-Coupling of *N*-Mesylamides by N–C Cleavage: Electronic Effect of the Mesyl Group. *Org. Lett.* **2017**, *19*, 1434−1437. (i) Liu, C.; Meng, G.; Szostak, M. *N*-Acylsaccharins as Amide-Based Arylating Reagents via Chemoselective N–C Cleavage: Pd-Catalyzed Decarbonylative Heck Reaction. *J. Org. Chem.* **2016**, *81*, 12023−12030. (j) Meng, G.; Shi, S.; Szostak, M. Palladium-Catalyzed Suzuki–Miyaura Cross-Coupling of Amides via Site-Selective N–C Bond Cleavage by Cooperative Catalysis. *ACS Catal.* **2016**, *6*, 7335−7339. (k) Cui, M.; Wu, H.; Jian, J.; Wang, H.; Liu, C.; Stelck, D.; Zeng, Z. Palladium-Catalyzed Sonogashira Coupling of Amides: Access to Ynones via C–N Bond Cleavage. *Chem. Commun.* **2016**, *52*, 12076−12079. (l) Wu, H.; Li, Y.; Cui, M.; Jian, J.; Zeng, Z. Suzuki Coupling of Amides via Palladium-Catalyzed C–N Cleavage of *N*-Acylsaccharins. *Adv. Synth. Catal.* **2016**, *358*, 3876−3880. (m) Shi, S.; Szostak, M. Decarbonylative Cyanation of Amides by Palladium Catalysis. *Org. Lett.* **2017**, *19*, 3095−3098. (n) Lei, P.; Meng, G.; Ling, Y.; An, J.; Szostak, M. Pd-PEPPSI: Pd-NHC Precatalyst for Suzuki–Miyaura Cross-Coupling Reactions of Amides. *J. Org. Chem.* **2017**, *82*, 6638−6646. (o) Meng, G.; Szostak, R.; Szostak, M. Suzuki–Miyaura Cross-Coupling of *N*-Acylpyrroles and Pyrazoles: Planar, Electronically Activated Amides in Catalytic N–C Cleavage. *Org. Lett.* **2017**, *19*, 3596−3599. (p) Meng, G.; Lalancette, R.; Szostak, R.; Szostak, M. *N*-Methylamino Pyrimidyl Amides (MAPA): Highly Reactive, Electronically-Activated Amides in Catalytic N–C(O) Cleavage. *Org. Lett.* **2017**, *19*, 4656−4659. (q) Osumi, Y.; Szostak, M. *N*-Acylsuccinimides: Twist-Controlled, Acyl-Transfer Reagents in Suzuki–Miyaura Cross-Coupling by N–C Amide Bond Activation. *Org.*

Biomol. Chem. **2017**, *15*, 8867−8871. (r) Lei, P.; Meng, G.; Ling, Y.; An, J.; Nolan, S. P.; Szostak, M. General Method for the Suzuki–Miyaura Cross-Coupling of Primary Amide-Derived Electrophiles Enabled by [Pd(NHC)(cin)Cl] at Room Temperature. *Org. Lett.* **2017**, *19*, 6510−6513. (s) Li, X.; Zou, G. Palladium-Catalyzed Acylative Cross-Coupling of Amides with Diarylborinic Acids and Sodium Tetraarylborates. *J. Organomet. Chem.* **2015**, *794*, 136–145. (t) Liu, C.; Li, G.; Shi, S.; Meng, G.; Lalancette, R.; Szostak, R.; Szostak, M. Acyl and Decarbonylative Suzuki Coupling of *N*-Acetyl Amides: Electronic Tuning of Twisted, Acyclic Amides in Catalytic Carbon–Nitrogen Bond Cleavage. *ACS Catal.* **2018**, *8*, 9131–9139. (u) Meng, G.; Szostak, M. Palladium/NHC (NHC = *N*-Heterocyclic Carbene)-Catalyzed B-Alkyl Suzuki Cross-Coupling of Amides by Selective N–C Bond Cleavage. *Org. Lett.* **2018**, *20*, 6789–6793. (v) Shi, S.; Szostak, M. Decarbonylative Borylation of Amides by Palladium Catalysis. *ACS Omega* **2019**, *4*, 4901–4907. (w) Zhou, T.; Li, G.; Nolan, S. P.; Szostak, M. [Pd(NHC)(acac)Cl]: Well-Defined, Air-Stable, and Readily Available Precatalysts for Suzuki and Buchwald–Hartwig Cross-coupling (Transamidation) of Amides and Esters by N–C/O–C Activation. *Org. Lett.* **2019**, *21*, 3304–3309.

(8) For Ni- and Pd-catalyzed cross-couplings of amides with aryl boronic esters or acids, See Section 3.10, references: 5b,o; 6a,b; 7a,c,f–h,j,n,o,q–s,t,u,w.

(9) For Ni- and Pd-catalyzed cross-couplings of amides with alkyl zinc reagents, See Section 3.10, references: 5d–f,m.

(10) Boit, T. B.; Weires, N. A.; Kim, J.; Garg, N. K. Nickel-Catalyzed Suzuki–Miyaura Coupling of Aliphatic Amides. *ACS Catal.* **2018**, *8*, 1003–1008.

(11) The Molander group has reported a dual-metal photoredox approach to the synthesis of alkyl–alkyl ketones using alkyltrifluoroborate salts and aliphatic acyl succinimides, see: Amani, J.; Alam, R.; Badir, S.; Molander, G. A. Synergistic Visible-Light Photoredox/Nickel-Catalyzed Synthesis of Aliphatic Ketones via N–C Cleavage of Imides. *Org. Lett.* **2017**, *19*, 2426–2429.

(12) The use of air-stable Ni(II) precatalysts represents a complementary strategy for avoiding glovebox manipulations, see: (a) Shields, J. D.; Gray, E. E.; Doyle, A. G. A Modular, Air-Stable Nickel Precatalyst. *Org. Lett.* **2015**, *17*, 2166–2169. (b) Magano, J.; Monfette, S. Development of an Air-Stable, Broadly Applicable Nickel Source for Nickel-Catalyzed Cross-Coupling. *ACS Catal.* **2015**, *5*, 3120–3123. (c) Standley, E. A.; Jamison, T. F. Simplifying Nickel(0) Catalysis: An Air-Stable Nickel Precatalyst for the Internally Selective Benzylation of Terminal Alkenes. *J. Am. Chem. Soc.* **2013**, *135*, 1585–1592. (d) Park. N. H.; Teverovskiy, G.; Buchwald, S. L. Development of an Air-Stable Nickel Precatalyst for the Amination of Aryl Chlorides, Sulfamates, Mesylates, and Triflates. *Org. Lett.* **2014**, *16*, 220–223. (e) Ge, S.; Hartwig, J. F. Highly Reactive, Single-Component Nickel Catalyst Precursor for Suzuki–Miyuara Cross-Coupling of Heteroaryl Boronic Acids with Heteroaryl Halides. *Angew. Chem., Int. Ed.* **2012**, *51*, 12837–12841.

(13) (a) Sather, A. C.; Lee, H. G.; Colombe, J. R.; Zhang, A.; Buchwald, S. L. Dosage Delivery of Sensitive Reagents Enables Glove-Box-Free Synthesis. *Nature* **2015**, *524*, 208–211. (b) Fang, Y.; Liu, Y.; Ke, Y.; Guo, C.; Zhu, N.; Mi, X.; Ma, Z.; Hu, Y. A New Chromium-Based Catalyst Coated with Paraffin for Ethylene Oligomerization and the Effect of Chromium State on Oligomerization Selectivity. *Appl. Cat. A* **2002**, *235*, 33–38. (c) Taber, D. F.; Frankowski,

K. J. Grubbs' Catalyst in Paraffin: An Air-Stable Preparation for Alkene Metathesis. *J. Org. Chem.* **2003**, *68*, 6047–6048.

(14) (a) Dander, J. E.; Weires, N. A.; Garg, N. K. Benchtop Delivery of Ni(cod)$_2$ using Paraffin Capsules. *Org. Lett.* **2016**, *18*, 3934–3936. (b) Dander, J. E.; Morrill, L. A.; Nguyen, M. M.; Chen, S.; Garg, N. K. Breaking Amide C–N Bonds in an Undergraduate Organic Chemistry Laboratory. *J. Chem. Ed.* **2019**, *96*, 776–780.

(15) Lei, P.; Meng, G.; Shi, S.; Ling, Y.; An, J.; Szostak, R.; Szostak, M. Suzuki–Miyaura Cross-Coupling of Amides and Esters at Room Temperature: Correlation with Barriers to Rotation Around C–N and C–O Bonds. *Chem. Sci.* **2017**, *8*, 6525–6530.

(16) See Section 3.8.2.3 for details.

(17) See Section 3.8.2.3 for full optimization details.

(18) TCI Chemicals is commercializing the capsules containing Ni(cod)$_2$ and Benz-ICy•HCl.

(19) (a) Vitaku, E.; Smith, D. T.; Njardarson, J. T. Analysis of the Structural Diversity, Substitution Patterns, and Frequency of Nitrogen Heterocycles among U.S. FDA Approved Pharmaceuticals. *J. Med. Chem.* **2014**, *57*, 10257–10257. (b) Hirata, T.; Funatsu, T.; Keto, Y.; Nakata, M.; Sasamata, M. Pharmacological Profile of Ramosetron, a Novel Therapeutic Agent for IBS. *Inflammopharmacology* **2007**, *15*, 5–9.

(20) Amide Derivatives featuring various *N*-substituents have been employed successfully in cross-coupling reactions. *N*-Bn-*N*-Boc derivatives were selected for the present study due to their utility in the glovebox methodology and ease of preparation.

Base-Mediated Meerwein–Ponndorf–Verley Reduction of Aromatic Ketones and

Heterocyclic Ketones

Timothy B. Boit,[†] Milauni M. Mehta, and Neil K. Garg.

4.1 Abstract

An experimental protocol to achieve the Meerwein–Ponndorf–Verley (MPV) reduction of ketones under mildly basic conditions is reported. The transformation is tolerant of a range of ketone substrates, including *O*- and *S*-containing heterocycles, is scalable, and shows potential to be used as platform to access enantioenriched products. These studies provide a general method for achieving the reduction of ketones under mildly basic conditions and offer an alternative protocol to more well-known Al-based MPV reduction conditions.

4.2 Introduction

The Meerwein–Ponndorf–Verley (MPV) reaction is an important and powerful tool for the reduction of ketones and aldehydes because of its chemoselectivity, mild reaction conditions, scalability, and low operational cost.[1] Discovered nearly a century ago,[2] the traditional MPV reduction employs an aluminum alkoxide catalyst generated from a secondary alcohol (most commonly isopropanol) to achieve the reversible transfer hydrogenation of carbonyl substrates (Figure 4.1).[3] This venerable reaction has been featured in the syntheses of several natural products[4] and spurred numerous experimental[5] and computational studies.[6] Despite the synthetic

utility of the traditional MPV reduction, several drawbacks exist. These include long reaction times, the need for a large excess of reducing agent, competing side reactions such as aldol condensation and the Tishchenko reduction of aldehydes, and low enantioselectivities in the case of intermolecular asymmetric variants.[1,3] Methodological advances to address these limitations include the use of additives,[7] microwave irradiation,[8] and the development of novel aluminum,[9] organoboron[10] and metal alkoxide catalysts (i.e. transition[11] and lanthanide[12]). A particularly efficient aluminum siloxide catalyst has been reported by the Krempner group.[9c]
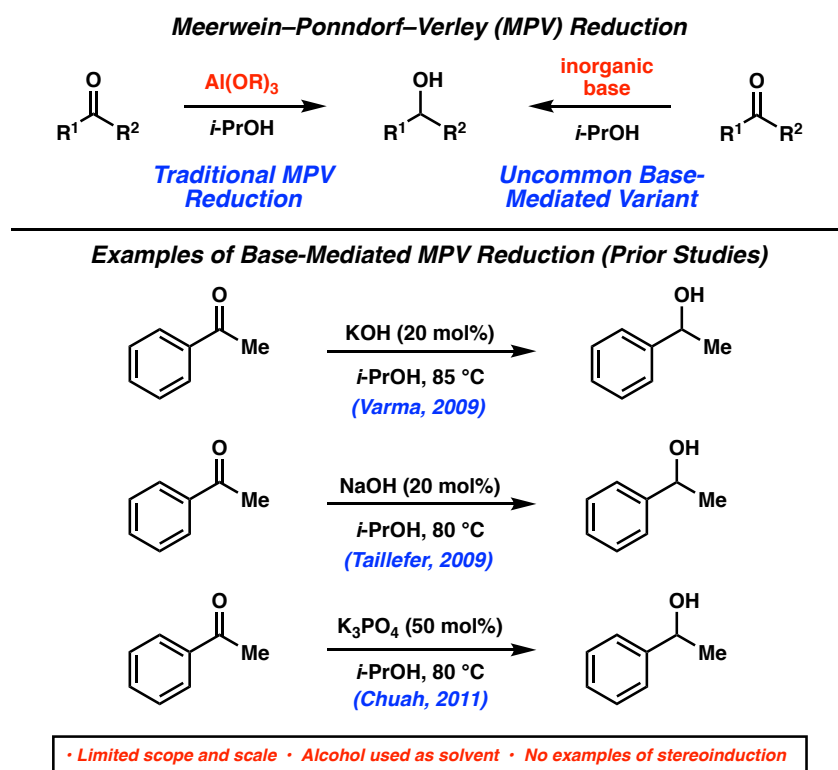
Figure 4.1. Traditional MPV reduction of ketones and base-mediated variant (prior studies).

A largely unexplored approach to the MPV-type reduction of carbonyls uses simple alkali metal alkoxides. (Figure 4.1).[13,14] This variant of the MPV reaction has several benefits including its avoidance of metal catalysts, operational simplicity, and compatibility with heteroatoms known

to inhibit metal catalysis.[3,13] Specifically, isopropoxide catalysts generated from strong alkali bases, such as NaOH[13a] and KOH[13b] and milder bases such as K_3PO_4,[13c] have been employed in the reduction of aldehydes and ketones. Nevertheless, a number of limitations of the base-mediated MPV reduction remain unaddressed including a limited scope and the reliance on *i*-PrOH as the solvent and hydride source.[15] Additionally, no examples of stereoselective base-mediated MPV reactions exist. We report the use of a simple potassium alkoxide reductant, generated in situ from the corresponding alcohol and K_3PO_4, for the reduction of a wide range of aromatic ketones. This methodology is tolerant of heterocycles, scalable, and shows potential for the asymmetric reduction of alkyl–aryl ketones.

4.3 Reaction Discovery and Optimization

To initiate our studies, we examined the reduction of dihydrochalcone (**4.1**) using alkyl–alkyl secondary alcohols and K_3PO_4, a readily available and mild base (Table 4.1).[16] Subjecting **4.1** to catalytic K_3PO_4 using isopropanol or 3-pentanol (**4.3**) (2.5 equivalents) in 1,4-dioxane at 80 °C provided none of the desired alcohol product **4.2** (entries 1 and 2).[16,17,18] Owing to the potential reversibility of the reaction,[1a–c,16] we turned to the use of aryl–alkyl reductants to bias the reaction equilibrium. Importantly, this class of alcohol enabled a greater control of the redox properties of the reductant. We evaluated alcohol **4.4** and the more electron-rich derivative **4.5** as reductants,[19] anticipating that the stability of the respective aryl ketone and doubly vinylogous amide byproducts would drive the forward reaction to yield **4.2**. Gratifyingly, the use of 2.5 equivalents of **4.4** or **4.5** provided **4.2** in 40% and 61% yield, respectively (entries 3 and 4). Employing reductant **4.5** at 120 °C furnished desired product **4.2** in 92% yield (entry 5). Finally, alcohol **4.2** was obtained in near quantitative yield by utilizing excess base (entry 6).

Table 4.1. Optimization of reaction conditions

Entry	Reductant	Equiv K$_3$PO$_4$	Temp (°C)	Yield[a]
1	i-PrOH	0.50	80	0%
2	3	0.50	80	0%
3	4	0.50	80	40%
4	5	0.50	80	61%
5	5	0.50	120	92%
6	5	4.0	120	99%
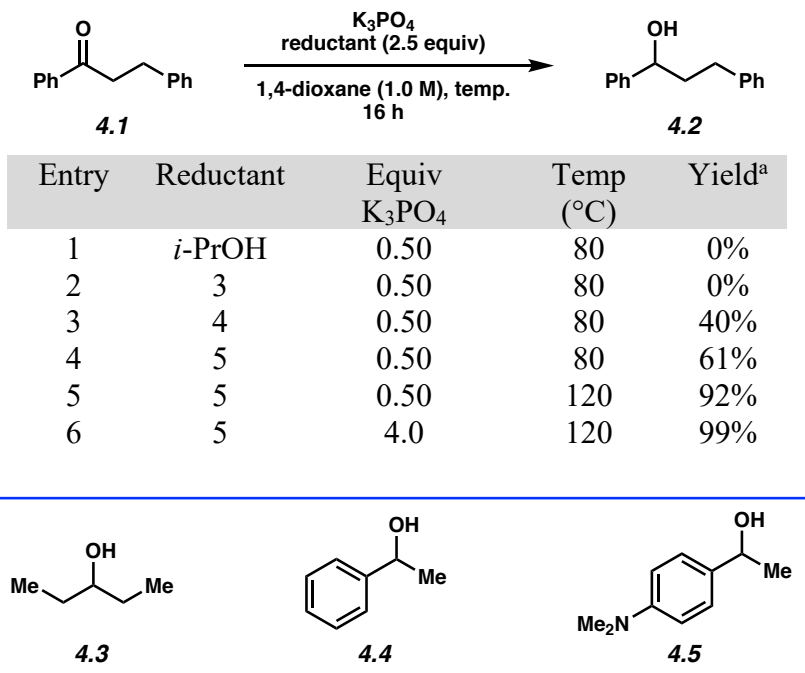
[a]General conditions unless otherwise stated: substrate **4.1** (1.0 equiv, 0.10 mmol), K$_3$PO$_4$ (0.50–4.0 equiv), reductant (2.5 equiv), and 1,4-dioxane (1.0 M) heated at 80–120 °C for 16 h in a sealed vial under an atmosphere of N$_2$. Yields determined by ^{1}H NMR analysis using 1,3,5-trimethoxybenzene as an external standard.

4.4 Scope of Methodology

With optimized conditions in hand, we examined a range of aryl ketone substrates in the reduction (Figure **4.2**). Linear and α-branched substrates smoothly underwent reduction, giving rise to alcohols **4.2** and **4.6–4.8** in good yields. Of note, steric bulk on the alkyl substituent of the ketone was tolerated, as shown by the successful reduction of *tert*-butyl phenyl ketone to furnish alcohol **4.8** in 83% yield. The reduction of α-tetralone to give α-tetralol (**4.9**) in 86% yield demonstrates competence of a cyclic ketone substrate in this transformation. Notably, we found that electron-rich aromatic ketones and those highly decorated with heteroatom substitutents underwent facile reduction, as demonstrated by the formation of alcohols **4.10** and **4.11** in 81%

and 87% yield, respectively. Finally, both electron-rich and electron-deficient benzophenone derivatives were suitable substrates, as shown by the production of alcohol products **4.12** and **4.13** in good yields.
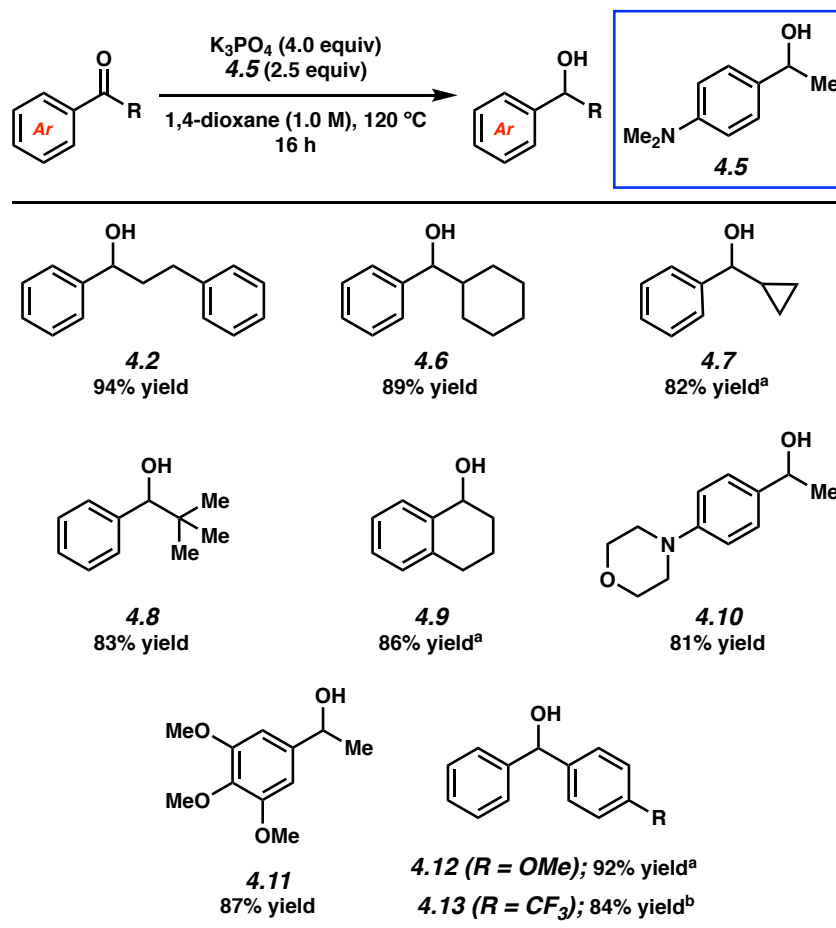
Figure 4.2. Scope of the base-mediated MPV reduction of aromatic ketones. Conditions: substrate (1.0 equiv, 0.10 mmol), K₃PO₄ (4.0 equiv), reductant (2.5 equiv), and 1,4-dioxane (1.0 M) heated at 120 °C for 16 h in a sealed vial under an atmosphere of N₂. Unless otherwise noted, yields reflect the average of two isolation experiments. [a]Yield determined by ¹H NMR analysis using hexamethylbenzene as an external standard. [b]Reaction heated at 80 °C for 16 h.

We next set out to evaluate the reactivity of a number of heterocyclic ketone substrates, as only a handful of examples of base-mediated MPV reductions of heterocyclic ketones have been previously reported (Figure **4.3**).[20] Benzofuran- and dibenzofuran-containing ketones underwent

reduction to provide alcohols **4.14** and **4.15** in 73% and 76% yield, respectively. Benzodioxole

and benzodioxane moieties were also well tolerated, as seen by the formation of alcohols **4.16** and

4.17 in good yields. Lastly, ketones bearing thiophenes were successfully employed, as judged by

the formation of benzothiophene **4.18** and tetrahydrobenzothiophene **4.19** in 70% and 73% yield,

respectively.[21]
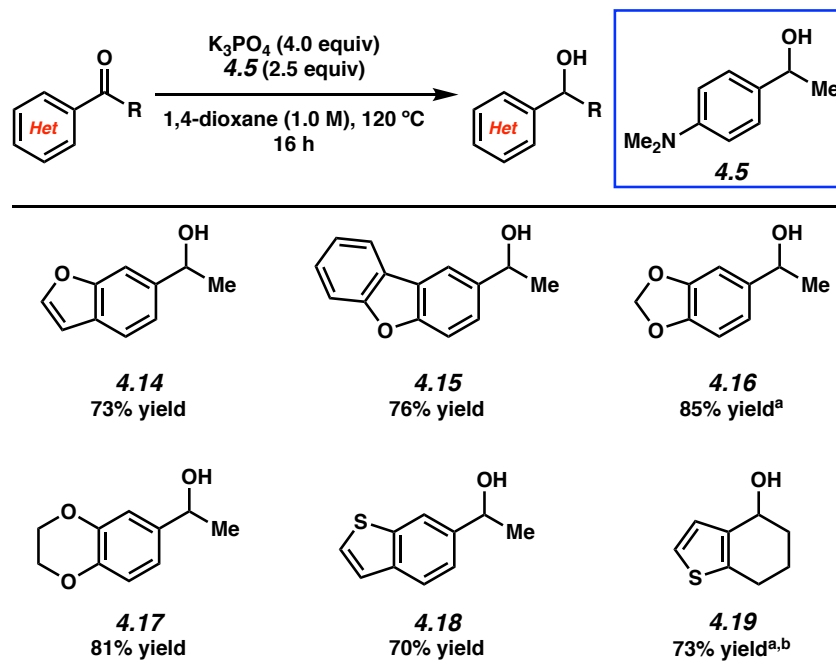
Figure 4.3. Scope of the base-mediated MPV reduction of heteroaromatic ketones. Conditions: substrate (1.0 equiv, 0.10 mmol), K$_3$PO$_4$ (4.0 equiv), reductant (2.5 equiv), and 1,4-dioxane (1.0 M) heated at 120 °C for 16 h in a sealed vial under an atmosphere of N$_2$. Unless otherwise noted, yields reflect the average of two isolation experiments. [a]Yield determined by ^{1}H NMR analysis using hexamethylbenzene as an external standard. [b]Reaction heated at 130 °C for 16 h.

4.5 Gram-Scale and Stereospecific Reductions

As a demonstration of the utility of the base-mediated MPV reduction of ketones, we

performed the additional studies shown in Figure **4.4**. In the first, we performed a gram-scale

reduction of acetyldibenzofuran **4.20**.[22] Carrying out the reaction at 130 °C for 24 h delivered

alcohol **4.15** in 66% yield, thus demonstrating the scalability of this methodology. Next, we questioned whether this reaction could be used for the synthesis of enantioenriched alcohols. Toward this end, we performed the reduction of phenylcyclohexyl ketone **4.21** using enantioenriched (*R*)-**4.5**. This proceeded to give alcohol (*S*)-**4.6** with 50% stereochemical transfer (96% *ee* of (*R*)-**4.5** → 48% *ee* (*S*)-**4.6**. This result underscores the potential of the base-mediated MPV reduction to generate enantioenriched products.[1e,12d,23]
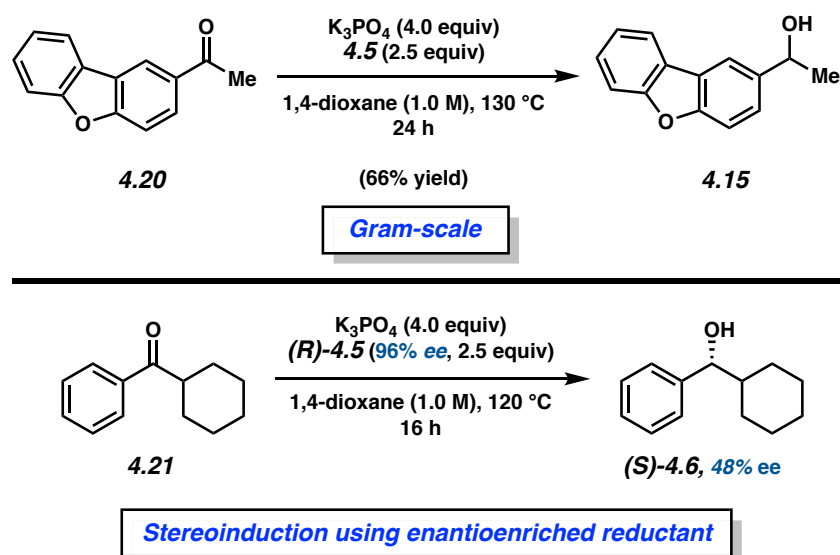
Figure 4.4. Gram-scale reduction and stereochemical transfer studies demonstrating the synthetic utility of the base-mediated MPV reduction. Conditions: substrate (1.0 equiv), K_3PO_4 (4.0 equiv), reductant (2.5 equiv), and 1,4-dioxane (1.0 M) heated at the indicated temperature and time in a sealed vial under an atmosphere of N_2.

4.6 Conclusions

In summary, we have developed the base-mediated MPV reduction of aromatic and heteroaromatic ketones. This methodology employs the simple combination of K_3PO_4 as a mild base and secondary alcohol **4.5** as the reductant. The transformation is tolerant of a range of ketone substrates, including *O*- and *S*-containing heterocycles, and avoids the hydride source being used

as the solvent. The reduction has been demonstrated on gram scale and shows potential to be used as platform to provide enantioenriched products. These studies provide a general platform for achieving the reduction of ketones under mildly basic MPV conditions and offer an alternative protocol to the more classic Al-based MPV reduction. We hope this study will enable the greater utilization of the uncommon base-mediated variant of the MPV reduction in chemical synthesis.

4.7 Experimental Section

4.7.1 Materials and Methods

Unless stated otherwise, reactions were conducted in flame-dried glassware under an atmosphere of nitrogen or argon and commercially obtained reagents were used as received. Not-commercially available ketone substrates were synthesized following protocols specified in Section A in the Experimental Procedures. Alcohols **4.5** and (*R*)-**4.5** were synthesized following protocols specified in Section B and C in the Experimental Procedures, respectively. 1,2-Dicholoroethane, 1,4-dioxane, and isopropanol were obtained from Fischer Scientific and purified by distillation. 3-Pentanol (**4.3**) and 1-phenylethanol (**4.4**) were obtained from Sigma-Aldrich and purified by distillation. Prior to use, 1,4-dioxane, isopropanol, 3-pentanol (**4.3**) and 1-phenylethanol (**4.4**) were degassed by sparging with N_2 for 1 h. Ketone **4.1**[24] and **4.36**[25] were prepared according to literature procedures. **4.22**, **4.28**, **4.29**, **4.30**, **4.31**, and **4.34** were obtained from Sigma-Aldrich. **4.26**, **4.21**, **4.27**, **4.32**, **4.35**, and **4.37** was obtained from Combi-Blocks. Ketone **4.26** was obtained from Oxchem. Ketone **4.33** was obtained from Alfa Aesar. Pd(PPh$_3$)$_4$ (99%) was obtained from Strem Chemicals. Acetyltrimethylsilane (**4.23**) (97%) was obtained from Sigma-Aldrich. Cesium fluoride (99%+) was obtained from Strem Chemicals. Potassium phosphate (K$_3$PO$_4$) was obtained from Acros. Reaction temperatures were controlled using an IKAmag temperature modulator, and unless stated otherwise, reactions were performed at room temperature (approximately 23 °C). Thin-layer chromatography (TLC) was conducted with EMD gel 60 F254 pre-coated plates (0.25 mm for analytical chromatography and 0.50 mm for preparative chromatography) and visualized using a combination of UV, anisaldehyde, iodine, and potassium permanganate staining techniques. Silicycle Siliaflash P60 (particle size 0.040–0.063 mm) was used for flash column chromatography. ^{1}H NMR spectra were recorded on Bruker

spectrometers (at 300, 400, 500, and 600 MHz) and are reported relative to residual solvent signals. Data for ^{1}H NMR spectra are reported as follows: chemical shift (δ ppm), multiplicity, coupling constant (Hz), integration. Data for ^{13}C NMR are reported in terms of chemical shift (at 75 and 125 MHz). IR spectra were recorded on a Perkin-Elmer UATR Two FT-IR spectrometer and are reported in terms of frequency absorption (cm^{-1}). DART-MS spectra were collected on a Thermo Exactive Plus MSD (Thermo Scientific) equipped with an ID-CUBE ion source and a Vapur Interface (IonSense Inc.). Both the source and MSD were controlled by Excalibur software v. 3.0. The analyte was spotted onto OpenSpot sampling cards (IonSense Inc.) using $CHCl_3$ or CH_2Cl_2 as the solvent. Ionization was accomplished using UHP He plasma with no additional ionization agents. The mass calibration was carried out using Pierce LTQ Velos ESI (+) and (–) Ion calibration solutions (Thermo Fisher Scientific). Optical rotations were measured with a Rudolf Autopol III Automatic Polarimeter. Trace metal analysis was determined by inductively coupled plasma mass spectrometry on an Agilent 8800 Triple Quadrupole ICP-MS instrument. The level of all analytes of interest was determined in MS/MS mode, measured using He in the collision/reaction cell using an environmental calibration standard (elements not included in this standard: B, Ti, Rb, Ru, Rh, Pd, Ir, and Pt). The quantification was done using the ICP-MS MassHunter WorkStation v4.3, through the QuickScan acquisition. Nitric acid was obtained from Fisher Scientific (A467500). Determination of enantiopurity was carried out on a Mettler Toledo SFC (supercritical fluid chromatography) or Agilent HPLC (high performance liquid chromatography) using Daicel ChiralPak IC–3 and Daicel ChiralPak OD–H columns. Data for SFC and HPLC spectra are reported in enantiomeric excess (ee). For SFC and HPLC chromatograms see Section 4.7.2.9 of Experimental Procedures.

4.7.2 Experimental Procedures

4.7.2.1 Syntheses of Ketone Substrates

Representative Procedure for the Synthesis of Ketone Substrates (synthesis of ketone 4.24 is used as an example).
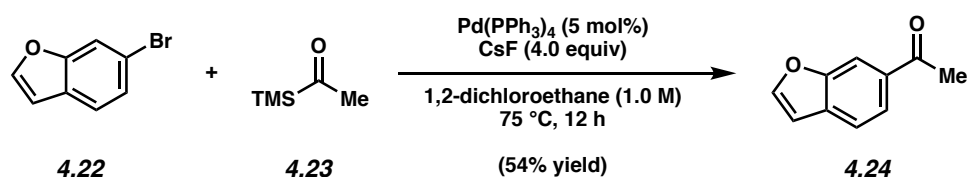
A flame-dried 1-dram vial was charged 6-bromobenzofuran (**4.22**) (130 mg, 0.660 mmol, 1.00 equiv) and a magnetic stir bar. In the glove box, CsF (401 mg, 2.64 mmol, 4.00 equiv) and Pd(PPh$_3$)$_4$ (38.1 mg, 0.0330 mmol, 0.0500 equiv) were added to the vial. The vessel was removed from the glove box and placed under an atmosphere of N$_2$ on the bench. Distilled 1,2-dichloroethane (0.700 mL, 1.00 M) and silane **4.23** (189 μL, 1.32 mmol, 2.0 equiv) were added and the vial was sealed with a Teflon-lined screw cap. The heterogeneous mixture was heated to 75 ºC for 12 h. After cooling to 23 ºC, the mixture was diluted with hexanes (0.5 mL), filtered over a plug of silica gel (1.00 cm OD x 5.00 cm, 10 mL EtOAc eluent), and the volatiles were removed under reduced pressure. The crude residue was purified by flash chromatography (19:1 Hexanes:EtOAc → 14:1 Hexanes:EtOAc) to yield ketone **4.24** (57.0 mg, 54% yield) as a yellow oil. Ketone **4.24**: R$_f$ 0.42 (5:1 Hexanes:EtOAc); ^{1}H NMR (600 MHz, CDCl$_3$): δ 8.13 (s, 1H), 7.89 (dd, J = 8.30, 1.38 Hz, 1H), 7.79 (d, J = 2.17 Hz, 1H), 7.66 (d, J = 8.30 Hz, 1H), 6.87–6.89 (m, 1H), 2.67 (s, 3H); ^{13}C NMR (125 MHz, CDCl$_3$): δ 197.8, 154.8, 148.4, 134.0, 132.0, 123.3, 121.2, 112.0, 107.0, 27.0; IR (film): 3118, 3003, 1673, 1425, 1271 cm^{-1}; HRMS-APCI (*m/z*) [M+NH$_4$]$^+$ calcd for C$_{10}$H$_{12}$O$_2$N$^+$, 178.08626; found 178.08536.

Note: Supporting information for the synthesis of ketone **4.36** has previously been reported.[25] The synthesis of the remaining substrate, **4.20**, is as follows:

Any modifications of the conditions shown in the representative procedure above are specified in the following scheme.

4.25   +   **4.23**   Pd(PPh₃)₄ (5 mol%)
CsF (4.0 equiv)

1,2-dichloroethane (1.0 M)
75 °C, 20 h
(77% yield)   **4.20**
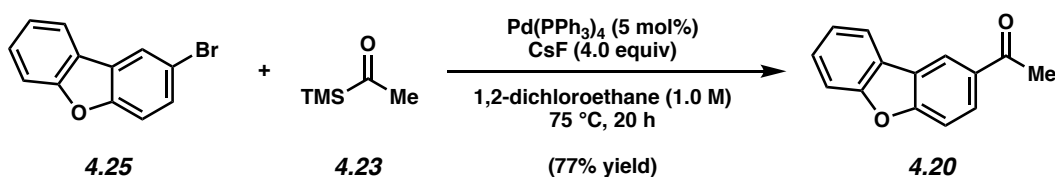
Ketone 20. Purification by flash chromatography (49:1 Hexanes:EtOAc) generated ketone **4.20** (263 mg, 77% yield) as a white solid. Ketone **4.20**: R_f 0.33 (9:1 Hexanes:EtOAc). Spectral data match those previously reported.[26]

4.7.2.2 Syntheses of Alcohol Reductant 4.5

4.26   LiAlH₄ (1.1 equiv)

THF (1.0 M), 0 °C → 23 °C
2 h
(93% yield)   **4.5**
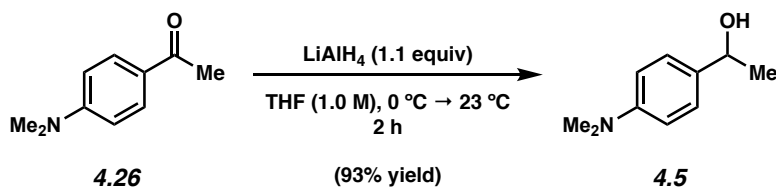
To a flame-dried flask equipped with a magnetic stir bar was added LiAlH₄ (2.56 g, 67.4 mmol, 1.10 equiv) in a glovebox. The flask was removed from the glovebox, THF (61.0 mL) was added, and the solution was cooled to 0 °C. To the solution was then added ketone **4.26** (2.00 g, 61.5 mmol each, 0.200 equiv) in 5 aliquots over 25 min. The reaction was then warmed to 23 °C. After stirring for 2 h, the reaction was cooled to 0 °C and quenched by the sequential addition of deionized water (5 mL), 10% aq. NaOH (7 ml), MeOH (20 mL), and deionized water (10 mL).

The mixture was then warmed to 23 °C and stirred for 30 min. The mixture was then filtered over a pad of celite (100 mL EtOAc eluent). The resulting organic layer was dried over Na_2SO_4, filtered, and the volatiles were removed under reduced pressure. The crude residue was purified by flash chromatography (5:1 Hexanes:EtOAc → 3:1 Hexanes:EtOAc) to yield alcohol **4.5** (9.42 g, 93% yield) as a white solid. Alcohol **4.5**: R_f 0.33 (3:1 Hexanes:EtOAc). Spectral data match those previously reported.[27]

4.7.2.3 Syntheses of Enantioenriched Alcohol Reductant (*R*)-4.5
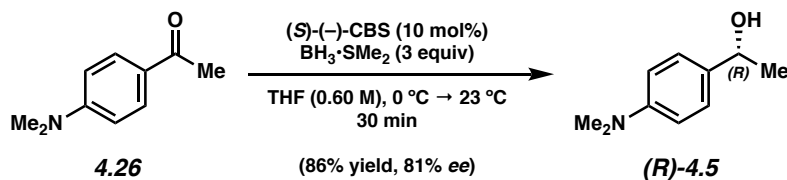
To a flame-dried flask equipped with a magnetic stir bar was added (S)-(–)-CBS catalyst (170 mg, 0.613 mmol, 0.100 equiv). The flask was removed from the glovebox and THF (6.13 mL) was added. Next, **4.26** (1.00 g, 6.13 mmol, 1.00 equiv) in a solution of THF (2.50 mL) was added to the reaction flask, which was then stirred to give a clear homogeneous solution and cooled to 0 °C. Subsequently, $BH_3 \cdot SMe_2$ (1.70 mL, 18.4 mmol, 3.00 equiv) was added (1 drop/2 sec) over 7.50 min. The reaction was stirred at 0 °C for 2 min, then warmed to 23 °C. After stirring for 30 min, the reaction was cooled to 0 °C and quenched by the dropwise addition of methanol (20 mL) and water (20 mL) and diluted with Et_2O (50 mL). The layers were separated and the aqueous layer was extracted with Et_2O (3 x 50 mL). The combined organic layers were washed with sat. aq. NH_4Cl (80 mL), sat. aq. $NaHCO_3$ (80 mL), and brine (80 mL). The organic layer was then dried over Na_2SO_4, filtered, and the volatiles were removed under reduced pressure. The crude residue was purified by flash chromatography (10:1 Hexanes:EtOAc → 3:1 Hexanes:EtOAc) to yield

alcohol (*R*)-**4.5** (871 mg, 86% yield, 81% ee) as a white solid. Alcohol (*R*)-**4.5**: R*f* 0.33 (3:1

Hexanes:EtOAc). The spectral data match those previously reported in the literature for *rac*-**4.5**.[27]

The SFC data match those reported in the Experimental Procedures Section 4.7.2.7.
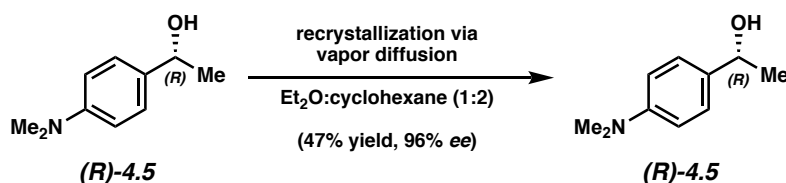
A solution of (*R*)-**4.5** (25.0 mg, 0.151 mmol, 1.00 equiv) in Et$_2$O (1.00 mL) was filtered through a

0.45 µm Millipore Millex PTFE filter into a 1-dram vial. The vial was then placed within a 20 mL

scintillation vial containing cyclohexane (2.00 mL). The scintillation vial was sealed and allowed

to stand at 23 °C for 24 h, which led to the formation of white crystals. This vapor diffusion

crystallization process was repeated three times to lead to the recovery of alcohol (*R*)-**4.5** (11.8

mg, 47% yield, 96% ee) as a white crystalline solid. $[\alpha]_D^{23.1} = +51.6$ (*c* = 1.00, CHCl$_3$). The spectral

data match those previously reported in the literature for *rac*-**4.5**.[27] The major enantiomer product

was assigned by comparison to published $[\alpha]_D$ values for (*R*)-**4.5**.[28]

4.7.2.4 Initial Survey of Reaction Conditions and Relevant Control Experiments
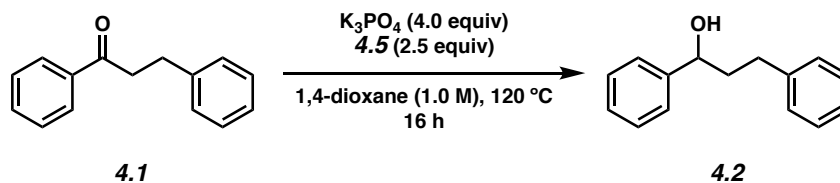
Representative Procedure for Base-Mediated MPV Reduction from Table 4.2 (reduction of

ketone 4.1 with alcohol 4.5 is used as an example). A 1-dram vial was charged with anhydrous

powdered K$_3$PO$_4$ (85.0 mg, 0.400 mmol, 4.00 equiv) and a magnetic stir bar. The vial and its

contents were flame-dried under reduced pressure, then allowed to cool under N_2. Ketone substrate **4.1** (21.0 mg, 0.100 mmol, 1.00 equiv) and alcohol reductant **4.5** (41.3 mg, 0.250 mmol, 2.50 equiv) were added. The vial was flushed with N_2, and then 1,4-dioxane (0.100 mL, 1.00 M) was added. Under a stream of N_2, the vial septum cap was quickly switched for a Teflon-lined screw cap, sealed, then further sealed with electrical tape. The reaction was stirred vigorously (800 rpm) at 120 °C for 16 h. After cooling to 23 °C, the mixture was diluted with hexanes (0.5 mL) and filtered over a plug of silica gel (1 cm OD x 5 cm, 10 mL EtOAc eluent). The volatiles were removed under reduced pressure and the yield of alcohol **4.2** was determined by ^{1}H NMR analysis with 1,3,5-trimethoxybenzene as an external standard.

Any modifications of the conditions shown in the representative procedure

above are specified below in Table 4.2.

Table 4.2. Survey of reaction conditions and relevant control experiments
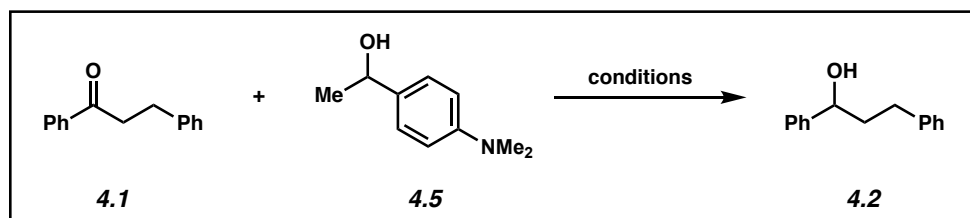
Reaction Conditions	Experimental Results[a]	
	4.1	4.2
4.5 (2.5 equiv), K$_3$PO$_4$ (4.0 equiv), dioxane (1.0 M), 120 °C, 16 h	0%	99%
4.5 (2.5 equiv), K$_3$PO$_4$ (4.0 equiv), dioxane (1.0 M), 80 °C, 16 h	0%	99%
4.5 (2.5 equiv), K$_3$PO$_4$ (4.0 equiv), dioxane (1.0 M), 120 °C, 3 h	<5%	98%
4.5 (2.5 equiv), K$_3$PO$_4$ (4.0 equiv), 2-Me THF (1.0 M), 80 °C, 16 h	0%	99%
4.5 (2.5 equiv), K$_3$PO$_4$ (4.0 equiv), *t*-amyl alcohol (1.0 M), 80 °C, 16 h	<5%	98%
4.5 (2.5 equiv), K$_3$PO$_4$ (4.0 equiv), *n*-heptane (1.0 M), 80 °C, 16 h	11%	89%
Control Experiments:		
4.5 (2.5 equiv), K$_3$PO$_4$ (4.0 equiv), dioxane (1.0 M), 120 °C, 16 h **Ran in the dark**	0%	99%
4.5 (2.5 equiv), K$_3$PO$_4$ (4.0 equiv), H$_2$O (2.0 equiv), dioxane (1.0 M), 120 °C, 16 h	<5%	95%
4.5 (2.5 equiv), K$_3$PO$_4$ (4.0 equiv), dioxane (1.0 M), 120 °C, 16 h **Ran under an atmosphere of air**	12%	88%

[a]Yields were determined by ^{1}H NMR analysis using 1,3,5-trimethoxybenzene as an external standard.

4.7.2.5 Trace Metal Analysis of Reagents

Representative Procedure for Trace Metal Analysis (preparation of K$_3$PO$_4$ is used as an example). A 15-mL conical tube was charged with K$_3$PO$_4$ (95.2 mg, 1.00 equiv) and the sample was diluted with milli-Q water (6.8 mL) to a final concentration of 1.4% (w/w). Subsequently, ICP-MS-grade 70% nitric acid (200 μl) was added to each sample (2% final nitric acid concentration).

Table 4.3. Trace metal analysis of K_3PO_4

Sample: K_3PO_4	
Metal	**Concentration (ppm) (average of two samples)**
Fe	0.00809
Al	0.000
Co	0.000
B	0.0240
Ti	0.0420
Mg	0.00189
Mn	7.84×10^{-5}
Sc	0.000
Rb	0.203
Ni	0.0303
Cu	0.000
Zn	0.000
Ru	9.46×10^{-6}
Rh	0.000
Pd	1.53×10^{-5}
Ag	0.000
Ir	1.17×10^{-6}
Pt	0.000

Table 4.4. Trace metal analysis of 1,4-dioxane

Sample: 1,4-dioxane	
Metal	Concentration (ppm) (average of two samples)
Fe	0.00369
Al	0.00384
Co	0.000130
B	0.00570
Ti	0.00250
Mg	0.01780
Mn	0.000151
Sc	0.00190
Rb	3.41×10^{-5}
Ni	0.354
Cu	0.000
Zn	0.000
Ru	0.000
Rh	0.000
Pd	1.06×10^{-5}
Ag	2.85×10^{-5}
Ir	0.000
Pt	0.000

Table 4.5. Trace metal analysis of alcohol reductant **4.5**

Sample: Alcohol Reductant 4.5	
Metal	Concentration (ppm) (average of two samples)
Fe	0.00352
Al	0.00121
Co	3.20×10^{-5}
B	0.0211
Ti	0.000642
Mg	0.0125
Mn	1.81×10^{-5}
Sc	0.000962
Rb	5.15×10^{-6}
Ni	0.113
Cu	0.000
Zn	0.000
Ru	0.000
Rh	9.31×10^{-7}
Pd	3.00×10^{-6}
Ag	7.91×10^{-6}
Ir	0.000
Pt	1.76×10^{-6}

4.7.2.6 Scope of Methodology
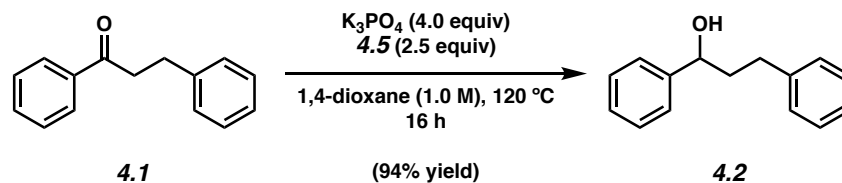
Representative Procedure for Base-Mediated MPV Reduction from Figure 4.2 (reduction of ketone 4.1 with alcohol 4.5 is used as an example). Alcohol 4.2. A 1-dram vial was charged with anhydrous powdered K_3PO_4 (85.0 mg, 0.400 mmol, 4.00 equiv) and a magnetic stir bar. The vial and its contents were flame-dried under reduced pressure, then allowed to cool under N_2. Ketone substrate **4.1** (21.0 mg, 0.100 mmol, 1.00 equiv) and alcohol reductant **4.5** (41.3 mg, 0.250 mmol, 2.50 equiv) were added. The vial was purged with N_2, and then 1,4-dioxane (0.100 mL, 1.00 M) was added. Under a stream of N_2, the vial septum cap was quickly switched for a Teflon-lined screw cap, sealed, then further sealed with electrical tape. The reaction was stirred vigorously (800 rpm) at 120 °C for 16 h. After cooling to 23 °C, the reaction was quenched by the addition of sat. aq. NH_4Cl (1.00 mL) and diluted with EtOAc (2.00 mL) and the layers were separated. The aqueous layer was extracted with EtOAc (3 x 2.00 mL) and the combined organic layers were passed through a plug (1.00 cm OD) of silica gel (3.00 cm tall) and Na_2SO_4 (3.00 cm tall) using EtOAc (10.0 mL) as eluent. The volatiles were removed under reduced pressure. The crude residue was purified by flash chromatography (99:1 Hexanes:EtOAc → 19:1 Hexanes:EtOAc) to yield alcohol **4.2** (20 mg, 94% yield, average of two experiments) as a clear oil. Alcohol **4.2**: R_f 0.32 (5:1 Hexanes:EtOAc). ^{1}H NMR (500 MHz, CDCl$_3$): δ 7.41–7.33 (m, 4H), 7.32–7.26 (m, 3H), 7.23–7.16 (m, 3H), 4.78–4.61 (m, 1H), 2.85–2.61 (m, 2H), 2.23–1.97 (m, 2H), 1.87 (d, J = 3.5 Hz, 1H). Spectral data match those previously reported.[29]

Any modifications of the conditions shown in the representative procedure above are specified in the following schemes, which depict all of the results shown in Figures 4.2 and 4.3.
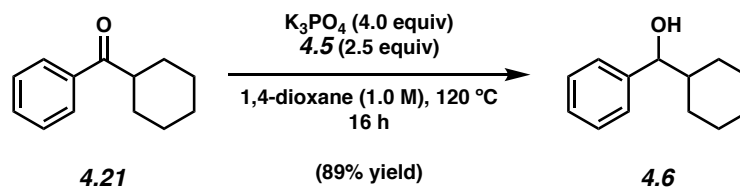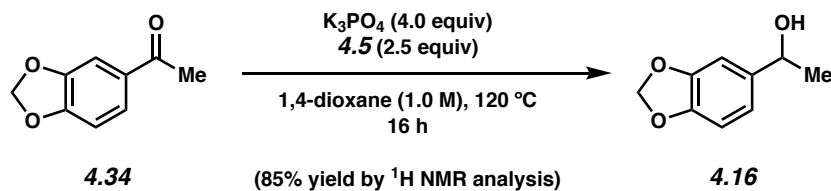

Alcohol 4.6. Purification by flash chromatography (99:1 Hexanes:EtOAc → 19:1 Hexanes:EtOAc) generated alcohol **4.6** (17 mg, 89% yield, average of two experiments) as a crystalline white solid. Alcohol **4.6**: R_f 0.39 (5:1 Hexanes:EtOAc).). ^{1}H NMR (500 MHz, CDCl$_3$): δ 7.38–7.25 (m, 5H), 4.37 (dd, J = 7.2 Hz, 3.3 Hz, 1H), 2.03–1.92 (m, 1H), 1.84–1.72 (m, 2H), 1.71–1.57 (m, 3H), 1.41–1.33 (m, 1H), 1.29–1.00 (m, 4H), 0.99–0.87 (m, 1H). Spectral data match those previously reported.[30]
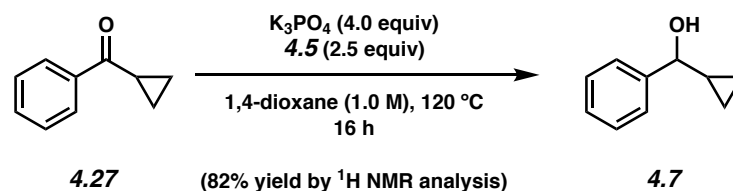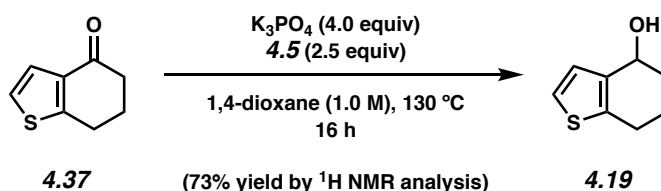

Alcohol 4.7. ^{1}H NMR analysis of the crude reaction mixture indicated an 82% yield of alcohol **4.7** relative to hexamethylbenzene external standard (average of two experiments). Purification by preparative thin-layer chromatography (3:1 Hexanes:EtOAc) provided an analytical sample of alcohol **4.7** as a clear oil. Alcohol **4.7**: R_f 0.30 (5:1 Hexanes:EtOAc). ^{1}H NMR (500 MHz, CDCl$_3$): δ 7.46–7.40 (m, 2H), 7.39–7.33 (m, 2H), 7.32–7.27 (m, 1H), 4.02 (dd, J = 8.3, 3.0, 1H), 1.90 (d, J

= 3.0, 1H), 1.28–1.18 (m, 1H), 0.69–0.61 (m, 1H), 0.60–0.52 (m, 1H), 0.52–0.44 (m, 1H), 0.42–0.34 (m, 1H). Spectral data match those previously reported.[31]
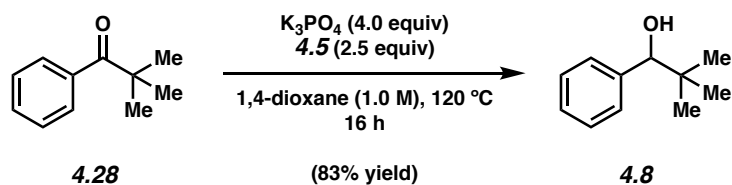

Alcohol 4.8. Purification by flash chromatography (24:1 Hexanes:EtOAc) generated alcohol **4.8** (14 mg, 83% yield, average of two experiments) as a white crystalline solid. Alcohol **4.8**: R_f 0.52 (5:1 Hexanes:EtOAc). ^{1}H NMR (500 MHz, CDCl$_3$): δ 7.35–7.30 (m, 4H), 7.29–7.26 (m, 1H), 4.40 (d, J = 2.8, 1H), 1.84 (d, J = 2.8, 1H), 0.93 (s, 9H). Spectral data match those previously reported.[32]
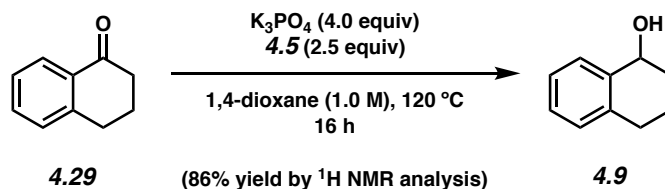
Alcohol 4.9. ^{1}H NMR analysis of the crude reaction mixture indicated an 86% yield of alcohol **4.9** relative to hexamethylbenzene external standard (average of two experiments). Purification by preparative thin-layer chromatography (9:1 PhH:Acetone) provided an analytical sample of alcohol **4.9** as a clear oil. Alcohol **4.9**: R_f 0.50 (9:1 PhH:Acetone). ^{1}H NMR (500 MHz, CDCl$_3$): δ 7.48–7.39 (m, 1H), 7.24–7.17 (m, 2H), 7.14–7.05 (m, 1H), 4.84–4.71 (m, 1H), 2.88–2.78 (m, 1H), 2.87–2.67 (m, 1H), 2.05–1.95 (m, 2H), 1.95–1.87 (m, 1H), 1.85–1.73 (m, 1H), 1.71–1.60 (m, 1H). Spectral data match those previously reported.[33]
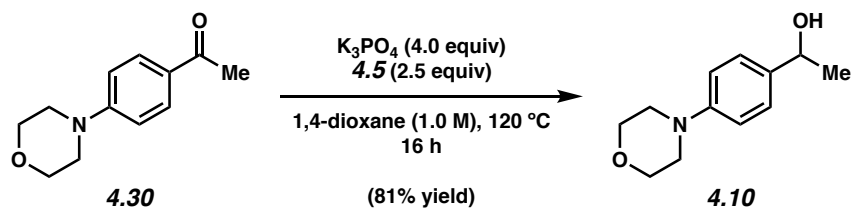
Alcohol 4.10. Purification by flash chromatography (2:2:1 CH_2Cl_2:Et_2O:Hexanes) generated alcohol **4.10** (17 mg, 81% yield, average of two experiments) as a pale yellow solid. Alcohol **4.10**: R_f 0.24 (1:1:1 CH_2Cl_2:Et_2O:Hexanes). ^1H NMR (500 MHz, $CDCl_3$): δ 7.33–7.28 (m, 2H), 6.93–6.87 (m, 2H), 4.85 (dq, J = 6.4, 3.5, 1H), 3.90–3.83 (m, 4H), 3.19–3.12 (m, 4H), 1.67 (d, J = 3.5, 1H), 1.48 (d, J = 6.4, 3H). Spectral data match those previously reported.[34]
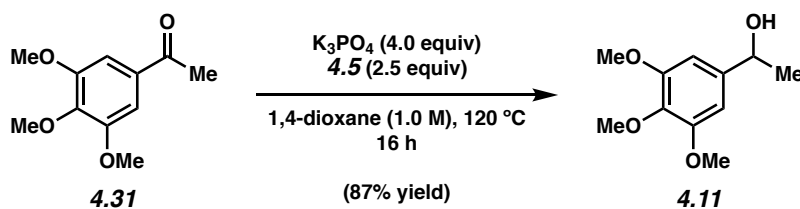
Alcohol 4.11. Purification by flash chromatography (9:1 Hexanes:EtOAc → 2:1 Hexanes:EtOAc) generated alcohol **4.11** (18 mg, 87% yield, average of two experiments) as a clear oil. Alcohol **4.11**: R_f 0.33 (1:1 Hexanes:EtOAc). ^1H NMR (500 MHz, $CDCl_3$): δ 6.60 (s, 2H), 4.89–4.77 (m, 1H), 3.86 (s, 6H), 3.83 (s, 3H), 1.99–1.80 (m, 1H), 1.48 (d, J = 6.4, 3H). Spectral data match those previously reported.[34]

4.32 — K$_3$PO$_4$ (4.0 equiv), **4.5** (2.5 equiv), 1,4-dioxane (1.0 M), 120 °C, 16 h — (92% yield by ^{1}H NMR analysis) → **4.12**
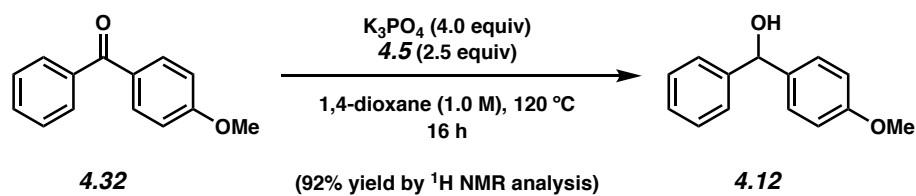
Alcohol 4.12. ^{1}H NMR analysis of the crude reaction mixture indicated a 92% yield of alcohol **4.12** relative to hexamethylbenzene external standard (average of two experiments). Purification by preparative thin-layer chromatography (3:3:2 CH$_2$Cl$_2$:Et$_2$O:Hexanes) provided an analytical sample of alcohol **4.12** as a pale yellow solid. Alcohol **4.12**: R$_f$ 0.70 (1:1:1 CH$_2$Cl$_2$:Et$_2$O:Hexanes). ^{1}H NMR (500 MHz, CDCl$_3$): δ 7.40–7.31 (m, 4H), 7.31–7.23 (m, 3H), 6.93–6.81 (m, 2H), 5.82 (d, J = 3.0, 1H), 3.79 (s, 3H), 2.15 (d, J = 3.4, 1H). Spectral data match those previously reported.[30]

4.33 — K$_3$PO$_4$ (4.0 equiv), **4.5** (2.5 equiv), 1,4-dioxane (1.0 M), 80 °C, 16 h — (84% yield) → **4.13**
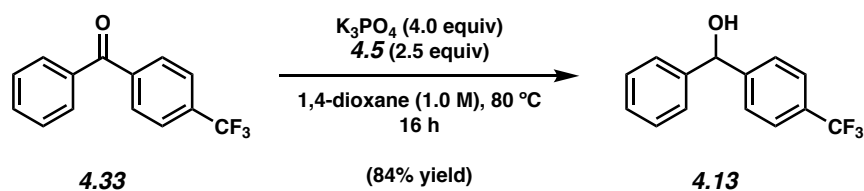
Alcohol 4.13. Purification by flash chromatography (9:1 Hexanes:Et$_2$O → 3:1 Hexanes:Et$_2$O) generated alcohol **4.13** (21 mg, 84% yield, average of two experiments) as a clear oil. Alcohol **4.13**: R$_f$ 0.30 (5:1 Hexanes:Et$_2$O). ^{1}H NMR (500 MHz, CDCl$_3$): δ 7.60 (d, J = 8.3, 2H), 7.51 (d, J = 8.3, 2H), 7.42–7.34 (m, 4H), 7.34–7.28 (m, 1H), 5.88 (s, 1H), 2.46–2.32 (m, 1H). Spectral data match those previously reported.[30]
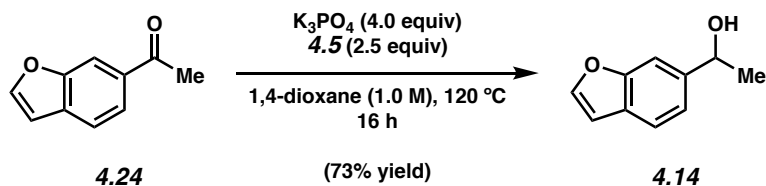
Alcohol 4.14. Purification by flash chromatography (90:9:1 → 15:9:1 Hexanes:PhH:Acetone) generated alcohol **4.14** (12 mg, 73% yield, average of two experiments) as a yellow oil. Alcohol **4.14**: R_f 0.39 (9:1 PhH:Acetone); ^{1}H NMR (500 MHz, C_6D_6): δ 7.50–7.46 (m, 1H), 7.35 (d, J = 8.1 Hz, 1H), 7.12 (ddd, J = 8.1, 1.4, 0.5 Hz, 1H), 6.35 (dd, J = 2.2, 1.1 Hz, 1H), 4.59 (q, J = 6.5 Hz, 1H), 1.29 (d, J = 6.5 Hz, 3H), 1.14, (br s, 1H); ^{13}C NMR (125 MHz, CDCl$_3$): δ 155.3, 145.4, 142.8, 126.9, 121.2, 120.6, 108.4, 106.5, 70.7, 25.6; IR (film): 3350, 2972, 2926, 1430, 1265 cm^{-1}; HRMS-APCI (*m/z*) [M + H]$^+$ calcd for $C_{10}H_{11}O_2^+$, 163.0754; found 163.0746.
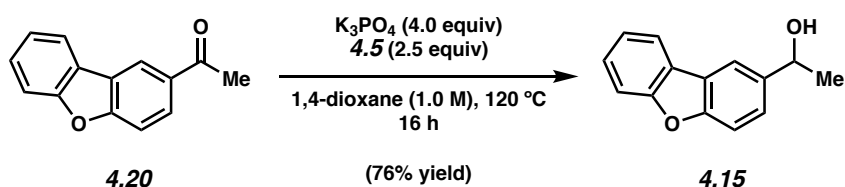
Alcohol 4.15. Purification by flash chromatography (90:9:1 → 25:9:1 Hexanes:PhH:Acetone) generated alcohol **4.15** (16 mg, 76% yield, average of two experiments) as a yellow solid. Alcohol **4.15**: R_f 0.35 (9:1 PhH:Acetone). ^{1}H NMR (400 MHz, CDCl$_3$): δ 8.03–7.91 (m, 2H), 7.60–7.51 (m, 2H), 7.50–7.43 (m, 2H), 7.35 (td, J = 7.5, 1.0, 1H), 5.09 (dq, J = 6.4, 3.3, 1H), 1.90 (d, J = 3.3, 1H), 1.60 (d, J = 6.4, 3H). Spectral data match those previously reported.[35]

4.34   (85% yield by ¹H NMR analysis)   **4.16**

Alcohol 4.16. ¹H NMR analysis of the crude reaction mixture indicated an 85% yield of alcohol **4.16** relative to hexamethylbenzene external standard. Purification by preparative thin-layer chromatography (13:1:1 PhH:Et$_2$O:CH$_3$CN) provided an analytical sample of alcohol **4.16** as a yellow oil. Alcohol **4.16**: R$_f$ 0.30 (13:1:1 PhH:Et$_2$O:CH$_3$CN); ¹H NMR (500 MHz, CDCl$_3$): δ 6.90 (s, 1H), 6.82 (dd, J = 8.1, 1.7 Hz, 1H), 6.77 (d, J = 8.1 Hz, 1H), 5.95 (s, 2H), 4.86–4.79 (m, 1H), 1.70 (d, J = 3.4 Hz, 1H), 1.46 (d, J = 6.4 Hz, 3H); ¹³C NMR (125 MHz, CDCl$_3$): δ 147.9, 147.0, 140.1, 118.8, 108.2, 106.2, 101.1, 70.4, 25.3; IR (film): 3361, 2972, 2890, 1487, 1240 cm^{-1}; HRMS-APCI (m/z) [M + H]$^+$ calcd for C$_9$H$_{11}$O$_3^+$, 167.0703; found 167.0699.

4.35   (81% yield)   **4.17**
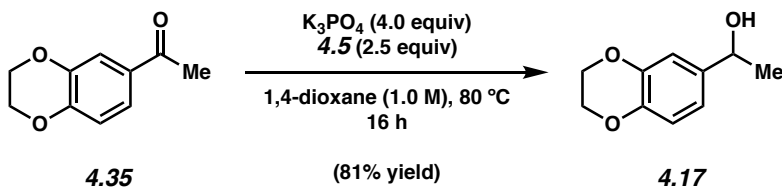
Alcohol 4.17. Purification by flash chromatography (98:1:1 → 28:1:1 PhH:Et$_2$O:CH$_3$CN) generated alcohol **4.17** (15 mg, 81% yield, average of two experiments) as a yellow oil. Alcohol **4.17**: R$_f$ 0.32 (13:1:1 PhH:Et$_2$O:CH$_3$CN). ¹H NMR (500 MHz, CDCl$_3$): δ 6.92–6.88 (m, 1H), 6.86–6.81 (m, 2H), 4.80 (dq, J = 6.4, 3.6, 1H), 4.25 (s, 4H), 1.69 (d, J = 3.6, 1H), 1.46 (d, J = 6.4, 3H). Spectral data match those previously reported.[36]

K₃PO₄ (4.0 equiv)

K₃PO₄ (4.0 equiv)
4.5 (2.5 equiv)
1,4-dioxane (1.0 M), 120 °C
16 h

4.36

(70% yield)

4.18
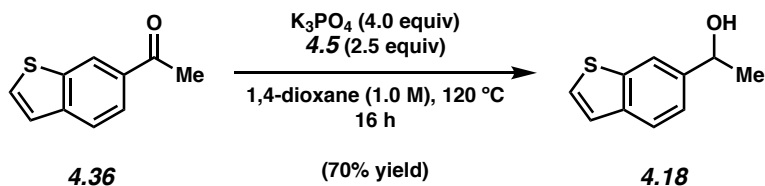
Alcohol 4.18. Purification by flash chromatography (90:9:1 → 40:9:1 Hexanes:PhH:Acetone) generated alcohol **4.18** (12 mg, 70% yield, average of two experiments) as a yellow oil. Alcohol **4.18**: R_f 0.38 (9:1 PhH:Acetone); ^{1}H NMR (500 MHz, CDCl₃): δ 7.91 (s, 1H), 7.80 (d, J = 8.2 Hz, 1H), 7.43 (d, J = 5.5 Hz, 1H), 7.38 (dd, J = 8.3, 1.3 Hz, 1H), 7.32 (d, J = 5.5 Hz, 1H), 5.10–5.0 (m, 1H), 1.85 (d, J = 3.4 Hz, 1H), 1.56 (d, J = 6.5 Hz, 3H); ^{13}C NMR (125 MHz, CDCl₃): δ 142.3, 140.1, 139.2, 126.6, 123.8, 123.7, 122.3, 119.2, 70.7, 25.5; IR (film): 3351, 2971, 1398, 1197, 1074 cm^{-1}; HRMS-APCI (*m/z*) [M]$^{+}$ calcd for C₁₀H₁₀OS^{+}, 178.0447; found 178.0437.

K₃PO₄ (4.0 equiv)
4.5 (2.5 equiv)
1,4-dioxane (1.0 M), 130 °C
16 h

4.37

(73% yield by ^{1}H NMR analysis)

4.19

Alcohol 4.19. ^{1}H NMR analysis of the crude reaction mixture indicated a 73% yield of alcohol **4.19** relative to hexamethylbenzene external standard. Purification by preparative thin-layer chromatography (1:1:1 Hexanes:Et₂O:CH₂Cl₂) provided an analytical sample of alcohol **4.19** as a white crystalline solid. Alcohol **4.19**: R_f 0.48 (1:1:1 Hexanes:Et₂O:CH₂Cl₂); ^{1}H NMR (500 MHz, CDCl₃): δ 7.10 (dt, J = 5.2, 0.7 Hz, 1H), 7.03 (d, J = 5.2 Hz, 1H), 4.82–4.75 (m, 1H), 2.89–2.79 (m, 1H), 2.77–2.67 (m, 1H), 2.06–1.94 (m, 2H), 1.93–1.79 (m, 2H), 1.64 (d, J = 7.0 Hz 1H); ^{13}C NMR (125 MHz, CDCl₃): δ 139.0, 138.1, 126.7, 122.9, 65.6, 32.5, 25.2, 20.1; IR (film): 3235,

2936, 2921, 1431, 982 cm^{-1}; HRMS-APCI (m/z) [M + H]$^+$ calcd for C$_8$H$_{11}$OS$^+$, 155.0525; found

155.0521.

4.7.2.7 Gram-Scale Reduction

4.20   (66% yield)   **4.15**
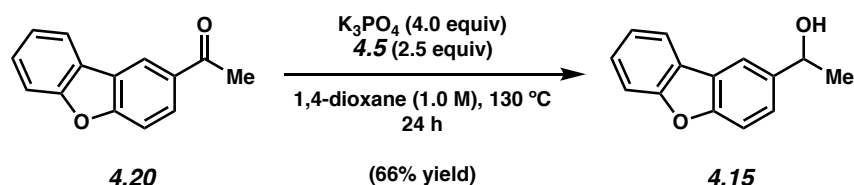
Alcohol 4.15. An 8-dram vial was charged with anhydrous powdered K$_3$PO$_4$ (4.04 g, 19.0 mmol,

4.00 equiv) and a magnetic stir bar. The vial and its contents were flame-dried under reduced

pressure, then allowed to cool under N$_2$. Ketone substrate **4.20** (1.00 g, 4.76 mmol, 1.00 equiv)

and alcohol reductant **4.5** (1.96 g, 11.9 mmol, 2.50 equiv) were then added. The vial was flushed

with N$_2$ and subsequently 1,4-dioxane (4.76 mL, 1.00 M) was added. Under a stream of N$_2$, the

vial septum cap was quickly switched for a Teflon-lined screw cap, sealed, then further sealed with

electrical tape. The reaction was then stirred vigorously (800 rpm) at 130 °C for 24 h. After cooling

to 23 °C, the reaction was quenched by the addition of sat. aq. NH$_4$Cl (8.00 mL) and diluted with

EtOAc (6.00 mL) and the layers were separated. The aqueous layer was extracted with EtOAc (3

x 6.00 mL) and the combined organic layers were passed through a plug (1.00 cm OD) of silica

gel (3.00 cm tall) and Na$_2$SO$_4$ (3.00 cm tall) using EtOAc (10.0 mL) as eluent. The volatiles were

removed under reduced pressure. The crude residue was purified by flash chromatography (60:9:1

Hexanes:PhH:Acetone → 5:9:1 Hexanes:PhH:Acetone) to yield alcohol **4.15** (664 mg, 66% yield)

as a yellow solid. Alcohol **4.15**: R$_f$ 0.32 (5:1 Hexanes:EtOAc). Spectral data match those

previously reported.[35]

4.7.2.8 Stereospecific Reduction
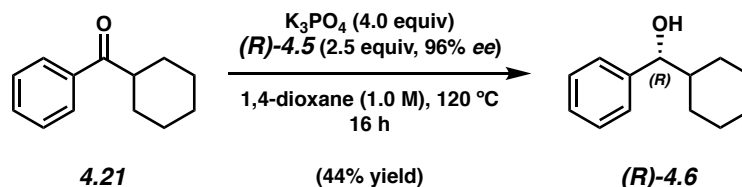
Alcohol (*R*)-4.6. A 1-dram vial was charged with anhydrous powdered K$_3$PO$_4$ (85.0 mg, 0.400

mmol, 4.00 equiv) and a magnetic stir bar. The vial and its contents were flame-dried under

reduced pressure, then allowed to cool under N$_2$. Ketone substrate **4.21** (18.8 mg, 0.100 mmol,

1.00 equiv) and alcohol reductant (*R*)-**4.5** (41.3 mg, 0.250 mmol, 2.50 equiv) were added. The vial

was purged with N$_2$ and subsequently, 1,4-dioxane (0.100 mL, 1.00 M) was added. Under a stream

of N$_2$, the vial septum cap was quickly switched for a Teflon-lined screw cap, sealed, then further

sealed with electrical tape. The reaction was stirred vigorously (800 rpm) at 120 °C for 16 h. After

cooling to 23 °C, the reaction was quenched by the addition of sat. aq. NH$_4$Cl (1.00 mL) and

diluted with EtOAc (2.00 mL) and the layers were separated. The aqueous layer was extracted

with EtOAc (3 x 2.00 mL) and the combined organic layers were passed through a plug (1.00 cm

OD) of silica gel (3.00 cm tall) and Na$_2$SO$_4$ (3.00 cm tall) using EtOAc (10.0 mL) as eluent. The

volatiles were removed under reduced pressure. The crude residue was purified by flash

chromatography (99:1 Hexanes:EtOAc → 19:1 Hexanes:EtOAc) to yield alcohol (*R*)-**4.6** (8.4 mg,

44% yield, 48% ee) as a white crystalline solid. Alcohol (*R*)-**4.6**: R$_f$ 0.39 (5:1 Hexanes:EtOAc).

$[\alpha]_D^{21.1}$ = +20.8 (*c* = 0.50, CHCl$_3$). The spectral data match those previously reported in the

literature for *rac*-**4.6**.[30] The major enantiomer product was assigned by comparison to published

$[\alpha]_D$ values for (*R*)-**4.6**.[37]

4.7.2.9 Verification of Enantiopurity

4.7.2.9.1 Chiral SFC & HPLC Assays of Alcohol Reductant

Table 4.6. Conditions and results of chiral SFC analysis of alcohol reductant **4.5**.
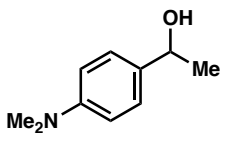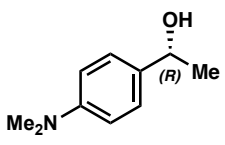
Compound	SFC Method Column/Temp. Abs. Wavelength	Solvent	Method Flow Rate	Retention Times (min)	Enantiomeric Ratio (er)
rac-4.5	Daicel ChiralPak IC-3/35 °C $\lambda_{abs} = 210$ nm	5% isopropanol in CO_2	3.5 mL/min	7.88/8.61	50:50
(R)-4.5	Daicel ChiralPak IC-3/35 °C $\lambda_{abs} = 210$ nm	5% isopropanol in CO_2	3.5 mL/min	7.58/8.22	98:2

Figure 4.5. SFC trace of *rac*-**4.5** (Table 4.6, Entry 1).
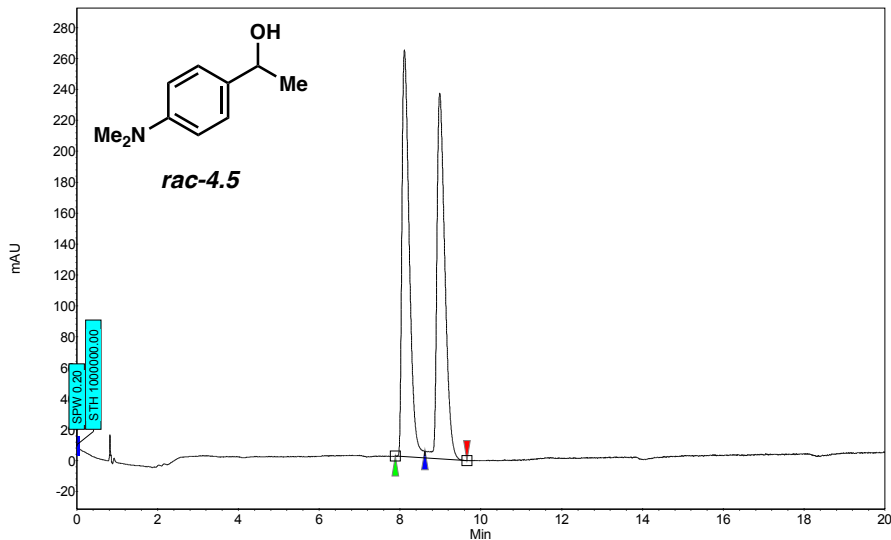
Index	Name	Start	Time	End	RT Offset	Quantity	Height	Area	Area
		[Min]	[Min]	[Min]	[Min]	[% Area]	[µV]	[µV.Min]	[%]
1	UNKNOWN	7.88	8.11	8.61	0.00	50.43	263.1	55.4	50.434
2	UNKNOWN	8.61	8.99	9.66	0.00	49.57	236.6	54.5	49.566
Total						100.00	499.7	109.9	100.000

Figure 4.6. SFC trace of (*R*)-**4.5** (Table 4.6, Entry 2).
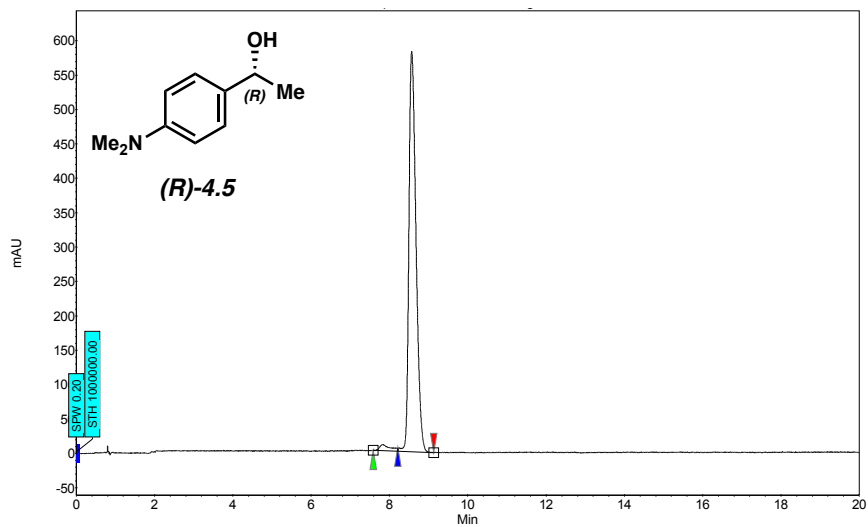
Index	Name	Start	Time	End	RT Offset	Quantity	Height	Area	Area
		[Min]	[Min]	[Min]	[Min]	[% Area]	[µV]	[µV.Min]	[%]
1	UNKNOWN	7.58	7.82	8.22	0.00	2.18	8.7	2.7	2.176
2	UNKNOWN	8.22	8.57	9.13	0.00	97.82	582.5	122.1	97.824
Total						100.00	591.1	124.8	100.000

231

4.7.2.9.2 Stereospecific Reduction of Ketone 4.6

Table 4.7. Conditions and results of chiral HPLC analysis of alcohol products.
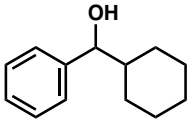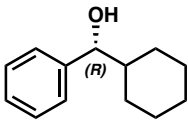
Compound	HPLC Method Column/Temp. Abs. Wavelength	Solvent	Method Flow Rate	Retention Times (min)	Enantiomeric Ratio (er)
rac-4.6	Daicel ChiralPak OD-H/23 °C λ_{abs} = 210 nm	10% isopropanol in Hexanes	1 mL/min	5.14/5.77	50:50
(R)-4.6	Daicel ChiralPak OD-H/23 °C λ_{abs} = 210 nm	10% isopropanol in Hexanes	1 mL/min	5.16/5.70	74:26

Figure 4.7. HPLC trace of *rac*-**4.6** (Table 4.7, Entry 1).
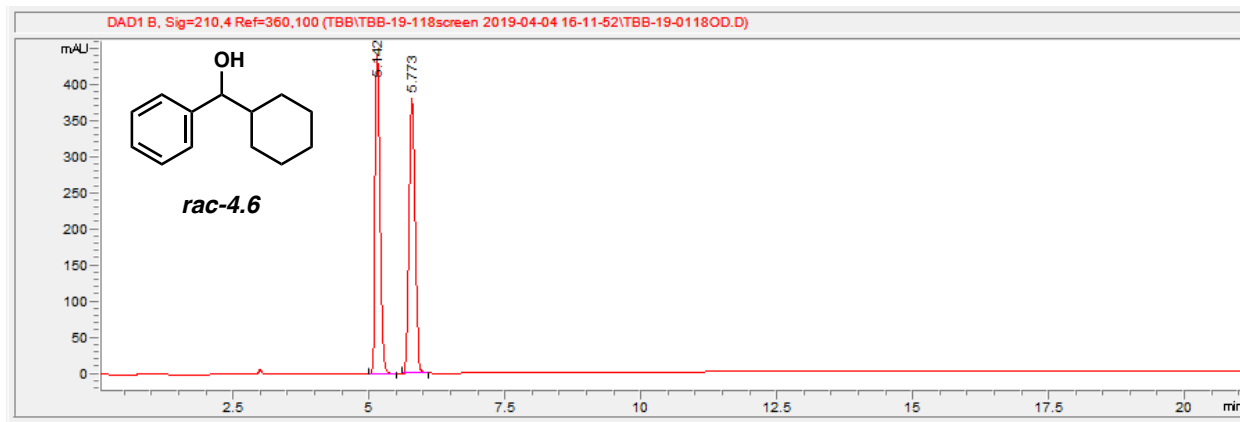
#	Time	Area	Height	Width	Area%	Symmetry
1	5.142	2774.2	442.1	0.0972	50.021	0.833
2	5.773	2771.9	380.2	0.113	49.979	0.836

Figure 4.8. HPLC trace of (*R*)-**4.6** (Table 4.7, Entry 2).
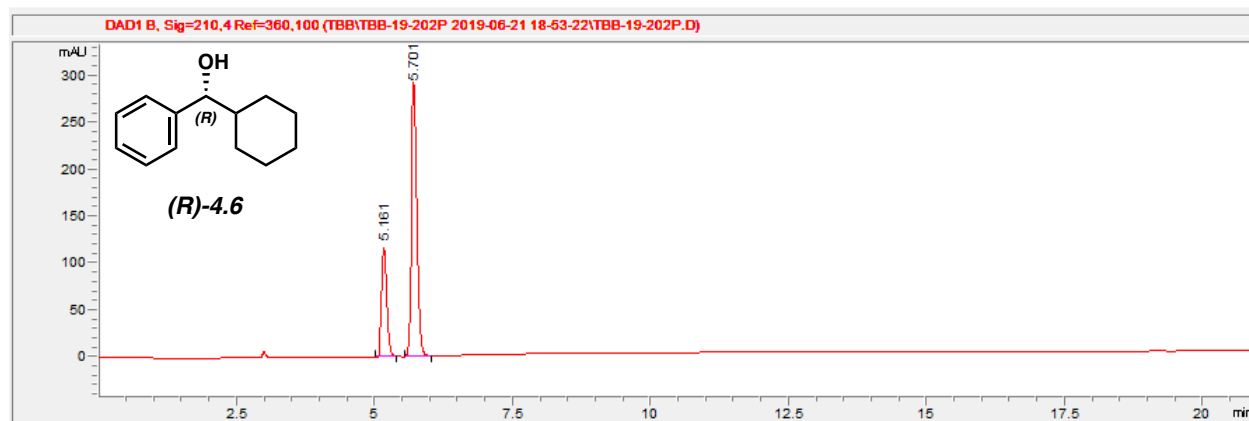
#	Time	Area	Height	Width	Area%	Symmetry
1	5.161	732.7	116.3	0.0975	25.919	0.834
2	5.701	2094.1	291.8	0.1107	74.081	0.837

4.8 Spectra Relevant to Chapter Four:

Base-Mediated Meerwein–Ponndorf–Verley Reduction of Aromatic Ketones and Heterocyclic Ketones

Timothy B. Boit,[†] Milauni M. Mehta, and Neil K. Garg.
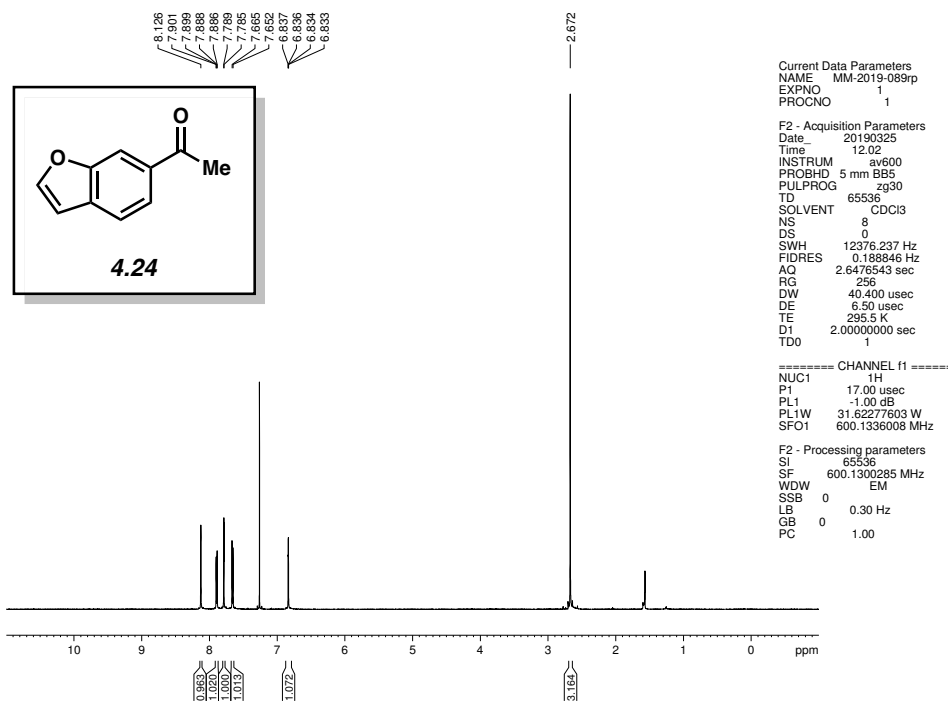
Figure 4.9 ^{1}H NMR (600 MHz, CDCl$_3$) of compound **4.24**.
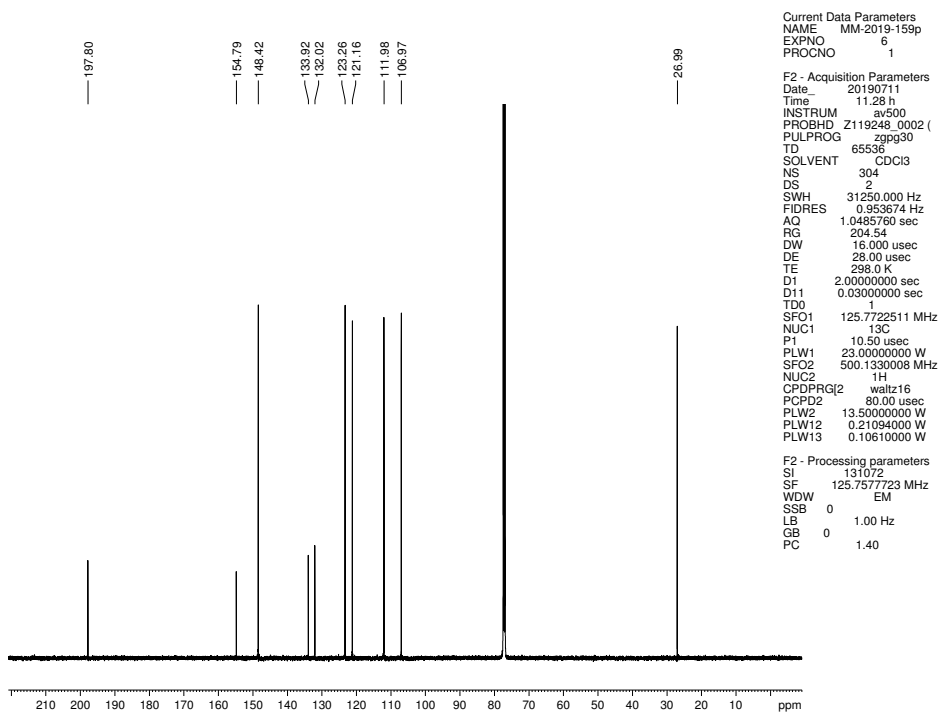
Figure 4.10 ^{13}C NMR (125 MHz, CDCl$_3$) of compound **4.24**.
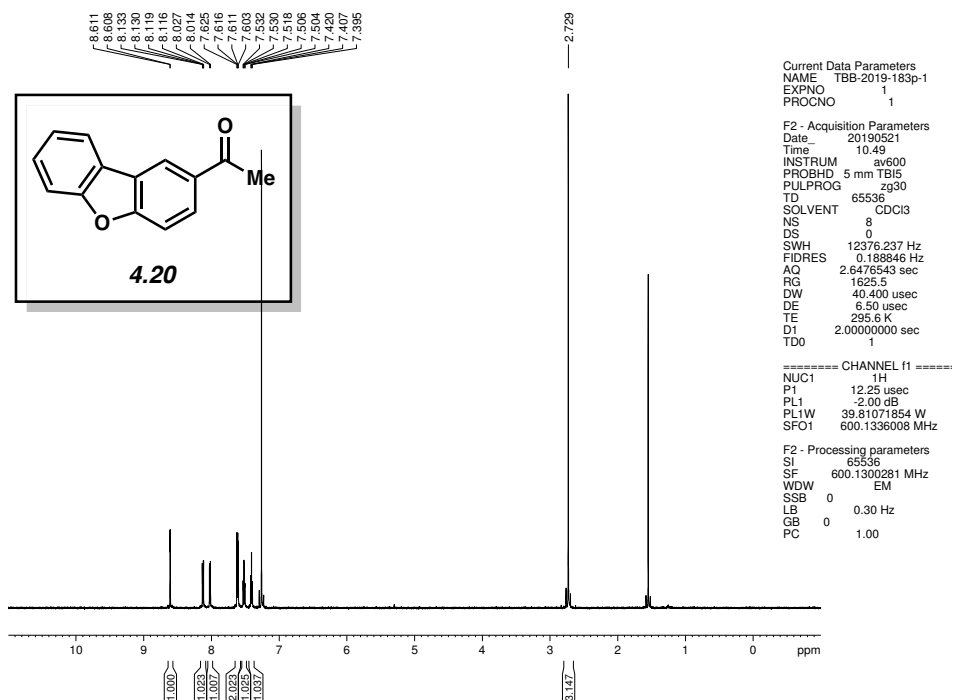
Figure 4.11 ^{1}H NMR (500 MHz, CDCl$_3$) of compound **4.20**.
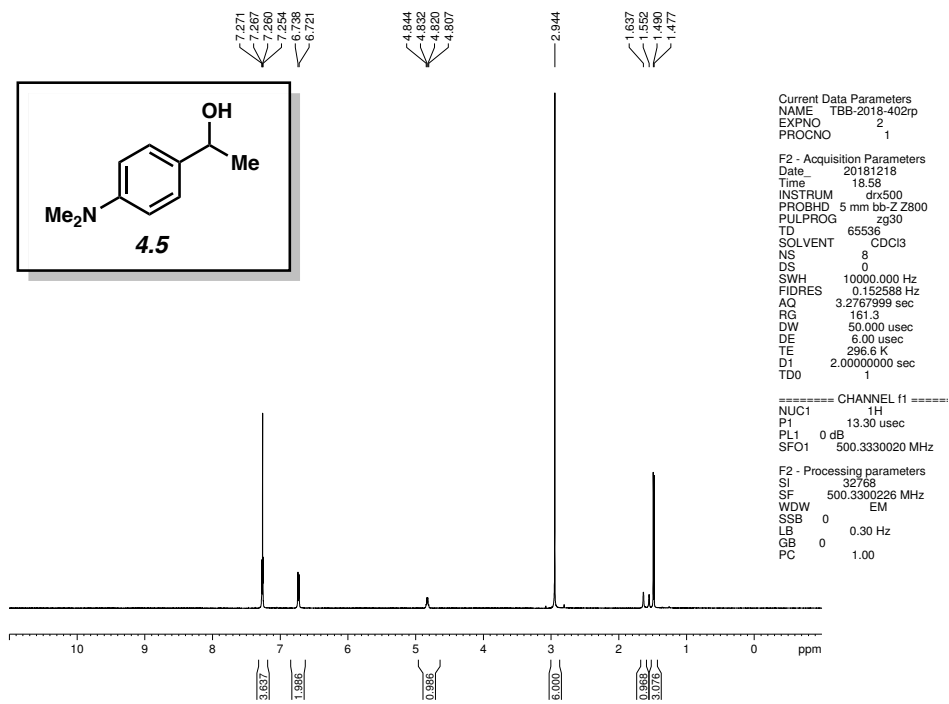
Figure 4.12 ^{1}H NMR (500 MHz, CDCl$_3$) of compound **4.5**.

236
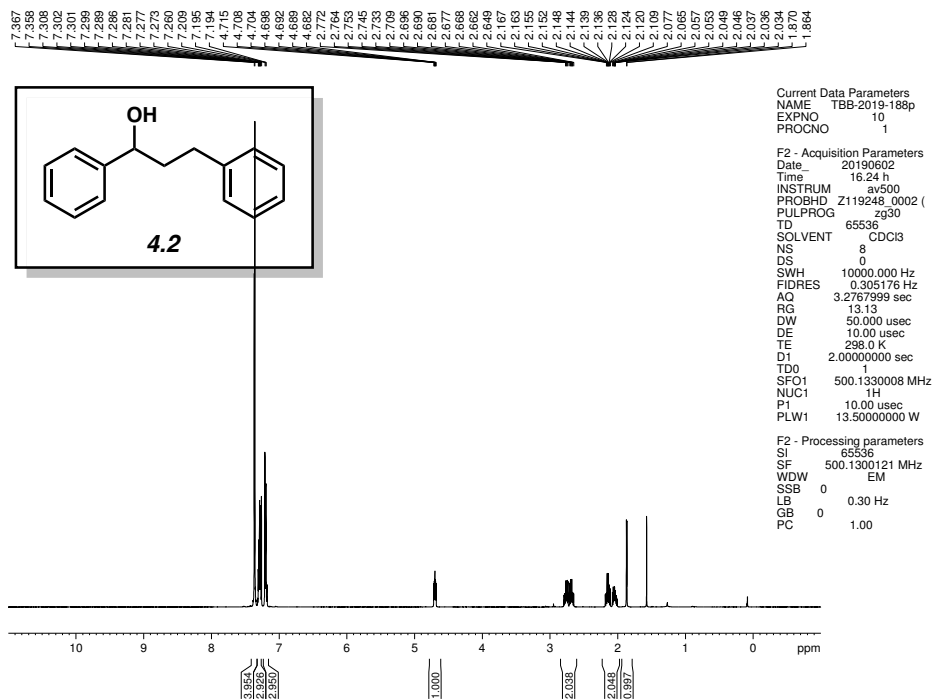
Figure 4.13 ¹H NMR (500 MHz, CDCl₃) of compound **4.2**.
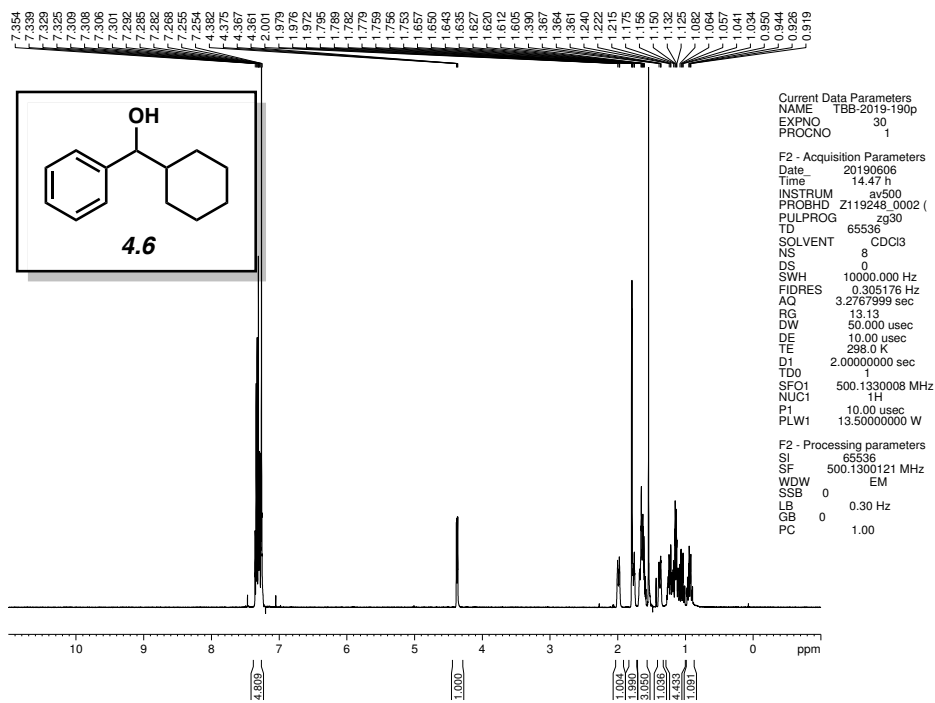
Figure 4.14 ¹H NMR (500 MHz, CDCl₃) of compound **4.6**.
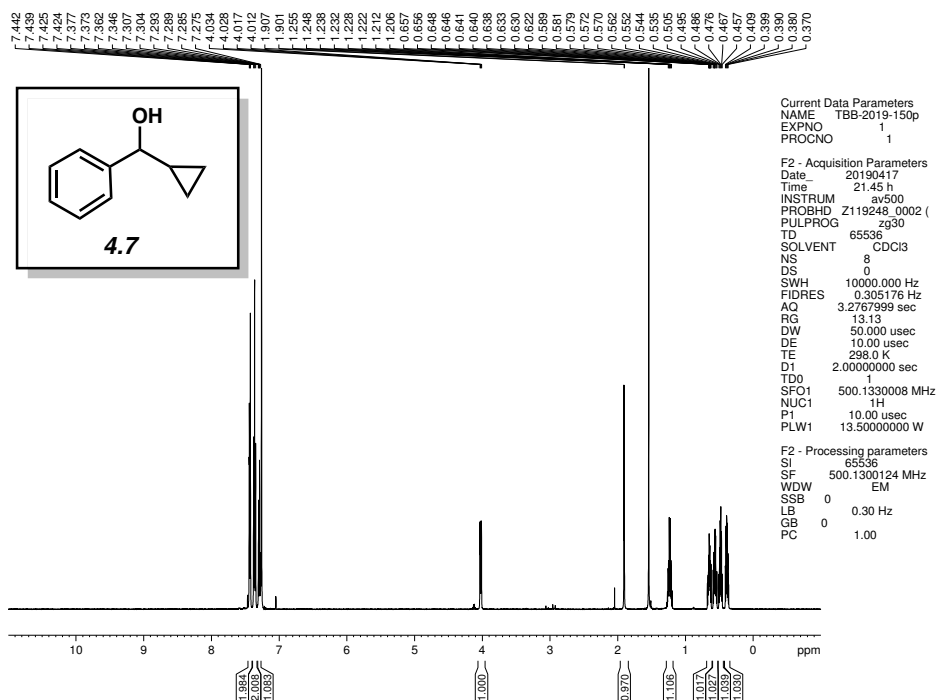
Figure 4.15 ^{1}H NMR (500 MHz, CDCl$_3$) of compound **4.7**.
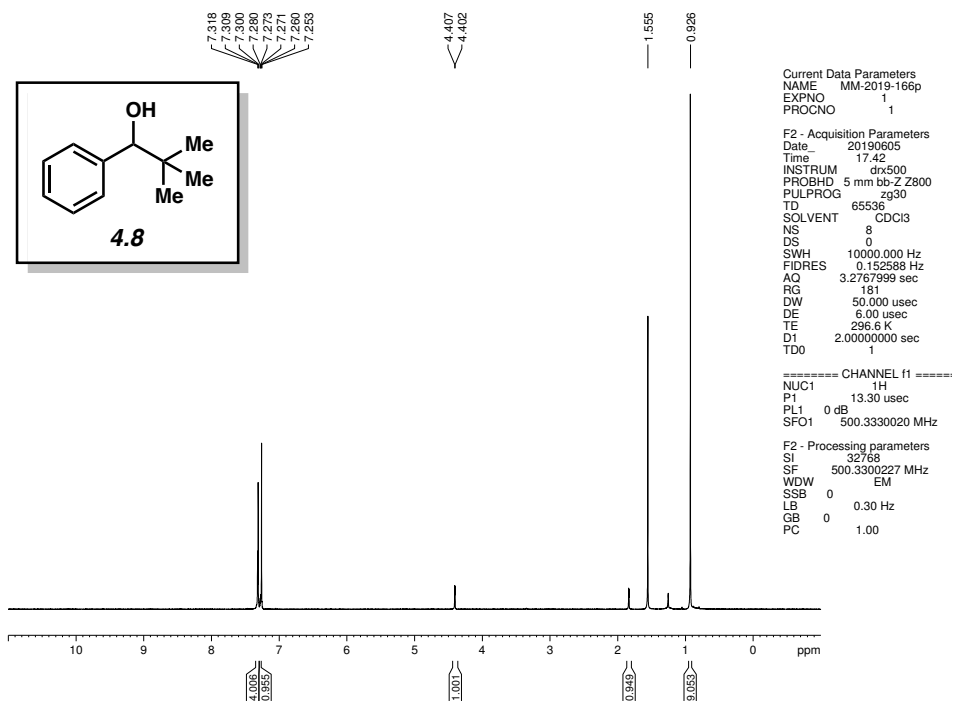
Figure 4.16 ^{1}H NMR (500 MHz, CDCl$_3$) of compound **4.8**.
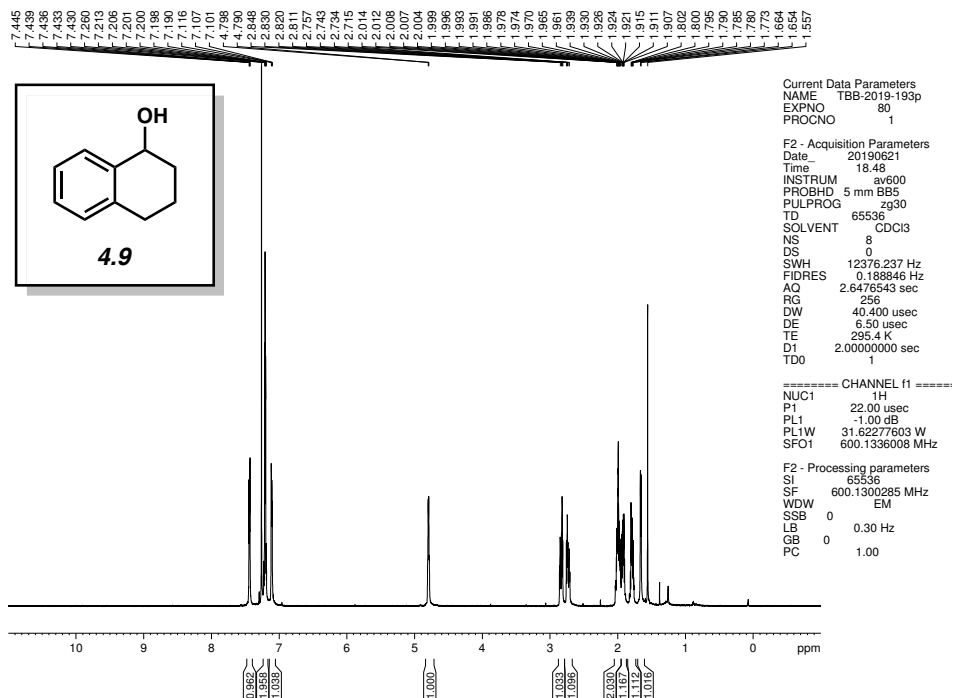
Figure 4.17 ^{1}H NMR (500 MHz, CDCl$_3$) of compound **4.9**.
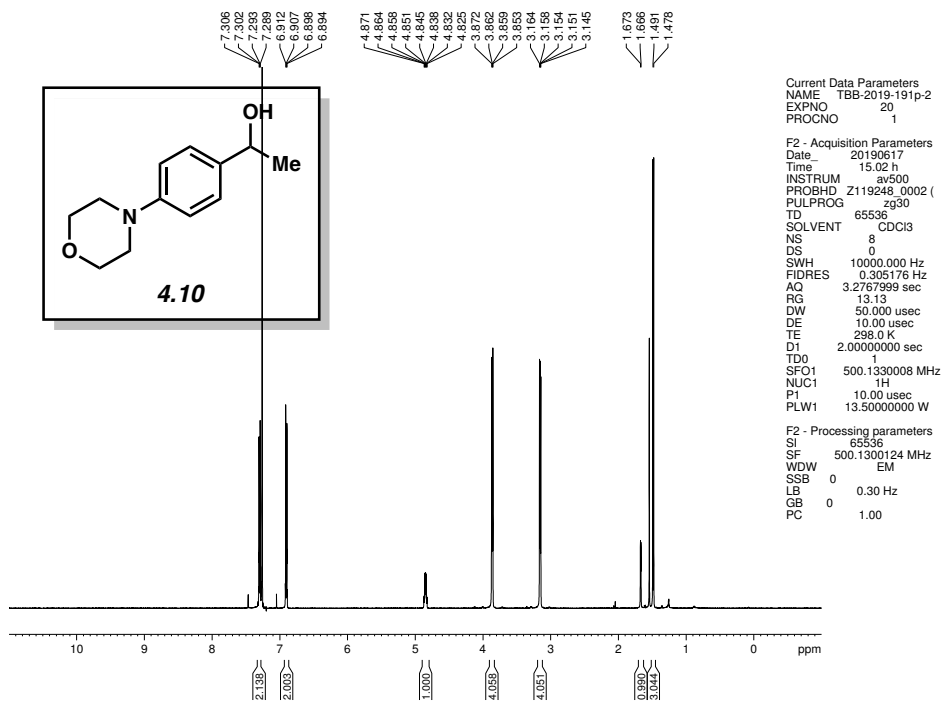
Figure 4.18 ^{1}H NMR (500 MHz, CDCl$_3$) of compound **4.10**.

239
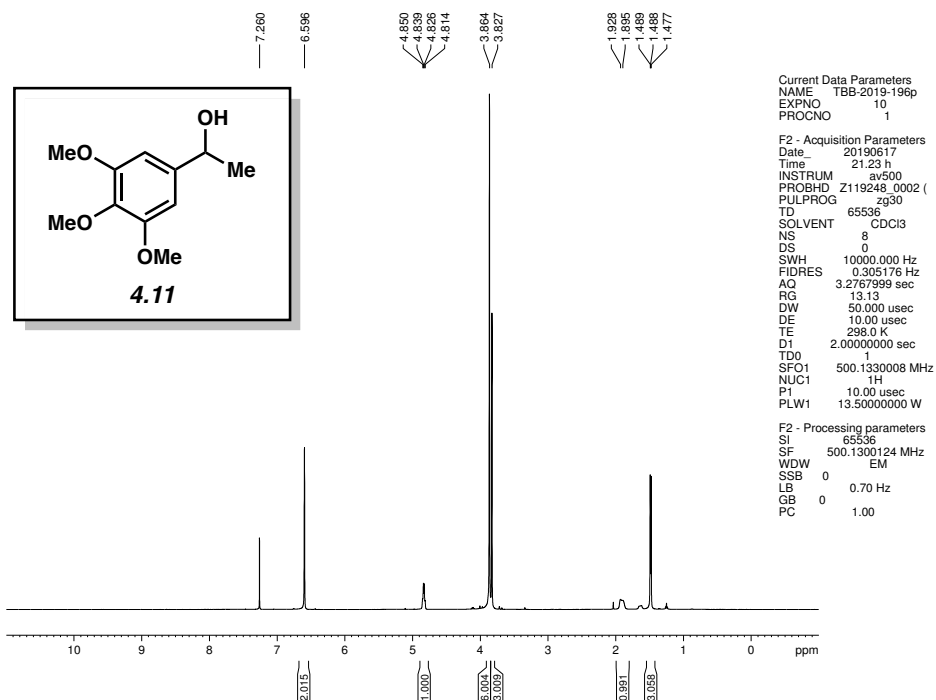
Figure 4.19 ¹H NMR (500 MHz, CDCl₃) of compound **4.11**.
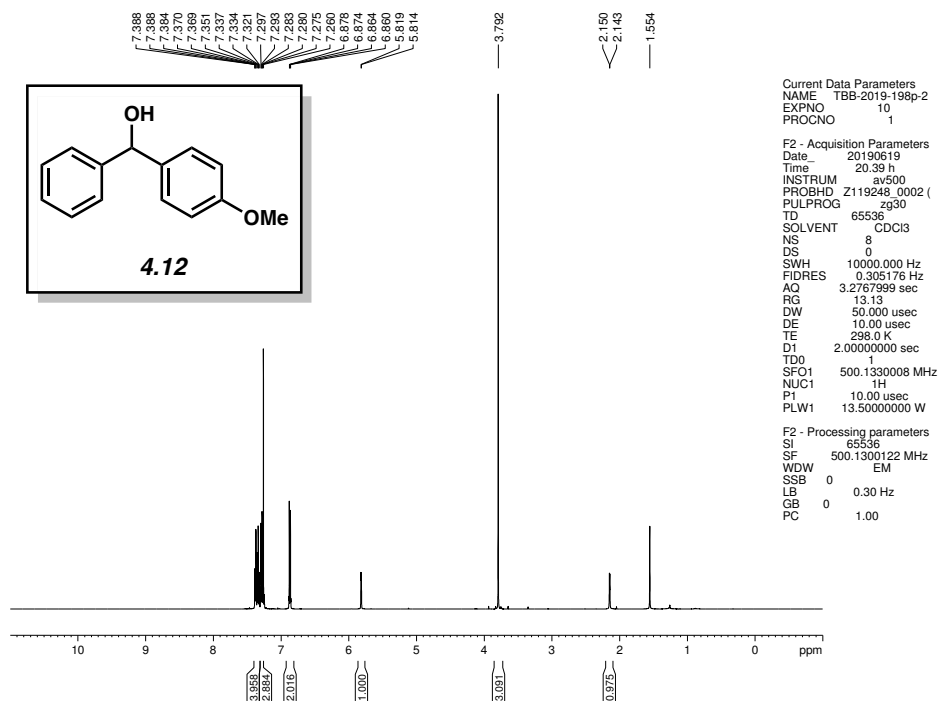
Figure 4.20 ¹H NMR (500 MHz, CDCl₃) of compound **4.12**.
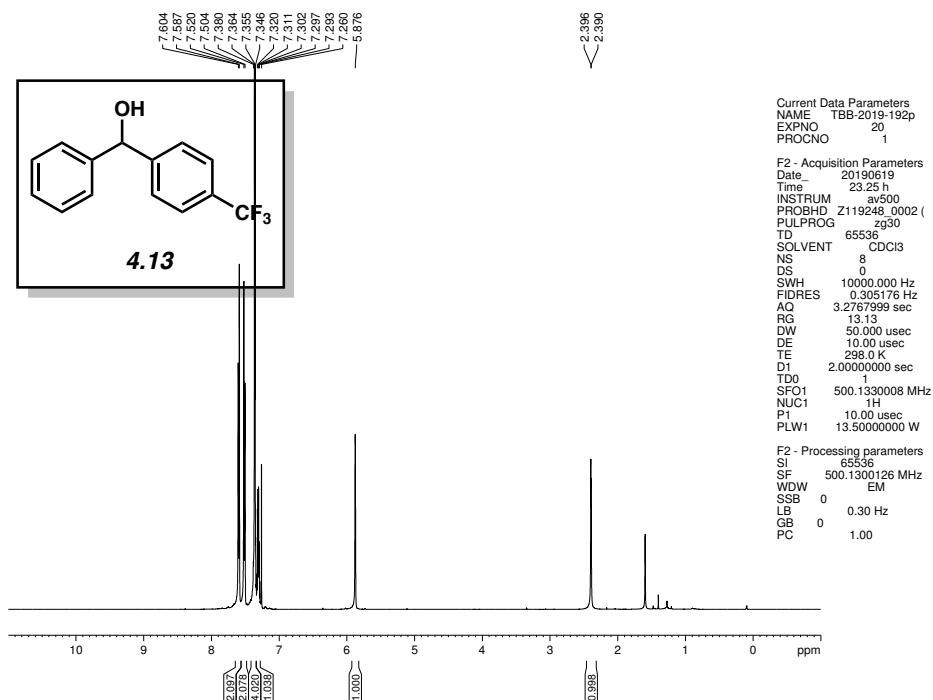
Figure 4.21 ¹H NMR (500 MHz, CDCl₃) of compound **4.13**.
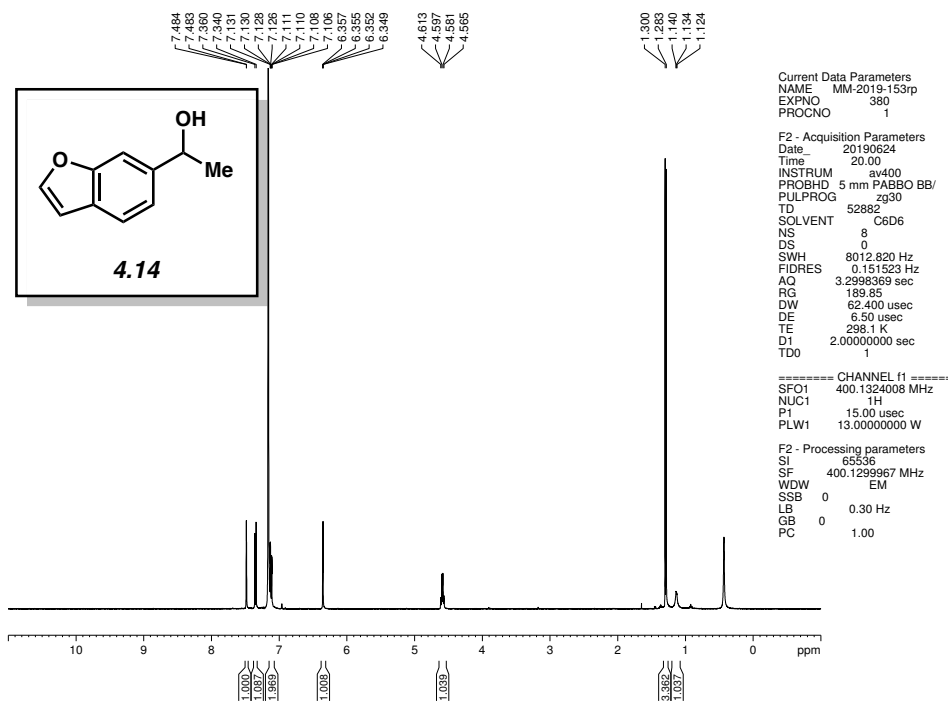
Figure 4.22 ¹H NMR (400 MHz, CDCl₃) of compound **4.14**.

241
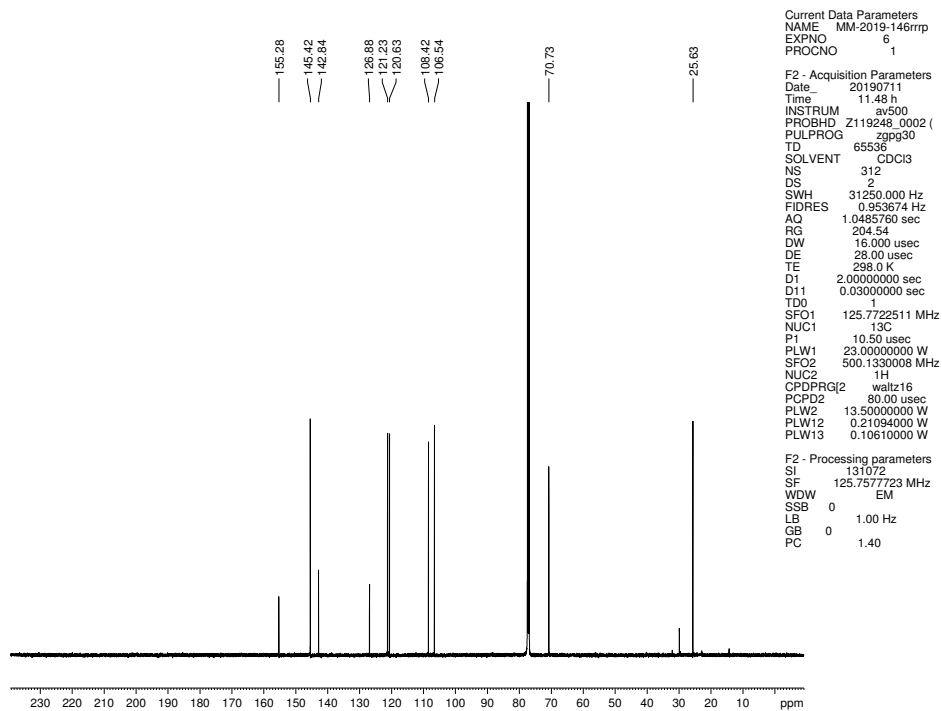
Figure 4.23 ^{13}C NMR (125 MHz, CDCl$_3$) of compound **4.14**.
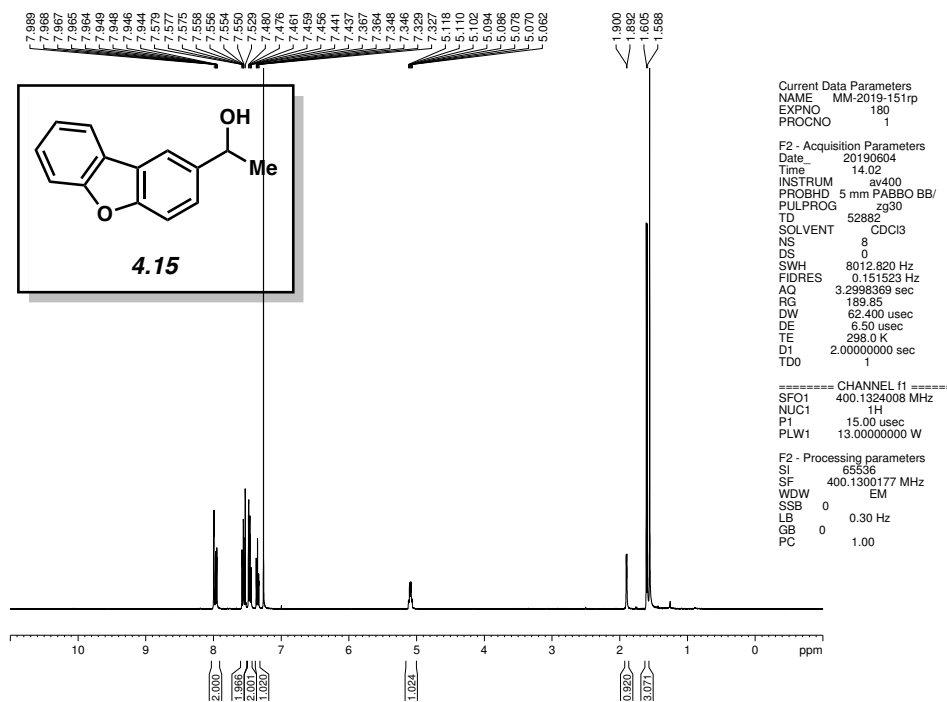
Figure 4.24 ^{1}H NMR (400 MHz, CDCl$_3$) of compound **4.15**.

242
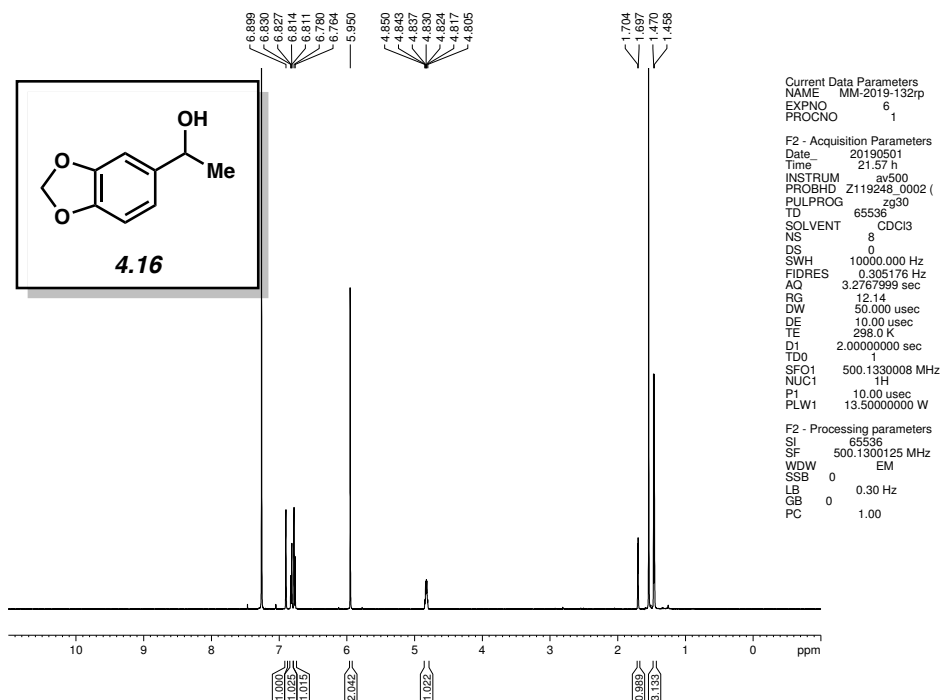
Figure 4.25 ¹H NMR (500 MHz, CDCl₃) of compound **4.16**.
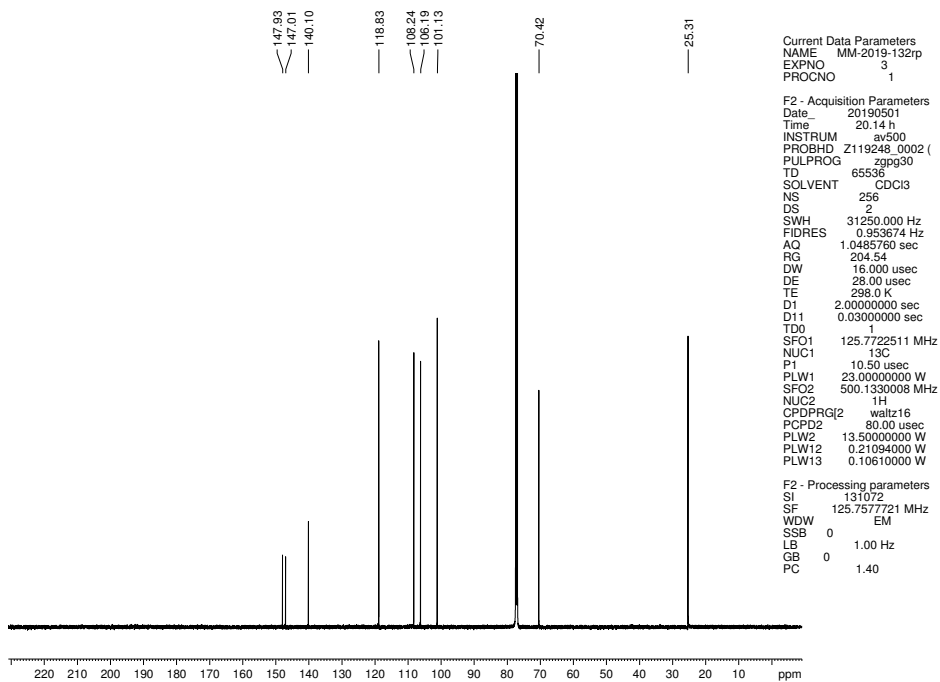
Figure 4.26 ¹³C NMR (125 MHz, CDCl₃) of compound **4.16**.
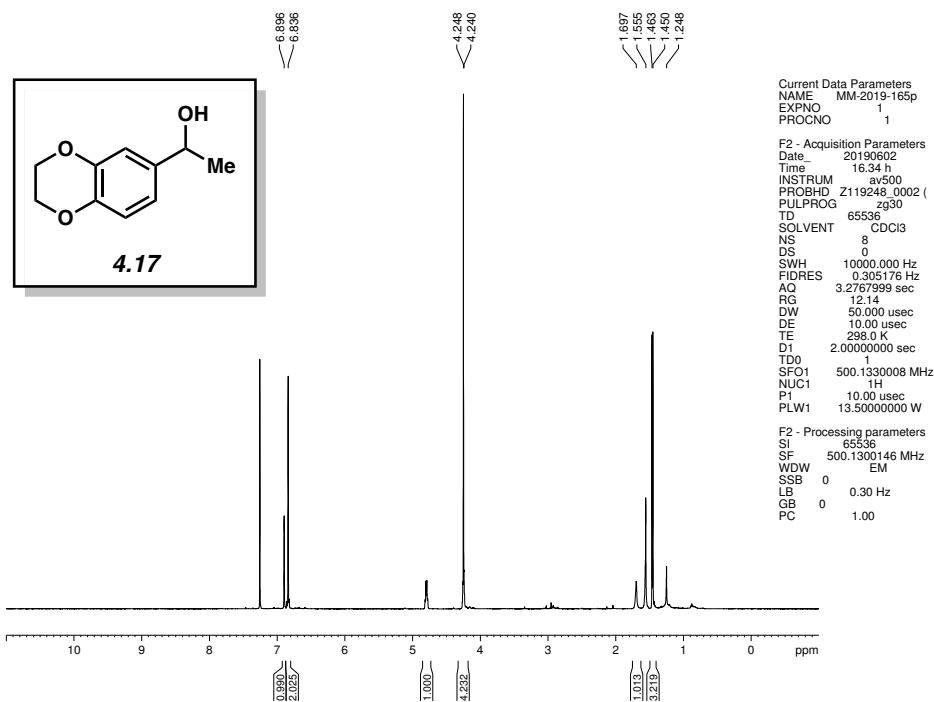
Figure 4.27 ^{1}H NMR (500 MHz, CDCl$_3$) of compound **4.17**.
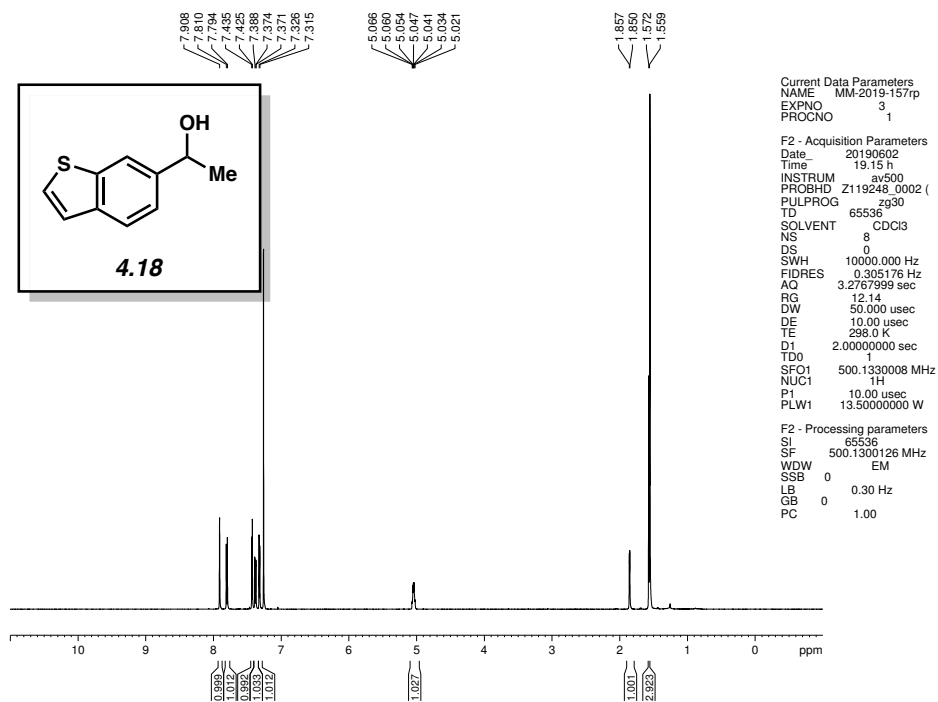
Figure 4.28 ^{1}H NMR (500 MHz, CDCl$_3$) of compound **4.18**.
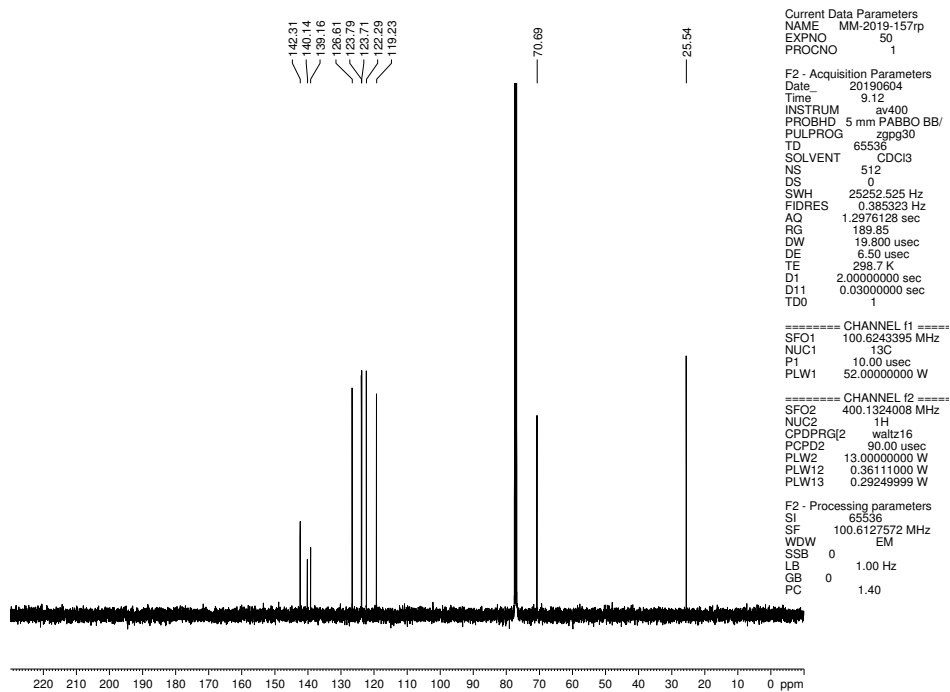
Figure 4.29 ^{13}C NMR (125 MHz, CDCl$_3$) of compound **4.18**.
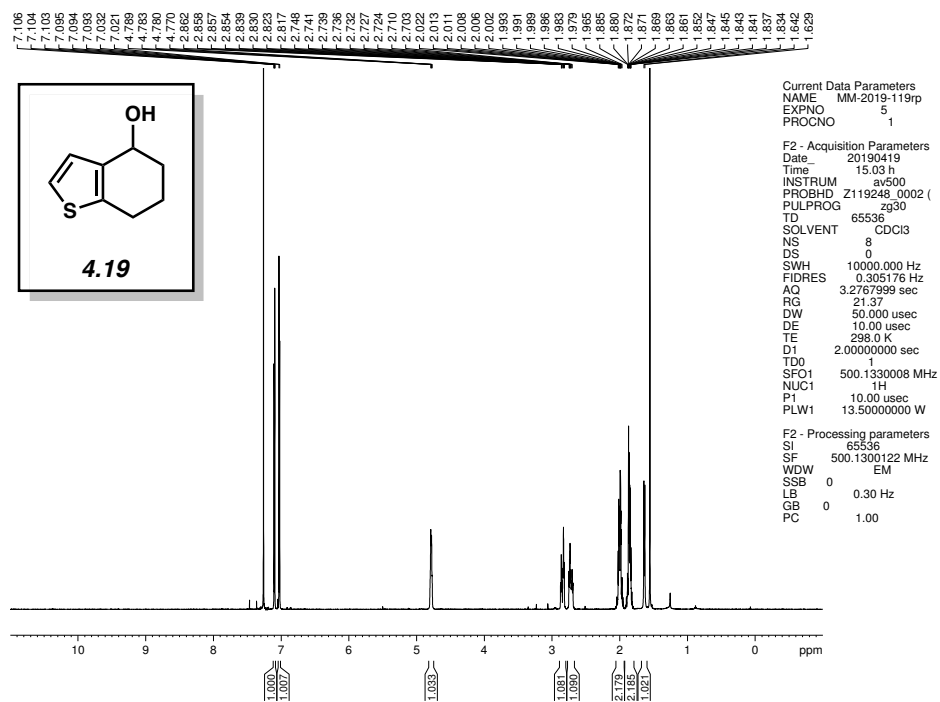
Figure 4.30 ^{1}H NMR (500 MHz, CDCl$_3$) of compound **4.19**.

245

138.95
138.06
126.74
122.90
65.63
32.50
25.16
20.05

Current Data Parameters
NAME   MM-2019-125p
EXPNO   3
PROCNO   1

F2 - Acquisition Parameters
Date_   20190419
Time   12.44 h
INSTRUM   av500
PROBHD Z119248_0002 (
PULPROG   zgpg30
TD   65536
SOLVENT   CDCl3
NS   128
DS   2
SWH   31250.000 Hz
FIDRES   0.953674 Hz
AQ   1.0485760 sec
RG   204.54
DW   16.000 usec
DE   28.00 usec
TE   298.0 K
D1   2.00000000 sec
D11   0.03000000 sec
TD0   1
SFO1   125.7722511 MHz
NUC1   13C
P1   10.50 usec
PLW1   23.00000000 W
SFO2   500.1330008 MHz
NUC2   1H
CPDPRG[2   waltz16
PCPD2   80.00 usec
PLW2   13.50000000 W
PLW12   0.21094000 W
PLW13   0.10610000 W

F2 - Processing parameters
SI   131072
SF   125.7577726 MHz
WDW   EM
SSB   0
LB   1.00 Hz
GB   0
PC   1.40

Figure 4.31 ¹³C NMR (125 MHz, CDCl₃) of compound **4.19**.

4.9 Notes and References

(1) For reviews, see: (a) Johnstone, R. A. W.; Wilby, A. H.; Entwistle, I. D. Heterogeneous Catalytic Transfer Hydrogenation and its Relation to Other Methods for Reduction of Organic Compounds. *Chem. Rev.* **1985**, *85*, 129–170. (b) Cha, J. S. Recent Developments in the Meerwein–Ponndorf–Verley and Related Reactions for the Reduction of Organic Functional Groups using Aluminum, Boron, and Other Metal Reagents: A Review. *Org. Proc. Res. Dev.* **2006**, *10*, 1032–1053. (c) de Graauw, C. F.; Peters, J. A.; van Bekkum, H.; Husken, J. Meerwein–Ponndorf–Verley Reductions and Oppenauer Oxidations: An Integrated Approach. *Synthesis* **1994**, 1007–1017. (d) Inch, T. D. Asymmetric Synthesis. *Synthesis* **1970**, *2*, 466–473. (e) Nishide, K.; Node, M. Recent Development of Asymmetric Syntheses Based on the Meerwein–Ponndorf–Verley Reduction. *Chirality* **2002**, *14*, 759–767. (f) Ooi, T.; Miura, T.; Itagaki, Y.; Ichikawa, H.; Maruoka, K. Catalytic Meerwein–Ponndorf–Verley (MPV) and Oppenauer (OPP) Reactions: Remarkable Acceleration of Hydride Transfer by Powerful Bidentate Aluminum Alkoxides. *Synthesis* **2002**, 279–291. (g) Zassinovich, G.; Mestroni, G. Asymmetric Hydrogen Transfer Reactions Promoted by Homogeneous Transition Metal Catalysts. *Chem. Rev.* **1992**, *92*, 1051–1069. (h) Wilds, A. L. Reduction with Aluminum Alkoxides. *Org. React.* **1944**, *2*, 178–223. (i) Djerassi, C. The Oppenauer oxidation. *Org. React* **1951**, *6*, 207–272.

(2) For seminal publications, see: (a) Meerwein, H.; Schmidt, R. Ein neues Verfahren zur Reduktion von Aldehyden und Ketonen. *Liebigs Ann.* **1925**, *444*, 221–238. (b) Verley, A. The Exchange of Functional Groups Between Two Molecules: The Passage of Ketones to

Alcohols and the Reverse. *Bull. Soc. Chim. Fr.* **1925**, *37*, 871–874. (c) Ponndorf, W. Z. The Reversible Exchange of Oxygen Between Aldehydes or Ketones on the One Hand and Primary or Secondary Alcohols on the Other Hand. *Angew. Chem.,* **1926**, *39*, 138–143.

(3) Woodward, R. B.; Wendler, N. L.; Brutschy, F. J. Quininone. *J. Am. Chem. Soc.* **1945**, *67*, 1425–1429.

(4) (a) Gammill, R. B. The Synthesis and Chemistry of Functionalized Furochromones. 2. The Synthesis, Sommelet-Hauser Rearrangement, and Conversion of 4,9-dimethoxy-7-[(methylthio)methyl]-5H-furo(3,2-g)benzopyran-5-one to Ammiol. *J. Org. Chem.* **1984**, *49*, 5035–5041. (b) Sano, T.; Toda, J.; Maehara, N.; Tsuda, Y. Synthesis of Erythrina and Related Alkaloids. 17. Total Synthesis of *dl*-Coccuvinine and *dl*-Coccolinine. *Can. J. Chem.* **1987**, *65*, 94–98. (c) Evans, D. A.; Reiger, D. L.; Jones, T. K.; Kaldor, S. W. Assignment of Stereochemistry in the Oligomycin/Rutamycin/Cytovaricin Family of Antibiotics. Asymmetric Synthesis of the Rutamycin Spiroketal Synthon. *J. Org. Chem.* **1990***, 55*, 6260–6268. (d) Toyota, M.; Odashima, T.; Wada, T.; Ihara, M. Application of Palladium-Catalyzed Cycloalkenylation Reaction to C_{20} Gibberellin Synthesis: Formal Syntheses of GA_{12}, GA_{111}, and GA_{112}. *J. Am. Chem. Soc.* **2000**, *122*, 9036–9037.

(5) (a) Doering, W. v. E.; Aschner, T. C. Mechanism of the Alkoxide-Catalyzed Carbinol–Carbonyl Equilibrium. *J. Am. Chem. Soc.* **1953***, 75*, 393–397. (b) Moulton, W. N.; Van Atta, R. E.; Ruch, R. R. Mechanism of the Meerwein–Ponndorf–Verley Reduction. *J. Org. Chem.* **1961**, *26*, 290–292. (c) Yager, B. J.; Hancock, C. K. Equilibrium and Kinetic Studies of the Meerwein–Ponndorf–Verley–Oppenauer (MPVO) Reaction. *J. Org. Chem.* **1965**, *30*, 1174–

1179. (d) Screttas, C. G.; Cazianis, C. T. Mechanism of Meerwein–Ponndorf–Verley type reductions. *Tetrahedron* **1978**, *34*, 933–940. (e) Ashby, E. C.; Argyropoulos, J. N. Single Electron Transfer in the Meerwein–Ponndorf–Verley Reduction of Benzophenone by Lithium Alkoxides. *J. Org. Chem.* **1986**, *51*, 3593–3597. (f) Shiner Jr., V. J.; Whittaker, D. Kinetics of the Meerwein–Ponndorf–Verley Reaction. *J. Am. Chem. Soc.* **1969**, *91*, 394–398.

(6) (a) Cohen, R.; Graves, C. R.; Nguyen, S. T.; Martin, J. M. L.; Ratner, M. A. The Mechanism of Aluminum-Catalyzed Meerwein−Schmidt−Ponndorf−Verley Reduction of Carbonyls to Alcohols. *J. Am. Chem. Soc.* **2004**, *126*, 14796–14803. (b) Boronat, M.; Corma, A.; Renz, M. Mechanism of the Meerwein−Ponndorf−Verley−Oppenauer (MPVO) Redox Equilibrium on Sn− and Zr−Beta Zeolite Catalysts. *J. Phys. Chem. B* **2006**, *110*, 21168–21174. (c) Sominsky, L.; Rozental, E.; Gottlieb, H.; Gedanken, A.; Hoz, S. Uncatalyzed Meerwein−Ponndorf−Oppenauer−Verley Reduction of Aldehydes and Ketones Under Supercritical Conditions. *J. Org. Chem.* **2004**, *69*, 1492–1496.

(7) (a) Kow, R.; Nugren, R.; Rathke, M. W. Rate Enhancement of the Meerwein–Ponndorf–Verley–Oppenauer Reaction in the Presence of Proton Acids. *J. Org. Chem.* **1977**, *42*, 826–827. (b) Akamanchi, K. G.; Varalakshmy, N. R. Aluminium Isopropoxide - TFA, a Modified Catalyst for Highly Accelerated Meerwein–Ponndorf–Verley (MPV) Reduction. *Tetrahedron Lett.* **1995**, *36*, 3571–3572. (c) Akamanchi, K. G.; Varalakshmy, N. R. Truly Catalytic Meerwein–Ponndorf–Verley (MPV) Reduction. *Tetrahedron Lett.* **1995**, *36*, 5085–5088.

(8) Barbry, D.; Torchy, S. Accelerated Reduction of Carbonyl Compounds under Microwave Irradiation. *Tetrahedron Lett.* **1997**, *38*, 2959–2960.

(9) (a) Graves, C. R.; Scheidt, K. A.; Nguyen, S. T. Enantioselective MSPV Reduction of Ketimines Using 2-Propanol and (BINOL)Al[III]. *Org. Lett.* **2006**, *8,* 1229–1232. (b) Campbell, E. J.; Zhou, H.; Nguyen, S. T. The Asymmetric Meerwein–Schmidt–Ponndorf–Verley Reduction of Prochiral Ketones with *i*PrOH Catalyzed by Al Catalysts. *Angew. Chem., Int. Ed.,* **2002***, 41,* 1020–1022. (c) McNerney, B.; Whittlesey, B.; Cordes, D. B.; Krempner, C. A Well-Defined Monomeric Aluminum Complex as an Efficient and General Catalyst in the Meerwein-PonndorfVerley Reduction. *Chem. - Eur. J.* **2014**, *20*, 14959−14964.

(10) (a) Midland, M. M.; Tramontano, A. B-Alkyl-9-borabicyclo[3.3.1]nonanes as Mild, Chemoselective Reducing Agents for Aldehydes. *J. Org. Chem*. **1978**, *43*, 1470–1471. (b) Chandrasekharan, J.; Ramachandran, P. V.; Brown, H. C. Diisopinocampheylchloroborane, a Remarkably Efficient Chiral Reducing Agent for Aromatic Prochiral Ketones. *J. Org. Chem.* **1985**, *50*, 5446–5448.

(11) Krohn, K.; Knauer, B. The Diastereoselectivity of Zirconium Alkoxide Catalysed Meerwein–Ponndorf–Verley Reductions. *Liebigs Ann.* **1995**, 1347–1351.

(12) (a) Kagan, H. B.; Namy, J. L. Lanthanides in Organic Synthesis. *Tetrahedron* **1986**, *42*, 6573–6614. (b) Namy, J. L.; Souppe, J.; Collin, J.; Kagan H. B. New Preparations of Lanthanide Alkoxides and their Catalytical Activity in Meerwein–Ponndorf–Verley–Oppenauer Reactions. *J. Org. Chem.* **1984**, *49*, 2045–2049. (c) Okano, T.; Matsuoka, M.; Konishi, H.;

Kiji, J. Meerwein–Ponndorf–Verley Reduction of Ketones and Aldehydes Catalyzed by Lanthanide Tri-2-propoxides. *Chem. Lett.* **1987**, 181–184. (d) Evans, D. A.; Nelson, S. G.; Gagné, M. R.; Muci, A. R. A Chiral Samarium-Based Catalyst for the Asymmetric Meerwein–Ponndorf–Verley Reduction. *J. Am. Chem. Soc.* **1993**, *115*, 9800–9801. (e) Molander G. A.; McKie, J. A. Samarium(II) Iodide Induced Sequential Intramolecular Nucleophilic Acyl Substitution and Stereospecific Intramolecular Meerwein–Ponndorf–Verley Reduction/Oppenauer Oxidation. *J. Am. Chem. Soc.* **1993**, *115*, 5821–5822. (f) Hu, X.; Kellogg, R. M. Asymmetric Reduction and Meerwein–Ponndorf–Verley Reaction of Prochiral Aromatic Ketones in the Presence of Optically Pure 1-aryl-2, 2-dimethylpropane-1, 3-diols. *Recl. Trav. Chim. Pays-Bas.* **1996**, *115*, 410–417.

(13) (a) Ouali, A.; Majoral, J.-P.; Caminade, A.-M.; Taillefer, M. NaOH-promoted Hydrogen Transfer: Does NaOH or Traces of Transition Metals Catalyze the Reaction?. *ChemCatChem* **2009**, *1*, 504–509. (b) Polshettiwar, V.; Varma, R. S. Revisiting the Meerwein–Ponndorf–Verley Reduction: A Sustainable Protocol for Transfer Hydrogenation of Aldehydes and Ketones. *Green Chem.* **2009**, *11*, 1313–1316. (c) Radhakrishan, R.; Do, D. M.; Jaenicke, S.; Sasson, Y.; Chuah, G.-K. Potassium Phosphate as a Solid Base Catalyst for the Catalytic Transfer Hydrogenation of Aldehydes and Ketones. *ACS Catal.* **2011**, *1*, 1631–1636.

(14) Mojtahedi, M. M.; Zkbarzadeh, E.; Sharifi, R.; Abaee, M. S. Lithium Bromide as a Flexible, Mild, and Recyclable Reagent for Solvent-Free Cannizzaro, Tishchenko, and Meerwein−Ponndorf−Verley Reactions. *Org. Lett.* **2007**, *9*, 2791–2793.

(15) Under the conditions reported by Chuah and coworkers (ref. 12c), only cyclohexanone, 4-*tert*-butyl cyclohexanone, and acetophenone were evaluated for reactivity using K_3PO_4/*i*-PrOH affording the respective alcohol products in 55%, 30%, and 38% yield.

(16) Subjecting dihydrochalcone (**4.1**) to previously reported conditions for the reduction of ketones using catalytic K_3PO_4 using *i*-PrOH as a solvent gave the desired product **4.2** in only 47% yield.

(17) Although 1,4-dioxane was chosen for these studies, we found other solvents could be employed (see section 4.7.2 for details).

(18) K_3PO_4 is roughly 10^3 less basic than NaOH and KOH. For the pKa of KH_2PO_4 and H_2O respectively, see: (a) Bruice, P. Y. *Organic Chemistry*. 6th ed. Boston: Prentice Hall, 2011. (b) Bordwell, F. G. Equilibrium Acidities in Dimethylsulfoxide Solution. *Acc. Chem. Res.* **1988**, *21*, 456–463.

(19) Using DFT calculations (M06-2X/6-31G(d)), we estimate that the conversion of **4.1** and **4.5** to **4.2** and reduced **4.5** is thermodynamically favorable by ~2 kcal/mol.

(20) Previous reports on the base-mediated MPV reductions of ketones using NaOH and KOH have shown only a handful of heterocyclic substrates undergoing reduction (see refs. 12a and 12b). The base-mediated MPV reduction of heterocyclic ketones using K_3PO_4 has not been previously reported.

(21) Subjecting *N*-containing heterocyclic ketones such as *N*-MOM 4-acetyl indole and 4-acetyl pyridine to base-mediated MPV reduction conditions led to lower yields of the products (20% and 11% yield, respectively).

(22) Dibenzofurans have found application in OLED's, bioactive molecules, and chemical probes: (a) Kim, S.-Y.; Hwang, S.-H.; Kim, Y.-K.; Jung, H.-J.; Lim, J.-O.; Han, S.-H.; Jeong, E.-J.; Park, J.-H.; Lee, E.-Y.; Lee, B.-R.; Lee, J.-H. Condensed-Cyclic Compound and Organic Light-Emitting Device. U.S. Patent 20180248127, Jul. 25, 2012. (b) Patpi, S. R.; Pulipati, L.; Yogeeswari, P.; Sriram, D.; Jain, N.; Sridhar, B.; Murthy, R.; Devi, T. A.; Kalivendi, S., V.; Kantevari, S. Design, Synthesis, and Structure–Activity Correlations of Novel Dibenzo[b,d]furan, dibenzo[b,d]thiophene, and *N*-Methylcarbazole Clubbed 1,2,3-triazoles as Potent Inhibitors of *Mycobacterium tuberculosis. J. Med. Chem.* **2012**, *55*, 3911–3922. (c) Liu, L.-X., Wang, X.-Q.; Yan, J.-M.; Li, Y.; Sun, C.-J.; Chen, W.; Zhou, H.-B.; Yang, X.-D. Synthesis and Antitumor Activities of Novel Dibenzo[b,d]furan–imidazole Hybrid Compounds. *Eur. J. Med. Chem.* **2013**, *66*, 423–437. (d) Lusic, H.; Uprety, R.; Deiter, A. Improved Synthesis of the Two-photon Caging Group 3-nitro-2-ethyldibenzofuran and its Application to a Caged Thymidine Phosphoramidite. *Org. Lett.* **2010**, *12*, 916–919.

(23) For select examples of intermolecular asymmetric MPV reductions of ketones, see: (a) Doering, W. E.; Young, R. W. Partially asymmetric Meerwein–Ponndorf–Verley reductions. *J. Am. Chem. Soc.* **1950**, *72*, 631. (b) Nandi, P.; Solovyov, A.; Okrut, A.; Katz, A. Al[III]–calix[4]arene Catalysts for Asymmetric Meerwein–Ponndorf–Verley Reduction. *ACS Catal.* **2014**, *4*, 2492–2495. (c) Wu, W.; Zou, S.; Lin, L.; Ji, J.; Zhang, Y.; Ma, B.; Liu, X.; Feng, X. Catalytic Asymmetric Meerwein–Ponndorf–Verley Reduction of Glyoxylates Induced by a Chiral N,N′-dioxide/Y(OTf)$_3$ Complex. *Chem. Commun.* **2017**, *53*, 3232–3235. (d) Ooi, T.; Miura, T.; Maruoka, K. Highly Efficient, Catalytic Meerwein–Ponndorf–Verley

Reduction with a Novel Bidentate Aluminum Catalyst. *Angew. Chem., Int. Ed.* **1998**, *37*, 2347–2349.

(24) Mori, A.; Miyakawa, Y.; Ohashi, E.; Haga, T.; Maegawa, T.; Sajiki, H. Pd/C-Catalyzed Chemoselective Hydrogenation in the Presence of Diphenylsulfide. *Org. Lett.* **2006**, *8*, 3279–3281.

(25) Ramgren, S. D.; Garg, N. K. Pd-Catalyzed Acetylation of Arenes. *Org. Lett.* **2014**, *16*, 824–827.

(26) Xiao, B.; Gong, T.-J.; Liu, Z.-J.; Liu, J.-H.; Luo, D.-F.; Xu, J.; Liu, L. Synthesis of Dibenzofurans via Palladium-Catalyzed Phenol-Directed C–H Activation/C–O Cyclization. *J. Am. Chem. Soc.* **2011**, *133*, 9250–9253.

(27) Guyon, C.; Baron, M.; Lemaire, M.; Popowycz, F.; Métay, E. Commutative Reduction of Aromatic Ketones to Arylmethylenes/Alcohols by Hypophosphites Catalyzed by Pd/C Under Biphasic Conditions. *Tetrahedron* **2014**, *70*, 2088–2095.

(28) Xu, J.; Wei, T.; Zhang, Q. Influences of Electronic Effects and Anions on the Enantioselectivity in the Oxazaborolidine-Catalyzed Asymmetric Borane Reduction of Ketones. *J. Org. Chem.* **2004**, *69*, 6860–6886.

(29) Genç, S.; Arslan, B.; Gülcemal, S.; Günnaz, S.; Çetinkaya, B.; Gülcemal, D. Iridium(I)-Catalyzed C–C and C–N Bond Formation Reactions via the Borrowing Hydrogen Strategy. *J. Org. Chem.* **2019**, *84*, 6286–6297.

(30) Gaykar, R, N.; Bhunia, A.; Biju, A. T. Employing Arynes for the Generation of Aryl Anion Equivalents and Subsequent Reaction with Aldehydes. *J. Org. Chem.* **2018**, *83*, 11333–11340.

(31) Zeng, H.; Wu, J.; Li, S.; Hui, C.; Ta, A.; Cheng, S.-Y.; Zheng, S.; Shang, G. Copper(II)-catalyzed Selective Hydroboration of Ketones and Aldehydes. *Org. Lett.* **2019**, *21*, 401–406.

(32) Rahaim Jr., R. J.; Maleczka Jr., R. E. C–O Hydrogenolysis Catalyzed by Pd-PMHS Nanoparticles in the company of Chloroarenes. *Org. Lett.* **2011**, *13*, 584–587.

(33) Puls, F.; Knölker, H.-J. Conversion of Olefins into Ketones by an Iron-catalyzed Wacker-type Oxidation using Oxygen as the Sole Oxidant. *Angew. Chem., Int. Ed.* **2018**, *57*, 1222–1226.

(34) Wang, S.; Huang, H.; Tsareva, S.; Bruneau, C.; Fischmeister, C. Silver-catalyzed Hydrogenation of Ketones under Mild Conditions. *Adv. Synth. Catal.* **2019**, *361*, 786–790.

(35) Patpi, S. R.; Pulipati, L.; Yogeeswari, P.; Sriram, D.; Jain, N.; Sridhari, B.; Murthy, R.; Devi T., A.; Kalivendi, S. V.; Kantevar, S. Design, Synthesis, and Structure–Activity correlations of Novel Dibenzo[b,d]furan, Dibenzo[b,d]thiophene, and N-Methylcarbazole Clubbed 1,2,3-Triazoles as Potent Inhibitors of Mycobacterium Tuberculosis. *J. Med. Chem.* **2012**, *55*, 3911–3922.

(36) Moine, E.; Dimier-Poisson, I.; Enguihard-Gueiffier, C.; Logé, C.; Pénichon, M.; Moiré, N.; Delebouzé, C.; Foll-Josselin, B.; Ruchaud, S.; Bach, S.; Gueiffier, A.; Debierre-Grockiego, F.; Denevault-Sabourin, C. Development of New Highly Potent Imidazo[1,2-b]pyridazines Targeting Toxoplasma Gondii Calcium-Dependent Protein Kinase 1. *Eur. J. Med. Chem.* **2015**, *105*, 80–105.

(37) Stepanenko, V.; De Jesús, M.; Correa, W.; Guzmán, I.; Vázquez, C.; de la Cruz, W.; Ortiz-Marciales, M.; Barnes, C. L. Enantioselective Reduction of Prochiral Ketones Using Spiroborate Esters as Catalysts. *Tetrahedron Lett.* **2007**, *48*, 5799–5802.

CHAPTER FIVE

Reductive Arylation of Amides via a Nickel-Catalyzed Suzuki–Miyaura Coupling and Transfer Hydrogenation Cascade

Timothy B. Boit,[†] Milauni M. Mehta,[†] Junyong Kim, Emma L. Baker and Neil K. Garg.

5.1 Abstract

We report a means to achieve the addition of two disparate nucleophiles to the amide carbonyl carbon in a single operational step. Our method takes advantage of non-precious-metal catalysis and allows for the facile conversion of amides to chiral alcohols via a one-pot Suzuki–Miyaura cross-coupling / transfer hydrogenation process. This study is anticipated to promote the development of new transformations that allow for the conversion of carboxylic acid derivatives to functional groups bearing stereogenic centers via cascade processes.

5.2 Introduction

The synthetic manipulation of carboxylic acid derivatives has become central to organic chemistry after more than a century of methodological development.[1] Though the field has a rich history, strategies for nucleophilic addition to carboxylic acid derivatives may be largely characterized by two primary mechanisms (Figure 5.1a). The first involves an addition-elimination sequence to produce carbonyl derivatives via a tetrahedral intermediate.[2] Notably, this traditional strategy has limitations in the context of organometallic nucleophiles, as the ketone products resulting from initial acyl substitution are susceptible to further nucleophilic attack to give achiral

alcohol products. Specialized acyl derivatives such as *N*-methyl-*N*-methoxy amides, or "Weinreb amides," are often required to avoid such undesired reactivity and necessitate two-step protocols.[2,3] A complementary approach employs transition metal catalysis,[4] where mild substrate activation affords an acyl-metal intermediate and allows for cross-coupling with a variety of nucleophiles.[4a,5] This alternative pathway differentiates the reactivity of the substrate from the product carbonyl to overcome the selectivity challenges mentioned above. An exciting opportunity offered by the latter strategy is the addition of a second, *different* nucleophile to the intermediate resulting from the initial cross-coupling reaction to generate chiral products. Cascade reactions of this type would provide efficient access to important chiral products in racemic or enantioenriched form from achiral starting materials.[6]

Despite the widely recognized importance of cross-couplings, methods to leverage this platform for the addition of disparate nucleophiles to carboxylic acid derivatives remain underexplored.[7] We envisioned that amides could provide a viable entry to address this challenge, given their recent popularization as cross-coupling handles.[4j–o,8,9] Amides have been shown to undergo a variety of couplings through the intermediacy of acyl-metal species using either non-precious or precious metal catalysis (e.g., Ni or Pd). Additionally, we viewed them as ideal substrates for one-pot cascade reactions, as their stability under non-metal catalyzed conditions could allow for the orchestration of orthogonal bond-forming events.[10] Dixon has reported an elegant intramolecular reductive cyclization of a tertiary lactam substrate mediated by Vaska's Ir complex,[11] however, no examples exist for the intermolecular addition of two distinct nucleophiles to amides using catalysis in a single operation.[12,13] Indeed, a reductive alkylation of aryl pyridyl esters reported by Chen and coworkers in 2019 represents the only known example of a carboxylic acid derivative undergoing direct catalytic addition of two nucleophiles through a cross-coupling

approach (Figure 5.1b).[14] Though mechanistically distinct and not involving acyl metal species, two additional relevant methodologies should be highlighted. Buchwald and coworkers have reported a copper-catalyzed reductive alkylation of symmetric anhydrides to afford enantioenriched secondary alcohols,[15] and more recently the Hoveyda group reported a copper-catalyzed asymmetric reductive allylation of nitriles to access enantioenriched homoallylic amines (Figure 5.1b).[16] Together, these examples illustrate some of the potential advantages of cascade reactions that add disparate nucleophiles to a single reactive center of an achiral substrate and uncover synergistic reactivity beyond the capabilities of one reaction manifold.[17]
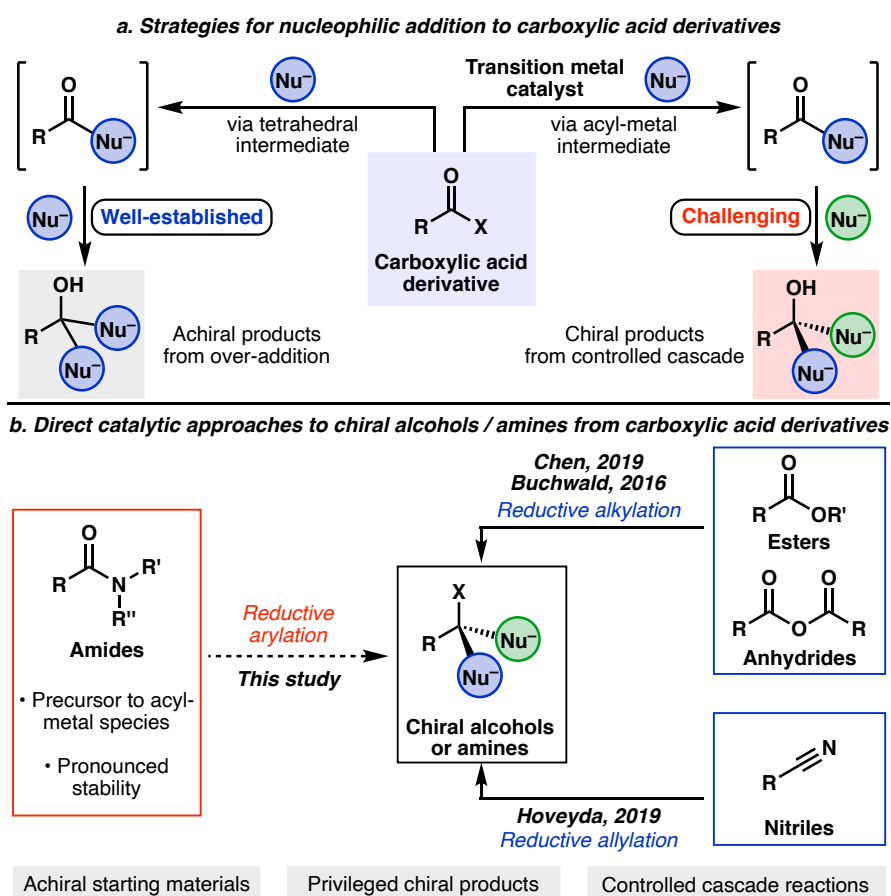
Figure 5.1. (a) Common reaction pathways for nucleophilic additions to carboxylic acid derivatives. (b) Direct catalytic approaches to chiral amines or alcohols from carboxylic acid derivatives.

In this manuscript, we describe a synthetic method for achieving the addition of two different nucleophiles to a carboxylic acid derivative using nickel catalysis.[18] The overall transformation relies on a Suzuki–Miyaura cross-coupling / transfer hydrogenation cascade reaction of amide starting materials to form a C–C and C–H bond,[19,20] consecutively, and ultimately furnish alcohol products (Figure 5.2).[21] The results presented herein not only reinforce the notion that amides are versatile building blocks for transition-metal catalyzed reactions, but also validate their utility as synthons for directly generating sp^3 carbon centers from the amide carbonyl.
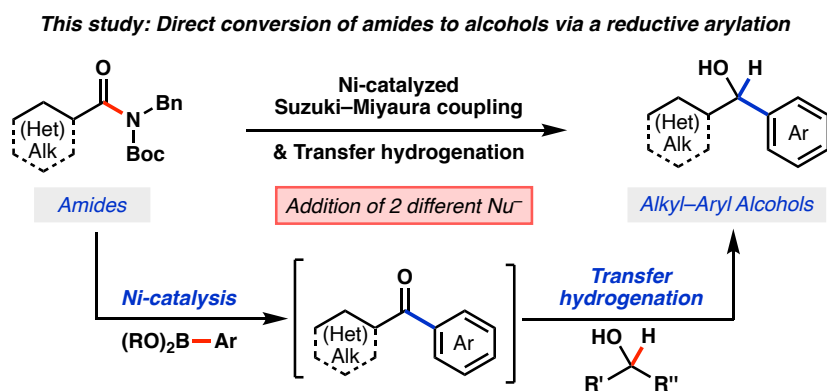
Figure 5.2. Overview of current study involving the conversion of aliphatic amides to alkyl–aryl alcohols via a Suzuki–Miyaura coupling / transfer hydrogenation cascade.

5.3 Reaction Discovery and Optimization

We initiated our study by examining the Ni-catalyzed Suzuki–Miyaura coupling and in situ reduction of dihydrocinnamic acid-derived amide **5.1** as shown in Figure 5.3.[19b] In the absence of a reducing agent, the Suzuki–Miyaura coupling with boronate **5.5** delivered ketone **5.3** in nearly quantitative yield (entry 1).[22,23,24] With the aim of developing the reductive variant, we questioned whether the use of a secondary alcohol reductant could effect the in situ transfer hydrogenation of ketone **5.3** to deliver alcohol **5.4**. In this regard, we attempted the use of *i*-PrOH as solvent, reminiscent of common Meerwein–Ponndorf–Verley (MPV) reduction conditions.[25,26]

Unfortunately, this change resulted in low yields of **5.4** (entries 2 and 3).[27] By shifting to the use of *i*-PrOH as an additive while using toluene as solvent, we obtained the desired product **5.4** in a slightly improved yield of 32%, with 18% of ketone **5.3** remaining (entry 4). Given our lab's recent success in using 1-4-(dimethylamino)phenyl)-1-ethanol (DMPE, **5.7**) in base-catalyzed MPV reductions,[28] we also tested this benzylic alcohol in our system.[29] By simply replacing *i*-PrOH with **5.7**, alcohol **5.4** was obtained in 51% yield (entry 5). Finally, switching the solvent to 1,4-dioxane (entry 6) and using boronate **5.6** in place of boronate **5.5** (entry 7) led to further improvements, delivering alcohol **5.4** in 82% yield.[30,31,32]

It is worth noting that these optimized conditions satisfy a challenging balance of reactivity required for the success of the amide to alcohol conversion. Specifically, reducing agent **5.7** does not significantly impede the nickel-catalyzed cross-coupling step, yet is reactive enough to efficiently reduce ketone **5.3**. Furthermore, as will be shown, other carbonyl functional groups are tolerated by the methodology's mild reducing conditions.

Figure 5.3. Evaluation of reaction conditions for the nickel-catalyzed Suzuki–Miyaura coupling / transfer hydrogenation cascade of amide **5.1** with phenyl boronates and reductants. Standard conditions unless otherwise noted: amide substrate (0.20 mmol, 1.0 equiv); phenyl boronate (0.50–0.80 mmol, 2.5–4.0 equiv); reductant (0.50 equiv, 2.5 equiv); K$_3$PO$_4$ (0.80 mmol, 4.0 equiv); H$_2$O (0.40 mmol, 2.0 equiv); Ni(cod)$_2$ (0.010–0.020 mmol, 5–10 mol%); **5.2** (0.020–0.040 mmol, 10–20 mol%); solvent (1.0 M); 120 °C; 16 h in a sealed vial. [a]Yield determined by ^{1}H NMR analysis using 1,3,5-trimethoxybenzene as an external standard.

5.4 Scope of the Aliphatic Amide Substrate and Robustness Screen

With optimized conditions in hand, we evaluated the scope of the reaction with respect to the aliphatic amide[33] coupling partner using phenyl boronate **5.6**, which afforded a range of alkyl–aryl alcohol products (Figure 5.4). Beginning with the parent dihydrocinnamic acid-derived amide substrate used in optimization studies (i.e., **5.1**), the reductive arylation furnished alcohol **5.4** in 76% isolated yield. Additionally, the use of an unbranched amide derived from decanoic acid provided alcohol **5.8** in 82% yield. Carrying out the reaction at 130 °C allowed for the reductive

arylation of sterically encumbered substrates, as demonstrated by the formation of alcohol **5.9** in 61% yield. The compatibility of carbocyclic amides with boronate **5.6** was explored as well and gave alcohols **5.10**–**5.14** in good yields. We also evaluated an amide substrate bearing an epimerizable stereocenter α to the amide carbonyl. As shown by the formation of alcohol **5.15** from the corresponding *trans* amide substrate, minimal erosion of stereochemistry was observed.[34] Of note, the ester moiety was not disturbed, demonstrating both the preferential cleavage of the amide C–N bond over the ester C–O bond and the mildness of the reducing conditions.[35] The tolerance of the methodology toward heterocycles was also determined. Notably, tetrahydropyrans, pyrrolidines, and piperidines, all of which are valuable in medicinal chemistry,[36] could be employed as evidenced by the synthesis of alcohols **5.16**–**5.20**, respectively.

With the aim of further improving the synthetic utility of the reductive arylation, we performed a robustness screen to assess the compatibility of the reaction with various functional groups and heterocycles (Figure 5.4).[37] Results indicated the tolerance of functional groups including tertiary alcohols, secondary anilines, and secondary amides, as demonstrated by moderate to good yields of alcohol **5.20** and appreciable recoveries of additives **5.22**–**5.24**, respectively. Additionally, heterocycles such as quinoline (**5.25**), dibenzofuran (**5.26**), and *N*-methyl indole (**5.27**) were found to be stable under our standard reductive arylation conditions with minimal to no inhibition of reactivity.[38] These results complement those presented in the scope of the reaction and further demonstrate the methodology's robustness toward several heteroatom-containing functional groups.
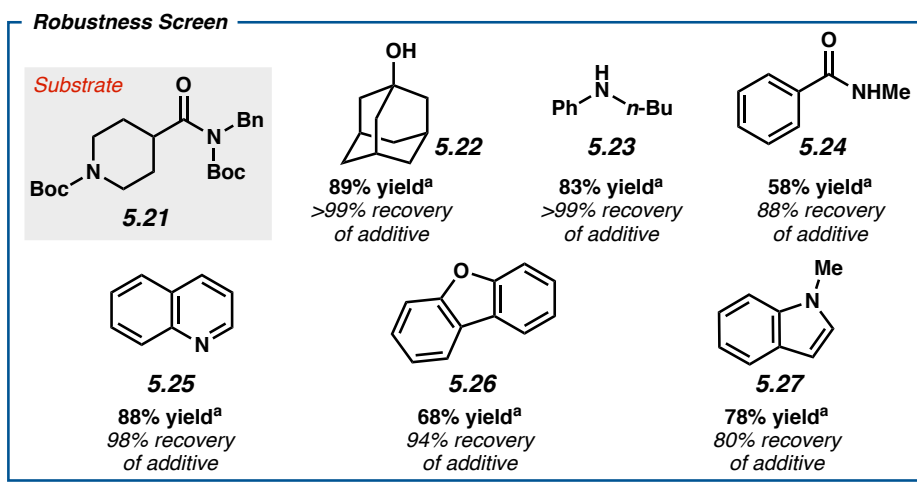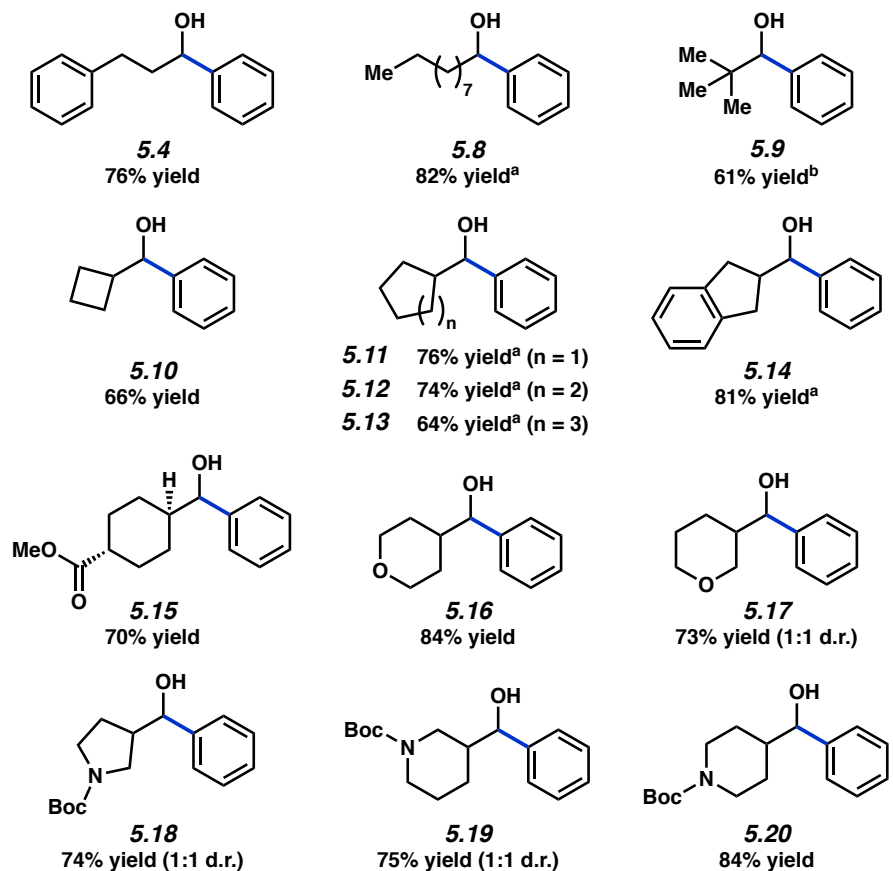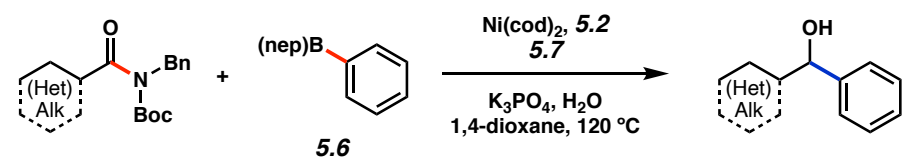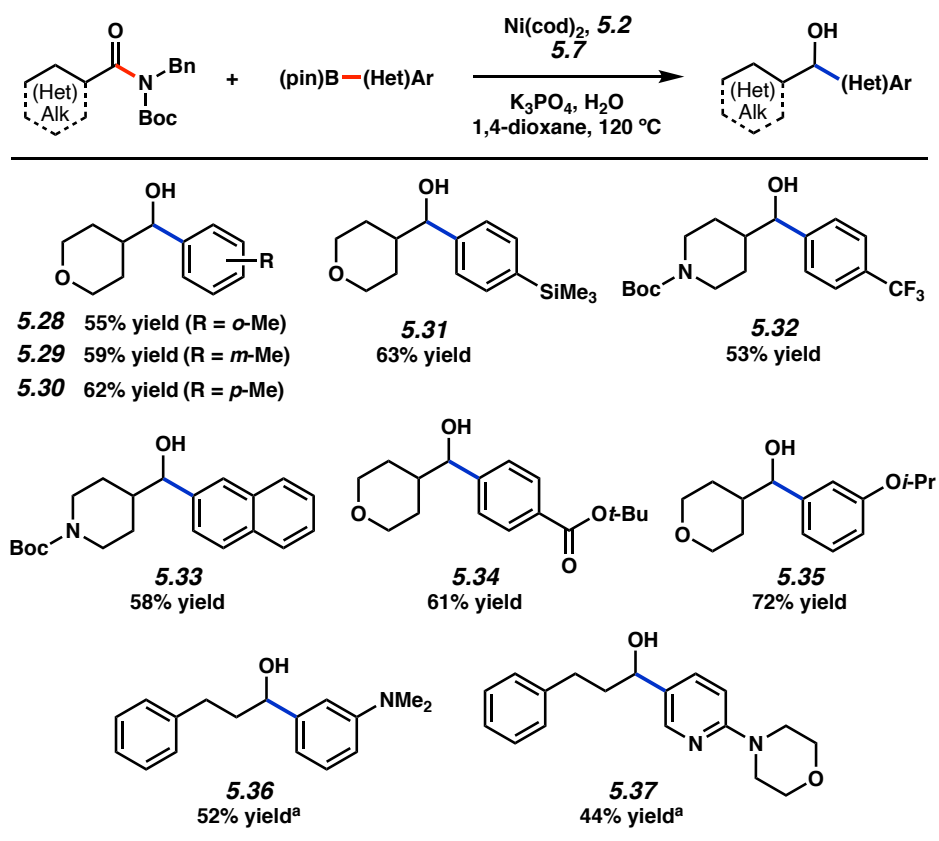
Figure 5.4. Scope of the reductive arylation of aliphatic amides and boronate **5.6**. Standard conditions unless otherwise noted: amide substrate (0.20 mmol, 1.0 equiv); phenyl boronate **5.6** (0.80 mmol, 4.0 equiv); 7 (0.50 mmol, 2.5 equiv); K_3PO_4 (0.80 mmol, 4.0 equiv); H_2O (0.40 mmol,

2.0 equiv); Ni(cod)$_2$ (0.020 mmol, 10 mol%); **5.2** (0.040 mmol, 20 mol%); solvent (1.0 M); 120 °C; 16 h. Unless otherwise noted, yields reflect the average of two isolation experiments. [a]Yield determined by ^{1}H NMR analysis using 1,3,5-trimethoxybenzene as an external standard. [b]Reaction ran at 130 °C.

5.5 Scope of Aryl Boronic Ester Coupling Partner

The scope of the aryl boronate component was also examined by coupling pinacol boronates with various amides (Figure 5.5).[31,39] Methyl substitution at the ortho, meta, or para positions of the aryl boronate was tolerated, as demonstrated by the formation of alcohols **5.28**–**5.30** in synthetically useful yields. We also evaluated aryl boronic ester nucleophiles bearing either a trimethylsilyl or trifluoromethyl group, which furnished alcohols **5.31** and **5.32**, respectively, in good yields. Additionally, a naphthyl boronate ester underwent the reductive arylation to afford alcohol **5.33** in 58% yield. We also tested several boronates that possess functional groups that have been demonstrated to be reactive to nickel catalysis. To our delight, an aryl ester,[35] an ether,[40] and a dimethyl amine were tolerated,[41] thus giving rise to alcohols **5.34**–**5.36**, respectively. Furthermore, a boronic ester containing a morpholinopyridine motif was employed to furnish alcohol **5.37**, showing the reaction's tolerance of this heteroatom-rich unit.[42]

Figure 5.5. Scope of the reductive arylation of aliphatic amides and aryl boronates. Standard conditions unless otherwise noted: amide substrate (0.20 mmol, 1.0 equiv); aryl boronate (0.80–1.2 mmol, 4.0–6.0 equiv); **5.7** (0.50 mmol, 2.5 equiv); K₃PO₄ (0.80 mmol, 4.0 equiv); H₂O (0.40 mmol, 2.0 equiv); Ni(cod)₂ (0.020–0.040 mmol, 10–20 mol%); **5.2** (0.040–0.080 mmol, 20–40 mol%); solvent (1.0 M); 120 °C; 16–24 h. Unless otherwise noted, yields reflect the average of two isolation experiments. [a]Yield determined by ¹H NMR analysis using 1,3,5-trimethoxybenzene as an external standard.

5.6 Synthetic Applications of the Methodology

The utility of this methodology was evaluated in the synthesis of known intermediates toward two bioactive compounds (Figure 5.6). In the first example (Figure 5.6a), amide **5.38** underwent reductive arylation with boronate **5.39**, despite the notable electron deficiency of this nucleophile. This delivered alcohol **5.40**, a precursor to a known γ-secretase modulator.[43] We also targeted the interception of a known route to fluoxetine,[44] the active ingredient in the blockbuster drug Prozac®. Toward this end, amide **5.42**, derived from the corresponding commercially

available carboxylic acid, was coupled with boronate **5.6** (Figure 5.6b). This transformation furnished alcohol **5.43** in 69% yield, providing facile access to a known intermediate in the synthesis of **5.44** from commercially available materials.[44] These results not only further demonstrate the viability of leveraging a cross-coupling approach to add two disparate nucleophiles into an amide carbonyl carbon, but also showcase the practical utility of this reductive arylation protocol in the synthesis of complex chiral molecules.
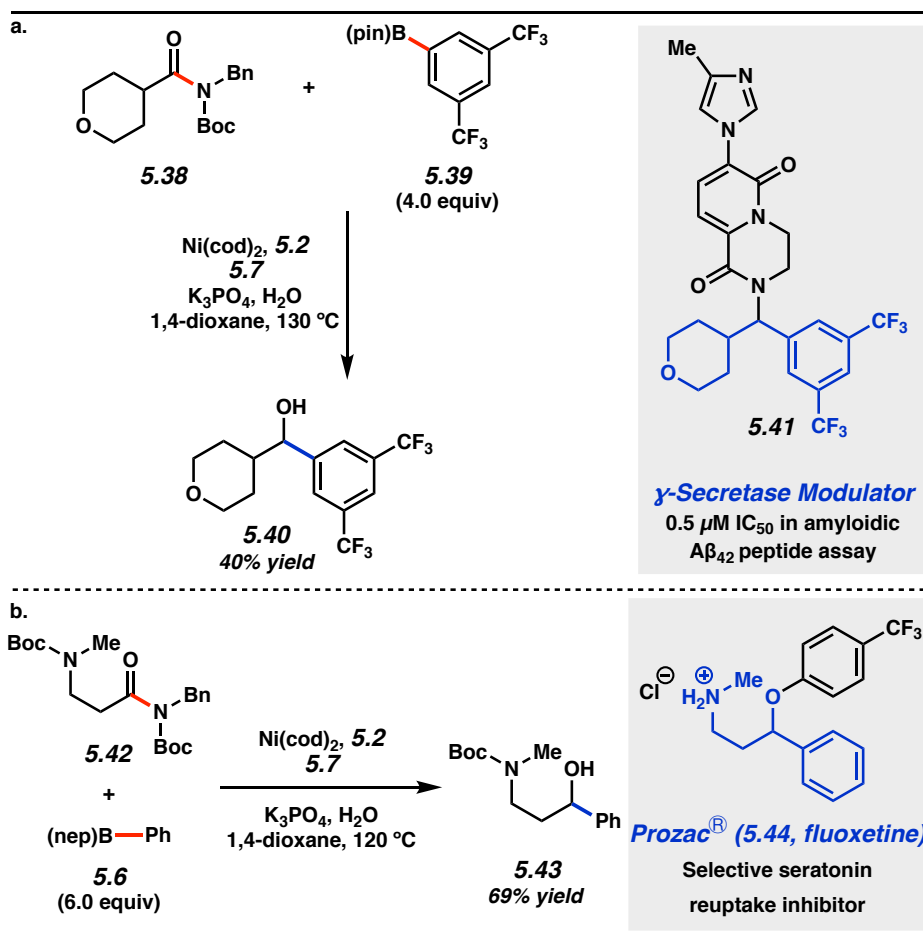
Figure 5.6. (a) Synthesis of alcohol **5.40**, an intermediate in the synthesis of γ-secretase modulator **5.41**. (b) Synthesis of alcohol **5.43**, intercepting a known synthetic route toward Prozac® (**5.44**, fluoxetine). See section 5.8.2.6 for details.

5.7 Conclusions

In summary, we have developed the first catalytic method for the direct intermolecular addition of two distinct nucleophiles to the amide carbonyl carbon. This transformation takes advantage of non-precious metal catalysis and allows for the facile conversion of amides to chiral alcohols via a cascade reaction involving Suzuki–Miyaura cross-coupling and subsequent transfer hydrogenation. The methodology has a broad scope with respect to both the amide and boronate cross-coupling partners. Additionally, it shows tolerance toward epimerizable stereocenters, select functional groups (i.e., alcohols, amines, esters, ethers, and secondary amides,) and a range of heterocycles. Moreover, the methodology can be used to access scaffolds of value to medicinal chemistry, as shown by the syntheses of **5.40** and **5.43**. This study validates the use of a cross-coupling approach to construct sp^3 carbon centers from the amide carbonyl carbon in a single operational step. We hope this study will prompt the development of additional processes that allow for the direct conversion of carboxylic acid derivatives to functional groups bearing stereogenic centers[45] via catalytic cascade processes.

5.8 Experimental Section

5.8.1 Materials and Methods. Unless stated otherwise, reactions were conducted in flame-dried glassware under an atmosphere of nitrogen or argon and commercially obtained reagents were used as received. Amide substrates were synthesized following protocols specified in Section A in the Experimental Procedures. Alcohol **5.7** was prepared according to literature procedure.[46] Boronate esters **5.5**, **5.59**–**5.61**, **5.63**–**5.65**, **5.67** and **5.68** were obtained from Combi-Blocks. Boronate ester **5.6** was obtained from TCI Chemicals. Boronate ester **5.39** was obtained from AK Scientific. Boronate esters **5.62** and **5.66** were prepared according to literature procedure.[47] $Ni(cod)_2$ and Benz-ICy•HCl (**5.2**) were obtained from Strem Chemicals. [(TMEDA)Ni(o-tolyl)Cl] was prepared according to literature procedure.[48] Ligand A (**5.71**) was prepared according to literature procedure.[49] Potassium phosphate (K_3PO_4) was obtained from Acros. 1,4-dioxane was obtained from Fisher Scientific and purified by distillation over sodium metal degassed by sparging with N_2 for 1 h. Paraffin wax (mp 53–57 °C ASTM D 87) was obtained from Sigma-Aldrich and used as received). 1,3,5-trimethoxybenzene was obtained from Alfa Aesar and used as received. Reaction temperatures were controlled using an IKAmag temperature modulator, and unless stated otherwise, reactions were performed at room temperature (approximately 23 °C). Thin-layer chromatography (TLC) was conducted with EMD gel 60 F254 pre-coated plates (0.25 mm for analytical chromatography and 0.50 mm for preparative chromatography) and visualized using a combination of UV, anisaldehyde, iodine, and potassium permanganate staining techniques. Silicycle Siliaflash P60 (particle size 0.040–0.063 mm) was used for flash column chromatography. ^1H NMR spectra were recorded on Bruker spectrometers (400, 500, and 600 MHz were allowed for our provided spectra) and are reported relative to residual solvent signals. Data for ^1H NMR spectra are reported as follows: chemical shift (δ ppm), multiplicity, coupling

constant (Hz), integration. Data for ^{13}C NMR are reported in terms of chemical shift (at 125 MHz).

IR spectra were recorded on a Perkin-Elmer UATR Two FT-IR spectrometer and are reported in terms of frequency absorption (cm^{-1}). DART-MS spectra were collected on a Thermo Exactive Plus MSD (Thermo Scientific) equipped with an ID-CUBE ion source and a Vapur Interface (IonSense Inc.). Both the source and MSD were controlled by Excalibur software v. 3.0. The analyte was spotted onto OpenSpot sampling cards (IonSense Inc.) using CHCl$_3$ or CH$_2$Cl$_2$ as the solvent. Ionization was accomplished using UHP He plasma with no additional ionization agents. The mass calibration was carried out using Pierce LTQ Velos ESI (+) and (–) Ion calibration solutions (Thermo Fisher Scientific). Determination of enantiopurity was carried out on a Mettler Toledo SFC (supercritical fluid chromatography) using Daicel ChiralPak AD–H columnn. Data for SFC are reported in enantiomeric excess (ee). For SFC chromatograms see section 5.8.2.11 of Experimental Procedures.

5.8.2 Experimental Procedures

5.8.2.1 Syntheses of Amide Substrates

Supporting information for the syntheses of amides **5.1**,[50] **5.45–5.48**,[50] **5.21**,[51] **5.38**,[51] **5.49–5.52**,[51] and **5.53**[52] have been published and spectral data match those previously reported.

5.50　　　　　**5.21**　　　　　**5.38**

5.51　　　　　**5.52**　　　　　**5.53**
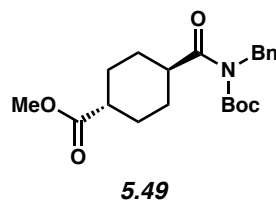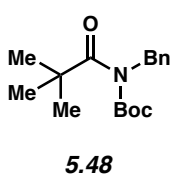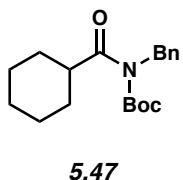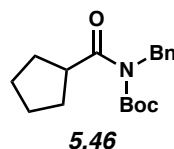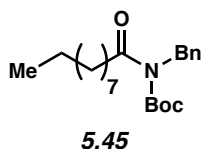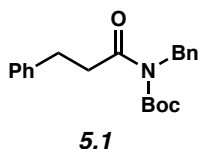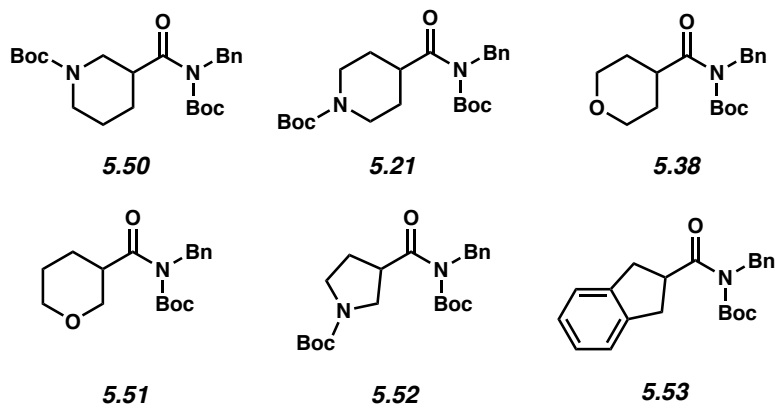
Syntheses for the remaining substrates shown in Figures 5.4 and 5.6 are as follows:

1. BnNH$_2$ (1.1 equiv)
   EDC•HCl (1.1 equiv)
   HOBt (1.1 equiv)
   Et$_3$N (1.1 equiv)
   DMF, 23 °C

2. Boc$_2$O (1.3 equiv)
   DMAP (0.10 equiv)
   CH$_3$CN, 23 °C

5.54　　　　(32% yield, 2 steps)　　　　**5.55**
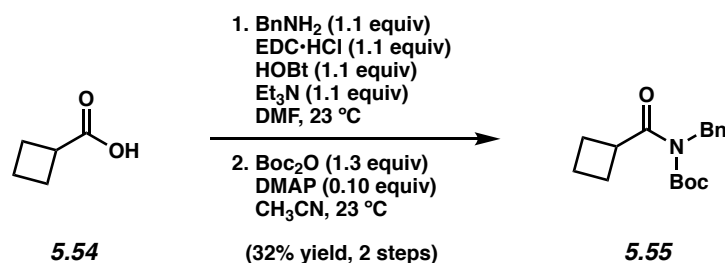
To a mixture of carboxylic acid **5.54** (65.0 mg, 0.650 mmol, 1.00 equiv), EDC•HCl (137 mg, 0.0720 mmol, 1.10 equiv), HOBt (109 g, 0.710 mmol, 1.10 equiv), triethylamine (0.100 mL, 0.710 mmol, 1.10 equiv), and DMF (5.00 mL, 0.130 M) was added benzylamine (78.0 µL, 0.710 mmol, 1.10 equiv). The resulting mixture was stirred at 23 °C for 17 h, and then diluted with deionized water (5 mL) and transferred to a separatory funnel with brine (5 mL). The aqueous layer was extracted with EtOAc (3 x 10 mL), then the organic layers were combined and washed with deionized water (3 x 10 mL), dried over Na$_2$SO$_4$, and evaporated under reduced pressure. The resulting crude material was used in the subsequent step without further purification.

To a flask containing the crude material from the previous step was added DMAP (8.00 mg, 0.0650 mmol, 0.100 equiv) followed by acetonitrile (4.00 mL, 0.160 M). Boc$_2$O (184 g, 0.850

mmol, 1.30 equiv) was added in one portion and the reaction vessel was flushed with N_2, then the reaction mixture was allowed to stir at 23 °C for 20 h. The reaction was quenched by addition of saturated aqueous NaHCO$_3$ (5 mL), transferred to a separatory funnel with EtOAc (10 mL) and H$_2$O (10 mL), and extracted with EtOAc (3 x 10 mL). The organic layers were combined, dried over Na$_2$SO$_4$, and evaporated under reduced pressure. The resulting crude residue was purified by flash column chromatography (29:1 Hexanes:EtOAc) to yield amide **5.55** (60.5 mg, 32% yield, over two steps) as a clear oil. Amide **5.55**: R_f 0.65 (5:1 Hexanes:EtOAc); ^{1}H NMR (600 MHz, C$_6$D$_6$): δ 7.30 (d, J = 7.5, 2H), 7.11 (t, J = 7.5, 2H), 7.03 (t, J = 7.5, 1H), 4.88 (s, 2H), 4.05 (quint, J = 8.3, 1H), 2.54–2.43 (m, 2H), 2.30–2.18 (m, 2H), 1.82–1.67 (m, 2H), 1.17 (s, 9H); ^{13}C NMR (125 MHz, CDCl$_3$): δ 178.0, 152.8, 138.6, 128.4, 127.6, 127.1, 83.0, 47.6, 41.4, 28.0, 25.8, 17.9; IR (film): 2980, 2869, 1732, 1687, 1144, 980 cm^{-1}; HRMS-APCI (m/z) [M + H]$^+$ calcd for C$_{17}$H$_{24}$NO$_3$$^+$, 290.17507; found 290.17377.

1. BnNH$_2$ (1.1 equiv)
   EDC·HCl (1.1 equiv)
   HOBt (1.1 equiv)
   Et$_3$N (1.1 equiv)
   DMF, 23 °C

2. Boc$_2$O (1.3 equiv)
   DMAP (0.10 equiv)
   CH$_3$CN, 40 °C

(60% yield, 2 steps)

5.56   **5.57**
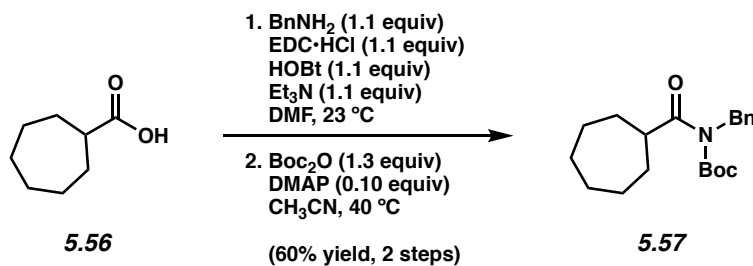
To a mixture of carboxylic acid **5.56** (1.00 g, 7.03 mmol, 1.00 equiv), EDC·HCl (1.48 g, 7.74 mmol, 1.10 equiv), HOBt (1.18 g, 7.74 mmol, 1.10 equiv), triethylamine (1.10 mL, 7.74 mmol, 1.10 equiv), and DMF (70 mL, 0.10 M) was added benzylamine (0.850 mL, 7.740 mmol, 1.10 equiv). The resulting mixture was stirred at 23 °C for 20 h, and then diluted with deionized water (100 mL) and transferred to a separatory funnel with EtOAc (30 mL) and brine (15 mL). The aqueous layer was extracted with EtOAc (3 x 100 mL), then the organic layers were combined

and washed with deionized water (4 x 100 mL), dried over Na_2SO_4, and evaporated under reduced pressure. The resulting crude solid material was used in the subsequent step without further purification.

To a flask containing the crude material from the previous step was added DMAP (85.9 mg, 0.703 mmol, 0.100 equiv) followed by acetonitrile (35.0 mL, 0.200 M). Boc_2O (1.99 g, 9.14 mmol, 1.30 equiv) was added in one portion and the reaction vessel was flushed with N_2, then the reaction mixture was allowed to stir at 40 °C for 16 h. The reaction was quenched by addition of saturated aqueous $NaHCO_3$ (100 mL), transferred to a separatory funnel with EtOAc (20 mL) and extracted with EtOAc (3 x 40 mL). The organic layers were combined, dried over Na_2SO_4, and evaporated under reduced pressure. The resulting crude residue was purified by flash chromatography (99:1 Hexanes:EtOAc → 9:1 Hexanes:EtOAc) to yield amide **5.57** as a white crystalline powder. Hot recrystallization of the purified product from *n*-heptane gave the recrystallized material (1.41 g, 60% yield over two steps) as white crystals. Amide **5.57**: mp: 57.7–62.8 °C; R_f 0.57 (5:1 Hexanes:EtOAc); ^1H NMR (500 MHz, $CDCl_3$): δ 7.32–7.27 (m, 2H), 7.25–7.20 (m, 3H), 4.85 (s, 2H), 3.59 (tt, J = 9.7, 3.9, 1H), 1.97–1.87 (m, 2H), 1.81–1.70 (m, 2H), 1.70–1.44 (m, 8H), 1.40 (s, 9H); ^{13}C NMR (125 MHz, $CDCl_3$): δ 180.8, 153.3, 138.7, 128.4, 127.6, 127.1, 83.0, 47.8, 45.8, 31.9, 28.4, 28.0, 26.7; IR (film): 2977, 2928, 2858, 1734, 1694, 1369, 1148 cm^{-1}; HRMS-APCI (*m/z*) [M + H]$^+$ calcd for $C_{20}H_{30}NO_3^+$, 332.22202; found 332.22098.
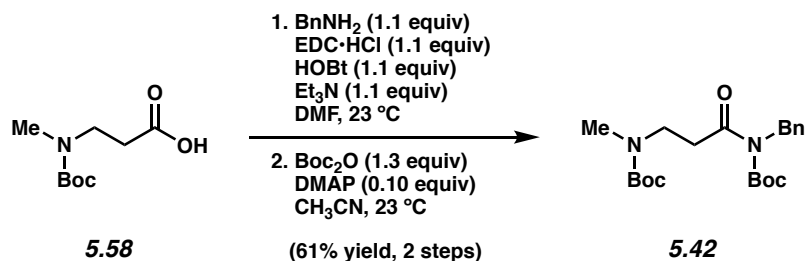
To a mixture of carboxylic acid **5.58** (500 mg, 2.46 mmol, 1.00 equiv), EDC•HCl (519 mg, 2.71 mmol, 1.10 equiv), HOBt (414 mg, 2.71 mmol, 1.10 equiv), triethylamine (0.380 mL, 2.71 mmol, 1.10 equiv), and DMF (25.0 mL, 0.100 M) was added benzylamine (0.300 mL, 2.71 mmol, 1.10 equiv). The resulting mixture was stirred at 23 ºC for 23 h, and then diluted with deionized water (100 mL) and transferred to a separatory funnel with EtOAc (30 mL) and brine (15 mL). The aqueous layer was extracted with EtOAc (3 x 80 mL), then the organic layers were combined and washed with deionized water (4 x 80 mL), dried over Na_2SO_4, and evaporated under reduced pressure. The resulting crude solid material was used in the subsequent step without further purification.

To a flask containing the crude material from the previous step was added DMAP (28.9 mg, 0.236 mmol, 0.100 equiv) followed by acetonitrile (12.0 mL, 0.200 M). Boc_2O (671 mg, 3.07 mmol, 1.30 equiv) was added in one portion and the reaction vessel was flushed with N_2, then the reaction mixture was allowed to stir at 23 ºC for 17 h. The reaction was quenched by addition of saturated aqueous $NaHCO_3$ (10 mL), transferred to a separatory funnel with EtOAc (20 mL) and extracted with EtOAc (3 x 40 mL). The organic layers were combined, dried over Na_2SO_4, and evaporated under reduced pressure. The resulting crude residue was purified by flash chromatography (19:1 Hexanes:EtOAc → 9:1 Hexanes:EtOAc) to yield amide **5.42** (0.57 g, 61% yield over two steps) as a clear oil. Amide **5.42**: R_f 0.38 (5:1 Hexanes:EtOAc); ^{1}H NMR (500 MHz, CDCl_3): δ 7.33–7.17 (m, 5H), 4.87 (br s, 2H), 3.55 (s, 2H), 3.15 (br s, 2H), 2.86 (br s, 3H),

1.45 (s, 9H), 1.40 (s, 9H); ^{13}C NMR (125 MHz, CDCl$_3$): δ 174.4, 155.7, 153.1, 138.3, 128.4, 127.6, 127.3, 83.5, 79.6, 79.5, 47.4, 45.6, 45.3, 37.2, 36.6, 35.0, 34.8, 28.6, 28.0; IR (film): 2977, 1734, 1691, 1368, 1145 cm^{-1}; HRMS-APCI (m/z) [M + H]$^+$ calcd for C$_{21}$H$_{33}$N$_2$O$_5^+$, 393.23840; found 393.23730.

*Note: **5.42** was obtained as a mixture of rotamers. These data represent empirically observed chemical shifts from the ^{1}H NMR and ^{13}C NMR spectra.*

5.8.2.2 Relevant Control Experiments
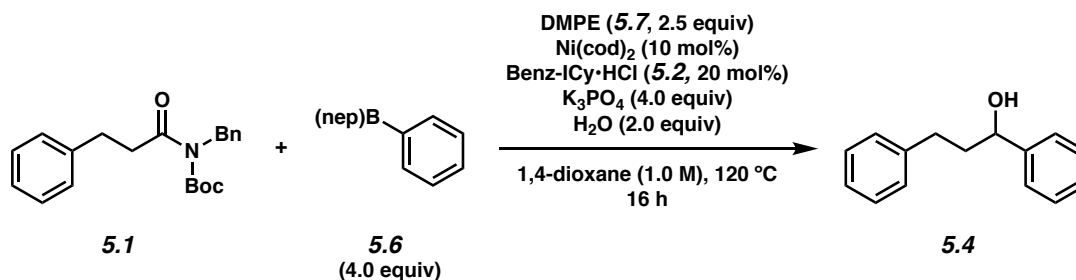
Representative Procedure for Conversion of Aliphatic Amides to Secondary Alcohols from Figure 3 (amide 5.1 and boronate ester 5.6 used as an example). A 1-dram vial was charged with anhydrous powder K$_3$PO$_4$ (170 mg, 0.800 mmol, 4.00 equiv) and a magnetic stir bar. The vial and its contents were flame-dried under reduced pressure and allowed to cool under N$_2$. Amide substrate **5.1** (67.9 mg, 0.200 mmol, 1.00 equiv), boronate ester nucleophile **5.6** (152 mg, 0.800 mmol, 4.00 equiv), and DMPE (**5.7**, 82.6 mg, 0.500 mmol, 2.50 equiv) were added. The vial was flushed with N$_2$ for 5 min, then water (7.21 μL, 0.400 mmol, 2.00 equiv), which had been sparged with N$_2$ for 10 min, was added. The vial was taken into a glovebox and charged with Ni(cod)$_2$ (5.50 mg, 0.0200 mmol, 10 mol%) and Benz-ICy•HCl (**5.2**, 12.8 mg, 0.0400 mmol, 20 mol%). Subsequently, 1,4-dioxane (200 μL, 1.00 M) was added. The vial was sealed with a Teflon-lined screw cap, removed from the glovebox, and stirred vigorously (800 RPM) at 120 ºC for 16 h. After

cooling to 23 ºC, the mixture was quenched by the addition of saturated aqueous NH$_4$Cl (1 mL) and extracted with EtOAc (3 x 2 mL). The combined organic layers were then filtered over a plug of silica gel (3 cm) and Na$_2$SO$_4$ (3 cm) using EtOAc (10 mL) as eluent. The volatiles were removed under pressure and the yield of alcohol **5.4** was determined by ^{1}H NMR analysis with 1,3,5-trimethoxybenzene as an external standard.

Any modifications of the conditions shown in the representative procedure above are specific below in Table 5.1.

Table 5.1. Relevant control experiments

Reaction Conditions	Experimental Results[a]		
	5.1	**5.3**	**5.4**
5.6 (4.0 equiv), DMPE (**5.7**, 4.0 equiv), K$_3$PO$_4$ (4.0 equiv), H$_2$O (2.0 equiv) 1,4-dioxane (1.0 M), 120 °C, 16 h	5%[b]	0%	0%
5.6 (4.0 equiv), DMPE (**5.7**, 4.0 equiv), K$_3$PO$_4$ (4.0 equiv), H$_2$O (2.0 equiv) Benz-ICy·HCl (**5.2**, 20 mol%), 1,4-dioxane (1.0 M), 120 °C, 16 h	0%[b]	0%	0%
5.6 (4.0 equiv), DMPE (**5.7**, 4.0 equiv), K$_3$PO$_4$ (4.0 equiv), H$_2$O (2.0 equiv) Ni(cod)$_2$ (10 mol%), 1,4-dioxane (1.0 M), 120 °C, 16 h	12%[b]	0%	0%

[a] Yields determined by 1H NMR analysis using 1,3,5-trimethoxybenzene as an external standard.
[b] Substantial amounts of the corresponding Boc-cleavage product (des-Boc amide starting material) were observed due to the elevated reaction temperature.

**5.8.2.3 General Procedures for Methodology**

5.8.2.3.1 General Procedure A. A 1-dram vial was charged with anhydrous powder K_3PO_4 (170 mg, 8.00 mmol, 4.00 equiv) and a magnetic stir bar. The vial and its contents were flame-dried under reduced pressure and allowed to cool under N_2. Amide substrate (0.200 mmol, 1.00 equiv), boronate ester nucleophile (152 mg, 0.800 mmol, 4.00 equiv), and DMPE (**5.7**, 82.6 mg, 0.500 mmol, 2.50 equiv) were added. The vial was flushed with N_2 for 5 min, then water (7.21 μL, 0.400 mmol, 2.00 equiv), which had been sparged with N_2 for 10 min, was added. The vial was taken into a glovebox and charged with Ni(cod)$_2$ (5.50 mg, 0.0200 mmol, 10 mol%) and Benz-ICy•HCl (**5.2**, 12.8 mg, 0.0400 mmol, 20 mol%). Subsequently, 1,4-dioxane (200 μL, 1.00 M) was added. The vial was sealed with a Teflon-lined screw cap, removed from the glovebox, and stirred vigorously (800 RPM) at 120 ºC for 16 h. After cooling to 23 ºC, the mixture was quenched by the addition of saturated aqueous NH_4Cl (1 mL) and extracted with EtOAc (3 x 2 mL). The combined organic layers were then filtered over a plug of silica gel (3 cm) and Na_2SO_4 (3 cm) using EtOAc (10 mL) as eluent and the volatiles were removed under pressure. The crude mixture was adsorbed onto silica gel (450 mg) under reduced pressure and purified by flash column chromatography on silica.

5.8.2.3.2 General Procedure B. A 1-dram vial was charged with anhydrous powder K_3PO_4 (170 mg, 8.00 mmol, 4.00 equiv) and a magnetic stir bar. The vial and its contents were flame-dried under reduced pressure and allowed to cool under N_2. Amide substrate (0.200 mmol, 1.00 equiv), boronate ester nucleophile (152 mg, 0.800 mmol, 4.00 equiv), and DMPE (**5.7**, 82.6 mg, 0.500 mmol, 2.50 equiv) were added. The vial was flushed with N_2 for 5 min, then water (7.21 μL, 0.400 mmol, 2.00 equiv), which had been sparged with N_2 for 10 min, was added. The vial was taken

into a glovebox and charged with Ni(cod)$_2$ (5.50 mg, 0.0200 mmol, 10 mol%) and Benz-ICy•HCl (**5.2**, 12.8 mg, 0.0400 mmol, 20 mol%). Subsequently, 1,4-dioxane (200 μL, 1.00 M) was added. The vial was sealed with a Teflon-lined screw cap, removed from the glovebox, and stirred vigorously (800 RPM) at 120 ºC for 16 h. After cooling to 23 ºC, the mixture was diluted with CH$_2$Cl$_2$ (1 mL) and washed with 2 M HCl (3 x 1 mL). The organic layer was then filtered over a plug of silica gel (3 cm) and Na$_2$SO$_4$ (3 cm) using EtOAc (10 mL) as eluent and the volatiles were removed under pressure. The crude mixture was adsorbed onto silica gel (450 mg) under reduced pressure and purified by flash column chromatography on silica.

5.8.2.3.3 General Procedure C. A 1-dram vial was charged with anhydrous powder K$_3$PO$_4$ (170 mg, 8.00 mmol, 4.00 equiv) and a magnetic stir bar. The vial and its contents were flame-dried under reduced pressure and allowed to cool under N$_2$. Amide substrate (0.200 mmol, 1.00 equiv), boronate ester nucleophile (228 mg, 1.20 mmol, 6.00 equiv), and DMPE (**5.7**, 82.6 mg, 0.500 mmol, 2.50 equiv) were added. The vial was flushed with N$_2$ for 5 min, then water (7.21 μL, 0.400 mmol, 2.00 equiv), which had been sparged with N$_2$ for 10 min, was added. The vial was taken into a glovebox and charged with Ni(cod)$_2$ (11.0 mg, 0.0400 mmol, 20 mol%) and Benz-ICy•HCl (**5.2**, 25.6 mg, 0.0800 mmol, 40 mol%). Subsequently, 1,4-dioxane (200 μL, 1.00 M) was added. The vial was sealed with a Teflon-lined screw cap, removed from the glovebox, and stirred vigorously (800 RPM) at 120 ºC for 16 h. After cooling to 23 ºC, the mixture was diluted with CH$_2$Cl$_2$ (1 mL) and washed with deionized H$_2$O (3 x 1 mL). The organic layer was then filtered over a plug of silica gel (3 cm) and Na$_2$SO$_4$ (3 cm) using EtOAc (10 mL) as eluent and the volatiles were removed under pressure. The crude mixture was adsorbed onto silica gel (450 mg) under reduced pressure and purified by flash column chromatography on silica.

Any modifications of the conditions shown in the representative procedures above are specified in the following schemes, which depict all of the results shown in Figures 5.4, 5.5, and 5.6.

5.8.2.4 Scope of Amide Substrates
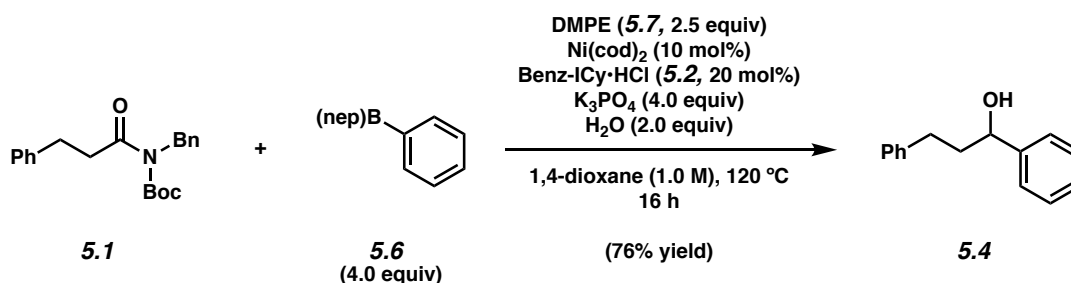
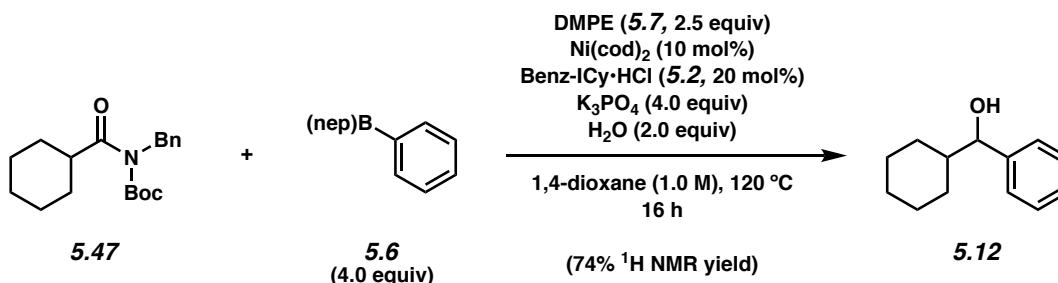**Alcohol 5.4.** Crude alcohol **5.4** was synthesized following General Procedure A. Purification by flash column chromatography (99:1 Hexanes:EtOAc → 19:1 Hexanes:EtOAc) afforded alcohol **5.4** (76% yield, average of two experiments) as a white solid. Alcohol **5.4**: R_f 0.34 (5:1 Hexanes:EtOAc). ^{1}H NMR (500 MHz, CDCl$_3$): δ 7.40–7.34 (m, 4H), 7.32–7.27 (m, 3H), 7.23–7.16 (m, 3H), 4.70 (app t, J = 6.5, 1H), 2.76 (ddd, J = 13.9, 10.0, 5.8, 1H), 2.68 (ddd, J = 13.9, 9.6, 6.4, 1H), 2.21–1.98 (m, 2H), 1.92 (br s, 1H). Spectral data match those previously reported.[53]
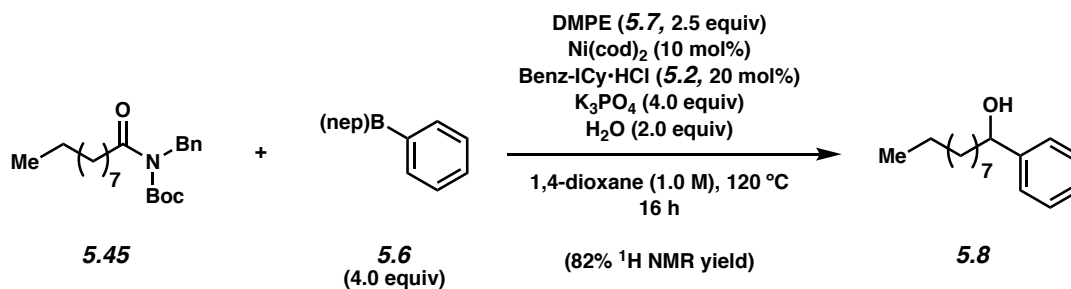
Alcohol 5.8. Crude alcohol **5.8** was synthesized following General Procedure A. ^{1}H NMR analysis of the crude reaction mixture indicated an 82% yield o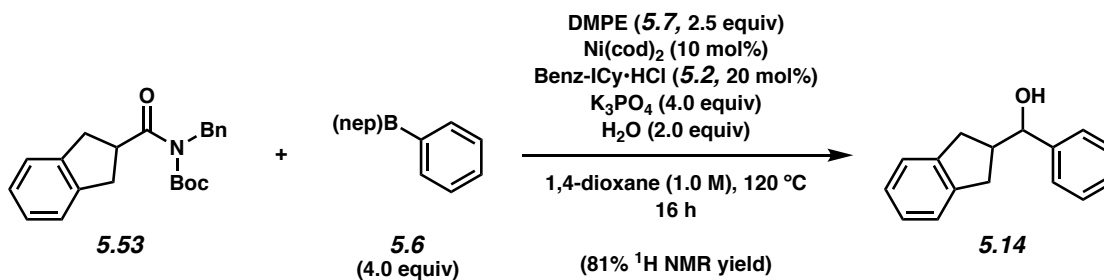f alcohol **5.8** relative to 1,3,5-trimethoxybenzene external standard. Sequential purification by preparative thin-layer chromatography (3:1 Hexanes:Et$_2$O, then 4:1 Hexanes:Acetone) provided an analytical sample of

alcohol **5.8** as a clear oil. Alcohol **5.8**: R_f 0.52 (5:1 Hexanes:EtOAc). ^{1}H NMR (500 MHz, CDCl$_3$):

δ 7.41–7.31 (m, 4H), 7.31–7.27 (m, 1H), 4.67 (dd, J = 7.5, 5.9, 1H), 1.87–1.75 (m, 2H), 1.75–1.65

(m, 1H), 1.49–1.36 (m, 1H), 1.36–1.16 (m, 13H), 0.87 (t, J = 6.8, 3H). Spectral data match those

previously reported.[54]
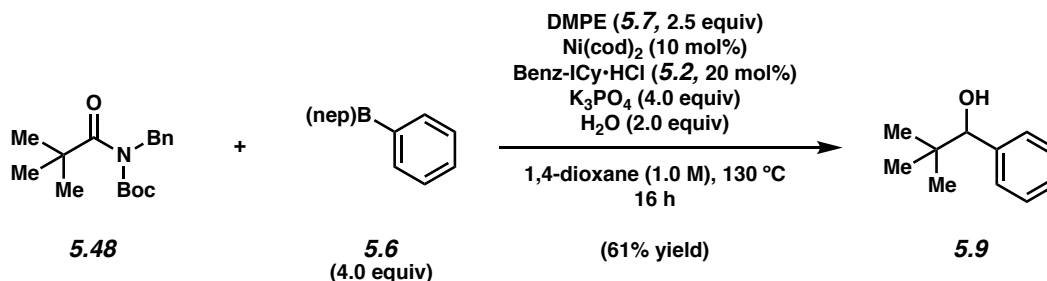
Alcohol 5.9. Crude alcohol **5.9** was synthesized following General Procedure A. Purification by

flash column chromatography (39:1 Hexanes:Et$_2$O → 6.5:1 Hexanes:Et$_2$O) afforded alcohol **5.9**

(61% yield, average of two experiments) as a clear oil. Alcohol **5.9**: R_f 0.48 (5:1 Hexanes:EtOAc).

^{1}H NMR (500 MHz, CDCl$_3$): δ 7.34–7.28 (m, 4H), 7.29–7.26 (m, 1H), 4.40 (s, 1H), 1.83 (s, 1H),

0.93 (s, 9H). Spectral data match those previously reported.[55]
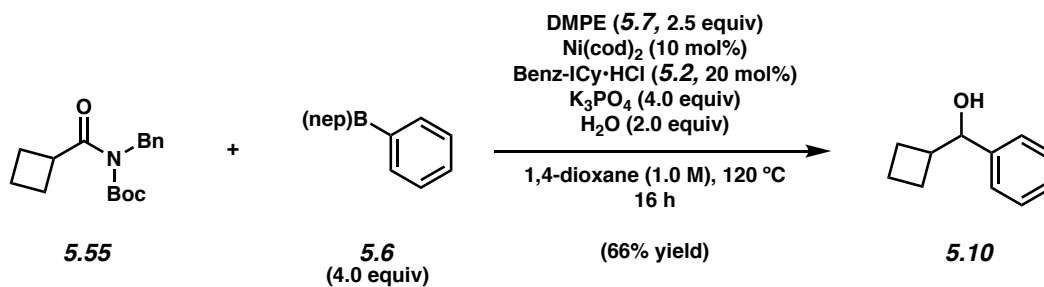
Alcohol 5.10. Crude alcohol **5.10** was synthesized following General Procedure A. Sequential

purification by flash column chromatography (98:1:1 Hexanes:CH$_2$Cl$_2$:Et$_2$O → 3:1:1

Hexanes:CH$_2$Cl$_2$:Et$_2$O) followed by preparative thin-layer chromatography (1:1:1

CH$_2$Cl$_2$:Et$_2$O:Hexanes) afforded alcohol **5.10** (66% yield, average of two experiments) as a clear

oil. Alcohol **5.10**: R_f 0.38 (5:1 Hexanes:EtOAc). ^{1}H NMR (500 MHz, CDCl$_3$): δ 7.37–7.30 (m, 4H), 7.30–7.24 (m, 1H), 4.58 (d, J = 8.0, 1H), 2.69–2.56 (m, 1H), 2.15–1.96 (m, 2H), 1.92–1.75 (m, 5H). Spectral data match those previously reported.[55]
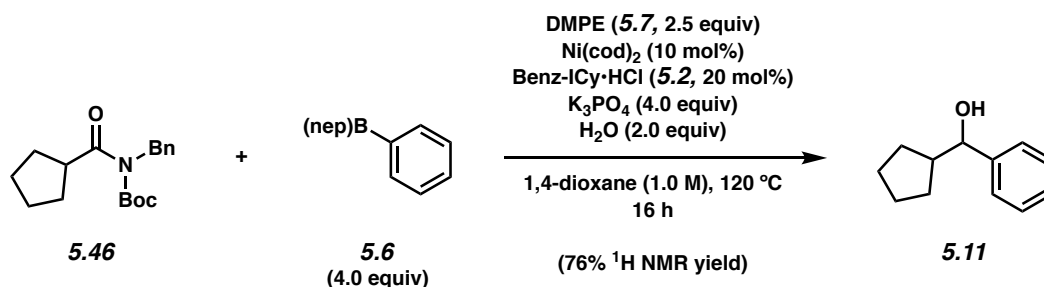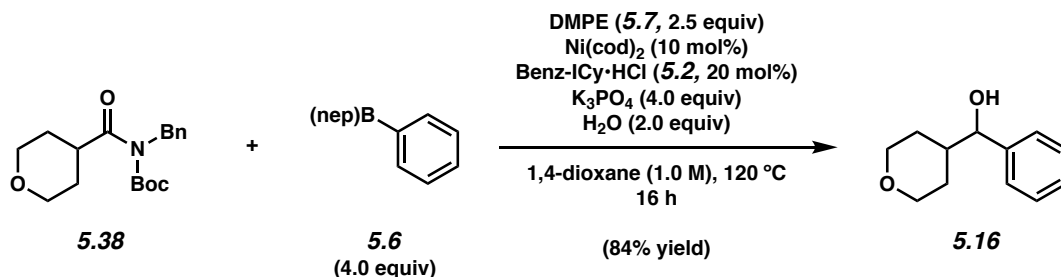

Alcohol 5.11. Crude alcohol **5.11** was synthesized following General Procedure A. ^{1}H NMR analysis of the crude reaction mixture indicated a 76% yield of alcohol **5.11** relative to 1,3,5-trimethoxybenzene external standard. Sequential purification by preparative thin-layer chromatography (5:1 Hexanes:EtOAc, then 5:1:1 Hexanes:CH$_2$Cl$_2$:Et$_2$O) afforded an analytical sample of alcohol **5.11** as a clear oil. Alcohol **5.11**: R_f 0.46 (5:1 Hexanes:EtOAc). ^{1}H NMR (500 MHz, CDCl$_3$): δ 7.36–7.26 (m, 5H), 7.30–7.27 (m, 1H), 4.41 (d, J = 8.5, 1H), 2.22 (app sext, J = 8.2, 1H), 1.95–1.78 (m, 2H), 1.70–1.63 (m, 1H), 1.54–1.44 (m, 3H), 1.42–1.33 (m, 1H), 1.19–1.10 (m, 1H). Spectral data match those previously reported.[56]

Alcohol 5.12. Crude alcohol **5.12** was synthesized following General Procedure A. ^{1}H NMR analysis of the crude reaction mixture indicated a 74% yield of alcohol **5.12** relative to 1,3,5-

trimethoxybenzene external standard. Alcohol **5.12**: R$_f$ 0.44 (5:1 Hexanes:EtOAc). Spectral data match those previously reported.[57]

Note: The ^{1}H NMR spectrum of the crude material obtained using the reaction conditions above is provided and matches previously reported ^{1}H NMR data.
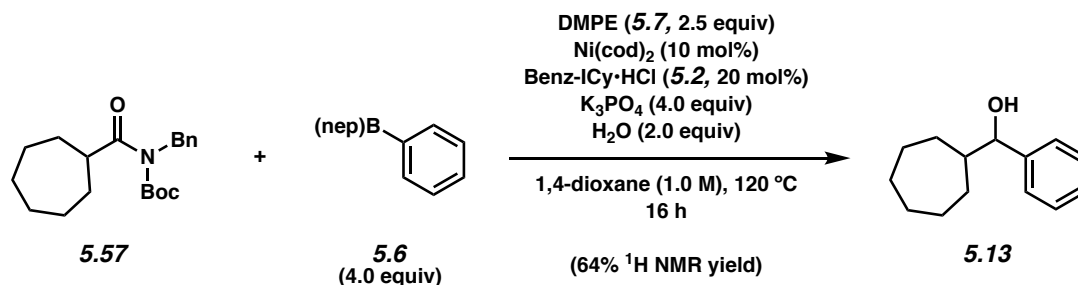
Alcohol 5.13. Crude alcohol **5.13** was synthesized following General Procedure A. ^{1}H NMR analysis of the crude reaction mixture indicated an 64% yield of alcohol **5.13** relative to 1,3,5-trimethoxybenzene external standard). Preparation of an authentic sample of alcohol **5.13** from cycloheptyl(phenyl)methanone (see section 5.8.2.7 for experimental details) allowed for direct comparison with the ^{1}H NMR spectrum of the crude reaction mixture and full characterization. Alcohol **5.13**: R$_f$ 0.57 (5:1 Hexanes:EtOAc); ^{1}H NMR (600 MHz, CDCl$_3$): δ 7.35–7.23 (m, 5H), 4.47 (d, J = 6.7, 1H), 1.93–1.82 (m, 2H), 1.79 (br s, 1H), 1.72–1.65 (m, 1H), 1.65–1.30 (m, 9H), 1.23–1.09 (m, 1H); ^{13}C NMR (125 MHz, CDCl$_3$): δ 144.0, 128.3, 127.5, 126.8, 79.4, 46.4, 31.2, 29.4, 28.6, 28.5, 26.9, 26.7; IR (film): 3378, 2917, 2852, 1492, 699 cm^{-1}; HRMS-APCI (*m/z*) [M + H]$^+$ calcd for C$_{14}$H$_{21}$O$^+$, 205.15869; found 205.15788.

Note: ^{1}H NMR and ^{13}C NMR spectra of the authentic material, as prepared in section 5.8.2.7, are provided. A ^{1}H NMR spectrum of the crude material obtained using the reaction conditions above is also provided and matches the ^{1}H NMR spectrum of the authentic material.

Reaction scheme: **5.53** + **5.6** (4.0 equiv), with (nep)B–phenyl. Conditions: DMPE (**5.7**, 2.5 equiv), Ni(cod)$_2$ (10 mol%), Benz-ICy·HCl (**5.2**, 20 mol%), K$_3$PO$_4$ (4.0 equiv), H$_2$O (2.0 equiv), 1,4-dioxane (1.0 M), 120 °C, 16 h, → **5.14** (81% ^{1}H NMR yield).

Alcohol 5.14. Crude alcohol **5.14** was synthesized following General Procedure A. ^{1}H NMR analysis of the crude reaction mixture indicated an 81% yield of alcohol **5.14** relative to 1,3,5-trimethoxybenzene external standard (average of two experiments). To the crude reaction mixture was added a teflon-coated magnetic stir bar and CH$_2$Cl$_2$ (1 mL). The solution was stirred, cooled to 0 °C, TFA (200 μL) was slowly added, and the contents were stirred at 0 °C for 1 h. The volatiles were then removed under reduced pressure to give the crude material, which was purified by flash column chromatography (99:1 Hexanes:EtOAc → 19:1 Hexanes:EtOAc). Treatment of the purified product with a solution (4 mL total volume, 1:1 v/v) of MeOH:2M KOH and stirring the resulting solution at 23 °C for 2 h afforded an analytical sample of alcohol **5.14** as a white solid. Alcohol **5.14**: R$_f$ 0.38 (5:1 Hexanes:EtOAc); ^{1}H NMR (500 MHz, CDCl$_3$): δ 7.43–7.29 (m, 5H), 7.23–7.22 (m, 1H), 7.14–7.11 (m, 3H), 4.63 (d, J = 8.5, 1H), 3.16 (dd, J = 16.0, 8.0, 1H), 3.06 (dd, J = 16.0, 8.0, 1H), 2.87 (app sext, J = 8.3, 1H), 2.69 (dd, J = 16.0, 8.0, 1H), 2.64 (dd, J = 16.0, 8.5, 1H); ^{13}C NMR (125 MHz, CDCl$_3$): δ 144.0, 143.2, 142.8, 128.7, 128.0, 126.7, 126.4, 126.3, 124.7, 124.5, 78.5, 47.3, 36.3, 36.1; IR (film): 3556, 3385, 3067, 3028, 2936 cm^{-1}; HRMS-APCI (m/z) [M + NH$_4$]$^+$ calcd for C$_{16}$H$_{20}$NO$^+$, 242.15394; found 242.15312.

*Note: **5.14** was obtained as a mixture of rotamers. These data represent empirically observed chemical shifts from the ^{1}H NMR and ^{13}C NMR spectra.*
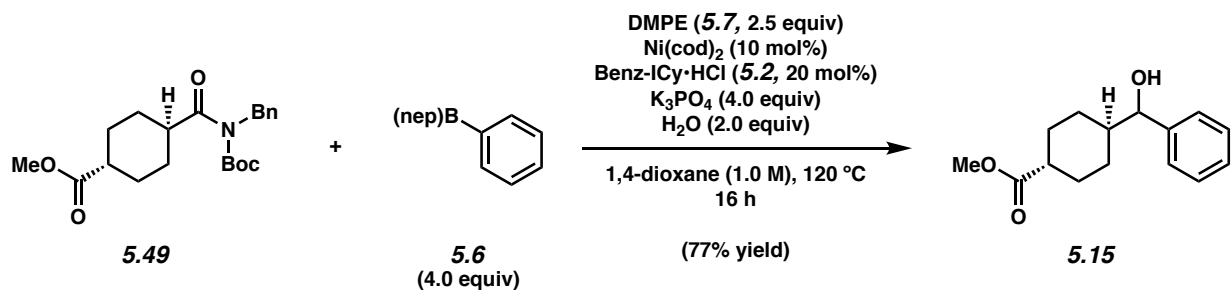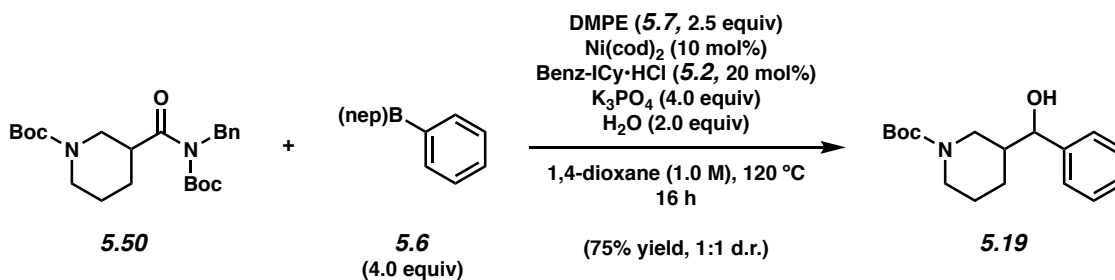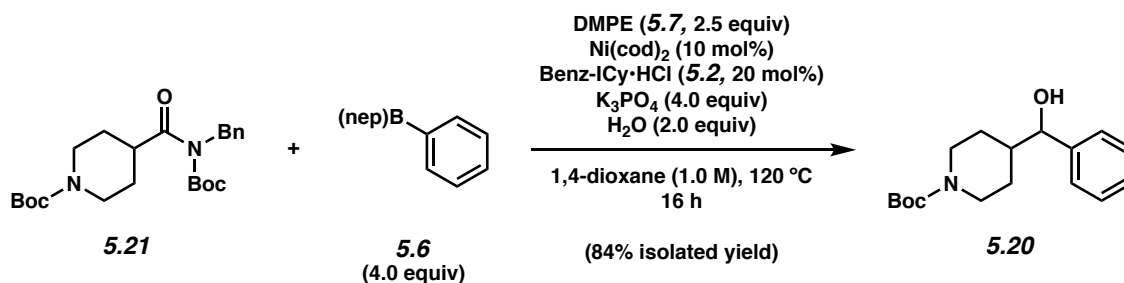
Alcohol 5.15. Crude alcohol **5.15** was synthesized following General Procedure A. Purification by flash column chromatography (99:1 Hexanes:Acetone → 9:1 Hexanes:Acetone) afforded a mixture of the trans and cis diastereomers of alcohol **5.15** (77% yield, 31:1 trans:cis diastereomers, average of two experiments) as a clear oil. Trans diastereomer alcohol **5.15**: R_f 0.22 (5:1 Hexanes:EtOAc); ^{1}H NMR (500 MHz, CDCl$_3$): δ 7.37–7.24 (m, 5H), 4.35 (d, J = 7.2, 1H), 3.63 (s, 3H), 2.20 (tt, J = 12.4, 3.6, 1H), 2.13–1.87 (m, 4H), 1.66–1.56 (m, 1H), 1.51–1.28 (m, 3H), 1.13–0.96 (m, 2H); ^{13}C NMR (125 MHz, CDCl$_3$): δ 176.6, 143.5, 128.4, 127.7, 126.7, 79.1, 51.6, 44.2, 43.3, 28.70, 28.68, 28.4, 27.9; IR (film): 3454, 2938, 1731, 1716, 1170 cm^{-1}; HRMS-APCI (m/z) [M + H]$^+$ calcd for C$_{15}$H$_{21}$O$_3^+$, 249.14852; found 249.14806.

Alcohol 5.16. Crude alcohol **5.16** was synthesized following General Procedure B. Purification by flash column chromatography (19:1 Hexanes:EtOAc → 3:1 Hexanes:EtOAc) afforded alcohol **5.16** (84% yield, average of two experiments) as a white solid. Alcohol **5.16**: R_f 0.23 (3:1 Hexanes:EtOAc). ^{1}H NMR (500 MHz, CDCl$_3$): δ 7.38–7.26 (m, 5H), 4.32 (d, J = 7.7, 1H), 3.98

(app dd, J = 11.6, 4.6, 1H), 3.86 (app dd, J = 11.6, 4.6, 1H), 3.34 (td, J = 11.8, 2.2, 1H), 3.25 (td, J = 11.9, 2.3, 1H), 2.21 (br s, 1H), 1.94–1.86 (m, 1H), 1.86–1.72 (m, 1H), 1.50–1.36 (m, 1H), 1.36–1.20 (m, 1H), 1.20–1.07 (m, 1H). Spectral data match those previously reported.[58]
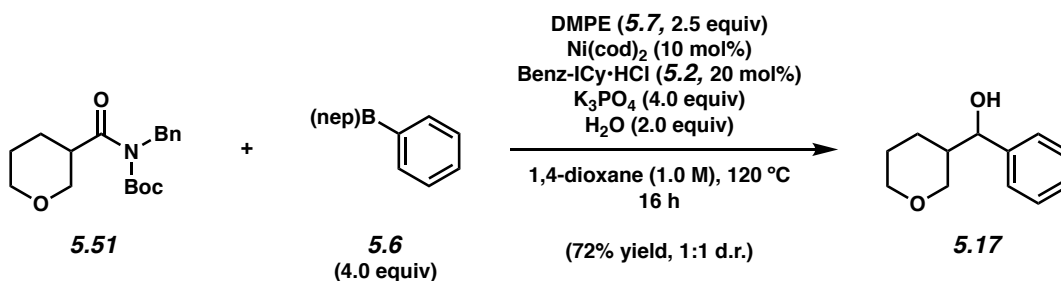
Alcohol 5.17. Crude alcohol **5.17** was synthesized following General Procedure B. Purification by flash chromatography (19:1 Hexanes:EtOAc → 1:1 Hexanes:EtOAc) afforded a mixture of diastereomers of alcohol **5.17** (72% yield, 1:1 d.r., average of two experiments) as a clear oil. Alcohol **5.17**: R_f 0.27 (3:1 Hexanes:EtOAc); ^{1}H NMR (500 MHz, CDCl$_3$): δ 7.37–7.26 (m, 10H), 4.50 (dd, J = 2.8, 7.0, 1H), 4.40 (dd, J = 2.9, 8.5, 1H), 4.16 (ddd, J = 1.8, 4.0, 11.3, 1H), 3.89–3.71 (m, 2H), 3.58 (ddd, J = 1.7, 4.0, 11.3, 1H), 3.49–3.30 (m, 3H), 3.20 (dd, J = 11.3, 9.4, 1H), 2.13, (d, J = 2.9, 1H), 2.10 (d, J = 3.0, 1H), 2.00–1.86 (m, 3H), 1.73–1.65 (m, 1H), 1.63–1.43 (m, 4H), 1.43–1.35 (m, 1H), 1.20–1.10 (m, 1H); ^{13}C NMR (125 MHz, CDCl$_3$, 19 of 20 observed): δ 143.1, 143.0, 128.60, 128.56, 128.0, 127.9, 126.7, 126.4, 76.6, 75.9, 70.8, 70.6, 68.6, 68.4, 43.0, 42.9, 26.4, 25.4, 25.3; IR (film): 3401, 2938, 2846, 1453, 1081 cm^{-1}; HRMS-APCI (m/z) [M + H]$^+$ calcd for C$_{12}$H$_{17}$O$_2$$^+$, 193.12231; found 193.12228.

*Note: **5.17** was obtained as a mixture of diastereomers. These data represent empirically observed chemical shifts from the ^{1}H NMR and ^{13}C NMR spectra.*
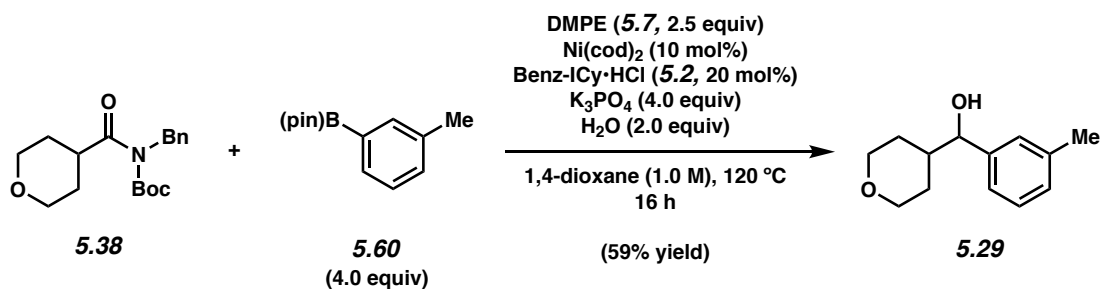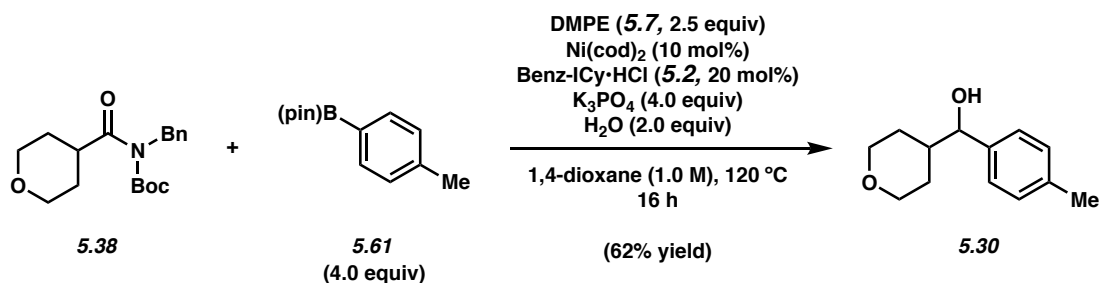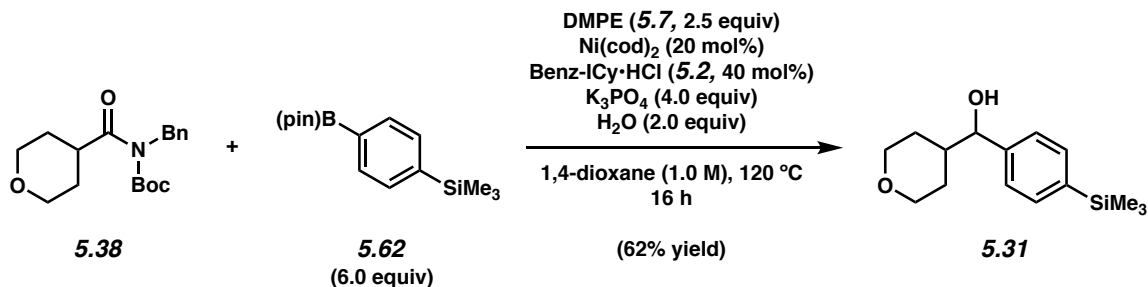
Alcohol 5.18. Crude alcohol **5.18** was synthesized following General Procedure B. Purification

by flash chromatography (19:1 Hexanes:EtOAc → 1:1 Hexanes:EtOAc) afforded a mixture of

diastereomers of alcohol **5.18** (74% yield, 1:1 d.r., average of two experiments) as a clear oil.

Alcohol **5.18**: R$_f$ 0.27 (9:1 PhH:Acetone). ^{1}H NMR (500 MHz, DMSO-d_6): 7.44–7.08 (m, 5H),

5.45–5.33 (m, 1H), 4.52–4.21 (m, 1H), 3.45–2.83 (m, 4H), 2.47–2.27 (m, 1H), 1.97–1.71 (m, 1H),

1.63–1.30 (m, 10H). Spectral data match those previously reported.[59]

*Note: **5.18** was obtained as a mixture of rotamers and diastereomers. These data represent*

empirically observed chemical shifts from the ^{1}H NMR spectra.

Alcohol 5.19. Crude alcohol **5.19** was synthesized following General Procedure B. Purification by

flash column chromatography (PhH → 9:1 PhH:Acetone) afforded a mixture of diastereomers of

alcohol **5.19** (75% yield, 1:1 d.r. average of two experiments) as a clear oil. Alcohol **5.19**: R$_f$ 0.44

(9:1 PhH:Acetone); ^{1}H NMR (500 MHz, CDCl$_3$, 49 of 50 observed): δ 7.81–7.26 (m, 10H), 4.50

(br s, 1H), 4.43 (d, J = 8.5, 1H), 4.16–2.46 (m, 7H), 2.24–1.51 (m, 10H), 1.49–1.31 (m, 18H),

1.22–1.09 (m, 1H); ^{13}C NMR (125 MHz, CDCl$_3$, 23 of 26 observed): δ 155.4, 155.0, 142.9, 128.57,

128.56, 127.93, 127.91, 126.7, 126.5, 79.7, 79.4, 76.5, 75.9, 46.7, 44.5, 43.1, 43.0, 28.6, 28.5, 27.0, 26.3, 24.8, 24.0; IR (film): 3422, 2975, 2930, 1665, 1424 cm^{-1}; HRMS-APCI (*m/z*) [M + H]$^+$ calcd for C$_{17}$H$_{26}$NO$_3$$^+$, 292.19072; found 292.18998.

*Note: **5.19** was obtained as a mixture of rotamers and diastereomers. These data represent empirically observed chemical shifts from the ^{1}H NMR and ^{13}C NMR spectra.*

Alcohol 5.20. Crude alcohol **5.20** was synthesized following General Procedure B. Purification by flash column chromatography (PhH → 9:1 PhH:Acetone) afforded alcohol **5.20** (84% yield, average of two experiments) as a clear oil. Alcohol **5.20**: R$_f$ 0.33 (9:1 PhH:Acetone). ^{1}H NMR (500 MHz, CDCl$_3$): 7.38–7.23 (m, 5H), 4.34 (d, *J* = 7.5, 1H), 4.29–3.81 (m, 2H), 2.77–2.38 (m, 2H), 2.26 (br s, 1H), 1.98–1.89 (m, 1H), 1.81–1.65 (m, 1H), 1.42 (s, 9H), 1.33–1.17 (m, 2H), 1.11 (app qd, *J* = 12.5, 4.4, 1H). Spectral data match those previously reported.[58]

5.8.2.5 Scope of Boronate Ester Nucleophiles
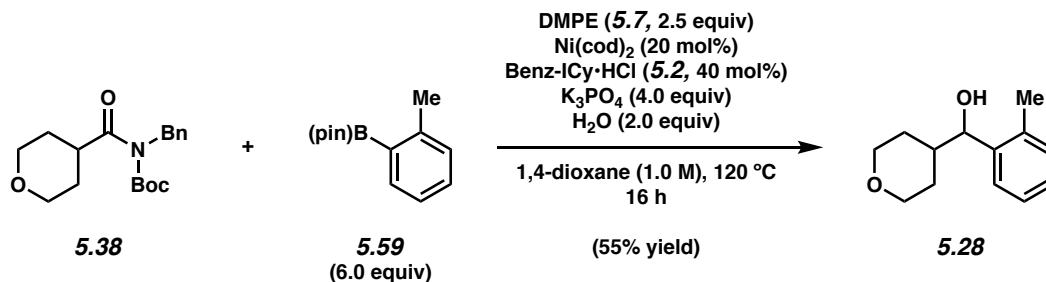
Alcohol 5.28. Crude alcohol **5.28** was synthesized following General Procedure B. Purification by flash column chromatography (19:1 Hexanes:EtOAc → 3:1 Hexanes:EtOAc) afforded alcohol **5.28** (55% yield, average of two experiments) as a crystalline solid. Alcohol **5.28**: mp: 62–64 °C; R_f 0.32 (2:1 Hexanes:EtOAc); ^{1}H NMR (500 MHz, CDCl$_3$): δ 7.42 (dd, J = 7.7, 1.3, 1H), 7.23 (td, J = 7.5, 1.5, 1H), 7.21–7.12 (m, 2H), 4.69 (d, J = 7.3, 1H), 4.03 (dd, J = 11.2, 4.5, 1H), 3.90 (dd, J = 11.5, 4.5, 1H), 3.37 (td, J = 9.5, 2.3, 1H), 3.29 (td, J = 9.5, 2.3, 1H), 2.35 (s, 3H), 1.96–1.83 (m, 2H), 1.71 (br s, 1H), 1.60–1.48 (m, 1H), 1.42 (qd, J = 12.5, 4.6, 1H), 1.22–11.5 (m, 1H); ^{13}C NMR (125 MHz, CDCl$_3$): δ 141.3, 135.3, 130.6, 127.5, 126.39, 126.36, 74.6, 68.1, 67.9, 42.2, 29.4, 29.2, 19.6; IR (film): 3420, 2951, 2847, 1090, 1016 cm^{-1}; HRMS-APCI (m/z) [M + H]$^+$ calcd for C$_{13}$H$_{19}$O$_2^+$, 207.13796; found 207.13823.
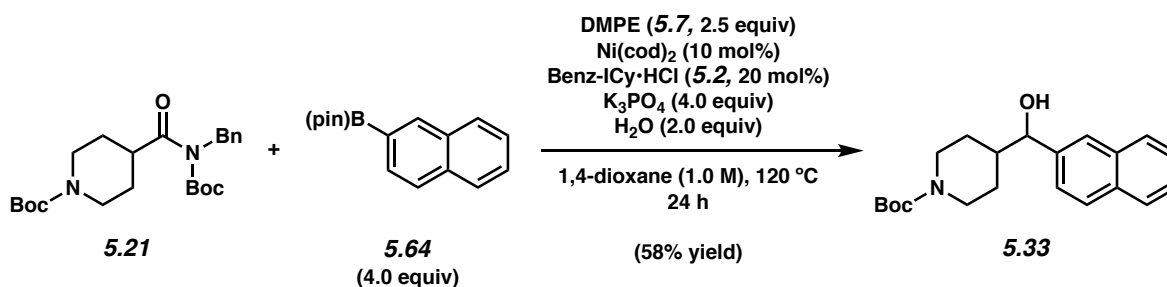

Alcohol 5.29. Crude alcohol **5.29** was synthesized following General Procedure B. Purification by flash chromatography (19:1 Hexanes:EtOAc → 3:1 Hexanes:EtOAc) afforded alcohol **5.29** (59%

yield, average of two experiments) as a white solid. Alcohol **5.29**: mp: 97–99 ºC; R_f 0.36 (2:1

Hexanes:EtOAc); ^{1}H NMR (500 MHz, CDCl$_3$): δ 7.23 (t, J = 7.5, 1H), 7.12–7.09 (m, 3H), 4.33

(d, J = 7.9, 1H), 4.02 (dd, J = 11.4, 4.4, 1H), 3.90 (dd, J = 11.4, 4.4, 1H), 3.37 (td, J = 11.9, 2.3,

1H), 3.29 (td, J = 11.9, 2.3, 1H), 2.36 (s, 3H), 1.93–1.90 (m, 1H), 1.89–1.79 (m, 2H), 1.47 (qd, J

= 12.2, 4.5, 1H), 1.32 (qd, J = 12.2, 4.6, 1H), 1.18–1.15 (m, 1H); ^{13}C NMR (125 MHz, CDCl$_3$): δ

143.0, 138.2, 128.7, 128.4, 127.4, 123.8, 79.1, 68.0, 67.8, 42.5, 29.5, 29.4, 21.6; IR (film): 3409,

2950, 2848, 1135, 1089, 1035 cm^{-1}; HRMS-APCI (m/z) [M + H]$^+$ calcd for C$_{13}$H$_{19}$O$_2$$^+$, 207.13796;

found 207.13826.

Alcohol 5.30. Crude alcohol **5.30** was synthesized following General Procedure B. Purification by

flash chromatography (19:1 Hexanes:EtOAc → 3:1 Hexanes:EtOAc) afforded alcohol **5.30** (62%

yield, average of two experiments) as a white solid. Alcohol **5.30**: mp: 71–74 ºC; R_f 0.25 (2:1

Hexanes:EtOAc); ^{1}H NMR (500 MHz, CDCl$_3$): δ 7.24–7.13 (m, 4H), 4.33 (d, J = 7.9, 1H), 4.02

(dd, J = 11.8, 4.4, 1H), 3.89 (dd, J = 11.2, 4.8, 1H), 3.37 (td, J = 11.9, 2.3, 1H), 3.28 (td, J = 11.9,

2.3, 1H), 2.34 (s, 3H), 1.94–1.91 (m, 1H), 1.86–1.79 (m, 1H), 1.46 (qd, J = 12.3, 4.7, 1H), 1.30

(qd, J = 12.3, 4.7, 1H), 1.17–1.13 (m, 1H); ^{13}C NMR (125 MHz, CDCl$_3$): δ 143.0, 137.6, 129.2,

126.7, 78.8, 68.0, 67.8, 42.5, 29.6, 29.3, 21.3; IR (film): 3410, 2950, 2847, 1089, 1033, 1017 cm^{-1}; HRMS-APCI (m/z) [M + H]$^+$ calcd for C$_{13}$H$_{19}$O$_2$$^+$, 207.13796; found 207.13823.
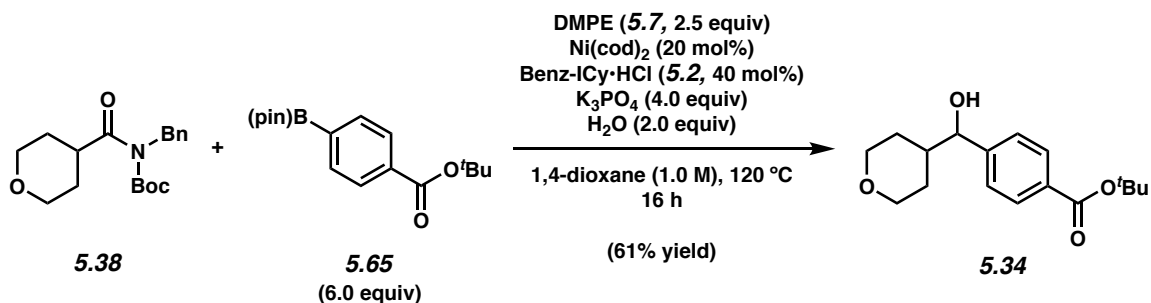
Alcohol 5.31. Crude alcohol **5.31** was synthesized following General Procedure B. Purification by flash chromatography (PhH → 9:1 PhH:Acetone) afforded alcohol **5.31** (62% yield, average of two experiments) as a clear oil. Alcohol **5.31**: R_f 0.26 (9:1 PhH:Acetone); ^{1}H NMR (500 MHz, CDCl$_3$): δ 7.51 (d, J = 8.1, 2H), 7.30 (d, J = 8.1, 2H), 4.37 (d, J = 7.5, 1H), 4.02 (dd, J = 11.4, 4.6, 1H), 3.90 (dd, J = 11.4, 4.6, 1H), 3.37 (td, J = 12.0, 2.3, 1H), 2.29 (td, J = 12.0, 2.3, 1H), 1.95–1.89 (m, 1H), 1.89–1.74 (m, 2H), 1.47 (app qd, J = 12.6, 4.7, 1H), 1.39–1.29 (m, 1H), 1.22–1.16 (m, 1H), 0.26 (s, 9H); ^{13}C NMR (125 MHz, CDCl$_3$): δ 143.5, 140.2, 133.6, 126.1, 79.0, 68.0, 67.8, 42.4, 29.4, 29.3, –0.98; IR (film): 3409, 2953, 2846, 1247, 831 cm^{-1}; HRMS-APCI (m/z) [M + K]$^+$ calcd for C$_{15}$H$_{24}$O$_2$SiK$^+$, 303.11771; found 303.11798.
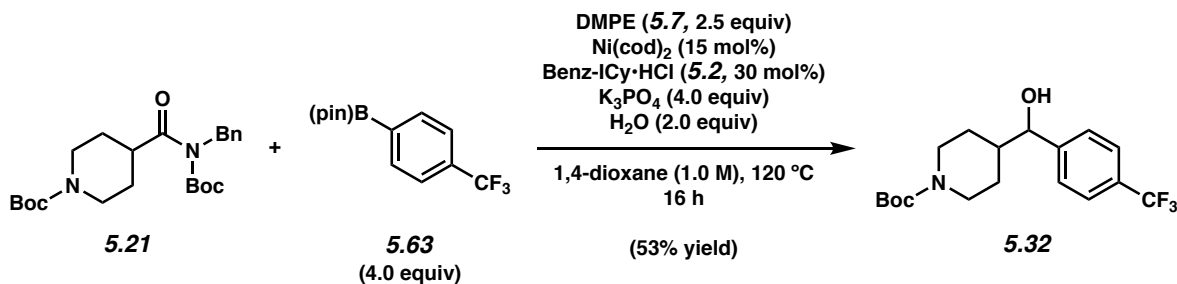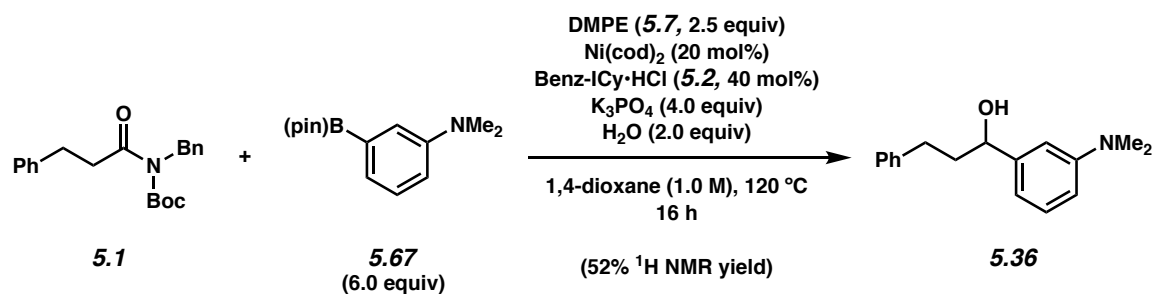

Alcohol 5.32. Crude alcohol **5.32** was synthesized following General Procedure B. Purification by flash chromatography (PhH → 9:1 PhH:Acetone) afforded alcohol **5.32** (53% yield, average of two experiments) as a clear oil. Alcohol **5.32**: mp: 140–143 ºC; R_f 0.29 (9:1 PhH:Acetone). ^{1}H NMR (500 MHz, CDCl$_3$): δ 7.61 (d, J = 8.3, 2H), 7.43 (d, J = 8.3, 2H), 4.48 (d, J = 7.1, 1H), 4.29–

3.93 (m, 2H), 2.77–2.45 (m, 2H), 2.01 (br s, 1H), 1.93–1.84 (m, 1H), 1.80–1.69 (m, 1H), 1.44 (s, 9H), 1.34–1.12 (m, 4H); ^{13}C NMR (125 MHz, CDCl$_3$): δ 154.9, 147.1, 130 (q, J = 32), 127.0, 125.4 (q, J = 3.6), 125.4, 125.3, 123.1, 79.6, 77.9, 43.7, 28.6, 28.4, 27.9; IR (film): 3418, 2932, 2859, 1666, 1325, 1162, 1125 cm^{-1}; HRMS-APCI (m/z) [M]$^+$ calcd for C$_{18}$H$_{24}$F$_3$NO$_3^+$, 359.17028; found 359.17126.

*Note: **5.32** was obtained as a mixture of rotamers. These data represent empirically observed chemical shifts from the ^{1}H NMR and ^{13}C NMR spectra.*
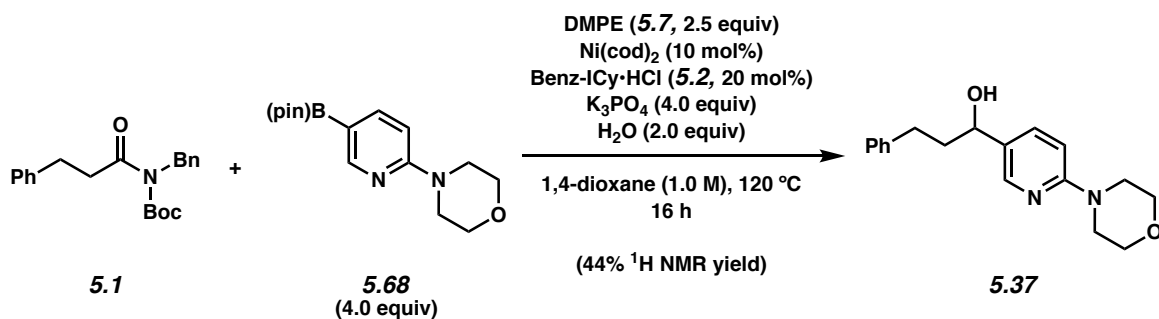

Alcohol 5.33. Crude alcohol **5.33** was synthesized following General Procedure B. Purification by flash chromatography (PhH → 9:1 PhH:Acetone) afforded alcohol **5.33** (58% yield, average of two experiments) as a clear oil. Alcohol **5.33**: R$_f$ 0.39 (9:1 PhH:Acetone); ^{1}H NMR (500 MHz, CDCl$_3$): δ 7.89–7.80 (m, 3H), 7.73, (s, 1H), 7.53–7.43 (m, 3H), 4.56 (d, J = 7.5, 1H), 4.17 (app d, J = 13.4, 1H), 4.04 (app d, J = 13.4, 1H), 2.68 (td, J = 12.9, 2.7, 1H), 2.58 (td, J = 12.9, 2.7, 1H), 2.04–1.98 (m, 1H), 1.89–1.82 (m, 1H), 1.43 (s, 9H), 1.36–1.15 (m, 4H); ^{13}C NMR (125 MHz, CDCl$_3$, 16 of 17 observed): δ 154.9, 140.5, 133.3, 133.2, 128.4, 128.0, 127.8, 126.4, 126.1, 125.7, 124.5, 79.4, 78.8, 43.5, 28.6, 28.4; IR (film): 3418, 2974, 2929, 2856, 1666, 1425, 1162 cm^{-1}; HRMS-APCI (m/z) [M + H]$^+$ calcd for C$_{21}$H$_{28}$NO$_3^+$, 342.20637; found 342.20615.

Alcohol 5.34. Crude alcohol **5.34** was synthesized following General Procedure B. Purification by flash chromatography (19:1 Hexanes:EtOAc → 3:1 Hexanes:EtOAc) generated alcohol **5.34** (61% yield, average of two experiments) as a clear oil. Alcohol **5.34**: R_f 0.18 (2:1 Hexanes:EtOAc); ^{1}H NMR (500 MHz, CDCl$_3$): δ 8.00–7.95 (m, 2H), 7.39–7.34 (m, 2H), 4.45 (d, J = 7.2, 1H), 4.01 (app dd, J = 11.4, 4.2, 1H), 3.90 (app dd, J = 11.4, 4.2, 1H), 3.35 (td, J = 12.0, 2.0, 1H), 3.27 (td, J = 12.0, 2.0, 1H), 1.91 (br s, 1H), 1.88–1.78 (m, 2H), 1.59 (s, 9H), 1.52–1.42 (m, 1H), 1.40–1.31 (m, 1H), 1.18–1.14 (m, 1H); ^{13}C NMR (125 MHz, CDCl$_3$): δ 165.7, 147.5, 131.6, 129.7, 128.5, 126.5, 81.2, 78.4, 68.0, 67.7, 42.6, 29.3, 29.1, 28.3; IR (film): 3417, 2953, 2848, 1710, 1292, 1117 cm^{-1}; HRMS-APCI (*m/z*) [M + H]$^+$ calcd for C$_{17}$H$_{25}$O$_4^+$, 293.17474; found 293.17416.
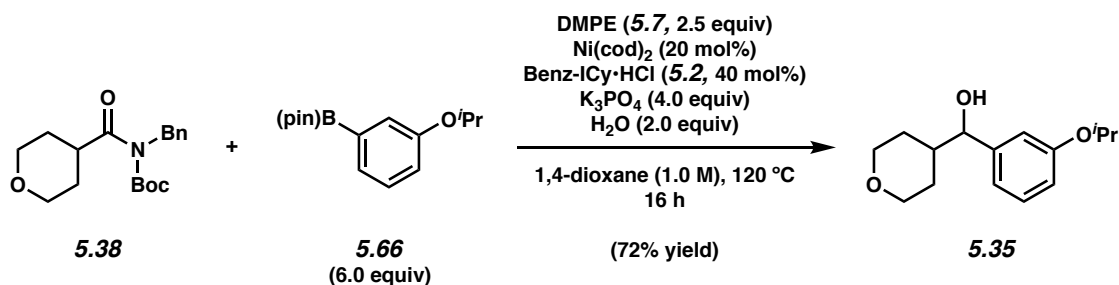
Alcohol 5.35. Crude alcohol **5.35** was synthesized following General Procedure B. Purification by flash chromatography (PhH → 9:1 PhH:Acetone) generated alcohol **5.35** (72% yield, average of two experiments) as a clear oil. Alcohol **5.35**: R_f 0.31 (9:1 PhH:Acetone); ^{1}H NMR (500 MHz, CDCl$_3$): δ 7.24 (t, J = 8.1, 1H), 6.87–6.84, (m, 2H), 6.81 (ddd, J = 8.1, 2.5, 0.85, 1H), 4.56 (sept,

J = 6.0, 1H), 4.32 (d, J = 7.6, 1H), 4.02 (app dd, J = 11.4, 4.2, 1H), 3.90 (app dd, J = 11.4, 4.2, 1H), 3.36 (td, J = 12.0, 2.2, 1H), 3.28 (td, J = 11.8, 2.2, 1H), 1.94–1.87 (m, 1H), 1.87–1.78 (m, 1H), 1.58 (br s, 1H) 1.46 (qd, J = 12.3, 4.6, 1H), 1.34 (d, J = 6.1), 1.33 (qd, J = 12.3, 4.4) (7H total), 1.23–1.15 (m, 1H); ^{13}C NMR (125 MHz, CDCl$_3$): δ 158.1, 144.7, 129.5, 118.9, 115.0, 114.3, 78.9, 69.9, 68.0, 67.8, 42.5, 29.4, 29.3, 22.2; IR (film): 3406, 2974, 2847, 1599, 1583, 1253, 1116 cm^{-1}; HRMS-APCI (m/z) [M]$^+$ calcd for C$_{15}$H$_{22}$O$_3$$^+$, 250.15635; found 250.15623.
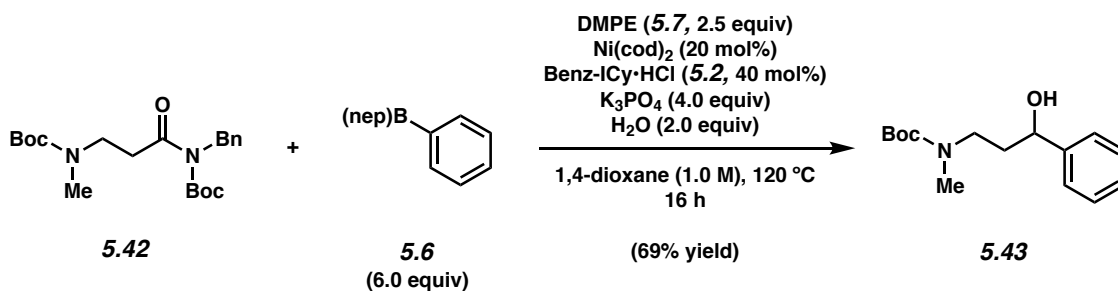

Alcohol 5.36. Crude alcohol **5.36** was synthesized following General Procedure C. ^{1}H NMR analysis of the crude reaction mixture indicated an 52% yield of alcohol **5.36** relative to 1,3,5-trimethoxybenzene external standard (average of two experiments). Purification by preparative thin-layer chromatography (9:1 PhH:Acetone) provided an analytical sample of alcohol **5.36** as a clear oil. Alcohol **5.36**: R$_f$ 0.54 (2:1 Hex:EtOAc); ^{1}H NMR (500 MHz, CDCl$_3$): δ 7.30–7.26 (m, 2H), 7.25–7.14 (m, 3H), 6.75–6.72 (m, 1H), 6.70 (app d, J = 7.5, 1H), 6.66 (ddd, J = 8.5, 2.6, 0.8, 1H), 4.62 (ddd, J = 8.3, 5.4, 3.3, 1H), 2.96 (s, 6H), 2.77 (ddd, J = 14.5, 9.8, 5.8, 1H), 2.69 (ddd, J = 14.5, 9.8, 6.4, 1H), 2.20–2.10 (m, 1H), 2.10–1.99 (m, 1H), 1.81 (d, J = 3.3, 1H); ^{13}C NMR (125 MHz, CDCl$_3$): δ 151.0, 145.7, 142.1, 129.4, 128.6, 128.5, 125.9, 114.3, 112.1, 110.1, 74.6, 40.8, 40.4, 32.3; IR (film): 3366, 3025, 2918, 2858, 2801, 1602, 1495, 697 cm^{-1}; HRMS-APCI (m/z) [M + H]$^+$ calcd for C$_{17}$H$_{22}$NO$^+$, 256.16959; found 256.16915.

Alcohol 5.37. Crude alcohol **5.37** was synthesized following General Procedure C. ^{1}H NMR analysis of the crude reaction mixture indicated a 44% yield of alcohol **5.37** and 56% yield of the corresponding ketone intermediate relative to 1,3,5-trimethoxybenzene external standard (average of two experiments). Preparation of an authentic sample of alcohol **5.37** (see section 5.8.2.7 for experimental details) allowed for direct comparison with the ^{1}H NMR spectrum of the crude reaction mixture and full characterization. Alcohol **5.37**: R_f 0.45 (3:1 PhH:Acetone); ^{1}H NMR (500 MHz, CDCl$_3$): δ 8.15 (d, J = 2.4, 1H), 7.55 (dd, J = 8.8, 2.4, 1H), 7.31–7.26 (m, 2H), 7.22–7.15 (m, 3H), 6.65 (d, J = 8.8, 1H), 4.65–4.59 (m, 1H), 3.83 (app t, J = 4.8, 4H), 3.50 (app t, J = 4.8, 4H), 2.76–2.58 (m, 2H), 2.20–2.10 (m, 1H), 2.06–1.95 (m, 1H), 1.78–1.68 (m, 1H); ^{13}C NMR (125 MHz, CDCl$_3$): δ 159.6, 146.3, 141.7, 135.8, 129.5, 128.56, 128.55, 126.1, 107.1, 71.6, 66.9, 45.8, 40.0, 32.2; IR (film): 3391, 3025, 2918, 2855, 1605, 1494, 1245 cm^{-1}; HRMS-APCI (*m/z*) [M + H]$^+$ calcd for C$_{18}$H$_{23}$N$_2$O$_2$$^+$, 299.17540; found 299.17471.

Note: ^{1}H NMR and ^{13}C NMR spectra of the authentic material, as prepared in section 5.8.2.7, are provided. A ^{1}H NMR spectrum of the crude material obtained using the reaction conditions above is also provided and matches the ^{1}H NMR spectrum of the authentic material.

5.8.2.6 Syntheses of Alcohols 5.40 and 5.43
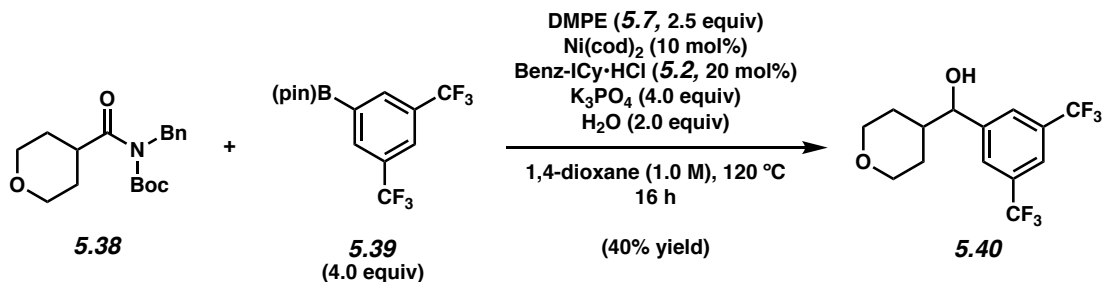
Alcohol 5.40. Crude alcohol **5.40** was synthesized following General Procedure B. Purification by

flash column chromatography (19:1 Hexanes:EtOac → 3:1 Hexanes:EtOAc) afforded alcohol **5.40**

(40% yield, average of two experiments) as a clear oil. Alcohol **5.40**: R_f 0.45 (2:1 Hexanes:EtOAc);

^{1}H NMR (500 MHz, CDCl$_3$): δ 7.81 (s, 1H), 7.78 (s, 2H), 4.58 (dd, J = 6.9, 3.5, 1H), 4.03 (app dd,

J = 11.6, 4.3, 1H), 3.95 (app dd, J = 11.6, 4.2, 1H), 3.36 (td, J = 12.1, 2.0), 3.32 (td, J = 12.1, 2.0)

(2H total), 2.08 (d, J = 3.5, 1H), 1.90–1.80 (m, 1H), 1.79–1.72 (m, 1H), 1.49 (qd, 12.3, 4.6), 1.43

(qd, J = 12.3, 4.7) (2H total), 1.29–1.19 (m, 1H); ^{13}C NMR (125 MHz, CDCl$_3$): δ 145.6, 131.8 (q,

J = 33), 126.8, 126.7, 124.5, 122.3, 121.8 (sept, J = 3.7), 77.5, 67.8, 67.6, 42.6, 29.1, 28.4; IR

(film): 3401, 2956, 2855, 1277, 1128 cm^{-1}; HRMS-APCI (m/z) [M + H]$^+$ calcd for C$_{14}$H$_{15}$F$_6$O$_2$$^+$,

329.09708; found 329.09637.

Alcohol 5.43. Crude alcohol **5.43** was synthesized following General Procedure B. Purification by

flash column chromatography (PhH → 9:1 PhH:Acetone) yield alcohol **5.43** (69% yield, average

of two experiments) as a clear oil. Alcohol **5.43**: R_f 0.48 (2:1 Hexanes:EtOAc); ^{1}H NMR (400

MHz, CDCl$_3$): δ 7.42–7.18 (m, 5H), 4.60 (br s, 1H), 4.33 (br s), 3.90 (br s), 3.47 (br s), 3.30–2.92

(m), 2.50 (br s), (total 3H), 2.87 (s, 3H), 2.00–1.88 (m, 1H), 1.88–1.67 (m, 1H), 1.47 (s, 9H).

Spectral data match those previously reported.[60]

*Note: **5.43** was obtained as a mixture of rotamers. These data represent empirically observed*

chemical shifts from the ^{1}H NMR spectrum.

5.8.2.7 Syntheses of Authentic Samples of Alcohols 5.13 and 5.37
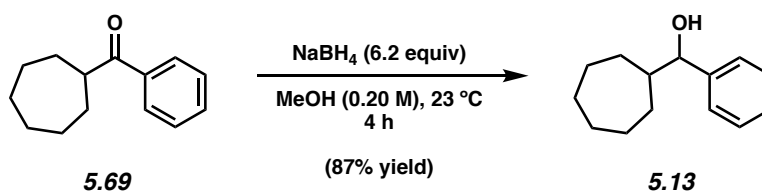
To a flame-dried 1-dram vial equipped with a magnetic stir bar was added the ketone **5.69**

(11.4 mg, 0.0560 mmol, 1.00 equiv) in MeOH. The solvent was then evaporated under reduced

pressure. The vial was then capped with a septum cap, and the atmosphere was purged with N$_2$.

To the vial was added MeOH (0.300 mL, 0.190 M) and the reaction was stirred to give a

homogeneous solution. NaBH$_4$ (6.80 mg, 0.180 mmol, 3.20 equiv) was added in a single portion

and the vial was stirred at 23 °C. After 1 h, NaBH$_4$ (6.40 mg, 0.170 mmol, 3.00 equiv) was added

in a single portion and the vial was stirred at 23 °C. After 3 h, the reaction was quenched with H$_2$O

(2 mL). The aqueous layer was extracted with EtOAc (4 x 3 mL), the combined organic layers

were dried over anhydrous MgSO$_4$, and the volatiles were removed under reduced pressure. The

resulting crude residue was purified by preparative thin-layer chromatography (5:1

Hexanes:EtOAc) to yield alcohol **5.13** as a clear oil (10.0 mg, 87% yield).

Note: See section 5.8.2.4 for chemical shifts from the ^{1}H NMR and ^{13}C NMR spectra.
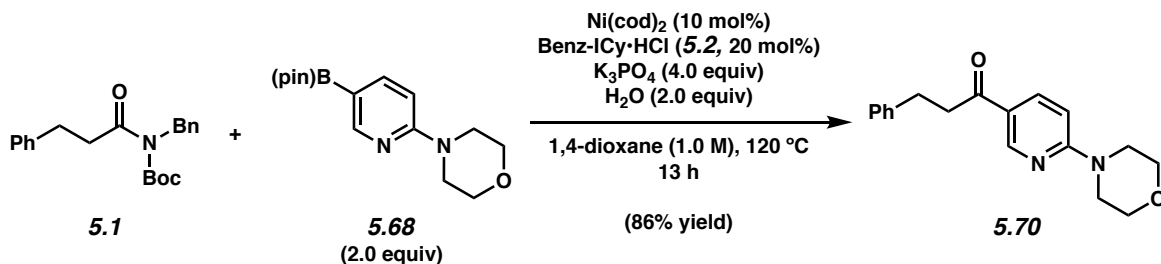
A 1-dram vial was charged with anhydrous powder K_3PO_4 (170 mg, 0.800 mmol, 4.00 equiv) and a magnetic stir bar. The vial and its contents were flame-dried under reduced pressure and allowed to cool under N_2. Amide substrate **5.1** (67.9 mg, 0.200 mmol, 1.00 equiv) and boronate ester nucleophile **5.68** (116 mg, 0.400 mmol, 2.00 equiv) were added. The vial was flushed with N_2 for 5 min, then water (7.21 μL, 0.400 mmol, 2.00 equiv), which had been sparged with N_2 for 10 min, was added. The vial was taken into a glovebox and charged with $Ni(cod)_2$ (5.50 mg, 10 mol%) and Benz-ICy•HCl (**5.2**, 12.8 mg, 20 mol%). Subsequently, 1,4-dioxane (200 μL, 1.00 M) was added. The vial was sealed with a Teflon-lined screw cap, removed from the glovebox, and stirred vigorously (800 RPM) at 120 ºC for 13 h. After cooling to 23 ºC, the mixture was quenched by the addition of saturated aqueous NH_4Cl (1 mL) and extracted with EtOAc (3 x 2 mL). The combined organic layers were then filtered over a plug of silica gel (3 cm) and Na_2SO_4 (3 cm) using EtOAc (10 mL) as eluent. The volatiles were removed under reduced pressure and the resulting crude residue was purified by flash column chromatography (9:1 Hexanes:EtOAc → EtOAc) to yield ketone **5.70** as a clear oil (10.0 mg, 87% yield). Alcohol **5.70**: ^{1}H NMR (500 MHz, CDCl₃): δ 8.78 (d, J = 2.3, 1H), 8.05 (dd, J = 9.1, 2.3, 1H), 7.32–7.28 (m, 2H), 7.26–7.18 (m, 3H), 6.60 (d, J = 9.1, 1H), 3.81 (t, J = 5.0, 4H), 3.67 (t, J = 5.0, 4H), 3.19 (t, J = 7.5, 4H), 3.05 (t, J = 7.5, 4H). Spectral data match those previously reported.[61]

5.70 → 5.37

NaBH₄ (2.7 equiv)

MeOH (0.30 M), 23 °C
4 h

(50% yield)
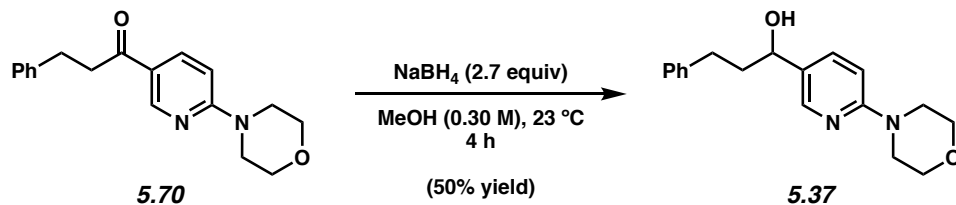
To a flame-dried 1-dram vial equipped with a magnetic stir bar was added NaBH₄ (17.0 mg, 0.450 mmol, 2.70 equiv). The ketone **5.70** (50.0 mg, 0.0170 mmol, 1.00 equiv) was dissolved in MeOH (0.60 mL, 0.30 M) and added to the vial. After 1 h, the reaction was quenched with H₂O (2 mL). The aqueous layer was extracted with EtOAc (4 x 3 mL), the combined organic layers were dried over anhydrous NaSO₄, and the volatiles were removed under reduced pressure. The resulting crude residue was purified by preparative TLC (1:1 Hexanes:EtOAc) to yield alcohol **5.37** as a clear oil (25.0 mg, 50% yield).

Note: See section 5.8.2.5 for chemical shifts from the ¹H NMR and ¹³C NMR spectra.

5.8.2.8 Robustness Screen

Table 5.2. Evaluation of functional group compatibility in the Suzuki–Miyaura coupling and transfer hydrogenation cascade
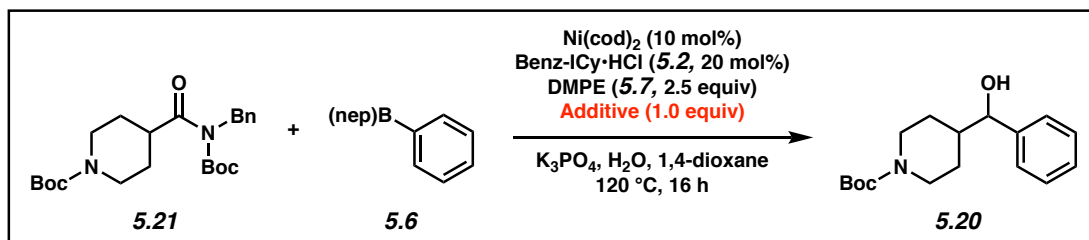
Entry	Additive	Yield of 5.20 (%)	Additive Remaining (%)	SM Remaining (%)	Entry	Additive	Yield of 5.20 (%)	Additive Remaining (%)	SM Remaining (%)
1	–	81	N.D.	0	9	(benzamide, NH₂)	13	0	0
2	(1-adamantanol, OH)	89	>99	0	10	(N-methylbenzamide, NHMe)	58	88	0
3	(Ph-NH-n-Bu)	83	>99	0	11	(Ph alkyne Et)	68	0	0
4	(Me-C(O)-O-t-Bu)	42	N.D.[b]	0	12	(Ph epoxide Ph)	22	18	0
5	(hydrocinnamaldehyde, H)	43	0	0	13	(quinoline, N)	88	98	0
6	(cyclohexyl CN)	0	0	0	14	(dibenzofuran)	68	94	0
7	(phenol, OH)	0	0	0	15	(benzofuran)	25	0	0
8	(benzoic acid, OH)	31	0	0	16	(N-methylindole, Me)	78	80	0

Conditions: amide **5.21** (0.20 mmol, 1.00 equiv), PhB(nep) (**5.6**, 0.80 mmol, 4.00 equiv), DMPE (**5.7**, 0.50 mmol, 2.50 equiv), additive (0.20 mmol, 1.00 equiv), Ni(cod)$_2$ (0.020 mmol, 10 mol%), Benz-ICy•HCl (**5.2**, 0.040 mmol, 20 mol%), K$_3$PO$_4$ (0.80 mmol, 4.00 equiv), H$_2$O (0.40 mmol, 2.00 equiv), and 1,4-dioxane (1.0 M) in a sealed vial at 120 °C for 16 h. Yields of coupled product, remaining additive, and remaining starting material were determined by ^{1}H NMR analysis using 1,3,5-trimethoxybenzene or hexamethylbenzene as an external standard.

5.8.2.9 Benchtop Variants of Methodology

5.8.2.9.1 Procedure A: Employing a paraffin wax encapsulation approach. Note: The supporting information for the preparation of Ni(cod)$_2$/Benz-ICy–paraffin capsules has been previously reported.[62]
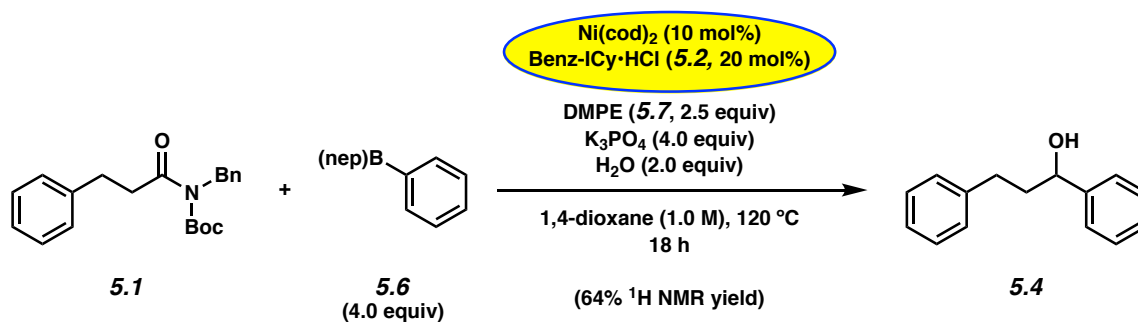
A 2-dram vial was charged with anhydrous powder K$_3$PO$_4$ (340 mg, 1.60 mmol, 4.00 equiv) and a magnetic stir bar (egg-shaped 3/8 x 3/16 in). The vial and its contents were flame-dried under reduced pressure and allowed to cool under N$_2$. The vial was then charged with amide substrate **5.1** (136 mg, 0.40 mmol, 1.00 equiv), boronate ester nucleophile **5.6** (304 mg, 1.60 mmol, 4.00 equiv), DMPE (**7**, 165 mg, 1.00 mmol, 2.50 equiv), and a paraffin wax capsule containing Ni(cod)$_2$ (11.0 mg, 0.0400 mmol, 10 mol%) and Benz-ICy•HCl (**5.2**, 25.5 mg, 0.0800 mmol, 20 mol%) were added. The vial was purged with N$_2$ and subsequently deionized water (14.0 µL, 0.80 mmol, 2.00 equiv) and 1,4-dioxane (0.400 mL, 1.00 M), which had been sparged with N$_2$ for 10 min, were added. The vial was capped with a Teflon-lined screw cap under a flow of N$_2$ and the reaction mixture was stirred vigorously (800 RPM) at 120 ℃ for 18 h. After removing the vial from heat, the reaction mixture was transferred to a 100 mL pear-shaped flask containing 2.0 g of silica gel with hexanes (6 mL) and CH$_2$Cl$_2$ (6 mL). The mixture was adsorbed onto the silica gel under reduced pressure and filtered over a plug of silica gel (4.0 cm OD x 3.0 cm, 300 mL of hexanes eluent to remove paraffin, then 250 mL of EtOAc eluent). The volatiles were removed under

reduced pressure. ^{1}H NMR analysis of the crude reaction mixture indicated a 64% yield of alcohol **5.4** relative to 1,3,5-trimethoxybenzene external standard (average of two experiments).

5.8.2.9.2 Procedure B: Employing an air-stable Ni(II) precatalyst
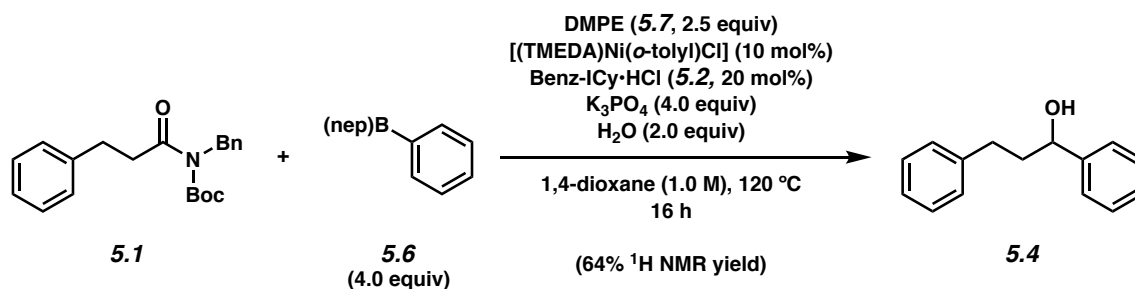
A 1-dram vial was charged with anhydrous powder K$_3$PO$_4$ (170 mg, 0.800 mmol, 4.00 equiv) and a magnetic stir bar. The vial and its contents were flame-dried under reduced pressure and allowed to cool under N$_2$. Amide substrate **5.1** (67.9 mg, 0.200 mmol, 1.00 equiv), boronate ester nucleophile **5.6** (152 mg, 0.800 mmol, 4.00 equiv), DMPE (**7**, 82.6 mg, 0.500 mmol, 2.50 equiv), [(TMEDA)Ni(*o*-tolyl)Cl]^{48} (6.03 mg, 0.0200 mmol, 10 mol%), and Benz-ICy•HCl (**5.2**, 12.8 mg, 0.0400 mmol, 20 mol%) were added. The vial was flushed with N$_2$ for 5 min, then water (7.21 µL, 0.400 mmol, 2.00 equiv) and 1,4-dioxane (200 µL, 1.00 M), which had been sparged with N$_2$ for 10 min, were added. The vial was capped with a Teflon-lined screw cap under a flow of N$_2$ and the reaction mixture was stirred vigorously (800 RPM) at 120 ºC for 16 h. After cooling to 23 ºC, the mixture was quenched by the addition of saturated aqueous NH$_4$Cl (1 mL) and extracted with EtOAc (3 x 2 mL). The combined organic layers were then filtered over a plug of silica gel (3 cm) and Na$_2$SO$_4$ (3 cm) using EtOAc (10 mL) as eluent. The volatiles were removed under reduced pressure. ^{1}H NMR analysis of the crude reaction mixture indicated a 64% yield of alcohol **4** relative to 1,3,5-trimethoxybenzene external standard.

5.8.2.10 Enantioselectivity Experiments

5.1

5.6
(4.0 equiv)

Ligand A (**5.71**, 20 mol%)
DMPE (**5.7**, 2.5 equiv)
Ni(cod)$_2$ (10 mol%)
K$_3$PO$_4$ (4.0 equiv)
H$_2$O (2.0 equiv)

1,4-dioxane (1.0 M), 120 °C
16 h

(36% ^{1}H NMR yield, 20% *ee*)

5.4
(Not absolute stereochemistry)

A 1-dram vial was charged with anhydrous powder K$_3$PO$_4$ (170 mg, 0.800 mmol, 4.00 equiv) and a magnetic stir bar. The vial and its contents were flame-dried under reduced pressure and allowed to cool under N$_2$. Amide substrate **5.1** (67.9 mg, 0.200 mmol, 1.00 equiv), boronate ester nucleophile **5.6** (152 mg, 0.800 mmol, 4.00 equiv), and DMPE (**5.7**, 82.6 mg, 0.500 mmol, 2.50 equiv) were added. The vial was flushed with N$_2$ for 5 min, then water (7.21 μL, 0.400 mmol, 2.00 equiv), which had been sparged with N$_2$ for 10 min, was added. The vial was taken into a glovebox and charged with Ni(cod)$_2$ (5.50 mg, 0.0200 mmol, 10 mol%) and Ligand A (**5.71**, 15.6 mg, 0.0400 mmol, 20 mol%). Subsequently, 1,4-dioxane (200 μL, 1.00 M) was added. The vial was sealed with a Teflon-lined screw cap, removed from the glovebox, and stirred vigorously (800 RPM) at 120 °C for 16 h. After cooling to 23 °C, the mixture was quenched by the addition of saturated aqueous NH$_4$Cl (1 mL) and extracted with EtOAc (3 x 2 mL). The combined organic layers were then filtered over a plug of silica gel (3 cm) and Na$_2$SO$_4$ (3 cm) using EtOAc (10 mL) as eluent. ^{1}H NMR analysis of the crude reaction mixture indicated a 36% yield of alcohol **5.4** relative to 1,3,5-trimethoxybenzene external standard. Purification by preparative thin-layer chromatography (4:1 Hexanes:EtOAc) provided an analytical sample of enantioenriched alcohol **5.4** as a clear oil.

The spectral data match those previously reported in section 5.8.2.4 of Experimental Procedures

for *rac*-**5.4**.

5.8.2.11 Verification of Enantioenrichment

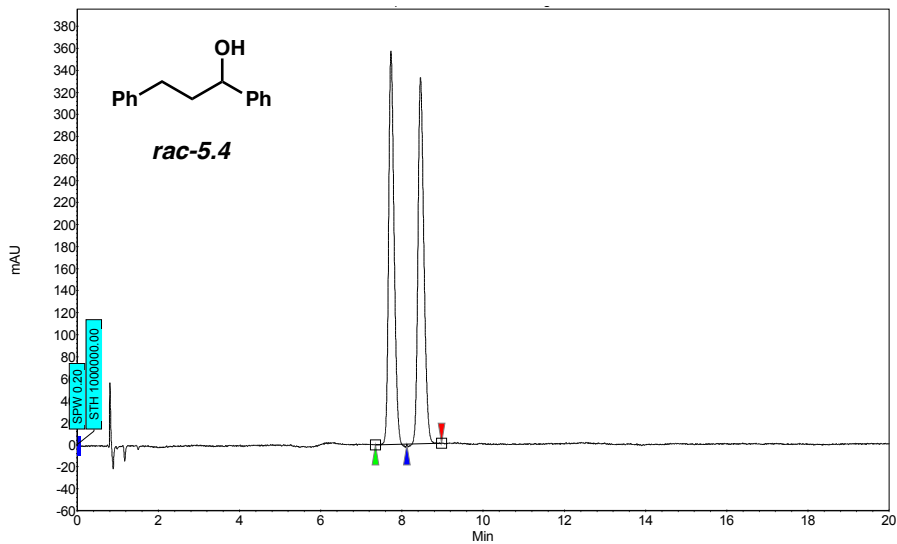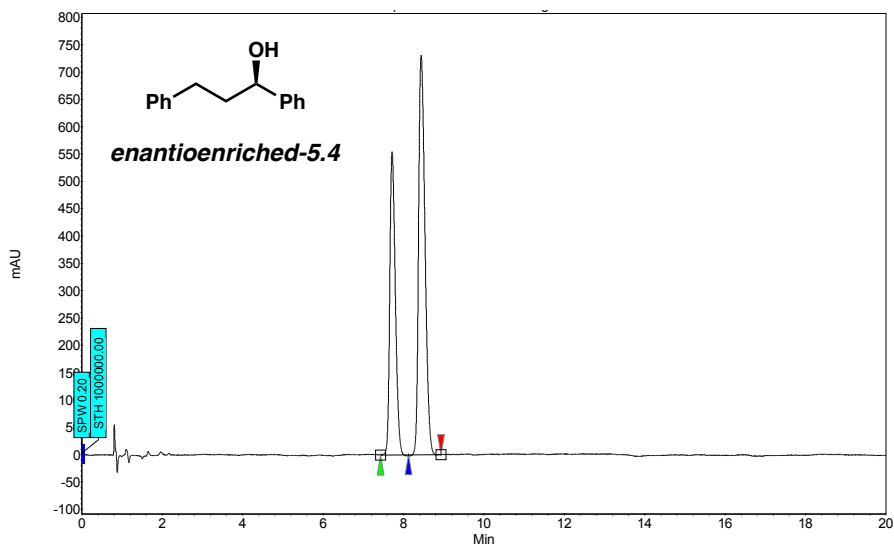*Table 5.3*. Conditions and results of chiral SFC analysis of alcohol products
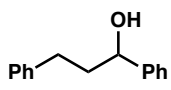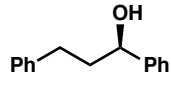
Compound	Method Column/Temp.	Solvent	Method Flow Rate	Retention Times (min)	Enantiomeric Ratio (er)
OH / Ph, Ph / *rac-5.4*	Daicel ChiralPak AD-H/35 °C	1% isopropanol in CO_2	3.5 mL/min	7.35/8.12	50:50
OH / Ph, Ph / *enantioenriched-5.4*	Daicel ChiralPak AD-H/35 °C	1% isopropanol in CO_2	3.5 mL/min	7.43/8.12	40:60

Figure 5.7. SFC trace of *rac*-**5.4** (Table 5.3, Entry 1).

Index	Name	Start	Time	End	RT Offset	Quantity	Height	Area	Area
		[Min]	[Min]	[Min]	[Min]	[% Area]	[µV]	[µV.Min]	[%]
1	UNKNOWN	7.35	7.73	8.12	0.00	49.91	357.5	55.6	49.913
2	UNKNOWN	8.12	8.46	8.98	0.00	50.09	332.4	55.8	50.087
Total						100.00	689.9	111.4	100.000

Figure 5.8. SFC trace of *enantionenriched*-**5.4** (Table 5.3, Entry 2).

Index	Name	Start	Time	End	RT Offset	Quantity	Height	Area	Area
		[Min]	[Min]	[Min]	[Min]	[% Area]	[µV]	[µV.Min]	[%]
1	UNKNOWN	7.43	7.72	8.12	0.00	39.72	554.9	88.6	39.725
2	UNKNOWN	8.12	8.44	8.94	0.00	60.28	731.0	134.5	60.275
Total						100.00	1285.9	223.1	100.000

304

5.8.2.12 Deuterium Incorporation Experiments

5.8.2.12.1 Preparation of deuterated reducing agent *d*-DMPE (*d*-5.7)
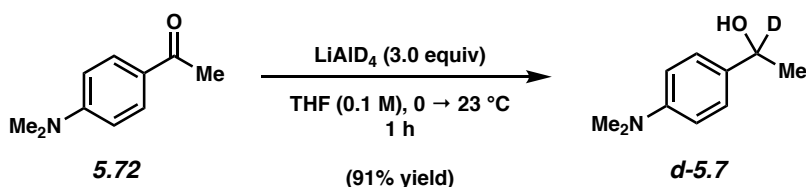
To a flame-dried flask equipped with a magnetic stir bar was added ketone **5.72** (50.0 mg, 0.307 mmol, 1.00 equiv) and THF (3.0 mL, 0.10 M). The flask was cooled to 0 °C and lithium aluminum deuteride (39 mg, 0.921 mmol. 3.00 equiv) was added in a single portion. The reaction was then warmed to 23 °C and stirred for 1 h. The reaction was cooled to 0 °C and quenched by the sequential addition of MeOH (5 mL), and deionized water (3 mL) and the resulting mixture was transferred to a separatory funnel with CH_2Cl_2 (10 mL) and water (10 mL). The aqueous layer was extracted with CH_2Cl_2 (3 x 10 mL), then the organic layers were combined, dried over Na_2SO_4, and evaporated under reduced pressure. Purification of the crude residue by flash chromatography (4:1 Hexanes:EtOAc) afforded deuterated alcohol **d-5.7** (46 mg, 91% yield) as a white solid. Alcohol **d-5.7**: R_f 0.33 (3:1 Hexanes:EtOAc). ^{1}H NMR (500 MHz, $CDCl_3$): δ 7.26 (d, *J* = 9.0, 2H), 6.73 (d, *J* = 9.0, 2H), 2.94 (s, 3 H), 1.62 (s, 1H), 1.48 (s, 3H).

5.8.2.12.2 Deuterium incorporation experiments using *d*-DMPE (*d*-5.7)
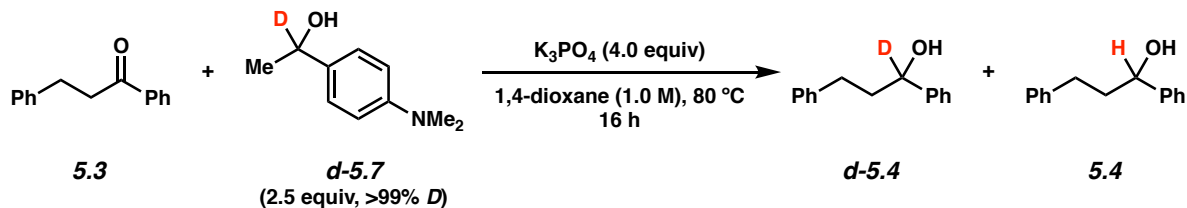
Conversion	Yield of *d*-5.4	Yield of 5.4
75%	75%	0%
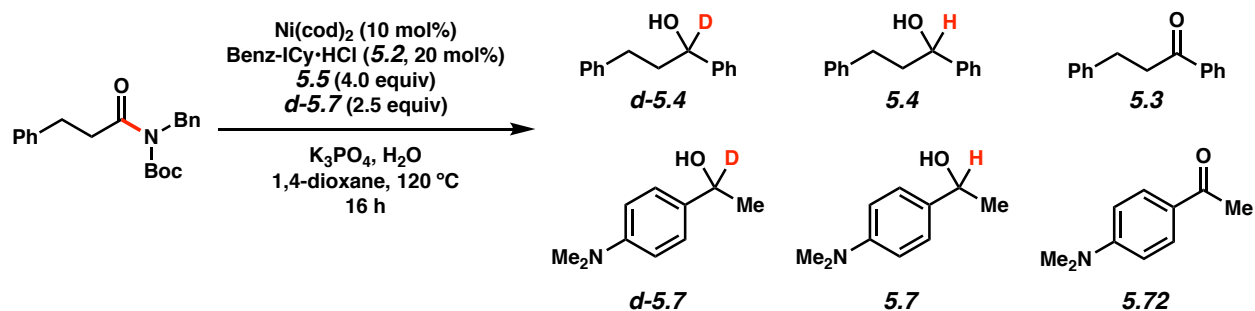
Conversion	Yield *d*-4	Yield 4	Yield 3	Yield *d*-7	Yield 7	Yield 72
100%	0%	72%	15%	58%	1%	30%
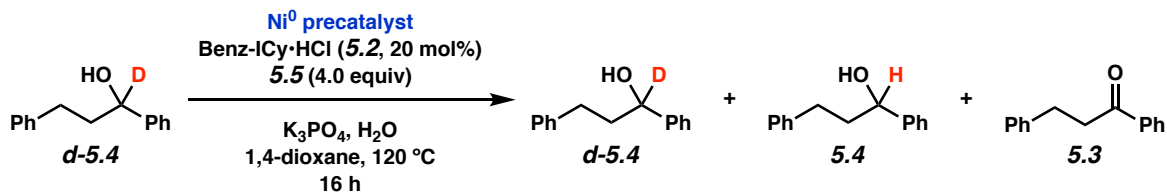
Ni⁰ precatalyst	Yield *d*-4	Yield 4	Yield 3
None	95%	0%	0%
Ni(cod)₂ (10 mol%)	12%	22%	20%

306

5.9 Spectra Relevant to Chapter Five:

Reductive Arylation of Amides via a Nickel-Catalyzed Suzuki–Miyaura Coupling and Transfer Hydrogenation Cascade

Timothy B. Boit,[†] Milauni M. Mehta,[†] Junyong Kim, Emma L. Baker and Neil K. Garg.

Angew. Chem., Int. Ed. **2021**, *60*, 2472–2477.
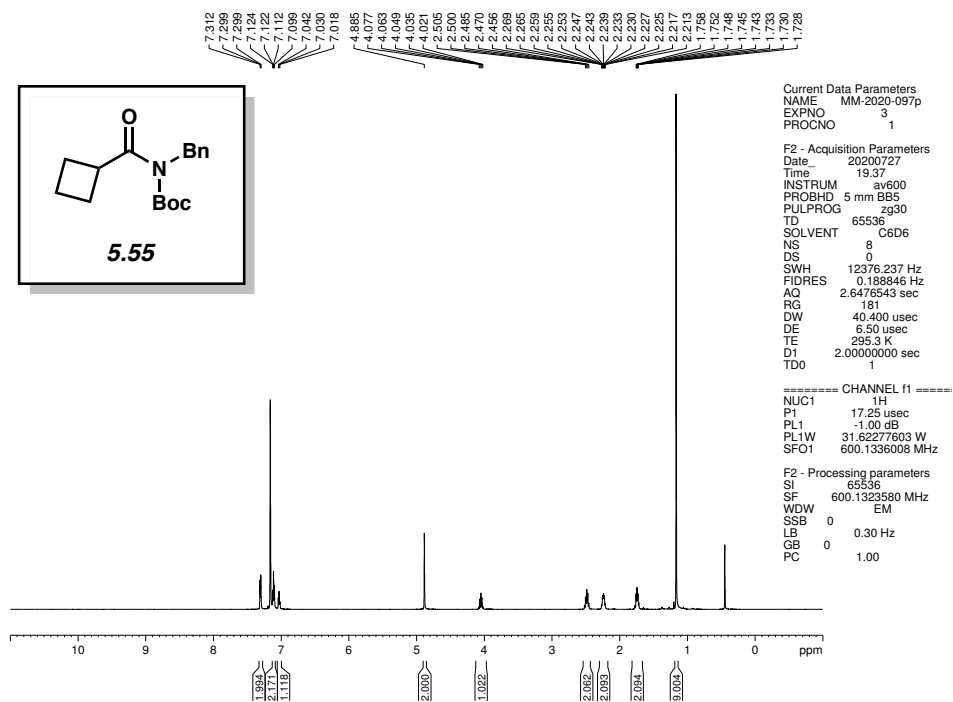
Figure 5.9 ^{1}H NMR (600 MHz, CDCl$_3$) of compound **5.55**.
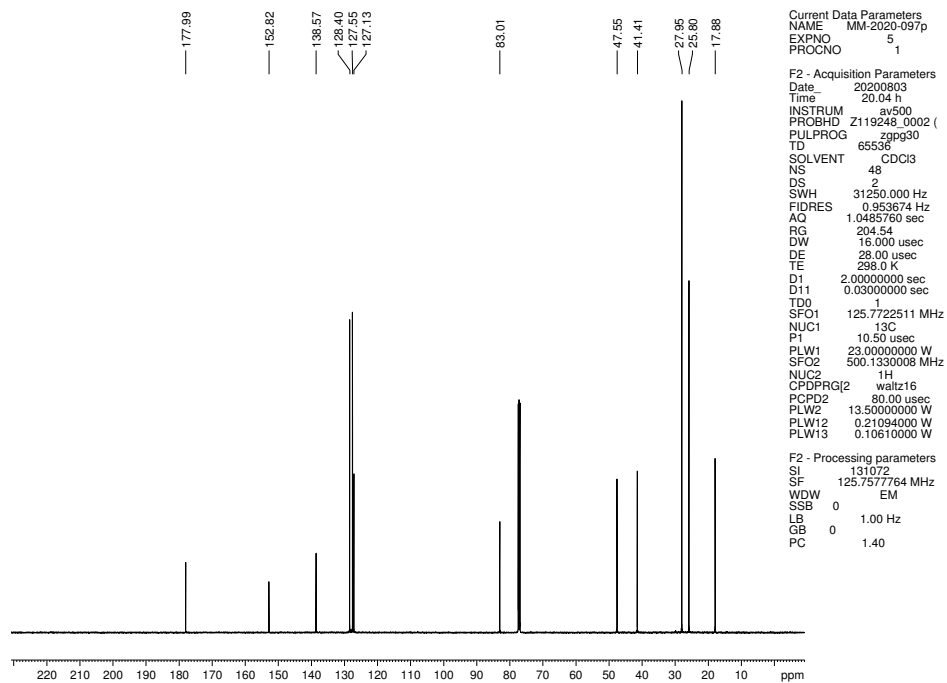
Figure 5.10 ^{13}C NMR (125 MHz, CDCl$_3$) of compound **5.55**.
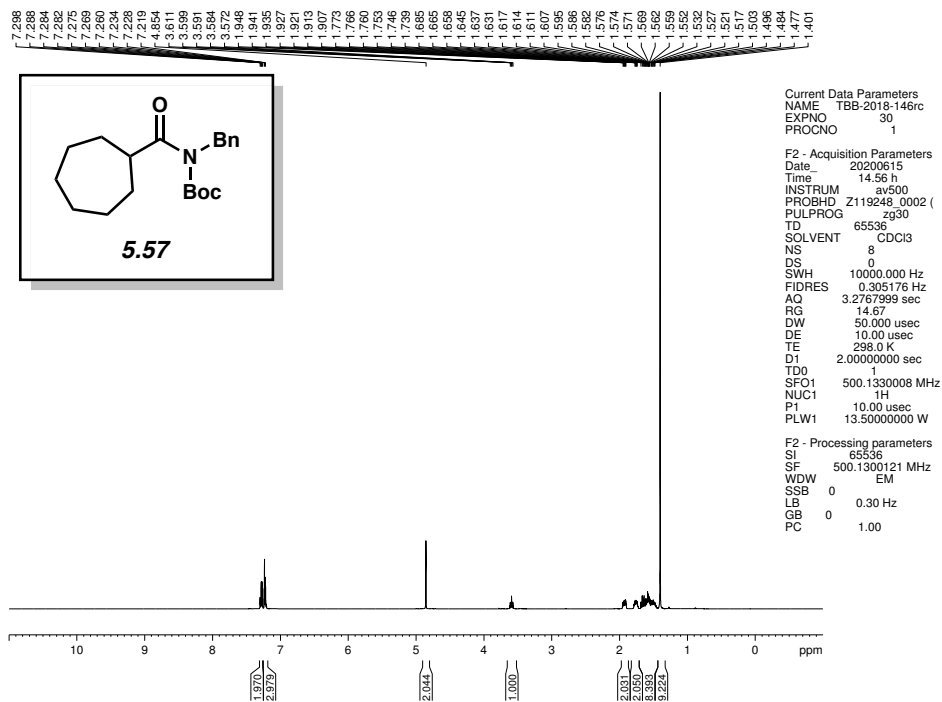
Figure 5.11 ^{1}H NMR (500 MHz, CDCl$_3$) of compound **5.57**.
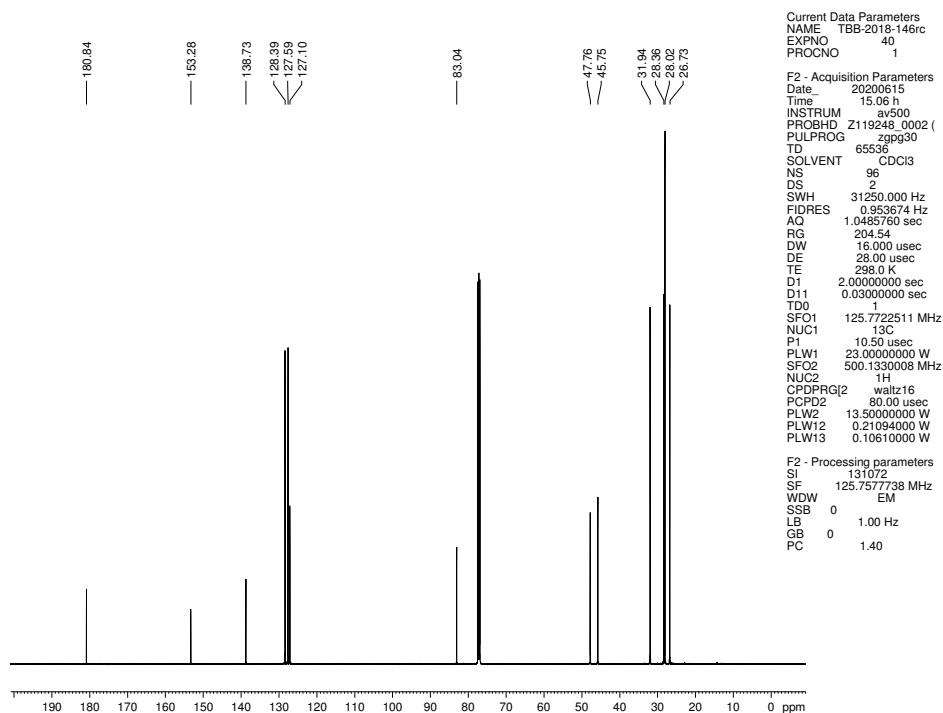
Figure 5.12 ^{13}C NMR (125 MHz, CDCl$_3$) of compound **5.57**.
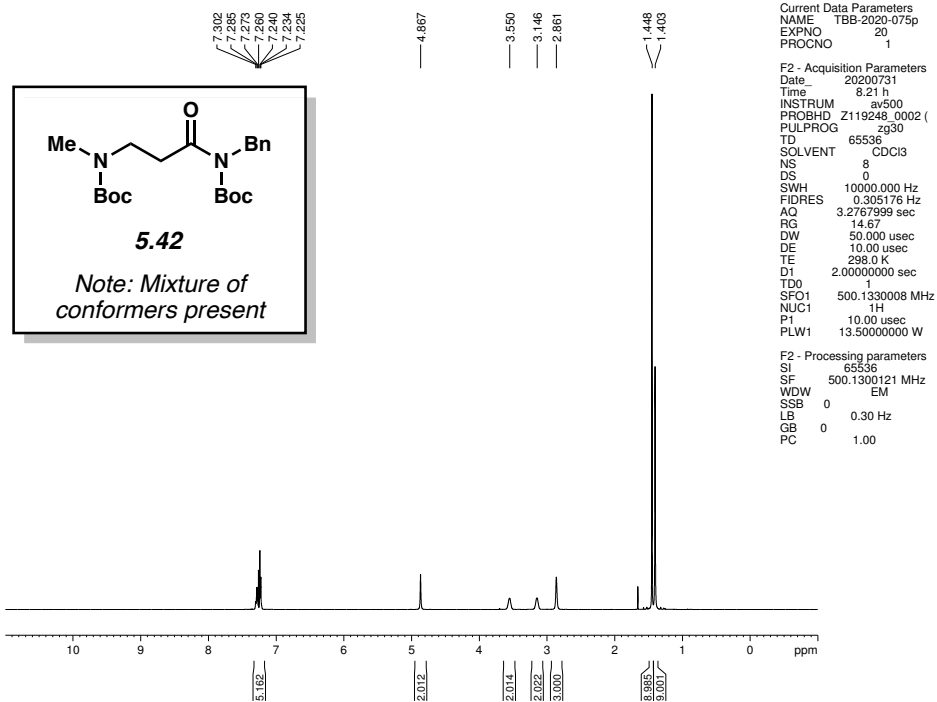
Figure 5.13 ^{1}H NMR (500 MHz, CDCl$_3$) of compound **5.42**.
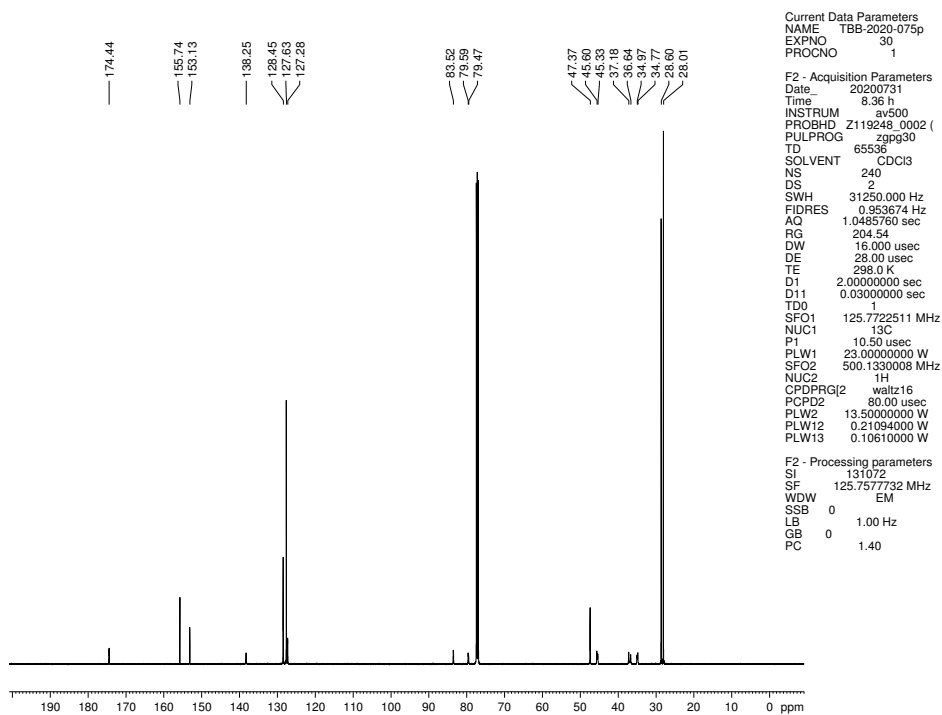
Figure 5.14 ^{13}C NMR (125 MHz, CDCl$_3$) of compound **5.42**.
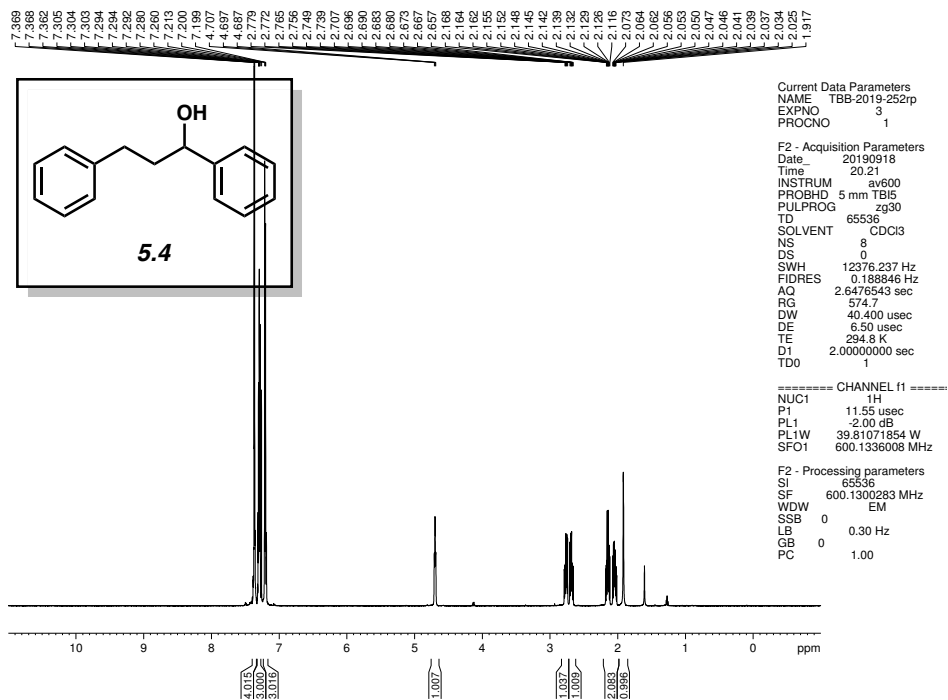
Figure 5.15 ^{1}H NMR (600 MHz, CDCl$_3$) of compound **5.4**.
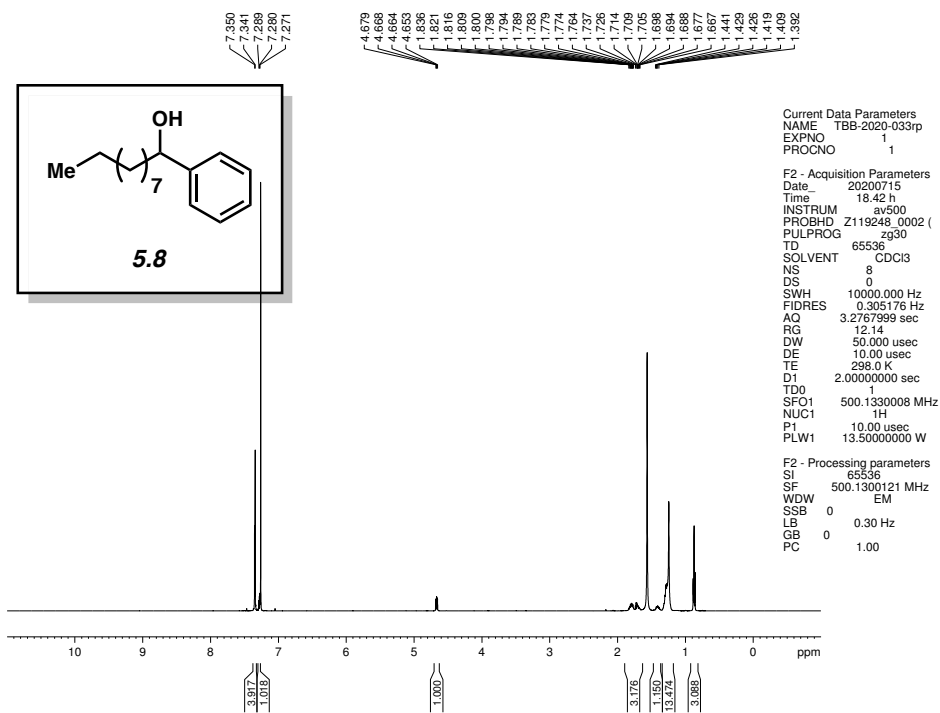
Figure 5.16 ^{1}H NMR (500 MHz, CDCl$_3$) of compound **5.8**.
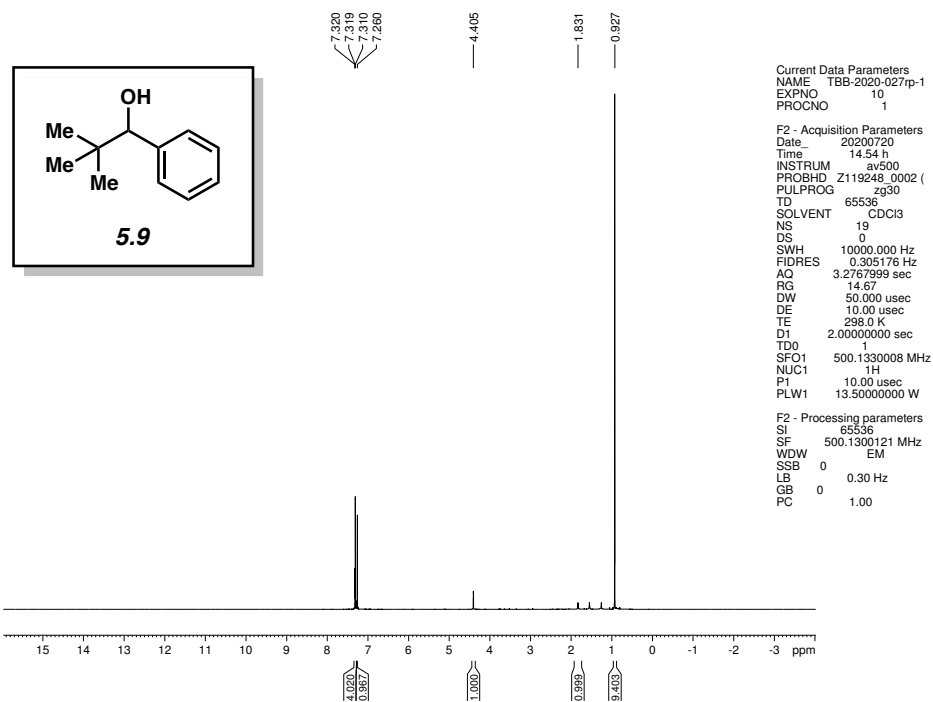
Figure 5.17 ^{1}H NMR (500 MHz, CDCl$_3$) of compound **5.9**.
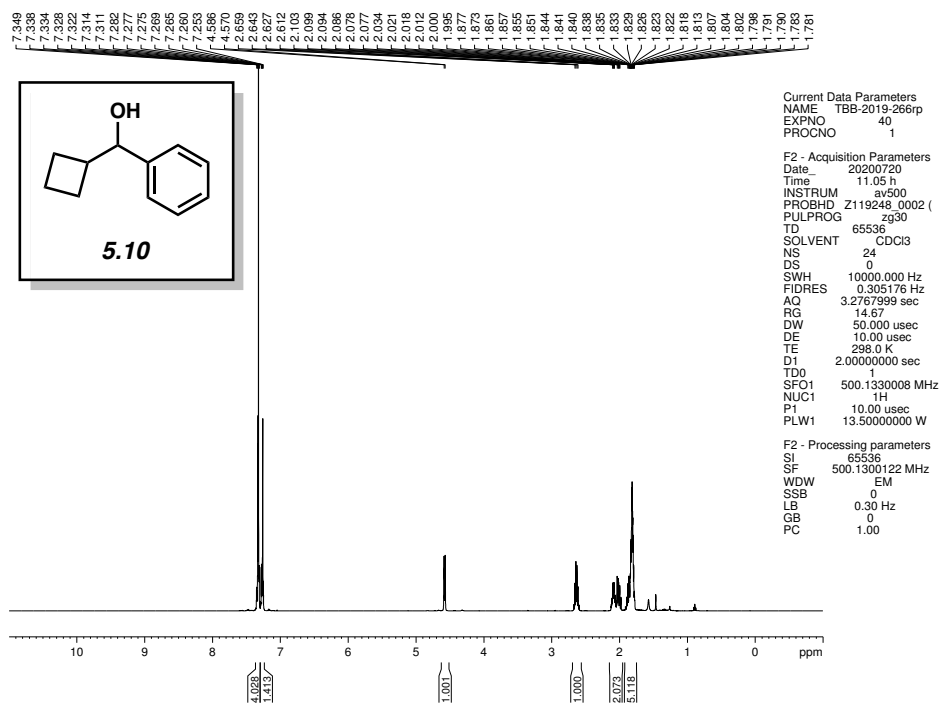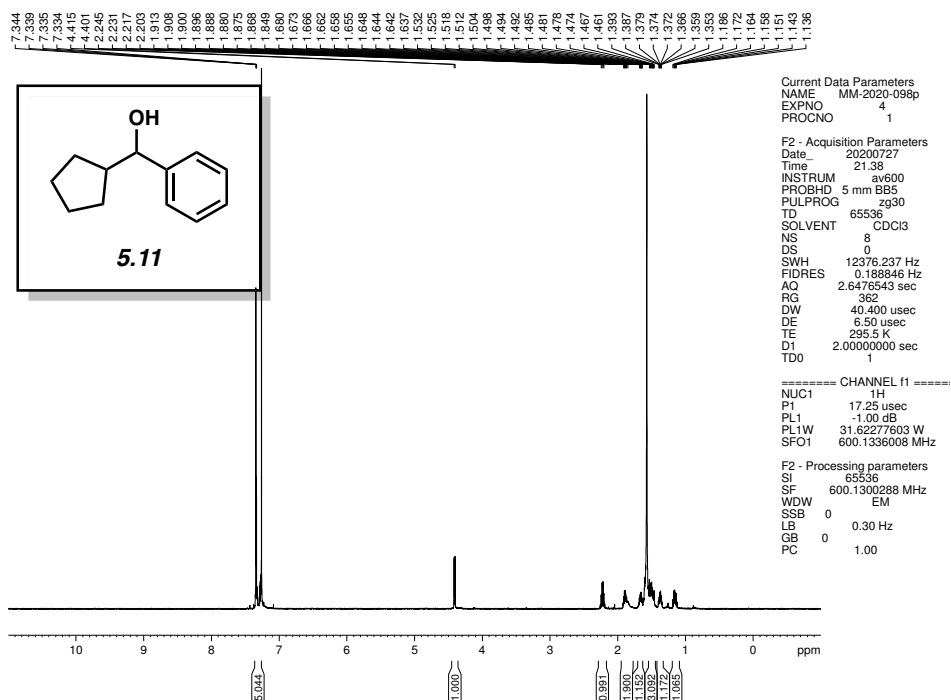

Figure 5.18 ^{1}H NMR (500 MHz, CDCl$_3$) of compound **5.10**.

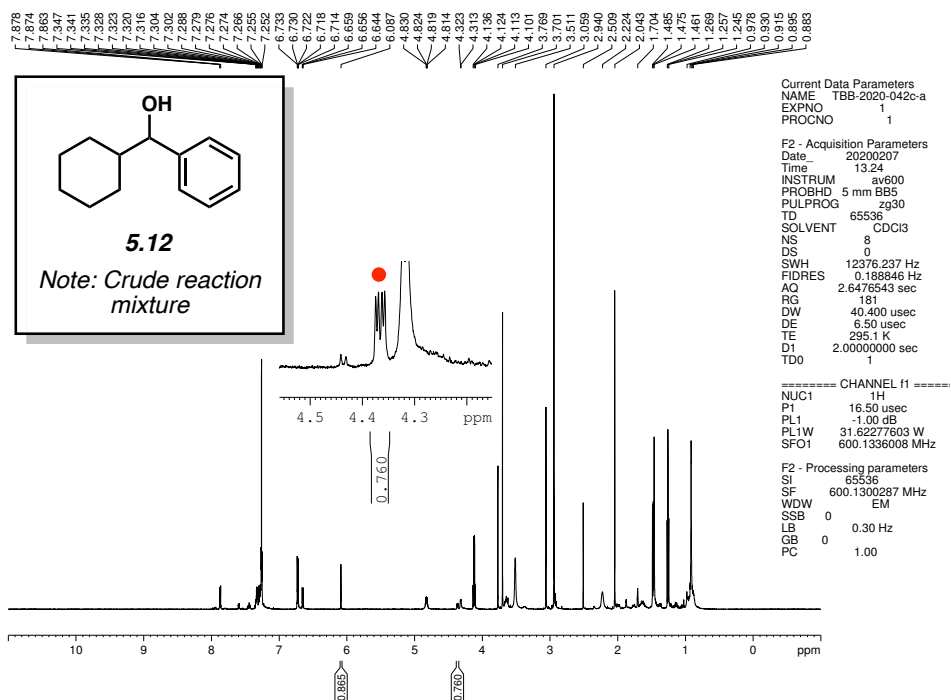Figure 5.19 ¹H NMR (600 MHz, CDCl₃) of compound **5.11**.

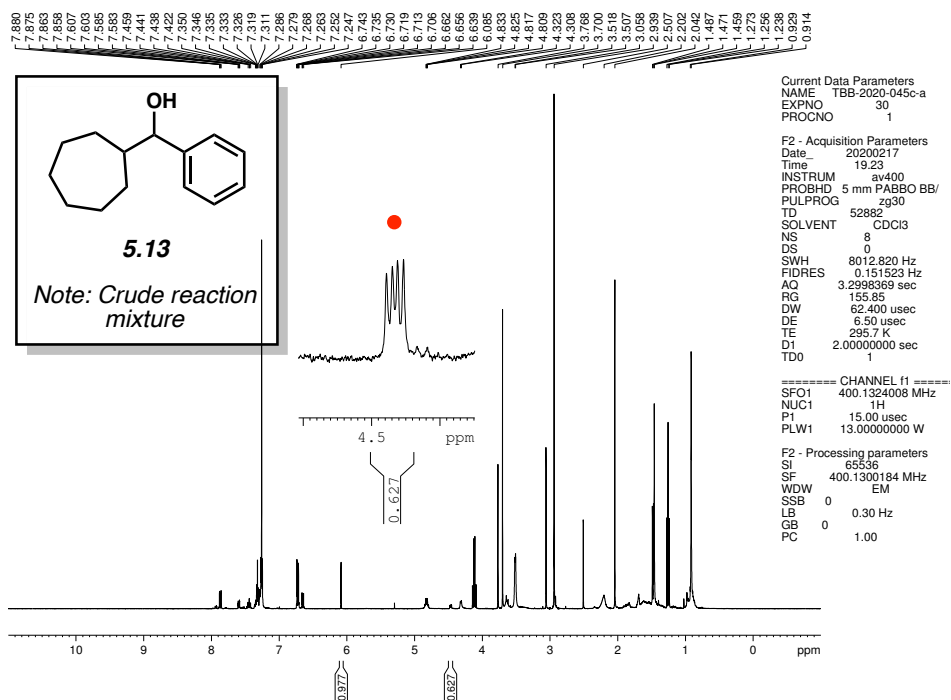Figure 5.20 ¹H NMR (600 MHz, CDCl₃) of compound **5.12**.

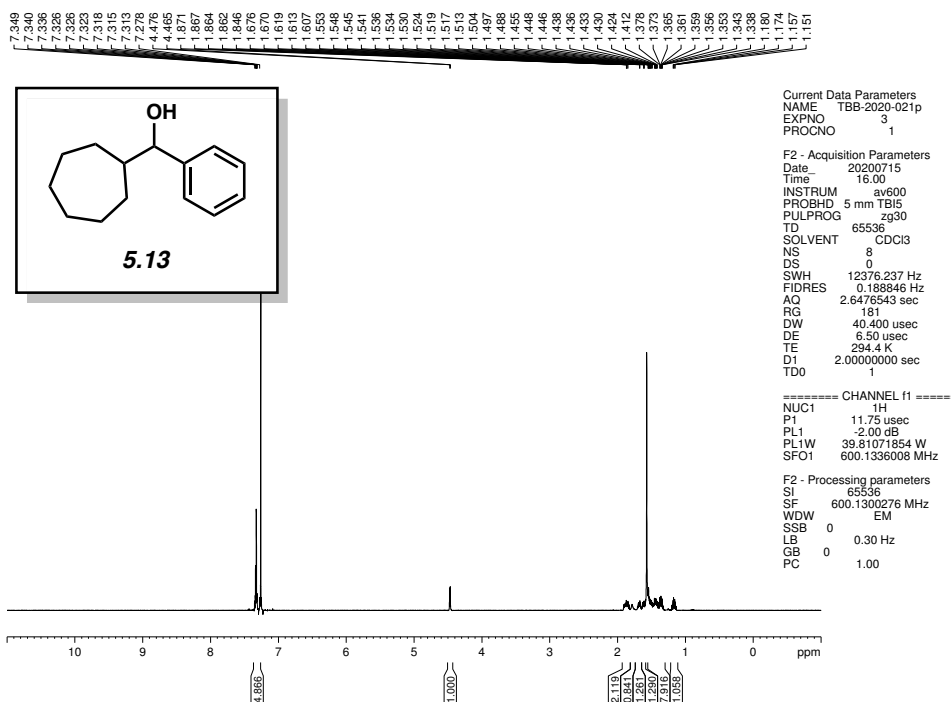*Figure 5.21* ¹H NMR (400 MHz, CDCl₃) of compound **5.13**.

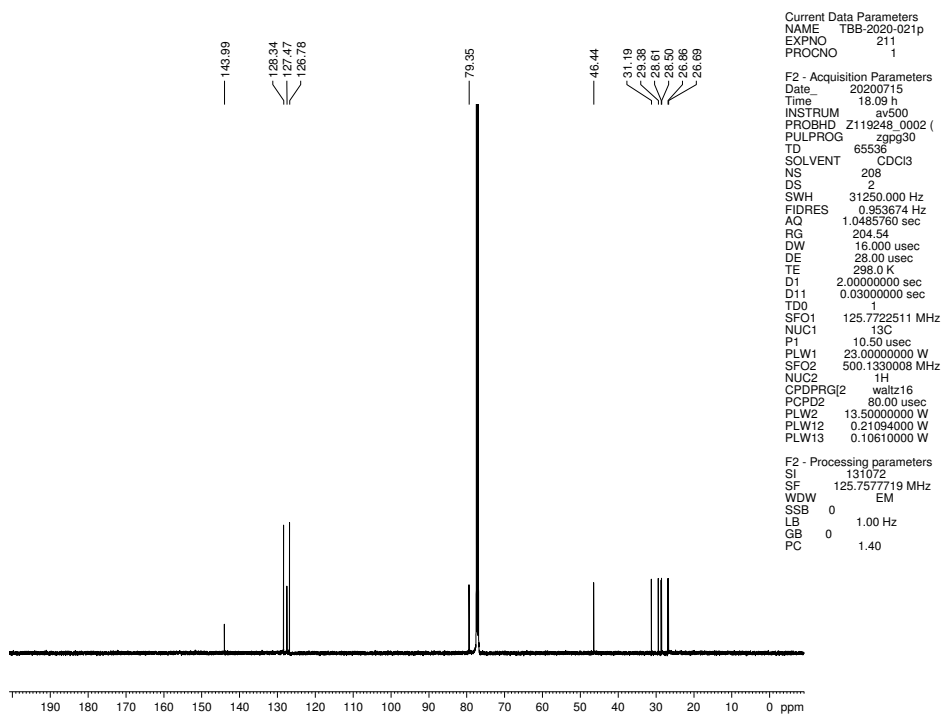*Figure 5.22* ¹H NMR (600 MHz, CDCl₃) of compound **5.13**.

Figure 5.23 ^{13}C NMR (125 MHz, CDCl$_3$) of compound **5.13**.

Figure 5.24 ^{1}H NMR (600 MHz, CDCl$_3$) of compound **5.14**.

Figure 5.25 ^{13}C NMR (125 MHz, CDCl₃) of compound **5.14**.

Figure 5.26 ^{1}H NMR (500 MHz, CDCl₃) of compound **5.15**.

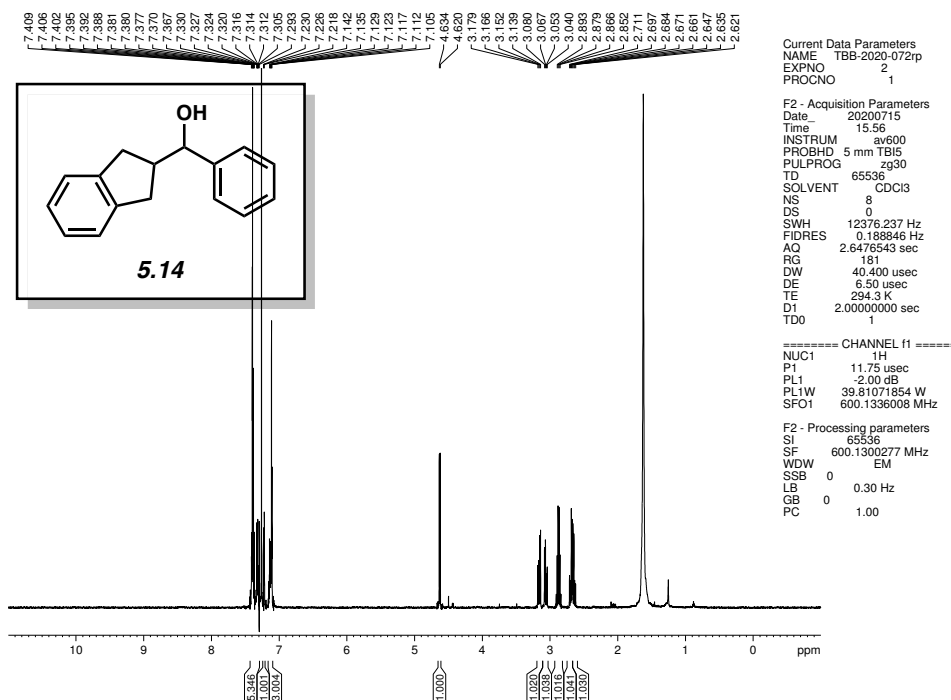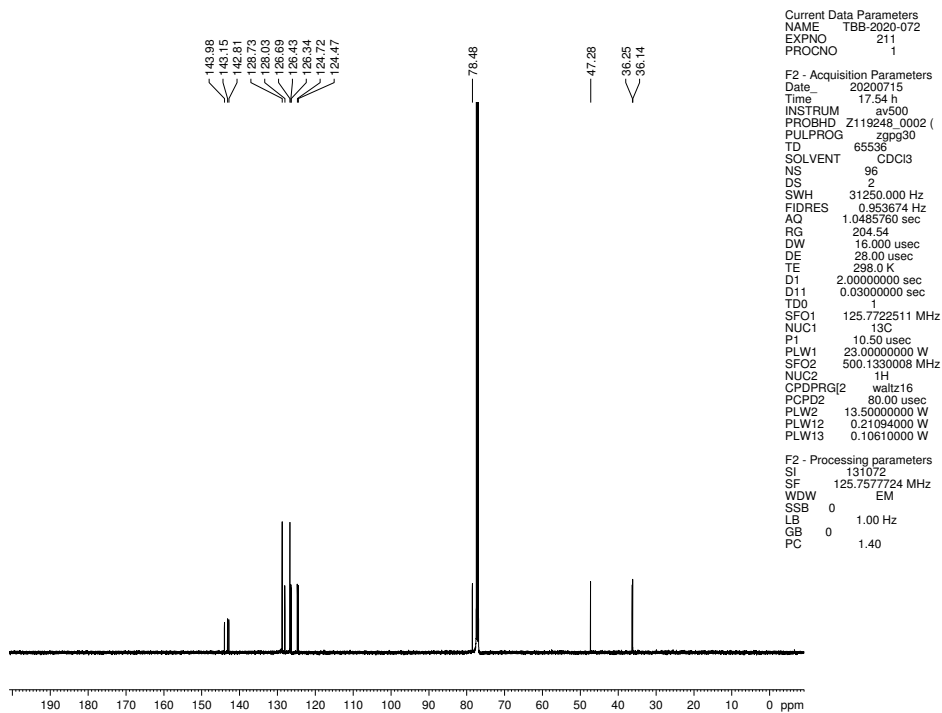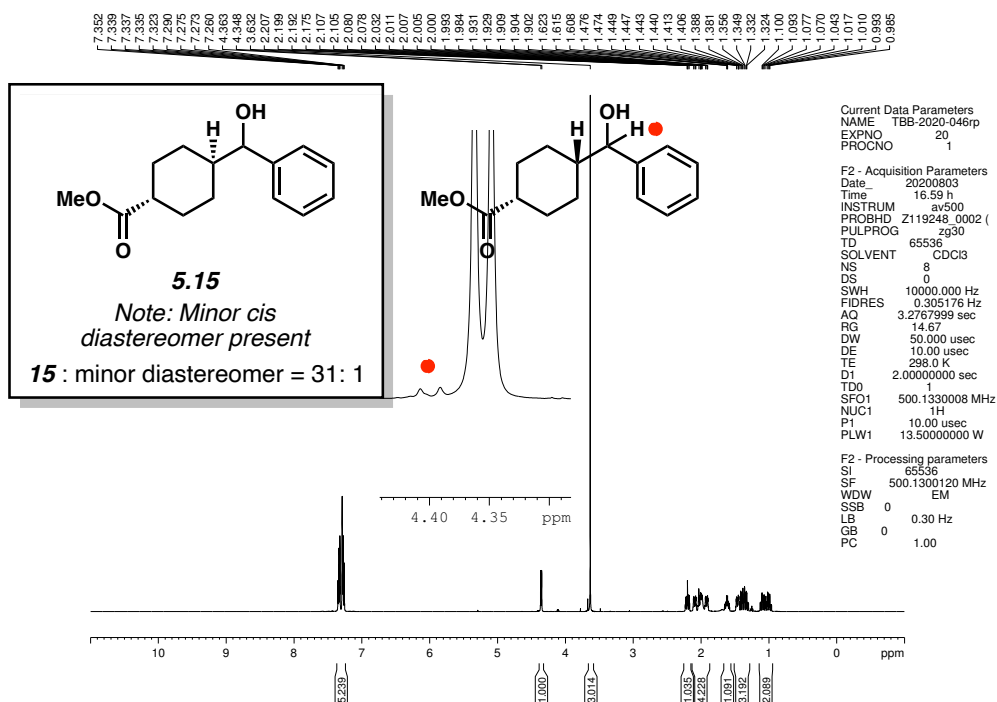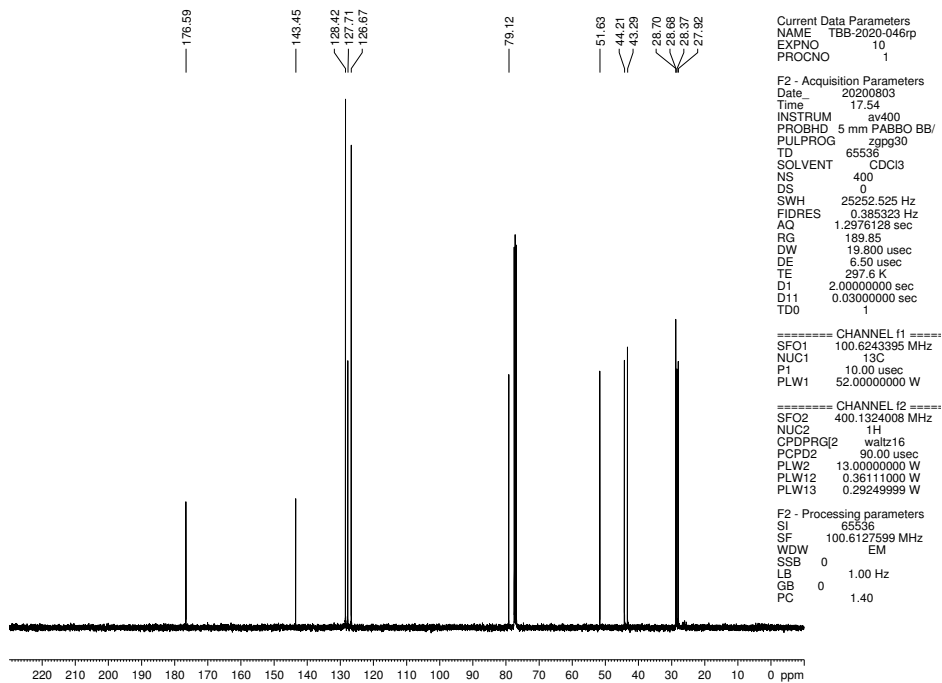*Figure 5.27* ^{13}C NMR (125 MHz, CDCl$_3$) of compound **5.15**.

Figure 5.28 ^{1}H NMR (500 MHz, CDCl$_3$) of compound **5.16**.

Peaks (ppm): 7.365, 7.360, 7.358, 7.355, 7.351, 7.349, 7.343, 7.341, 7.336, 7.335, 7.329, 7.303, 7.296, 7.289, 7.281, 7.274, 7.260, 4.503, 4.498, 4.489, 4.484, 4.410, 4.399, 4.393, 3.809, 3.802, 3.424, 3.405, 3.401, 3.398, 3.395, 3.383, 3.377, 3.375, 3.354, 3.218, 3.200, 3.196, 3.177, 2.134, 2.128, 2.098, 2.092, 1.943, 1.936, 1.925, 1.917, 1.910, 1.578, 1.557, 1.540, 1.532, 1.524, 1.503, 1.495, 1.490, 1.482

OH

5.17

Note: Mixture of diastereomers present

Integrals: 10.000 | 1.042, 1.009, 1.024 | 2.097, 1.091, 1.089 | 1.015, 1.000, 3.133, 1.381, 4.305, 1.076, 1.055

Figure 5.29 ^{1}H NMR (500 MHz, CDCl₃) of compound **5.17**.

Peaks (ppm): 143.11, 142.95, 128.60, 128.56, 127.97, 127.89, 126.68, 126.40, 76.55, 75.85, 70.81, 70.59, 68.57, 68.41, 43.01, 42.88, 26.36, 25.35, 25.25

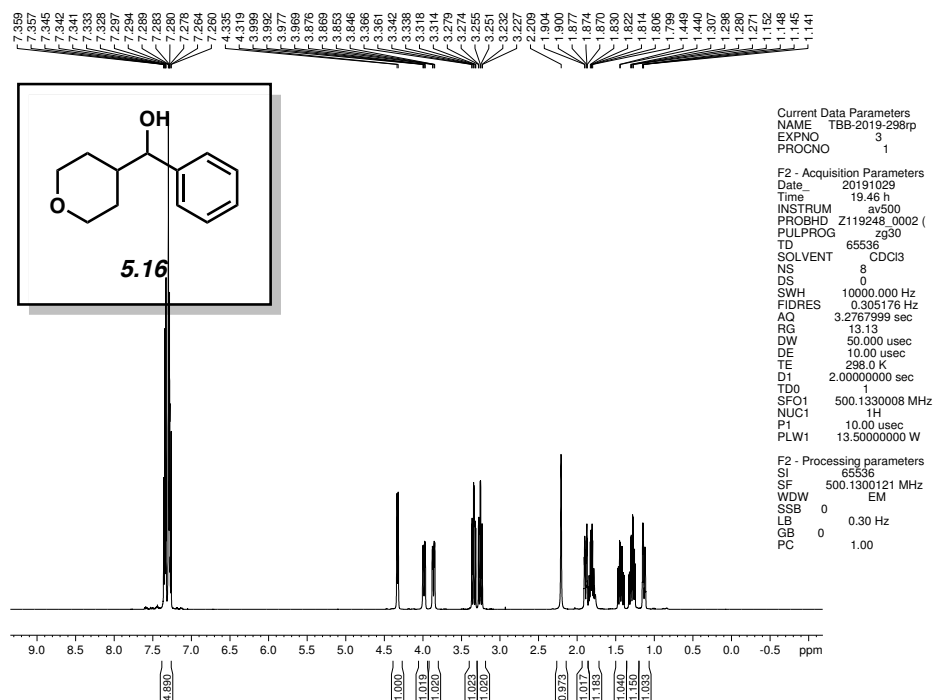*Figure 5.30* ^{13}C NMR (125 MHz, CDCl₃) of compound **5.17**.

318

Figure 5.31 ^{1}H NMR (500 MHz, CDCl$_3$) of compound **5.18**.
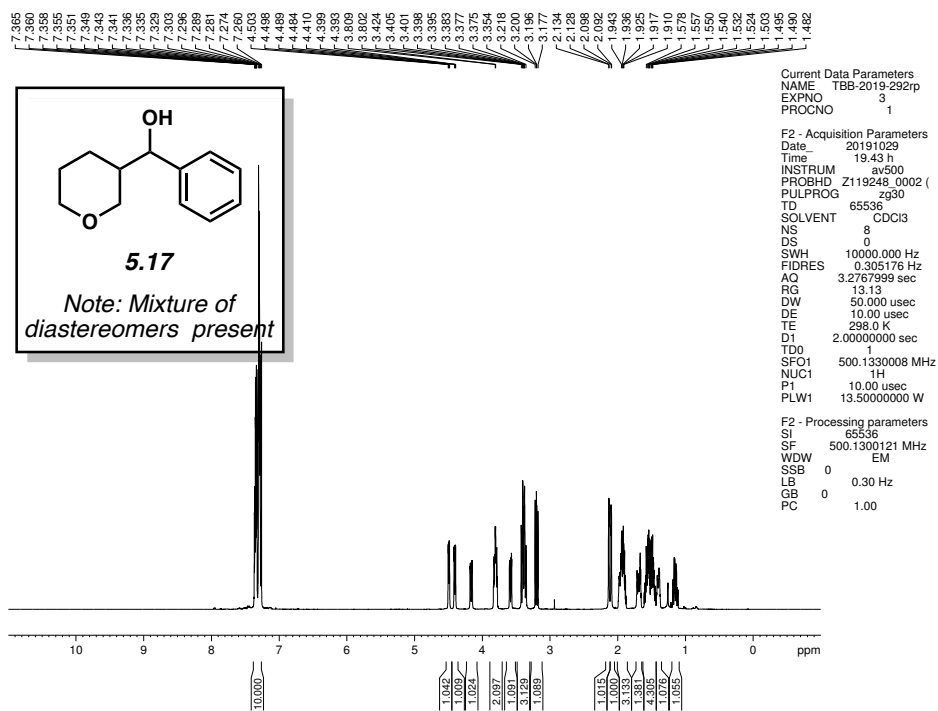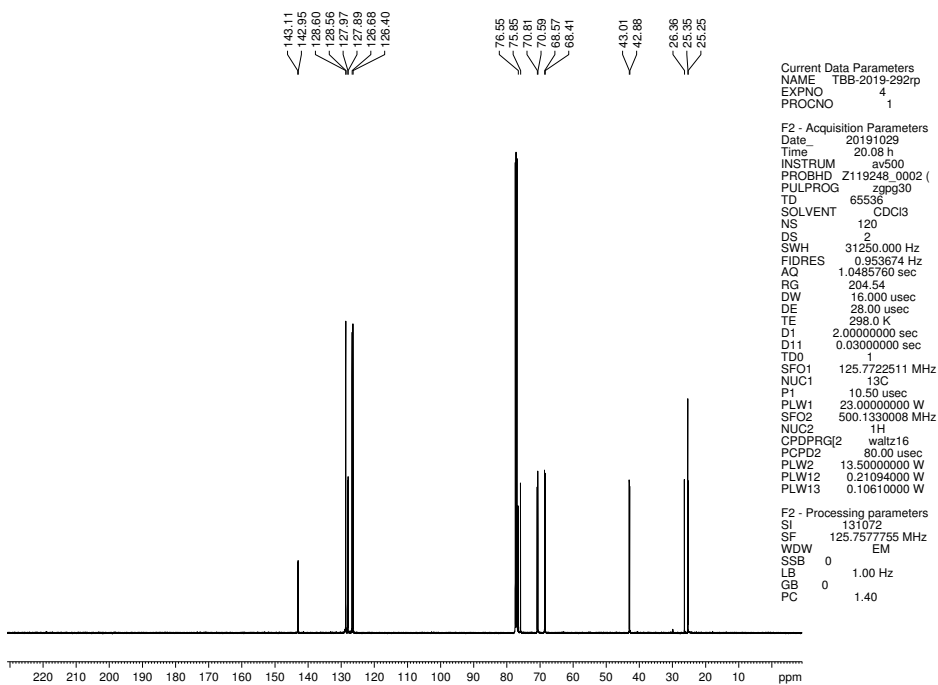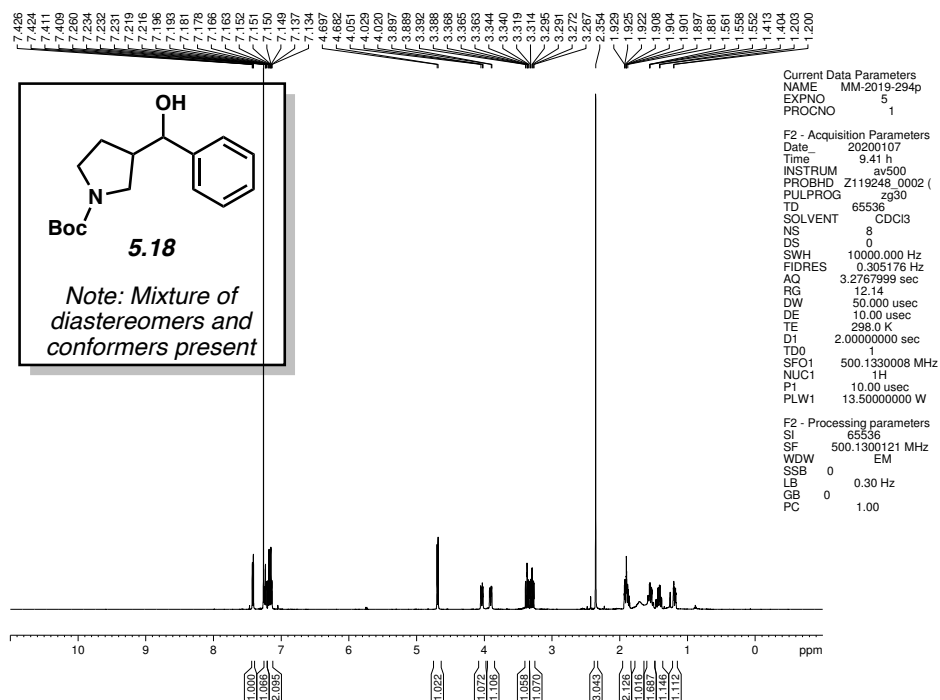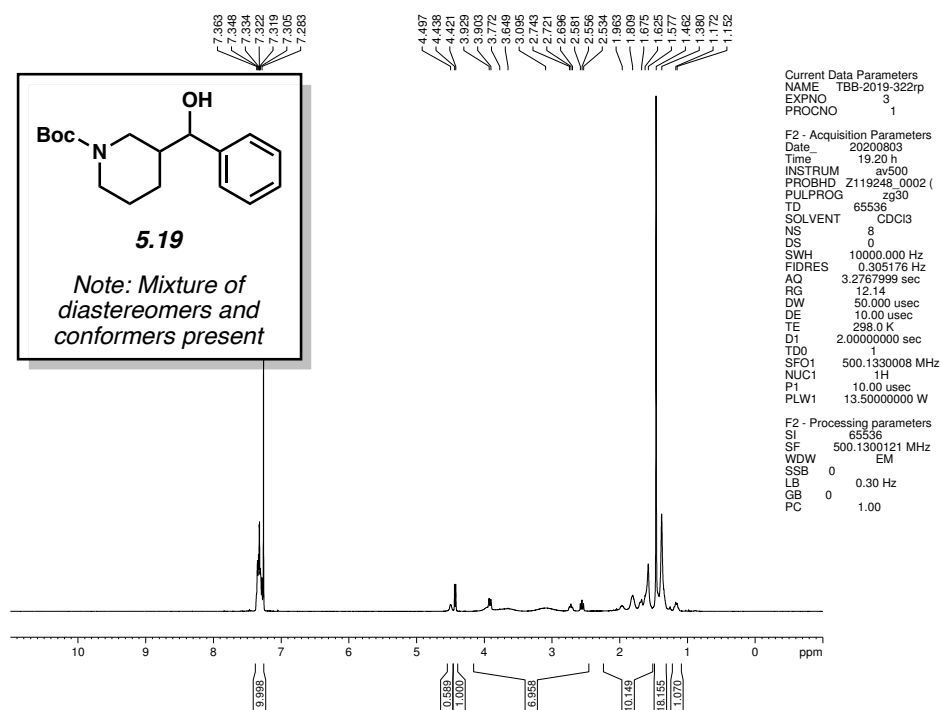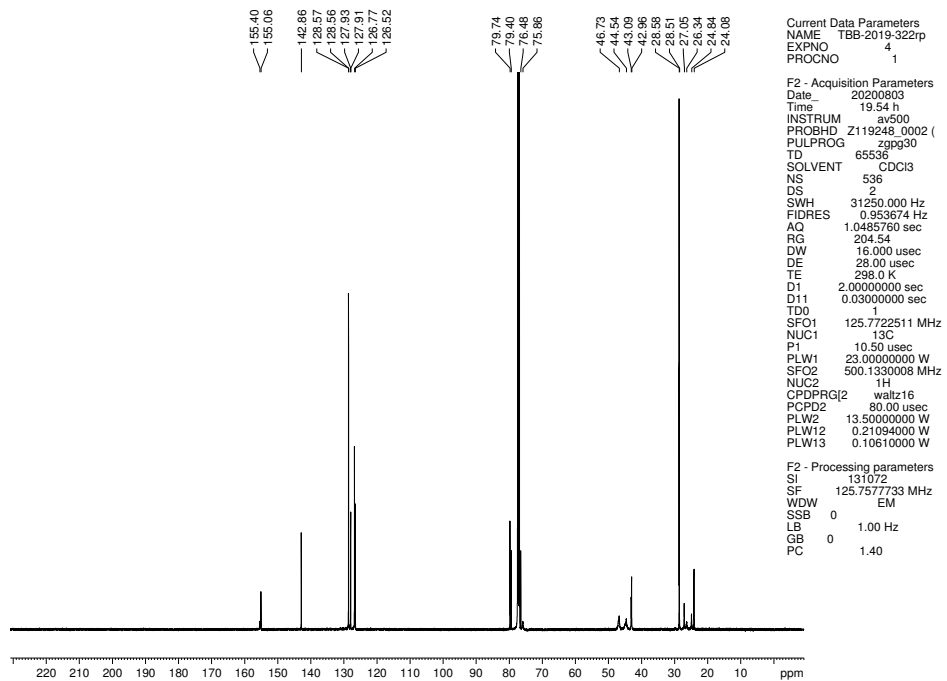

Figure 5.32 ^{1}H NMR (500 MHz, CDCl$_3$) of compound **5.19**.

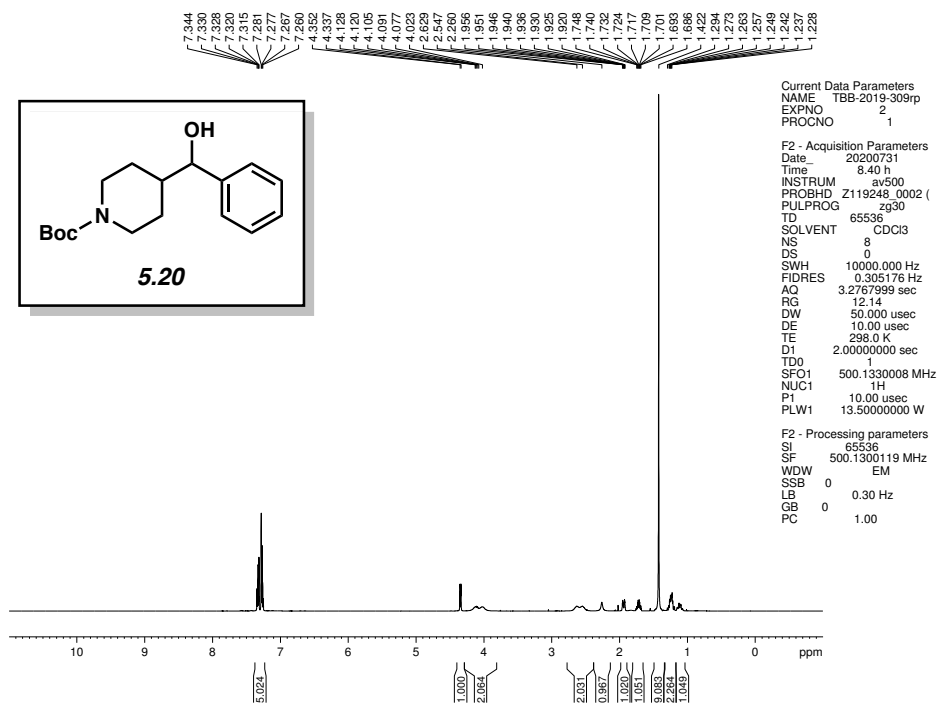*Figure 5.33* ^{13}C NMR (125 MHz, CDCl$_3$) of compound **5.19**.

Figure 5.34 ^{1}H NMR (500 MHz, CDCl$_3$) of compound **5.20**.

Peaks (ppm): 7.426, 7.424, 7.411, 7.409, 7.260, 7.234, 7.232, 7.231, 7.219, 7.216, 7.196, 7.193, 7.181, 7.178, 7.166, 7.163, 7.152, 7.151, 7.150, 7.149, 7.137, 7.134, 4.697, 4.682, 4.051, 4.029, 4.020, 3.897, 3.889, 3.392, 3.388, 3.368, 3.365, 3.363, 3.344, 3.340, 3.319, 3.314, 3.295, 3.291, 3.272, 3.267, 2.354, 1.929, 1.925, 1.922, 1.908, 1.904, 1.901, 1.897, 1.881, 1.561, 1.558, 1.552, 1.413, 1.404, 1.203, 1.200

Current Data Parameters
NAME   MM-2019-294p
EXPNO   5
PROCNO   1

F2 - Acquisition Parameters
Date_   20200107
Time   9.41 h
INSTRUM   av500
PROBHD   Z119248_0002 (
PULPROG   zg30
TD   65536
SOLVENT   CDCl3
NS   8
DS   0
SWH   10000.000 Hz
FIDRES   0.305176 Hz
AQ   3.2767999 sec
RG   12.14
DW   50.000 usec
DE   10.00 usec
TE   298.0 K
D1   2.00000000 sec
TD0   1
SFO1   500.1330008 MHz
NUC1   1H
P1   10.00 usec
PLW1   13.50000000 W

F2 - Processing parameters
SI   65536
SF   500.1300121 MHz
WDW   EM
SSB   0
LB   0.30 Hz
GB   0
PC   1.00

Integrals: 1.000, 1.086, 2.095, 1.022, 1.072, 1.106, 1.058, 1.070, 3.043, 2.126, 1.016, 1.687, 1.146, 1.112

Figure 5.35 ¹H NMR (500 MHz, CDCl₃) of compound **5.28**.

Peaks (ppm): 141.25, 135.28, 130.60, 127.51, 126.39, 126.36, 74.57, 68.09, 67.91, 42.19, 29.36, 29.25, 19.59

Current Data Parameters
NAME   MM-2019-294p
EXPNO   190
PROCNO   1

F2 - Acquisition Parameters
Date_   20200106
Time   18.38
INSTRUM   av400
PROBHD   5 mm PABBO BB/
PULPROG   zgpg30
TD   65536
SOLVENT   CDCl3
NS   512
DS   0
SWH   25252.525 Hz
FIDRES   0.385323 Hz
AQ   1.2976128 sec
RG   189.85
DW   19.800 usec
DE   6.50 usec
TE   296.9 K
D1   2.00000000 sec
D11   0.03000000 sec
TD0   1

======== CHANNEL f1 =====
SFO1   100.6243395 MHz
NUC1   13C
P1   10.00 usec
PLW1   52.00000000 W

======== CHANNEL f2 =====
SFO2   400.1324008 MHz
NUC2   1H
CPDPRG[2   waltz16
PCPD2   90.00 usec
PLW2   13.00000000 W
PLW12   0.36111000 W
PLW13   0.29249999 W

F2 - Processing parameters
SI   65536
SF   100.6127584 MHz
WDW   EM
SSB   0
LB   1.00 Hz
GB   0
PC   1.40

Figure 5.36 ¹³C NMR (125 MHz, CDCl₃) of compound **5.28**.

Figure 5.37 ^{1}H NMR (600 MHz, CDCl$_3$) of compound **5.29**.

Figure 5.38 ^{13}C NMR (125 MHz, CDCl$_3$) of compound **5.29**.

322

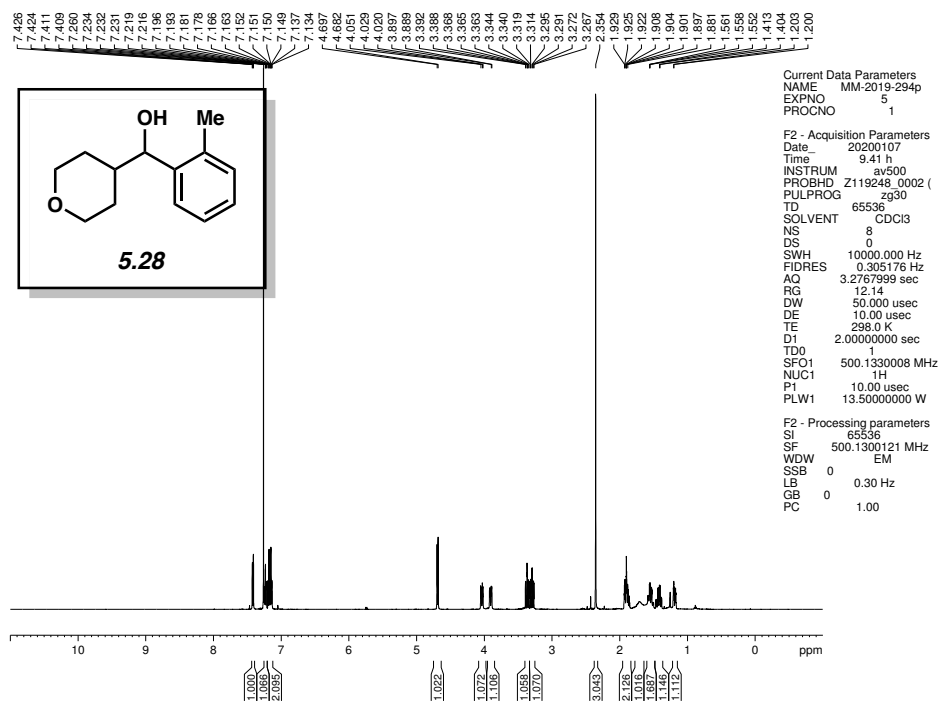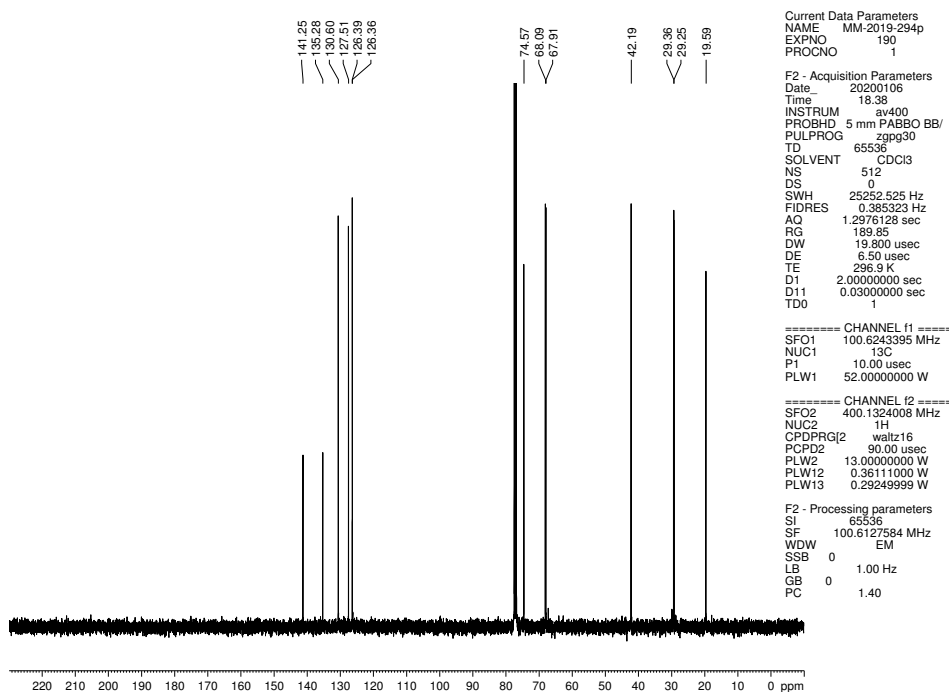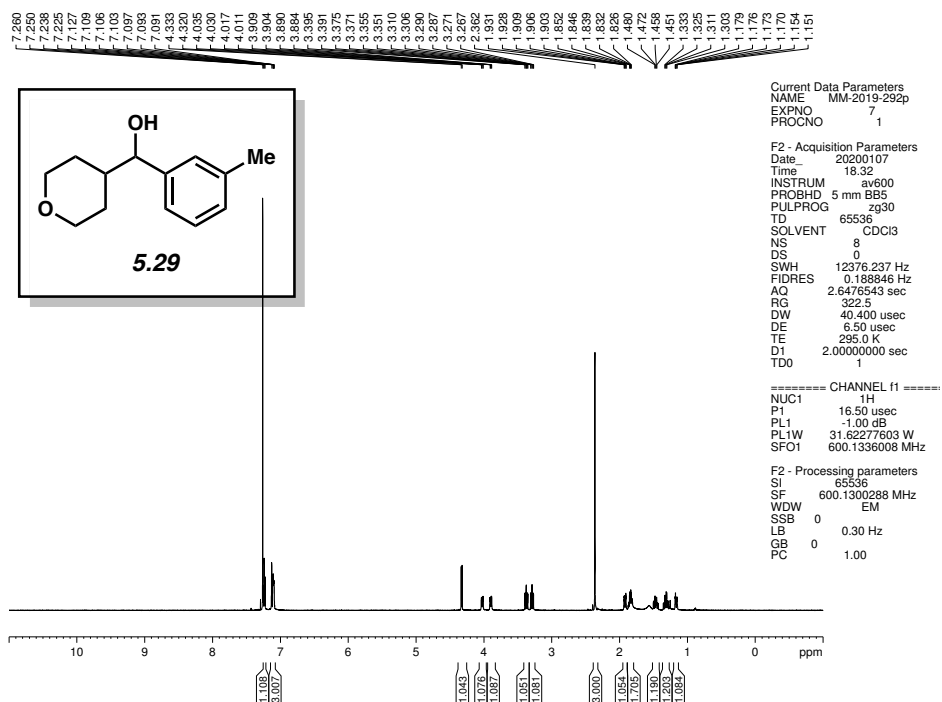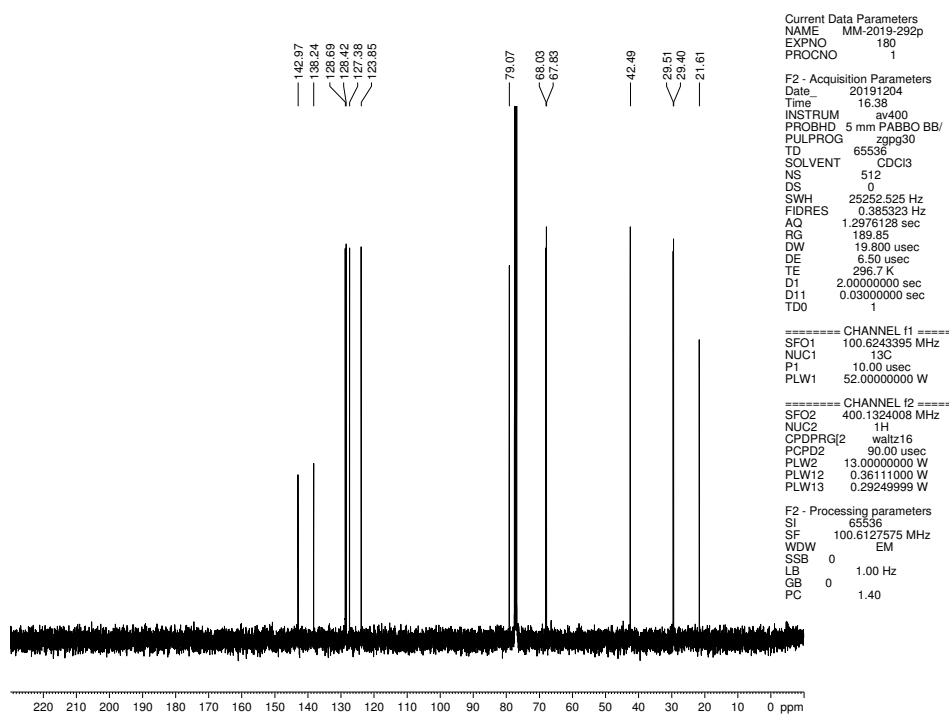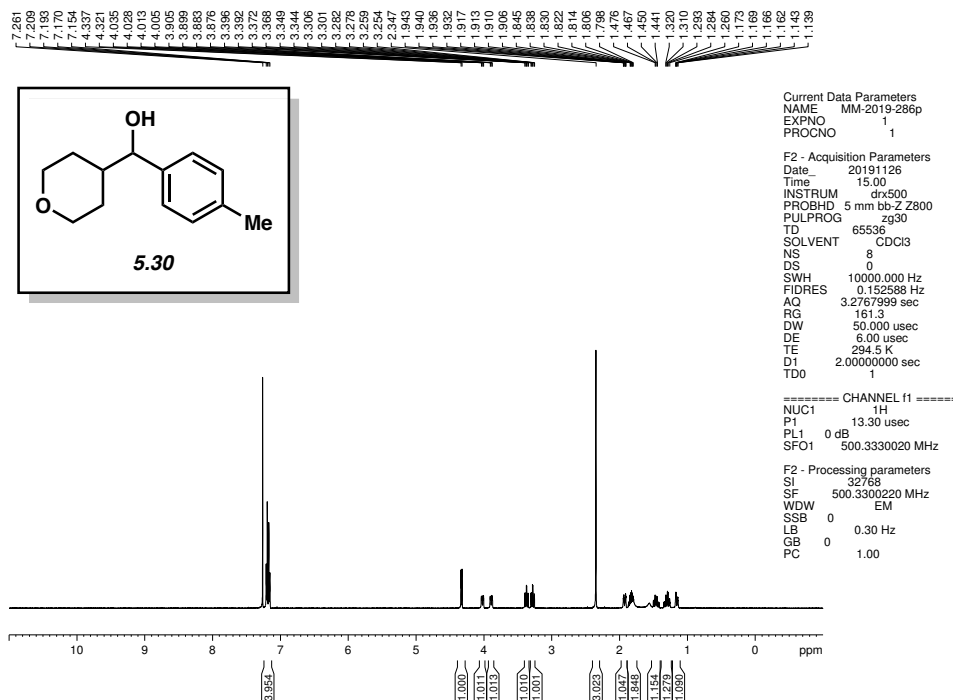*Figure 5.39* ¹H NMR (500 MHz, CDCl₃) of compound **5.30**.
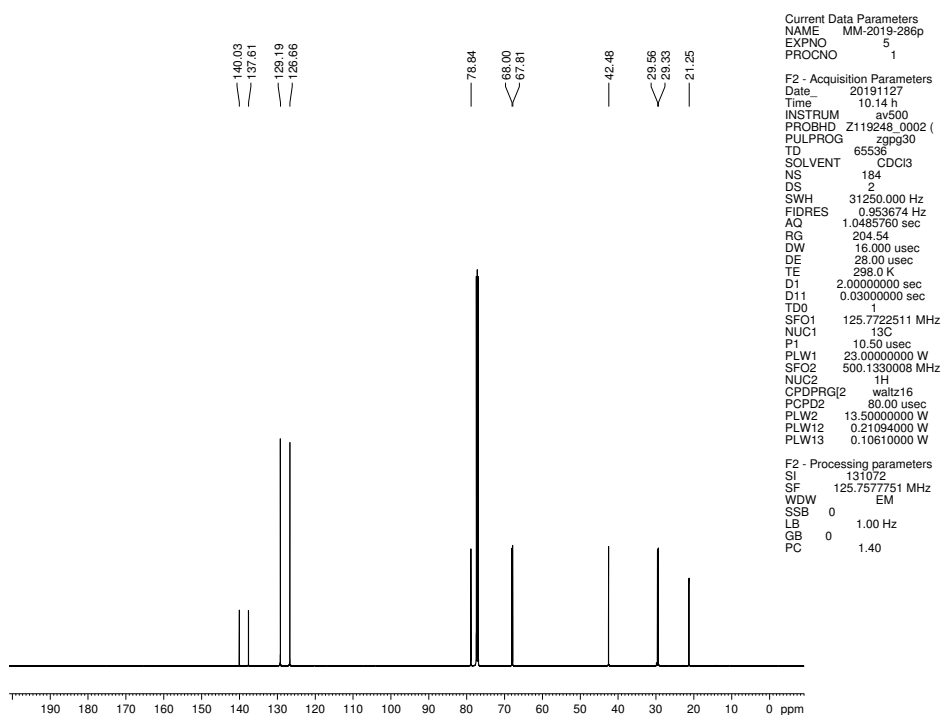

Figure 5.40 ¹³C NMR (125 MHz, CDCl₃) of compound **5.30**.
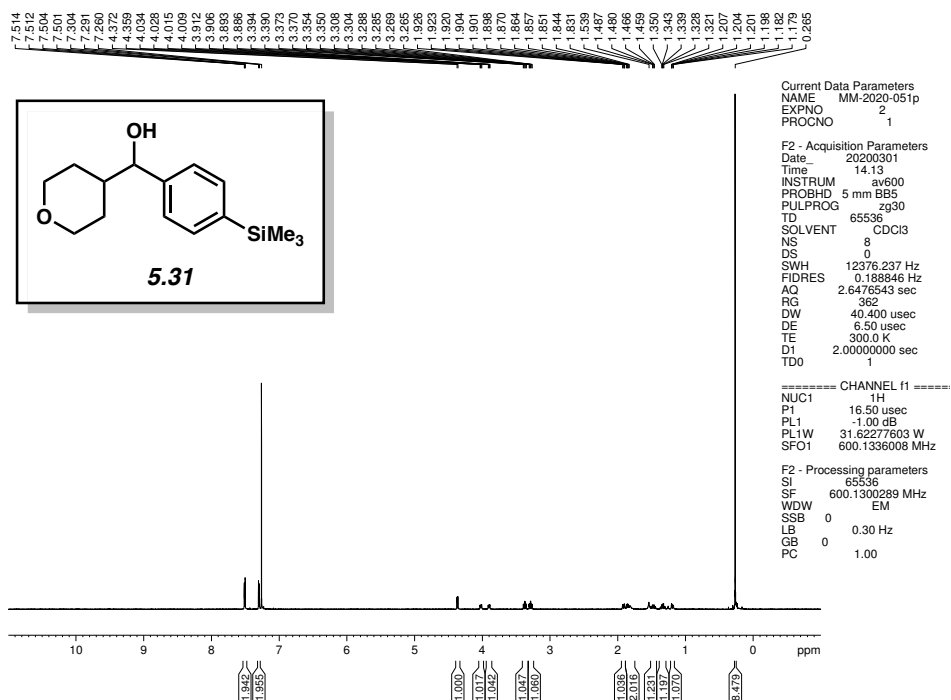
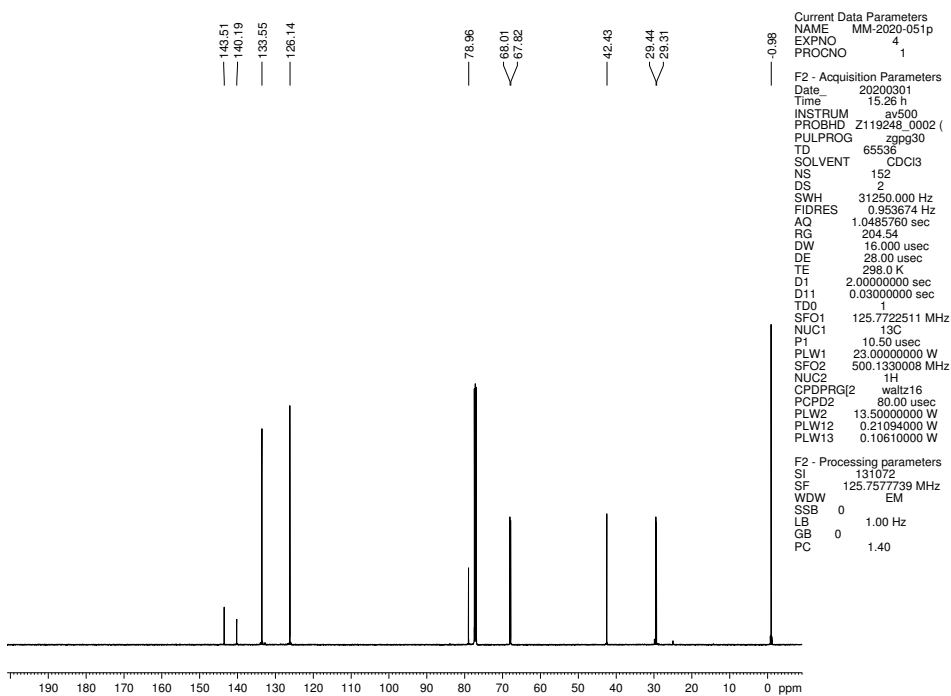*Figure 5.41* ^{1}H NMR (600 MHz, CDCl$_3$) of compound **5.31**.

Figure 5.42 ^{13}C NMR (125 MHz, CDCl$_3$) of compound **5.31**.
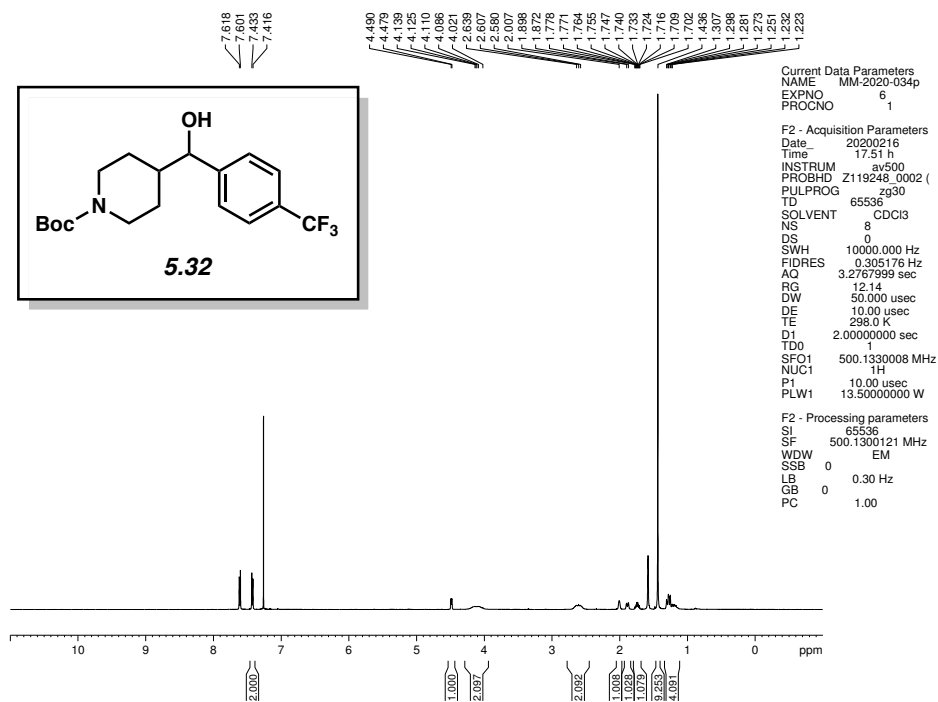
Figure 5.43 ^{1}H NMR (500 MHz, CDCl$_3$) of compound **5.32**.

Figure 5.44 ^{13}C NMR (125 MHz, CDCl$_3$) of compound **5.32**.

Figure 5.45 ^{1}H NMR (500 MHz, CDCl₃) of compound **5.33**.

Figure 5.46 ^{13}C NMR (125 MHz, CDCl₃) of compound **5.33**.

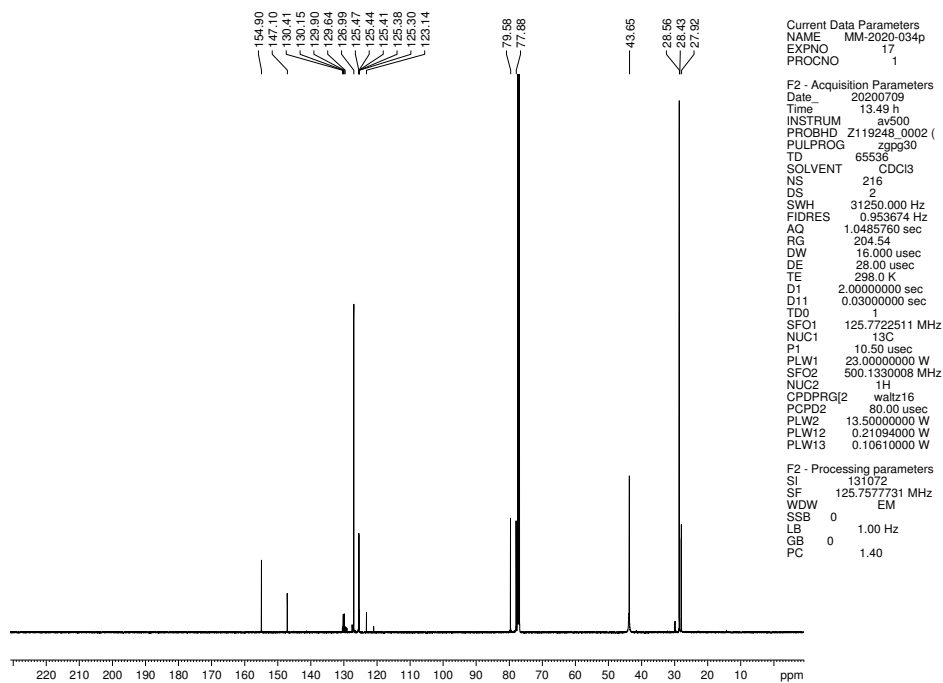*Figure 5.47* ¹H NMR (500 MHz, CDCl₃) of compound **5.34**.

Figure 5.48 ¹³C NMR (100 MHz, CDCl₃) of compound **5.34**.

Figure 5.49 ^{1}H NMR (500 MHz, CDCl$_3$) of compound **5.35**.

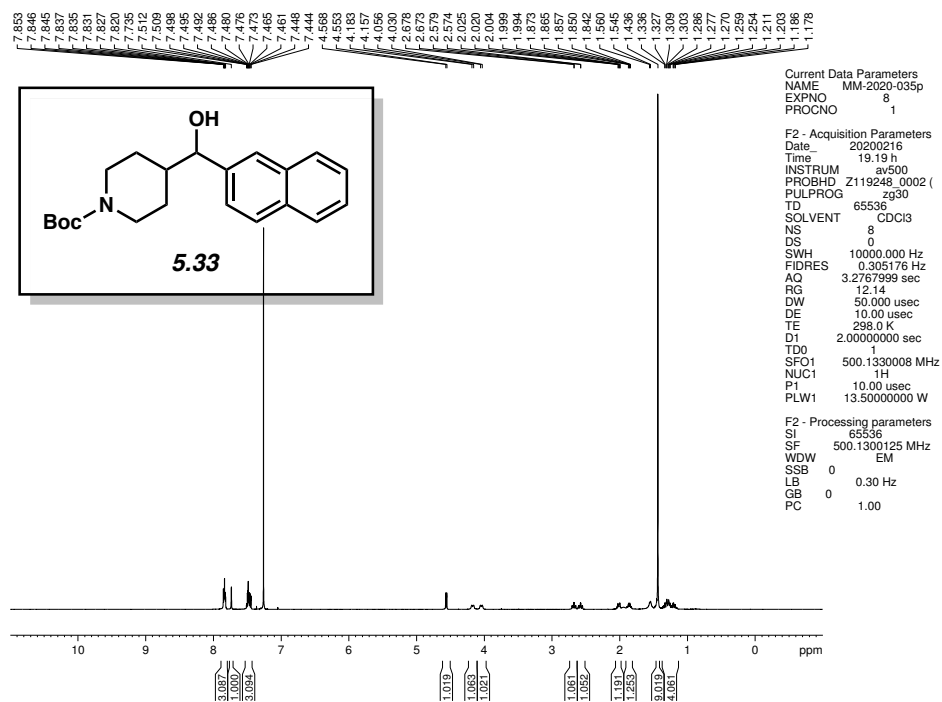*Figure 5.50* ^{13}C NMR (125 MHz, CDCl$_3$) of compound **5.35**.
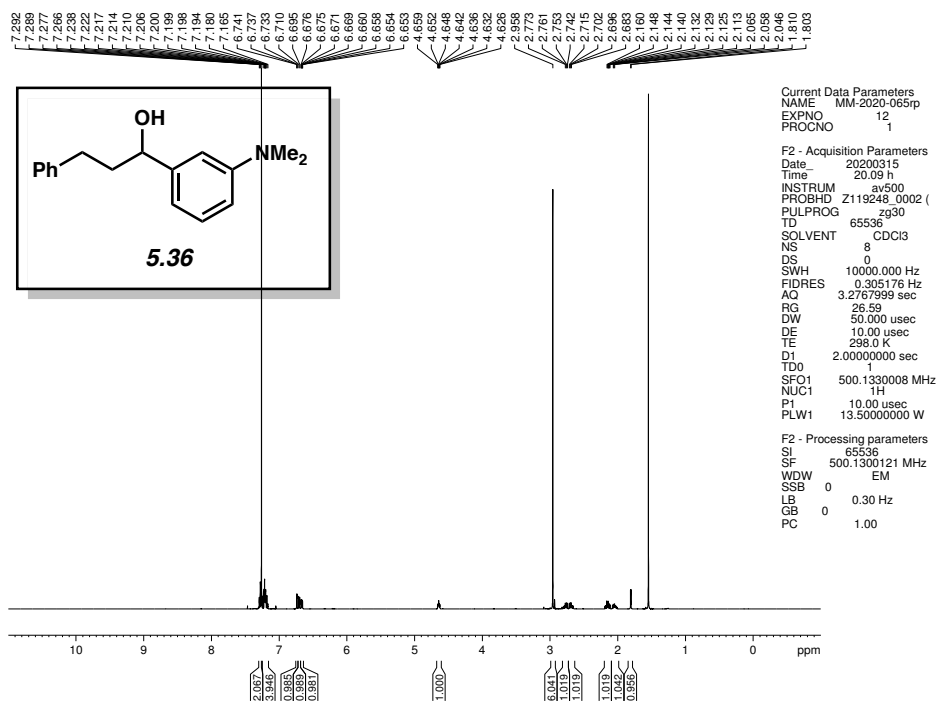
Figure 5.51 ¹H NMR (500 MHz, CDCl₃) of compound **5.36**.
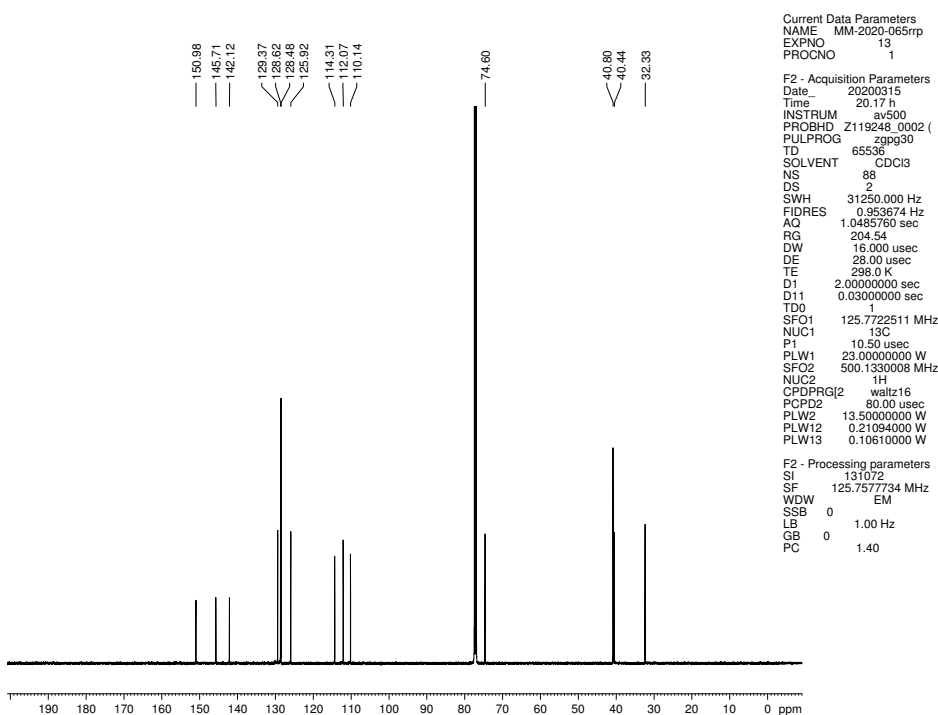
Figure 5.52 ¹³C NMR (125 MHz, CDCl₃) of compound **5.36**.
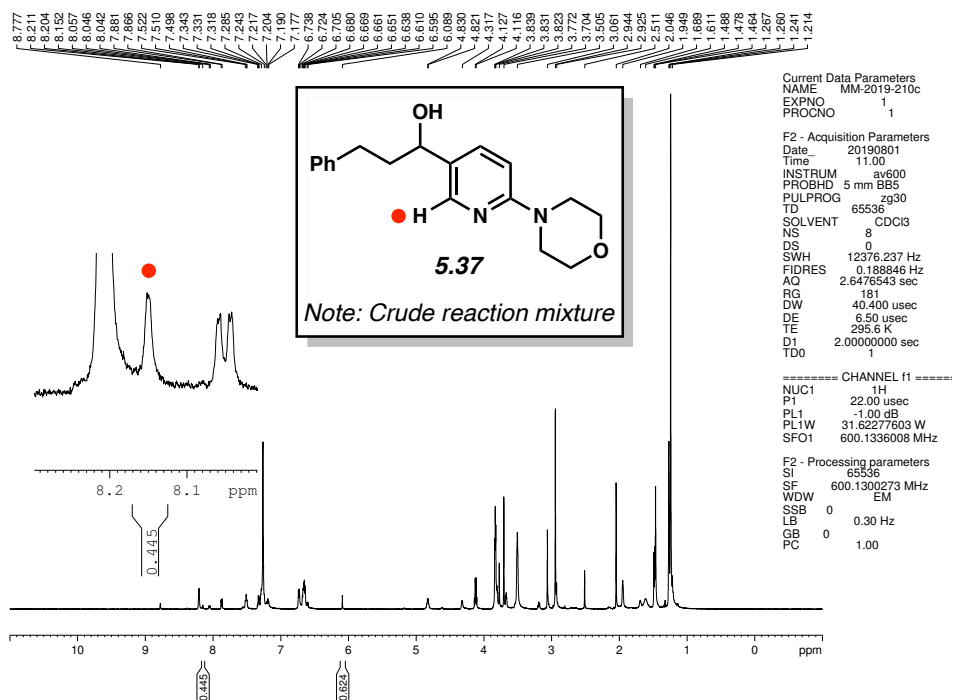
Figure 5.53 ^{1}H NMR (600 MHz, CDCl$_3$) of compound **5.37**.
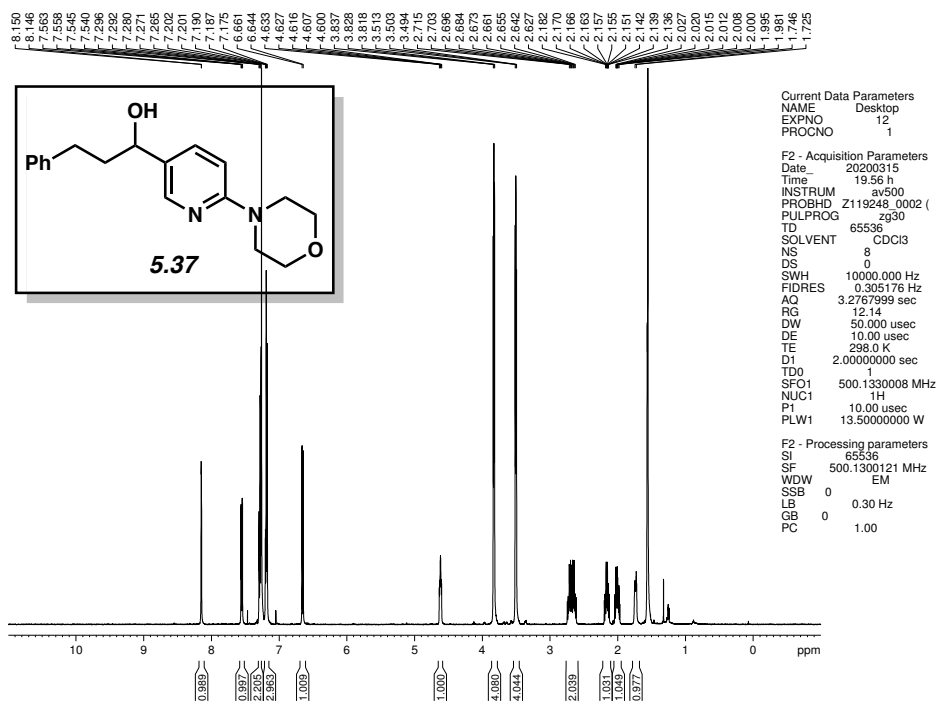
Figure 5.54 ^{1}H NMR (500 MHz, CDCl$_3$) of compound **5.37**.
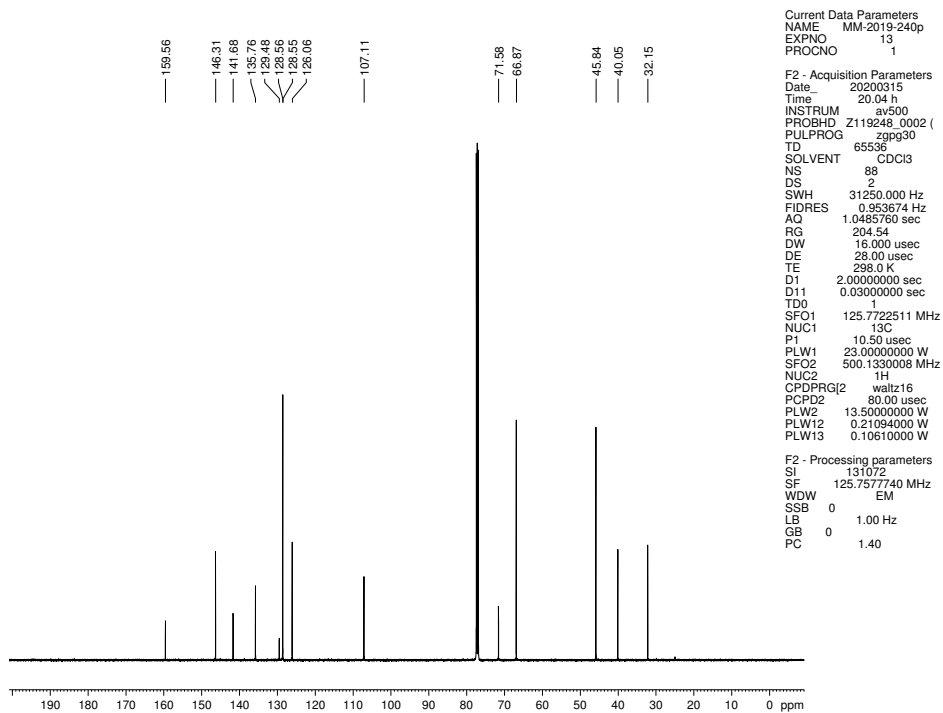
Figure 5.55 ^{13}C NMR (125 MHz, CDCl$_3$) of compound **5.37**.

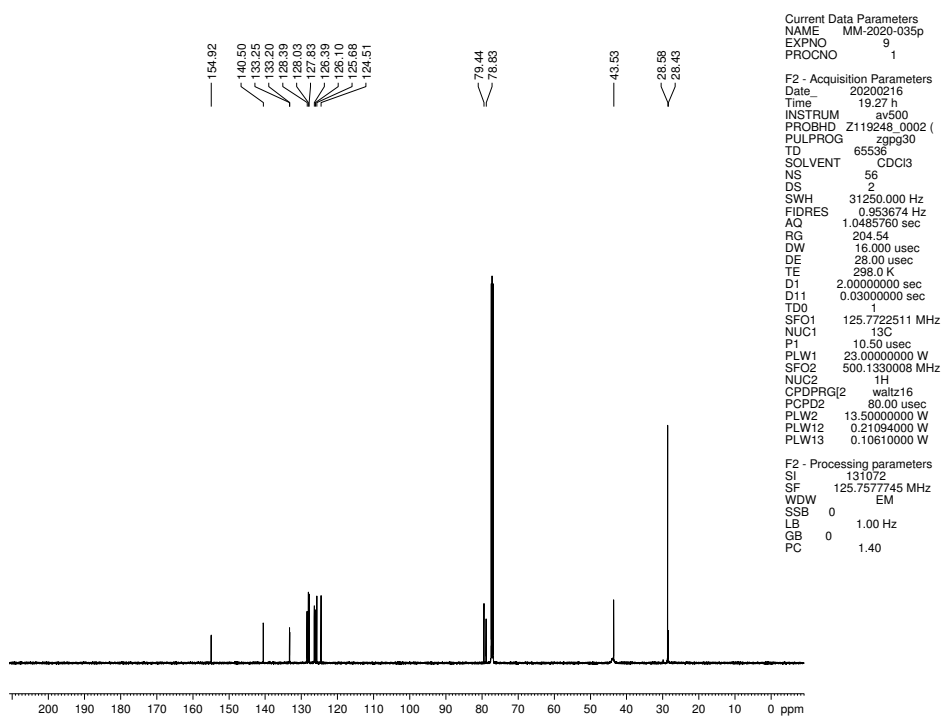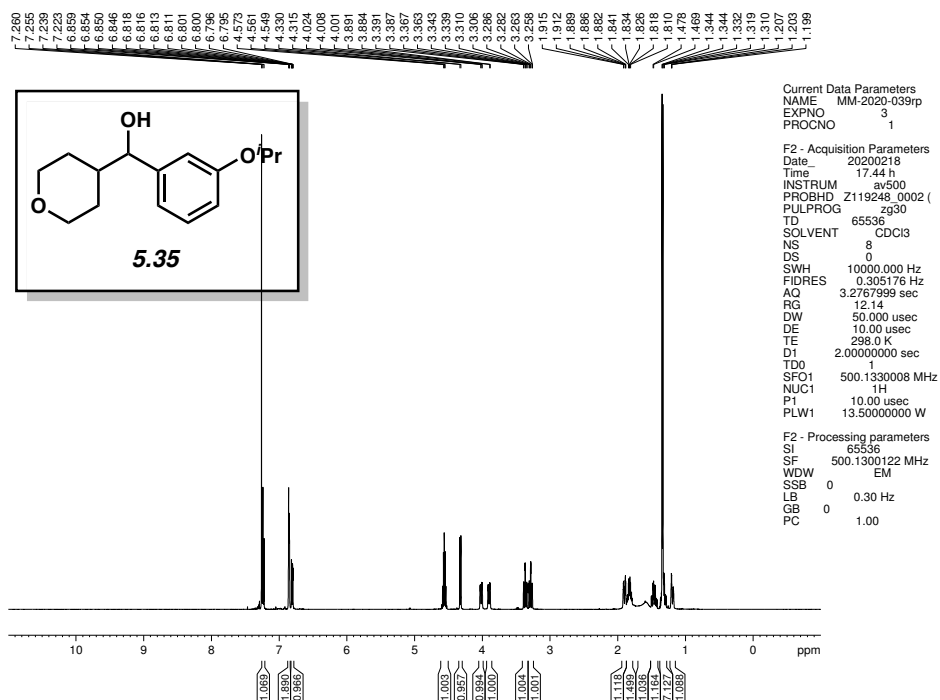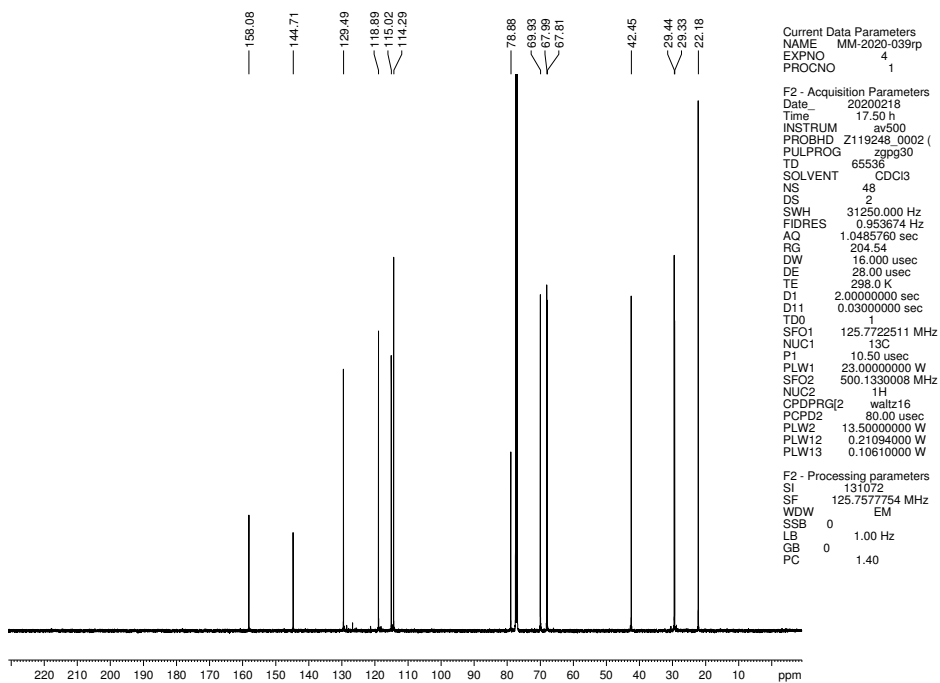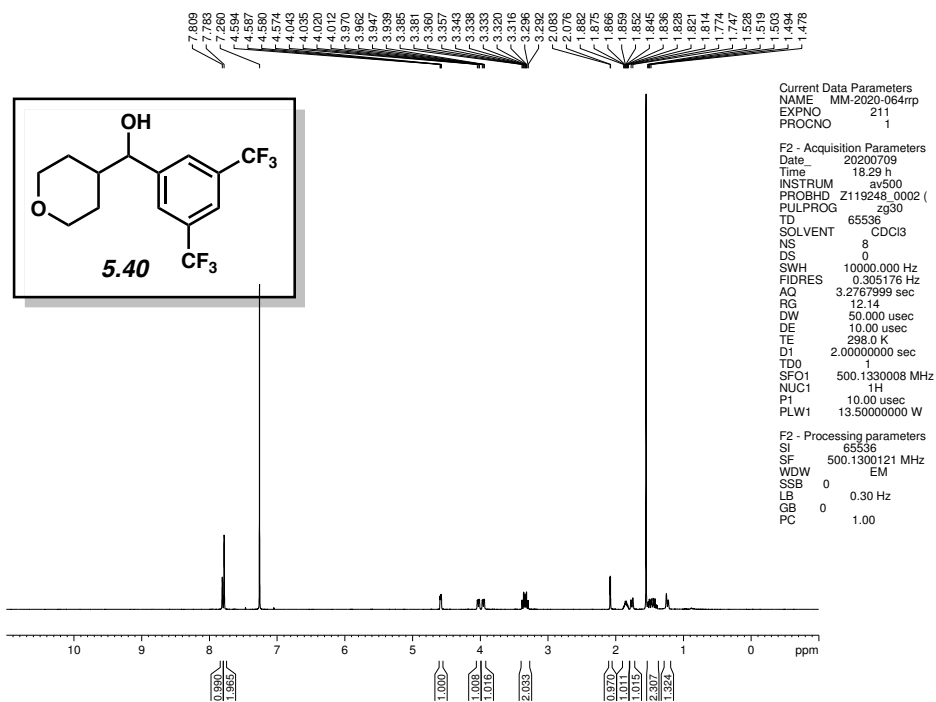*Figure 5.56* ^{1}H NMR (500 MHz, CDCl$_3$) of compound **5.40**.
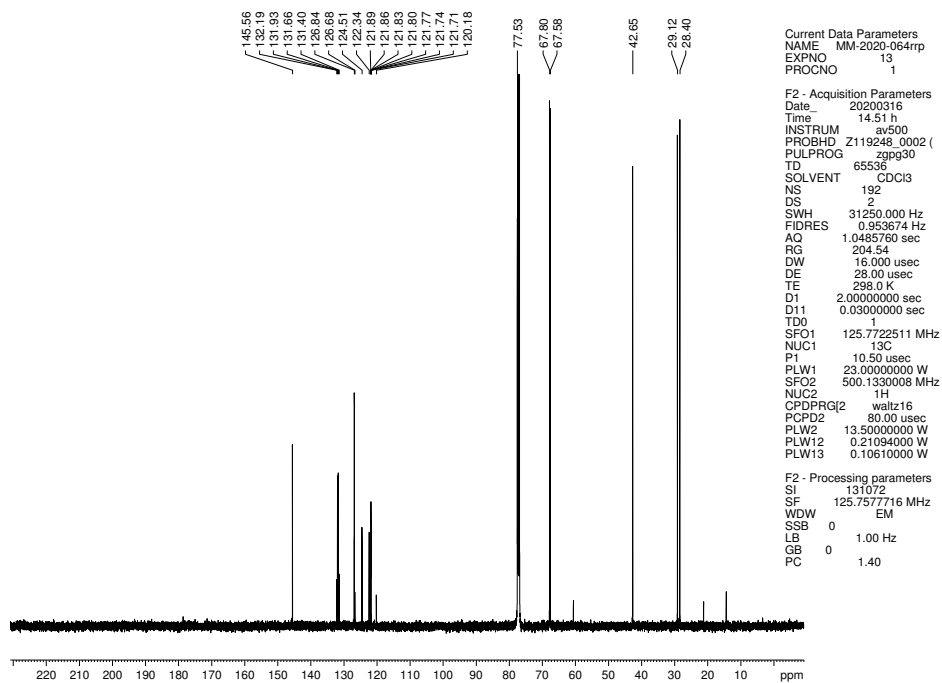
Figure 5.57 ^{13}C NMR (125 MHz, CDCl$_3$) of compound **5.40**.

OH

Boc—N

Me

5.43

Note: Mixture of conformers present

5.054

1.019   2.821   3.000   0.267   2.304   9.036

Figure 5.58 ^{1}H NMR (400 MHz, CDCl$_3$) of compound **5.43**.

Figure 5.59 ^{1}H NMR (500 MHz, CDCl$_3$) of compound **5.70**.

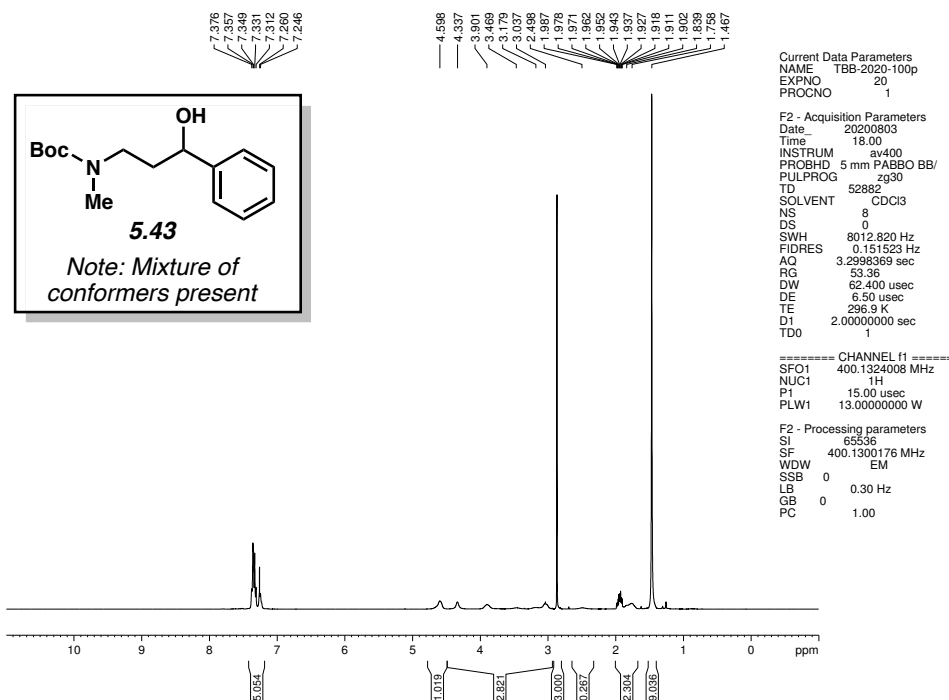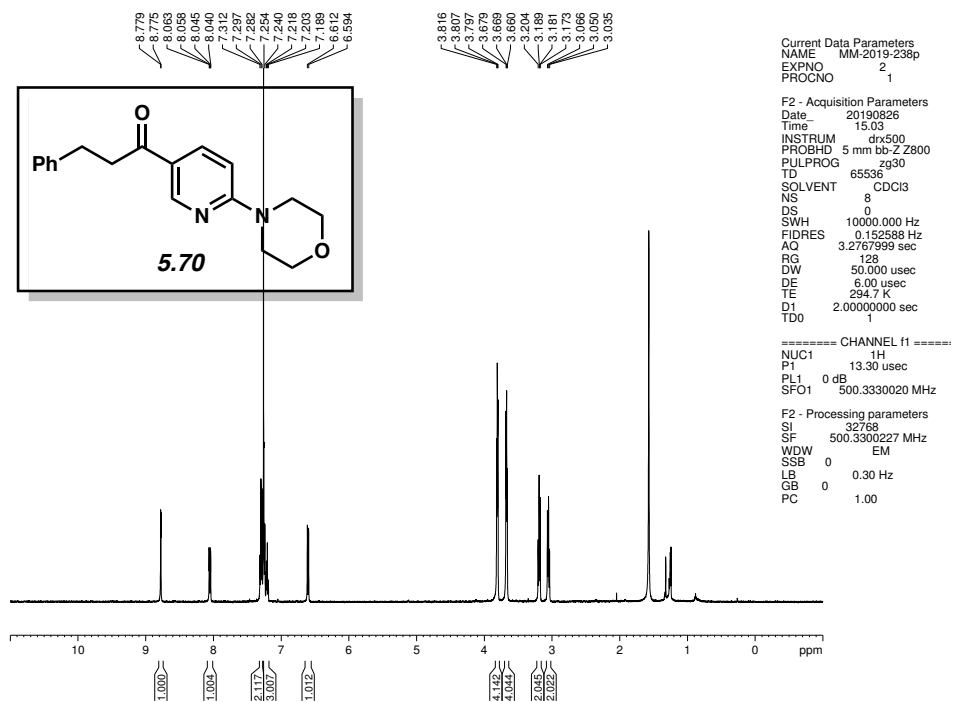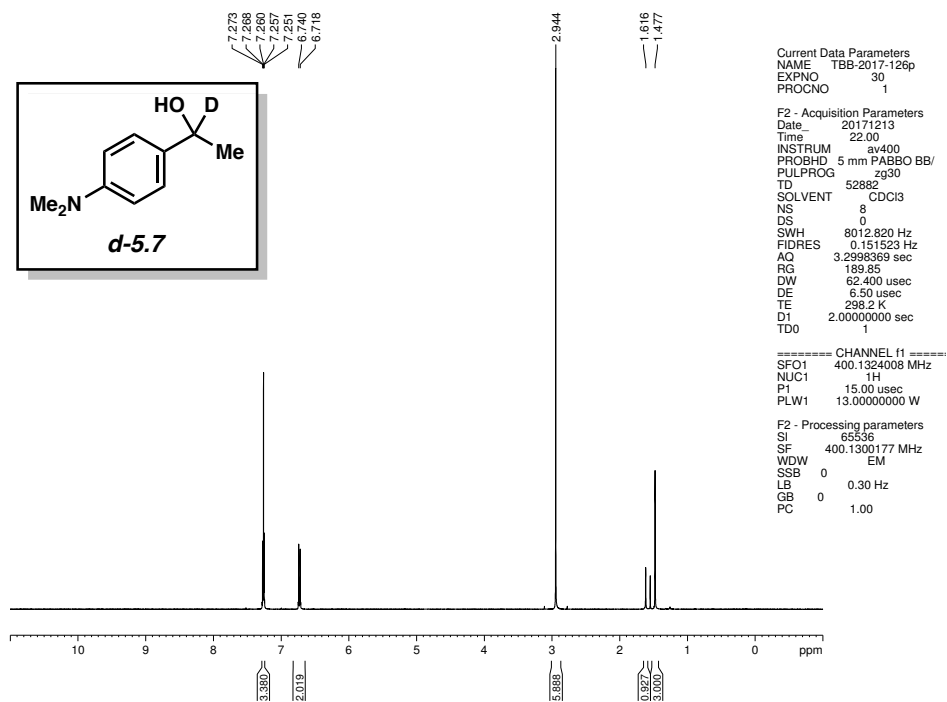*Figure 5.60* ^{1}H NMR (400 MHz, CDCl$_3$) of compound *d*-**5.7**.

5.10 Notes and References

(1) Larock, R. C. *Comprehensive Organic Transformations: A Guide to Functional Group Preparation*; 2nd Ed. John Wiley & Sons: New York, 1997.

(2) For the classic Weinreb amide synthesis of ketones from amides via a tetrahedral intermediate, see: Nahm, S.; Weinreb, S. M. *N*-Methoxy-*N*-methylamides as Effective Acylating Agents *Tetrahedron Lett.* **1981**, *22*, 3815–3818.

(3) For a related synthetic method that allows for the addition of two nucleophiles to substituted ureas, thus affording ketone products, see: Heller, S. T.; Newton, J. N.; Fu, T.; Sarpong, R. One-pot Unsymmetrical Ketone Synthesis Employing a Pyrrole-Bearing Formal Carbonyl Dication Linchpin Reagent. *Angew. Chem., Int. Ed.* **2015**, *54*, 9839–9843.

(4) For representative reviews and publications on the non-decarbonylative transition metal-catalyzed cross-coupling of carboxylic acid derivatives, see: (a) Liebeskind, L. S.; Srogl, J. Thiol Ester−Boronic Acid Coupling. A Mechanistically Unprecedented and General Ketone Synthesis. *J. Am. Chem. Soc.* **2000**, *122*, 45, 11260–11261. (b) Cheng, H.-G.; Chen, H.; Liu, Y.; Qianghui, Z. The Liebeskind–Srogl Cross-Coupling Reaction and its Synthetic Applications. *Asian J. Org. Chem.* **2008**, *7*, 490–508. (c) Johnson, J. B.; Rovis, T. Enantioselective Cross-Coupling of Anhydrides with Organozinc Reagents: The Controlled Formation of Carbon−Carbon Bonds through the Nucleophilic Interception of Metalacycles. *Acc. Chem. Res.* **2008**, *41*, 327–338. (d) Gooßen, L. J.; Rodriguez, N.; Gooßen, K. Carboxylic Acids as Substrates in Homogeneous Catalysis. *Angew. Chem., Int. Ed.* **2008**, *47*, 3100–3120. (e) Albano, G.; Aronica, L. A. Acyl Sonogashira Cross-Coupling: State of the Art and Application to the Synthesis of Heterocyclic Compounds. *Catalysts* **2020**, *10,* 25–61. (f)

Blangetti, M.; Rosso, H.; Prandi, C.; Deagostino, A.; Venturello, P. Suzuki-Miyaura Cross-Coupling in Acylation Reactions, Scope and Recent Developments. *Molecules* **2013**, *18*, 1188–1213. (g) Hirschbeck, V.; Gehrtz, P. H.; Fleischer, I. Metal-Catalyzed Synthesis and Use of Thioesters: Recent Developments. *Chem. Eur. J.* **2018**, *24*, 7092–7107. (h) Ogiwara, Y.; Sakai, N. Acyl Fluorides in Late-Transition-Metal Catalysis. *Angew. Chem., Int. Ed.* **2020**, *59*, 574–594. (i) Gooßen, L. J.; Gooßen, K.; Rodriguez, N.; Blanchot, M.; Linder, C.; Zimmermann, B. New Catalytic Transformations of Carboxylic Acids. *Pure Appl. Chem.* **2008**, *80*, 1725–1733. (j) Meng, G.; Shi, S.; Szostak, M. Cross-Coupling of Amides by N–C Bond Activation. *Synlett* **2016**, *27*, 2530–2540. (k) Liu, C.; Szostak, M. Twisted Amides: From Obscurity to Broadly Useful Transition-Metal-Catalyzed Reactions by N−C Amide Bond Activation. *Chem. Eur. J.* **2017**, *23*, 7157–7173. (l) Dander, J. E.; Garg, N. K. Breaking Amides using Nickel Catalysis. *ACS Catal.* **2017**, *7*, 1413–1423. (m) Takise, R.; Muto, K.; Yamaguchi, J. Cross-Coupling of Aromatic Esters and Amides. *Chem. Soc. Rev.* **2017**, *46*, 5864–5888. (n) Meng, G.; Szostak, M. N-Acyl-Glutarimides: Privileged Scaffolds in Amide N–C Bond Cross-Coupling. *Eur. J. Org. Chem.* **2018**, 2352–2365. (o) Buchspies, J.; Szostak, M. Recent Advances in Acyl Suzuki Cross-Coupling. *Catalysts* **2019**, *9,* 53–75.

(5) Hu, J.; Zhao, Y.; Liu, J.; Zhang, Y.; Shi, Z. Nickel-Catalyzed Decarbonylative Borylation of Amides: Evidence for Acyl C−N Bond Activation. *Angew. Chem., Int. Ed.* **2016**, *55*, 8718–8722.

(6) These cascade reactions could involve either one or two catalytic steps. For discussion on the definitions of cascade and tandem processes, see: (a) Fogg, D. E.; dos Santos, E. N. Tandem

Catalysis: A Taxonomy and Illustrative Review. *Coord. Chem. Rev.* **2004**, *248*, 2365–2379.

(b) Hayashi, Y. Pot Economy and One-Pot Synthesis. *Chem. Sci.* **2016**, *7*, 866–880.

(7) For representative examples of one-pot, sequential protocols for the reductive functionalization of amides, see: (a) Meyers, A.; Comins, D. *N*-Methylamino Pyridyl Amides (mapa) II. An Efficient Acylating Agent for Various Nucleophiles and Sequential Addition to Unsymmetrical *tert*-Alcohols. *Tetrahedron Lett.* **1978**, *19*, 5179–5182. (b) Oda, Y.; Sato, T.; Chida, N. Direct Chemoselective Allylation of Inert Amide Carbonyls. *Org. Lett.* **2012**, *14*, 950–953. (c) Zheng, X.; Liu, J.; Ye, C.-X.; Wang, A.; Wang, A.-E.; Huang, P.-Q. SmI$_2$-Mediated Radical Coupling Strategy to Securinega Alkaloids: Total Synthesis of (−)-14, 15-Dihydrosecurinine and Formal Total Synthesis of (−)-Securinine. *J. Org. Chem.* **2015**, *80*, 1034–1041. (d) Dander, J. E.; Giroud, M.; Racine, S.; Darzi, E. R.; Alvizo, O.; Entwistle, D.; Garg, N. K. Chemoenzymatic Conversion of Amides to Enantioenriched Alcohols in Aqueous Medium. *Commun. Chem.* **2019**, *2*, 82. (e) Ong, D. Y.; Fan, D.; Dixon, D. J.; Chiba, S. Transition-Metal-Free Reductive Functionalization of Tertiary Carboxamides and Lactams for α-Branched Amine Synthesis. *Angew. Chem., Int. Ed.* **2020**, *59*, 11903–11907.

(8) Kaiser, D.; Bauer, A.; Lemmerer, M.; Maulide, N. Amide Activation: An Emerging Tool for Chemoselective Synthesis. *Chem. Soc. Rev.* **2018**, *47*, 7899–7925.

(9) Hie, L.; Fine Nathel, N. F.; Shah, T.; Baker, E. L.; Hong, X.; Yang, Y.-F.; Liu, P.; Houk, K. N.; Garg, N. K. Conversion of Amides to Esters by the Nickel-Catalysed Activation of Amide C–N Bonds. *Nature* **2015**, *524*, 79–83

(10) Pauling, L.; Corey, R. B. Configurations of Polypeptide Chains with Favored Orientations Around Single Bonds: Two New Pleated Sheets. *Proc. Natl. Acad. Sci. USA* **1951**, *37*, 729–740.

(11) Gabriel, P.; Gregory, A. W.; Dixon, D. J. Iridium-Catalyzed Aza-Spirocyclization of Indole-Tethered Amides: An Interrupted Pictet–Spengler Reaction. *Org. Lett.* **2019**, *21*, 6658–6662.

(12) For examples of one-pot, *sequential* reductive functionalizations of tertiary amides, see: (a) Gregory, A. W.; Chambers, A.; Hawkins, A.; Jakubec, P.; Dixon, D. J. Iridium-Catalyzed Reductive Nitro-Mannich Cyclization. *Chem. Eur. J.* **2015**, *21,* 111–114. (b) Tan, P. W.; Seayad, J.; Dixon, D. J. Expeditious and Divergent Total Syntheses of Aspidosperma Alkaloids Exploiting Iridium (I)-Catalyzed Generation of Reactive Enamine Intermediates. *Angew. Chem., Int. Ed.* **2016**, *55*, 13436–13440. (c) Xie, L-G.; Dixon, D. J. Tertiary Amine Synthesis via Reductive Coupling of Amides with Grignard Reagents. *Chem. Sci.* **2017**, *8*, 7492–7497. (d) Fuentes de Arriba, Á. L.; Lenci, E.; Sonawane, M.; Formery, O.; Dixon, D. J. Iridium-Catalyzed Reductive Strecker Reaction for Late-Stage Amide and Lactam Cyanation. *Angew. Chem., Int. Ed.* **2017**, *56*, 3655–3659. (e) Xie, L.-G.; Dixon, D. J. Iridium-Catalyzed Reductive Ugi-Type Reactions of Tertiary Amides. *Nat. Commun.* **2018**, *9*, 2841. (f) Gabriel, P.; Xie, L.-G.; Dixon, D. J. Iridium-Catalyzed Reductive Coupling of Grignard Reagents and Tertiary Amides. *Org. Synth.* **2019**, *96*, 511–527. (g) T. Rogova, P. Gabriel, S. Zavitsanou, J. A. Leitch, F. Duarte, D. J. Dixon. Reverse Polarity Reductive Functionalization of Tertiary Amides via a Dual Iridium-Catalyzed Hydrosilylation and Single Electron Transfer Strategy. *ACS Catal.* **2020**, *10,* 11438–11447. (h) For a review, see: Matheau-Raven, D.; Gabriel, P.; Leitch, J. A.; Almehmadi, Y. A.; Yamazaki, K.; Dixon, D. J. Catalytic

Reductive Functionalization of Tertiary Amides using Vaska's Complex: Synthesis of Complex Tertiary Amine Building Blocks and Natural Products. *ACS Catal.* **2020**, *10*, 8880–8897.

(13) Although definitions for step count vary widely in the literature, here we employ the term "operational step" to indicate the number of reagent additions. Cascade reactions involving a single operational step enjoy certain practical advantages, such as operational simplicity, over complementary cascade reactions requiring multiple reagent additions. Moreover, cascade reactions involving one operational step present additional challenges to the organic chemist including the design of reaction conditions suitable for both transformations.

(14) Wu, X.; Li, X.; Huang, W.; Wang, Y.; Xu, H.; Cai, L.; Qu, J.; Chen, Y. Direct Transformation of Aryl 2-Pyridyl Esters to Secondary Benzylic Alcohols by Nickel Relay Catalysis. *Org. Lett.* **2019**, *21*, 2453–2458.

(15) Bandar, J. S.; Ascic, E.; Buchwald, S. L. Enantioselective CuH-Catalyzed Reductive Coupling of Aryl Alkenes and Activated Carboxylic Acids. *J. Am. Chem. Soc.* **2016**, *138*, 5821–5824.

(16) Zhang, S.; del Pozo, J.; Romiti, F.; Mu, Y.; Torker, S.; Hoveyda, A. Delayed Catalyst Function Enables Direct Enantioselective Conversion of Nitriles to NH_2-Amines. *Science* **2019**, *364*, 45–51.

(17) Further advantages of cascade reactions in regard to efficiency include the avoidance of intermediate purification, improved atom economy, and reduced waste generation. For general reviews on cascade reactions, see: (a) Ref. 6. (b) Tietze, L. F.; Brasche, G.; Gericke, K. *Domino Reactions in Organic Synthesis*, Wiley-VCH, Weinheim, **2006.** (c) Tietze, L. F.;

Beifuss, U. Sequential Transformations in Organic Chemistry: A Synthetic Strategy with a Future. *Angew. Chem., Int. Ed.* **1993**, *32*, 131–163. (d) Tietze, L. F. Domino Reactions in Organic Synthesis. *Chem. Rev.* **1996**, *96*, 115–136. (e) Ho, T.-L. *Tandem Organic Reactions*, Wiley, New York, **1992**. (f) Bunce, R. A. Recent Advances in the Use of Tandem Reactions for Organic Synthesis. *Tetrahedron* **1995**, *51*, 13103–13159. (g) Trost, B. M. The Atom Economy–A Search for Synthetic Efficiency. *Science* **1991**, *254*, 1471–1477. (h) Trost, B. M. Atom Economy—A Challenge for Organic Synthesis: Homogeneous Catalysis Leads the Way. *Angew. Chem., Int. Ed.* **1995**, *34*, 259–281. (i) Nicolaou, K. C.; Edmonds, D. J.; Bulger, P. G. Cascade Reactions in Total Synthesis. *Angew. Chem., Int. Ed.* **2006**, *45*, 7134–7186. (j) Romiti, F.; del Pozo, J.; Paioti, P. H. S.; Gonsales, S. A.; Li, X.; Hartrampf, F. W. W.; Hoveyda, A. Different Strategies for Designing Dual-Catalytic Enantioselective Processes: From Fully Cooperative to Non-Cooperative Systems. *J. Am. Chem. Soc.* **2019**, *141*, 17952–17961. (k) Jones, A.; Stoltz, B. M.; May, J. A.; Sarpong, R. S. Toward a Symphony of Reactivity: Cascades Involving Catalysis and Sigmatropic Rearrangements. *Angew. Chem., Int. Ed.* **2014**, *535*, 2556–2591.

(18) For reviews on nickel catalysis see: (a) Tasker, S. Z.; Standley, E. A.; Jamison, T. F. Recent Advances in Homogeneous Nickel Catalysis. *Nature* **2014**, *509*, 299–309. (b) Rosen, B. M.; Quasdorf, K. W.; Wilson, D. A.; Zhang, N.; Resmerita, A.-M.; Garg, N. K.; Percec, V. Nickel-Catalyzed Cross-Couplings Involving Carbon–Oxygen Bonds. *Chem. Rev.* **2011**, *111*, 1346–1416.

(19) For our laboratory's nickel-catalyzed Suzuki–Miyaura couplings of amides, see: (a) Weires, N. A.; Baker, E. L.; Garg, N. K. Nickel-Catalysed Suzuki–Miyaura Coupling of Amides. *Nat.*

Chem. **2016**, *8*, 75–79. (b) Boit, T. B.; Weires, N. A.; Kim, J.; Garg, N. K. Nickel-Catalyzed Suzuki–Miyaura Coupling of Aliphatic Amides. *ACS Catal.* **2018**, *8*, 1003–1008.

(20) Johnstone, R. A. W.; Wilby, A. H.; Entwistle, I. D. Heterogeneous Catalytic Transfer Hydrogenation and its Relation to Other Methods for Reduction of Organic Compounds. *Chem. Rev.* **1985**, *85*, 129−170.

(21) This catalytic reductive *arylation* protocol complements the known catalytic reductive *alkylation* and reductive *allylation* methods shown in Figure 5.1b.

(22) Despite its air-sensitivity, Ni(cod)$_2$ has been used in more than 800 synthetic methodology studies (see ref 23a). Moreover, it has been used in several process research studies, suggesting its value in manufacturing. For select studies, see: (a) Dawson, D. D.; Jarvo, E. R. Stereospecific Nickel-Catalyzed Cross-Coupling Reactions of Benzylic Ethers with Isotopically-Labeled Grignard Reagents. *Org. Process Res. Dev.* **2015**, *19*, 1356–1359. (b) Liu, J.; Gao, S.; Chen, M. Preparation of Bifunctional Allylboron Reagent and Application to Aldehyde Allylboration. *Org. Process Res. Dev.* **2019**, *23*, 1659–1662.

(23) For the use of Ni(cod)$_2$ on the benchtop, paraffin wax encapsulation has proven to be an effective strategy, including for the Suzuki–Miyaura coupling of aliphatic amides; see: a) Dander, J. E.; Weires, N. A.; Garg, N. K. *Org. Lett*. **2016**, *18*, 3934–3936. (b) Mehta, M. M.; Boit, T. B.; Dander, J. E.; Garg, N. K. Ni-Catalyzed Suzuki–Miyaura Cross-Coupling of Aliphatic Amides on the Benchtop. *Org. Lett.* **2020**, *22*, 1–5.

(24) In our prior studies, we have shown that the Suzuki–Miyaura coupling of aliphatic amides requires high temperatures, presumably to facilitate the transmetalation step.

(25) For seminal publications, see: (a) Meerwein, H.; Schmidt, R. Ein neues Verfahren zur Reduktion von Aldehyden und Ketonen. *Liebigs Ann*. **1925**, *444*, 221−238. (b) Verley, A. The Exchange of Functional Groups Between Two Molecules. The Passage of Ketones to Alcohols and the Reverse. *Bull. Soc. Chim. Fr*. **1925**, *37*, 871−874. (c) Ponndorf, W. Z. Der reversible Austausch der Oxydationsstufen zwischen Aldehyden oder Ketonen einerseits und primären oder sekundären Alkoholen anderseits. *Angew. Chem*. **1926**, *39*, 138−143.

(26) For reviews, see: (a) Cha, J. S. Recent Developments in Meerwein−Ponndorf−Verley and Related Reactions for the Reduction of Organic Functional Groups Using Aluminum, Boron, and Other Metal Reagents: A Review. *Org. Process Res. Dev*. **2006**, *10*, 1032−1053. (b) de Graauw, C. F.; Peters, J. A.; van Bekkum, H.; Huskens, J. Meerwein-Ponndorf-Verley Reductions and Oppenauer Oxidations: An Integrated Approach. *Synthesis* **1994**, 1007−1017. (c) Inch, T. D. Asymmetric Synthesis. *Synthesis* **1970**, 466−473. (d) Nishide, K.; Node, M. Recent Development of Asymmetric Syntheses Based on the Meerwein-Ponndorf-Verley Reduction. *Chirality* **2002**, *14*, 759−767. (e) Ooi, T.; Miura, T.; Itagaki, Y.; Ichikawa, H.; Maruoka, K. Catalytic Meerwein–Ponndorf–Verley (MPV) and Oppenauer (OPP) Reactions: Remarkable Acceleration of the Hydride Transfer by Powerful Bidentate Aluminum Alkoxides. *Synthesis* **2002**, 279−291. (f) Wilds, A. L. *Org. React*. **2011**, *2*, 178−223. (g) Djerassi, C. The Oppenauer Oxidation. *Org. React*. **2011**, *6*, 207−272.

(27) When using *i*-PrOH as the solvent, up to 39% yield of the corresponding ester product was observed by ^{1}H NMR.

(28) Boit, T. B.; Mehta, M. M.; Garg, N. K. Base-Mediated Meerwein–Ponndorf–Verley Reduction of Aromatic and Heterocyclic Ketones. *Org. Lett*. **2019**, *21*, 6447–6451.

(29) We anticipated that the stability of the doubly vinylogous amide byproduct resulting from oxidation of DMPE (**5.7**) would drive the transfer hydrogenation reaction forward.

(30) (a) Verheyen, T.; van Turnhout, L.; Vandavasi, J. K.; Isbrandt, E. S.; De Borggraeve, W. M.; Newman, S. G. Ketone Synthesis by a Nickel-Catalyzed Dehydrogenative Cross-Coupling of Primary Alcohols. *J. Am. Chem. Soc.* **2019**, *141*, 6869–6874. (b) Bera, S.; Bera, A.; Banerjee, D. Nickel-Catalyzed Hydrogen-Borrowing Strategy: Chemo-Selective Alkylation of Nitriles with Alcohols. *Chem. Commun.* **2020**, *56*, 6850–6853. (c) Berini, C.; Brayton, D. F.; Mocka, C.; Navarro, O. Homogeneous, Anaerobic (N-Heterocyclic Carbene)-Pd or -Ni Catalyzed Oxidation of Secondary Alcohols at Mild Temperatures. *Org. Lett.* **2009**, *11*, 4244–4247.

(31) It should be noted that for subsequent evaluation of the scope of the methodology, boronates derived from both pinacol and neopentyl glycol were used. We generally recommend the use of boronates derived from neopentyl glycol. However, the superior commercial availability of boronates derived from pinacol can sometimes be advantageous.

(32) Notably, the reductive arylation of amide **5.1** could be performed on the benchtop by employing either (a) a paraffin wax capsule charged with the precatalyst/ligand combination, $Ni(cod)_2$/Benz-ICy•HCl, or (b) the air-stable Ni(II) precatalyst [(TMEDA)Ni(*o*-tolyl)Cl]. See section 5.8.2.9 for details.

(33) When amides derived from benzoic acids were employed, using a $Ni(cod)_2$ / SIPr catalyst/ligand system and 3-pentanol as the alcohol reductant in toluene at 50 °C for 16 h, the corresponding ester was observed in 85% yield as determined by ^{1}H NMR analysis using hexamethylbenzene as an external standard.

(34) Notably, under our standard Suzuki–Miyaura coupling conditions of the parent amide, epimerization of the stereocenter α to the amide carbonyl is observed affording a mixture of *cis* and *trans* diastereomers (see ref. 19b.)

(35) For transition metal-catalyzed cleavage of the acyl C–O bond of esters, see: (a) Muto, K.; Yamaguchi, J.; Musaev, D. G.; Itami, K. Decarbonylative Organoboron Cross-Coupling of Esters by Nickel Catalysis. *Nat. Commun.* **2015**, *6*, 7508. (b) LaBerge, N. A.; Love, J. A. Nickel-Catalyzed Decarbonylative Coupling of Aryl Esters and Arylboronic Acids. *Eur. J. Org. Chem.* **2015**, 5546–5553. (c) Halima, T. B.; Vandavasi, J. K.; Shkoor, M.; Newman, S. G. A Cross-Coupling Approach to Amide Bond Formation from Esters. *ACS Catal.* **2017**, *7*, 2176–2180. (d) Kruckenberg, A.; Wadepohl, H.; Gade, L. H. Bis(diisopropylphosphinomethyl)amine Nickel(II) and Nickel(0) Complexes: Coordination Chemistry, Reactivity, and Catalytic Decarbonylative C–H Arylation of Benzoxazole. *Organometallics* **2013**, *32*, 5153–5170. (e) Yue, H.; Guo, L.; Liao, H.-H.; Cai, Y.; Zhu, C.; Rueping, M. Catalytic Ester and Amide to Amine Interconversion: Nickel-Catalyzed Decarbonylative Amination of Esters and Amides by C–O and C–C Bond Activation. *Angew. Chem., Int. Ed.* **2017**, *56*, 4282–4285. (f) Yu, H.; Guo, L.; Lee, S.-C.; Liu, X.; Rueping, M. Selective Reductive Removal of Ester and Amide Groups from Arenes and Heteroarenes through Nickel-Catalyzed C–O and C–N Bond Activation. *Angew. Chem., Int. Ed.* **2017,** *56*, 3972–3976. (g) Halima, T. B.; Zhang, W.; Yalaoui, I.; Hong, X.; Yang, Y.; Houk, K. N.; Newman, S. G. Palladium-Catalyzed Suzuki–Miyaura Coupling of Aryl Esters. *J. Am. Chem. Soc.* **2017**, *139*, 1311–1318. (h) Halima, T. B.; Masson-Makdissi, J.; Newman, S. G. Nickel-Catalyzed Amide Bond Formation from Methyl Esters. *Angew. Chem., Int. Ed.* **2018**, *57*,

12925–12929. (i) Zheng, Y.-L.; Newman, S. G. Methyl Esters as Cross-Coupling Electrophiles: Direct Synthesis of Amide Bonds. *ACS Catal.* **2019**, *9*, 4426–4433. (j) Zheng, Y.-L.; Newman, S. G. Nickel-Catalyzed Domino Heck-Type Reactions Using Methyl Esters as Cross-Coupling Electrophiles. *Angew. Chem., Int. Ed.* **2019**, *58*, 18159–18164.

(36) Vitaku, E.; Smith, D. T.; Njardarson, J. T. Analysis of the Structural Diversity, Substitution Patterns, and Frequency of Nitrogen Heterocycles Among US FDA Approved Pharmaceuticals: Miniperspective. *J. Med. Chem.* **2014**, *57*, 10257–10274.

(37) Collins, K. D.; Glorius, F. A Robustness Screen for the Rapid Assessment of Chemical Reactions. *Nat. Chem.* **2013**, *5*, 597–601.

(38) The robustness screen was carried out using amide **5.21** and boronate **5.6**, with one equivalent of additive. Additives **5.22**–**5.27** were recovered in near quantitative yields and did not significantly hinder the reductive arylation reaction. See section 5.8.2.8 for details.

(39) The amide coupling partner was varied in order to simplify isolation of purified products.

(40) For nickel-catalyzed cleavage of the aryl C–O bond of aryl ethers, see: (a) Wenkert, E.; Michelotti, E. L.; Swindell, C. S. Nickel-Induced Conversion of Carbon-Oxygen into Carbon-Carbon bonds. One-Step Transformations of Enol Ethers into Olefins and Aryl Ethers into Biaryls. *J. Am. Chem. Soc*. **1979**, *101*, 2246–2247. (b) Wenkert, E.; Michelotti, E. L.; Swingdell, C. S.; Tingoli, M. Transformation of Carbon-Oxygen into Carbon-Carbon Bonds Mediated by Low-Valent Nickel Species. *J. Org. Chem.* **1984**, *49*, 4894–4899. (c) Dankwardt, J. W. Nickel-Catalyzed Cross-Coupling of Aryl Grignard Reagents with Aromatic Alkyl Ethers: An Efficient Synthesis of Unsymmetrical Biaryls. *Angew. Chem., Int. Ed.* **2004**, *43*, 2428–2432. (d) Guan, B.-T.; Xiang, S.-K.; Wu, T.; Sun, Z.-P.; Wang, B.-Q.; Zhao, K.-Q.;

Shi, Z.-J. Methylation of Arenes via Ni-Catalyzed Aryl C–O/F Activation. *Chem. Commun.* **2008**, 1437–1439. (e) Tobisu, M.; Shimasaki, T.; Chatani, N. Nickel-Catalyzed Cross-Coupling of Aryl Methyl Ethers with Aryl Boronic Esters. *Angew. Chem., Int. Ed.* **2008**, *47*, 4866–4869. (f) Sergeev, A. G.; Hartwig, J. F. Selective, Nickel-Catalyzed Hydrogenolysis of Aryl Ethers. *Science* **2011**, *322*, 439–443.

(41) For the nickel-catalyzed cleavage of the aryl C–N bond of dimethylanilines, see: Cao, Z.-C.; Xie, S.-J.; Fang, H.; Shi, Z.-J. Ni-Catalyzed Cross-Coupling of Dimethyl Aryl Amines with Arylboronic Esters Under Reductive Conditions. *J. Am. Chem. Soc.* **2018**, *140*, 13575−13579.

(42) When boronates bearing para electron-donating groups were employed, a significant amount of the ketone intermediate was observed. For example, the coupling of amide **5.1** with p-NMe$_2$Ph–B(pin) under our standard reaction conditions gave the corresponding ketone and alcohol in 17% and 42% yields, respectively.

(43) Rombouts, F. J. R.; Trabanco-Suárez, A. A.; Gijsen, H. J. M.; Macdonald, G. J.; Bischoff, F. P.; Alonso-de Diego, S.-A.; Velter, A. I.; Van Roosbroeck, Y. E. M. Substituted 3,4-Dihydro-2H-pyrido[1,2-a]pyrazine-1,6-dione Derivatives Useful for the Treatment of (Inter Alia) Alzheimer's Disease. (Janssen Pharmaceuticals, Inc.), WO2013171712A1, **2013**.

(44) Zhao, S.; Guo, Y.; Han, E.-J.; Luo, J.; Liu, H.-M.; Liu, C.; Xie, W.; Zhang, W.; Wang, M. Copper (II)-Catalyzed Trifluoromethylation of Iodoarenes Using Chen's Reagent. *Org. Chem. Front.* **2018**, *5,* 1143–1147.

(45) An exciting opportunity lies in catalytic asymmetric variants of our strategy. In an encouraging preliminary result, we have found that the use of a chiral NHC ligand allows for the synthesis of **5.4** in 36% yield and 20% ee. See sections 5.8.2.10 and 5.8.2.11 for details.

(46) Boit, T. B.; Mehta, M. M.; Garg, N. K. Base-mediated Meerwein–Ponndorf–Verley reduction of aromatic and heteroaromatic ketones. *Org. Lett.* **2019**, *21*, 6447–6451.

(47) Fier, P. S.; Luo, J.; Hartwig, J. F. Copper-mediated fluorination of arylboronate esters. Identification of a copper(III) fluoride complex. *J. Am. Chem. Soc.* **2013***, 135,* 2552–2559

(48) Shields, J. D.; Gray, E. E.; Doyle, A. G. A modular air-stable nickel precatalyst. *Org. Lett.* **2020**, *17*, 2166–2169.

(49) He, W.; Zhao, W.; Zhou, B.; Liu, H.; Li, X.; Li, L.; Li, J.; Shi, J. Synthesis of C_2-symmetric benzimidazolium salts and their application in palladium-catalyzed enantioselective intramolecular α-arylation of amides. *Molecules* **2016**, *21*, 742–748.

(50) Hie, L.; Baker, E. L.; Anthony, S. M.; Desrosiers, J. -N.; Senanayake, C.; Garg, N. K. Nickel-catalyzed esterification of aliphatic amides. *Angew. Chem., Int. Ed.* **2016**, *65*, 15129–15132.

(51) Boit, T. B.; Weires, N. A.; Kim, J.; Garg, N. K. Nickel-catalyzed Suzuki–Miyaura coupling of aliphatic amides. *ACS Catal.* **2018**, *8*, 1003–1008.

(52) Dander, J. E.; Baker, E. L.; Garg, N. K. Nickel-catalyzed transamidation of aliphatic amide derivatives. *Chem. Sci.* **2017**, *8*, 6433–6438.

(53) Lamani, M.; Ravikumara, G. S.; Prabhu, K. R. Iron(III) chloride-catalysed aerobic reduction of olefins using aqueous hydrazine at ambient temperature. *Adv. Synth. Catal*. **2012**, *354*, 1437–1442.

(54) Genc, S.; Arslan, B.; Gulcemal, S.; Gunnaz, S.; Cetinkaya, B.; Gulcemal, D. Iridium(I)-catalyzed C–C and C–N bond forming reactions via the borrowing hydrogen strategy. *J. Org. Chem.* **2019**, *84*, 6286–6297.

(55) Rahaim, R. J.; Maleczka, R. E. C–O hydrogenolysis catalyzed by Pd-PMHS nanoparticles in the company of chloroarenes. *Org. Lett*. **2011**, *13*, 584–587.

(56) Kabalka, G. W.; Wu, Z.; Ju, W. Alkylation of aromatic aldehydes with alkylboron chloride derivatives. *Tetrahedron* **2001**, *57*, 1663–1670.

(57) Gaykar, R. N.; Bhunia, A.; Biju, A. T. Employing arynes for the generation of aryl anion equivalents and subsequent reaction with aldehydes. *J. Org. Chem*. **2018**, *83*, 11333–11340.

(58) Orjales, A.; Mosquera, R.; Toledo, A.; Pumar, M. C.; Garcia, N.; Cortizo, L.; Labeaga, L.; Innerarity, A. Syntheses and binding studies of new [(aryl)(aryloxy)methyl]piperidine derivatives and related compounds as potential antidepressant drugs with high affinity for serotonin (5-HT) and norepinephrine (NE) transporters. *J. Med. Chem*. **2003**, *46*, 5512–5532.

(59) Van Orden, L. J.; Van Dyke, P. M.; Saito, D. R.; Church, T. J.; Chang, R.; Smith, J. A. M.; Martin, W. J.; Jaw–Tsai, S.; Strangeland, E. L. A novel class of 3-(phenoxy-phenyl-methyl)-pyrrolidines as potent and balanced norepinephrine and serotonin reuptake inhibitors: synthesis and structure-activity relationships. *Bioorg & Med Chem. Lett.* **2013**, *23*, 1456–1461.

(60) Jakobsson, J. E.; Gronnevik, G.; Riss, P. J. Organocatalyst-assisted Ar–[18]F bond formation: a universal procedure for direct aromatic radiofluorination. *Chem. Commun.* **2017**, *53*, 12906–12909.

(61) Perner, R. J.; Gu, Y.-G.; Lee, C.-H.; Bayburt, E. K.; McKie, J.; Alexander, K. M.; Kohlhaas, K. L.; Wismer, C. T.; Mikusa, J.; Jarvis, M. F.; Kowaluk, E. A.; Bhagwat, S. S. 5,6,7-Trisubstituted 4-Aminopyrido[2,3-*d*]pyrimidines as novel inhibitors of adenosine kinase. *J. Med. Chem*. **2003**, *46*, 5249–5257.

(62) Mehta, M. M.; Boit, T. B.; Dander, J. E.; Garg, N. K. Ni-catalyzed Suzuki–Miyaura cross-coupling of aliphatic amides on the benchtop. *Org. Lett.* **2020**, *22*, 1–5.